universität wien

DISSERTATION

Titel der Dissertation

„Challenges and solutions of modelling landslide susceptibility in heterogeneous regions – preparing maps for spatial planning in Lower Austria“

Verfasserin

Mag. Helene Petschko

angestrebter akademischer Grad

Doktorin der Naturwissenschaften (Dr. rer. nat.)

Wien, 2014

Studienkennzahl lt. Studienblatt:	A 091 452
Dissertationsgebiet lt. Studienblatt:	Geographie
Betreuer:	Univ.-Prof. Dipl.-Geogr. Dr. Thomas Glade

„Man can learn nothing unless he (she) proceeds from the known to the unknown“.
(Claude Bernard, 1813-1878)

Acknowledgements

Many people played a role in the research and writing process of this thesis and I want to take the opportunity here to express my gratitude to all of them.

Univ.-Prof. Dipl-Geogr. Dr. Thomas Glade was giving me the opportunity and was encouraging me to work on this topic and the related project MoNOE. He was providing me insight and guidance through the research world and the field of natural hazards internationally and in Austria. Thomas thanks for this big chance, your guidance, encouragement and your trust in me.

I am very grateful for continuous support throughout my PhD years from Dr. Rainer Bell. Rainer thanks a lot for all the guidance, advice, talks, quick answers to short termed requests, patience, moral support and collaboration at numerous occasions in research and teaching.

Furthermore, I would like to say thank you to Prof. Dr. Alexander Brenning for all his advice over the years and his willingness to collaborate. Alex, thanks for your guidance, the opportunity for stimulating research stays with the University of Waterloo and all your support.

This thesis was prepared within the project MoNOE (Method development for landslide susceptibility maps for Lower Austria) funded by the Provincial Government of Lower Austria. I want to express my gratitude for very fruitful collaboration and discussions with all the people involved in the project, namely Dr. Joachim Schweigl, Dipl. Ing. Michael Bertagnoli, Mag. Harald Steininger, Ingrid Czech, Dipl. Ing. Gilbert Pomaroli, DI Martin Hois, Dr. Philip Leopold, Dr. Gerhard Heiss and Mag. Herwig Proske.

This thesis would have not been possible without the magnificent availability of data. I'm very grateful for the generous provision of data by the Geological Survey of Austria (Dr. Heinrich Maria, Dipl.-Ing. Dr. Arben Kociu, Dr. Nils Tilch) and Lower Austria (Dr. Joachim Schweigl, Ing. Michael Pernerstorfer), the subunits of the Austrian Torrent and Avalanche Control (DI Johann Grafinger, DI Christian Amberger and DI Heinrich Grünwald) and the Geoinformation Service of the Provincial Government of Lower Austria (Ing. Jürgen Zornig, DI Rainer Prager MSc. (GIS), DI Michael Pregesbauer).

I'm very grateful for the opportunity to gain a wonderful research and training experience in the field of landslide susceptibility analysis with the team of CNR at IRPI in Perugia, Fausto Guzzetti, Paola Reichenbach, Mauro Cardinali, Federica Fiorucci, Mauro Rossi and Ivan Marchesini. This period and the inputs I got were very fruitful for my PhD research.

All current and former ENGAGEies, Catrin, Stefan, Karin, Rainer, Ronny, Christine (E.-H.), Melanie, Benni, Roxana, Christine (G.), Kirsten, Maria and Margreth, I would like to thank for fruitful discussions, good advice, an open ear, lots of fun and laughter, and understanding during my PhD time.

All my friends, with Heike, Iris, Astrid, Birke and Catrin leading the way, and all people I might have forgot, but who helped me during all this time, I want to thank for their listening and understanding on innumerable occasions.

Ein ausgesprochen großer Dank geht auch an meine Familie. All eure Unterstützung in all meinen Projektchen, zu wissen, dass da immer jemand ist auf den/die ich zählen kann wenn mal der Hut brennt und das Zuhause mit jederzeit offenen Türen hat mich hier hin gebracht, nun auch dieses große Projekt Dissertation abschließen zu können. Mama, Papa, Josef, Irene, Johannes, Petra und Giggi vielen herzlichen Dank euch allen dafür!

Dear Jason, I want to thank you for all your support in so many different ways which helped me incredibly a lot in this challenging time to keep on track. Here we go to the future ;)

Table of Contents

Acknowledgements

Table of Contents ..... **i**

List of Figures ..... **v**

List of Tables ..... **viii**

1. Introduction **1**

1.1 Motivation 2

1.2 Thesis outline 3

2. Landslide and susceptibility mapping – theory, state of the art and research gaps **4**

2.1 Landslide types and processes 4

2.1.1 Landslide classification and features 4

2.1.2 Considerations on systems theory and basic concepts 10

2.1.3 Landslide triggers and predisposing factors 15

2.1.4 Human impact on landslides and their mapping 19

2.2 Landslide inventory mapping 21

2.3 Landslide susceptibility modelling 25

2.4 Assessment of the quality of landslide susceptibility maps 32

2.4.1 Quality of input data 33

2.4.2 Quality of statistical model form 34

2.4.3 Quality of final susceptibility map – visualizing prediction uncertainties 35

2.5 Landslide susceptibility maps and spatial planning 35

2.6 Research gaps and challenges analyzing large areas 38

3. Hypotheses and research objectives **44**

4. Lower Austria – a province and its heterogeneity **47**

4.1 General facts and environmental factors 47

4.2 Geology, geomorphology and soils 51

4.3 Landslides 55

4.4 Human impact on landslides 58

4.5 Spatial planning and landslide hazard mitigation strategies 60

5. Materials..... 64

5.1 Available data and their characteristics 64

5.2 Landslide inventories 65

5.3 New data generated during the dissertation 66

6. Methods – from landslide mapping to susceptibility modelling, performance assessment and visualization 69

6.1 Landslide inventory mapping..... 72

6.1.1 Comparison of relative landslide age and current land cover 73

6.1.2 Automated derivation of main scarps from polygons 75

6.1.3 Tests on minimum requirements on landslide inventories for ..... statistical landslide susceptibility modelling.....75

6.1.4 Effectiveness estimate - comparison of landslide polygons and ..... points in the main scarp 76

6.2 Landslide susceptibility modelling – facing the heterogeneity of large regions..... 77

6.2.1 Generalized additive models (GAM) 77

6.2.2 Model design for large heterogeneous study areas 77

6.2.3 Statistical model performance assessment – repeated ..... *k*-fold cross-validation.....78

6.2.4 Assessment of spatially varying prediction uncertainties.....79

6.3 Number and thresholds of susceptibility classes suitable for planning purposes..... 79

6.4 Analysis of different dimensions of human impact on landslides 80

6.4.1 Landslide persistence analysis.....81

6.4.2 Influence on catchment area 81

7. Results..... 82

7.1 Landslide inventory mapping..... 82

7.1.1 Comparison of relative landslide age and current land cover 83

7.1.2 Automated derivation of main scarps from polygons 83

7.1.3 Tests on minimum requirements on landslide inventories ..... for statistical landslide susceptibility modelling 84

7.1.4 Effectiveness estimate - comparison of landslide polygons and ..... points in the main scarp 86

7.2 Landslide susceptibility modelling – facing the heterogeneity of large regions..... 86

7.2.1 Generalized additive models (GAM) and model design for large heterogeneous study areas 86
7.2.2 Statistical model performance assessment – repeated *k*-fold cross-validation 87
7.2.3 Assessment of spatially varying prediction uncertainties 88
7.3 Number and thresholds of susceptibility classes suitable for planning purposes 89
7.4 Analysis of different dimensions of human impact on landslides 92
7.4.1 Landslide persistence analysis 92
7.4.2 Influence on catchment area 92
8. Discussion of the methods, results and hypotheses 94
8.1 Effectiveness, minimum requirements and limitations of landslide inventory mapping on LiDAR DTM derivatives 95
8.1.1 Where within the landslide should be sampled? 97
8.2 Landslide susceptibility of heterogeneous regions – modelling, performance assessment and uncertainties 99
8.2.1 Modelling assumption of uniformitarianism 99
8.2.2 K-fold cross-validation 100
8.2.3 Spatially varying prediction uncertainties 101
8.2.4 Communication of uncertainties by visualization 102
8.3 Human impact on landslides and landslide susceptibility assessments 103
8.3.1 What is an adequate sample size for statistical modelling? 104
9. Conclusions 106
10. Innovations - Solutions 109
11. Perspectives 110
12. References 112
Annex A-1
A. Synopsis of the Publications / Manuscripts A-3
A.1. Landslide inventories for regional early warning systems A-7
A.2. Assessment of landslide age, landslide persistence and human impact using airborne laser scanning DTMs A-15
A.3. Landslide susceptibility modeling with generalized additive models – facing the heterogeneity of large regions A-39
A.4. Landslide inventories for reliable susceptibility maps A-47

A.5. Landslide susceptibility maps for spatial planning in Lower Austria ..A-55

A.6. Assessing the quality of landslide susceptibility maps – case study Lower Austria A-63

A.7. Landslide inventory mapping for large regions – effectiveness of visually analyzing LiDAR DTM derivatives (subm.).....A-89

A.8. Relative age estimation at landslide mapping on LiDAR derivatives – revealing the applicability of land cover data in statistical susceptibility modeling A-123

B. Tables A-131

C. Maps A-135

D. German and English Summary A-143

D.1. Zusammenfassung A-143

D.2. Summary.....A-145

E. Eidesstattliche Erklärung A-147

F. Curriculum Vitae A-149

List of Figures

Figure 2.1 Schematic of a rotational slide (a) and of a translational slide (b) (modified from Highland and Bobrowsky 2008, after Varnes 1978). 5

Figure 2.2 Schematic illustration of a complex slide (rotational slide evolved into an earth flow) illustrating commonly used labels for the parts of a landslide (modified from Highland and Bobrowsky 2008, after Varnes 1978) 6

Figure 2.3 The rise and fall of selected concepts in geomorphology and related fields (own adaption after Orme (2002)) 13

Figure 2.4 Slope stability states and destabilizing factors (based on Crozier, 1986) 15

Figure 2.5 Disposition triggering concept, modified following Kienholz et al. (2004), translated and modified after Zimmermann et al. (1997). (Note: arrows indicate direction of increasing values)..... 18

Figure 2.6 Factors influencing slope stability of a building site on a hillslope (After Worley Consultants Ltd. 1987 in Selby 1993) 20

Figure 4.1 Location and lithology of the study area and the three test districts, Amstetten and Waidhofen/Ybbs in the West and Baden in the East (black outline), in Lower Austria. Source: altered from Petschko et al. 2014c... 48

Figure 4.2 (a) Mean annual precipitation rate (1971-2000), (b) Mean annual air temperature (1991-2000). Source: Hydrographischer Dienst des Landes Niederösterreich (Hydrographic Service of Lower Austria 2011) 48

Figure 4.3 Topography and districts of Lower Austria (Vogl 2008). 49

Figure 4.4 Mean monthly precipitation (Prec.) and mean monthly temperature (Temp.) for four selected areas in Lower Austria. Source: Vogl, 2008 50

Figure 4.5 Area of the lithological units of Lower Austria in km² and number of reported slides per lithological unit as reported in the Building Ground Register of Lower Austria. BM = Bohemian Massif, M = Molasse Zone, TI = intramontane Basins, WBZ = Waschbergzone, FLZ = Flysch Zone, KLZ = Klippen Zone, AU = Austroalpine Unit, PM = Permo-Mesozoic rocks (overlying the Austroalpine ingeous rocks); Source: adapted from Schwenk 1992. 56

Figure 4.6 Typical earth- and debris slides of some lithological units (a) slide in Molasse Zone at Strengberg, (b) the village "Waitzendorf" located on a slide in Molasse with Schlier, (c) translational slide in the Rheno-danubian Flysch Zone at Brand, (d) rotational slide/flow in the Rheno-danubian Flysch Zone at Stössing, (e) slide in Austroalpine Unit (Limestone, Marls) at Dippelreith, (f) slide in Austroalpine Unit (with Dolostone) at Kleinzell. Pictures taken by: (a), (b), (c), (f) Petschko (2010, 2011, 2012); (d) Bertsch (2009); (e) BGR (2006). Source: Petschko et al., 2014c 57

Figure 4.7 Examples of damage reported in the Building Ground Register of the Geological Survey of Lower Austria. a) Slide on farmland (pasture) in Purgstall triggered by thaw in 1978; b) Slide in the district Wien Umgebung on a land fill; c) slide in a forest in Loich occurred in 1989; d)

Cracks in a house caused by a slide in 1968 in the district Melk; e) Slide in Waidhofen/Ybbs damaging a road in 1992. Picture source: Reports of the Building Ground Register. 59

Figure 4.8 Earth slide at Kleinsierndorf (Weinviertel) at a field which the topography was modified during the "Kommasierung" in the past (date unknown), triggered August 2010. Pictures taken by Petschko (2010) . 60

Figure 4.9 Hazard zonation plan extract from eHORA for Ybbsitz (Waidhofen/Ybbs). Source: Hora, 2014 62

Figure 5.1 Existing landslide inventories in Lower Austria. a) Points of the Building Ground Register (red triangles); b) Polygons, lines or points of the GEORIOS database of the Geological Survey of Austria; c) Landslide mapped in the hazard zonation plan of the Austrian Service for Torrent and Avalanche control. 65

Figure 6.1 Materials used for the landslide inventory mapping: (a) LiDAR DTM hillshade map with 315° azimuth angle; (b) LiDAR DTM hillshade map with 135° azimuth angle; (c) LiDAR DTM hillshade map with 45° azimuth angle; (d) Orthophoto (25cm x 25cm) acquired between 2000-2004; (e) Orthophoto (12,5cm x 12,5cm) acquired between 2007-2008; (f) Slope angle map derivative from the LiDAR DTM; (g) 4m spaced contour lines derived from the LiDAR DTM. Source: DTM and orthophotos: Provincial Government of Lower Austria; Landslide mapping: own survey. Figure: Petschko et al. 2014a 72

Figure 6.2 Schematic drawing of geomorphological changes with increasing relative landslide age of an idealized landslide (based on McCalpin (1984) and Keaton and DeGraff (1996). A = active, reactivated, suspended or dormant-historic; B = dormant-young; C = dormant-mature; D = dormant-old. Source: Bell et al. (2012) 74

Figure 7.1 Comparison of the landslide inventory mapped on Airborne Laserscanning (ALS) LiDAR DTM derivatives with existing inventories in Lower Austria. Source: Petschko et al. 2010 83

Figure 7.2 Comparison of landslide susceptibility maps derived using (a) points from the Building Ground Register, (b) points sampled randomly within the landslide polygon and (c) points sampled randomly within the main scarp. (d) Landslide inventory of the district Amstetten and Waidhofen/Ybbs. Source: Petschko et al. (2013). 85

Figure 7.3 Landslide susceptibility maps classified according to different percentage of landslides within each susceptibility class. The versions correspond to the versions listed in Table 7.1 and Table 7.2. The naming of the classes represents the naming decided on with the stakeholders in the project MoNOE. 90

Figure 7.4 Final susceptibility map for the study area in Lower Austria. Source: altered from Petschko et al. (2014c) 91

Figure 7.5 Landslide persistence, landslide size and land cover type in Waidhofen/Ybbs. Source: Bell et al. (2012) 93

Figure C.1 Map of the Building Ground Register of the Geological Survey of Lower Austria. Source: Geological Survey of Lower Austria A-135

Figure C.2 Explanatory variable: catchment area A-135

Figure C.3 Explanatory variable: catchment height A-136
Figure C.4 Explanatory variable: convergence index (10m radius) A-136
Figure C.5 Explanatory variable: convergence index (50m radius) A-137
Figure C.6 Explanatory variable: Curvature A-137
Figure C.7 Explanatory variable: Euclidian distance to nappe boundary A-138
Figure C.8 Explanatory variable: East versus West exposition (Eastness) A-138
Figure C.9 Explanatory variable: North versus South exposition (Northness) ... A-139
Figure C.10 Explanatory variable: Permeability (0cm - 20cm) A-139
Figure C.11 Explanatory variable: Minimum permeability (0cm - 100cm) A-140
Figure C.12 Explanatory variable: Slope angle A-140
Figure C.13 Explanatory variable: Euclidian distance to tectonic line A-141
Figure C.14 Explanatory variable: Topographic wetness index A-141
Figure C.15 Explanatory variable: Void space (0cm – 20cm) A-142
Figure C.16 Explanatory variable: Void space (mean 0cm – 100cm) A-142

I tried my best, to identify and cite all sources of the pictures and figures. In case any copyright infringement occurred I would politely like to ask the copyright holder to contact me.

List of Tables

Table 4.1 Lithological units of Lower Austria: landslides and topography (Source: Petschko et al. 2014c) 52

Table 5.1 Overview on data generated within the thesis for the different study areas: (1) the test study area including the districts Amstetten, Baden and Waidhofen/Ybbs and (2) the study area mainly covering Lower Austria (15,835km²) 67

Table 6.1 Overview on analysis steps and methods used within this study. Similarly to a flow chart the steps are listed chronologically from top to the bottom according to when it was done within this analysis. Overlapping cells within different steps (columns, e.g. landslide inventory and modelling) indicate an interrelationship of the methods used for assessing the respective hypothesis. In brackets the study area of the respective analysis is indicated: AMBNWY = Amstetten, Baden and Waidhofen/Ybbs; WY = Waidhofen/Ybbs; WB = Wilhelmsburg; NOE = entire study area. Furthermore, the respective hypothesis (H1 – H5) and the publication addressing this (A.1 – A.8, according to the list given in the annex) are given. LR = Logistic regression; GAM = Generalized additive models..... 70

Table 7.1 Versions of visually analyzed susceptibility maps visualized using different threshold values according to the percentage of landslides included in the high and low susceptibility class 89

Table 7.2 List of percentage of landslides included in the susceptibility class and percentage of the total area covered by the susceptibility class (visualized in Fig. 7.3)..... 89

Table B.1 Variable frequency of variables used linearly (N) or with a smoothing function (S) applying spatial k-fold cross validation (spCV) and k-fold cross validation with random subsampling (CV). The grey shaded cells mark the variable usage in the global model used to compute the susceptibility map. A-132

1. Introduction

Every year naturally and anthropogenically triggered landslides are causing fatalities or damage on houses, linear infrastructure (roads, train tracks) or farmland. While only few data is available to describe the total count of fatalities worldwide, a study of reported fatalities between the years 2004 – 2010 allows a first estimation (Petley 2012). Globally, information on 2620 landslides causing 32,322 documented fatalities was collected (Petley 2012). While the hot spots of these landslides and fatalities are located in Asia, in Europe and the United States these numbers might be considered as comparably low (Petley 2012). Perhaps the awareness of possible impacts of landslides is considered being low, and this natural hazard is often underestimated by people and governing authorities, due the limited affected local areas (Committee on the review of the national landslide hazards mitigation strategy, board on earth sciences and resources, division on earth and life studies 2004; Hervás 2003).

Similarly, in Austria damage and fatalities caused by landslides (debris flows and slides) occurred in the past, while the awareness was considered as rather low. Events such as in 2005 in Gasen and Haslau or in 2009 in Feldbach or in the province of Lower Austria, with a total number of around 4000 landslide events brought the possible effects of landslides to the mind of authorities, residents and the media (Abteilung Feuerwehr und Zivilschutz, Amt der NÖ Landesregierung 2010; BMLFUW 2010; Damm et al. 2010; Hornich and Adelwöhrer 2010; Schwarz and Tilch 2008). These events increased the demand for tools (e.g. landslide susceptibility maps) to consider not only debris flows, avalanches and floods but also sliding and rock fall processes in provincial spatial planning (Pomaroli et al. 2011; Rudolf-Miklau 2007). This describes an ongoing transformation from post-disaster recovery practices to introducing pre-disaster mitigation strategies in Austria (Alexander 2002; Petschko et al. 2014c).

Generally, landslide susceptibility describes the likelihood of a landslide event occurring in an area on the basis of the local terrain conditions (Brabb 1984). Implementing these new tools in spatial planning would be beneficiary aiming at the avoidance of the hazard by preventing development in undesirable locations or undesirable types of development (Cascini 2008; Pomaroli et al. 2011; Sapountzaki et al. 2011; Schwab et al. 2005). Furthermore, they might contribute to a better understanding and awareness regarding landslide susceptibility including the existence of remaining susceptibility even after installing mitigation measures (Committee on the review of the national landslide hazards mitigation strategy, board on earth sciences and resources, division on earth and life studies 2004).

With this thesis I want to contribute to the research in the field of providing landslide susceptibility maps prepared for implementation in spatial planning strategies. This includes the evaluation of effective methods for landslide inventory mapping, the assessment of the quality of landslide susceptibility maps questioning

the appropriateness and limitations of these maps for use in a planning framework, and exploring approaches to accommodate the needs of map users.

1.1 Motivation

Landslide susceptibility maps have a huge potential for being implemented in spatial planning strategies. They provide spatially comprehensive and coherent information on the landslide susceptibility of an investigated area (Brabb 1984; Glade et al. 2005; Guzzetti et al. 2006; Guzzetti et al. 2000; Varnes 1984). However, only few examples are known to date, where landslide susceptibility maps have been prepared for large, heterogeneous regions in a comparable manner and implemented in spatial planning strategies (e.g. Bălteanu et al. 2010; Van Den Eeckhaut et al. 2007; Piacentini et al. 2012; Wills et al. 2011).

Furthermore, these maps are resulting from modelling and immediately create a decisive reality for the users of the map (Egner and Pott 2010). The users of the map might not know about the uncertainties behind the rather definite looking boundaries between different landslide susceptibility classes. This leads to a perception of the maps as a reality, a partitioning of the land according to susceptibility classes more or less prone to future landslides (Egner 2012). However, all models are always only a simplification of the reality and uncertainties can only be minimized but never be eliminated. In other words, *"all models are wrong, but some are useful"* (Box 1979). Therefore, there is a demand for a detailed analysis and communication of the quality of the landslide susceptibility map. Quality in terms of the input data (landslide inventory), the model performance and reliability of the (usually) classified susceptibility map.

Hence, the motivation of this study is:

- Gaining knowledge on the past occurrence and distribution of landslides within a large study area
- Detecting possible future affected areas/slopes within a large heterogeneous study area where more detailed (geotechnical) analysis is necessary or strongly recommended
- Providing a landslide susceptibility map comparable for an entire province, optimized for its implementation in spatial planning, aiding easy interpretation and well informed decisions of a municipality
- Assessing and visualizing uncertainties of the landslide susceptibility map that might be informative or decisive during the planning process
- Supporting the transformation from the reaction to events, to the avoidance of damage and better preparedness to possible landslide events with user-friendly map products prepared on a planning scale but for large regions

As study area the province of Lower Austria (19,186 km²) was selected. In this province, a wide range of landslide processes occurs, e.g. debris flows, rock falls,

earth slides as defined after Cruden and Varnes (1996). Provincial reports highlight that earth and debris slides regularly cause damage on houses and farmland (Schweigl and Hervás 2009). The landslide size and density varies throughout the province.

Therefore, aiming at better preparedness and avoidance of damage due to landslide events, a project called "Method development of landslide susceptibility modelling for Lower Austria (MoNOE)" was initiated by the Geological Survey and the Department of Spatial Planning and Regional Policy of the Provincial Government of Lower Austria. The objective was, to provide landslide susceptibility maps for the processes earth and debris slides and rock falls for the entire province on a scale of 1:25,000. These maps will be implemented in the spatial planning procedure of every municipality of Lower Austria, as first information on possible landslide susceptibility where more detailed slope stability analysis is necessary. This project gave room and the opportunity for the present thesis analyzing and presenting the modelling and generation of landslide susceptibility maps for earth and debris slides on a scale of 1:25,000 for Lower Austria. Lower Austria portrays a very interesting study area given the size, the analysis scale and the possible implementation of the results in spatial planning strategies.

1.2 Thesis outline

Being a cumulative dissertation this thesis is containing both, a monographic part presenting the framework of the thesis showing how the different publications and manuscript are all part of a greater research question, and the publications and manuscript themselves. In the monographic part the theory and state of the art of landslide susceptibility research, the hypotheses of this study, a description of the study area and the materials used are described in detail giving a framework for the research. While the focus is more on the theoretical background and presentation of the research objective, the methods, the results and a synthesizing discussion of the different methodologies, results and hypotheses closed by conclusions of the entire research done and research perspectives are also presented. A more extensive discussion of the different methodologies used within all the analysis steps is furthermore provided in the respective publication or manuscript in the annex.

The individual articles published in international journals, books or as conference proceeding contributions are collected in the synopsis of the publications and manuscripts in the annex. As the publications present the methods and results of the studies in full detail, a respective reference to this work was included writing these passages in the monographic part. Although the publications were coauthored by other researchers, the referenced passages were written and analyzed solely by the author of this thesis. More detailed descriptions of the contributions of the different authors are given for each publication the annex. All together forms the dissertation and portrays the scientific contribution of this research.

2. Landslide and susceptibility mapping – theory, state of the art and research gaps

2.1 Landslide types and processes

Landslide is only one out of several terms which are used nearly simultaneously in literature to describe masses moving down a slope. While the term landslide is the most popular expression (Dikau 1996), the terms mass movement, mass wasting, slope failure, or slope movements might also be found in literature (Brunsden 1985; Crozier 1986; Cruden 1991; Terzaghi and Peck 1967; Varnes 1978). Throughout this manuscript the term landslide is used describing a *"movement of a mass of rock, debris or earth down a slope"* (Cruden 1991) or maybe more generally worded *"a downward and outward movement of slope forming materials under the influence of gravity"* (Varnes 1978). Varnes has advocated the term slope movement with the latter definition.

2.1.1 Landslide classification and features

Landslides of different types occur in a variety of materials and form different processes. To distinguish between different types the velocity and mechanism of the movement, the material, the mode of deformation, the geometry of the moving mass and the water content have to be analyzed (Selby 1993). Unsurprisingly, a large number of different classifications of landslide types and processes exist, strongly influenced by the field they emerged from (geology, (geo-) engineering, geomorphology; Crozier 1986). New landslide classification schemes are still coming up, however the first classification suggestions were already presented around 80 years ago, amongst others, by (Varnes 1978) Sharpe (1938), Ward (1945), Campbell (1951), Varnes (1958, 1978), Hutchinson (1968, 1977, 1988), Skempton and Hutchinson (1969) and Crozier (1973) (as summarized by Crozier (1986)). Newer classification schemes were proposed by Cruden and Varnes (1996), Dikau et al. (1996) and most recently by Hungr et al. (2013).

The classification most generally accepted in the international landslide community and also applied in this study is the one proposed by Varnes (1978) and published abbreviated by Cruden and Varnes (1996). It distinguishes between different types of material (bedrock and predominantly coarse or fine soils) and types of movement (fall, topple, slide, spread, flow and complex). Combining these, for example to "earth slide", 16 different types of landslides are classified (Tab. 2.1). The material types describe the material before its displacement by a landslide (Cruden and Varnes

1996). Bedrock is defined as intact, hard material that was found in its original place. In contrast, debris and earth, both summed up to soil, are containing 20 to 80 percent of coarse and more than 80 percent of particles smaller than 2mm respectively (Cruden and Varnes 1996; Dikau 1996).

Tab. 2.1 Abbreviated classification of landslides (Cruden and Varnes 1996; Varnes 1978)

Type of Movement	*Type of material*		
	Bedrock	*Engineering soils*	
		Predominantly coarse	*Predominantly fine*
Fall	Rock fall	Debris fall	Earth fall
Topple	Rock topple	Debris topple	Earth topple
Slide Rotational	Rock slide	Debris slide	Earth slide
Translational			
Spread	Rock spread	Debris spread	Earth spread
Flow	Rock flow	Debris flow	Earth flow
Complex	Combination of two or more principal types of movement		

Slides are characterized by the presence of a surface of rupture or relatively thin zones of intense shear strain (Cruden and Varnes 1996). They can be distinguished according to the shape of the shearing plane in "translational slides" and "rotational slides" (Fig. 2.1; Varnes 1978). While "rotational slides" show a semicircular shear surface, the shear surface of translational slides is planar (Dikau 1996). "Rotational slides" might also be referred to as "slumps" (Selby 1993; Varnes 1978).

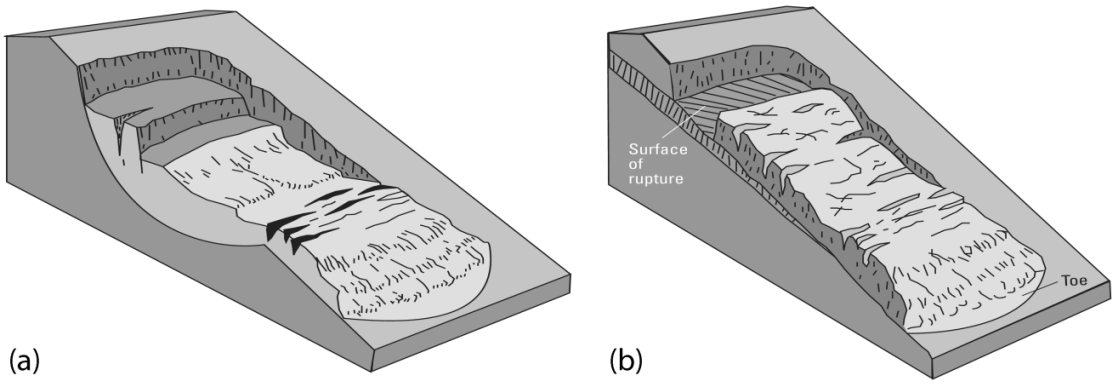

Figure 2.1 Schematic of a rotational slide (a) and of a translational slide (b) (modified from Highland and Bobrowsky 2008, after Varnes 1978).

Landslides show specific morphological features which are decisive detecting and distinguishing landslides in the field, on aerial photographs, orthophotos or from digital elevation models (DTMs, Fig. 2.2, Tab. 2.2). These features might be found of different dimensions (size, depth, number) depending on the current landslide type and size. They can be found in either, the depletion zone, where the displaced material lies below the original ground surface, and the accumulation zone, where

additional material is deposited from the landslide as can be observed by an increase of the elevation of the original ground surface (Cruden and Varnes 1996).

The overall morphology of the depletion zone is characerized by a concave profile and planar curvature. It includes the crown, main scarp, minor scarp(s), main body, surface of rupture and flank of a landslide (Fig. 2.2). Starting from the crown the depletion zone expands until the toe of the surface of rupture (Fig. 2.2). The undisplaced material of the crown is located next to the highest parts of the main scarp (Cruden and Varnes 1996). The main scarp is probably the most distinct discernible feature of a landslide. Located at the upper edge of a landslide the main scarp is a steep surface of undisturbed ground giving a glance on the original surface of rupture (Cruden and Varnes 1996). However, it does not necessarily portray the initial point of movement in the landslide. This usually remains unknown (Cruden and Varnes 1996). Minor scarps can be found slope downwards and have a similarly steep surface as main scarps but are located within the displaced material (Cruden and Varnes 1996). The boundary between the displaced material and the original surface is termed the surface of rupture (Fig. 2.2; Cruden and Varnes 1996).

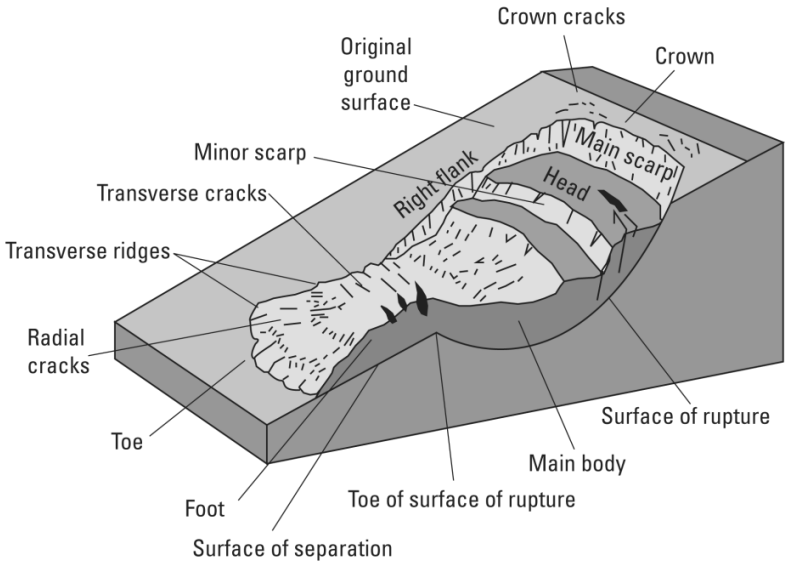

Figure 2.2 Schematic illustration of a complex slide (rotational slide evolved into an earth flow) illustrating commonly used labels for the parts of a landslide (modified from Highland and Bobrowsky 2008, after Varnes 1978)

In contrast to the depletion zone, the accumulation zone generally shows a convex profile and planar curvature. However, this general form can be disturbed by transverse and radial cracks and ridges. The feature most distant from the main scarp that represents the lower end of the displaced material of the landslide is termed the toe (Varnes 1978). The accumulation zone expands from the toe of the surface of rupture to the landslide toe (Cruden and Varnes 1996; Fig. 2.2).

For more detailed information on characteristic features of each landslide section please refert to Table 2.2 (Rib and Liang 1978). Only a selection of landslide types (rotational and translational slides, rock and debris slides and soil (earth) flow) is presented in this thesis, as only these types were analysed (Tab. 2.2).

In the following rotational and translational slides are characterized in more detail, providing a basis for the applied landslide mapping criteria. Characteristic for rotational slides are backwards-tilted surfaces in the upper part of the slide (head) oriented toward the scarps and forming crevasses (so called Nackentälchen; Cruden and Varnes 1996; Dikau 1996; Rib and Liang 1978). Within these, small ponds, which can form from obstruction of overland flow, can be observed in the field or on remote sensing imagery (Buma and van Asch 1996; Varnes 1978). Using contour lines (from topographic maps or derived from DTMs) areas of rotational slides are characterized by irregular, wavy and in the scarp areas closely spaced, curved contour lines (Rib and Liang 1978). This morphology arises from the movement mechanism and the evolvement of minor scarps, ridges and cracks. Furthermore, some material might move downwards the slope in discrete blocks caused by transverse cracks (Buma and van Asch 1996). Whereas other landslide types might be bond to the presence of specific material, rotational slides can occur in a broad range of parent materials (Buma and van Asch 1996).

In contrast to rotational slides translational may be very different according to the material they occur in. Translational earth slides, or slab slides as termed by Dikau et al. (1996), occur in soils, weathered from clays, mudrocks and silty clays (Ibsen et al. 1996). Characteristically, translational earth slides are highly influenced by the pedological or geological structure. Generally spoken, the surface of rupture usually evolves along discontinuities or in a shear zone where permeable and impermeable layers are superimposed on each other (Ibsen et al. 1996). This might occur at a surface of unweathered or lightly weathered bedrock, a pedogenic horizon or a structural surface (Ibsen et al. 1996). Ridges or waves might form at the toe of a slab slide by bucking, wedging or heaving processes when the block of material is comparably thin (Ibsen et al. 1996). Relative to their length and width and compared to rotational slides, translational earth slides are usually shallow (Ibsen et al. 1996). As their movement is strongly related to the water content and therefore the groundwater level, the movement shows seasonality with faster movement during wet months (Ibsen et al. 1996).
Another type of translational slides is debris slides. They occur in unconsolidated material (colluvium or weathered portions of usually densely fractured rock masses) and are rather shallow (0.5m - 1.5m; Corominas 1996; Varnes 1978). The failure occurs at the contact zone of bedrock, regolith cover and at discontinuity planes such as bedding planes or schistosity (Corominas 1996). Water plays a role for the start of the movement but intense rainfall and earthquakes are more important for the initiation (Corominas 1996). Therefore, also the aspect of the slope is decisive, as it has an influence on the moisture conditions (Crozier 1986). Furthermore, the presence or absence of vegetation cover and the steepness of the slope play an important role (Corominas 1996).

Tab. 2.2 Summary of features characterizing and aiding the recognition of selected landslide types (according to the classification used in Dikau 1996), modified after Rib and Liang (1978)

Landslide type	*Landslide sections*						
	Crown	Main scarp	Flanks	Head	Body	Foot	Toe
Slide (rotational)	Has cracks that tend to follow facture patterns in the original rock, in debris or soil cracks are mostly curved concave toward the slide	Steep, bare, concave toward slide and commonly high; may show striae and furrows on surface running from crown to head; may be vertical in upper part	Have striae with strong vertical component near head and strong horizontal component near foot; have scarp height that decreases toward foot; may be higher than original ground surface between foot and toe; have 'en echelon' cracks that outline slide in early stages	Remnants of land surface flatter than original slope or even tilted into hill, creating at base of main scarp depressions in which perimeter ponds form; has transverse cracks, minor scarps, grabens, fault blocks; bedding attitude different from surrounding; trees lean uphill	Consists of original slump blocks generally broken into smaller masses; has longitudinal cracks, pressure ridges and occasional over thrusting; commonly develops small pond just above the foot	Commonly transverse cracks developing over the foot line and transverse pressure ridges developing below the foot line; has zone of uplift, no large individual blocks and trees that lean downhill	Often a zone of earth flow of lobate form in which material is rolled over and buried; has trees that lie flat or at various angles and are mixed into the toe material; in rock there is little or no flow, often nearly straight and close to the foot may have steep front
Slide (translational)	Has cracks most of which are nearly vertical and tend to follow the contour of the slope	Nearly vertical in upper part and nearly planar and gently sloping in lower part	Low scarps with vertical cracks that usually diverge downhill	Relatively undisturbed and has no rotation	Usually composed of single or few units; is undisturbed except for common tension cracks that show little or no vertical displacement		Flows or overrides ground surface

Landslide type	*Landslide sections*						
	Crown	Main scarp	Flanks	Head	Body	Foot	Toe
Rock slide, debris slide, mudslide*	Consists of loose material and has cracks between blocks	Usually stepped according to spacing of joints or bedding planes; has irregular surface in upper part and is planar or gently sloping in lower pan	Irregular	Many blocks of rock, debris or soil	Rough surface of many blocks some of which may be in approximately their original attitude but lower if movement was slow, shows flow structure		Consists of an accumulation zone of rock, debris or soil; spreading and lobate; often consists of material rolled over and buried
Soil flow	Few cracks	Steep and concave toward slide; may have a variety of shapes in outline; nearly straight, gentle arc, circular or bottle-shaped			Conical heap of soil, equal in volume to the head region		Spreading and lobate

*Note: While the term mudslide is used in the European context, the term earthflow is more common in North America.

Recently a new version of the classification scheme proposed by Cruden and Varnes (1996) was published by Hungr et al. (2013). This new classification scheme was done to incorporate up to date findings characterizing the landslide processes and to introduce general geological and geoengineering terms (Hungr et al. 2013). It contains 32 different types of landslide processes and gives room for user customization creating a term best appropriate for the landslide processes dealt with. Furthermore, the compatibility of the wording with the old classification system of Varnes (1978) and Cruden and Varnes (1996) was taken care of (Hungr et al. 2013). This should prevent misunderstandings reading and comparing old and recent literature (Hungr et al. 2013). However, this is a very recent development, published after the landslide inventory mapping was done for this study. Therefore, this new classification is not considered or applied here.

Naturally, distinguishing these idealized landslide forms and types in nature can be challenging (Crozier 1986). One process observed in the nature might represent multiple processes according to the classification (Dikau 1996). Therefore, often a mix of movement and material types is combined to a complex landslide e.g. a rotational earth slide-earth flow (Cruden and Varnes 1996).

2.1.2 Considerations on systems theory and basic concepts

The theoretical background of this thesis can be aligned with the paradigm of the systems theory which was introduced to geomorphology with the quantitative revolution initiated by Arthur N. Strahler (1952; 1950). In the 1950s and 1960s Arthur Strahler and Richard Chorley recognized the relevance of the general systems theory based on Bertalanffy (1956; 1950) to geomorphology (Chorley 1962; Chorley and Kennedy 1971; Strahler 1980; Strahler 1950). The systems approach or theory reached wider acceptance with publications of Richard Chorley (1962) and later a book published by him together with Barbara Kennedy (1971). Since, the systems approach has been dominating the physical geography and geomorphology (Egner 2010). Nowadays, this theory developed to an implicit theory used by many physical geographers and geomorphologists, but not reflected, questioned or analyzed in the daily research practice (Egner and Von Elverfeldt 2009; Von Elverfeldt and Glade 2011; Von Elverfeldt and Keiler 2008; Scheidegger 1992). Whereas this "old" systems theory still influences the way of thinking, recently new trends evolved in this field considering nonlinearity and complexity in geomorphology (Von Elverfeldt and Glade 2011; Keiler 2011; Phillips 2009a). Both is briefly introduced and reflected on in this chapter providing a theoretical background of this research and the perspective of an emerging research field.

Traditionally a system is defined as *"a structured set of objects and/or attributes. These objects and attributes consist of components or variables (i.e. phenomena which are free to assume variable magnitudes) that exhibit discernible relationships with one another and operate together as a complex whole, according to some observed pattern."* (Chorley and Kennedy 1971). Therefore, using systems theory looking at

the objects of interest we look at interacting elements and transformation processes, influenced by inputs from the environment and its produced outputs (except in morphological systems; Egner and Von Elverfeldt 2009; Von Elverfeldt and Glade 2011).

Focusing on physical geography, Richard Chorley and Barbara Kennedy distinguish four different structural types of inanimate systems (Chorley and Kennedy 1971): (a) morphological systems; (b) cascading systems; (c) process-response systems and (d) control systems. Some additions introducing morphologic evolutionary systems to this classification were done later e.g. by Slaymaker (1991) and Dikau (1998). The main difference between these system types is the degree of complexity increasing from morphological systems to control systems (Chorley and Kennedy 1971):

Morphological systems consist of the physical elements of the system, e.g. slope geometry including amongst others slope angle, slope aspect, permeability or soil depth (Chorley and Kennedy 1971; Von Elverfeldt and Keiler 2008). The degree and direction of relationship between these elements can be assessed with correlation analysis (Chorley and Kennedy 1971). At cascading systems additionally to the physical elements also the input, throughput and output of the subsystems in form of energy or mass (e.g. water, sediment) is analyzed (Chorley and Kennedy 1971; Von Elverfeldt and Keiler 2008). Regulators might influence the flow, or cause storage of energy or mass. Therefore, the relationship of input and output is of high interest analyzing cascading systems. The combination of cascading and morphological systems using regulators or storage (e.g. internal friction angle of slope material as part of the morphological system) describes process-response systems (Chorley and Kennedy 1971). A control system describes a process-response system where humans change the system intentionally and controlled, e.g. influencing the regulators in a cascading system (e.g. changing the slope geometry to install technical landslide mitigation measures; Chorley and Kennedy 1971; Von Elverfeldt and Keiler 2008). All these relatively low-complexity systems interact with higher-level structures of plants, animals, and human societies (Chorley and Kennedy 1971). A more detailed definition and description of these system types can be found in Chorley and Kennedy (1971) and is discussed amongst others by Slaymaker (1991), Dikau (1998), Hugget (2007), Von Elverfeldt and Keiler (2008) and Von Elverfeldt and Glade (2011).

In this understanding, describing a system necessitates knowing the parts and the relationships between the parts (Egner and Von Elverfeldt 2009; Slaymaker 1991). Furthermore, the surrounding environment has a high influence on the system, possibly changing the links between the system elements and determining the systems behavior (Von Elverfeldt and Glade 2011). When this input and output of mass and energy is balanced, e.g. by self-adjustment or self-regulatory processes of the elements and variables within a system, the system can be assumed as being in equilibrium (Bracken and Wainwright 2006; Von Elverfeldt and Glade 2011). However, this is only one out of many equilibrium concepts in geomorphology as reviewed by Bracken and Wainwright (2006) and Phillips (2006a; Von Elverfeldt and Glade 2011). Generally, the aim of a geomorphic system might be described as to

reach this equilibrium, constantly balancing the interaction with its environment (Von Elverfeldt and Glade 2011). This equilibrium thinking is still present in research on geomorphology (Bracken and Wainwright 2006; Von Elverfeldt and Glade 2011).

Furthermore, in the framework of systems theory the concepts of causality, scales and reductionism are applied. Causality describes that one cause has one effect, which is reproducible and repeatable (e.g. changes in the environment cause changes within the system; Embleton-Hamann et al. 2013). Within scales, the concepts of "graded time" and "steady time" are leading the way within which linear and causal relationships and equilibria are assumed (Von Elverfeldt and Glade 2011). Trying to describe and understand the reality better, looking at the 'reality' using subsections of space and time (the reductionist view) and summing this up to the larger entity is assumed to be appropriate (Von Elverfeldt and Glade 2011; Sarewitz and Pielke 1999).

This general paradigm of systems theory is the basis for landslide susceptibility, hazard or risk analysis. Different concepts alongside the systems theory are of importance for this thesis. These are the concepts of uniformitarianism and the quantitative, nearly mechanic, understanding of landslide mechanisms. With the quantitative revolution in the 1950s and 1960s many long known concepts from other disciplines (e.g. engineering, soil science, geology, and statistics) which included a quantitative approach found a place in geomorphology (Orme 2002). Landslide processes are considered to occur in a system that might be defined in physics as open complex but organized (Huggett 2007). More precisely, in this thesis systems are looked at as open process-response systems or in case of human interference as control systems (Chorley and Kennedy 1971; Huggett 2007; Slaymaker 1991). Therefore, knowing the input to the system, the output can be estimated using different models (or) describing the system itself as detailed as possible. Applying this to landslides, knowing the rainfall or earthquake intensity (as input to the system) and the details of the slope (e.g. mechanics, hydrology, topography) the output (e.g. sediment) could be defined. According to this basic concept physically based models are facilitated to describe and model landslide processes.

"The present is the key to the past" or in other words "the past is the key to the future" is the core assumption of the concept of uniformitarianism after James Hutton (1726-1797) (Fig. 2.3; Carrara et al. 1995; Orme 2002). This was later adapted and published by Charles Lyell (geologist, 1797-1875) which is probably why nowadays the uniformitarianism is mainly attributed to him (Orme 2002). Using quantitative methods for analyzing geomorphic processes is the point of intersection between the uniformitarianism concept and quantitative methods. Many statistical tests and models were already provided before 1900 (Orme 2002). However, nowadays geomorphologists still rediscover those methods, as for example rather recently in landslide susceptibility modelling. This concept is an important basic principle for many statistical or also physically based modelling approaches which are very frequently used by geomorphologists (e.g. Carrara et al. 1995). It is

facilitated by analyzing the characteristics of past geomorphic processes to learn about possible future processes and effects.

The "mass movement theory" or concept dating back to 1773 has its foundations in Coulomb's equation on slope stability (Fig. 2.3; Orme 2002):

$$\tau = c + \sigma \tan(\varphi) \qquad (1),$$

where τ is the shear strength, c is the non-directional cohesion per unit area, the effective normal stress on the slide plane is σ and φ is the internal friction angle (Crozier 1986; Orme 2002). This equation was refined (e.g. Collin 1846; Mohr 1872; 1871; Orme 2002) and found wider acceptance in the science of soil mechanics in writings of Terzaghi, Fellenius and Krey (e.g. Skempton 1979; Terzaghi 1925). However, some years went by, until this rather mathematical concept of describing the internal mechanics of landslides was introduced in geomorphology in the 1960s (Fig. 2.3, Leopold et al. 1964; Orme 2002).

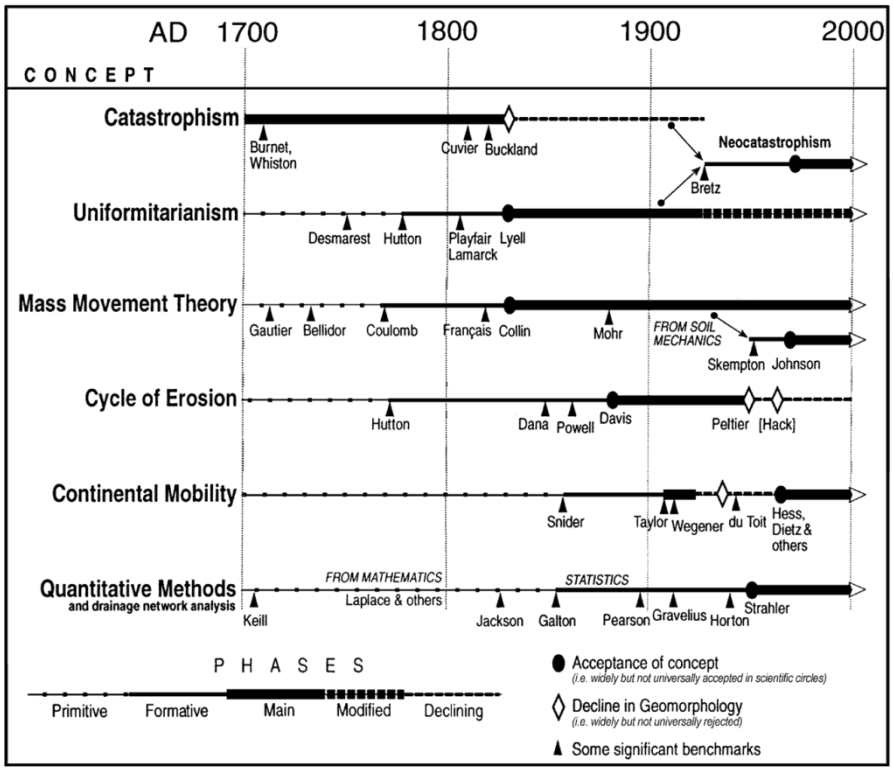

Figure 2.3 The rise and fall of selected concepts in geomorphology and related fields (own adaption after Orme (2002))

While limitations of the systems theory approach were outlined already earlier (Scheidegger 1992; Schumm and Lichty 1965) systems theory has only recently been studied in more detail with a tendency towards a theory of nonlinear complex or chaotic systems (as described amongst others by (Bak 1996; Dikau 2006; Von Elverfeldt 2012; Keiler 2011; Lam 2000; Murray et al. 2014; Phillips 2011; Phillips

2009a; Phillips 2009b; Phillips 2006a; Phillips 2006b; Phillips 1999; Phillips 1992a; Phillips 1992b). These new additions are changing the focus from systems in equilibrium states towards systems in nonequilibrium states showing nonlinear, complex, chaotic, emergent and/or self-organized behavior (Hergarten 2002; Phillips 1992a; Phillips 1992b; Schumm 1991). They give a different, maybe additional, picture on how geomorphic processes work and comment on inconsistencies in the old approach.

Von Elverfeldt and Glade (2011) discuss some discrepancies in detail providing an outlook on possible ways to meet these challenges. These inconsistencies include the undefined way to delineate a system or the contradictions of the systems approach with the causality (cause-effect relationships) concept. The exact way of distinguishing between parts within and outside of a system remains unclear and the identification of all parts of a system is challenging (Brunotte 2002; Von Elverfeldt and Keiler 2008). A possible solution to this challenge is describing the system boundaries according to differences in the flux of energy and mass between inside and outside the system (Christopherson 2006; Von Elverfeldt and Keiler 2008). However, the delineation of system boundaries in contrast to the environment is impossible describing geomorphic systems as open systems, with interactions between the (sub-) systems (Von Elverfeldt and Glade 2011; Von Elverfeldt and Keiler 2008). The majority of geomorphic systems are considered to be open systems, as energy and mass are constantly exchanged within the system and external with the environment (Von Elverfeldt and Keiler 2008; Huggett 2007; Schrott 2002). Furthermore, they are nested and connected as the output of a system may be the input of another system (Schrott 2002). This is troublesome for selecting the way of thinking in systems, as their delineation is challenging. Additionally, the traditional understanding of causality is violated within systems theory as interactions and more than one possible effect out of one cause are possible (e.g. morphological convergence of forms Brunsden and Thornes 1979; Von Elverfeldt 2012).

Besides, newly to geomorphology introduced concepts of nonlinearity, chaos and complexity alter the main interest of geomorphological research as for example emergence might occur, meaning in short after ARISTOTLE “The whole is more than the sum of its parts” (Von Elverfeldt and Keiler 2008; Embleton-Hamann et al. 2013; Phillips 1999). This suggests, that applying a reductionist approach, or trying to define all the elements of a system is not enough. Therefore, the focus of geomorphological research should be moving away from analyzing these external influences on the system (such as triggers of landslides) to analyzing the internal (maybe even self-organizing) processes within the system itself (Von Elverfeldt and Glade 2011). This transition from the idea of a (steady-state) equilibrium, zonal and mature forms and external causality of geomorphic processes to the recognition of multiple potential characteristic or equilibrium forms and self-organized system (re)action is generally seen as a broadening of approaches, not as a replacement of former ideas (Von Elverfeldt and Glade 2011; Phillips 2009a).

Whereas this new developments in geomorphic systems theory summarized as second-order systems theory (Egner and Von Elverfeldt 2009) are of high interest

aiming towards a better understanding e.g. of landslide processes, it has to pointed out that this thesis is grounded in the previously described "traditional" systems approach (after Chorley and Kennedy 1971).

2.1.3 Landslide triggers and predisposing factors

Slope stability is commonly described distinguishing three stability states: (1) stable, (2) marginally stable and (3) actively unstable (Crozier 1986). The transition from one stability state into the other is influenced by preparatory, triggering and predisposing factors, while controlling factors define the movement form, rate and duration (Fig 2.4; Crozier 1986; Glade and Crozier 2005). This transition from a stable or even marginally stable state to an actively unstable state is caused by changes in the distribution of resistance (shear strength) and shear stresses within the slope (Crozier 1986).

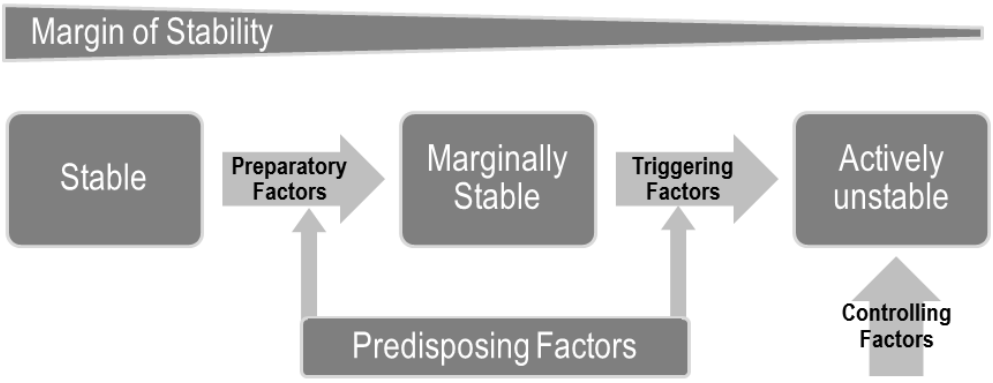

Figure 2.4 Slope stability states and destabilizing factors (based on Crozier, 1986)

The amount of shear strength and shear stress is dependent on the type of material, more specifically on its cohesion and internal friction angle (Crozier 1986). While the cohesion gives a measure for the shear strength independent of any weight imposed on the shear surface, the internal friction angle gives the shear strength resulting from the weight of the material acting on the shear plane as normal stress (Crozier, 1986). Therefore, the weight not only provides shear strength, it also produces shear stress depending on the shear plane angle (Crozier 1986). Additionally, the pore water pressure is of importance for slope stability. Under saturated conditions, e.g. resulting from a (ground)water table above the shear plane, the pore water pressure is positive leading to a reduction of the resistance within the slope (Crozier 1986). In contrast to this, the pore water pressure is negative in unsaturated conditions due to the tension coming from the attached water. Therefore, in unsaturated conditions the pore water pressure provides an increase in shear strength (Crozier 1986). In short, besides the type of material the availability and amount of water within the slope is decisive for its stability. The different reasons for high or low water

availability, permeability and void space are discussed in detail in literature, e.g. Crozier (1986), Selby (1993) or Glade et al. (2005).

Thresholds of slope stability play an important role in this transition of stability states. Schumm describes geomorphic thresholds as *"a threshold of landform stability that is exceeded either by intrinsic change of the landform itself, or by a progressive change of an external variable"* (Schumm 1979). The core of this concept is that abrupt changes in the system are not always related to a change in an external variable but the geomorphic threshold might be exceeded by normal development of a landscape (Schumm 1979). In detail he distinguishes between extrinsic and intrinsic thresholds: (a) Extrinsic thresholds describe the point at which the response of the system to an external influence, or relatively fast acting preparatory factors, occurs (Schumm 1979). This external influence (e.g. change in climate or land-use) might change progressively and without its presence the threshold would not be crossed and no change within the system might occur (Schumm 1979). (b) Intrinsic thresholds might be exceeded by slow preparatory factors such as long-term progressive weathering (Crozier 1986; Glade and Crozier 2005; Kirkby 1973; Schumm 1979). These describe changes occurring without a change in an external variable (Schumm 1979).

In detail, predisposing factors are distinguished from preparatory ones by their static opposed to a dynamic behavior (Glade and Crozier 2005). Predisposing factors influence the margin of stability inherently and act as a catalyst to allow other destabilizing factors to act more effectively (characteristics of different slope material e.g. weathering mechanism and speed, bedding and dipping; Glade and Crozier, 2005). The dynamic preparatory factors are defined as factors that reduce the margin of stability of a slope over time without actually initiating movement and placing the slope in a marginally stable state (Crozier 1986; Glade and Crozier 2005). Preparatory factors affected by weathering, climate change and tectonic uplift may act slowly over time. In contrast, factors such as deforestation or over steeping due to erosion may act relatively quicker over time (Glade and Crozier 2005). Triggering factors (e.g. rainfall, earthquakes, additional water supply) initiate the movement of the slope by transferring the slope system from a marginally stable state into an actively unstable state (Crozier 1986). However, the action of a triggering factor can only partially be attributed to the actual cause of a landslide (Crozier 1986). Many more destabilizing (preparatory or predisposing) factors may have reduced the shear strength and/or piled up the shear stresses so that the trigger factor was just the last bit missing to initiate landslide movement (Crozier 1986).

More detailed summaries and examples of destabilizing mechanisms and factors can be found manifold in literature (e.g. Brunsden 2001; Brunsden 1993; Crozier 1986; Dikau 1996; Selby 1993). These include natural processes and triggers and anthropogenic influences on slope stability, i.e. the slope material and water supply. The natural processes are summarized here (Tab.2.3). For specific anthropogenic influences refer to section 2.1.4.

The ability of landforms to change, known as sensitivity to change, is varying spatially and temporally (Brunsden 2001). Therefore, stability is a function of temporal and spatial distributions of forces changing the balance of shear stress and shear strength (Brunsden 1990). Only if triggering events meet a marginally stable system, which is highly influenced by predisposing and preparatory factors, an event might be triggered (Fig. 2.5). This variability in disposition and triggering events is decisive for the occurrence of a landslide event (Zimmermann et al. 1997).

Tab. 2.3 Classification of preparatory and triggering processes of landslides (after Brunsden 1993)

External process group	*Causal processes*	*Description*	*Specific effect on stability state of the slope system (examples only). Changes in:*
Weathering: physical, chemical and biological	Physical properties Chemical properties Horizonation	Changes in particle size Cation exchange, cementation Internal layers and basal surface, development of weak discontinuities	Density, unit weight strength, strength, permeability, vertical and spatial strength variation, total stress, critical depth, friction, cleft water pressure
	Regolith thickness	Weathering > erosion, accumulation in hollows and foot of slope, soil ripening	
Erosion fluvial, glacial and coastal, material removal from the face or base of slope	Geometrical change	Relief, height, length, angle, aspect	Total stresses, permeability, strength
	Unloading	Removal of lateral support, expansion, swelling, fissuring, strain softening, stress concentration	
Ground subsidence	Undermining	Mechanical eluviation of fines, solution, leaching, removal of cement, seepage erosion, backsapping, piping	Strength, physical support, consolidation, water concentration, pore water pressure
Deposition of fluvial, glacial and mass movement New material added to face or top of slope	Loading Undrained	Solifluction, mudsliding, rockfall, deltaic addition, talus accumulation	Water content, weight, strength, stress

	loading		Underconsolidation, pore pressure
Shocks and vibrations, seismic activity	Vertical and horizontal movements	Shocks of varying frequency, magnitude, intensity, duration, disturbance to intergranular bonds and cements, water-table change	Horizontal stress, strength, excess pressures
Air fall of loess, tephra	Mantling with fine regolith. Addition of fine components to soil	New slope created with strong discontinuity beneath	Strength, water content, water pressures
Water regime change, geomorphological or meteorological	Perched water tables, surface saturation	Piping flooding, lake bursts	Water pressures
	Water table and pressure change	"Wet" rainfall years, intense precipitation, snow and ice melt, drawdown	Excess pressures, water-table, pore pressure, weight
Complex "follow on" or run out processes after initial failure, bank collapse, seismic slope failure	Liquefaction, remoulding, fluidization, air layer lubrication, cohesionless grain flow		Strength, water distribution, consolidation, friction

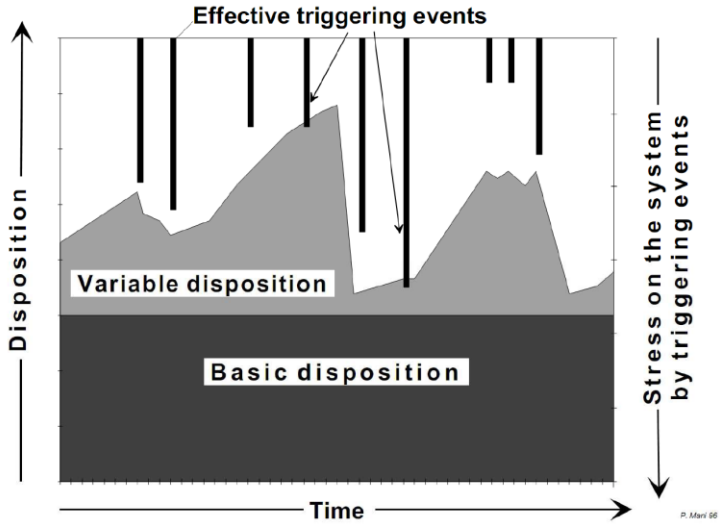

Figure 2.5 Disposition triggering concept, modified following Kienholz et al. (2004), translated and modified after Zimmermann et al. (1997). (Note: arrows indicate direction of increasing values).

2.1.4 Human impact on landslides and their mapping

Human drivers of landscape change are significant in most biomes of the world (Spencer et al. 2009). Amongst these, the observed human impact on landslides and their mapping is twofold. On the one hand, there is the globally reported human impact on landslide activity (preparatory or triggering factors). On the other hand, human activity may influence the visibility of landslides in the field or on remote sensing imagery.

Besides natural processes, also human interference and activity may generate preparatory or even triggering factors causing slope instability. Brunsden (2001) distinguished between morphological, material and hydrological controls which are influenced by anthropogenic activity (Tab. 2.4).

Tab. 2.4 Anthropogenic preparatory and triggering causes of landslides (after Brunsden (2001))

System specification	*Morphological control*		*Material control*		*Hydrological control*	
	Construction		*Structure*	*Fabric*	*Ground water*	*Surface water*
Preparation process	Cut / fill	Blasting Vibration	Pile, Rock anchor, Pin, Retain, Reinforce	Chuman, Shotcrete, Compact, Grout	Tunnel, Drain, Supply, Sewer	Catch, Store, Drain, Supply
Forcing functions	Planning, Dynamic growth of city and infrastructure, Maintenance and control					
Specification change	Load, Unload, Slope form	Permeability strength	Bulk strength voids	Erosion strength voids	Height, Pressure, Internal erosion, Weep hole, Efficiency, Chemistry	Volume erosion
e.g. direct trigger	Critical stress	Critical strength	Critical stress and strength			
e.g. landslide response	All forms of slide	Rock falls and slides	All forms		Rotation Non-circular	Debris flow

Human impact on landslides as a source of vibration, undercutting of possibly unstable slopes due to construction of buildings or roads, filling landforms or loading of material on the slope, the additional supply of water or drainage of water into a different area or land use change (e.g. deforestation) was reported and analyzed all over the world (e.g. Andrecs et al. 2007; Bai et al. 2010; Beguería 2006a; Bonachea et al. 2010; Borga et al. 2005; Bruschi et al. 2013; Van Den Eeckhaut et al. 2010; García-Ruiz et al. 2010; Glade 2003; Goetz 2012; Guthrie 2002; Krejci et al. 2002; Larsen 2008; Preuth et al. 2010; Regmi et al. 2014; Zezere et al. 1999).

On example of anthropogenic interference in a slope system is the construction of buildings or roads. Any construction may have large effects on the hydrological and soil mechanical slope characteristics which might ultimately cause a slope failure (Fig. 2.6). Multiple changes listed in Table (2.4) occur during construction work: slope undercut and fill, additional supply of water from the roof, or a potential leakage of underground services and vegetation clearance (Fig. 2.6).

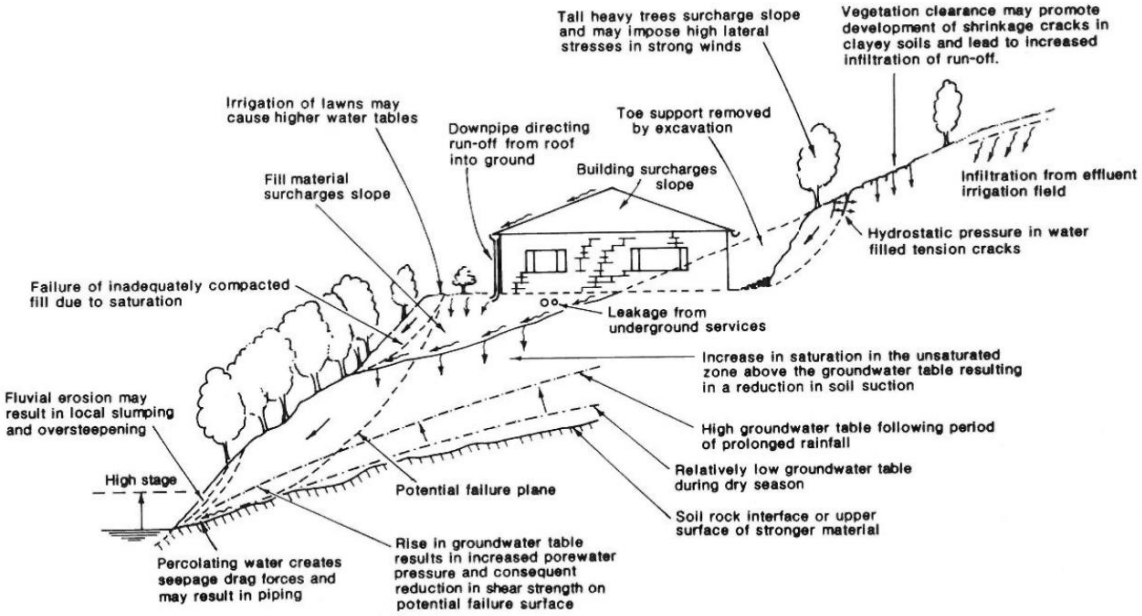

Figure 2.6 Factors influencing slope stability of a building site on a hillslope (After Worley Consultants Ltd. 1987 in Selby 1993)

Human impact on geomorphic processes including landslide initiation was previously analyzed quantitatively (1) from exploratory analysis of landslide inventories (e.g. Glade 1996; Zezere et al. 1999), (2) from geoarchives (sediments cores (lakes, estuaries (Bonachea et al. 2010; Glade 2003)), (3) by statistical analysis of the proximity to or presence of construction works (infrastructure, roads, houses; e.g. Chung and Leclerc 2003; Tien Bui et al. 2012; Yalcin et al. 2011) or land use/cover change (e.g. Beguería 2006a; Guns and Vanacker 2012), or (4) by introducing a human impact proxy such as the GDP (general gross product; Cendrero et al. 2006), population density (Remondo et al. 2005), building density, road density or land price in the landslide susceptibility analysis (Zhao et al. 2010). These studies revealed all different kinds of human impact on landslide initiation and showed some ways of incorporating these in regional analysis. Furthermore, it was pointed out that after stopping the anthropogenic interference its effects on the slope stability remain detectable for many years (Beguería 2006a). This may occur, although the roots of newly upcoming vegetation were found to provide a stabilizing effect on slope stability, or although technical stabilizing methods were installed (e.g. Glade 2003). Therefore, considering the possible effects of human impact besides natural predisposing and preparatory factors influencing the slope stability in the planning process is of high importance.

Additionally, human impact influences the persistence of landslide morphology and therefore the visibility of landslides either in the field or on any kind of remote sensing imagery. Due to farming or building activity the morphological footprint of landslides might be not visible anymore after a short period (e.g. within a year; Bell et al. 2012). This influence of anthropogenic activity on the visibility and persistence of landslide morphology was reported e.g. by Fiorucci et al. (2011), Guzzetti et al. (2003), Matthews et al. (1997) and was analyzed in Lower Austria within this study (refer to Bell et al. 2012). This influence renders the assessment of the (relative) age of landslides with dating methods almost impossible (Lang et al. 1999). Furthermore, it portrays a limitation concerning the completeness of landslide inventories which is discussed in more detail later.

More details on anthropogenic interference types on slope stability in the study area Lower Austria are presented in section 4.4.

2.2 Landslide inventory mapping

Landslide inventories are storing the location of landslides in an area and give information on previous landslide occurrence in a region (Guzzetti et al. 2000). Therefore, a landslide inventory is the simplest form of landslide zonation, considering that many new landslides might occur as a reactivation of old landslides (Crozier 1986; Deadman 2014). The drawback is though, that the inventories are not showing possibly future affected areas outside of mapped landslides (Fell et al. 2008; Guzzetti et al. 2000; van Westen et al. 2008).

Aside from that, landslide inventories are prerequisites for analyzing landslide processes, their activity, magnitude and frequency, predisposing and preparatory factors, landslide susceptibility, and also contribute to related vulnerability and risk analysis (Fell et al. 2008; Ghosh et al. 2012; Guzzetti et al. 2000; Soeters and Van Westen 1996). Furthermore, their availability is crucial for assessing the success and predictive power of the applied models used to derive landslide susceptibility, hazard or risk maps (Beguería 2006b; Chung and Fabbri 2003).

Independent from the planned purpose of the landslide inventory, its quality regarding complete or substantially complete spatial and temporal information on landslide occurrence in the past (Malamud et al. 2004), amount of stored information (e.g. date of occurrence, trigger, caused damage), positional accuracy of the mapped landslide and correctness in the assigned landslide type/age/extent is decisive for its usability (Ardizzone et al. 2002; Galli et al. 2008; Glade et al. 2005; Guzzetti et al. 2012; Petschko et al. 2014a; Soeters and Van Westen 1996; van Westen et al. 2008). However, the positional accuracy of single landslides is the minimum and maybe most important information stored in an inventory (Aleotti and Chowdhury 1999; Fell et al. 2008; Malamud et al. 2004). Wrong locations of landslides clearly affect the reliability of the modelling or model performance results (Malamud et al. 2004; van Westen et al. 2008). This is of importance if the resulting e.g. susceptibility

maps are applied within land use development plans or zonings (Petschko et al. 2014a).

In general two different types of landslide inventories are distinguished: event and historical landslide inventory (Malamud et al. 2004). An event inventory portrays all landslides that occurred after a specific trigger event and allow the analysis of rainfall thresholds or other triggering events (e.g. earthquakes; Guzzetti et al. 2000; Malamud et al. 2004). Historical inventories are cumulative inventories containing all landslides that are visible on the analyzed (multi temporal) imagery (Malamud et al. 2004). Usually the date or time and circumstances of the triggering of each of these landslides are unknown (Guzzetti et al. 2000). Furthermore, the landslides might be several hundred or even thousands of years old (Guzzetti et al. 2000).

The general principle of inventory mapping/detection methods is the mapping of discernible features (Tab. 2.2) that remain after a landslide has occurred (Carrara and Merenda 1976; Guzzetti 2005; McCalpin 1984; Wieczorek 1984). The wide and growing availability of geographical information system (GIS) software and the constant development of new technologies revolutionize methods for landslide inventory mapping permanently (Guzzetti et al. 2012). Guzzetti et al. (2012) and Van Westen et al. (2008) gave a profound overview on different landslide inventory mapping techniques, which is why here only a brief selection of the most important and maybe promising methods is presented: Landslide inventories may be assembled by the evaluation of historical archives, literature research or inquires at local public organizations or private consultants (CNR-IRPI-Turin 1998; Glade et al. 2001; Guzzetti et al. 2000; Ibsen and Brunsden 1996; Pereira et al. 2014; Röhrs and Dix 2010; Rossi et al. 2010b; Schwenk 1992). Furthermore, inventories may be mapped in the field using geomorphological field mapping (Brardinoni et al. 2003; Brunsden 1993; Brunsden 1985; Carrara and Merenda 1976; Zezere et al. 1999), GPS or more advanced tools such as GPS equipped binoculars (e.g. Santangelo et al. 2010).

Preparing a landslide inventory more effectively for larger areas was enabled with the availability of desktop mapping methods analyzing remotely sensed satellite, SAR (synthetic aperture radar) or LiDAR (light detection and range) data including aerial photographs (Guzzetti et al. 2012; Tarolli 2014; van Westen et al. 2008). Naturally, these desktop mapping methods are accompanied by field campaigns reviewing the mapping results. These mapping methods include geomorphological mapping on aerial photographs (Carrara et al. 2003; Duman et al. 2005; Mantovani et al. 1996; Van Westen and Lulie Getahun 2003; Zanutta et al. 2006) and on high resolution remote sensing imagery such as (stereoscopic) optical satellite imagery (e.g. Ardizzone et al. 2013; Fiorucci et al. 2011), imagery derived from ground based or space borne SAR (synthetic aperture radar; e.g. Cigna et al. 2012; Colesanti and Wasowski 2006; Herrera et al. 2010; Rott and Nagler 2006) and airborne or terrestrial laser scanning data (ALS, TLS; e.g. (Jaboyedoff et al. 2010; McKean and Roering 2004; Petschko et al. 2014a; Schulz 2004; Tarolli 2014). Most recently however, the traditional geomorphological mapping is complemented by semi-automated detection of landslides and change detection on the basis of high resolution satellite data (e.g. Barlow et al. 2006; Fiorucci et al. 2011; Harp et al.

2011; Mondini et al. 2011a; Mondini et al. 2011b; Tarolli 2014; Whitworth et al. 2005), by object-oriented approaches analyzing digital elevation models (DTM) and optical satellite data (Martha et al. 2012; Martha et al. 2010), by analyzing movement using DInSAR and sub-pixel offset techniques (differential SAR interferometry; (Singleton et al. 2014; Wasowski and Bovenga 2014) and by change monitoring using multi temporal ALS and/or TLS LiDAR data (Burns et al. 2010; Ventura et al. 2011).

The advantage of SAR or LiDAR data is the independence from the weather and vegetation conditions, as the presence of clouds or forest does not affect the data acquisition of the terrain underneath (e.g. Anders and Seijmonsbergen 2008; Bell 2007; Chigira et al. 2004; Eeckhaut et al. 2007; Glenn et al. 2006; Haneberg et al. 2005; Schulz 2004; Singleton et al. 2014). The list of references shows that the area wide availability of airborne LiDAR DTMs rose significantly recently. This started a revolution in geomorphology and mapping landslides using LiDAR DTMs were identified as one of the most promising methods available (Anders and Seijmonsbergen 2008; Guzzetti et al. 2012; Tarolli 2014). It allows a new level of spatial coverage paired with high precision in the positioning accuracy of the landslide feature which is beneficiary mapping a historical landslide inventory (Guzzetti et al. 2012; Petschko et al. 2010). Besides visual interpretation of LiDAR DTM derivatives more advanced methods were developed performing semi-automated or object-oriented detection of landslides or landslide features (scarps) according to their distinct morphology (e.g. van Asselen and Seijmonsbergen 2006; Booth et al. 2009; Dalyot et al. 2008; Van Den Eeckhaut et al. 2012; McKenna et al. 2008; Tarolli et al. 2010).

Although higher spatial and temporal resolution of landslide inventories can be achieved with new data it might never be possible to consider an inventory as fully complete. The quality of a landslide inventory is influenced by the subjectivity involved in the mapping and limitations associated with the available data (e.g. archive, aerial photograph, satellite imagery, LiDAR), the mapping approach (mapping in the field, digitizing analogue or digital data sources, or (semi-) automated mapping) and with anthropogenic activities influencing the persistence and visibility of landslide morphology (Ardizzone et al. 2002; Bell et al. 2012; Cardinali et al. 2000; Fiorucci et al. 2011; Guzzetti et al. 2000; van Westen et al. 2008; Van Westen et al. 1999). Therefore, Malamud et al. (2004) introduced the concept of a substantial complete inventory representing a randomly incomplete inventory. Accordingly, substantial complete inventories may not be complete in time or spatially, but they portray the characteristics of all landslides in the analyzed region properly (Malamud et al. 2004). In short, it is assumed that a representative set of landslides is available without a mapping bias, e.g. in one geological or land cover unit (e.g. forest).

A possible source for mapping errors is the possibility of morphological convergent geomorphic forms. While the morphology might look like a landslide (scarp) the process resulting in the form might have been very different including natural and anthropogenic processes (Antonini et al. 2002). An example for morphological

convergence is the misinterpretation of old quarries for landslide features. This may often only be solved by checks on supplementary imagery or in the field or by information provided from the local people (Ramml et al. 2014; Fig. 2.7). Often the old quarries were also used as a dump for debris which might give the impression of a landslide toe on the imagery (Fig. 2.7).

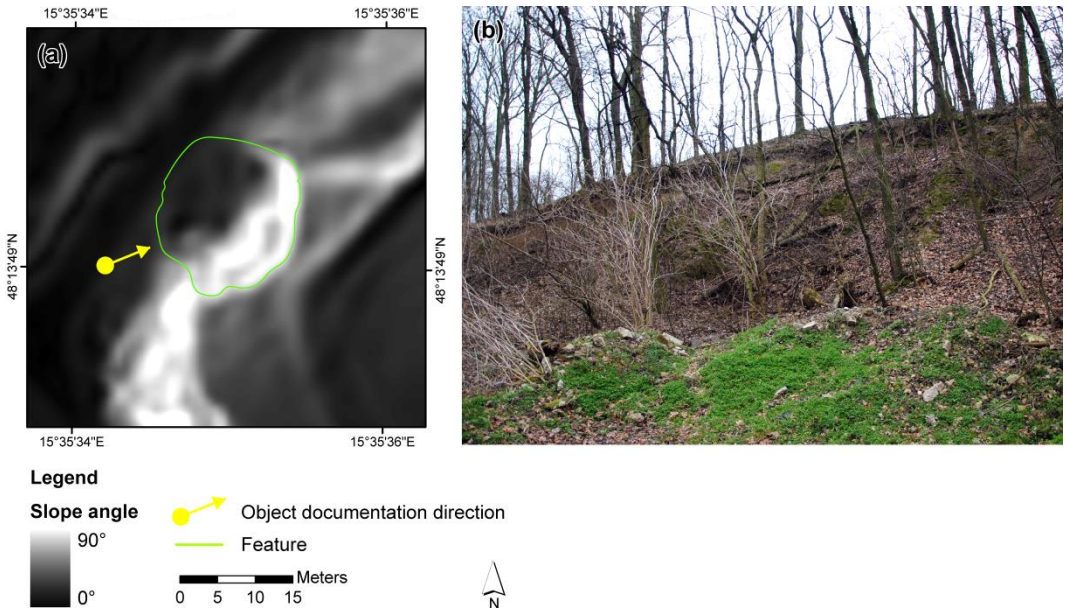

Figure 2.7 Example for morphological convergence of an earth slide with a small old quarry for construction stones close to a village visible on LiDAR derivatives and in the field. Source: DTM: Provincial Government of Lower Austria; Photo taken by Petschko, 2012.

2.3 Landslide susceptibility modelling

The term landslide susceptibility has been defined many times in literature (Brabb 1984; Crozier and Glade 2005; Dai and Lee 2002; Fell et al. 2008; Guzzetti 2005; Guzzetti et al. 1999; Remondo et al. 2003; Santacana et al. 2003; Soeters and Van Westen 1996). In this study we use the definition most closely related to statistical analysis of landslide susceptibility. Brabb (1984) defines landslide susceptibility as the likelihood of a landslide occurring in an area with given local terrain attributes. Or as Guzzetti (2005) described, it "*is the probability of spatial occurrence of slope failures, given a set of geo-environmental conditions*". The time frame including the frequency of the occurrence of landslides is explicitly not taken into account (Fell et al. 2008). Therefore, these maps can only answer the question Where? but not When? landslides might occur which is opposed to landslide hazard analysis including landslide magnitude and frequency.

Within the landslide risk management cycle (after Alexander 2002; Alexander 2000) landslide susceptibility analysis may be seen as initial step highlighting areas highly prone to landslides where detailed analysis of the hazard or even risk may be aspired (Corominas et al. 2013; Van Westen et al. 1997). It is a crucial step in the pre-disaster preparation phase as a landslide susceptibility map shows areas which might be affected by landslides (Crozier and Glade 2005; Fell et al. 2008). While a large number of landslide susceptibility mapping approaches are tested and developed constantly, the number of studies analyzing landslide hazard, especially on regional scale is limited (Corominas et al. 2013). The biggest challenge in hazard analysis is the estimation of the occurrence time of future landslides (Corominas et al. 2013; Soeters and Van Westen 1996; Van Westen et al. 2006; Zêzere et al. 2004).

Assessing the landslide susceptibility can be done with a large range of methods generally grouped in heuristic, statistical and deterministic (physically based or geotechnical) methods (Soeters and Van Westen 1996). Usually, the estimation of the possible future location of landslides is based on the conditions (e.g. local terrain attributes) of past landslides (Carrara 1993; Varnes 1984). However, the way how this information is included in the analysis differs significantly between the methods. Heuristic methods are based on the expert opinion of a geomorphologist to classify the susceptibility/hazard either by geomorphic analysis or by qualitative map combination (Soeters and Van Westen 1996). The expert identifies the explanatory factors for the landslides in the area and also assigns weights to each factor according to its importance (Brabb 1984; Cascini 2005; Crandell et al. 1979; Dai and Lee 2002; Evans and King 1998; Hungr et al. 2005; Nilsen et al. 1979; Van Westen et al. 1997). Therefore, heuristic methods include a high degree of subjectivity, which lowers the reproducibility of the method, although an expert performed the zoning (Van Westen et al. 1997).

Statistical methods are considered as more objective, as the importance of each explanatory variable is assigned by the statistical relationship of the variable with the landslide distribution (Fell et al. 2008; Van Westen et al. 1997). The result gives

a probability of landslide (initiation) occurrence. Taylor et al. (1977) identified probabilities as "the only rational basis for assessment" as "there is no such thing as a 100% safe slope, whether natural or man-made" (Crozier 1986). A large range of bivariate to multivariate methods such as logistic regression (LR), frequency ratio, weights of evidence and machine learning techniques such as artificial neuronal networks or support vector machines deriving the relationship between landslides and the explanatory variables has been applied amongst others by Carrara et al. (1995), Chung and Fabbri (2003), Chung and Fabbri (1999), Claessens et al. (2006), Davis et al. (2006), Van Den Eeckhaut et al. (2009b), Van Den Eeckhaut et al. (2006), Dikau (1996), Den Eeckhaut et al. (2010), Felicísimo et al. (2012), Lee et al. (2007), Nefeslioglu et al. (2008), Neuhäuser et al. (2012), Piacentini et al. (2012), Pradhan (2013), Pradhan and Lee (2009), Remondo et al. (2003), Rossi et al. (2010a), Santacana et al. (2003), Schicker and Moon (2012), Sterlacchini et al. (2011), Vorpahl et al. (2012), Yesilnacar and Topal (2005), Yilmaz (2009) and Zezere (2002). These include a number of studies comparing different statistical and/or machine learning techniques mainly based on model performance measures. Furthermore, the applicability, usability, required input data and interpretability was considered in some comparisons (Van Den Eeckhaut et al. 2009a; Guzzetti et al. 2006; Rossi et al. 2010a). These models rely strongly on the input data: its positional accuracy, geomorphological relevance, the completeness and availability of the explanatory variables and their spatial and temporal scale.

Deterministic or also called physically based models aim to portray all soil mechanical and hydrological processes within the slope which is why these slope stability models were considered as white box models (Carrara 1983; Soeters and Van Westen 1996). Problems associated with using these models is the dependency on a large amount of data, lack of knowledge on processes within the soil and oversimplification of the processes of slope stability (Soeters and Van Westen 1996; Van Westen et al. 1997). The models currently found in literature range in the detail of considering slope mechanical and hydrological processes and possible feedbacks and influences from vegetation and rainfall (e.g. Bathurst et al. 2006; Baum et al. 2005; Van Beek and Van Asch 2004; Duncan 1992; Goodman and Shi 1985; Kuriakose et al. 2009; Nadim et al. 2005; Potts 2003; Thiebes et al. 2013). Prominent models are SHALSTAB (shallow slope stability model (Dietrich et al. 1998)), SINMAP (stability index mapping, (Pack et al. 2005; Pack et al. 1998)), SHETRAN (Ewen et al. 2000), TRIGRS (Transient Rainfall Infiltration and Grid based Regional Slope Stability (Baum et al. 2002)), STARWARS and PROBSTAB (storage and redistribution of water in agricultural and re-vegetated slopes coupled with probability of stability (Van Beek 2002; Van Beek and Van Asch 2004)), CHASM (combined hydrology-slope stability model (Anderson et al. 2008)), and GEOtop-Fs (Simoni et al. 2008). Furthermore, first methods including physically based models into statistical models were tested by Goetz et al. (2011).

While this large range of different landslide susceptibility modelling methods exists and is applied simultaneously, recommendations on which model is preferable for what study area or aimed analysis output are rare. The model comparisons usually

only show low differences of the model performance measure balancing between insignificant or overfitted results. Instead, recommendations are given dependent on the analysis scale and only on the three general groups of methods (heuristic, statistical or physically based; Fell et al. 2008).

Summarized, aiming at objective and reproducible results for large study areas (>10,000km²) at medium scale (1:100,000 – 1:25,000; Fell et al. 2008) statistical approaches are favorable for landslide susceptibility modelling. Objective and reproducible results are particularly important implementing the final susceptibility map in spatial or land use planning strategies. Selecting a specific statistical susceptibility model may be based on the several model comparisons available in literature (references please see above). However, it has to be kept in mind that the model performance might not only depend on the model itself. It may differ between study areas depending on their heterogeneity or homogeneity of topography and/or geotechnical characteristics and on the specific sample used for the modelling (Petschko et al. 2014c). Also, a combination of results from different modelling approaches was tested in literature resulting in improved model performance measures (Choi et al. 2012; Rossi et al. 2010a). However, this procedure was stated to be serious contradictory with the philosophy of the approaches (Gokceoglu 2012). Furthermore, it was considered questionable due to multicollinearity of the results obtained from the different models (Gokceoglu 2012). Therefore, one model has to be selected. This model selection may be based on the model's capability to generalize, the interpretability of the results, data handling, requirements and usability at a specific study area size and geomorphic plausibility of the results (Cascini 2008; Guzzetti et al. 2006). The capability to generalize includes a low tendency to overfitting, which occurs when the model is trained too close to the modelling sample and the comparison with new data reveals the failure of the model to generalize. This is shown by a mismatch of the new data with the distribution of the highest susceptible classes.

Previous studies showed, while more flexible machine learning algorithms often tend to overfit, linear models (e.g. logistic regression, generalized linear models (GLM)) cannot portray possible nonlinearity in the relationship between landslide occurrence and the explanatory variables (Brenning 2005; Goetz et al. 2011; Nefeslioglu et al. 2008). Other methods, such as the weights of evidence model have the disadvantage of the need to classify the explanatory variables which might introduce an unwanted bias into the modelling (Schicker and Moon 2012). Generalized additive models were identified as a compromise between the flexibility of machine learning approaches and the ability to generalize of linear models (Brenning 2008; Goetz et al. 2011). GAMs are an extension of a GLM by a smoothing function in the regression equation and therefore can portray the nonlinearity and non-monotonic relationship between landslide occurrence and explanatory variables (Brenning 2009; Goetz et al. 2011; Hastie and Tibshirani 1990; Vorpahl et al. 2012). Furthermore, GAMs are less prone to overfitting than machine learning, random forest or regression tree approaches (Brenning 2009; Goetz et al. 2011; Hastie and Tibshirani 1990; Vorpahl et al. 2012). Therefore, GAMs are considered as the more

appropriate model form, rather than GLM, although the model performance is only slightly better (Goetz et al. 2011; Marmion et al. 2009; Vorpahl et al. 2012). GAMs are not new to spatial modelling, as they have been used widely in ecology (Vorpahl et al. 2012; Yee and Mitchell 1991; for a review refer to Guisan et al. 2002) and geomorphology (Marmion et al. 2009). In landslide susceptibility modelling the GAM has recently been introduced and applied with satisfactory results of model performance measures (Brenning 2008; Goetz et al. 2011; Jia et al. 2008; Park and Chi 2008; Vorpahl et al. 2012; Zhao et al. 2010).

In statistical modelling a subsample of landslide and non-landslide points/grid cells has to be drawn instead of using all grid cells of the landslide polygons and outside the landslides. Different approaches regarding the amount of sampled grid cells per landslide and the location of these can be found in literature (Nefeslioglu et al. 2008; Regmi et al. 2014). Their main difference is the location: either within the entire landslide polygon or main scarp (e.g. Atkinson et al. 1998; Dai and Lee 2002; Fernández et al. 2003; Regmi et al. 2014), from a zone in the vicinity of the landslide almost representing pre-failure conditions (so called seed cells, e.g. Bai et al. 2008; Suzen and Doyuran 2004) or from a derived pre hillslope gradient within the main scarp (Van Den Eeckhaut et al. 2006). Naturally, all of these approaches have a significant effect on the resulting landslide susceptibility map and its allowed interpretation. Nevertheless, not all landslide susceptibility studies state on how the sampling of how many grid cells was performed (Nefeslioglu et al. 2008). Moreover, all these methods assume to know the point of the initiation of the landslide. However, as discussed by Regmi et al. (2014) there are many possible locations of the first movement e.g. at the slope toe, slope head or the center of the slope. Independently from where the landslide initiates it can expand in any direction (upslope, downslope, sidewise; Regmi et al. 2014). This is impossible to map on remote sensing imagery, especially analyzing large regions (Regmi et al. 2014).

Another issue where lots of different information is available is the appropriate sample size used within statistical susceptibility modelling. The answer to this question lies more within the applied model and model design than there would be a general solution. This was shown by positive examples of fitting a susceptibility model with a small sample size (e.g. Demoulin and Chung 2007; Van Den Eeckhaut et al. 2006). However, extensive tests with *k*-fold cross-validation within this study applying GAMs identified a minimum sample size of around 400 landslide and non-landslide samples (Petschko et al. 2014c).

Corominas et al. (2013) provide an extensive overview on preparatory, predisposing and triggering factors of landslides applied in landslide susceptibility or hazard assessments as listed in Tab. 2.5. Modelling landslide susceptibility at least information on the topography should be available. Furthermore, spatial information on the local geology, soils, geomorphology, hydrology, land use and other anthropogenic factors and on possible triggers such as earthquakes and weather (rainfall, snowfall) is beneficiary, if available in an appropriate resolution and quality (Tab. 2.5, Corominas et al. 2013).

Tab. 2.5 Overview of predisposing, preparatory or triggering factors of landslides and their relevance in landslide susceptibility and hazard assessment for different landslide types (R = rockfalls, S = shallow landslides and debris flows, L = large, slow moving landslides). The relevance is indicated as C (crucial), H (highly important), M (moderately important), and L (less important). The type of factor is indicated as either P (preparatory and/or predisposing factor) or T (triggering factor) (Corominas et al. 2013)

Group	*Parameters*	*Relevance for landslide susceptibility and hazard assessment*	*Type of factor*		*Landslide type*		
			P	T	R	S	L
Topography	Elevation, internal relief	Elevation differences result in potential energy for slope movements	*		H	C	H
	Slope gradient	Slope gradient is the predominant factor in landslides	*	*	C	C	C
	Slope direction	Might reflect differences in soil moisture and vegetation, and plays an important role in relation to discontinuities	*		C	M	M
	Slope length, shape, curvature, roughness	Indicator of slope hydrology, important for runout trajectory modelling	*		C	H	H
	Flow direction and accumulation	Used in slope hydrological modelling, e.g. for the wetness index	*		M	C	H
Geology	Rock types	Determine the engineering properties of rock types	*		C	H	C
	Weathering	Types of weathering (physical/chemical), depth of weathering, individual weathering zones and age of cuts are important factors	*		C	H	H
	Discontinuities	Discontinuity sets and characteristics, relation with slope directions and inclination	*		C	M	H
	Structural aspects	Geological structure in relation to the slope angle/direction	*		H	H	H
	Faults	Distance from active faults or widths of fault zones	*		H	H	H
Soils	Soil types	Origin of the soil determines its properties and geometry	*		L	C	H
	Soil depth	In surficial formations, depth determines the potential movable volume	*		L	C	H
	Geotechnical properties	Grain size, cohesion, friction angle, bulk density	*		L	C	H
	Hydrological properties	Pore volume, saturated conductivity, PF curve	*		L	H	H
Hydrology	Groundwater	Spatial and temporal variations in depth to groundwater table, perched groundwater tables, wetting fronts, pore water pressure, soil suction	*	*	L	H	H
	Soil moisture	Spatial and temporal variations in soil moisture content	*	*	L	H	H
	Hydrological components	Interception, evapotranspiration, throughfall, overland flow, infiltration, percolation, etc.	*	*	M	H	H
	Stream network and drainage density	Buffer zones around streams; in small scale assessment, drainage density may be used as an indicator for type of terrain	*		L	H	H
Geomorphology	Geomorphological	Alpine, glacial, periglacial, denudational.	*		H	H	H

	environment	Coastal, tropical, etc.						
	Old landslides	Material and terrain characteristics have changed, making these locations more prone to reactivations	*		M	H	C	
	Past landslide activity	Historical information on landslide activity is often crucial for determining landslide hazards and risk	*		C	C	C	
Land use and anthropogenic factors	Current land use	Type of land use/land cover, vegetation type, canopy cover, rooting depth, root cohesion, weight	*		H	H	H	
	Land use changes	Temporal variations in land use/land cover	*	*	M	C	H	
	Transportation infrastructure	Buffers around roads in sloping areas with road cuts	*		M	H	H	
	Buildings	Slope cuts made for building construction	*	*	M	H	H	
	Drainage and irrigation networks	Leakages from such networks may be an important cause of landslides	*	*	L	H	H	
	Quarrying and mining	These activities alter the slope geometry and stress distribution. Vibrations due to blasting can trigger landslides	*	*	H	H	H	
	Dams and reservoirs	Reservoirs change the hydrological conditions. Tailing dams may fail	*	*	L	H	H	
Earthquakes and volcanoes	Seismicity	Earthquake magnitude/frequency relations, historical intensity maps linked with co-seismic landslide inventories		*	C	C	C	
	Fault mechanism	Fault locations, fault type, length of fault rupture, buried or exposed, distance from fault, hanging wall/footwalls	*	*	H	H	H	
	Volcano type	Height and composition of volcanic edifice, magma chamber stability	*	*	M	H	H	
	Volcanic eruption types	Lateral explosions, collapse of magma chambers, pyroclastic flows, lahars	*	*	M	H	H	
Weather and climate	Precipitation	Daily or continuous data, weather patterns, magnitude/frequency relations, IDF curves, rainfall thresholds, antecedent rain, PADF curves		*	C	C	C	
	Temperature	Important influence on hydrology and the condition of vegetation. Rapid temperature changes, snowmelt, frost-thaw cycles, permafrost	*	*	H	H	H	

Validation, or model performance assessment is a key and meanwhile also a standard procedure in landslide susceptibility modelling.

As Chung and Fabbri stated *"Without some kind of validation, the prediction model and image are totally useless and have hardly any scientific significance."* (Chung and Fabbri 2003, p. 460).

While Chung and Fabbri use the term "validation" widely, they point out the nature of the term as a term-of-art in goodness-of-fit testing (Chung and Fabbri 2008). Further, they emphasize, that no connotation of absolute "truth" in the strictest

sense is intended by the usage of this term (Sterman et al. 1994). This applies also for the usage of the term within this thesis.

Knowing about the model performance, is not only of importance for the scientist him/herself but also helpful to communicate the model quality to non-specialists such as spatial planners or majors (Chung and Fabbri 2003). This measure on the significance of the model results is usually obtained in all spatial data analyses related to planning of multi-purpose use of space for human activity (Chung and Fabbri 2003).

The model performance can be assessed quantitatively using different estimation techniques and performance measures or qualitatively considering expert knowledge of a particular study area (Petschko et al. 2014c). Assessing the model performance quantitatively a test sample of landslide and non-landslide cells independent from the sample used for the modelling is crucial (Chung and Fabbri 1999). This test sample can be assembled subsampling by time (year of occurrence), space (part of the study area) or randomly (Chung and Fabbri 2003). Furthermore, it may consist of only one landslide grid cell, as done in the leave one out validation (Demoulin and Chung 2007), or it may be a percentage of grid cells of all sampled cells, as done in single hold-out validation.

Single hold-out validation is probably the most popular sampling method applied in landslide susceptibility modelling (e.g. Beguería 2006b; Brenning 2005; Chung and Fabbri 2003; Chung and Fabbri 1999; Van Den Eeckhaut et al. 2006; Fabbri et al. 2003; Frattini et al. 2010; Remondo et al. 2003; Rossi et al. 2010a). The data set (or original sample) is split in one single training and test sample. While the model is fitted with the training sample, the test sample is used to determine the model performance. The distribution of the landslide and non-landslide cells is compared to the distribution of the susceptibility probability and a single performance measure is estimated. However, this single estimate does not provide a measure of the precision of the estimator and is highly dependent on the sample used for modelling and testing the susceptibility model (Petschko et al. 2014c). The strength and reliability of the model performance can only be evaluated comparing it to other performance assessments resulting from another sample (Chung and Fabbri 2003).

Repeated *k*-fold cross-validation provides a standardized framework to perform the repetition of the sampling process. *K*-fold cross-validation creates different subsets or partitions (folds) of the data set as training and test samples (Brenning 2012a; Brenning 2012b). The model is fitted with *k*-1 training samples and its performance is assessed using the remaining fold as test sample. This procedure is done as long as each fold was used as a test sample once. After this first validation run the folds are partitioned differently and the process is repeated. With this assessment the effect of the sampling on the model performance can be assessed resulting in a range, instead of a single performance measure (Petschko et al. 2014c). It allows the determination of the precision of the performance estimator and was performed recently in spatial and landslide susceptibility modelling (Brenning 2012b; Petschko et al. 2014c; von Ruette et al. 2011; Vorpahl et al. 2012).

Several quantitative performance measures were tested in the landslide susceptibility modelling context: success/prediction rate (Chung and Fabbri 2008; Chung and Fabbri 2003), confusion matrix or error rates (Beguería 2006b; Brenning 2005), cost curves (Frattini et al. 2010), Cohen's kappa (κ) index (Cohen 1960; Van Den Eeckhaut et al. 2006; Rossi et al. 2010a), spatial agreement (Sterlacchini et al. 2011) and most prominently the area under receiver operating characteristic curve (AUROC) value based on ROC plots (Beguería 2006b; Brenning 2005; Frattini et al. 2010).

2.4 Assessment of the quality of landslide susceptibility maps

"There are known knowns. These are the things we know that we know. There are known unknowns. That is to say, there are things that we now know we don't know. But there are also unknown unknowns. These are the things we do not know we don't know." Donald Rumsfeld in Spiegelhalter and Riesch (2011).

This quote nicely summarizes the knowns and unknowns we face also in geomorphology according to the current paradigm of systems theory. Gathering information about the known knowns and the known unknowns, or maybe even the unknown unknowns might be one general aim of research. Aiming at a reliable landslide susceptibility map these knowns and unknowns have to be analyzed and possibly communicated to provide a map of good quality. This is particularly of importance when it comes to the application of the resulting susceptibility map in spatial planning (Petschko et al. 2014c). Considerations on different aspects of quality in landslide susceptibility modelling were reviewed in the publication by (Petschko et al. 2014c; A.6). The following subsections contain large parts of this review in Petschko et al. (2014c; p. 96-98; A.6,).

Every display of a map is associated with constructing a decisive reality (Egner and Pott 2010) for the users of the map (e.g. municipality, spatial planner). The map becomes a reality for the reader despite the background or knowledge of the person (Egner and Pott 2010). Therefore, boundaries or spatial extents of different classes shown in a map might be interpreted very strictly. In contrast to this, it is known that every model (or map) is only an approximation of the reality and is inherently riddled with uncertainties (Petschko et al. 2014c). While this might be clear for scientists, other users of the map might have to be reminded about that. In this context a detailed and transparent assessment and communication of the quality of the landslide susceptibility map is necessary.

This very generic term of quality may be interpreted differently depending on the research field. By extension quality may have a different meaning on the several stages of landslide susceptibility modelling as described, amongst others, by Carrara (1993), Carrara et al. (1995), Ardizzone et al. (2002), and Guzzetti et al. (2006). In

this study, good quality refers to input data, a model or result (e.g. susceptibility map) which includes relatively low uncertainties of any kind (Petschko et al. 2014c). As Carrara et al. (1999) state many processes and conditions leading to landslide occurrence are known and mappable, known but not collectable, or are simply unknown.

Commonly a basic distinction between aleatory and epistemic uncertainties is done in engineering and risk assessment (Hill et al. 2013; Hoffman and Hammonds 1994; Oberkampf et al. 2004; Roy and Oberkampf 2011). Epistemic uncertainties refer to the imperfect understanding of the complexity of landslides arising from the missing knowledge (Ardizzone et al. 2002; Hoffman and Hammonds 1994; Hora 1996; Kunz et al. 2011; Oberkampf et al. 2004). Generally stated subgroups of epistemic uncertainty are input uncertainty, parametric uncertainty and structural or model form uncertainty (Rougier and Beven 2013; Roy and Oberkampf 2011). These uncertainties can be reduced by doing more research on the subject to improve knowledge (Spiegelhalter and Riesch 2011). In contrast to this, aleatory uncertainties are unavoidable uncertainties arising from the natural variability and/or randomness of the natural hazard process (Rougier 2013; Rougier and Beven 2013). While these distinctions can be applied, many more different groups may be found in literature depending on the study objectives which will not be reviewed here (Hora 1996; Roy and Oberkampf 2011).

In the following, different aspects of quality will be discussed by addressing uncertainty issues associated with statistical modelling regarding input data (parametric uncertainty), model performance (model form uncertainty) and the final susceptibility map (Petschko et al. 2014c). Details on other types of uncertainties, which might be more important for other types of susceptibility assessment (e.g. deterministic) or on the propagation of uncertainties, can be found amongst others in Draper (1995), Helton et al. (2010), Hoffman and Hammonds (1994), Karam (2005), Oberkampf et al. (2004) and Rougier (2013).

2.4.1 Quality of input data

Every modelling result can only be as good as the input data used for the modelling. Therefore, a good quality of the final landslide susceptibility map may be achieved by a good quality of the input data (Petschko et al. 2014c). Aspects such as geomorphological relevance, appropriate spatial resolution and accuracy of the geo-environmental as well as the landslide inventory data are generally listed as important (van Westen et al. 2008). However, achieving a fully complete data set may be impossible. Chung and Fabbri (1999) stated *"no matter how good the information available may be, the database will always contain incomplete information"* (Chung and Fabbri 1999, p. 1397).

Sources of parametric uncertainty are subjectivity, level of experience of the mapper, measuring errors or imprecision in computer algorithms, all occurring during the preparation (mapping or measuring) of all input data (Ardizzone et al. 2002; Baeza

et al. 2010; Carla et al. 1997; Elith et al. 2002; Mosleh 1986; van Westen et al. 2008; van Westen et al. 2005). Furthermore, the possibility of not being able to incorporate all explanatory variables that contribute to landslide occurrence has to be kept in mind (Guzzetti et al. 2006). This might happen due to lack of knowledge or limited availability of data and poses a challenge for susceptibility assessments (Ardizzone et al. 2002; Carrara et al. 1999; van Westen et al. 2005). Usually, parametric uncertainty can rarely be reduced and has to be assessed otherwise. However, their quantitative assessment is challenging which is why estimates on the completeness of e.g. a landslide inventory including details on the collecting and mapping method are very important (Ardizzone et al. 2002; Oberkampf et al. 2004; Roy and Oberkampf 2011). Based on that information, the further usage of all data and the feasible interpretation of the result have to be decided on (Petschko et al. 2014c).

2.4.2 Quality of statistical model form

Models are used to analyze complex processes in nature by simplification of reality. Therefore, some discrepancies regarding the ability to explain all the processes involved in landslide occurrence should not be surprising (Rougier and Beven 2013). Besides a high dependence on the input data, the assumptions included in the model design define the limitations of the model, its result and the allowed interpretation of it. This describes the so called model form uncertainty, which is rather challenging to quantify. However, one commonly applied solution is the quantitative assessment of the model performance with quantitative or qualitative model validation procedures (Roy and Oberkampf 2011).

Quantitative model validation procedures include various performance measures and estimation techniques as already introduced in section 2.3. Facilitating these performance measures, the transferability of a model within the study area can be analyzed (Petschko et al. 2014c). Depending on the partitioning method (randomly or spatially) in *k*-fold cross-validation the non-spatial transferability of a model onto a different, independent random sample, and the spatial transferability of a model into a spatially separate area can be assessed. The measure of spatial transferability gives the capability of the model to generalize empirical relationships learned from the training sample and to transfer these relationships to other regions (with similar geotechnical characteristics (Guzzetti et al. 2006)) while the predictive performance should remain high (Brenning 2005; von Ruette et al. 2011). In this study the (non-) spatial transferability is used besides the AUROC value to describe the model form uncertainty (Petschko et al. 2014c).

Qualitative model performance assessment is less wide spread in landslide susceptibility research, at least it is not very often stated on. Qualitative methods may include analysis of the geomorphic plausibility of the map and of the input variables (Bell 2007; Demoulin and Chung 2007). This qualitative analysis is done by an expert knowing the particular study area and focuses more on the geomorphic plausibility of the map from the expert point of view.

Besides epistemic uncertainties, aleatory uncertainties can occur in the modelling stage as a form of deviance (or discrepancy) of the model results to the conditions in nature occur (Petschko et al. 2014c). These arise due to the natural variability of the process (e.g. landslide) which cannot be captured in detail, even if all parameters would be known perfectly (Elith et al. 2002; Rougier and Beven 2013).

2.4.3 Quality of final susceptibility map – visualizing prediction uncertainties

One model form uncertainty which is of specific interest when landslide susceptibility maps are implemented in spatial planning, is the prediction uncertainty (Petschko et al. 2014c). It is arising from using a statistical model which gives a single probability value for each unit of the prediction surface (grid cells, slopes or terrain units) used for displaying the landslide susceptibility in a map (Guzzetti et al. 2006). These individual probability values represent the estimated conditional mean value of the predicted probability (Hosmer and Lemeshow 2000; Petschko et al. 2014c). Accordingly, each predicted probability value has a standard error which gives a prediction uncertainty or possible range of probability estimates (Guzzetti et al. 2006). This standard error can be used to calculate the upper and lower confidence limits e.g. at 95% confidence. Displaying those on a map, gives the possible range of landslide susceptibility probability for each prediction surface.

While the estimation of the standard error was presented in previous research (e.g. Van Den Eeckhaut et al. 2009c; Guzzetti et al. 2006; Rossi et al. 2010a; Sterlacchini et al. 2011), the calculation of confidence limits and possible overlaps of different susceptibility probabilities was pending (Petschko et al. 2014c). Possible overlaps of susceptibility classes (low, medium or high) of classified susceptibility maps of the predicted probability with the upper and lower confidence limit are of specific interest in the planning framework (Petschko et al. 2014c).

"The details in which the figure differs from its mathematical prototype are more important and more interesting than the features in which it agrees" (Thompson 1942, p. 1026-1029).

However, this type of model form uncertainty expressed for classified susceptibility maps is clearly dependent on the selected number of classes and threshold values for the classification (Petschko et al. 2014c).

2.5 Landslide susceptibility maps and spatial planning

Landslide susceptibility maps are valuable tools to be implemented in spatial planning, as they portray information on landslide susceptibility on a grid cell or slope unit level for an entire area. Land use management or planning, spatial

planning or aerial zoning are almost synonymously used terms. All these methods are aiming to the avoidance of future damage by preventing development in undesirable locations, or undesirable development forms (Schwab et al. 2005). Their main purpose is to intervene in settlement development to guide residential, commercial and industrial development away from susceptible areas (Chung and Leclerc 2003).

Generally, when implementing landslide susceptibility maps in spatial planning, their scale should be appropriate for displaying the information needed at a particular planning level (Cascini 2008). Furthermore, the objectives of the map and the scale of the available data affect the selection of an appropriate scale of the susceptibility map (Fell et al. 2008). In literature small to detailed scales and related study area sizes are suggested (Tab. 2.6; Cascini 2005; Fell et al. 2008; Soeters and Van Westen 1996): (1) analyzing on small scale (< 1:100,000) is advised for a study area size larger than 10,000 km², (2) a medium scale (1:100,000 to 1:25,000) is suggested for a study area size between 1,000 km² and 10,000 km², (3) large scale analysis is recommended for areas between 10 km² to 1,000 km² and (4) detailed scale is usually used in analysis of several hectares to tens of square kilometers.

With regional zoning as the purpose, the resulting landslide susceptibility maps are only suitable for information or advisory for the users. No statutory use is feasible (Tab. 2.7; Fell et al. 2008). Basic and intermediate zoning levels are recommended focusing on geomorphological and landslide inventory mapping and landslide density and simple correlation analysis.

Implementing the resulting maps from basic or intermediate zoning in land use or spatial planning, the limited expressiveness of the maps has to be considered (Fell et al. 2008). The accuracy of the susceptibility zoning boundaries is limited and the resulting maps might only be used as information where more detailed geotechnical assessment of the landslide hazard is necessary (Fell et al. 2008). For local zoning and especially performing detailed zoning more advanced methods such as physically based or statistical models (e.g. logistic regression or discriminant analysis) are recommended (Tab. 2.6 and Tab. 2.7; Fell et al. 2008).

While numerous examples of landslide susceptibility maps and different modelling methods are presented in literature, it is less obvious how many of these were actually implemented in spatial planning strategies. This is striking as the potential usage of landslide susceptibility maps to avoid losses due to landslide events has already been pointed out 30 years ago (Varnes 1984). Therefore, at first glance there is a misbalance in state of the art and its implementation. However, there are many examples globally where landslide susceptibility maps are published in a Web-GIS platform or via a web mapping service (Tab. 2.8).

Tab. 2.6 Landslide zoning mapping scales and their application (Fell et al. 2008)

Scale description	*Indicative range of scales*	*Examples of zoning application*	*Typical area of zoning*
Small	< 1:100,000	Landslide inventory and susceptibility to inform policy makers and the general public	> 10,000 km²
Medium	1:100,000 to 1:25,000	Landslide inventory and susceptibility zoning for regional development; or very large scale engineering projects. Preliminary level hazard mapping for local areas	1,000 – 10,000 km²
Large	1:25,000 to 1:5,000	Landslide inventory, susceptibility and hazard zoning for local areas. Intermediate to advanced level hazard zoning for regional development. Preliminary to intermediate level risk zoning for local areas and the advanced stages of planning for large engineering structures, roads and railways.	10 – 1,000 km²
Detailed	> 1:5,000	Intermediate and advanced level hazard and risk zoning for local and site-specific areas and for the design phase of large engineering structures, roads and railways.	1 ha – 10 km²

Tab. 2.7 Recommended types and levels of zoning and zoning map scales related to landslide zoning purpose (simplified after Fell et al. (2008))

Scale description	*Zoning methods*				*Zoning levels*			*Purpose*
	Inventory	Susceptibility	Hazard	Risk	Basic	Intermediate	Advanced	
Small	*				*			Regional zoning - Information
Medium	*	*	(*)		*	(*)		Regional zoning - Information - Advisory
Large	*	*	*	*	*	*	*	Local zoning - Information - Advisory - Statutory
Detailed	[*]	(*)	*	*	[*]	(*)	*	Site specific zoning - Information - Advisory - Statutory - Design

Notes: * Applicable; (*) May be applicable; [*] Not recommended or not commonly used.

In many of these countries (e.g. Great Britain, Germany (Bavaria, Swabian Alb) or Georgia) the landslide susceptibility maps are used for deriving recommendations or a first indication of landslide hazard for spatial planning (Tab. 2.8). However, a few countries or provinces, with Switzerland leading the way (South Tyrol, Philippines, France, Flemish Ardennes and the district of North Vancouver), introduced legal restrictions of land use types and development within each susceptibility class implemented by spatial planning (Tab. 2.8).

This review in Table 2.8 aims to show a range of applications in land use planning but it might not be exhaustive. Many landslide susceptibility maps might be prepared and maybe also used in local planning processes, but are not reported in science publications or in English on the web.

However, the best maps are of no use if their content is not communicated properly to the potential users. To increase the acceptance of landslide mitigation measures, or preventative planning, participative or community based approaches have proved highly effective (Anderson and Holcombe 2013; Pearce 2005; Pearce 2003; Schwab et al. 2005). This includes involvement of the stakeholders already at an early stage of the project and training in reading maps and understanding the processes (Anderson and Holcombe 2013; DeGraff 2012; Fabbri and Chung 2009; Pearce 2003; Schwab et al. 2005). However, the translation of the results from science to policy making includes some pitfalls (DeGraff 2012). Regulations need to be worded in a way where no interpretation or gradation is allowed which is the contradictory to what science does (DeGraff 2012). For a sustainable reduction of losses continuous involvement in the implementation of landslide susceptibility or hazard maps and education of the users is required from the scientists (DeGraff 2012; Schwab et al. 2005).

2.6 Research gaps and challenges analyzing large areas

In all stages of landslide susceptibility modelling some research gaps and challenges can be identified considering the analysis of a large, heterogeneous study area with incomplete available landslide inventories. Taking into account the respective state of the art (refer to sections 2.1 - 2.5) these research gaps and the challenges faced within this study in the context of the implementation of the resulting maps in municipal spatial planning strategies are summarized in the following:

Statistical modelling methods are highly dependent on the input data selected to characterize the slope stability. Starting from the input data and the landslide inventory, a lot of research has been done on mapping landslides on different imagery (e.g. aerial photographs, satellite images, LiDAR hillshades) and with different methods (stereoscopic photo interpretation, visual analysis, (semi-) automated change or landslide detection). Furthermore, their respective limitations and restrictions regarding completeness and uncertainties arising from the used imagery were reported (e.g. Guzzetti et al. 2012).

Tab. 2.8 Mapping method (Heuristic (HE), statistic (ST), physically based (PB)), Map type (Inventory (INV), Susceptibility (SUS), Hazard (HAZ) or Risk (RIS)); *only with costs available

Method	*Map type*	*Country / Province / Location*	*Scale*	*Area (km²)*	*Landslide type*	*Way of implementation in spatial planning*	*Web GIS / WMS*	*Source*
HE	INV	Czech Republic	1:10,000 - 1:50,000	78,866	Slides, creep, flows, falls	Information for municipal authorities.	Yes	Česká geologická služba 2014; Krejci et al. 2002
HE	INV	Germany (Baden-Württemberg)	1:50,000	35,752	Slides, falls, dolines, sinkholes, subsidence	Information for governmental and municipal authorities, citizens and companies to allow for preventative spatial and land use planning.	Yes (*)	Landesamt für Geologie, Rohstoffe und Bergbau (LGRB) 2014; Ruch 2014
HE	INV	Italy	1:10,000	301,338	Slides, falls, flows, spreads, sinkholes	Information for municipal authorities.	Yes	Trigila and Iadanza 2008
HE	RIS	France	1:10,000 - 1:25,000	n.i.	n.i.	Municipalities, collaboration with insurance companies; specific rules for land use regulations and urbanism, nonobservance of the PPR has legal consequences	No	Malet and Maquaire 2009
HE	SUS	California	1:100,000	423,970	Slides	Identification of hot spots for further action	No	Wills et al. 2011
HE	SUS	Czech Republic		78,866		Information for municipal authorities.	Yes	Česká geologická služba 2014
HE	SUS	Georgia	1:100,000	69,700	n.i.	Ranking of municipalities for hot spots of risk reduction measures	No	Gaprindashvili 2011
HE	SUS	Great Britain	1:50,000	243,610	Falls, topples, slides,	Recommendations and advice for public or a specialist for further actions for each susceptibility class (5 classes).	Yes	British Geological Survey 2014; Gibson et al. 2012

					flows.			
HE	SUS	Ireland (Bréifne Area, East Coast, Cork area)	1:50,000	n.i.	Bedrock slides, peat slides, falls and flows	Maps are used informative and do not impose statutory measures. Not embraced yet for entire country.	Yes	Geological Survey of Ireland 2014a; Geological Survey of Ireland 2014b
HE	SUS	Philippines	1:50,000	298,170 (1,634 cities and municipalities)	n.i.	Used in municipalities to identify areas susceptible to various hazards such as flooding or landslides to lessen or mitigate potential damage or losses from these events by preparedness planning.	Yes	Mines and Geosciences Bureau 2011; 2008
HE	SUS	Poland (Flysch Carpathians)	1:200,000	n.i.	Slides	n.i.	No	Dlugosz 2009
HE	SUS	Romania	1:200,000	238,391	Slides, flows	Supplying basic information on slope stability of construction sites. Development planning,	No	Bălteanu et al. 2010
HE, PB	HAZ	Austria	1:2,000 - 1:5,000	83,855 (only settlements)	Torrential processes, Flows, falls	Basics for consideration in municipal development planning. If hazard zones are included in the final area zoning plan, their consideration in the planning of new building zones is legally mandatory.	Yes	Rudolf-Miklau 2007
HE, PB	INV, HAZ	South Tyrol (Italy)	1:5,000 - 1:10,000	7,400	Slides, falls, flows, spreads, sinkholes, flooding, avalanches, erosion	Hazard zonation plans with classes legally implemented in spatial planning processes. Prepared only in areas close to settlements.	Yes	Autonome Provinz Bozen - Südtirol 2012a; Autonome Provinz Bozen - Südtirol 2012b
PB	RIS	North Vancouver (BC, Canada)	n.i.	160.76	Slides	Slope Hazard Development Permit Areas introduced in 2012 in the new Official Community Plan	Yes	District of North Vancouver 2014; Tappenden 2014

PB	SUS	Germany (Bavaria)	1:25,000	70,553	Slides, flows, falls	Recommendations and advice for public or a specialist for further actions for each susceptibility class. Including legal implementation in provincial spatial planning.	Yes	Bayerisches Landesamt für Umwelt (LfU) 2013; Bayerisches Landesamt für Umwelt (LfU) 2012
PB	SUS	Switzerland	1:25,000 - 1:50,000	41,285	Slides, avalances, falls, flows	Overview maps resulting from the project SilvaProtect-CH indicating areas which have to be considered in the more detailed zoning on a scale of 1:5,000. Furthermore, the government uses these and the maps from "ShowMe" to decide on funding priorities for the calculation of landslide susceptibility maps. The slide maps show the initiation and runout zone.	Yes	Heil et al. 2014; Losey and Wehrli 2013; Schweizerische Eidgenossenschaft 2014
PB	SUS	Switzerland	1:5,000	41,285	Slides, avalances, falls, flows	Hazard archives and maps have to be considered within land use planning done by the Cantons.	Yes	Heil et al. 2014; Kanton Bern 2014
ST	SUS	Austria (Burgenland)	1:25,000	3,962	Slides	Land management planning – prevention and remediation of landslides. Recommendations for each susceptibility class for planning and building of new infrastructure.	No	Leopold 2012
ST	SUS	Flemish Ardennes, Belgium	1:10,000 (10m x 10m)	720	Slides	Land management planning – prevention and remediation of landslides. Imposes obligations and limitations on the development plan.	Yes	Van Den Eeckhaut et al. 2007; Van Den Eeckhaut et al. 2006; Malet and Maquaire 2009
ST	SUS	Germany (Swabian Alb)	1:350,000	10,000	Slides	Consideration of slide susceptibility map in the regional development planning of the region Neckar-Alb. Recommendations for each susceptibility class for planning and building of new infrastructure.	No	Bell 2007
ST	SUS	Philippines	1:10,000	218 municipalities	n.i.	Used in municipalities to identify areas susceptible to various hazards such as flooding or landslides to lessen or mitigate potential damage or losses from these events by preparedness planning.	Yes	Mines and Geosciences Bureau 2011

However, the effectiveness of each method mapping a landslide inventory indicating single landslides for a large study area on high resolution scale (around 1:5,000) is not quantified in a standardized way. Working in larger study areas may go along with a limited availability of an abundant landslide inventory sufficiently complete for statistical modelling. Additionally, in large study areas the mapping of all landslides visible on the imagery might not be feasible given limited resources and a large number of landslides to be mapped. Furthermore, the minimum number of landslides required and their mapping type (point or polygon) necessary to derive reliable landslide susceptibility maps by statistical modelling methods remains unclear. Therefore, mapping a sufficiently complete landslide inventory most effectively and optimized for its usage in statistical susceptibility modelling generates another challenge.

While the need of information on landslide susceptibility is widely agreed on and landslide susceptibility modelling methods have been tested in various study areas globally, model designs facing the heterogeneity of a study area are not reported on. Independent of the study area size, the area might show a high heterogeneity regarding its topography, morphology and geotechnical characteristics. This may include variations of the main predisposing, preparatory or triggering factors within the study area which might not be portrayed properly in one single model. This is independent on which statistical model is used for the analysis. The variety of available methods and the differences in the characterization of slope stability in different study areas worldwide, pose a challenge on the identification of a globally valid and applicable method (Van Westen et al. 2006). In detail, ensuring the feasibility of comparing the resulting landslide susceptibility map over the entire area is challenging and a research gap which has not been answered yet. Selecting an appropriate study design, mapping and modelling method was a challenge in this study given the study area size (15,850km²) and the aimed output map scale of 1:25,000.

Tables 2.6 and 2.7 give clear suggestions which methods should be applied for the respective aimed output scale and study area size. However, this study in Lower Austria steps out of line, given the study area size and the aimed output map scale. Looking at the scale, this study is of medium scale, but looking at the area, it is considered as a small scale study (Cascini 2008; Fell et al. 2008). Additionally, for the purpose of regional zoning on a scale of 1:25,000, statistical (advanced) methods of assessing the landslide susceptibility are indicated as not applicable (Fell et al. 2008).

Nevertheless, given the application of the resulting maps in a planning strategy the usage of statistical methods seems the only suitable solution. They are stated to be more objective, traceable and reproducible than heuristic methods and require less detailed data than physically based models. Furthermore, given the potential implementation of the resulting landslide susceptibility map in spatial planning strategies, the provision of an interpretable model and the comparability of the maps all over the province are of high importance. This allows the identification of hot spots where action needs to be taken on a province level. Still, statistically modelling

of a heterogeneous area clearly poses a challenge on the data preparation, modelling and computational capacities which were faced within this study.

Different aspects of quality of landslide susceptibility maps or models, such as thematic consistency, high model performance and prediction skills and prediction uncertainties, have been defined before (Guzzetti et al. 2006). Furthermore, the need for the assessment or validation of model performance is pursued in the last ten years (Chung and Fabbri 2003). However, the assessment of the model performance showing the possible range of performance measures and its transferability, changing the sample used for the modelling has not been tested systematically. Also, the thematic consistency was not described quantitatively. While the spatially varying prediction uncertainties have been shown by visualizing the standard error of the predicted probability (e.g. Guzzetti et al. 2006), their influence on a classified map has not been assessed yet. Although providing information or the assessment of the uncertainties involved in the modelling is of importance to be communicated to the users of the map, ways of communicating these uncertainties with the users of the landslide susceptibility map have not been explored in this field. An estimate on where the largest uncertainties can be expected might be considered as very helpful for the planning process.

Providing an easy interpretable map was another challenge. The susceptibility information should be detailed enough for its interpretation within municipalities on a scale of 1:25,000 to aid the identification of areas with the need for more detailed slope stability analysis. This required a decision on how many susceptibility classes and which thresholds should be used for building the classes. Also the way how the maps would be presented to the municipalities to ascertain their acceptance and usability was subject of the project within which this thesis was written.

In statistical landslide susceptibility modelling it is assumed that all explanatory variables relevant for the landslide occurrence are known. Similarly, the possible incompleteness of the explanatory variables for the modelling due to limited data availability was stated earlier (Guzzetti et al. 2006). Theoretically it is known that human impact may play a major role in landslide initiation. Some solutions have already been presented to include possible human impact on landslide initiation in the modelling (e.g. including a distance to roads variable or human impact index, refer to section 2.1.5). However, these might not take into account the several facets of human impacts including influences and changes of the landslide catchment area by installing drainages or roads. On top of that, spatial consideration of these facets in a regional susceptibility assessment would be necessary to better estimate the actual landslide susceptibility.

3. Hypotheses and research objectives

Five hypotheses were tested within this thesis, which were arising from the identified research gaps and challenges. These are presented in the following with their respective research objectives and main expected outcomes.

The **first hypothesis** (H1) arises from the need of effectively mapping a landslide inventory in a large study area:

A landslide inventory mapped on the basis of LiDAR DTM derivatives and orthophotos shows remarkably better precision and accuracy of the landslide location and delineation compared to existing landslide inventories. Furthermore, mapping points in the main scarp only increases the inventory mapping effectiveness and achieves comparably reliable landslide susceptibility maps with three classes in terms of model performance and visualization.

Therefore, the objectives are

- mapping a landslide inventory using polygons and points (set in the main scarp only)
- the comparison of the resulting inventory with previously existing inventories
- assessing the mapping effectiveness by comparing the resources needed during the mapping and the benefit arising from the mapped inventory
- to analyze the reliability of the resulting landslide susceptibility map by comparing of the model performance and visualization of the classified susceptibility map using samples in the landslide polygon or the point mapped in the main scarp

Analyzing this is expected to result in the identification of an effective landslide inventory mapping method using LiDAR DTM derivatives suitable for statistical landslide susceptibility modelling and the creation of a classified susceptibility map.

The **second hypothesis** (H2) embraces modelling in large, topographical and geotechnical heterogeneous regions:

Modelling the landslide susceptibility of a large heterogeneous area for maps with a scale of 1:25,000 requires a special consideration of the geotechnical and topographical conditions and their heterogeneity in the study area as the predominant preparatory and predisposing factors change with the conditions.

The objectives are accordingly:

- defining a model design taking into account the heterogeneity of the study area
- statistically modelling the landslide susceptibility using automated stepwise variable selection to assess the variable selection frequency within each modelling domain

From this analysis the identification of an appropriate model design allowing the comparison of the landslide susceptibility across the entire study area (all homogeneous modelling domains) characterizing each domain is expected.

The **third hypothesis** (H3) challenges common model evaluation in landslide susceptibility modelling:

Established model performance measures change with the selection of a new random or spatial sample of landslide and non-landslide points (cells). Splitting the sample into k subsamples and repeating this sampling process multiple times results in a range opposed to a single value of performance measures.

The arising objectives are:

- performing a spatial and non-spatial k-fold cross-validation
- assessing the spatial and non-spatial transferability of the model by analyzing the interquartile range of the resulting performance measure
- estimating the thematic consistency of the model summarizing the variable frequency of each model repetition

The resulting measures of spatial and non-spatial transferability and of the thematic consistency assist in evaluating the quality of the landslide susceptibility model and study design used to generate the susceptibility map.

The **fourth hypothesis** (H4) addresses uncertainties arising from the usage of a statistical model for estimating the probability of landslide occurrence:

The uncertainties of the predicted probabilities vary spatially according to the standard error of the predicted probability. Comparing classified landslide susceptibility maps derived within the 95% confidence interval results in overlaps of different susceptibility classes.

This includes the objectives:

- deriving the upper and lower confidence interval limits with 95% confidence for the predicted probabilities
- assessing the overlaps in the classified susceptibility map comparing the maps of the upper and lower confidence limits with the predicted mean probability of landslide occurrence

The results of this analysis will aid a better communication of uncertainties to stakeholders, as the class overlaps can easily be presented in a map along with the original susceptibility map. It proposes the methodology for a first important step towards open communication of uncertainties instead of giving an impression of certainty.

The **final hypothesis** (H5) examines the human impact and the possibility to map it spatially:

The human impact on landslides can be mapped and implemented in a statistical susceptibility modelling approach for large areas.

The objectives to this hypothesis are:

- identifying different human impact present in the study area and its appearance on remote sensing imagery
- mapping human impact on landslides and estimate landslide persistence
- analyze the human influence on the catchment size of a slope

The analysis of this hypothesis will increase the knowledge on human impact occurring within the study area and the dimensions of it. It will aid to identify limitations of mapping landslides on the basis of one data source only and of including the human impact into spatial modelling approaches.

4. Lower Austria – a province and its heterogeneity

4.1 General facts and environmental factors

Lower Austria has a total size of 19,186km² of which 15,835km² comprise the study area (Statistik Austria, 2014). Furthermore, a test study area was assigned covering the districts of Amstetten (1187km²), Baden (754km²) and Waidhofen/Ybbs (131km²; Fig. 4.1). This smaller area was used for the development of a study design of landslide mapping and susceptibility modelling. The three districts represent nearly all lithological, land use and topographical characteristics of Lower Austria (Fig. 4.1, Fig. 4.3). Each district is characterized by a different amount of landslides recorded in the archive of the Geological Survey of Lower Austria (refer to section 4.3). Not all analysis done in the test districts was performed for the large study area. Within the methods section the study area analyzed will be stated clearly.

In 2012 Lower Austria had 1,618,592 inhabitants with the highest population density in the districts around Vienna and the cities Krems, St.Pölten and Wr. Neustadt (Statistik Austria 2014). The southern districts Lilienfeld and Scheibbs and the northern districts Zwettl, Horn and Waidhofen/Thaya have the lowest population density (28.5 i/km² - 40.2 i/km²; Statistik Austria 2014). The village located at the lowest elevation is Engelhartstetten (143masl) and Annaberg is the highest located village of Lower Austria (976masl). The highest elevations are in the south of the province at the mountain peaks of Schneeberg (2075masl), Rax (2007masl) and Ötscher (1893masl).

Lower Austria is located in a transition zone from the maritime climate of Western Europe to the continental climate of Eastern Europe (Machalek 1986). The maritime climate is characterized by temperate summers, relatively mild winters and front precipitation. Unlike, the continental climate shows more seasonal temperature variations with cold winters and comparably warm summers. While precipitation is generally less frequent it usually is from convective origin (Machalek 1986). This transition is well visible in the distribution of the mean annual precipitation (1971-2000) and the mean annual air temperature (Fig. 4.2; 1991-2000). The mean annual precipitation rate increases from the northeast (400-500mm) to the southwest regions (1600-1700mm) while the mean annual temperature decreases from around 10°C to 5°C (Fig. 4.2; Hydrographic Service of Lower Austria 2011).

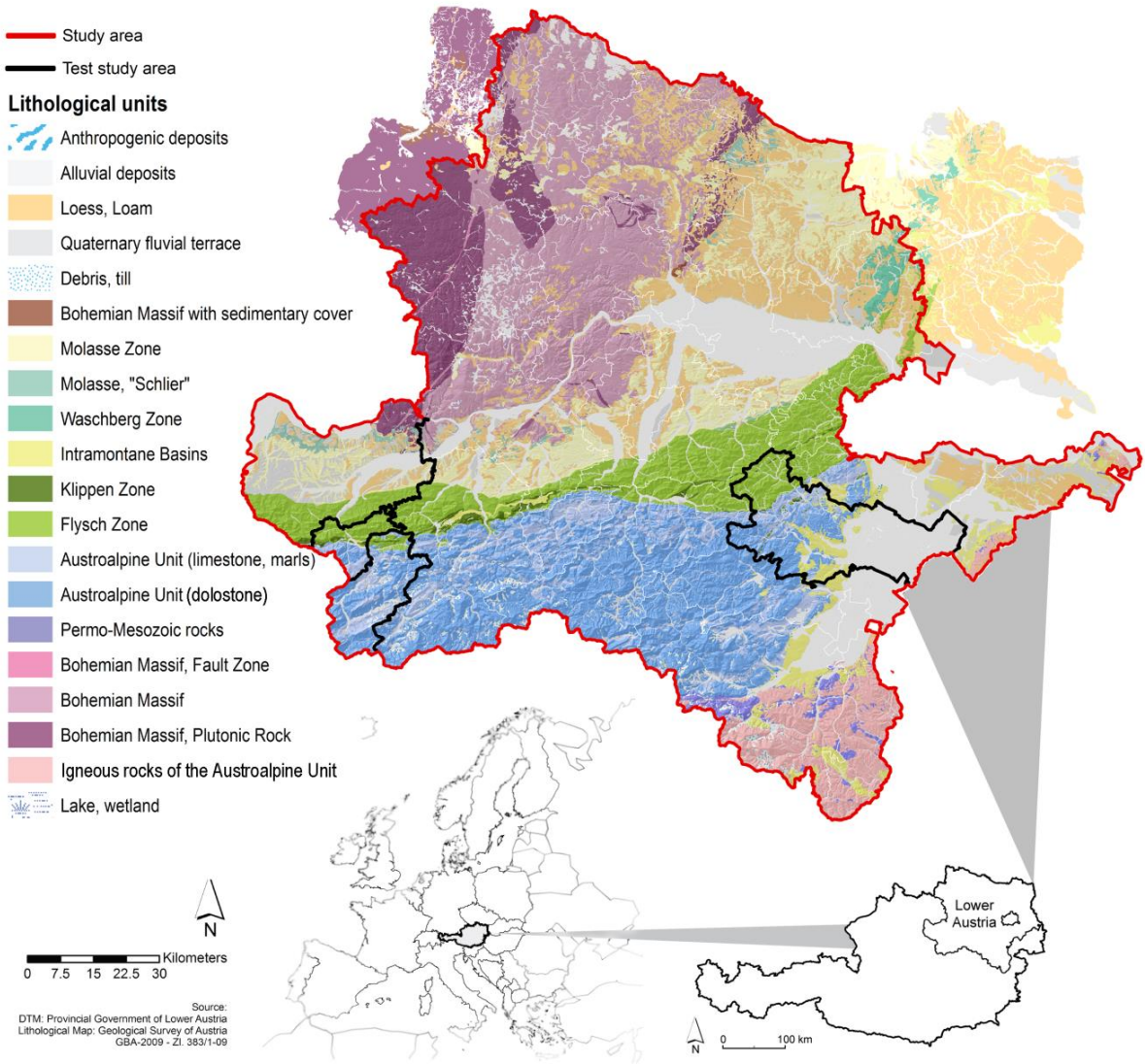

Figure 4.1 Location and lithology of the study area and the three test districts, Amstetten and Waidhofen/Ybbs in the West and Baden in the East (black outline), in Lower Austria. Source: altered from Petschko et al. 2014c

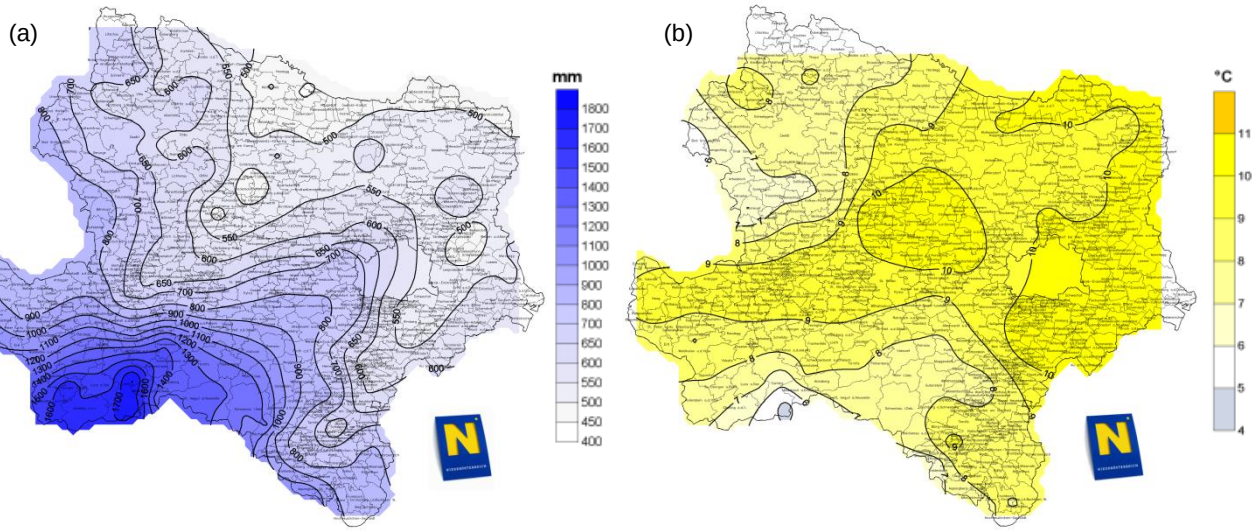

Figure 4.2 (a) Mean annual precipitation rate (1971-2000), (b) Mean annual air temperature (1991-2000). Source: Hydrographischer Dienst des Landes Niederösterreich (Hydrographic Service of Lower Austria 2011)

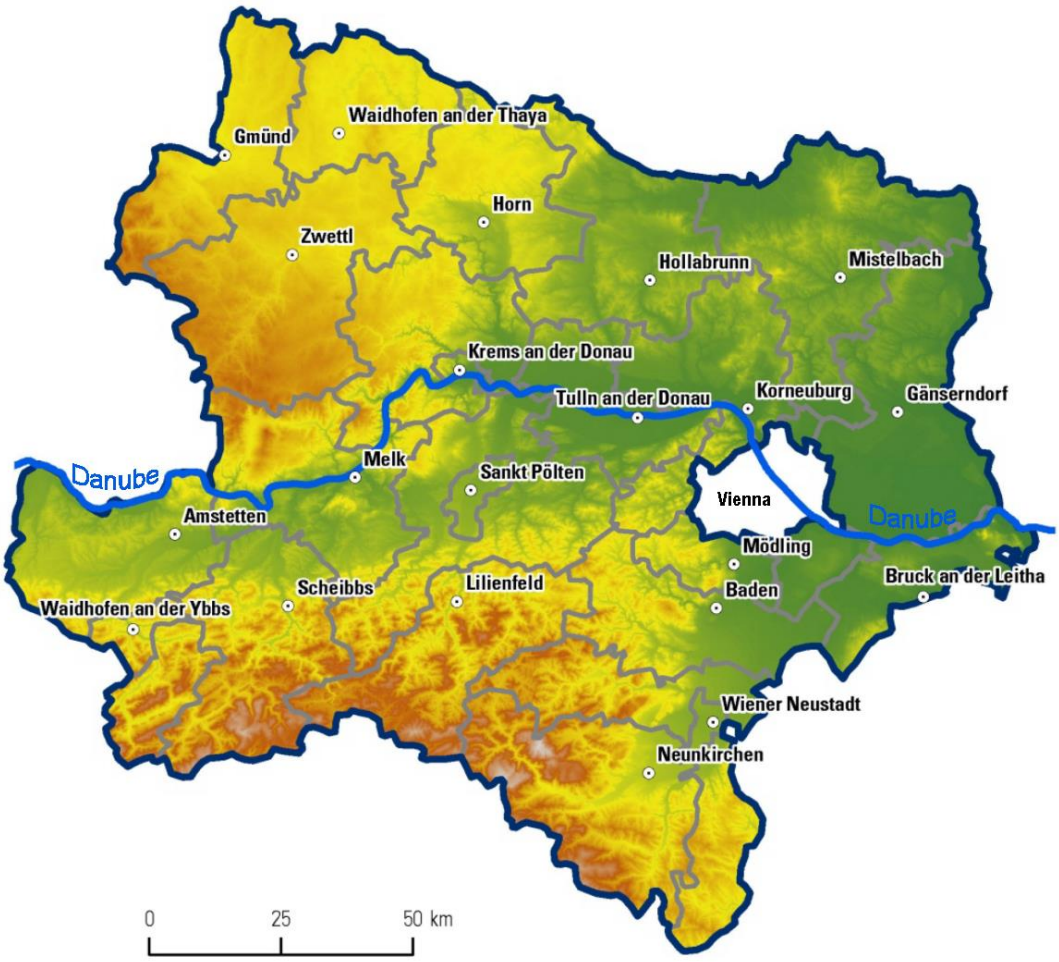

Figure 4.3 Topography and districts of Lower Austria (Vogl 2008).

Lower Austria is commonly divided according to different topographical conditions. Variation in climate is illustrated by describing conditions of four main regions in the province: the Waldviertel, the Weinviertel, the Alpen and the Alpenvorland (alpine foreland). The Waldviertel describes the area northwest of the Danube mainly in the Bohemian Massif (Fig. 4.1 and Fig. 4.3). The Weinviertel is located east of the Waldviertel, also north of the Danube and is outlined by the rivers Thaya, March and Danube. South of the Danube the alpine foreland (Alpenvorland) and the Alpen (the alps) are located, characterized by a more mountainous topography and higher elevations.

The mean monthly temperatures are rather similar between all these regions, with a maximum difference of 2°C in July (Fig. 4.4). The Weinviertel is the warmest region and the Alpen are the coldest region of Lower Austria (Fig. 4.4; Vogl 2008). Unlike, the precipitations rates show large differences (Fig. 4.4). The largest amount of precipitation falls in the alps, while the lowest amount of precipitation was recorded for the Weinviertel. Generally, the graph shows a clear peak of precipitation and temperature in July and the summer months June and August (Vogl 2008). The most of the landslides occurrence (shallow and rotational slides) have also been reported within these months (Schwenk 1992).

June and July have the most days with thunderstorms, with around five to six days (Zentralanstalt für Meteorologie und Geodynamik (ZAMG) 2014). The Alpenvorland and the Weinviertel both typically have more than five days with thunderstorms in June and July (ZAMG 2014). The longest duration of a snow cover with more than 1cm was recorded for the Waldviertel (station Zwettl, 73.3 days; ZAMG, 2014). However, the largest thickness of snow has been documented for the Alpen (station Reichenau/Rax, 70cm; station Waidhofen/Ybbs, 84 cm; ZAMG 2014). Precipitation in form of snow is generally most likely from November to March (ZAMG 2014; Vogl, 2008).

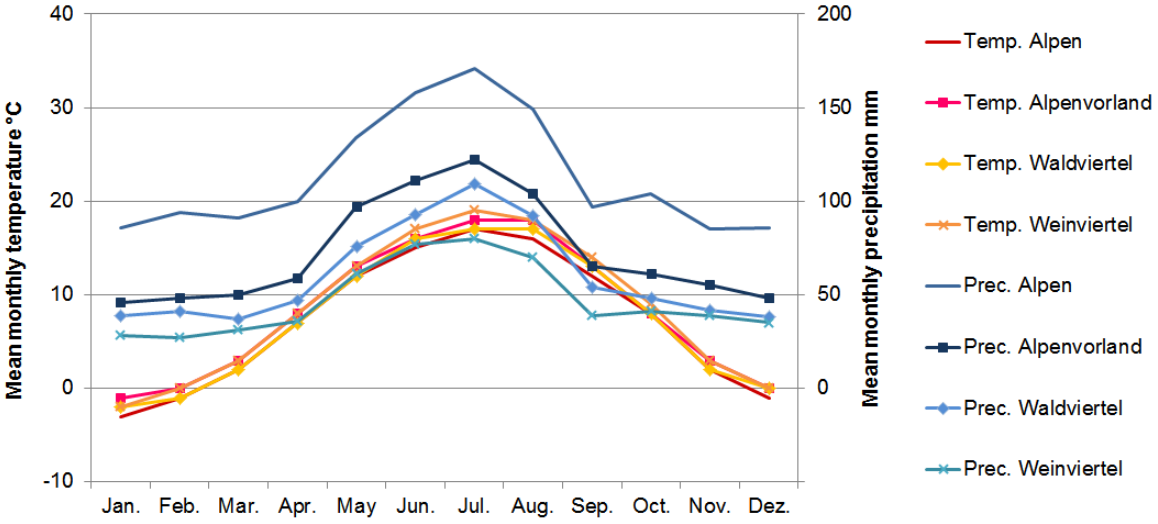

Figure 4.4 Mean monthly precipitation (Prec.) and mean monthly temperature (Temp.) for four selected areas in Lower Austria. Source: Vogl, 2008

In addition to climate, land use gives a diverse picture over the Lower Austria and adds to the heterogeneity of the province. In 2008, 39.2% of the area of Lower Austria was covered in forest and about half of the province was used as agricultural land. Overall, 58.8% of the area has been assigned as permanent settlement area (Vogl 2008). Land use is generally distributed unevenly across the province. The relatively steeper slopes in the south in the Alpen are predominantly forested (with coniferous and deciduous trees) while the areas more north close to the Danube (Alpenvorland) and north northeast of that in the Weinviertel are mainly used as agricultural land growing crops and wine (Eder et al. 2011).

Only little spatially traceable information on land use or land cover changes in Lower Austria is available. Land use or land cover changes are documented in some areas since the medieval but are still observed throughout the province. Studies in Lower Austria (the municipality of Ybbsitz and in the Vienna Woods) have reported past land cover changes of different extent (Fritz 2005; Johann 2005; Lettner and Wrbka 2011). These are very different in the West of the province (Ybbsitz) from the East of the province (Vienna Woods). In the West in Ybbsitz arable fields were

mainly converted to meadows and pasture and an increase in forest during 1822 to 2006 was observed (Lettner and Wrbka 2011). Furthermore, from late mediaeval times to the mid- 19th century the influence of the ironware industry had widespread consequences for the land use development in this area in form of deforestation of large areas (Lettner and Wrbka 2011).

In the Vienna Woods deforestation was also an issue. The forests were cleared due to the need of fire wood in the city of Vienna (Johann 2005) and to provide more land for the expansion of settlements (Fritz 2005). However, in the 20th century the value of the forest for the environment and recreation was acknowledged. Therefore, further deforestation was tamed to preserve the forest. In recent years still the expansion of settlement areas is of high importance. Nowadays, the main observed land cover change in the Vienna Woods is from meadow to settlement area as the vicinity to Vienna attracted many new inhabitants (Fritz 2005). Unfortunately this relatively detailed information on land use or land cover change is only scarcely available throughout the province.

4.2 Geology, geomorphology and soils

The variation of material and topographic characteristics across Lower Austria is strongly related to the diverse lithology (Fig. 4.1; Petschko et al. 2012). As shown on a lithological map compiled on a scale of 1:200,000 the lithological units and therewith the predominant material types vary greatly from north to south (Fig. 4.1; Schnabel 2002). 20 different lithological units can be distinguished showing different geotechnical characteristics as indicated by the different predominant material type (Tab. 4.1). More detailed data on the geotechnical characteristics of the study area are not available abundantly.

The Bohemian Massif in the north is characterized by Paragneiss, Mica-schist, Phyllite, Orthogneiss, Gföhl Gneiss, Granulite and Granite (Tab. 4.1). Around the Bohemian Massif, Loess and Loam can be found which is mainly comprised of sand, loam, loess-loam and drifting sand. The Molasse Zone south of the Bohemian Massif is unique because of its high content of marl, sand, gravel and silt while in the alluvial deposits marl and slit are usually not found. A special type of the Molasse Zone is the Schlier Zone which has high amounts of fine grained sandy-silty marl and a rather low slope angle with about 5°-10° (Schweigl and Hervás 2009). Through the center of Lower Austria a comparably thin band of the Rheno-danubian Flysch Zone accompanied by the Klippen Zone stretches from west to east briefly past Vienna (Fig. 4.1). The Flysch Zone is characterized by a large content of interbedded sandstone, marlstone and mudstone. The Klippen Zone is built of red to green shales and marls of the Cretaceous (Wessely 2006).

Table 4.1 Lithological units of Lower Austria: landslides and topography (Source: Petschko et al. 2014c)

Code	*Merged units*	*Name*	*Material*[+]	*Area (km²)*	*No. of slides*	*Landslide density (No./km²)*	*Median slope angle (°)*
1	0124	Anthropogenic deposits		2.93	0	0	3.1
2	02297	Alluvial deposits	Gravel, sand	3739.17	194	0.05	0.9
10	10	Loess,Loam	Sand, loam, loess-loam, drifting sand	2849.22	329	0.12	2.8
24	0124	Quaternary fluvial terrace	Gravel, sand, loess loam	747.79	222	0.30	2.2
35	35	Debris, till	Debris, till, scree material, rock avalanche material	217.19	177	0.81	16.6
37	3786	Bohemian Massif with sedimentary cover	Sandstone, claystone, conglomerate	30.95	0	0	12.2
39	39	Molasse Zone	Marl, sand, gravel, silt	1462.46	428	0.29	4.7
58	58	Molasse, Schlier	Fine sandy-silty marl in the circum-Alpine Tertiary basins	117.43	501	4.27	4.8
86	3786	Waschberg Zone	Marl, sand, limestone, clay	123.50	52	0.42	5.8
104	104	Intramontane Basins	Sand, gravel, breccia, clay, marl	737.26	291	0.39	5.2
120	120	Mélange Zone, Klippen Zone	Dominantly penninic metasediments and phiolites as well as insignificant Austroalpine elements, Ybbsitzer and Grestener Klippen Zone	73.46	404	5.50	11.9
126	126	Rheno-danubian Flysch Zone	Interbedded sandstone, marlstone to mudstone, marl	1365.96	6281	4.60	12.6
179	179	Austroalpine Unit with limestone, marls and sandstone	Limestone, marl, shale, sandstone, gypsum, conglomerate	785.85	1636	2.08	20.2
191	191	Austroalpine Unit with dolostone	Dolostone, limestone	2148.57	1419	0.66	27.1

Code	Merged units	Name	Material[+]	Area (km²)	No. of slides	Landslide density (No./km²)	Median slope angle (°)
230	230	Permo-Mesozoic rocks (overlying the Austroalpine ingeous rocks)	Carbonate Rocks, siliciclastics, porphyry (mostly metamorphics)	116.43	88	0.76	19.5
239	239	Igneous rocks of the Austroalpine Unit	Orthogneiss, Paragneiss, Mica-schist, Phyllite	614.35	586	0.95	15.1
251	251259	Bohemian Massif, Fault Zone	Tectonic fault zone	11.81	0	0	7.0
259	251259	Bohemian Massif	Paragneiss, mica-schist, Phyllite, Orthogneiss, Gföhl Gneiss, Granulite	2398.93	227	0.09	6.1
276	276	Bohemian Massif, plutonic rock	Granite, plutonic rock	1606.85	52	0.03	6.5
297	02297	Lake, wetland	Limnic sediments, wetland	38.77	2	0.05	3.5

[+] sorted according to frequency of occurrence, after geological map

The Klippen zone is also the contact area of the Flysch with the Austroalpine Unit, which contains limestone, limestone with marls and dolostone further south. In the south of Lower Austria Permo-Mesozoic rocks (overlying the Austroalpine ingeous rocks) and igneous rocks of the Austroalpine Unit are dominant. These include carbonate rocks, siliciclastics, porphyry (mostly metamorphics), Orthogneiss, Paragneiss, Mica-schist and Phyllite (Tab. 4.1). Each of these groups of material types inhibits specific characteristics regarding weathering, soil formation and soil depths (further details can be found in Wessely 2006). These have a large influence on the general susceptibility of these units to landslides.

Furthermore, a number of nappe boundaries and tectonic lines are present in the study area (Fig. C.7 and Fig. C.13 in the annex). Along tectonic lines the soil formation might be faster which leads to the presence of a larger soil thickness favorable for landslides (Schwenk 1992). Around fault lines the material might be strongly tectonically influenced, reworked and mechanically fragmented leading to a lower shear strength (Crozier 1986; Petschko et al. 2014c).

Nappe boundaries have been reported in the past as important additional preparatory factor for the occurrence of landslides in Lower Austria. It was found, that earth and debris slides occur with higher density close to nappe boundaries as these indicate a distinct difference in the material and permeability (Schnabel, 1985). The most prominent example is the nappe boundary of the Austroalpine Unit with limestone overlaying the Rheno-danubian Flysch Zone. Many landslides have been reported at this boundary due to the higher water permeability of the Austroalpine limestone lying on top of denser sandstones and marlstones of the Flysch Zone with comparably low water permeability (Schnabel 1985). This can result in increased soil water availability at the boundary zone and the development of boundary springs (Schnabel 1985).

The geomorphology of the province is mainly influenced by the presence of the Alps, the alpine foreland, the Danube, the Bohemian Massif in the northwest and the Loess and Loam in the northeast and around the Danube. The rivers in the study area, with the Danube leading the way, are well known for regular minor to major flooding events (as recently occurred in June 2013 and May 2014) which also had an effect on landform formation in the pre river regulation era.

While the slopes of the undulating hills in the Flysch and Klippen Zone are well known for their susceptibility to landslides and landslides are the main geomorphic processes in these units, the other lithological units exhibit other main geomorphic processes. In the Bohemian Massif mainly different types of granite and gneiss weathering, such as spheroidal weathering, and their resulting forms are of geomorphic interest (Huber 1999; Steininger 1999). The Loess and Loam area shows loess specific landforms and is more prone to erosional processes. These processes formed sunken lanes or sinkholes which still characterize the landscape (Gottschling 2006; Wiesbauer and Mazzucco 1995). In the Austroalpine Unit with limestone and marls landslides, mainly rock fall and debris flows (Gottschling 2006; Schwenk

1992), karst phenomena and the location at the boarder of the Würm glaciation are of geomorphological interest (van Husen 1987; Ivy-Ochs et al. 2008).

As a simple proxy of the topographic characteristics and the morphology of the lithological units the median slope angle was calculated from the DTM. The alluvial deposits are the flattest areas in the study area with a median slope angle lower than 1° (Tab. 4.1). In contrast, the Austroalpine Unit with dolostone has the steepest slopes with a median slope angle of 27° (Tab. 4.1).

Apart from the lithology, the soil types also vary greatly within the study area. In a recent study 21 soil regions were identified within Lower Austria and presented on a map with a scale of 1:900,000 (Wenzel et al. 2013). These regions describe the assembly of different groups of soil types. In this study only the main different soil types are described for the four earlier introduced regions of Lower Austria.

In the Weinviertel, Chernozems are the predominant soil type. The Waldviertel mainly consists of Cambisols and Luvisols. It is typical here that there is higher clay content in the subsoil than the topsoil (IUSS Working Group WRB 2006; Wenzel et al. 2013). South of the Danube, the Alpenvorland is characterized by the presence of Stagnosols and Gleysols which indicate (periodically) high water availability and the formation of saturated zones in the soil (IUSS Working Group WRB 2006). Even further south, in the Austroalpine Unit in the Alps, Rendzic Leptosols and Regosols may be found (Wenzel et al. 2013). In the valleys Fluvisols are abundant (Wenzel et al., 2013).

These soil groups show differences regarding the void space, clay content and permeability on which data was compiled for Lower Austria in 2011 (Fig. C.10, C.11, C.15, and C.16 in the annex; Eder et al. 2011).

4.3 Landslides

With the lithology also the predominant landslide types found within the study area change. This large range of landslide types includes rock falls, earth falls, earth slides, debris slides, earth flows and debris flows. While earth and debris slides can be found all over the province, rock fall and debris flows occur typically in the southern region within the Austroalpine Unit. As only earth and debris slides are within the scope of this study some more details on reported earth and debris slides will be given in this section.

The Geological Survey of Lower Austria collects reports on damaging landslide events (rock falls, debris flows, and earth and debris slides) since the late 1950ies. These reports include a description of the location of the event, the size, extent, possible triggers of the landslide and the caused damage (Gottschling 2006; Schwenk 1992). This archive called “Building Ground Register” was maintained to have information on previous events and on the process history and therefore on the

eligibility of parcels of land for settlement development (Schwenk 1992). Nowadays this archive is available digitally in form of a geodatabase with points set at the location of each reported event and respective reports in PDF format (Schweigl and Hervás 2009).

The incompleteness of this landslide inventory is beyond question as it is dependent on the reporting of a landslide event. Since 1965 the number of reported landslide events increased significantly (Schwenk 1992). In this year a new law on the Natural Disaster Fund was introduced in Austria which included the possibility to apply for funding from the Natural Disaster Fund for costs of necessary repair work after a landslide event (Schwenk 1992). To be able to receive the funding, the Geological Survey of Lower Austria has to survey the reported landslides and to decide whether it was a natural disaster (Schwenk 1992). However, not all occurrences are reported, as small landslides might have been levelled by the farmer without asking for financial aid (Schwenk 1992). By the end of 2009 around 1800 landslides were documented in this archive (Petschko et al. 2013).

Earth and debris slides mainly occur in lithological units containing a high amount of clay minerals and their weathering products (Gottschling 2006). These rocks include clay marl, marl, clayey sandstone, clay schist, phyllit, mica schist and gneiss (Gottschling 2006). The distribution of the landslides over the different lithological units of the study area shows a high proportion of slides that occurred in the Flysch and Klippen Zone (Fig. 4.5). Comparing this to the total area of the lithological units, a high slide density can be observed here (Schwenk 1992). In the Bohemian Massif by far the fewest slides are reported in the Building Ground Register (Fig. 4.5). The high number of landslides in the Flysch and Klippen Zone, and in the Austroalpine Unit and the Molasse Zone is related to the occurrence of large amounts of clays and marls in these units (Schwenk 1992).

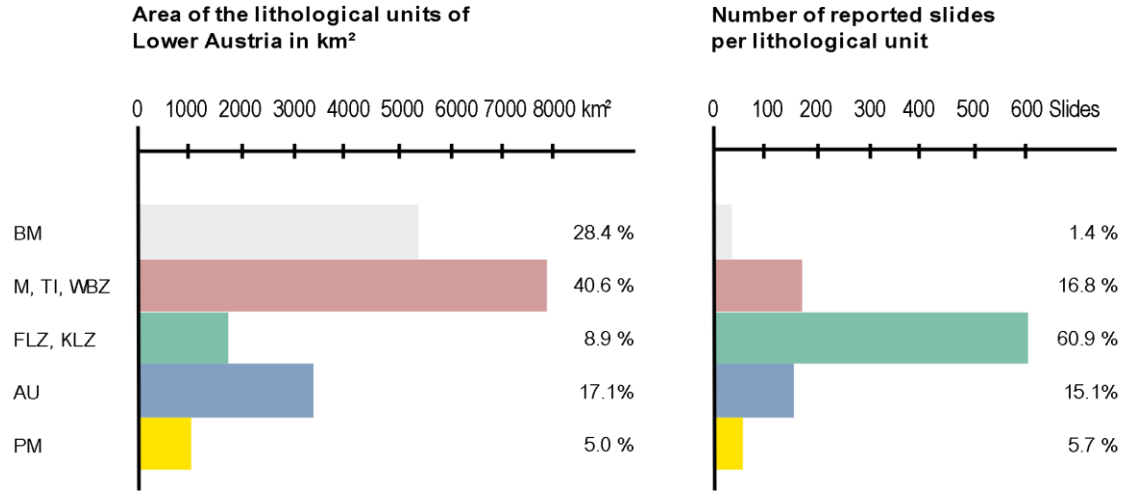

Figure 4.5 Area of the lithological units of Lower Austria in km² and number of reported slides per lithological unit as reported in the Building Ground Register of Lower Austria. BM = Bohemian Massif, M = Molasse Zone, TI = intramontane Basins, WBZ = Waschbergzone, FLZ = Flysch Zone, KLZ = Klippen Zone, AU = Austroalpine Unit, PM = Permo-Mesozoic rocks (overlying the Austroalpine ingeous rocks); Source: adapted from Schwenk 1992.

Additional to the different observed landslide density, also the characteristics of the sliding process and morphology is different between the lithological units (Fig. 4.6). While in the Molasse Zone landslides already occur at a slope angle of 5° - 10°, in the Flysch Zone the slope angle can be much steeper (15°-25°; Schweigl and Hervás 2009). Furthermore, the earth and debris slides show different characteristics in terms of size and depth. The largest slides were reported in the Molasse Zone and the Permo-Mesozoic rocks (Schwenk 1992). In general, 35% of the reported slides were smaller than 500m² and 40 % are larger than 500m² and smaller than 3,000m². The slide depth was mainly between one and three meters (Schwenk 1992).

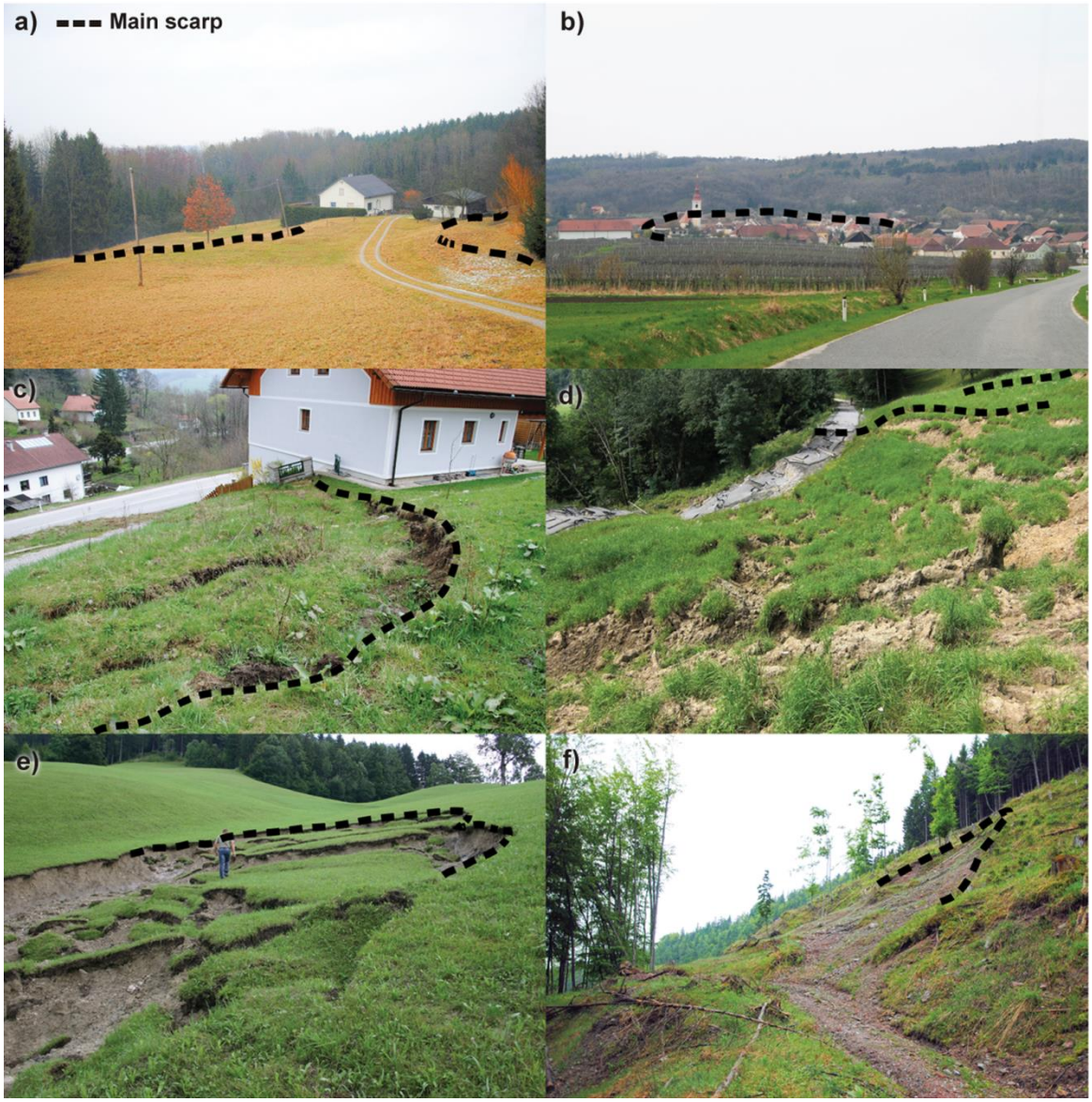

Figure 4.6 Typical earth- and debris slides of some lithological units (a) slide in Molasse Zone at Strengberg, (b) the village "Waitzendorf" located on a slide in Molasse with Schlier, (c) translational slide in the Rheno-danubian Flysch Zone at Brand, (d) rotational slide/flow in the Rheno-danubian Flysch Zone at Stössing, (e) slide in Austroalpine Unit (Limestone, Marls) at Dippelreith, (f) slide in Austroalpine Unit (with Dolostone) at Kleinzell. Pictures taken by: (a), (b), (c), (f) Petschko (2010, 2011, 2012); (d) Bertsch (2009); (e) BGR (2006). Source: Petschko et al., 2014c

The main trigger for landslides in Lower Austria is a high amount of wetness in the upper soil. This may mainly be induced by heavy rainfall or storm events (in over 90% of the reported events), such as occurred in Spring and Summer 1965/66, July 1975, June 2009 and May 2014, or during exceptionally warm thaw in spring (Schwenk, 1992; Abteilung Feuerwehr und Zivilschutz, Amt der NÖ Landesregierung, 2010; BMLFUW, 2010; noe.ORF.at, 2014). Furthermore, in about 30% of the slide events, human activities are stated as preparatory factor for the slide (Schwenk 1992, refer to section 4.4). While earthquakes occur within the entire province (Eisinger et al. 1992; Lenhardt 2006), their importance or contribution as predisposing or triggering factor of landslides has not been analyzed yet.

Although the median of the slides are not very big and do not travel far they caused considerable economic losses throughout the province (Schwenk 1992). Most of the reported slides occurred in pastures and meadows (85%), while 13% occurred in forest and only few slides occurred on agricultural land. Once the slides reach a certain size and depth, even farmland (pasture, agricultural land) cannot be used anymore without remediation measures (Fig 4.7). Furthermore, about 50% of the slides reportedly affected roads or forestry paths either by the deposition of material on the road or by subsidence of the ground and the road (Fig. 4.7; Schwenk 1992).

Moreover, in many cases houses were affected by the slides forming crevasses in the walls and floors which led to the evacuation of the houses or farms and in more than 30 cases to the resettlement of the families (Fig. 4.7; Schwenk 1992).

4.4 Human impact on landslides

Reportedly, earth and debris slides in Lower Austria have not only been triggered in natural conditions, they have also been caused by human activities in Lower Austria (Schwenk 1992, Gottschling 2006). Every year many landslides are triggered by road construction, cut or fill of material at the construction of houses, changes of the surface and subsurface slope hydrology by the construction of roads or drainages, and logging activities (Gottschling 2006). The vibration caused by the impact of bombs during the Second World War might have also been a trigger for earth and debris slides in the past as observed in the field, although no written reports exist.

Amongst these the most frequently reported anthropogenic influence on earth and debris slides in Lower Austria is the construction of forestry roads and paths (Schwenk 1992). This influence might trigger a landslide immediately after the undercutting or filling of the slope, or might change the slope hydrology and concentrate runoff at a new place slowly preparing the slope for instability (Borga et al. 2005; Schwenk 1992).

Similarly, the presence of sunken lanes, which are rather common in the Loess and Loam lithology and to a lesser extent in the Flysch Zone, may contribute to triggering landslides by changing the path of runoff (Wiesbauer and Mazzucco 1995).

Furthermore, drainage pipes commonly installed in pasture or farmland can contribute to slope instability. The drainage pipes can lead to the transport of water to an unfavorable location resulting in triggering or reactivating a slide (refer to section 6.4 and 7.4 for more details).

Figure 4.7 Examples of damage reported in the Building Ground Register of the Geological Survey of Lower Austria. a) Slide on farmland (pasture) in Purgstall triggered by thaw in 1978; b) Slide in the district Wien Umgebung on a land fill; c) slide in a forest in Loich occurred in 1989; d) Cracks in a house caused by a slide in 1968 in the district Melk; e) Slide in Waidhofen/Ybbs damaging a road in 1992. Picture source: Reports of the Building Ground Register.

A less reported, but probable, human influence on the predisposition of landslides may be the modification of local topography by levelling of agricultural fields for easier machine handling (Schwenk 1992). Starting from 1890 very small parcels of land, as they were common at that time, were merged into bigger fields to maximize the yield (Österreichisches Institut für Wirtschaftsforschung 1955). During this process in Austria called "Kommassierung" (i.e. land merging), many fields were levelled and the topography was changed substantially (Kainz 1979; Kraus 1997; Müllner 1990). The occurrence of landslides is rarely associated with this practice, as the landslide may occur many years later. However, during fieldwork of a slide in Kleinsierndorf, a local farmer reported about the "Kommassierung" process that occurred in the field where the landslide occurred (Fig. 4.8). He pointed out similarities between the previous boundaries of the fields and the main scarp of the earth slide. However, further research needs to be done to investigate this relationship.

Figure 4.8 Earth slide at Kleinsierndorf (Weinviertel) at a field which the topography was modified during the "Kommasierung" in the past (date unknown), triggered August 2010. Pictures taken by Petschko (2010)

4.5 Spatial planning and landslide hazard mitigation strategies

Austria and Lower Austria have developed several strategies for hazard mitigation. They are designed to be applied before and after the occurrence of natural hazards. At federal and provincial level there are three important laws aimed at avoiding natural hazards and providing financial aid for remediation measures.

First, the provincial spatial planning law of Lower Austria is of high importance for the avoidance of fatalities and economic losses (Landtag von Niederösterreich 1976; Pomaroli et al. 2011). It was first introduced in 1968 and later refined in 1976, which is the current version focused on establishing a high level of protection against natural hazards (Pomaroli et al. 2011). It generally defines municipal spatial planning and addresses the allowed area zoning types (e.g. housing, industry, shops,

grassland) within the area zoning plan prepared by each municipality. This area zoning plan is aimed to show development plans for the municipality for about the next 30 years.

Additionally, it addresses allowed zoning in areas where natural hazards are known. Concerning natural hazards, this spatial planning law is one of the most restrictive spatial planning laws in Austria, as it can prohibit settlement development in areas where the exposure to natural hazards is known (Gottschling 2002; Pomaroli et al. 2011).

"Areas which are due to their natural conditions not suitable for development can not be zoned as building land. These include amongst others areas which (1) are located within flooding areas, (2) have a low load capacity of the ground and (3) are prone to slides, rock falls, subsidence, torrential hazards or avalanches" (Landtag von Niederösterreich 1976; Pomaroli et al. 2011).

In these cases, the municipal council can decide on a prohibition on building on undeveloped land even if it was assigned as building land (Landtag von Niederösterreich 1976). However, in practice the spatial planning law is not interpreted in its strictest sense as the basic information on the location of potential natural hazards was unknown at the time of the introduction of the spatial planning law (Pomaroli et al. 2011). The current practice rather evaluates where actual landslides, flooding events or avalanches are known and not where a potential susceptibility to these hazards is present (Pomaroli et al. 2011).

Secondly, the preparation of hazard zonation plans aiding the identification of natural hazards was legally introduced in Austria in 1975 based on the Forest Act of 1975 (Rudolf-Miklau 2007). This map is prepared by a decentralized agency called Austrian Service for Torrent and Avalanche Control (Rudolf-Miklau 2007). Further tasks of this agency are the design and installation of active prevention measures and watershed management (Rudolf-Miklau 2007). The hazard zonation plans are an important source for identifying hazardous areas in settlements or close by. They are prepared nationwide for areas in and around settlements to identify potential landslide, avalanche or torrential process hazards on a scale of 1:2000 (Rudolf-Miklau 2007).

The hazard zonation plans distinguish between red and yellow hazard zones, blue reservation areas and purple and brown reference areas (Rudolf-Miklau 2007). Red hazard zones are assigned for areas where the threat of the hazard is very high and the costs of the construction of preventative measures are too high (Rudolf-Miklau 2007). Therefore, building is not recommended in red hazard zones (Rudolf-Miklau 2007). Yellow hazard zones show areas where the permanent use for living or transportation may be affected regularly by the hazard. In these zones, building of houses or roads might be allowed if special construction types to mitigate the hazards are considered (Rudolf-Miklau 2007). Blue reservation areas and purple reference areas are mainly concerned with the construction of mitigation or flood retention measures (Rudolf-Miklau 2007).

While mainly torrential processes (e.g. debris flows) and avalanches are analyzed and mapped assigning red and yellow hazard zones, landslides of the type earth or debris slide or rock falls are marked as brown reference area (Rudolf-Miklau 2007). Brown reference areas indicate the presence of rock fall or earth or debris slides without stating on the hazard (magnitude and frequency) itself (Rudolf-Miklau 2007). However, hazards of the brown reference areas are not assessed with the same detail as hazards within the red and yellow hazard zones (Pomaroli et al. 2011). Building in areas affected by slides is not restricted in the same way as in areas affected by debris flows or avalanches, as spatially abundant information on the earth and debris slide susceptibility is missing (Pomaroli et al. 2011).

As soon as the hazard zonation plan is integrated in the municipal zonation plan it is legally binding and has to be taken into account for development planning done by the municipality. With the web-based GIS platform "eHORA" all the information and maps provided for hazard zonation for floods, torrential processes and landslides is available publicly for entire Austria (Fig. 4.9; Federal Ministry of Agriculture, Forestry, Environment and Water Management 2014).

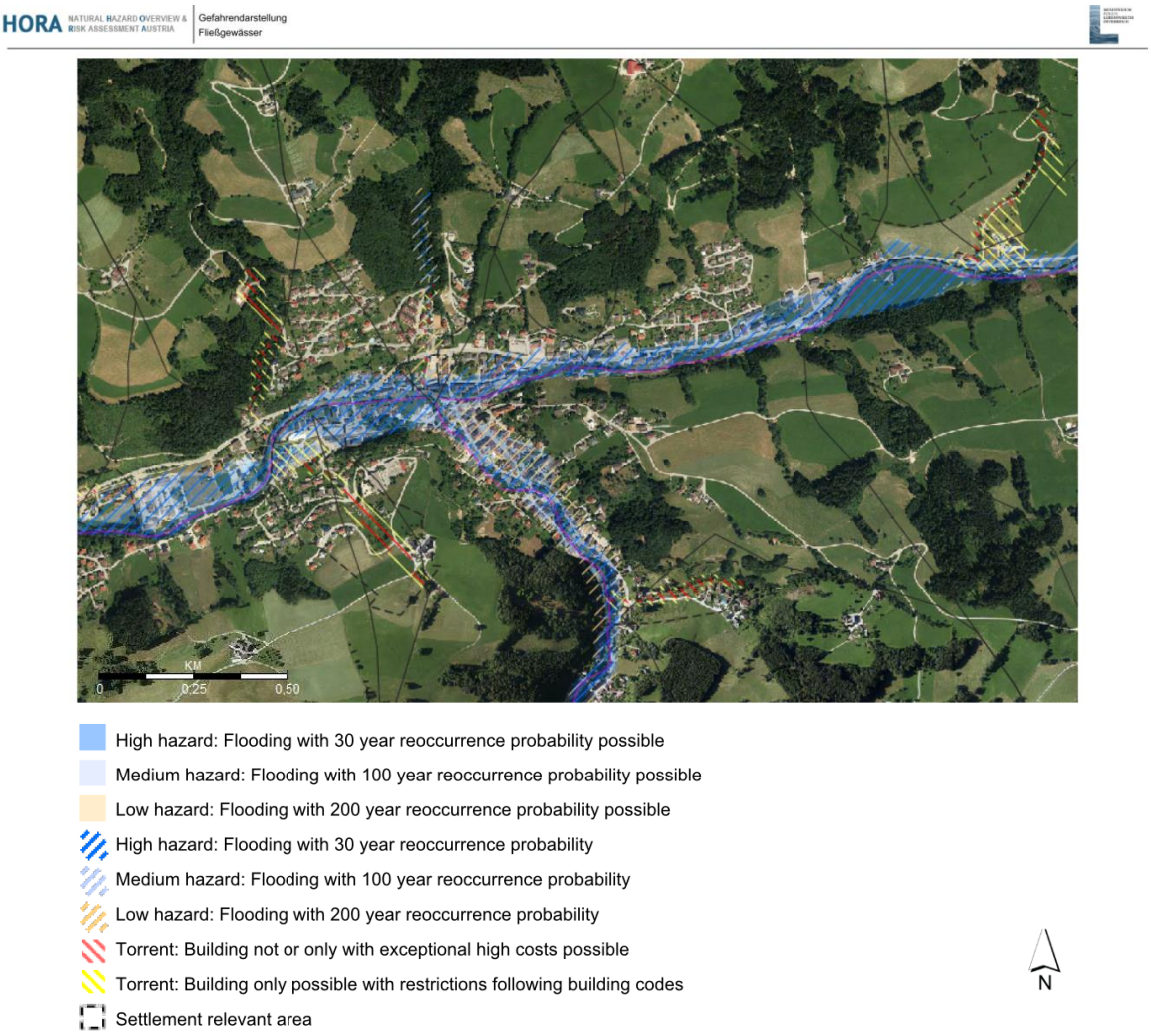

Figure 4.9 Hazard zonation plan extract from eHORA for Ybbsitz (Waidhofen/Ybbs). Source: Hora, 2014

Thirdly, a law meant to provide financial aid for affected people by installing the Natural Disaster Fund in 1966 is also of importance. This fund was introduced in 1966 after severe damages due to natural hazards in Austria (Gottschling 2002). The current version of the Natural Disaster Fund law (BGBl. 201/1996) defines a natural disaster and the examining authorities in case of losses due to a natural hazard event (Federal Ministry of Finance 2014a). This tax financed fund was established to cover costs for natural hazard prevention measures or costs for remediation measures after the occurrence of natural hazards (Federal Ministry of Finance 2014a). It affects not only the people but also the practice of the Geological Survey and the Austrian Service for Torrent and Avalanche Control. Three quarters of the funds of the Natural Disaster Fund are invested in preventative measures against natural hazards analyzed and realized by the Austrian Service for Torrent and Avalanche Control (Federal Ministry of Finance 2012). In 2013 approximately nine percent of the fund was attributed to investment in new equipment for local fire brigades. 18% was spent on remediation measures of private persons (4.5%), the nine provinces (3.5%), municipalities (9%) and the nation (1%) (Federal Ministry of Finance 2014b).

In cases of damage on private property, the provinces are the main authority in charge for assessing the amount of loss and the presence of a natural disaster. Furthermore, the distribution of the fund to the people is administrated by the province (Federal Ministry of Finance 2014b).

Application for this funding is completed through the municipal government, who contact the damage committee and an expert (e.g. Geological Survey of the province) for assessing the presence of a natural disaster (Gottschling 2002). A private person can apply for the funding once the remediation costs are estimated (Gottschling 2002). Private persons can expect financial aid to cover 20% - 30%, or in very severe cases up to 80% of the remediation costs, which is provided by the province (Federal Ministry of Finance 2012). Municipalities or the province itself may receive a refund of up to 50% of the costs for remediation works needed to repair buildings or roads (Federal Ministry of Finance 2012).

5. Materials

5.1 Available data and their characteristics

The mapping, analysis and modelling of landslides in Lower Austria was based on the availability of a high resolution LiDAR (Light Detection and Range) digital elevation model (DTM) with a spatial resolution of 1m x 1m. This LiDAR DTM was acquired within entire Lower Austria between 2006 and 2009. Four different LiDAR sensors were applied, as the flight campaigns were operated by different experts and in different years: Riegl LMS-Q560 (Riegl 2010), ALTM 3100 (Optech 2008a), ALTM Gemini (Optech 2008b) and Leica ALS50 (Amt der NÖ Landesregierung 2013; Leica Geosystems 2003; Petschko et al. 2014a). While the density of the point cloud is unknown it can be generally stated that the resulting DTM is of high quality with a low amount of distortions or data gaps where resampling was applied by the provincial government of Lower Austria.

In addition to the high resolution DTM, orthophotos, as well as data on land cover, geology and soil also supported the research of landslides. Two sets of orthophotos were used for exploring landslides in test districts (Petschko et al. 2014a). The orthophotos had a spatial resolution of 25cm and 12.5cm and were taken between 2000-2004 and 2007-2008 (Amt der NÖ Landesregierung 2013). Complete coverage of the entire study was available with orthophotos that had a 25cm spatial resolution (Amt der NÖ Landesregierung 2013).

Information on the land cover of the province was provided by a supervised land cover classification of satellite imagery (Bell et al. 2012). A composite of satellite images from Aster, Landsat TM5, Landsat TM7 and ALOS/AVNIR of the years 2007 and 2008 was used to cover the entire province (Bell et al. 2012). The classification was performed on a spatial resolution of 15m (Bell et al. 2014; Bell et al. 2012).

While geological maps are available with a scale of 1:50,000 in selected areas in Lower Austria, a geological map with a scale of 1:200,000 was applied within this study (Petschko et al. 2014c; Schnabel 2002). Although this is a rather small scale given the aimed map output scale of 1:25,000, it was the only dataset available covering the entire study area. Furthermore, for the applied study design (refer to section 6.2.3) the available scale was not of disadvantage.

Within any landslide susceptibility model information on the soil characteristics is on the wish list of input variables as the soil properties have an effect on the infiltration capacity and water storage in the soil (refer to section 2.1.3; Crozier 1986). In this study soil data on the permeability (mm d^{-1}; average value of the top 20 cm, and minimum value within 100 cm profiles) and void space (%; average value of the top 20 cm, and average of 100 cm profiles) was available with a spatial

resolution of 50m (Eder et al. 2011; Petschko et al. 2014c). These data might be considered as a proxy for the infiltration capacity (Petschko et al. 2014c).

As learned from the description of the study area tectonics and the presence of nappe boundaries are important for soil development and landslide initiation in the study area. Data on fault lines and nappe boundaries was available as vector data derived from geological maps in the scale of 1:50,000 (Kurz 2012).

5.2 Landslide inventories

Data on the Building Ground Register was provided by the Geological Survey of Lower Austria. All registered landslides and their respective reports were available starting from 1953 to end of 2009. In the past the location of the landslides was identified as a point on a map of the scale 1:50,000 (Fig. 5.1). However, with the availability of orthophotos a more precise positioning of the point indicating a landslide became possible. In total, information on 1878 landslides was available for this study. For more details on this inventory please refer to section 4.3.

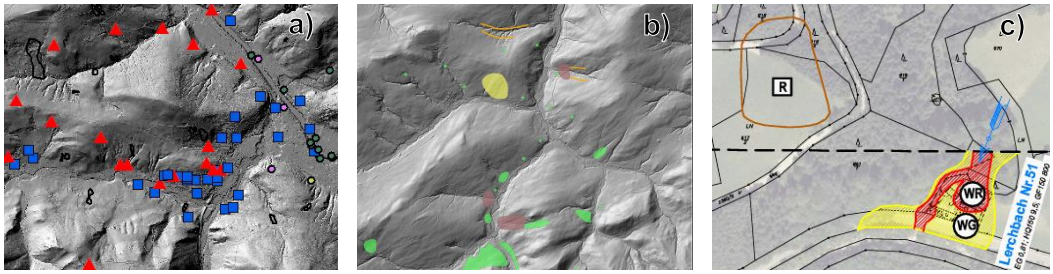

Figure 5.1 Existing landslide inventories in Lower Austria. a) Points of the Building Ground Register (red triangles); b) Polygons, lines or points of the GEORIOS database of the Geological Survey of Austria; c) Landslide mapped in the hazard zonation plan of the Austrian Service for Torrent and Avalanche control.

Additionally, vector data originating from a database called "GEORIOS – GEORIsiken OeSterreich" compiled by the Geological Survey of Austria was available. It includes polygons, lines or points of landslides found in old manuscript geological maps, archives, field work, project reports, surveys, literature, theses and the geological map in the scale of 1:50,000 (Fig. 5.1; Kociu et al. 2007). The information available on very different scales (1:10,000 – 1:200,000) was compiled and digitized on a scale of 1:50,000 in vector format (Kociu et al, 2007). No information on landslide age or the circumstances of the landslide initiation was available. This inventory is rather incoherent given the multitude and dependency of different sources. Accordingly, in some areas in Lower Austria no information on landslides is given (Kociu 2013). In total the GEORIOS database for Lower Austria contains 3257 polygons, lines or points on landslides (at 17.11.2009).

Moreover, the Austrian Service for Torrent and Avalanche Control collects information on landslides. In the hazard zonation plans mainly debris flows and torrential processes are focused on. However, some information on earth and debris slides is included in the hazard zonation plans if an earth or debris slide occurred during the time of the creation of the map or if clear indicators for slide activity were discernible in the field (Fig. 5.1). These earth or debris slides are indicated within the hazard zonation plan on a scale of 1:2000. Nevertheless, the hazard zonation plans are restricted to areas in the vicinity of settlements (Rudolf-Miklau 2007). Therefore, no information on earth and debris slides was available outside settlement areas.

The Map of Quaternary Sediments (Untersweg et al. 2008; 1:50,000) was used as another source of information on the location of landslides. It includes polygons of landslides mapped on a scale of 1:50,000. However, also within this map, not all of Lower Austria was mapped by the same person, which resulted in a different density of information on landslides within this data source. The Map of Quaternary Sediments is the result of a project on raw materials aiming at a nation-wide inventory of sand and gravel deposits (Untersweg et al. 2008). Therefore, it is obvious that mapping landslides or their deposits was not the primary purpose of this map.

5.3 New data generated during the dissertation

A list of new data generated during the dissertation is given in the following, to provide a clear distinction of which data was available before, and which data is a result of the analysis of this thesis.

As parts of the thesis were addressing the test study area (covering the districts Amstetten, Baden and Waidhofen/Ybbs) and other parts were analyzed for the entire study area of 15,835km² the data generated is indicated respectively in Table 5.1. For example landslide polygons were only mapped for the test study area, while landslide points were mapped for the entire study area. Furthermore, the landslide susceptibility and uncertainty analysis was mainly done for the entire study area (which is covering the test districts and the rest of Lower Austria).

The mapped landslide points were used as response variable for the statistical modelling. Several derivatives were generated from the LiDAR DTM within SAGA GIS using the RSAGA package within R (Brenning 2011) to aid as explanatory variables and as proxies for geomorphic and hydrological processes: slope angle, slope aspect (transformed to represent the east versus west and north versus south using the sine and cosine of the aspect), catchment area, catchment height, convergence index (10m, 50m), curvature and topographic wetness index (Tab. 5.1; Petschko et al. 2014c). The relevance of most of these derivatives was reported on before by Van Westen et al. (2008). The large importance of slope angle for slope stability was described and discussed in detail in slope stability literature (e.g.

Crozier 1986). The inclusion of slope aspect may reflect both, a proxy for bedding orientation as well as the differences in intensity of solar radiation (Van Westen et al. 2008). The differences in solar radiation result in variations of local temperature, evaporation and therefore soil moisture (Van Westen et al. 2008).

Table 5.1 Overview on data generated within the thesis for the different study areas: (1) the test study area including the districts Amstetten, Baden and Waidhofen/Ybbs and (2) the study area mainly covering Lower Austria (15,835km²)

Data	*Amstetten, Baden and Waidhofen / Ybbs*	*Entire study area (15,835km²)*
Landslide polygons including differentiation of landslide types, relative age and mapping certainty	Yes	No
Landslide points in main scarp	Yes	Yes (but only for AM, BN, WY mapped by the author)
Derived main scarps of landslides	Yes	No
DTM derivatives: hillhade (315°, 135° and 45° azimuth angle), contour lines (4m spacing), slope angle (1m and 10m grid cell);	Yes	No
Derivatives with 10m grid cell size: east versus west, north versus south, catchment area, catchment height, convergence index (10m, 50m), curvature, topographic wetness index	Not only for this area	Yes
Euclidian distance to nappe boundaries and Euclidian distance to tectonic lines	Not only for this area	Yes
Landslide susceptibility map	Not only for this area	Yes
Variable frequency	Not only for this area	Yes
Thematic consistency index	Not only for this area	Yes
Transferability index	Not only for this area	Yes
Uncertainty index of susceptibility map	Not only for this area	Yes

The curvature variable was used to portray local variations in the morphology as it was calculated with a radius of three grid cells (Petschko et al. 2014c). On that scale local convex and concave surfaces are shown which can influence wetness conditions. Opposed to the curvature the convergence index was calculated once with a 10m radius and once with a 50m radius to portray the morphology on a smaller scale and to identify specific locations on a slope where landslides occurred in the past. Additionally, the catchment height variable can aid this identification of the position

of a landslide on a slope as it shows the distance from the ridge (Petschko et al. 2014c).

The topographic wetness index was reported as a proxy for the soil moisture and additionally also the ground water level (Beven and Kirkby 1979; Seibert et al. 2007). As more detailed information on the potential soil moisture was not available this variable was used as a proxy (Petschko et al. 2014c). Similarly, catchment area was calculated for the sub-catchments to derive the contributing area on a more local scale (Petschko et al. 2014c).

Furthermore, fault lines and nappe boundaries were available for this study. As reported earlier in the study area section, the proximity to fault lines and nappe boundaries was reported as an important preparatory factor for landslides in Lower Austria. Therefore, the Euclidean distance from the respective features was derived within a raster based approach (Petschko et al. 2014c).

All data necessary for the landslide susceptibility modelling was resampled to a spatial resolution of 10m x 10m (refer to figures in Annex C; Petschko et al. 2014c). Given the aimed map output scale of 1:25,000 a grid cell size of 25m (1/1000 of the scale factor; Calvello et al. 2013) might have been more appropriate. However, a resampling to 10m x 10m was done considering the detailed resolution and information on the topography provided by the LiDAR DTM and the coarse resolution of the soil data (50m x 50m; Petschko et al. 2014c). Given the coarse resolution of the soil data the decision on a better resolution might be troublesome. However, by deciding on an output spatial resolution of 10m x 10m it is possible to take advantage of the high resolution of the topographic data while avoiding wrong signals in the modelling from a higher resolution (e.g. 2m x 2m; Van Westen et al. 2008). Naturally, the performed resampling of the soil data is only an artificial improvement, which does not increase its data accuracy (Petschko et al. 2014c).

6. Methods – from landslide mapping to susceptibility modelling, performance assessment and visualization

The preparation of a landslide susceptibility map with a statistical approach and the assessment of its quality involve several steps: (1) Data preparation including the assembling or mapping of a landslide inventory and the identification of geomorphic relevant explanatory variables; (2) statistical modelling with determining the explanatory variables characterizing the landslide susceptibility in the study area best; (3) assessing the model performance and other facets of quality of the landslide susceptibility model (e.g. transferability or thematic consistency); (4) deriving the spatially varying prediction uncertainty; (5) transferring the model and the spatially varying prediction uncertainty to all grid cells within the study area; and (6) building the landslide susceptibility classes using interpretable and meaningful threshold values of the predicted probability and assigning colors to each class (Tab. 6.1). To assess these different steps several methods were applied within this study for different (test) study areas (Tab. 6.1). The interrelationships of different methods are indicated in Table 6.1 by cells overlapping two columns. This table emphasizes how the parts of the analysis are strongly interwoven, with implications on the final interpretation of the map and its uncertainties.

Different study areas within Lower Austria were used to establish a methodology for the entire province as indicated in Table 6.1. These study areas were the district Waidhofen/Ybbs, a catchment close to Wilhelmsburg, the test districts Amstetten, Baden and Waidhofen/Ybbs and the entire study area within Lower Austria (15,835km², Tab. 6.1). Some hypotheses (the first and fifth hypothesis) are addressed with multiple methods or steps of a susceptibility assessment as indicated in Table 6.1.

In the following sections a brief overview on the methods used within this study is given to introduce the main applied principles. The details on the methods used to assess each hypothesis are provided in full length within the publications (printed in the annex A.1 to A.8) as indicated for each method in Tab. 6.1.

Table 6.1 Overview on analysis steps and methods used within this study. Similarly to a flow chart the steps are listed chronologically from top to the bottom according to when it was done within this analysis. Overlapping cells within different steps (columns, e.g. landslide inventory and modelling) indicate an interrelationship of the methods used for assessing the respective hypothesis. In brackets the study area of the respective analysis is indicated: AMBNWY = Amstetten, Baden and Waidhofen/Ybbs; WY = Waidhofen/Ybbs; WB = Wilhelmsburg; NOE = entire study area. Furthermore, the respective hypothesis (H1 – H5) and the publication addressing this (A.1 – A.8, according to the list given in the annex) are given. LR = Logistic regression; GAM = Generalized additive models

<table>
<tr><th>Landslide inventory mapping (LiDAR DTM derivatives)</th><th>Statistical landslide susceptibility modelling</th><th>Assessment of the human impact</th><th>User optimized visualization</th></tr>
<tr><td></td><td></td><td>Literature research for possible human impacts on landslides documented in Lower Austria (NOE; H5)</td><td rowspan="3"></td></tr>
<tr><td rowspan="2">Mapping of landslides by visual interpretation of LiDAR DTM derivatives (AMBNWY; H1; A.1, A.2, A.4, A.7, A.8)

Comparison of the mapped inventory with existing inventories (WY; A.1)</td><td></td><td>Identifying possible human impact in the catchment of the landslide (AMBNWY, WB; H5; A.2)</td></tr>
<tr><td colspan="2">Estimating the relative age of landslides by visual interpretation of landslide morphology and vegetation cover as a basis for the selection of explanatory variables matching the characteristics of the landslides stored in the inventory used for the modelling (AMBNWY; H2; A.8)</td></tr>
<tr><td>Comparison of landslide mapping effectiveness using an effectiveness estimate (AMBNWY; H1; A.7)</td><td colspan="2">Tests on minimum requirements on landslide inventory for statistical modelling (H1) :
- Number of samples (GAM, NOE; A.6)
- Form of samples (one point within main scarp or landslide body; LR, AUROC; visual comparison; AMBNWY; A.4)</td></tr>
</table>

Landslide inventory completeness: Assessment of the **landslide persistence** using LiDAR DTM derivatives, orthophotos of different acquisition date and the Building Ground Register (WY; H5; A.2)

Facing the **heterogeneity** of the study area by a suited model design (AMBNWY, NOE; H2; A.3; A.6)

Analysis of the **quality** of the landslide susceptibility model and map (NOE; A.6):

- Model performance (AUROC)
- Model transferability (T)
- Thematic consistency (C)

→ ***k*-fold (spatial) cross-validation** (H3)

- Spatially varying prediction uncertainty

→ Estimation of **the confidence interval** limits of the predicted probability and analysis of the **overlaps** of susceptibility classes of the susceptibility maps (H4)

Identification of **number of classes (NOE; A.5)**

Classification of resulting landslide susceptibility maps using interpretable and meaningful **threshold values** of the predicted probability. (NOE; A.5)

Selection of colors allowing easy interpretation of the map indicating possibly affected areas. (NOE; A.5)

6.1 Landslide inventory mapping

The landslide inventory mapping was mainly performed on the basis of visual interpretation of LiDAR DTM derivatives (hillhade (315°, 135° and 45° azimuth angle), contour lines (4m spacing), slope angle (1m and 10m grid cell)) and orthophotos (Ardizzone et al. 2007; Schulz 2004; Fig. 6.1). Here the general approach used for mapping landslides is given. More details related to the mapping conducted for each research paper can be found in Annex A.1 (Petschko et al. 2010), Annex A.4 (Petschko et al. 2013), Annex A.7 (Petschko et al. 2014a) and Annex A.8 (Petschko et al. 2014b).

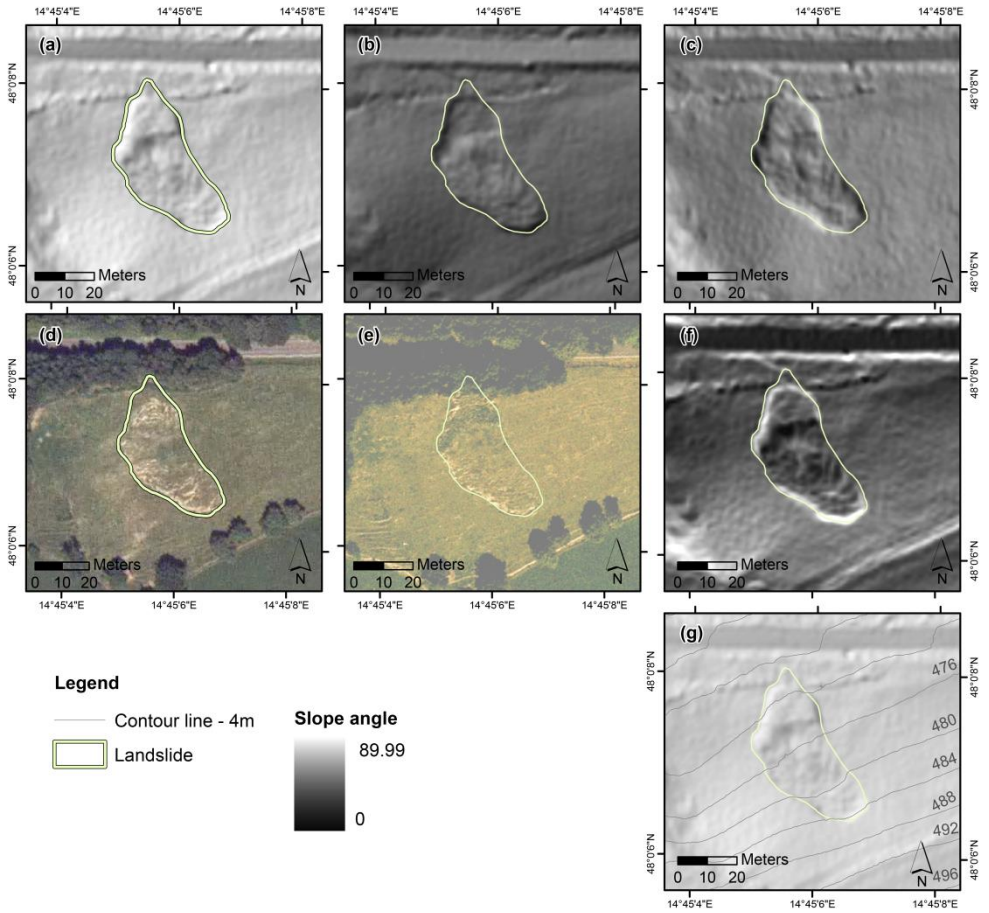

Figure 6.1 Materials used for the landslide inventory mapping: (a) LiDAR DTM hillshade map with 315° azimuth angle; (b) LiDAR DTM hillshade map with 135° azimuth angle; (c) LiDAR DTM hillshade map with 45° azimuth angle; (d) Orthophoto (25cm x 25cm) acquired between 2000-2004; (e) Orthophoto (12,5cm x 12,5cm) acquired between 2007-2008; (f) Slope angle map derivative from the LiDAR DTM; (g) 4m spaced contour lines derived from the LiDAR DTM. Source: DTM and orthophotos: Provincial Government of Lower Austria; Landslide mapping: own survey. Figure: Petschko et al. 2014a

During the visual interpretation of the LiDAR DTM derivatives, morphological features discernible after the occurrence of a landslide (Tab. 2.2; Rib and Liang 1978) were detected and outlined with a polygon and with a point in the main scarp of the

landslide. The hillshades of the different azimuth angle were used to avoid shades covering landslide features hindering the delineation of the landslide boundary (Schulz 2004). The contour lines were specifically helpful to identify concave and convex features defining the main scarp and the landslide toe. Furthermore, the slope map was used to interpret steep areas which also indicate scarps, ridges or the landslide toe (Ardizzone et al. 2007). While the morphology is directly visible from the LiDAR DTM derivatives, the orthophoto was used to avoid misinterpretation due to morphological convergence (Antonini et al. 2002).

Furthermore, for selected areas extensive field checks of the mapping were carried out. These field checks were prepared with print outs of orthophotos and of the LiDAR DTM derivatives superimposed with the delineated landslide polygon or point. In the field, the delineation of the landslide polygon and its assigned landslide type was checked looking for silent witnesses of previous and recent slide activity (e.g. drunken forest, cracks, scarps). This field work was very important for improving the accuracy of the mapping and for learning more about the processes and their morphology.

The polygons were mapped representatively within each lithological unit, to obtain a substantially complete landslide inventory. Despite that, the points were set in every landslide visible on the LiDAR DTM derivatives. Generally, only clearly discernible features showing both, the main scarp and the toe, with a size larger than 100m² were mapped (Petschko et al. 2014a).

While points were only set in landslides of the type earth or debris slide, several landslide types were mapped as polygons: earth and debris slides, earth flows, complex landslides and area with slides (Petschko et al. 2013). The landslide types were classified according to the classification based on Varnes (1984) and Cruden and Varnes (1996). Furthermore, the attributes of certainty of mapping regarding the delineation of the polygon and the assignment of the landslide type and the estimation of the relative age of the landslide (refer to section 6.1.1) were evaluated and added in the feature attribute table for each landslide polygon (Petschko et al. 2014a).

A visual comparison of the mapped polygons with the location of landslides from existing landslide inventories (e.g. BGR, GEORIOS) was done during the mapping to evaluate the need for mapping a new inventory from LiDAR data (Petschko et al. 2010). During this comparison overlaps of the mapped landslide with a landslide of an inventory were identified and stated in the feature attribute table.

6.1.1 Comparison of relative landslide age and current land cover

Within this study the potential to estimate the relative landslide age using LiDAR DTM derivatives and orthophotos was tested for the mapped landslide polygons. The aim of this analysis was to aid the selection of explanatory variables, as a successful

distinction between relative landslide ages might allow insights into characteristics of (very young) landslides at their occurrence.

The relative age estimation of the landslides was based on an approach proposed by McCalpin (1984), interpreting the freshness of the morphology and the vegetation cover of the landslides (Bell et al. 2012; Petschko et al. 2014b). It is assumed that the older the landslide becomes the less distinctive are the different features of a landslide (main and minor scarp, ridges, and toe) visible on any imagery (McCalpin 1984). The landslide is exposed to erosion and weathering processes which "wash out" the original distinct features. A drainage system evolves and usually (except in cases of agricultural land use) the vegetation regrows (Fig. 6.2; McCalpin 1984). Four different relative ages were distinguished: very young, young, old and very old. Fresh morphology and no vegetation at least within the main scarp characterized very young landslides. Very old landslides show a smooth morphology and a dense vegetation cover (e.g. forest; Petschko et al. 2014b).

A comparison with recent land cover data was done with a raster based approach within ArcGIS (9.3). The landslide polygons were used for masking the land cover data. The resulting data set gave the information on the land cover within the mapped landslides only. The percentage of pixel covered by the different land cover types was derived for each relative landslide age.

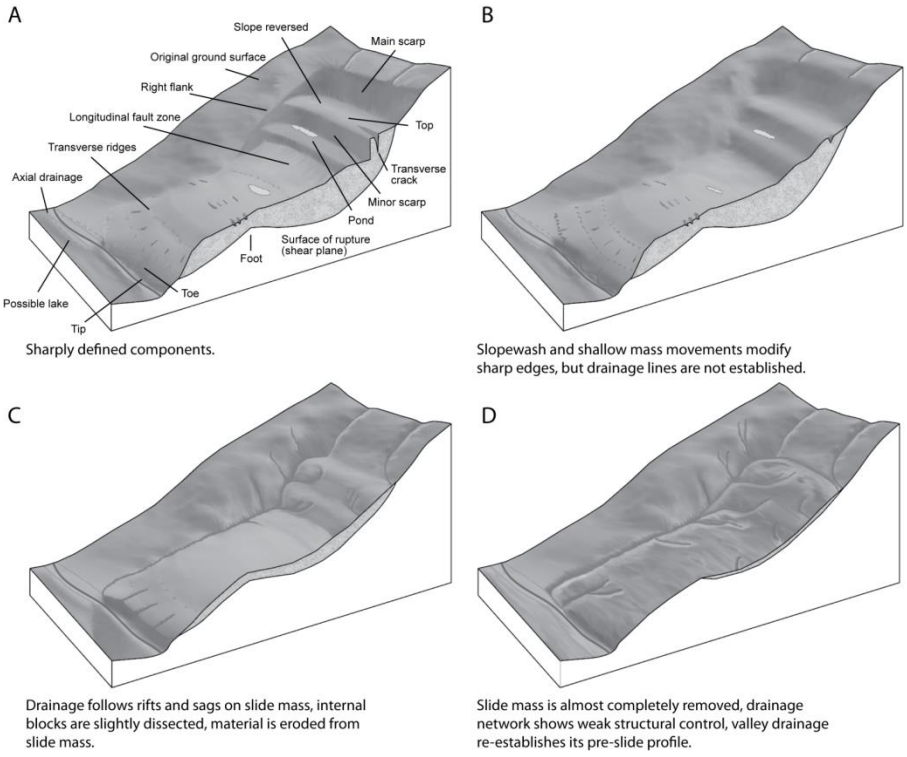

Figure 6.2 Schematic drawing of geomorphological changes with increasing relative landslide age of an idealized landslide (based on McCalpin (1984) and Keaton and DeGraff (1996). A = active, reactivated, suspended or dormant-historic; B = dormant-young; C = dormant-mature; D = dormant-old. Source: Bell et al. (2012)

6.1.2 Automated derivation of main scarps from polygons

As many statistical modelling approaches model with the grid cells (or one grid cell sampled) within the main scarp, the extent of the main scarp often needs to be known. An approach of the automated derivation of the main scarps of landslides using the mapped polygons was tested, as the time available for the mapping of the polygons was limited, and a high effectiveness of the mapping was a focus of this work (Petschko et al. 2014a).

The automatic derivation of the main scarps was done by a raster based approach masking the DTM by the landslide polygons (Petschko et al. 2014a). Then the elevation range within each landslide polygon was identified and a dynamic threshold value of the percentage of the elevation range was used to assign the main scarp area in a GIS environment. With this dynamic threshold value it can be assured that the characteristics and different sizes of all landslides are taken into account. Different threshold values of the elevation range were analyzed to identify the best fitting one for the actual size of the mapped main scarps in the test districts (Petschko et al. 2014a).

6.1.3 Tests on minimum requirements on landslide inventories for statistical landslide susceptibility modelling

The following requirements for statistical modelling of landslide susceptibility were assessed,

1. Where within the landslide should be sampled?
2. What is an adequate sample size for statistical modelling?

The landslide part (main scarp or the entire body) needed for the modelling was analyzed by trying to answer the question “Is the information on the entire landslide polygon necessary for the modelling and the resulting classified susceptibility map or is it adequate for obtaining a susceptibility map with three classes to sample (or map) a point in the main scarp only?” for the study area (AMBNWY; Petschko et al. 2013). Naturally, selecting a point in a different location of the landslide polygon highly influences the general allowed interpretation of the resulting landslide susceptibility map. However, aiming at a high mapping effectiveness mapping points in the main scarp only would enhance the mapping speed and allow the mapping of larger areas within shorter time.

To assess this two logistic regression (LR) models were fitted using one random sample grid cell within the entire landslide body and one random sample within the derived main scarp respectively (Petschko et al. 2013). The model performance was assessed deriving the AUROC value from comparing the resulting susceptibility map with the sampled grid cells within the entire landslide body. Furthermore, given the aimed output presentation of the susceptibility map with three classes, the classified susceptibility map was compared visually according to the differences between the

maps (Petschko et al. 2013). The visual comparison addressed the extent and spatial distribution of the susceptibility classes and their similarity at ridges and valleys.

The minimum required sample size was assessed by evaluating the performance of landslide susceptibility models trained and testing for a range of sample sizes. This assessment was conducted in the Flysch Zone, which is highly susceptible to landslides. A generalized additive model (GAM) was applied using *k*-fold cross-validation with 5 folds and 20 repetitions (for more details please refer to section 6.2) and the sample size was reduced stepwise from 12562 to 6400, 3200, 1600, 800, 400, 200, 100 and to 50 sampled cells (Petschko et al. 2014c). While the training sample was reduced constantly, the test sample stayed constant with a sum of 2000 landslide and non-landslide sample cells (Petschko et al. 2014c). To assess the changes in the model performance the median AUROC value and the interquartile range (IQR) of the AUROC value were determined for each sample size. Also the thematic consistency was evaluated (Petschko et al. 2014c). The thematic consistency assesses the similarity of the variable selection between different model runs. A high thematic consistency is obtained for models selecting the same set of explanatory variables in all model runs (refer to section 6.2.3).

6.1.4 Effectiveness estimate - comparison of landslide polygons and points in the main scarp

Assessing the effectiveness of mapping landslides with a polygon or with a point was done semi-quantitatively comparing the respective inventory with the defined requirements on a landslide inventory for different analysis types (e.g. statistical susceptibility modelling, hazard or risk analysis; Petschko et al. 2014a). From this comparison an effectiveness estimate was derived by taking into account the ratio of the number of landslides mapped, the used resources given by the person months (working 40h/week) and the study area size (Petschko et al. 2014a). Furthermore, a detailed catalogue of which aspects or information of an inventory are important for a given analysis type was developed and used to assign weights for the inventory. This weight was included in the calculation of the effectiveness estimate (Petschko et al. 2014a).

Additionally, the two landslide inventories were compared regarding their substantial completeness within the lithological units and the median slope angle represented by the polygons and the points set in the main scarp (Petschko et al. 2014a).

6.2 Landslide susceptibility modelling – facing the heterogeneity of large regions

6.2.1 Generalized additive models (GAM)

The analysis of identifying the minimum requirements on the information of the landslide inventory (point or polygon) was performed using the logistic regression model. Therewith, the intercept and a regression coefficient were determined for each explanatory variable describing the relationship between the landslide occurrence and the explanatory variables (Petschko et al. 2013).

Generalized additive models are a nonlinear extension of logistic regression models. Basically, the linear regression coefficient for each explanatory variable is exchanged with a nonlinear empirically fitted smooth function (Hastie and Tibshirani 1990; Petschko et al. 2014c). A GAM allows the combination of linear and nonlinear smoothing functions to describe the relationship between landslide occurrence and the explanatory variables (Petschko et al. 2014c).

Within a backward and forward stepwise variable selection the model decided on whether to include the variable or not, and if it was included, with which form (linear or nonlinear) the relationship with the response variable was explained best. This method was used to avoid the variable selection performed by an expert, as after Box (1976):

"Since all models are wrong the scientist cannot obtain a "correct" one by excessive elaboration. On the contrary following William of Occam he should seek an economical description of natural phenomena." (Box 1976, p. 792).

Accordingly, the Aikake Information Criteria (AIC) used within the automated stepwise variable selection measures the goodness-of-fit but seeks for a model with low complexity to obtain a parsimonious model (Akaike 1974).

6.2.2 Model design for large heterogeneous study areas

Characterizing study areas that show a high heterogeneity regarding their topography and geotechnical conditions is important for providing landslide susceptibility maps that are informative and comparable over the entire study area. Using the lithological map as proxy for geotechnical characteristics in the area it was assumed that the main explanatory variables might change within the lithological units (Petschko et al. 2012). Therefore, the lithological units were merged into homogeneous modelling domains which formed the basis for splitting the study area (Petschko et al. 2014c).

The difference of selected explanatory variables within the modelling domains was tested by fitting a GAM using stepwise variable selection within each modelling

domain. Furthermore, to have a result independent of the sampling the variable selection frequency was summarized after the repeated *k*-fold cross-validation (Heckmann et al. 2014; Petschko et al. 2014c; von Ruette et al. 2011).

After the modelling within the modelling domains, the landslide susceptibility maps were merged adjusting each map by the sampling rate. This step was necessary to account for the general relative landslide susceptibility of each modelling domain (Petschko et al. 2014c).

6.2.3 Statistical model performance assessment – repeated k-fold cross-validation

Assessing the model performance independent of a random sample was done by systematically applying a repeated *k*-fold cross-validation within each modelling domain (Petschko et al. 2014c).

Spatial and non-spatial (random) subsampling was performed to assess the spatial and non-spatial transferability (Kohavi 1995; Townsend Peterson et al. 2007). *K*-fold cross-validation describes a systematic technique to derive a number (*k,* here $k = 5$) of subsamples and fitting the model with *k*-1 fold and testing the model with the remaining fold to obtain a performance measure (Kohavi 1995; Petschko et al. 2014c). As the partitioning might also have an influence on the performance measure, the partitioning was repeated r times (here: r = 20) and the median and interquartile range of the 20 outcomes was calculated (Petschko et al. 2014c).

The area under the receiver operating characteristic curve (AUROC) value was used as performance measure. It compares the sensitivity of a model (proportion of true positives) with the specificity (or 1-specificity, the false positives rate; Hosmer and Lemeshow 2000). AUROC values can range from 0 to 1 indicating random agreement of predictions and observations (AUROC values between 0-0.5) or perfect discrimination (AUROC = 1; Brenning 2005; Petschko et al. 2014c).

The spatial and non-spatial transferability of the GAM was assessed within each modelling domain computing a transferability index *T* (Petschko et al. 2014c). Generally, the spatial and non-spatial transferability can be expressed with the IQR of the AUROC value obtained by the *k*-fold cross-validation. The computation of the transferability index was necessary to account for the varying sample size of all modelling domains and to allow the comparison of the transferability among the modelling domains (Petschko et al. 2014c). It takes into account the estimated standard error of the AUROC value and the IQR of the AUROC values within the domain (Petschko et al. 2014c). The higher the index value *T* the lower the (spatial or non-spatial) transferability of the model (Petschko et al. 2014c).

The thematic consistency is also of importance for describing the model quality (Guzzetti et al. 2006). Such as the transferability index it shows the models sensitivity to sample variation expressed by variation in variable selection (Petschko

et al., 2014c). A high thematic consistency is considered when in every model run the same set of variables is selected. Formalizing this concept a thematic consistency index *C* based on the Gini impurity index was obtained (Petschko et al. 2014c). A value of *C* close to zero indicates a good thematic consistency, while a value close to 1 shows poor thematic consistency (Petschko et al. 2014c).

6.2.4 Assessment of spatially varying prediction uncertainties

Giving an idea on the spatially varying prediction uncertainties visualized on a map was a very important step within this analysis aiming at transparent communication of uncertainties within this modelling approach. While the spatially varying prediction uncertainties only represent one out of many model form uncertainties it also has implications on the final spatial distribution of susceptibility classes.

The predicted probability value is usually used to display the landslide susceptibility resulting from one model run only. However, it is only a mean out of a range of possible probability values for the occurrence of landslides. Assessing this range, the 95% confidence interval can be derived using the standard error of the prediction. The spatially varying prediction uncertainties were obtained by deriving the upper and lower confidence limit of the predicted probability within the 95% confidence interval (Petschko et al. 2014c).

Therefore, the standard error of the prediction was transferred to every grid cell within the study area (NOE) by a lookup table (Petschko et al. 2014c). The R^2 value was derived between the looked up standard errors and the actual standard errors to assess the success of this procedure (Petschko et al. 2014c).

The grids of the upper and lower confidence limit and of the predicted probability were classified in three classes using the same threshold values (Petschko et al. 2014c). The three classified susceptibility maps were then analyzed regarding overlaps of different susceptibility classes (Petschko et al. 2014c).

6.3 Number and thresholds of susceptibility classes suitable for planning purposes

Landslide susceptibility maps are usually implemented using classes of susceptibility (e.g. low, medium, high) instead of the full range of values resulting from the modelling. This should give a basis for rather definitive decisions on if an expert on slope stability has to be consulted or not. Therefore, the classified map is contradictory to the probabilistic assessment of the landslide susceptibility where definitive predictions of stability are prevented (Crozier 1986).

Regarding the number of landslide susceptibility classes many different approaches can be found in literature. Many scientific papers distinguish between up to 10 or twelve classes (e.g. Chung and Fabbri 2003; Goetz et al. 2011), whereas others present susceptibility maps with seven, five or four classes (e.g. Van Den Eeckhaut et al. 2006; Rossi et al. 2010a; Santacana et al. 2003; Zezere 2002).

In the project MoNOE within which this thesis was written, the basic considerations for the decision on the number of susceptibility classes were: (1) cartographic considerations: the colors of the map should be monopolar to not give a wrong impression of stable and severely unstable slopes. Furthermore, the colors should be clearly distinguishable; (2) every susceptibility class is related to clear recommendations for action for the mayor who is in charge of the spatial planning in the municipality. Differentiating between more than three recommendations might lead to a simplification of them by the users of the map which had to be avoided (Bell et al. 2013).

Concerning the colors of the map, it was proposed to avoid the traffic light colors (red, yellow, green) to avoid misinterpretation and confusion with the landslide hazard zonation map of the Austrian Service for Torrent and Avalanche Control. The resulting landslide susceptibility maps represent a first indication of areas where more detailed investigation of the slope stability is necessary. This is contradictory to the hazard zonation maps. Therefore, this difference should also be portrayed by the color choice avoiding colors that look too alarming (e.g. red) or not serious enough (e.g. green; Bell et al. 2013).

Classifying the susceptibility map Fell et al. (2008) recommend relative susceptibility descriptors, which can be obtained by statistical models, to include the largest possible number of landslides in the highest susceptibility class. However, the spatial area covered by this class should be as small as possible. Accordingly, the number or percentage of landslides was determined by masking the resulting unclassified susceptibility map with the landslide grid cells. This gave the opportunity to quickly assign and visualize different threshold values of the landslide probability within ArcGIS (9.3). A range of threshold values and number of classes was tested and compared visually with the location of the mapped landslides. The visual appearance of the resulting classified susceptibility maps and the coverage of the area were of high importance. Therefore, this was analyzed and compared for 17 areas within different modelling domains.

6.4 Analysis of different dimensions of human impact on landslides

The literature research and field work within the study area gave insight in a range of possible impacts of human activity on the predisposing or triggering factors of landslides but also on the visibility of landslides on different remote sensing imagery

(refer to section 4.4). Within this thesis two of these were assessed within small study areas (Waidhofen/Ybbs and a landslide at Wilhelmsburg) as presented here.

6.4.1 Landslide persistence analysis

The persistence of the landslide morphology on the LiDAR DTM derivatives was evaluated by the comparison of landslides visible on the orthophoto or in the Building Ground Register with their visibility on the LiDAR imagery (Bell et al. 2012). A minimum persistence was defined for landslides visible in the LiDAR DTM derivatives and where the date of occurrence was known from different data sources (Bell et al. 2012). A maximum persistence was defined in cases where the landslide was visible on orthophotos, or its exact location was known from archive data, but the landslide was not visible on the LiDAR DTM derivatives anymore (Bell et al. 2012). The landslides showing a minimum or maximum persistence were analyzed regarding their land cover type and their size.

6.4.2 Influence on catchment area

In a very local study of two landslides (recently reactivated in 2009) the influence of human activity on changing the predisposing and preparatory factors of landslide occurrence was analyzed. Field studies showed that the natural watershed of the landslide might have been altered by the construction of a culvert close to a farmhouse in combination with the presence of an old sunken lane south of the landslide. This was analyzed in more detail using GRASS GIS (7.0) deriving the watershed boundaries for the study area in Wilhelmsburg (south of St. Pölten). The natural and the artificially enlarged watershed were computed using the r.carve and r.watershed tool of GRASS GIS (7.0).

7. Results

As the results and related discussions are presented in full detail in the publications in the annex (A.1 – A.8, Bell et al. 2013; Bell et al. 2012; Petschko et al. 2014c; Petschko et al. 2014a; Petschko et al. 2014b; Petschko et al. 2013; Petschko et al. 2012; Petschko et al. 2010), in this section the most important results are presented to supply an overview and a basis for the discussion.

7.1 Landslide inventory mapping

In total 2014 landslide polygons and 3994 points in the main scarp of the landslide were mapped in the test districts Amstetten, Baden and Waidhofen/Ybbs. Thereof, 694 slide polygons and 1061 landslide points were identified within the district Waidhofen/Ybbs. The largest district of the test study area Amstetten counted 1213 landslide polygons and 2709 landslide points. According to the mapping results the district Baden is less prone to landslides as only 107 polygons and 219 points indicating landslide presence were mapped (Petschko et al. 2014a).

1834 of all landslide polygons were identified and delineated with high certainty, which were used for further analysis, e.g. of the relative landslide age, or the susceptibility modelling. The main mapped landslide type within the test districts was earth and debris slides (75.7%), followed by "area with slides" (20.3%) and earth flows (3.8%; Petschko et al. 2014a).

In Lower Austria 13,166 earth and debris slide points were mapped of which 12,889 earth and debris slides lie within the study area of this thesis. Only for the districts Amstetten, Baden and Waidhofen/Ybbs the mapping was performed by the author of this thesis. For the other districts the author acted as an advisor of the mapping (Petschko et al. 2014a).

The comparison of the existing inventories from the Geological Survey of Austria and Lower Austria and the Austrian Service for Torrent and Avalanche control showed big differences between the inventories (Fig. 7.1). The GEORIOS database provided by the Geological Survey of Austria contains information of very different detail and resolution. As visible in Figure 7.1 some polygons stretch out over multiple valleys and catchments indicting an area with slides. This information is not suitable for statistical landslide susceptibility modelling. In detail 37% of the landslides mapped interpreting the LiDAR DTM derivatives were found within the GEORIOS database. 17% of the slides were located within landslides mapped in the Map of Quaternary Sediments and only 4% of the mapped landslides were showing landslides of the Building Ground Register. While 6% of the landslides were covered by more than one inventory, 36% of the mapped landslides did not show any overlap or clear similarity to the existing inventories.

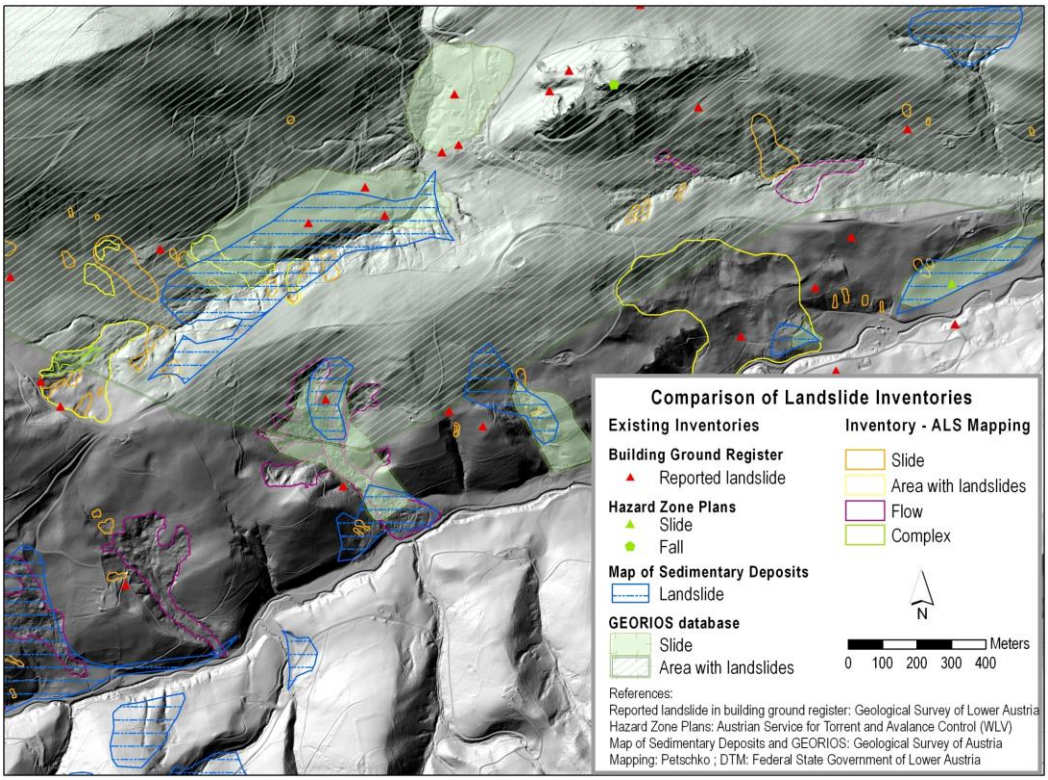

Figure 7.1 Comparison of the landslide inventory mapped on Airborne Laserscanning (ALS) LiDAR DTM derivatives with existing inventories in Lower Austria. Source: Petschko et al. 2010

7.1.1 Comparison of relative landslide age and current land cover

The mapped landslides' relative ages were mainly estimated to be old (48%) or young (34%). 8% of the landslide were estimated as very young, and 10% were assigned as very old (Petschko et al. 2014b). 75% of the mapped landslides were identified as earth or debris slide. Of these 64% are located in forested land cover types. In contrast to this, only 13% of the very young landslides contain forested grid cells while 83% of the very young landslides are covered by farmland (arable land, fallow land, grassland and rough pasture (Petschko et al. 2014b)). However, 65% of the very old landslides are forested. This showed a clear tendency: the younger the landslides were considered, the lower the percentages of forest cover were within these landslides (Petschko et al. 2014b).

7.1.2 Automated derivation of main scarps from polygons

Different percentage values of the elevation range were tested to automatically derive the main scarps from the landslide polygons (30%, 35%, 40%). The percentage representing the mapped main scarps best was the 35% of the elevation range. These

gave the closest representation of the mapped main scarps (cf. Fig.4 in Petschko et al. 2014a (A.7)).

The size (area in m²) of the derived main scarps was clearly smaller than of the landslide polygons. Also the median slope angle within the main scarps differed from the median slope angle of the entire mapped landslide polygons. The main scarps were steeper, which matched the general understanding of the slope angle distribution within a landslide (Varnes, 1984; Petschko et al. 2014a). Additionally, the comparison between the minimum and maximum values of the slope angle within the derived main earth and debris slide scarps and the mapped points in the main scarp indicated an overlap of the slope angle characteristics between both datasets (Petschko et al. 2014a).

These results emphasize the need to clearly communicate on where the landslide points were set within the landslide inventory as it may influence the modelling result and it's allowed interpretation. Furthermore, the comparison of the median slope angle shows the heterogeneity of the study area and of the earth and debris slides within (Petschko et al. 2014a).

7.1.3 Tests on minimum requirements on landslide inventories for statistical landslide susceptibility modelling

Comparing the resulting AUROC value from fitting a model with the points in the main scarp (AUROC = 0.84) and with a point sampled within the entire polygon (AUROC = 0.87) shows only minor differences in the model performance (Petschko et al. 2013). From a model performance point of view, using the points mapped in the main scarp gives just as good results as using the points within the polygon (Petschko et al. 2013).

Comparing the resulting landslide susceptibility maps with three classes visually shows changes in the extent of the high susceptibility class (Fig., 7.2; Petschko et al. 2013). The overall impression of both maps is similar, indicating similar slopes and slope parts with similar susceptibility classes (Petschko et al. 2013).

Reducing the sample size resulted in decreasing median AUROC values and in increasing interquartile ranges of the AUROC value. However, even the smallest sample size still achieved an acceptable median AUROC value (0.76) and therefore a good discrimination between slide and non-slide grid cells (cf. Fig. 6 in Petschko et al. 2014c). A distinct change of the model performance and the IQR of the AUROC occurred at a sample size of about 400 (spatial cross-validation) and 200 (non-spatial cross-validation). There, the IQR of the AUROC sharply increased as the sample size decreased indicating a decreasing (spatial) transferability of the model. Furthermore, the thematic consistency of the model decreased with smaller sample sizes (Petschko et al. 2014c).

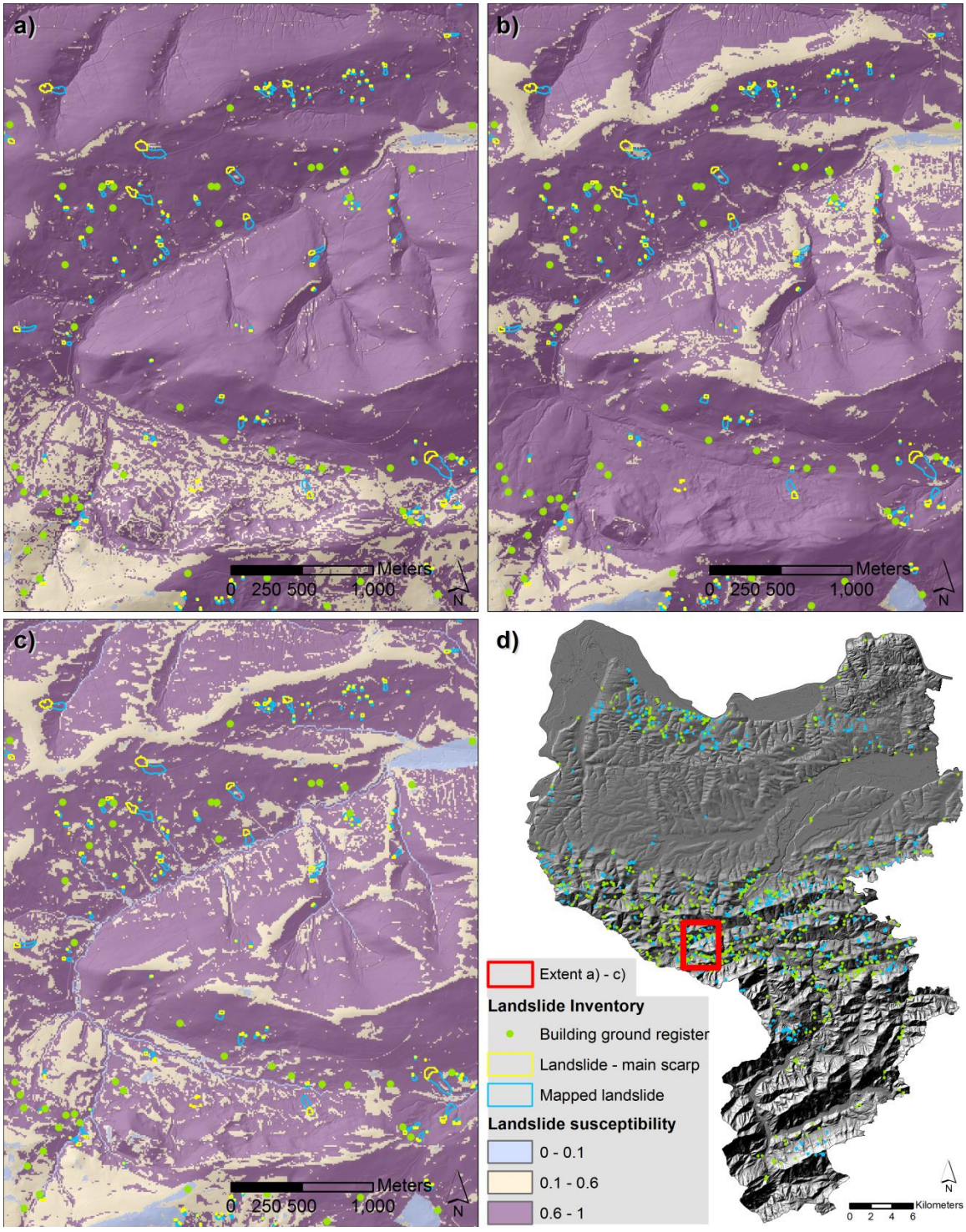

Figure 7.2 Comparison of landslide susceptibility maps derived using (a) points from the Building Ground Register, (b) points sampled randomly within the landslide polygon and (c) points sampled randomly within the main scarp. (d) Landslide inventory of the district Amstetten and Waidhofen/Ybbs. Source: Petschko et al. (2013).

7.1.4 Effectiveness estimate - comparison of landslide polygons and points in the main scarp

Additionally to the comparison of the model performance and the visualization of the map also other criteria for selecting either a point mapped in the main scarp or information from the entire landslide polygon were analyzed. Mapping the 1834 landslide polygons lasted 4 person months compared to 1.5 person months that were needed for mapping the points in the main scarp (Petschko et al. 2014a). The mapping rate was 459 and 2663 landslides per person month respectively (Petschko et al. 2014a).

The resulting effectiveness estimate (Ee_{ia}) was 6.9 and 57.5 for mapping polygons or points in the main scarp respectively, for statistical susceptibility modelling obtaining a susceptibility map with three classes (Petschko et al. 2014a). While the value itself is of minor interest, the difference between the values is more expressive. It outlines the higher effectiveness of mapping points in the main scarp of earth and debris slides rather than polygons for the analysis type of statistical landslide susceptibility modelling. Consequently, the mapping of points in the main scarp of earth or debris slides was the preferable and acceptable method (refer to section 7.1.3) for the susceptibility assessment in Lower Austria (Petschko et al. 2014a).

Compared to other analysis types (e.g. morphological analysis, hazard or risk analysis) the effectiveness estimates gave a different picture. The effectiveness of mapping points is decreasing and even below zero (ranging from -31 to -12.5), as the points cannot provide enough information for these types of analysis (Petschko et al. 2014a). In contrast to this, the effectiveness of mapping the landslides with polygons is doubling from hazard to risk analysis (1.3 to 2.6; Petschko et al. 2014a). Summarized, this analysis showed that none of the mapped inventories was perfect for the assessed analysis types (Petschko et al. 2014a).

7.2 Landslide susceptibility modelling – facing the heterogeneity of large regions

7.2.1 Generalized additive models (GAM) and model design for large heterogeneous study areas

Generalized additive models were successfully applied to perform the landslide susceptibility modelling and proved as a step forward regarding a better characterization of the earth and debris slides within the study area. The stepwise variable selection resulted in a selection of variables transformed with a smoother function in 65% of the cases (Petschko et al. 2014c). However, the selection of linear or nonlinear terms differed within the modelling domains (Tab. B.1 in the Annex). In some domains the linear form of the variables was preferred while in other domains

the variables were mainly included using a smoother function (Petschko et al. 2014c; Tab. B.1 in the Annex).

From this table the study design of modelling within the different modelling domains was confirmed. It shows the selection of different explanatory variables during the different model runs on the one hand and on the other hand within each modelling domain. However, using all landslide grid cells (derived from points mapped in the main scarp) for modelling the susceptibility used for compiling the landslide susceptibility map the variable slope was selected in all but one modelling domain. This emphasizes the importance of slope angle as a predisposing factor to landslide occurrence.

7.2.2 Statistical model performance assessment – repeated k-fold cross-validation

The resulting AUROC range from testing the *k*-fold cross-validation with spatial and random subsampling was smaller for the non-spatial cross-validation over all cross-validation repetitions and modelling domains (Petschko et al. 2014c). Additionally, the generally similar median AUROC values were slightly higher for the non-spatial cross-validation than the spatial cross-validation (Petschko et al. 2014c). Out of all modelling domains the alluvial deposits including lakes and wetland domain had the highest median AUROC values of 0.98 (spatial) and 0.99 (non-spatial cross-validation; Petschko et al. 2014c). All median AUROC values were higher than 0.74 except from the Permo-Mesozoic rocks domain (Petschko et al. 2014c).

The spatial and non-spatial transferability varied significantly within the different modelling domains (refer to Table 3 in publication A.6). A poor transferability was assigned at $T_{sp} > 0.10$ and $T_{nsp} > 0.04$ and was found for the three modelling domains with the smallest sample size (Petschko et al. 2014c). While generally a better transferability was observed for domains with larger sample sizes and/or higher landslide densities, this did not apply for all modelling domains (e.g. the Austroalpine Unit with dolostone, $T_{sp} = 0.098$). The best spatial transferability ($T_{sp} < 0.03$) was found for the igneous rocks of the Austroalpine Unit, the Molasse Zone and the Schlier Zone (Petschko et al. 2014c).

Generally, topographic variables were selected more often within the automated variable selection than available variables on soil properties (Petschko et al. 2014c). While the slope angle variable was selected in 15 out of 16 modelling domains using all landslide grid cells for the modelling, the minimum permeability was not used in any domain (refer to Table 2 in A.6; Petschko et al. 2014c).

While this finding only represents the result of a specific random sample (using all landslide grid cells within the main scarp) the spatial and non-spatial *k*-fold cross-validation gave a more balanced view on the relative variable-selection frequency and importance (Tab. B.1 in the annex; Petschko et al. 2014c). In spatial and non-spatial cross-validation the slope angle was selected in 91.8% and 95.7% of the model

repetitions (Petschko et al. 2014c). While catchment height was in general an important variable for both cross-validation approaches (selected in 55.6% (spatial) and 65% (non-spatial) of the models), the Euclidian distance to nappe boundaries was more important in spatial cross-validation (selected in 74.2% of the models; Petschko et al. 2014c). The variables of void space (mean 0-100cm) and void space (0-20cm) were of minor importance as they were selected by less than 1% of the models (Petschko et al. 2014c).

Generally, the thematic consistency was found to be stronger within the non-spatial cross-validation having less variable training sets than spatial cross-validation (refer to Table 3 in A.6; Petschko et al. 2014c). Nearly half of the modelling domains (seven) had a strong thematic consistency within non-spatial cross-validation. Within the spatial cross-validation the thematic consistency was strong for only a quarter of the modelling domains (Petschko et al. 2014c).

A relation between the thematic consistency and small sample size and poor spatial transferability was observed. However, the median AUROC values were unrelated in spatial cross-validation (Petschko et al. 2014c). In non-spatial cross-validation no relation was found between the sample size, transferability and the thematic consistency. However, the thematic consistency increased with lower median AUROC values (Petschko et al. 2014c).

7.2.3 Assessment of spatially varying prediction uncertainties

The range of the standard error of the predicted probability was different in the modelling domains. The largest range was observed within the Bohemian Massif with plutonic rock (0.37–16.24 (on the logit scale); Petschko et al. 2014c). Furthermore, the R^2 obtained to estimate the success of the lookup table used to transfer the standard error to all grid cells varied significantly (refer to Table 3 in A.6; Petschko et al. 2014c). It showed a range from 0.51 (Melange Zone) to 0.9 (in Loess, Loam; Petschko et al. 2014c).

No overlaps of different susceptibility classes in the susceptibility maps of the lower (LCLI) and upper confidence limit (UCLI) and the predicted probability (PP) were found for 85% of the study area (Petschko et al. 2014c). However, for the remaining 25% of the study area seven different types of overlaps of susceptibility classes grouped in three types were identified. Ranked according to their percentage of the coverage of the study area these include the overlap of (1) the low susceptibility class with the medium class (PP → UCLI: 6%; LCLI → PP: 5%); (2) the medium class with the high susceptibility class (PP → UCLI: 2%; LCLI → PP: 2%) and (3) the overlap of the low susceptibility class with the high class (LCLI → UCLI: 0.4%; PP → UCLI: 0.03%; LCLI → PP: 0.02%; Petschko et al. 2014c).

7.3 Number and thresholds of susceptibility classes suitable for planning purposes

According to the basic considerations on the appropriate number of landslide susceptibility classes, three susceptibility classes were observed to be of most practical use (Bell et al. 2013). While this decision was taken by the stakeholders within the project, it was based on a number of discussions with scientific input provided also from the author of this thesis.

Avoiding the confusion of the resulting maps with the hazard zonation plan of the Austrian Torrent and Avalanche Control the colors white, yellow and orange were selected to visualize the three susceptibility classes. They allow a good readability as the distinction between the colors is easy. Furthermore, confusion with other maps (such as topographic maps) is prevented (Bell et al. 2014).

Regarding the identification of an appropriate threshold value to obtain a classified susceptibility map a list of threshold values representing the percentage of landslides within the susceptibility class was tested (Tab. 7.1 and Tab. 7.2). This was done by visual comparison of the resulting susceptibility map with the general topography and the landslide inventory for different modelling domains (Fig. 7.3).

Table 7.1 Versions of visually analyzed susceptibility maps visualized using different threshold values according to the percentage of landslides included in the high and low susceptibility class

Landslide susceptibility map version	*Percentage of landslides within the susceptibility class*		
	"low"	"medium"	"high"
1	1	19	80
2	5	15	80
3	1	24	75
4	5	20	75
5	1	29	70
6	5	25	70

Table 7.2 List of percentage of landslides included in the susceptibility class and percentage of the total area covered by the susceptibility class (visualized in Fig. 7.3)

Susceptibility class	*Version 1*		*Version 2*		*Version 4*		*Version 6*	
	Percent earth and debris slides included	Percent study area covered	Percent earth and debris slides included	Percent study area covered	Percent earth and debris slides included	Percent study area covered	Percent earth and debris slides included	Percent study area covered
Low	1	60.9	5	75.2	5	75.2	5	75.2
Medium	19	28.9	15	14.6	20	16.7	25	18.4
High	80	10.2	80	10.2	75	8.1	70	6.4

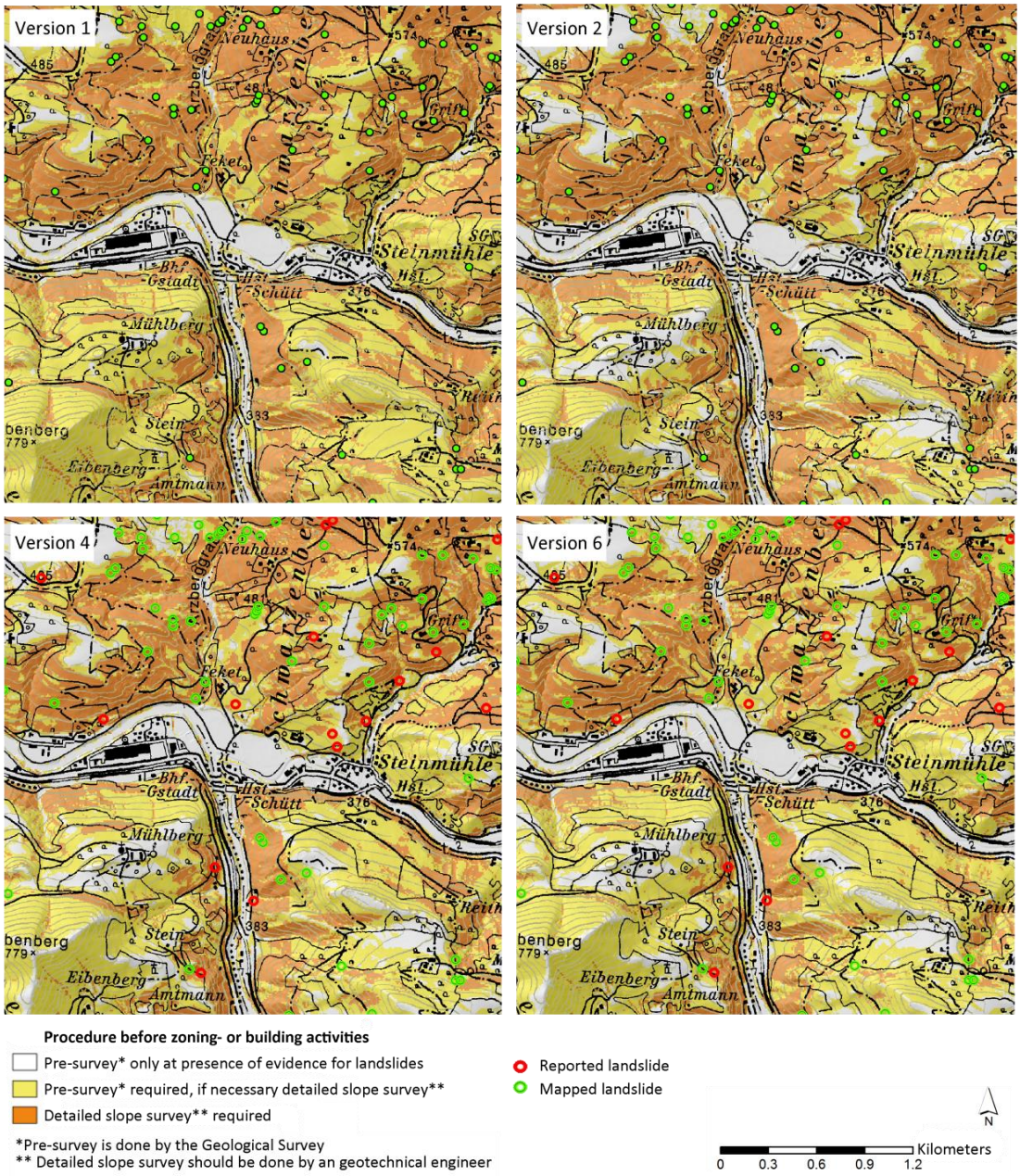

Figure 7.3 Landslide susceptibility maps classified according to different percentage of landslides within each susceptibility class. The versions correspond to the versions listed in Table 7.1 and Table 7.2. The naming of the classes represents the naming decided on with the stakeholders in the project MoNOE.

The visual appearance shown in Figure 7.3 gave an indication of the effect of selecting the one or the other threshold value on the planning practice and readability of the map. The best compromise between covering least of the area with a high susceptible class while containing as many landslides as possible was found in the map resulting from Version 6 (Tab. 7.1 and Tab. 7.2). The thresholds of this map were set to contain 70% of the earth and debris slides within the high susceptible class and 5% of the slides within the low susceptible class. These classes cover 6.4% and 75.2% of the entire study area respectively (Fig. 7.4). However, it has to be kept

in mind at the interpretation of the map that even within the low susceptibility class 5% of the slides are contained. This is an expression of the uncertainties of the modelling approach and the classification of the map, which has to be communicated with the users of the map.

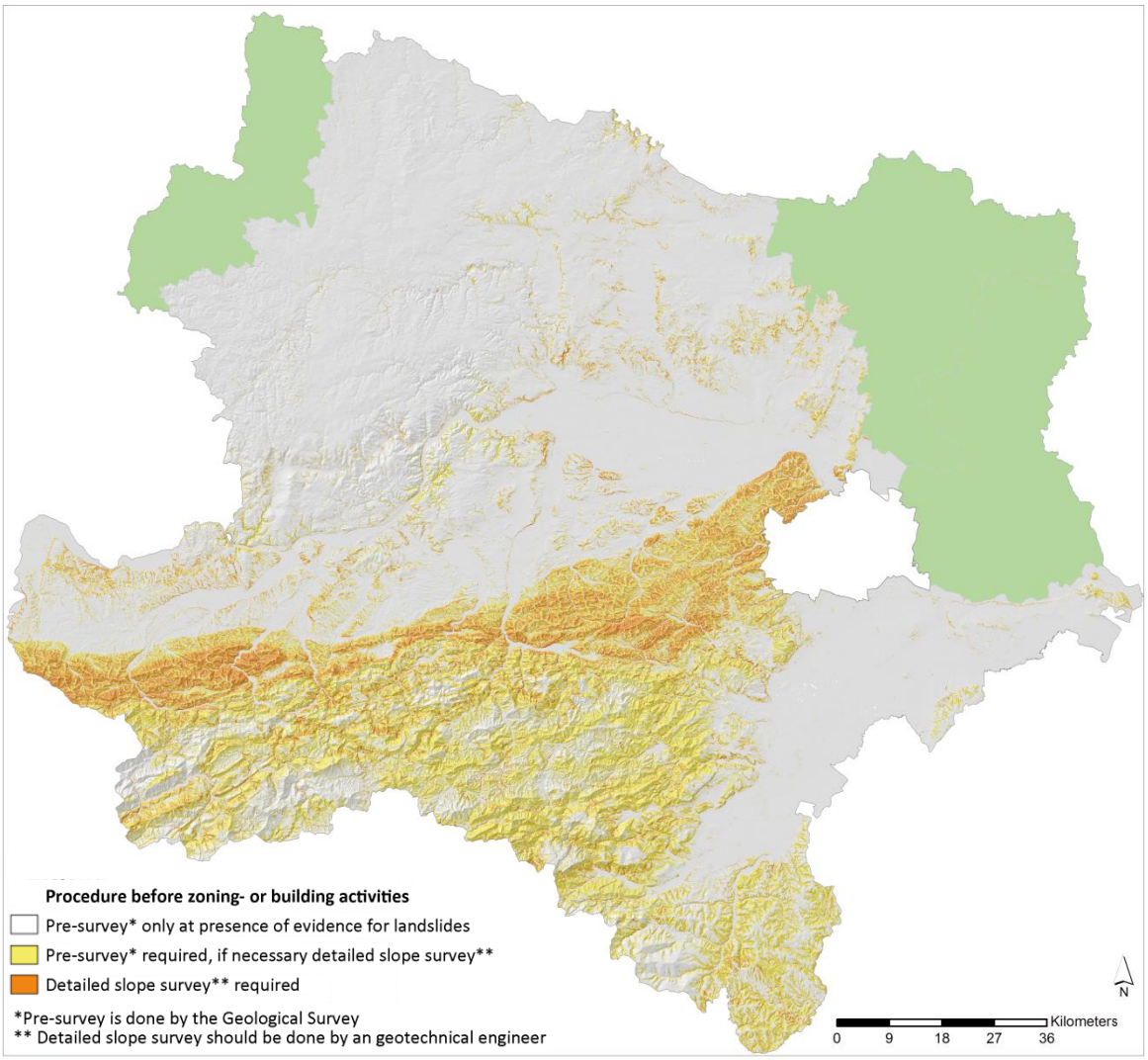

Figure 7.4 Final susceptibility map for the study area in Lower Austria. Source: altered from Petschko et al. (2014c)

One way of implicit communication is the naming of the susceptibility classes. Within the project MoNOE the naming was proposed to transport actions instead of susceptibility levels (Bell et al. 2014). Accordingly the title of the legend is not "Landslide susceptibility" but "Procedure before zoning or building activities". The single classes are named after the action the mayor has to take before zoning activities: (1) the low susceptibility class is named "Pre-survey* only at the presence of evidence for landslides"; (2) the medium susceptible class indicates "Pre-survey* required, if necessary detailed slope survey**" and (3) the high susceptible class is named "Detailed slope survey** required" (Bell et al. 2014). One star "*" indicates that the pre-survey is done by the Provincial Geological Survey; two stars "**"

indicate that the detailed slope survey should be done by a geotechnical engineer (Bell et al. 2014). These maps were handed to the mayors by the Provincial Government with a brief description of the maps and their allowed interpretation (Bell et al. 2014).

7.4 Analysis of different dimensions of human impact on landslides

7.4.1 Landslide persistence analysis

The dependency of the landslide persistence on the land cover was analyzed in Waidhofen/Ybbs. For 31 out of 694 earth and debris slides information on the landslide age was available, either absolute or estimated on the basis of their visibility on orthophotos (Bell et al. 2012). The morphology of 27 of these slides was not visible on the LiDAR DTM derivatives anymore. The majority of these were located in forest free land. In detail 48% of the slides were located in grassland and 23% were located in agricultural land at the time of their occurrence (Bell et al. 2012). However, the comparison with the land cover map resulting from satellite data showed that 16% of the slides occurred in forested land (Bell et al. 2012). Compared to all slides mapped in this area this percentage is only half as large, as 38% of all 694 slides were located in forest (Bell et al. 2012).

The morphological footprint of nine of the 27 slides disappeared within one year only mainly due to planation (Fig. 7.5; Bell et al. 2012). Farming activity and the importance of the forest free land as grassland or pasture were observed as the reason for the rather quick anthropogenic change of the morphology (Bell et al. 2012). While no slide located in mixed forest disappeared within one year, no clear trend between the land cover type and the landslide persistence could be found for the earth and debris slides mapped in Waidhofen/Ybbs (Fig. 7.5; Bell et al. 2012). According to the minimum persistence the morphology of slides located within all land cover types was still visible on the LiDAR DTM derivatives (Fig. 7.5).

7.4.2 Influence on catchment area

During fieldwork, the installed culvert and the route of the sunken lane was mapped in detail. This was used in the GRASS GIS analysis of the watershed. The natural watershed of the landslides was derived resulting in a size of 0.1km². Taking into account the anthropogenically installed channels, culverts and the sunken road, the watershed area was increased anthropogenically by 0.05km² (Bell et al. 2012). Unfortunately there is no information on the landslide activity before the installation of the culvert. Also the age of the sunken lane is unknown. However, this

increase in the watershed area by half of the original area might have led to a water surplus causing increased landslide activity or reactivation (Bell et al. 2012).

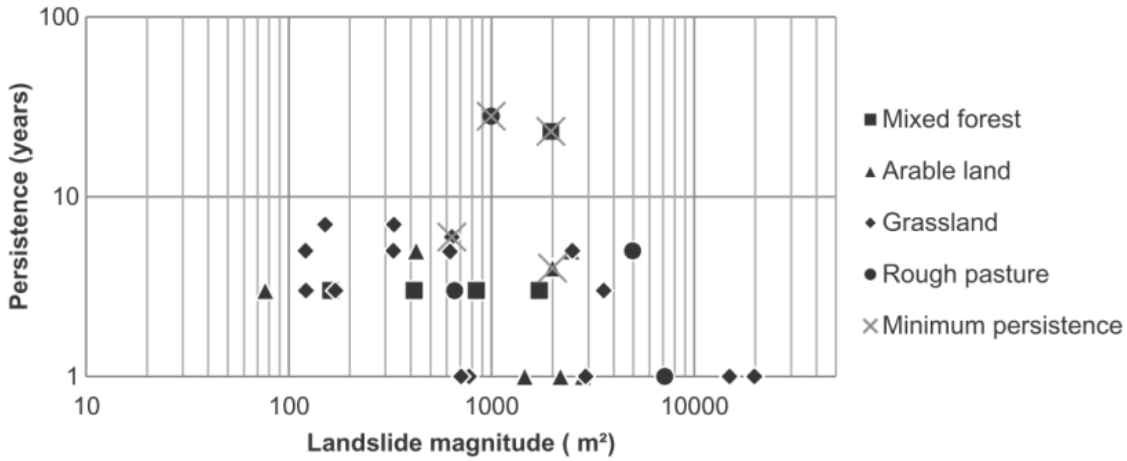

Figure 7.5 Landslide persistence, landslide size and land cover type in Waidhofen/Ybbs. Source: Bell et al. (2012)

8. Discussion of the methods, results and hypotheses

Five hypotheses around the mapping of landslides and modelling of landslide susceptibility and assessing its quality were formulated at the beginning of this study. The respective methodology to test the hypothesis and arising objectives and its results were presented in the previous sections. In this section the applied methodology, obtained results and the implications on the hypothesis are discussed in detail. Much of the presented discussion content was already presented in the publications printed in the annex. These parts are cited accordingly. Furthermore, the discussion might partly refer to methodology or results which were not presented in full detail in this monographic part of the thesis. These may be found in the copies of the full publications in the annex. Additionally, within this section the single publications or manuscripts are put into context with each other and the wider research field of landslide susceptibility modelling.

Every modelling precedes a detailed analysis of the characteristics of the study area and the available data. In line with the statement "garbage in, garbage out" used in computer science, the selection of geomorphologically meaningful and relevant datasets for statistical modelling is a crucial step to avoid meaningless results. Therefore, several different analyses were carried out within this study, to get to know the study area and landslide inventory better and to give a statistical assessment of the model performance. Only the combined use of mapping and modelling methodologies enabled deriving findings on the most effective landslide inventory mapping method for statistical analysis, on the appropriate pre-selection of explanatory variables and on the estimation of the achieved and necessary completeness of the inventory. However, all the applied methods inherit assumptions and limitations originate from the data availability or the selected modelling method. These limitations and their implications on the hypotheses shall be discussed in more detail in the following.

8.1 Effectiveness, minimum requirements and limitations of landslide inventory mapping on LiDAR DTM derivatives

A larger effectiveness of mapping landslide on the basis of high resolution LiDAR DTM derivatives for statistical susceptibility analysis was identified for mapping points in the main scarp rather than entire polygons. This finding was based on the analysis of the proposed effectiveness estimate (Petschko et al. 2014a) and the comparison of model performance of using different inventory sampling strategies (Petschko et al. 2013).

The final landslide inventory, which was mapped for Lower Austria, can be described as a historical inventory because it contains information on landslides that occurred in the past, probably after several triggering events (Malamud et al. 2004). A major limitation of historical inventories is the inability to link the landslide processes to specific event triggers. An event inventory representing all landslides occurred after a trigger event would be beneficiary for analyzing the landslide process and the triggering conditions in more detail (Van Westen et al. 2006).

For mapping an event inventory other methods than the visual interpretation of the LiDAR derivatives might be more suitable due to high acquisition costs of LiDAR data (Petschko et al. 2014a). Alternatives may include the visual or stereoscopic interpretation of aerial photographs (Cardinali et al. 2000), semi-automated mapping by change detection using satellite imagery (Ardizzone et al. 2013; Mondini et al. 2011a; Mondini et al. 2011b) or new reconnaissance mapping methods, e.g. GPS equipped binoculars (Santangelo et al. 2010). Automated approaches to detect landslides on satellite imagery proved to be of high effectiveness as it is possible to map a large number of landslides very fast (Guzzetti et al. 2012; Mondini et al. 2011b; Petschko et al. 2014a). However, their main drawback is the limited capability to detect single landslides instead of pixel or polygons covering the entire vegetation-free area (Petschko et al. 2014a). Unfortunately, while modelling the landslide susceptibility over large and heterogeneous areas, the information on the landslide density and single landslide events is crucial (Petschko et al. 2014c). Therefore, often a visual interpretation of the detected areas has to follow, which reduces the effectiveness of the mapping (Van Den Eeckhaut et al. 2012).

The general subjectivity of the mapping performed by experts has to be remembered. Ardizzone et al. (2002), Van Den Eeckhaut et al. (2005) and Van Westen et al. (1999) showed with their studies that the resulting inventories mapped by different geomorphologists can differ widely. This can clearly be attributed being an epistemic uncertainty. Not only may this uncertainty exist in the landslide inventory mapping, but also other data used to represent landslide conditions may have their own mapping subjectivities, such as the class boundaries drawn in a lithological map.

Another drawback of the landslide inventory built for this thesis is the limited knowledge on the ages corresponding to the mapped landslides. The relative age of

landslide may be estimated for historical landslide inventories, which were mapped from LiDAR derivatives, by comparing landslide morphological characteristics (Bell et al. 2012). This estimation of the relative landslide age aided the selection of appropriate explanatory variables that were used to feed the automated stepwise variable selection. The comparison of the land cover of landslides of different relative age revealed important insight into the sustainability of including recent land cover data in susceptibility modelling. The estimation of the relative age and comparison of the land cover in the landslide polygons of different relative ages pointed out how the recent land cover data does probably not reflect the past land cover. The recent land cover of very young and very old landslides was clearly different from each other. Furthermore, while the very young landslides mainly occurred in non-forested land, more than half of all mapped landslides independent of their relative age were covered by forest. This mismatch of land cover properties within the landslide inventory emphasizes the need to omit data on recent land cover from the statistical landslide susceptibility analysis. Naturally, it has to be pointed out, that this finding is only applicable in the specific setting of the study area (e.g. topography, geology, vegetation, climate (Antonini et al. 2002; Petschko et al. 2014b)).

However, the relative age estimation methodology proposed by McCalpin (1984) might also carry some uncertainties depending on the setting of the landslide (e.g. climate, topography). During field work some landslides were observed which were considered being of very old age due to the age of the trees. However, the morphological footprint of some of these made look the landslide much younger than observed in the field. This was described as a "conservation effect" as the young morphology was conserved under forest. Furthermore, no correlation to actual ages could be done due to missing data. This could probably be obtained carrying out dating techniques such as summarized by Lang et al. (1999). However, the combined interpretation of orthophotos and LiDAR DTM derivatives proved effective as it allows the identification of relative age of landslides due to vegetation growth on the landslide (Petschko et al. 2014b).

Furthermore, it should also be stated that very young and young landslides might also occur in forested land (Petschko et al. 2014b). Due to the resolution or date of the orthophotos and possible effects of shadows it might be possible, that vegetation free areas cannot be observed. A study performed on six event landslide inventories in Switzerland (in the Flysch Zone) found 50% of the landslides occurred in forested terrain (Rickli and Graf 2009). Additionally, it is possible that landslides under forest reactivate (Van Den Eeckhaut et al. 2009b).

The question might arise, if the mapping of the landslides in the entire area was necessary? Other studies analyzed ways to map all landslides within a sample area and transfer the fitted model to the entire study area (Calvello et al. 2013). Also, also more sophisticated mapping techniques derived from geospatial sampling methods sound appealing to avoid the mapping of an entire area and to increase the mapping effectiveness. For example, methods patterned on the quadrat count method that is widely used in ecology could be applied (Christman 2000; Ver Hoef 2002; Krebs 1999; Thompson 2012). This method includes mapping all landslides in a limited number

of quadrats (of a specific size) randomly located in the study area and using the mapped information to fit a model which is transferred to the remaining area (Thompson 2012). Other studies used the information of landslide distribution in sample terrain mapping units and transferred that to the terrain units of the entire study area to obtain a landslide probability map used for susceptibility modelling (Calvello et al. 2013). These methods allow calibrating and validating a model used to transfer the landslide distribution zoning maps to the entire area with only a small landslide inventory only (Calvello et al. 2013).

Although these geospatial sampling techniques are very useful for some applications, in heterogeneous study areas such as Lower Austria they might be very challenging (Petschko et al. 2014a). The variable characteristics of lithology, morphology, landslide size and density and land cover demand flexibility from the geospatial sampling technique to identify a satisfactory and still applicable sampling scheme (Petschko et al. 2014a). In the specific setting of Lower Austria, the applied study design requests details on the landslide density of each modelling domain (Petschko et al. 2014c). Additionally, the lithological units (modelling domains) are of irregular shape and the landslide density changes from east to west (Petschko et al., 2014a). Besides, results from the spatial cross-validation showed a clear variation of the model performance measure (AUROC value) between the different partitions and model runs (Petschko et al. 2014c). The applied methodology simulates exactly the setting of applying any geospatial sampling technique. Besides a variation of the spatial transferability within one modelling domain, the spatial transferability also varied between all the modelling domains (Petschko et al. 2014c). These findings emphasize the difficult nature of applying geospatial sampling techniques to heterogeneous study areas (Petschko et al. 2014a).

8.1.1 Where within the landslide should be sampled?

In the state of the art in landslide susceptibility modelling section, the different approaches of including information on landslides in statistical susceptibility modelling were introduced. As learned from literature sampling only one grid cell randomly per landslide body or main scarp is often done, but excludes information on the magnitude of landslides (Regmi et al. 2014). Modelling with the information of all grid cells of the body or main scarp was found to result in better model performance values (ROC) than modelling with only one sampled grid cell (Regmi et al. 2014). However, the decision for sampling one grid cell only in the main scarp is usually done in landslide susceptibility modelling. This is often based on considerations on increasing mapping effectiveness (Petschko et al. 2014a), on avoiding uncertainty related to mapping landslide polygon boundaries (Van Den Eeckhaut et al. 2006; Malamud et al. 2004), on reducing spatial autocorrelation of the landslide samples and on providing equal treatment of small and large landslides (Atkinson et al. 1998; Beguería 2006b; Carrara 1993; Claessens et al. 2006; Dai and Lee 2002; Van Den Eeckhaut et al. 2006; Felicísimo et al. 2012; Guns and Vanacker 2012; Heckmann et al. 2014; Petschko et al. 2014c; Remondo et al.

2003; Schicker and Moon 2012). The statements of the authors that were for representing landslides with a single point contrast the findings of Regmi et al. (2014). They highlight that mapping errors and the possibility of autocorrelation are key drawbacks of using all grid cells from the landslides. Moreover, no general guideline on best practice is available in literature. A comparison of sampling points/grid cells in the initiation, the transport or deposition zone only, gave very different landslide susceptibility maps (Vorpahl et al. 2012). Both highlights the importance of stating where the grid cells were sampled as it has clear implications on the interpretation of the map. A landslide susceptibility map modelled with grid cells sampled in the main scarp do by definition not show the downslope movement and runout of the landslide (Demoulin and Chung 2007).

Chung and Fabbri (2003) were well aware of the limitations of using information from the main scarps only for the modelling. They recommend the simulation of the possible deposit areas of future landslides by methods such as cellular automata (Packard and Wolfram 1985). This evolved to general practice in landslide susceptibility modelling as reflected by several publications (LfU - Bayerisches Landesamt für Umwelt 2007; Liener and Hunziker 2008; Liener and Kienholz; van Westen et al. 2008).

As found in the present study, the statistical model performance measure (AUROC) did not change significantly from modelling with a grid cell sampled within the main scarp or sampled within the entire landslide body (Petschko et al. 2013). In contrast to the findings of Vorpahl et al. (2012), the visualization of the landslide susceptibility map was found to be similar. Only slight changes were seen in the high susceptibility class, covering a smaller area in the map resulting from using the grid cells in the main scarp only. This clearly has to be attributed to the visualization with three susceptibility classes and has to be tested for maps with a different number of classes or threshold values (Petschko et al. 2013).

According to the presented results and the discussion the first hypothesis of this study

"A landslide inventory mapped on the basis of LiDAR DTM derivatives and orthophotos shows remarkably better precision and accuracy of the landslide location and delineation compared to existing landslide inventories. Furthermore, mapping points in the main scarp only increases the inventory mapping effectiveness and achieves comparably reliable landslide susceptibility maps with three classes in terms of model performance and visualization."

can be confirmed.

8.2 Landslide susceptibility of heterogeneous regions – modelling, performance assessment and uncertainties

The proposed study design of fitting a susceptibility model within different modelling domains was a step forward regarding characterization of the landslide susceptibility in the study area. The findings of the variable selection confirm that within each model domain different variables were selected (Petschko et al. 2014c). Furthermore, the different characteristics of explanatory variables (e.g. slope angle) were described by other authors (Blahut et al. 2010; Muenchow et al. 2012). Additionally, not only the list of selected variables but also the form (linear or nonlinear with applying a smoothing function) of their consideration in the model changed within the different modelling domains. A similar finding was obtained in ecology studies for modelling species distribution within different modelling domains instead of the entire area at once (Osborne and Suárez-Seoane 2002). In that study, the resulting model performance measures (AUROC values) of modelling in model domains were higher than of fitting one model for the entire study area (Osborne and Suárez-Seoane 2002). These and the results of the variable selection presented in this thesis confirm the hypothesis (H2):

"Modelling the landslide susceptibility of a large heterogeneous area for maps with a scale of 1:25,000 requires a special consideration of the geotechnical and topographical conditions and their heterogeneity in the study area as the predominant preparatory and predisposing factors change with the conditions.".

The model design allows taking into account variations in geotechnical and topographical characteristics which also influence the landslide susceptibility.

8.2.1 Modelling assumption of uniformitarianism

Generalized additive models were used to include possible nonlinearity in the relationship between the explanatory and response variables. This is a simple try to move away from linear models and relationships to nonlinear models, a direction given by the new trends in systems theory (Von Elverfeldt and Glade 2011; Phillips 2006b).

However looking at the theoretical background of this thesis grounded in traditional systems theory, some questions arise regarding the main assumption of the modelling: All modelling approaches (heuristic, statistical or physically based) assume that what we learned from the past also applies for the future and that all details of nature can be identified and included in a model if there is enough time for research (Von Elverfeldt and Keiler 2008; Embleton-Hamann et al. 2013; Phillips 1999). Looking at the emerging trends in systems theory such as self-organization or complexity (Hergarten 2002; Keiler 2011; Lam 2000) these assumptions seem outdated. However, no general answer or solution has been found yet for this topic. Instead the field of uncertainty research is growing recently. More and more

researchers have a closer look on the different types of uncertainty (epistemic and aleatory) involved in their modelling and try to assess or quantify those (Hill et al. 2013). Both, the new trends in the theoretical basis of geomorphology and the uncertainty analysis have to be followed closely. New theoretical insights might open the field to new methodologies which allow a better representation of natural processes leading to slope stability or instability.

Besides a possibly changing theoretical background of the thesis it is questionable if the assumption "the past is the key to the future" still applies in times of global environmental change. Cendrero et al. (2006) point out that starting from the middle of the last century humans seem to be the dominating geomorphic agent with geomorphic process rates increasing by one or more orders of magnitude. What does this mean for the assumption of the past is the key to the future? Land use change (deforestation, afforestation, extension of settlement areas into mountainous terrain) which goes along with increased human activity is known to have a large influence on slope stability (Selby, 1993). Basing the analysis of the susceptibility (or hazard) on past events and their predisposing, preparatory and triggering factors only, might not be representative for the future behavior of landslide processes (Cendrero et al., 2006). Furthermore, the possible effects of climate change on the land use are not very well understood. A number of studies proclaim implications of climate change on natural hazards in general and on landslides (Van Beek 2002; Dixon and Brook 2007; Innocenti and Albrito 2011; Keiler et al. 2010; Stoffel et al. 2014). Yet, the statements on the extent of the change and its effects on the landslide process are unclear or even contradictory from different studies (Crozier 2010; Huggel et al. 2012; Huggel et al. 2010; Liggins et al. 2010). On top of all that, the possibility has to be considered, that the most important explanatory variable might still be missing in the analysis as it might not be known yet (Guzzetti et al. 2006; Petschko et al. 2014c).

8.2.2 K-fold cross-validation

The model form uncertainty was assessed by computing the spatial and non-spatial transferability and the thematic consistency of the model (Petschko et al. 2014c). Spatial and non-spatial repeated *k*-fold cross-validation was performed to learn about the differences of the results from these methods and to identify a preferable method. The results showed comparable median AUROC values, but better transferability and thematic consistency for non-spatial cross-validation (Petschko et al. 2014c). This was confirmed by a small range in the AUROC values obtained from non-spatial cross-validation opposed to a larger range of AUROC values resulting from spatial cross-validation (Petschko et al. 2014c). Therefore, non-spatial cross-validation might be preferred for future analysis.

However, Chung and Fabbri (2008) state that model performance assessments using random subsampling may have a tendency to estimate overoptimistic results. Furthermore, by assessing the spatial transferability, more can be learned about the

effect of using a sample of a small area for obtaining the landslide susceptibility map for the entire area. Additionally, spatial cross-validation was recommended for spatial data showing spatial autocorrelation (Brenning 2012b; Brenning 2005). Therefore, a spatial assessment of the transferability is clearly recommended (Petschko et al. 2014c).

Generally it has to be taken into account that the AUROC value is clearly dependent on the selection of the study area and the size of areas naturally not susceptible to landslides. More comparable AUROC values can be achieved by masking low-lying flat areas from the analysis as done by Van Den Eeckhaut et al. (2009a) and Goetz et al. (2011). Additionally, it may lead to smaller AUROC ranges and differences between the AUROC values of all model domains (Petschko et al. 2014c). The analysis should only be done in areas with similar characteristics of explanatory variables for landslide occurrence (e.g. related to topography or land cover; Guzzetti et al. (2006)). The spatial cross-validation will be more difficult or even fail if the training and test sample are not comparable (e.g. the test sample is missing a land cover unit; Guzzetti et al. 2006, Petschko et al. 2014c).

Summarizing the results and discussion on the hypothesis (H3), which is

"Established model performance measures change with the selection of a new random or spatial sample of landslide and non-landslide points (cells). Splitting the sample into k subsamples and repeating this sampling process multiple times results in a range opposed to a single value of performance measures."

this hypothesis can be approved.

8.2.3 Spatially varying prediction uncertainties

The visualization of the spatially varying prediction uncertainties and their effect on the classified susceptibility map are a clear step forward from previous landslide susceptibility studies (Guzzetti et al. 2006; Van Den Eeckhaut et al. 2009c; Rossi et al. 2010a; Sterlacchini et al. 2011). The presentation of a map of the class overlaps along with the original susceptibility map is easily done and rather easy to interpret (Petschko et al. 2014c). It can give a simple picture of the effect of the involved uncertainties on a grid cell level (Guzzetti et al. 2006; Luoto et al. 2010). However, the method of transferring the standard error on all grid cells has its own uncertainties (Petschko et al. 2014c). These uncertainties were estimated by obtaining the R^2 value calculated from a comparison of the trained and tested standard error on the existing samples (Petschko et al. 2014c). The results give different R^2 values of the modelling domains indicating the success of the lookup table (Petschko et al. 2014).

Other types of spatial uncertainties comparing results from different modelling methods were analyzed in literature. Sterlacchini et al. (2011) and Tilch et al. (2011) analyzed the changes of the susceptibility between different models on a grid cell

basis and also showed the variation in the assigned landslide susceptibility. However, the spatially varying prediction uncertainties of the single statistical modelling methods were not taken into account in these analyses.

8.2.4 Communication of uncertainties by visualization

In the context of this study, the resulting landslide susceptibility maps were implemented in spatial planning strategies. In that case, a misinformation about the "real" susceptibility class may result in an underestimation of the landslide susceptibility by the mayor or land owner (Petschko et al. 2014c). In these cases knowing about possible class overlaps might help to direct more caution or detailed slope stability investigations more straight forward (Petschko et al. 2014c). Furthermore, information on areas without class overlaps is also given, which might help to avoid additional costs for geotechnical investigations (Elith et al. 2002; Petschko et al. 2014c).

The preparation of a map showing susceptibility class overlaps may lead to a better understanding and acceptance of involved uncertainties (Petschko et al. 2014c). It forms a first step towards open communication of research results, their uncertainties and limitations with user-friendly explanations or visualizations (Petschko et al. 2014c). This aids raising awareness and knowledge about uncertainties and is a starting point for discussions on acceptable levels of uncertainty in the decision making process (Brierley 2009; Hill et al. 2013; Knuepfer and Petersen 2002; Rogers 2006).

It remains unclear whether information on uncertainties is wanted by the stakeholders or not, as contradictory and controversial statements can be found in literature. While a rising confidence in modelling results was observed if uncertainties were presented to policy makers (Brugnach et al. 2006), others found that the stakeholders have no interest in the uncertainties of the modelling result (Klimeš and Blahůt 2012). In ecological modelling Elith et al. (2002) reported about the benefit of visualizing uncertainty to inform decision makers. With not giving an impression of certainty, the users learned about areas with extreme error, including areas with very low uncertainties in the modelling (Elith et al. 2002).

Maybe it is less about communicating the uncertainties in general, but more about an appropriate way of communicating them? The way of communication (e.g. by a map, interactive GIS platform or a text) should suit the understanding of the users and should allow nearly intuitive understanding of the involved uncertainties (Kunz et al. 2011). Clearly, the presentation of the uncertainties in an appropriate way has to be prepared by the scientists themselves to avoid misunderstandings or misleading oversimplification (Petschko et al. 2014c).

Nevertheless, the findings of the study show that overlaps of susceptibility classes occurred with a spatial variation. Therefore, the hypothesis (H4)

"The uncertainties of the predicted probabilities vary spatially according to the standard error of the predicted probability. Comparing classified landslide susceptibility maps derived within the 95% confidence interval results in overlaps of different susceptibility classes."

can be confirmed.

8.3 Human impact on landslides and landslide susceptibility assessments

The literature research and the analysis of the human impact in the study area gave new insight into the dimension of human impact on landslide initiation and landslide visibility in Lower Austria. The analysis of landslide catchment and the human impact on it showed the influence of the culvert on the catchment area. Furthermore, it revealed the weakness of including DTM derivatives in the landslide susceptibility modelling as these do not show channels and culverts that may be under ground. Additionally, the human impact was shown to be of high spatial and temporal variability and density, making it impalpable for a spatial consideration in regional landslide susceptibility assessments.

The analysis of the landslide persistence revealed a very fast human impact. It showed that the morphology of some landslide features was not visible on the LiDAR DTM derivatives or the orthophoto within a year (Bell et al. 2012). Reportedly, in agricultural land the farmers quickly level the land after a landslide event to ensure the agricultural use (Bell et al. 2012; Fiorucci et al. 2011). This has clear implications on the completeness of the inventory, which is of importance for the statistical susceptibility modelling and performance assessment (Petschko et al. 2014a). The landslide inventory mapped from LiDAR DTM derivatives may have a bias of an unknown extent due to missing landslides in agricultural/not-forested land (Bell et al. 2012; Petschko et al. 2014c).

The limited landslide persistence also affects the results of the relative age estimation as mainly young and very young landslides might be missing. The missing morphological and vegetation footprint make the landslide mapping and age estimation impossible from the available data sources (Petschko et al. 2014a; Petschko et al. 2014b). This might result in a bias of the landslide inventory, towards less mapped landslides within agricultural land. However, the existence of this bias has to be analyzed in further analysis which was beyond the scope of this study.

8.3.1 What is an adequate sample size for statistical modelling?

While the presence of a bias is unclear, it is clear that within statistical modelling and model performance assessment a minimum number of landslide samples are needed. The performed analysis with *k*-fold cross-validation within 16 modelling domains and the tests of minimizing the sample size within the Flysch Zone gave some idea on a minimum sample size necessary for the applied methodology. From the *k*-fold cross-validation a trend towards the larger the sample the better the transferability and thematic consistency of the model could be observed (Petschko et al. 2014c). Also other studies showed this relationship between model performance and sample size (Heckmann et al. 2014; Hjort and Marmion 2008; Stockwell and Peterson 2002). However, not all modelling domains followed this trend (Petschko et al. 2014c). The transferability index was less strongly related to the sample size than the thematic consistency (Petschko et al. 2014c). Consequently giving a recommendation on the minimum sample size is not as easy as expected from the results of the *k*-fold cross-validation within the modelling domains (Petschko et al. 2014c). According to the results, a dependency of the obtained quality estimates (transferability index, consistency index and prediction uncertainty) on the modelling domain size and landslide density might be present (Petschko et al. 2014c). Furthermore, the local terrain conditions and their homogeneity in the modelling domain might be of importance (Petschko et al. 2014c). These possible dependencies might be the reason for a blurry signal regarding minimal sample size from comparing the results from the modelling domains (Petschko et al. 2014c).

A more systematic assessment of the effect of reducing the sample size on the model performance was performed within the Flysch Zone (Petschko et al. 2014c). The median AUROC values generally remained satisfactory high even with having only 50 samples available (Petschko et al. 2014c). However, the interquartile range of the AUROC value increased indicating a decreasing transferability of the model (Petschko et al. 2014c). According to these findings a minimum sample size of 400 slide and non-slide grid cells might be recommended for the methods applied in this study. Using a sample size of 400 gives a substantially better transferability of the model and a high median AUROC value compared to using smaller sample sizes (200, 100, 50 landslide and non-landslide samples; Petschko et al. 2014c). Furthermore, the thematic consistency is satisfactory high (Petschko et al. 2014c).

Some studies using a variety of susceptibility modelling methods have illustrated that landslide susceptibility can be successfully modelled from very small samples (Demoulin and Chung 2007; Van Den Eeckhaut et al. 2006). The model performance assessment was changed to a leave one out strategy which yielded satisfactory model performance measures (Demoulin and Chung 2007). Accordingly, a different modelling and performance assessment method might be more successful in correctly computing landslide susceptibility and advised for smaller sample sizes (Petschko et al. 2014c). Nevertheless, with a small sample size it might be more difficult to obtain a substantially complete sample representing all local terrain conditions (e.g. land cover units; Heckmann et al. 2014; Malamud et al. 2004).

Summarizing the results of this study and Heckmann et al. (2014), a range of the transferability and thematic consistency of the model was found that could not be avoided with large sample sizes (Heckmann et al. 2014; Petschko et al. 2014c). Therefore, the analysis of the proposed quality measures (transferability and thematic consistency index, spatially varying prediction uncertainties) is recommended for any landslide susceptibility analysis (Heckmann et al. 2014; Petschko et al. 2014c). This is necessary to give an indication on the model form uncertainties defining the quality of the landslide susceptibility model and map (Petschko et al. 2014c).

Resuming, at the current state the hypothesis (H5)

"The human impact on landslides can be mapped and implemented in a statistical susceptibility modelling approach for large areas."

cannot be approved. However, the objectives of this hypothesis were reached by the analysis of the landslide persistence and the influence of a culvert on a landslide catchment.

9. Conclusions

Effective landslide inventory mapping on the basis of high resolution LiDAR DTM derivatives was performed within Lower Austria. Analyzing the proposed effectiveness estimate, the imperfection of all mapped inventories of different type (mapped polygons or points in the main scarp) became evident. While mapping of landslide points in the main scarp instead of entire landslide polygons only was found effective for statistical landslide susceptibility modelling, the mapping of different relative landslides ages, some of very old age, has to be kept in mind. This is particularly of importance during the pre-selection of explanatory variables for the statistical susceptibility modelling. More than half of the mapped slides were forested but the majority of young slides occurred on arable land. This contradiction led to the concluding proposal of omitting recent land cover data in statistical landslide susceptibility modelling in cases where the relative (or absolute) landslide age is unknown. This avoids the introduction of an unwanted bias into the modelling.

The quality of the inventory might be considered high because of its high precision in the location of the landslides. However, the analysis of the landslide persistence presented the sources of incompleteness of the mapped inventory. A definitive statement on the quality of the inventory cannot be made as long as the possible bias within the landslide inventory mapped from LiDAR DTM derivatives and orthophotos is not analyzed in more detail.

Within this study a reasonably feasible study design was successfully applied within a heterogeneous study area. Dividing heterogeneous areas into modelling domains by geotechnical or topographical characteristics allows the comparison of the resulting susceptibility map over the entire study area. Furthermore, it gives the flexibility to characterize the landslide susceptibility of each modelling domain appropriately. This procedure is therefore recommended even for global landslide susceptibility assessments.

While the implementation of the human impact in spatial statistical susceptibility models was not possible, new insights on the dimension of human impact were gained from the analysis. The human impact might be much more manifold as generally assumed. Within this study it was shown that the human impact acts not only on the triggering of landslides but also on their visibility in remote sensing imagery. This leads to incomplete landslide inventories, which might even carry a bias towards areas close to settlements. Furthermore, the different facets are difficult to portray within spatial landslide susceptibility analysis. The effect of a small culvert on the catchment area was exemplified. Unfortunately due to the data acquisition mechanism, culverts are usually not included in DTMs. The human impact varies spatially and temporally and is sometimes “invisible” using standard data sets. Therefore, currently human impacts cannot directly be included in the susceptibility modelling.

The systematic assessment of the landslide susceptibility model performance revealed a range of performance assessments even for very large samples of landslide and non-landslide grid cells. As this range cannot be avoided it is important to analyze it for every landslide susceptibility assessment and to communicate on this range. Other authors even recommended obtaining an assembled susceptibility map by using the median susceptibility value of all landslide susceptibility maps computed during the *k*-fold cross-validation (e.g. Heckmann et al. 2014). According to this model performance assessment, the model applied within the modelling domains might be considered as of high quality in most domains. The model form uncertainty expressed by the transferability and thematic consistency index is considered as rather low for most domains, especially those with a large sample size.

The assessment of the spatially varying prediction uncertainty gave confidence in the modelling results as for 85% of the study area no class overlaps of the maps from the upper and lower confidence limit and the predicted probability were found. However, for the remaining 15% of the study area seven different types of class overlaps including overlaps of the low with the high susceptibility class were obtained. These areas have to be considered and analyzed with care in the field in cases during area zoning activities.

All this modelling, model performance and spatially varying uncertainty assessment and visualization of the map are of no use if the results are not communicated in a user-friendly manner. The first step is an easy interpretable map providing clear instructions for actions instead of blurry statements on relative susceptibility levels. Deriving the threshold values for the three susceptibility classes according to the percentage of landslides within the susceptibility class proved of high benefit during the communication with stakeholders. Furthermore, can a well thought choice of the colors of the susceptibility classes avoid confusion of the landslide susceptibility maps with the hazard zoning maps available in Austria.

Despite some stakeholders claim that they do not want any information on uncertainties, the belief of the author of this thesis is that a communication and training regarding dealing with uncertainties has to be initiated from science and provided to the public. Only by starting to know about uncertainties and their dimension well informed weighting of accepted uncertainties can start and lead to well informed decisions of the stakeholders. Here it is the task of the scientists to empower the policy-makers and stakeholders.

Generally, the limited expressiveness of the resulting landslide susceptibility maps has to be kept in mind. As Fell et al. (2008) pointed out the statutory use of regional landslide susceptibility maps is not feasible. They can only be used as a first indication of areas possibly susceptible to landslides where more detailed slope stability investigation has to follow. Furthermore, a remaining susceptibility is included in the low susceptibility class as 5% of the landslides are contained in it. In the MoNOE project this was taken care of by the naming of the susceptibility classes by actions.

Implementing the resulting landslide susceptibility maps in spatial planning strategies is highly recommended, as it raises awareness towards the susceptibility to landslides and can aid the prevention of damage due to landslide processes.

10. Innovations - Solutions

Within this section the scientific progress in the field of landslide inventory mapping and susceptibility modelling is outlined. The key innovations and solutions found within the study are briefly described in the following.

With this research, considerations on the purpose of the landslide inventory for the aimed analysis led to the definition of an effectiveness estimate. This and the analysis of using points sampled in different locations of the landslide resulted in the identification of an effective method to map landslides over a large area (>10,000km²) on the basis of LiDAR DTM derivatives with high precision, information on single landslide events and the minimum information needed for spatial susceptibility modelling. This new landslide inventory gave information on the landslide distribution over the entire province. However, the analysis of the landslide persistence and human impact on the visibility of landslide morphology revealed sources of incompleteness of the inventory. Moreover, deeper insight into the speed of this human impact was gained.

While the minimum type of information of a landslide was identified as a point set in the main scarp, the minimum number of samples available was only identified for the specific method and setting in the study area. Resulting from the tests performed in the Flysch Zone a minimum number of 400 samples can be recommended using generalized additive models. These findings match the findings of Heckmann et al. (2014). However, a more extensive analysis in areas of different topographic characteristics would be necessary. An influence of the topography and heterogeneity of the study area on the minimum sample size for the presented study design is anticipated.

The interpretation of the relative age of the landslides based on the LiDAR DTM derivatives and a concept of McCalpin (1984) gave valuable insight into the characteristics landslide inventory. Furthermore, the comparison with recent land cover data aided the selection of explanatory variables for the statistical susceptibility modelling. This analysis clearly showed the potential of the combined analysis of LiDAR DTM derivatives and orthophotos.

The proposed model design of modelling in homogeneous model domains proved to aid a better characterization of the study area and its slope stability. This model design has large potential for future analysis of large and heterogeneous regions globally. Furthermore, it assures the comparability of the susceptibility over the different model domains.

The resulting landslide susceptibility maps for Lower Austria are a valuable addition to the existing planning instruments such as the hazard zonation plan of the Austrian Service for Torrent and Avalanche Control or the HORA platform. The landslide susceptibility maps originating from this study give spatial information on

where the occurrence of main scarps of earth and debris slides is probable. These processes were not covered extensively by previously available hazard zonation plans. Furthermore, the susceptibility maps are available for the entire study area, not only for settlement areas. This gives a better planning guide also for the design of forestry roads or other linear infrastructure.

Within this study a more robust and structured assessment of the model performance was provided by the *k*-fold cross-validation. Furthermore, the potential of testing the spatial transferability by spatial cross-validation was demonstrated. The proposed methods of spatial transferability and thematic consistency assessment provide a framework for comprehensive analysis of the quality of susceptibility maps.

Furthermore, the model form uncertainties were visualized in a map providing information on uncertainty instead of giving an impression of certainty. This assessment of the spatially varying prediction uncertainties might aid future applications of results from statistical susceptibility modelling. By showing the uncertainties on a map the discussion on the accepted degree of uncertainties can start and the public authorities are enabled to better informed decisions.

While it was not possible to integrate the human impact as a predisposing factor spatially into the statistical susceptibility modelling, the analysis showed another dimension of it. The human impact on the predisposing factors might be even more manifold as already presented in the literature. The analysis in Wilhelmsburg showed that a small culvert, which might not be represented properly in a DTM, could change the catchment area substantially. As many of these culverts are expected in the study area a detailed mapping would be necessary to integrate these into the spatial modelling properly.

11. Perspectives

The perspectives for this study are manifold and reach from more detailed and extensive analysis of different aspects covered within this study to the extension of the modelling towards a hazard or even risk map.

Reconfirmed from the experience of this research, high quality input data is really what matters in statistical landslide susceptibility analysis. Much more could be learned about the landslide initiation conditions (e.g. rainfall, land cover, land cover changes) if event landslide inventories would be available. This allows the assessment of landslide magnitude and frequency relations necessary for the landslide hazard analysis.

Although the AUROC values stayed satisfactory high while reducing the sample size substantially, its effects on the appearance of the landslide susceptibility map are

unknown. This comparison of the landslide susceptibility map derived from different sample sizes used within a test study area would be highly informative. Evaluating the geomorphic plausibility of the different maps is of high importance and might reveal new insights and maybe answers to the question about a minimum sample size necessary for statistical susceptibility modelling.

Furthermore, more details on human impact, and its spatial and temporal differing importance could enhance the susceptibility modelling. Much more needs to be known about when and which human impact alters the predisposing and preparatory factors in a way that a landslide might be triggered. Furthermore, the tam span how long human interference in the slope system is of importance is of high interest. Old aerial photographs and the LiDAR DTM might be a valuable source of spatial information on road construction, impact of bombs (e.g. during the Second World War) or the construction of drainages in the slope. Additionally, local studies monitoring slope stability of a slope affected by human impact might provide better insights into the temporal aspect.

Moreover, not only the predisposing factors might be influenced, but also the morphological footprint of a landslide. The rates of morphological change due to human impact (maybe of different kind (e.g. ploughing, levelling)) after landslide occurrence are of high interest e.g. for analyzing surface roughness within landslides. The analysis of multi temporal DTMs on a test study site might give valuable insight in the geomorphometry of a landslide under anthropogenic influence. However, as learned from the Building Ground Register, many hazards only occur after anthropogenic activity. This is where anticipatory spatial planning and building activity is demanded from the local authorities to prevent damage from landslides.

Another important explanatory variable besides the human impact is land cover. Very often only the recent land cover type is taken into account in the analysis, which might introduce an unwanted bias into the modelling. However, much more interesting might be information on areas which experienced land cover changes over a specific time span. Also the different types of changes (e.g. forest to pasture, or pasture to forest) are of high interest in combination with landslide occurrence and landslide susceptibility modelling. This information could also be extracted from the interpretation of old orthophotos. Furthermore, old forest inventory maps might be available in the region and could give information on this.

Something that has to be kept in mind is the need for a regular update of landslide susceptibility maps. Changing environmental conditions (e.g. logging, construction of roads, levelling and general changes in topography) might alter the predisposing factors sustainably. Furthermore, as the resulting susceptibility maps were implemented in municipal spatial planning the periodic review is advised (DeGraff 2012). This ensures the usage of state of the art methodology for generating these rather decisive susceptibility maps used in the planning process (DeGraff 2012).

12. References

Abteilung Feuerwehr und Zivilschutz, Amt der NÖ Landesregierung (2010) Zusammenfassung Ereignisse 2009. http://www.noe.gv.at/Land-Zukunft/Katastrophenschutz/Archiv/zusammenfassung_ereignisse_2009.wai.html. Accessed 9 Dec 2010

Akaike H (1974) A new look at the statistical model identification. IEEE Transactions on Automatic Control 19:716–723.

Aleotti P, Chowdhury R (1999) Landslide hazard assessment: summary review and new perspectives. Bulletin of Engineering Geology and the Environment 58:21–44.

Alexander D (2002) Principles of Emergency Planning and Management. Terra Publishing, Harpenden, Hertfordshire, England

Alexander D (2000) Scenario methodology for teaching principles of emergency management. Disaster Prevention and Management 9:89–97.

Amt der NÖ Landesregierung (2013) Niederösterreich Atlas. In: Niederösterreich Atlas. http://atlas.noe.gv.at. Accessed 28 Oct 2013

Anders NS, Seijmonsbergen H (2008) Laser Altimetry and Terrain Analysis - A revolution in Geomorphology. GIM International 36–39.

Anderson M, Holcombe L, Flory R, Renaud J-P (2008) Implementing low-cost landslide risk reduction: A pilot study in unplanned housing areas of the Caribbean. Natural Hazards 47:297–315.

Anderson MG, Holcombe E (2013) Community-Based Landslide Risk Reduction: Managing Disasters in Small Steps. The World Bank, Washington D.C.

Andrecs P, Hagen K, Lang E, et al. (2007) Dokumentation und Analyse der Schadensereignisse 2005 in den Gemeinden Gasen und Haslau (Steiermark). 75.

Antonini G, Ardizzone F, Cardinali M, et al. (2002) Surface deposits and landslide inventory map of the area affected by the 1997 Umbria-Marche earthquakes. Boll Soc Geol It Volume speciale n.1:843–853.

Ardizzone F, Cardinali M, Carrara A, et al. (2002) Impact of mapping errors on the reliability of landslide hazard maps. Natural Hazards and Earth System Sciences 2:3–14.

Ardizzone F, Cardinali M, Galli M, et al. (2007) Identification and mapping of recent rainfall-induced landslides using elevation data collected by airborne Lidar. Natural Hazards and Earth System Sciences 637–650.

Ardizzone F, Fiorucci F, Santangelo M, et al. (2013) Very-High Resolution Stereoscopic Satellite Images for Landslide Mapping. In: Margottini C, Canuti P, Sassa K (eds) Landslide Science and Practice. Springer Berlin Heidelberg, pp 95–101

Van Asselen S, Seijmonsbergen AC (2006) Expert-driven semi-automated geomorphological mapping for a mountainous area using a laser DTM. Geomorphology 78:309–320. doi: doi: DOI: 10.1016/j.geomorph.2006.01.037

Atkinson P, Jiskoot H, Massari R, Murray T (1998) Generalized linear modelling in geomorphology. Earth Surface Processes and Landforms 23:1185–1195.

Autonome Provinz Bozen - Südtirol (2012a) Beschluss der Landesregierung Autonome Provinz Bozen - Südtirol: Abänderung der Richtlinien zur Erstellung der

Gefahrenzonenpläne gemäß Landesraumordnungsgesetz, Landesgesetz vom 11.August 1997, Nr. 13, Artikel 22/bis. 82.

Autonome Provinz Bozen - Südtirol (2012b) Gefahrenzonen: Landesregierung für Beachtung langjähriger Erfahrung. Autonome Provinz Bozen - Südtirol - Pressemitteilungen 1.

Baeza C, Lantada N, Moya J (2010) Influence of sample and terrain unit on landslide susceptibility assessment at La Pobla de Lillet, Eastern Pyrenees, Spain. Environmental Earth Sciences 60:155–167. doi: 10.1007/s12665-009-0176-4

Bai S-B, Wang J, Lü G-N, et al. (2010) GIS-based logistic regression for landslide susceptibility mapping of the Zhongxian segment in the Three Gorges area, China. Geomorphology 115:23–31. doi: 10.1016/j.geomorph.2009.09.025

Bai SB, Wang J, Zhang FY, et al. (2008) Prediction of Landslide Susceptibility Using logistic Regression: A Case Study in Bailongjiang River Basin, China. Jinan Shandong, China, pp 647–651

Bak P (1996) How nature works. The science of self-organized criticality. Springer

Bălteanu D, Chendeş V, Sima M, Enciu P (2010) A country-wide spatial assessment of landslide susceptibility in Romania. Geomorphology 124:102–112.

Barlow J, Franklin S, Martin Y (2006) High spatial resolution satellite imagery, DEM derivatives, and image segmentation for the detection of mass wasting processes. Photogrammetric Engineering and Remote Sensing 72:687–692.

Bathurst JC, Burton A, Clarke BG, Gallart F (2006) Application of the SHETRAN basin-scale, landslide sediment yield model to the Llobregat basin, Spanish Pyrenees. Hydrol Process 20:3119–3138. doi: 10.1002/hyp.6151

Baum RL, Coe JA, Godt JW, et al. (2005) Regional landslide-hazard assessment for Seattle, Washington, USA. Landsldes 2:266–279.

Baum RL, Savage WZ, Godt JW (2002) TRIGRS - A Fortran porgram for transient rainfall infiltration and grid based regional slope stability analysis. 61.

Bayerisches Landesamt für Umwelt (LfU) (2013) GeoFachdatenAtlas des Bodeninformationssystems Bayern. In: GeoFachdatenAtlas (Bodeninformationssystem Bayern). http://www.bis.bayern.de/bis/. Accessed 25 Jun 2014

Bayerisches Landesamt für Umwelt (LfU) (2012) Gefahrenhinweiskarte Bayerische Alpen - Schutz vor Georisiken: Erfahrung und praktische Umsetzung. 40.

Van Beek LPH (2002) Assessment of the influence of changes in landuse and climate on landslide activity in a mediterranean environment. Dissertation, University of Utrecht

Van Beek LPH, Van Asch TW. (2004) Regional Assessment of the Effects of Land-Use Change on Landslide Hazard By Means of Physically Based Modelling. Natural Hazards 31:289–304. doi: 10.1023/B:NHAZ.0000020267.39691.39

Beguería S (2006a) Changes in land cover and shallow landslide activity: A case study in the Spanish Pyrenees. Geomorphology 74:196–206. doi: doi: 10.1016/j.geomorph.2005.07.018

Beguería S (2006b) Validation and Evaluation of Predictive Models in Hazard Assessment and Risk Management. Nat Hazards 37:315–329. doi: 10.1007/s11069-005-5182-6

Bell R (2007) Lokale und regionale Gefahren- und Risikoanalyse gravitativer Massenbewegungen an der Schwäbischen Alb. Rheinische Friedrich-Wilhelms-Universität Bonn

Bell R, Glade T, Granica K, et al. (2013) Landslide susceptibility maps for spatial planning in Lower Austria. In: Sassa K, Margottini C, Canuti P (eds) Landslide Science and Practice. Springer, pp 467–472

Bell R, Petschko H, Proske H, et al. (2014) Methodenentwicklung zur Gefährdungsmodellierung von Massenbewegungen in Niederösterreich – MoNOE - Endbericht. 235.

Bell R, Petschko H, Röhrs M, Dix A (2012) Assessment of landslide age, landslide persistence and human impact using airborne laser scanning digital terrain models. Geografiska Annaler: Series A, Physical Geography 94:135–156. doi: 10.1111/j.1468-0459.2012.00454.x

Bertalanffy L von (1956) General systems theory. General Systems 1:1–10.

Bertalanffy L von (1950) An outline of general systems theory. Brit J Philos Sci 1:134–165.

Beven KJ, Kirkby MJ (1979) A physically based, variable contributing area model of basin hydrology. Hydrological Sciences Bulletin 24:43–69.

Blahut J, van Westen CJ, Sterlacchini S (2010) Analysis of landslide inventories for accurate prediction of debris-flow source areas. Geomorphology 119:36–51. doi: 10.1016/j.geomorph.2010.02.017

BMLFUW (2010) Nachhaltig geschützt - Naturgefahrenmanagement im Unwetterjahr 2009. Bundesministerium für Land- und Forstwirtschaft, Umwelt und Wasserwirtschaft (Lebensministerium), Wien

Bonachea J, Bruschi VM, Hurtado MA, et al. (2010) Natural and human forcing in recent geomorphic change; case studies in the Rio de la Plata basin. Science of the Total Environment 408:2674–2695.

Booth AM, Roering JJ, Perron JT (2009) Automated landslide mapping using spectral analysis and high-resolution topographic data: Puget Sound lowlands, Washington, and Portland Hills, Oregon. Geomorphology 109:132–147.

Borga M, Tonelli F, Fontana G, Cazorzi F (2005) Evaluating the influence of forest roads on shallow landsliding. Ecological modelling 187:85–98.

Box EP (1979) Robustness in the strategy of scientific model building. Robustness in Statistics

Box EP (1976) Science and Statistics. Journal of the American Statistical Association 71:791–799.

Brabb EE (1984) Innovative approaches to landslide hazard mapping. Toronto, Canada, pp 307–324

Bracken LJ, Wainwright J (2006) Geomorphological equilibrium: myth and metaphor? Transactions of the Institute of British Geographers 31:167–178. doi: 10.1111/j.1475-5661.2006.00204.x

Brardinoni F, Slaymaker O, Hassan MA (2003) Landslide inventory in a rugged forested watershed: a comparison between air-photo and field survey data. Geomorphology 54:179–196.

Brenning A (2005) Spatial prediction models for landslide hazards: review, comparison and evaluation. Natural Hazards and Earth System Sciences 5:853–862.

Brenning A (2008) Statistical Geocomputing combining R and SAGA: The Example of Landslide susceptibility Analysis with generalized additive Models. SAGA—Seconds Out 19:23–32.

Brenning A (2012a) Spatial cross-validation and bootstrap for the assessment of prediction rules in remote sensing: the R package "sperrorest."Munich, Germany, pp 5372–5375

Brenning A (2012b) Improved spatial analysis and prediction of landslide susceptibility: Practical recommendations. Landslides and Engineered Slopes: Protecting Society through Improved Understanding. CRC Press/Balkema, Banff, Canada, pp 789–794

Brenning A (2011) RSAGA: SAGA Geoprocessing and Terrain Analysis in R.

Brenning A (2009) Benchmarking classifiers to optimally integrate terrain analysis and multispectral remote sensing in automatic rock glacier detection. Remote Sensing of Environment 113:239–247. doi: 10.1016/j.rse.2008.09.005

Brierley G (2009) Communicating Geomorphology. J of Geography in Higher Educ 33:3–17. doi: 10.1080/03098260802576899

British Geological Survey (2014) Property hazard information | Landslides (slope instability) | GeoSure | British Geological Survey (BGS). http://www.bgs.ac.uk/products/geosure/landslidesPHI.html. Accessed 1 May 2014

Brugnach M, Tagg A, Keil F, Lange WJ (2006) Uncertainty Matters: Computer Models at the Science–Policy Interface. Water Resources Management 21:1075–1090. doi: 10.1007/s11269-006-9099-y

Brunotte E (2002) Lexikon der Geographie. Spektrum, Heidelberg, Berlin

Brunsden D (1985) Landslide types, mechanisms, recognition, identification. In: Morgan CS (ed)pp 19–28

Brunsden D (1993) Mass movement; the research frontier and beyond: a geomorphological approach. Geomorphology 7:85–128. doi: 10.1016/0169-555X(93)90013-R

Brunsden D (1990) Tablets of stone: toward the ten commandments of geomorphology. Zeitschrift für Geomorpholgie 1–37.

Brunsden D (2001) A critical assessment of the sensitivity concept in geomorphology. Catena 42:99–123.

Brunsden D, Thornes JB (1979) Landscape sensitivity and change. Transactions of the Institute of British Geographers 4:463–484.

Bruschi VM, Bonachea J, Remondo J, et al. (2013) Land Management Versus Natural Factors in Land Instability: Some Examples in Northern Spain. Environmental Management 52:398–416. doi: 10.1007/s00267-013-0108-7

Buma J, van Asch T (1996) Slide (rotational). Landslide recognition: identification, movement, and clauses 43.

Burns WJ, Coe JA, Kaya BS, Ma L (2010) Analysis of Elevation Changes Detected from Multi-Temporal LiDAR Surveys in Forested Landslide Terrain in Western Oregon. Environmental & Engineering Geoscience 16:315–341.

Calvello M, Cascini L, Mastroianni S (2013) Landslide zoning over large areas from a sample inventory by means of scale-dependent terrain units. Geomorphology 33–48. doi: 10.1016/j.geomorph.2012.10.026

Cardinali M, Ardizzone F, Galli M, et al. (2000) Landslides triggered by rapid snow melting: the December 1996 – January 1997 event in Central Italy. In: Claps P, Siccardi F (eds) Proceedings 1st Plinius Conference. Bios Publisher, Cosenza, Maratea, pp 439–448

Carla R, Carrara A, Bitelli G (1997) Comparison of techniques for generating digital terrain models from contour lines. International Journal of Geographical Information Science 11:451–473.

Carrara A (1993) Uncertainty in evaluating landslide hazard and risk. Prediction and Perception of Natural Hazards. Kluwer Academic Publishers, Netherlands, pp 101–109

Carrara A (1983) Multivariate models for landslide hazard evaluation. Mathematical Geology 15:403–426.

Carrara A, Cardinali M, Guzzetti F, Reichenbach P (1995) GIS technology in mapping landslide hazard. In: Carrara A, Guzzetti F (eds) Geographical Information Systems in Assessing Natural Hazards. Kluwer Academic Publishers, Dordrecht, Netherlands, pp 135–175

Carrara A, Crosta G, Frattini P (2003) Geomorphological and historical data in assessing landslide hazard. Earth Surface Processes and Landforms 28:1125–1142. doi: 10.1002/esp.545

Carrara A, Guzzetti F, Cardinali M, Reichenbach P (1999) Use of GIS technology in the prediction and monitoring of landslide hazard. Natural Hazards 20:117–135.

Carrara A, Merenda L (1976) Landslide inventory in northern Calabria, southern Italy. Geol Soc Amer Bull 87:1153–1162. doi: doi: DOI: 10.1016/0148-9062(76)91932-X

Cascini L (2005) Risk assessment of fast landslide—from theory to practice. Proceedings of the International Conference on "Fast Slope Movements — Prediction and Prevention for Risk Mitigation."Pàtron Editore, Naples, Italy, pp 33–52

Cascini L (2008) Applicability of landslide susceptibility and hazard zoning at different scales. Engineering Geology 102:164–177. doi: 10.1016/j.enggeo.2008.03.016

Cendrero A, Remondo J, Bonachea J, et al. (2006) Sensitivity of landscape evolution and geomorphic processes to direct and indirect human influence. Geografia Fisica e Dinamica Quaternaria 29:125–137.

Česká geologická služba (2014) Svahové nestability (Slope instability). In: Map applications of the Czech Geological Survey. http://mapy.geology.cz/svahove_nestability/. Accessed 5 May 2014

Chigira M, Duan F, Yagi H, Furuya T (2004) Using an airborne laser scanner for the identification of shallow landslides and susceptibility assessment in an area of ignimbrite overlain by permeable pyroclastics. Landslides 1:203–209. doi: 10.1007/s10346-004-0029-x

Choi J, Oh H-J, Lee H-J, et al. (2012) Combining landslide susceptibility maps obtained from frequency ratio, logistic regression, and artificial neural network models using ASTER images and GIS. Engineering Geology. doi: 10.1016/j.enggeo.2011.09.011

Chorley RJ (1962) Geomorphology and general systems theory. 10.

Chorley RJ, Kennedy BA (1971) Physical Geography: A Systems Approach. Prentice-Hall, Londn

Christman MC (2000) A Review of Quadrat-Based Sampling of Rare, Geographically Clustered Populations. Journal of Agricultural, Biological, and Environmental Statistics 5:168–201. doi: 10.2307/1400530

Christopherson RW (2006) Geosystems: An introduction to physical geography. Prentice-Hall, Upper Saddle River

Chung CF, Leclerc Y (2003) Use of quantitative techniques for zoning landslide hazard.

Chung CJ, Fabbri AG (2008) Predicting landslides for risk analysis–Spatial models tested by a cross-validation technique. Geomorphology 94:438–452.

Chung CJ., Fabbri AG (2003) Validation of spatial prediction models for landslide hazard mapping. Natural Hazards 30:451–472.

Chung CJF, Fabbri AG (1999) Probabilistic prediction models for landslide hazard mapping. Photogrammetric Engineering and Remote Sensing 65:1389–1399.

Cigna F, Bianchini S, Casagli N (2012) How to assess landslide activity and intensity with Persistent Scatterer Interferometry (PSI): the PSI-based matrix approach. Landslides 10:267–283. doi: 10.1007/s10346-012-0335-7

Claessens L, Verburg P, Schoorl J, Veldkamp A (2006) Contribution of Topographically Based Landslide Hazard Modelling to the Analysis of the Spatial Distribution and Ecology of Kauri (Agathis australis). Landscape Ecol 21:63–76. doi: 10.1007/s10980-005-5769-z

CNR-IRPI-Turin (1998) Determinazione delle fasce fluviali di alcuni corsi d'acqua lombardi ai fini urbanistici: Torrente Stafora. Final report. CNR-IRPI-Turin, Torino, Italy

Cohen J (1960) A coefficient of agreement for nominal scales. Educational and Psychological Measurement 20:37–46.

Colesanti C, Wasowski J (2006) Investigating landslides with space-borne Synthetic Aperture Radar (SAR) interferometry. Engineering Geology 88:173–199. doi: 10.1016/j.enggeo.2006.09.013

Collin A (1846) Recherches Expe´rimentales sur les Glissements Spontane´s des Terrains Argileux. Carilian-Goeury et V. Dal- mont, Paris

Committee on the review of the national landslide hazards mitigation strategy, board on earth sciences and resources, division on earth and life studies NRC (2004) Partnerships for reduching landslide risk - Assessment of the national landslide hazards mitigaton strategy. National Academy Press, Washington, D.C.

Corominas J (1996) 5.5 DEBRIS SLIDE. Landslide recognition: identification, movement, and clauses 97.

Corominas J, Westen C, Frattini P, et al. (2013) Recommendations for the quantitative analysis of landslide risk. Bulletin of Engineering Geology and the Environment. doi: 10.1007/s10064-013-0538-8

Crandell DR, Mullineaux DR, Miller CD (1979) Volcanic-hazards studies in the Cascade Range of the western United States. In: Sheets PD, Grayson DK (eds) Volcanic activity and human ecology. Academic Press, pp 195–219

Crozier MJ (1986) Landslides: causes, consequences & environment. Croom Helm, London; Sydney; Dover, New Hampshire

Crozier MJ (2010) Deciphering the effect of climate change on landslide activity: A review. Geomorphology

Crozier MJ, Glade T (2005) Landslide hazard and risk: issues, concept and approach. In: Glade T, Crozier MJ, Anderson MG (eds) Landslide Hazard and Risk. John Wiley & Sons Inc., Chichester, England, pp 1–40

Cruden DM (1991) A simple definition of a landslide. Bulletin of Engineering Geology and the Environment 43:27–29.

Cruden DM, Varnes DJ (1996) Landslide types and processes. In: Turner AK, Schuster RL (eds) Landslides, Investigation and Mitigation. Transportation Research Board Special Report 247, Washington D.C, pp 36–75

Dai FC, Lee CF (2002) Landslide characteristics and slope instability modeling using GIS, Lantau Island, Hong Kong. Geomorphology 42:213–228.

Dalyot S, Keinan E, Doytsher Y (2008) Landslide Morphology Analysis Model Based on LiDAR and Topographic Dataset Comparison. Surveying and Land Information Science 68:155–170.

Damm A, Eberhard K, Patt A (2010) Risikowahrnehmung von Erdrutschen: Ergebnisse einer empirischen Untersuchung in der Südoststeiermark. 30.

Davis JC, Chung C-J, Ohlmacher GC (2006) Two models for evaluating landslide hazards. Computers & Geosciences 32:1120–1127. doi: 10.1016/j.cageo.2006.02.006

Deadman B (2014) How Politics Buries Science in Landslide Mapping. In: NBC News. http://www.nbcnews.com/news/investigations/how-politics-buries-science-landslide-mapping-n73256. Accessed 16 Apr 2014

DeGraff JV (2012) Solving the dilemma of transforming landslide hazard maps into effective policy and regulations. Natural Hazards and Earth System Science 12:53–60. doi: 10.5194/nhess-12-53-2012

Demoulin A, Chung C-JF (2007) Mapping landslide susceptibility from small datasets: A case study in the Pays de Herve (E Belgium). Geomorphology 89:391–404. doi: 10.1016/j.geomorph.2007.01.008

Van Den Eeckhaut M, Kerle N, Poesen J, Hervás J (2012) Object-oriented identification of forested landslides with derivatives of single pulse LiDAR data. Geomorphology 173-174:30–42. doi: 10.1016/j.geomorph.2012.05.024

Van Den Eeckhaut M, Moeyersons J, Nyssen J, et al. (2009a) Spatial patterns of old, deep-seated landslides: A case-study in the northern Ethiopian highlands. Geomorphology 105:239–252.

Van Den Eeckhaut M, Muys B, Van Loy K, et al. (2009b) Evidence for repeated re-activation of old landslides under forest. Earth Surface Processes and Landforms 34:352–365. doi: 10.1002/esp.1727

Van Den Eeckhaut M, Poesen J, Vandekerckhove L, et al. (2010) Human–environment interactions in residential areas susceptible to landsliding: the Flemish Ardennes case study. Area 42:339–358.

Van Den Eeckhaut M, Poesen J, Verstraeten G (2007) Opstellen van een gevoeligheidskaart met betrekking tot massabewegingen (masstransport) voor de Vlaamse Ardennen. Departement Leefmilieu, Natuur en Energie, Afdeling Land en Bodembescherming, Ondergrond, Natuurlijke Rijkdommen

Van Den Eeckhaut M, Poesen J, Verstraeten G, et al. (2005) The effectiveness of hillshade maps and expert knowledge in mapping old deep-seated landslides. Geomorphology 67:351–363.

Van Den Eeckhaut M, Reichenbach P, Guzzetti F, et al. (2009c) Combined landslide inventory and susceptibility assessment based on different mapping units: an example from the Flemish Ardennes, Belgium. Natural Hazards and Earth System Sciences 9:507–521.

Van Den Eeckhaut M, Vanwalleghem T, Poesen J, et al. (2006) Prediction of landslide susceptibility using rare events logistic regression: a case-study in the Flemish Ardennes (Belgium). Geomorphology 76:392–410.

Dietrich WE, Dietrich R, Real de Asua R, et al. (1998) A validation study of the shallow slope stability model, SHALSTAB, in forested lands of Northern California. 59.

Dikau R (1996) Landslide recognition: identification, movement, and clauses. Wiley

Dikau R (1998) The need for field evidence in modelling landform evolution. In: Hergarten S, Neugebauer HJ (eds) Process Modelling and Landform Evolution. Springer, Berlin, pp 3–12

Dikau R (2006) Komplexe Systeme in der Geomorphologie. Mitteilungen der Österreichischen Geographischen Gesellschaft 148:125–150.

District of North Vancouver (2014) GEOweb - Hazards. In: District of North Vancouver's GIS Website. http://www.geoweb.dnv.org/applications/hazardsapp/. Accessed 1 May 2014

Dixon N, Brook E (2007) Impact of predicted climate change on landslide reactivation: case study of Mam Tor, UK. Landslides 4:137–147. doi: 10.1007/s10346-006-0071-y

Dlugosz M (2009) Landslide susceptibility zoning in the Polish Flysch Carpathians. Zeitschrift für Geomorphologie, Supplementary Issues 2:49–56.

Draper D (1995) Assessment and Propagation of Model Uncertainty. Journal of the Royal Statistical Society Series B (Methodological) 57:45–97. doi: 10.2307/2346087

Duman TY, Çan T, Emre \Ö, et al. (2005) Landslide inventory of northwestern Anatolia, Turkey. Engineering Geology 77:99–114.

Duncan JM (1992) State-of-the-art: static stability and deformation analysis. Stability and performance of slopes and embankments-II. Geotechnical Engineering Division Special Publication 31:222–266.

Eder A, Sotier B, Klebiner K, et al. (2011) Hydrologische Bodenkenndaten der Böden Niederösterreichs (HydroBodNÖ) (Data on hydrological soil characteristics of soils in Lower Austria). 185.

Den Eeckhaut MV, Marre A, Poesen J (2010) Comparison of two landslide susceptibility assessments in the Champagne–Ardenne region (France). Geomorphology 115:141–155. doi: 10.1016/j.geomorph.2009.09.042

Eeckhaut MVD, Poesen J, Verstraeten G, et al. (2007) Use of LIDAR-derived images for mapping old landslides under forest. Earth Surf Process Landforms 32:754–769. doi: 10.1002/esp.1417

Egner H (2010) Theoretische Geographie. WBG (Wissenschaftliche Buchgesellschaft), Darmstadt, Deutschland

Egner H (2012) Riskante Räume: Zur Konstruktion verräumlichter Risken und Sicherheiten.

Egner H, Von Elverfeldt K (2009) A bridge over troubled waters? Systems theory and dialogue in geography. Area 41:319–328. doi: 10.1111/j.1475-4762.2008.00874.x

Egner H, Pott A (2010) Risiko und Raum: Das Angebot einer Beobachtungstheorie. In: Egner H, Pott A (eds) Geographische Risikoforschung - Zur Konstruktion verräumlichter Risiken und Sicherheiten. Franz Steiner Verlag, Stuttgart, pp 9–35

Eisinger U, Gutdeutsch R, Hammerl C (1992) Beiträge zur Erdbebengeschichte von Niederösterreich. Amt der NÖ Landesregierung, Landesamtsdirektion, Wien

Elith J, Burgman MA, Regan HM (2002) Mapping epistemic uncertainties and vague concepts in predictions of species distribution. Ecological modelling 157:313–329.

Von Elverfeldt K (2012) Systems Theory in Geomorphology. Challenges, Epistemological Consequences and Practical Implications. Springer, Dordrecht, Netherlands

Von Elverfeldt K, Glade T (2011) Systems theory in Geomorphology. A challenge. Zeitschrift für Geomorphologie, Supplementary Issues 55:87–108.

Von Elverfeldt K, Keiler M (2008) Offene Systeme und ihre Umwelt. Systemperspektiven in der Geomorphologie. In: Egner H, Ratter BMW, Dikau R (eds) Umwelt als System – System als Umwelt? Systemtheorie auf dem Prüfstand. oekom verlag, Deutschland, pp 75–102

Embleton-Hamann C, Von Elverfeldt K, Keiler M (2013) Geomorphologie in Stichworten. Band 1: Theorie, Methoden, endogene Prozesse, 7th ed. Borntraeger, Berlin, Stuttgart

Evans NC, King JP (1998) The natural terrain landslide study - Debris avalanche susceptibility. 96.

Ewen J, Parkin G, O'Connell P (2000) SHETRAN: Distributed River Basin Flow and Transport Modeling System. J Hydrol Eng 5:250–258. doi: 10.1061/(ASCE)1084-0699(2000)5:3(250)

Fabbri AG, Chung CJ (2009) Training decision-makers in hazard spatial prediction and risk assessment: ideas, tools, strategies and challenges. pp 285–296

Fabbri AG, Chung CJF, Cendrero A, Remondo J (2003) Is prediction of future landslides possible with a GIS? Natural Hazards 30:487–503.

Federal Ministry of Agriculture, Forestry, Environment and Water Management (2014) eHORA - Natural Hazard Overview & Risk Assessment Austria. http://www.hora.gv.at/. Accessed 22 May 2014

Federal Ministry of Finance (2014a) Katastrophenfondsgesetz 1996, 10.Bericht des Bundesministeriums für Finanzen. 12.

Federal Ministry of Finance (2012) Der Katastrophenfonds in Österreich.

Federal Ministry of Finance (2014b) BMF - Fiscal Federalism. In: Budget and Economic Policy. https://english.bmf.gv.at/budget-economic-policy/Fiscal-Federalism.html#Natural_Disaster_Fund_. Accessed 22 May 2014

Felicísimo ÁM, Cuartero A, Remondo J, Quirós E (2012) Mapping landslide susceptibility with logistic regression, multiple adaptive regression splines, classification and regression trees, and maximum entropy methods: a comparative study. Landslides 10:175–189. doi: 10.1007/s10346-012-0320-1

Fell R, Corominas J, Bonnard C, et al. (2008) Guidelines for landslide susceptibility, hazard and risk zoning for land use planning. Engineering Geology 102:85–98. doi: doi: DOI: 10.1016/j.enggeo.2008.03.022

Fernández T, Irigaray C, El Hamdouni R, Chacón J (2003) Methodology for landslide susceptibility mapping by means of a GIS. Application to the Contraviesa area (Granada, Spain). Natural Hazards 30:297–308.

Fiorucci F, Cardinali M, Carlà R, et al. (2011) Seasonal landslide mapping and estimation of landslide mobilization rates using aerial and satellite images. Geomorphology 129:59–70. doi: doi: DOI: 10.1016/j.geomorph.2011.01.013

Frattini P, Crosta G, Carrara A (2010) Techniques for evaluating the performance of landslide susceptibility models. Engineering geology 111:62–72.

Fritz P (2005) Die Wienerwald-Konferenz. In: Brunner K, Schneider P (eds) Umwelt Stadt - Geschichte des Natur- und Lebensraumes Wien. Böhlau Verlag Ges.m.b.H. & Co.KG, Wien - Köln - Weimar, pp 351–354

Galli M, Ardizzone F, Cardinali M, et al. (2008) Comparing landslide inventory maps. Geomorphology 94:268–289. doi: doi: DOI: 10.1016/j.geomorph.2006.09.023

Gaprindashvili G (2011) Report on the 1st project of AES Geohazards Stream. 15.

García-Ruiz JM, Beguería S, Alatorre LC, Puigdefábregas J (2010) Land cover changes and shallow landsliding in the flysch sector of the Spanish Pyrenees. Geomorphology 124:250–259. doi: doi: 10.1016/j.geomorph.2010.03.036

Geological Survey of Ireland (2014a) GSI Web - Landslide Susceptibility. In: Landslide Susceptibility. https://www.gsi.ie/Programmes/Quaternary+Geotechnical/Projects/Landslide+Susceptibility.htm. Accessed 1 May 2014

Geological Survey of Ireland (2014b) GSI Landslides Viewer. In: Irish landslides database. http://spatial.dcenr.gov.ie/GeologicalSurvey/LandslidesViewer/index.html. Accessed 1 May 2014

Ghosh S, van Westen CJ, Carranza EJM, et al. (2012) Generating event-based landslide maps in a data-scarce Himalayan environment for estimating temporal and magnitude probabilities. Engineering Geology 128:49–62.

Gibson AD, Culshaw MG, Dashwood C, Pennington CVL (2012) Landslide management in the UK—the problem of managing hazards in a “low-risk” environment. Landslides 10:599–610. doi: 10.1007/s10346-012-0346-4

Glade T (2003) Landslide occurrence as a response to land use change: a review of evidence from New Zealand. Catena 297–314.

Glade T (1996) The temporal and spatial occurrence of landslide-triggering rainstorms in New Zealand. Heidelberger Geographische Arbeiten 104:237–250.

Glade T, Anderson MG, Crozier, M.J. (2005) Landslide Hazard and Risk. John Wiley & Sons, Ltd, Chichester, England

Glade T, Crozier MJ (2005) The nature of landslide hazard impact. In: Glade T, Anderson M, Crozier, M.J. (eds) Landslide Hazard and Risk. John Wiley & Sons, Ltd, Chichester, England, pp 43–74

Glade T, Frances F, Albini P (2001) The use of historical data in natural hazard assessments. Kluwer Academic Publishers

Glenn NF, Streutker DR, Chadwick DJ, et al. (2006) Analysis of LiDAR-derived topographic information for characterizing and differentiating landslide morphology and activity. Geomorphology 73:131–148.

Goetz JN (2012) Natural and anthropogenic controls of landslides on Vancouver Island. Master thesis, University of Waterloo

Goetz JN, Guthrie RH, Brenning A (2011) Integrating physical and empirical landslide susceptibility models using generalized additive models. Geomorphology 129:376–386.

Gokceoglu C (2012) Discussion on "Combining landslide susceptibility maps obtained from frequency ratio, logistic regression, and artificial neural network models using ASTER images and GIS" by Choi et al. (2012), Engineering Geology, 124, 12–23. Engineering Geology 129-130:104–105. doi: 10.1016/j.enggeo.2012.01.008

Goodman RE, Shi G (1985) Block theory and its applications to rock engineering. Prentice Hall, Englewood Cliffs, New Jersey, USA

Gottschling P (2006) Massenbewegungen. Geologie der Bundesländer - Niederösterreich. Geologische Bundesanstalt, Wien, pp 335–340

Gottschling P (2002) Risikomanagement bei Naturgefahren aus der Sicht eines Landesdienstes. Berichte der Geologischen Bundesanstalt Berichte der Geologischen Bundesanstalt:20–22.

Guisan A, Edwards TC, Hastie T (2002) Generalized linear and generalized additive models in studies of species distributions: setting the scene. Ecological modelling 157:89–100.

Guns M, Vanacker V (2012) Logistic regression applied to natural hazards: rare event logistic regression with replications. Natural Hazards and Earth System Science 12:1937–1947. doi: 10.5194/nhess-12-1937-2012

Guthrie RH (2002) The effects of logging on frequency and distribution of landslides in three watersheds on Vancouver Island, British Columbia. Geomorphology 43:273–292. doi: doi: 10.1016/S0169-555X(01)00138-6

Guzzetti F (2005) Landslide hazard and risk assessment. Dissertation, Rheinischen Friedrich-Wilhelms-Universität Bonn

Guzzetti F, Cardinali M, Reichenbach P, Carrara A (2000) Comparing Landslide Maps: A Case Study in the Upper Tiber River Basin, Central Italy. Environmental Management 25:247–263. doi: 10.1007/s002679910020

Guzzetti F, Carrara A, Cardinali M, Reichenbach P (1999) Landslide hazard evaluation: a review of current techniques and their application in a multi-scale study, Central Italy. Geomorphology 31:181–216.

Guzzetti F, Mondini A, Cardinali M, et al. (2012) Landslide inventory maps: New tools for an old problem. Earth-Science Reviews 112:42–66. doi: 10.1016/j.earscirev.2012.02.001

Guzzetti F, Reichenbach P, Ardizzone F, et al. (2006) Estimating the quality of landslide susceptibility models. Geomorphology 81:166–184.

Guzzetti F, Reichenbach P, Cardinali M, et al. (2003) The impact of landslides in the Umbria region, central Italy. Natural Hazards and Earth System Science 3:469–486.

Haneberg WC, Creighton AL, Medley EW, Jonas DA (2005) Use of LiDAR to assess slope hazards at the Lihir gold mine, Papua New Guinea.

Harp EL, Keefer DK, Sato HP, Yagi H (2011) Landslide inventories: The essential part of seismic landslide hazard analyses. Engineering Geology

Hastie T, Tibshirani R (1990) Generalized additive models. Chapman & Hall/CRC, London

Heckmann T, Gegg K, Gegg A, Becht M (2014) Sample size matters: investigating the effect of sample size on a logistic regression susceptibility model for debris flows. Natural Hazards and Earth System Science 14:259–278. doi: 10.5194/nhess-14-259-2014

Heil B, Petzold I, Romang H, Hess J (2014) The common information platform for natural hazards in Switzerland. Natural Hazards 70:1673–1687. doi: 10.1007/s11069-010-9606-6

Helton JC, Johnson JD, Oberkampf WL, Sallaberry CJ (2010) Representation of analysis results involving aleatory and epistemic uncertainty. International Journal of General Systems 39:605–646. doi: 10.1080/03081079.2010.486664

Hergarten S (2002) Self-organized criticality in earth systems. Springer

Herrera G, Notti D, García-Davalillo JC, et al. (2010) Analysis with C- and X-band satellite SAR data of the Portalet landslide area. Landslides 8:195–206. doi: 10.1007/s10346-010-0239-3

Hervás J (2003) Lessons Learnt from Landslide Disasters in Europe. 101.

Highland LM, Bobrowsky P (2008) The landslide handbook - A guide to understanding landslides. U.S. Geological Survey, Reston, Virginia

Hill LJ, Sparks RSJ, Rougier JC (2013) Risk assessment and uncertainty in natural hazards. In: Rougier JC, Sparks RSJ, Hill LJ (eds) Risk and uncertainty assessment for natural hazards. Cambridge University Press, Cambridge, pp 1–18

Hjort J, Marmion M (2008) Effects of sample size on the accuracy of geomorphological models. Geomorphology 102:341–350. doi: 10.1016/j.geomorph.2008.04.006

Ver Hoef J (2002) Sampling and geostatistics for spatial data. Ecoscience 9:152–161.

Hoffman FO, Hammonds JS (1994) Propagation of uncertainty in risk assessments: the need to distinguish between uncertainty due to lack of knowledge and uncertainty due to variability. Risk Analysis 14:707–712.

Hora SC (1996) Aleatory and epistemic uncertainty in probability elicitation with an example from hazardous waste management. Reliability Engineering & System Safety 54:217–223.

Hornich R, Adelwöhrer R (2010) Landslides in Styria in 2009 / Hangrutschungsereignisse 2009 in der Steiermark. Geomechanics and Tunnelling 3:455–461. doi: 10.1002/geot.201000042

Hosmer DW, Lemeshow S (2000) Applied logistic regression. Wiley, New York, NY

Huber KH (1999) Zum Formenschatz der Granitverwitterung und -abtragung im nordwestlichen Waldviertel. In: Steininger F (ed) Erdgeschichte des Waldviertels, 2nd ed. Waldviertler Heimatbund, Horn, pp 113–132

Huggel C, Clague JJ, Korup O (2012) Is climate change responsible for changing landslide activity in high mountains? Earth Surf Process Landforms 37:77–91. doi: 10.1002/esp.2223

Huggel C, Salzmann N, Allen S, et al. (2010) Recent and future warm extreme events and high-mountain slope stability. Philosophical Transactions of the Royal Society A: Mathematical, Physical and Engineering Sciences 368:2435–2459. doi: 10.1098/rsta.2010.0078

Huggett R (2007) A history of the systems approach in geomorphology. Géomorphologie: relief, processus, environnement 145–158.

Hungr O, Corominas J, Eberhardt E (2005) Estimating landslide motion mechanisms, travel distance and velocity. In: Hungr O, Fell R, Couture R, Eberhardt E (eds) State of the Art Report (SOA4). Taylor & Francis, Vancouver, Canada, pp 99–128

Hungr O, Leroueil S, Picarelli L (2013) The Varnes classification of landslide types, an update. Landslides. doi: 10.1007/s10346-013-0436-y

Van Husen D (1987) Die Ostalpen in den Eiszeiten. Geologische Bundesantalt, Wien

Hydrographischer Dienst des Landes Niederösterreich (Hydrographic Service of Lower Austria) (2011) Wasserstandsnachrichten und Hochwasserprognosen Niederösterreich. http://www.noel.gv.at/Externeseiten/wasserstand/wiskiwebpublic/maps_N_0.htm ?entryparakey=N. Accessed 2 Mar 2011

Ibsen ML, Brunsden D (1996) The nature, use and problems of historical archives for the temporal occurrence of landslides, with specific reference to the south coast of Britain, Ventnor, Isle of Wight. Geomorphology 15:241–258.

Ibsen ML, Brunsden D, Bromhead E (1996) 53 SLAB SLIDE. Landslide recognition: identification, movement, and clauses 78.

Innocenti D, Albrito P (2011) Reducing the risks posed by natural hazards and climate change: the need for a participatory dialogue between the scientific community and policy makers. Environmental Science & Policy 14:730–733. doi: 10.1016/j.envsci.2010.12.010

IUSS Working Group WRB (2006) World reference base for soil resources: a framework for international classification, correlation and communication. Food and Agriculture Organization of the United Nations (FAO), Rome

Ivy-Ochs S, Kerschner H, Reuther A, et al. (2008) Chronology of the last glacial cycle in the European Alps. Journal of Quaternary Science 23:559–573. doi: 10.1002/jqs.1202

Jaboyedoff M, Oppikofer T, Abellán A, et al. (2010) Use of LIDAR in landslide investigations: a review. Natural Hazards 61:5–28. doi: 10.1007/s11069-010-9634-2

Jia G, Tian Y, Liu Y, Zhang Y (2008) A static and dynamic factors-coupled forecasting model of regional rainfall-induced landslides: A case study of Shenzhen. Science in China Series E: Technological Sciences 51:164–175. doi: 10.1007/s11431-008-6013-2

Johann E (2005) Das Holz-Zeitalter. Die städtische Holzversorgung vom 17. bis zum 19. Jahrhundert. In: Brunner K, Schneider P (eds) Umwelt Stadt - Geschichte des Natur- und Lebensraumes Wien. Böhlau Verlag Ges.m.b.H. & Co.KG, Wien - Köln - Weimar, pp 170–175

Kainz I (1979) Die Entwicklung der Kommassierung im nordöstlichen Niederösterreich. Diplomarbeit, Wirtschaftsuniversität

Kanton Bern (2014) Geoportal des Kantons Bern / Naturgefahrenkarten. In: Naturgefahrenportal Kanton Bern. http://www.map.apps.be.ch/pub/synserver?project=a42pub_gk5&userprofile=geo &language=de. Accessed 5 May 2014

Karam KS (2005) Landslide hazards assessment and uncertainties. PhD Thesis, Massachusetts Institute of Technology

Keiler M (2011) Geomorphology and Complexity – inseparably connected? Zeitschrift für Geomorphologie, Supplementary Issues 55:233–257. doi: 10.1127/0372-8854/2011/0055S3-0060

Keiler M, Knight J, Harrison S (2010) Climate change and geomorphological hazards in the eastern European Alps. Philosophical Transactions of the Royal Society A:

Mathematical, Physical and Engineering Sciences 368:2461–2479. doi: 10.1098/rsta.2010.0047

Kienholz H, Krummenacher B, Kipfer A, Perret S (2004) Aspects of integral risk managment in practice - considerations with respect to mountain hazards in Switzerland. Österreichische Wasser- und Abfallwirtschaft 56:43–50.

Kirkby MJ (1973) Landslides and weathering rates. Geología applicata e idrogeologia 8:171–183.

Klimeš J, Blahůt J (2012) Landslide risk analysis and its application in regional planning: an example from the highlands of the Outer Western Carpathians, Czech Republic. Natural Hazards. doi: 10.1007/s11069-012-0339-6

Knuepfer PL., Petersen JF (2002) Geomorphology in the public eye: policy issues, education, and the public. Geomorphology 47:95–105. doi: 10.1016/S0169-555X(02)00089-2

Kociu A (2013) Fragen zu GEORIOS Daten.

Kociu A, Kautz H, Tilch N, et al. (2007) Massenbewegungen in Österreich. Jahrbuch der Geologischen Bundesanstalt. Geologische Bundesanstalt, Wien, pp 215–220

Kohavi R (1995) A study of cross-validation and bootstrap for accuracy estimation and model selection. pp 1137–1145

Kraus R (1997) Kommassierung gestern - heute - morgen: Hintergründe und Problematik der Agrarverfahren mit besonderer Berücksichtigung Niederösterreichs. WWF Österreich, Wien

Krebs CJ (1999) Ecological Methodology, 2nd edition. Addison-Wesley Educational Publishers Inc., Benjamin Cummings, Menlo Park, CA

Krejci O, Jurova Z, Rybar J (2002) Slope instability hazard evaluation in the Flysch Western Carpathians (Czech Republic). In: McInnes RG, Jakeways J (eds) Instability - Planning and Management. Thomas Telford Publ., London, pp 305–312

Kunz M, Grêt-Regamey A, Hurni L (2011) Visualization of uncertainty in natural hazards assessments using an interactive cartographic information system. Natural Hazards 59:1735–1751. doi: 10.1007/s11069-011-9864-y

Kuriakose SL, van Beek LPH, van Westen CJ (2009) Parameterizing a physically based shallow landslide model in a data poor region. Earth Surface Processes and Landforms 34:867–881. doi: 10.1002/esp.1794

Kurz W (2012) Erstellung einer digitalen, strukturgeologischen, tektonischen Karte von Niederösterreich (Endbericht). 14.

Lam L (2000) How nature self-organizes - Active walks in complex systems. Skeptic 71–77.

Landesamt für Geologie, Rohstoffe und Bergbau (LGRB) (2014) Ingenieurgeologische Gefahrenhinweiskarte von Baden-Württemberg - Kartenviewer. In: Ingenierugeologische Gefahrenhinweiskarte von Baden-Württemberg. http://geogefahren.lgrb-bw.de/. Accessed 6 May 2014

Landtag von Niederösterreich (1976) NÖ Raumordnungsgesetz 1976 (NÖ ROG 1976). 66.

Lang A, Moya J, Corominas J, et al. (1999) Classic and new dating methods for assessing the temporal occurrence of mass movements. Geomorphology 30:33–52.

Larsen MC (2008) Rainfall-triggered landslides, anthropogenic hazards, and mitigation strategies. Advances in Geosciences 14:147–153.

Lee S, Ryu J-H, Kim I-S (2007) Landslide susceptibility analysis and its verification using likelihood ratio, logistic regression, and artificial neural network models: case study of Youngin, Korea. Landslides 4:327–338. doi: 10.1007/s10346-007-0088-x

Leica Geosystems (2003) ALS50 Airborne Laser Scanner, product description. 10.

Lenhardt W (2006) Erdbeben. Geologie der Bundesländer - Niederösterreich. Geologische Bundesanstalt, Wien, pp 259–265

Leopold LB, Wolman MG, Miller JP (1964) Fluvial processes in geomorphology. Freeman, San Francisco

Leopold P (2012) Kriechbewegungen in den neogenen Beckensedimenten des Burgenlandes. Verbreitung, Vergleich natürlicher Einflussfaktoren, Bewegungsmechanismen und Auslöser. Dissertation, Universität Wien

Lettner C, Wrbka T (2011) Historical Development of the Cultural Landscape at the Northern Border of the Eastern Alps: General Trends and Regional Peculiarities. In: Balázs P, Konkoly-Gyuró E (eds)Universtiy of West Hungary Press, Sopron, Hungary, pp 109–121

LfU - Bayerisches Landesamt für Umwelt (2007) Vorhaben: "Gefahrenhinweiskarte Oberallgäu."75.

Liener S, Hunziker G (2008) Simulation of shallow landslide based on detailed elevation models. INTERPRAEVENT 2008 - Conference Proceedings. Dornbirn, Austria, pp 248–249

Liener S, Kienholz H Modellierung von flachgründigen Rutschungen mit dem Modell SLIDISP. INTERPRAEVENT 2000 - Conference Proceedings. Villach, Austria, pp 259–269

Liggins F, Betts RA, McGuire B (2010) Projected future climate changes in the context of geological and geomorphological hazards. Philosophical Transactions of the Royal Society A: Mathematical, Physical and Engineering Sciences 368:2347–2367. doi: 10.1098/rsta.2010.0072

Losey S, Wehrli A (2013) Schutzwald in der Schweiz. Vom Projekt SilvaProtect-CH zum harmonisierten Schutzwald. 29.

Luoto M, Marmion M, Hjort J (2010) Assessing spatial uncertainty in predictive geomorphological mapping: A multi-modelling approach. Computers & Geosciences 36:355–361. doi: 10.1016/j.cageo.2009.07.008

Machalek A (1986) Klima und Bioklima von Niederösterreich: Dokumentation des Arbeitskreises 1 der Akademie für Umwelt und Energie, Bioklimaforschung und Umweltmeteorologie. 87.

Malamud BD, Turcotte DL, Guzzetti F, Reichenbach P (2004) Landslide inventories and their statistical properties. Earth Surf Process Landforms 29:687–711. doi: 10.1002/esp.1064

Malet JP, Maquaire O (2009) Risk assessment methods of landslides. 29.

Mantovani F, Soeters R, Van Westen CJ (1996) Remote sensing techniques for landslide studies and hazard zonation in Europe. Geomorphology 15:213–225.

Marmion M, Hjort J, Thuiller W, Luoto M (2009) Statistical consensus methods for improving predictive geomorphology maps. Computers & Geosciences 35:615–625. doi: 10.1016/j.cageo.2008.02.024

Martha TR, Kerle N, Jetten V, et al. (2010) Characterising spectral, spatial and morphometric properties of landslides for semi-automatic detection using object-

oriented methods. Geomorphology 116:24–36. doi: 10.1016/j.geomorph.2009.10.004

Martha TR, Kerle N, van Westen CJ, et al. (2012) Object-oriented analysis of multi-temporal panchromatic images for creation of historical landslide inventories. ISPRS Journal of Photogrammetry and Remote Sensing 67:105–119. doi: 10.1016/j.isprsjprs.2011.11.004

Matthews JA, Brunsden D, Frenzel B, et al. (1997) Rapid Mass Movement as a Source of Climatic Evidence for the Holocene. Gustav Fischer Verlag, Stuttgart

McCalpin J (1984) Preliminary age classification of landslides for inventory mapping. Moscow, Idaho, pp 99–111

McKean J, Roering J (2004) Objective landslide detection and surface morphology mapping using high-resolution airborne laser altimetry. Geomorphology 57:331–351. doi: 10.1016/S0169-555X(03)00164-8

McKenna JP, Lidke DJ, Coe JA (2008) Landslides Mapped from LIDAR Imagery, Kitsap County, Washington. US Geological Survey Open-File Report 1292:81.

Mines and Geosciences Bureau (2011) Geological Database Information System of the Philippines. http://gdis.denr.gov.ph/mgbviewer/. Accessed 30 Apr 2014

Mines and Geosciences Bureau (2008) Landslide susceptibility map of Malbug Quadrangle.

Mohr O (1872) Beiträge zur Theorie des Erddruckes. Zeitschrift für Architektur und Ingenieurwesen 18:67–245.

Mohr O (1871) Beiträge zur Theorie des Erddruckes. Zeitschrift für Architektur und Ingenieurwesen 17:344.

Mondini AC, Chang K-T, Yin H-Y (2011a) Combining multiple change detection indices for mapping landslides triggered by typhoons. Geomorphology 134:440–451. doi: 10.1016/j.geomorph.2011.07.021

Mondini AC, Guzzetti F, Reichenbach P, et al. (2011b) Semi-automatic recognition and mapping of rainfall induced shallow landslides using optical satellite images. Remote Sensing of Environment 115:1743–1757. doi: doi: 10.1016/j.rse.2011.03.006

Mosleh A (1986) Hidden sources of uncertainty: judgment in the collection and analysis of data. Nuclear Engineering and Design 93:187–198.

Muenchow J, Brenning A, Richter M (2012) Geomorphic process rates of landslides along a humidity gradient in the tropical Andes. Geomorphology 139-140:271–284. doi: 10.1016/j.geomorph.2011.10.029

Müllner H (1990) Kommassierung: Verfahren, Mängelbehebung, Kosten. Amt der NÖ Landesregierung, Wien

Murray AB, Coco G, Goldstein EB (2014) Cause and effect in geomorphic systems: Complex systems perspectives. Geomorphology 1–9. doi: 10.1016/j.geomorph.2014.03.001

Nadim F, Einstein H, Roberds W (2005) Probabilistic stability analysis for individual slopes in soil and rock. State of the Art Report (SOA3). Proceedings of the International Conference on "Landslide Risk Management."Taylor & Francis, Vancouver, Canada, pp 63–98

Nefeslioglu HA, Gokceoglu C, Sonmez H (2008) An assessment on the use of logistic regression and artificial neural networks with different sampling strategies for

the preparation of landslide susceptibility maps. Engineering Geology 97:171–191. doi: 10.1016/j.enggeo.2008.01.004

Neuhäuser B, Damm B, Terhorst B (2012) GIS-based assessment of landslide susceptibility on the base of the Weights-of-Evidence model. Landslides 9:511–528. doi: 10.1007/s10346-011-0305-5

Nilsen TJ, Wright RH, Vlasic TC, Spangle WE (1979) Relative slope stability and land-use planning in the San Francisco Bay region, California. 96.

Oberkampf WL, Helton JC, Joslyn CA, et al. (2004) Challenge problems: uncertainty in system response given uncertain parameters. Reliability Engineering & System Safety 85:11–19. doi: 10.1016/j.ress.2004.03.002

Optech (2008a) ALTM 3100. 2.

Optech (2008b) ALTM Gemini. 2.

Orme AR (2002) Shifting paradigms in geomorphology: the fate of research ideas in an educational context. Geomorphology 47:325–342.

Osborne PE, Suárez-Seoane S (2002) Should data be partitioned spatially before building large-scale distribution models? Ecological Modelling 157:249–259.

Österreichisches Institut für Wirtschaftsforschung (1955) Die Kommassierung - Ein Mittel zur Steigerung der Landwirtschaftserträge. 7.

Pack RT, Tarboton DG, Goodwin CN (1998) The SINMAP approach to terrain stabiltiy mapping.

Pack RT, Tarboton DG, Goodwin CN, Prasad A (2005) SINMAP 2 - A stability index approach to terrain stability hazard mapping. 73.

Packard NH, Wolfram S (1985) Two-dimensional cellular automata. Journal of Statistical Physics 38:901–946.

Park N -W., Chi K -H. (2008) Quantitative assessment of landslide susceptibility using high-resolution remote sensing data and a generalized additive model. International Journal of Remote Sensing 29:247–264. doi: 10.1080/01431160701227661

Pearce L (2005) The value of public participation during a hazard, impact, risk and vulnerability (HIRV) analysis. Mitigation and Adaptation Strategies for Global Change 10:411–441.

Pearce L (2003) Disaster management and community planning, and public participation: how to achieve sustainable hazard mitigation. Natural hazards 28:211–228.

Pereira S, Zêzere JL, Quaresma ID, Bateira C (2014) Landslide incidence in the North of Portugal: Analysis of a historical landslide database based on press releases and technical reports. Geomorphology In Press. doi: 10.1016/j.geomorph.2014.02.032

Petley D (2012) Global patterns of loss of life from landslides. Geology. doi: 10.1130/G33217.1

Petschko H, Bell R, Glade T (2014a) Landslide inventory mapping for large regions – effectiveness of visually analyzing LiDAR DTM derivatives. Landslides subm.

Petschko H, Bell R, Glade T (2014b) Relative age estimation at landslide mapping on LiDAR derivatives – revealing the applicability of land cover data in statistical susceptibility modelling. Landslide Risk Mitigation toward a Safer Geoenvironment. Springer, p In Press

Petschko H, Bell R, Leopold P, et al. (2013) Landslide inventories for reliable susceptibility maps in Lower Austria. In: Margottini C, Canuti P, Sassa K (eds) Landslide Science and Practice. Springer, pp 281–286

Petschko H, Bell, R., Brenning A, Glade T (2012) Landslide susceptibility modeling with generalized additive models - facing the heterogeneity of large regions. In: Eberhardt E, Froese C, Turner AK, Leroueil S (eds)Taylor & Francis, Banff, Alberta, Canada, pp 769–777

Petschko H, Brenning A, Bell R, et al. (2014c) Assessing the quality of landslide susceptibility maps – case study Lower Austria. Nat Hazards Earth Syst Sci 14:95–118. doi: 10.5194/nhess-14-95-2014

Petschko H, Glade T, Bell R, et al. (2010) Landslide inventories for regional early warning systems.

Phillips JD (2009a) Changes, perturbations, and responses in geomorphic systems. Progress in Physical Geography 33:17–30. doi: 10.1177/0309133309103889

Phillips JD (2006a) Deterministic chaos and historical geomorphology: a review and look forward. Geomorphology 76:109–121.

Phillips JD (2009b) Landscape evolution space and the relative importance of geomorphic processes and controls. Geomorphology 109:79–85.

Phillips JD (1999) Earth Surface Systems - Complexity, Order and Scale. Blackwell Publishers

Phillips JD (2011) Emergence and pseudo-equilibrium in geomorphology. Geomorphology 132:319–326. doi: doi: 10.1016/j.geomorph.2011.05.017

Phillips JD (2006b) Evolutionary geomorphology: thresholds and nonlinearity in landform response to environmental change. Hydrology & Earth System Sciences 10:

Phillips JD (1992a) The end of equilibrium? Geomorphology 5:195–201. doi: 10.1016/0169-555X(92)90002-6

Phillips JD (1992b) Nonlinear dynamical systems in geomorphology: revolution or evolution? Geomorphology 5:219–229. doi: 10.1016/0169-555X(92)90005-9

Piacentini D, Troiani F, Soldati M, et al. (2012) Statistical analysis for assessing shallow-landslide susceptibility in South Tyrol (south-eastern Alps, Italy). Geomorphology 151–152:196–206. doi: 10.1016/j.geomorph.2012.02.003

Pomaroli G, Bell R, Glade T, et al. (2011) Darstellung der Gefährdung durch gravitative Massenbewegungen im Bundesland Niederösterreich als Grundlage der Raumplanung. Wildbach- und Lawinenverbau, Zeitschrift für Wildbach-, Lawinen-, Erosions- und Steinschlagschutz 74:198–212.

Potts DM (2003) Numerical analysis: a virtual dream or practical reality? Géotechnique 53:535–573.

Pradhan B (2013) A comparative study on the predictive ability of the decision tree, support vector machine and neuro-fuzzy models in landslide susceptibility mapping using GIS. Computers & Geosciences 350–365. doi: 10.1016/j.cageo.2012.08.023

Pradhan B, Lee S (2009) Landslide risk analysis using artificial neural network model focusing on different training sites. International Journal of Physical Sciences 4:001–015.

Preuth T, Glade T, Demoulin A (2010) Stability analysis of a human-influenced landslide in eastern Belgium. Geomorphology 120:38–47.

Ramml CF, Hofmann T, Wimmer-Frey I (2014) Ziegelöfen und Lehmabbaue der politischen Bezirke Mistelbach und Gänserndorf (Niederösterreich): Geschichte und Geologie. Geologische Bundesanstalt (GBA), Wien

Regmi NR, Giardino JR, McDonald EV, Vitek JD (2014) A comparison of logistic regression-based models of susceptibility to landslides in western Colorado, USA. Landslides 11:247–262. doi: 10.1007/s10346-012-0380-2

Remondo J, Bonachea J, Cendrero A (2005) A statistical approach to landslide risk modelling at basin scale: from landslide susceptibility to quantitative risk assessment. Landslides 2:321–328. doi: 10.1007/s10346-005-0016-x

Remondo J, González A, De Terán JRD, et al. (2003) Validation of landslide susceptibility maps; examples and applications from a case study in Northern Spain. Natural Hazards 30:437–449.

Rib HT, Liang T (1978) Recognition and identification. In: Schuster RL, Krizek RJ (eds) Landslide Analysis and Control. National Academy of Sciences, Washington, pp 34–80

Rickli C, Graf F (2009) Effects of forests on shallow landslides–case studies in Switzerland. For Snow Landsc Res 82:33–44.

Riegl (2010) LMS-Q560 Airborne Laser Scanner for Full Waveform Analysis. Austria, Japan, USA

Rogers KH (2006) The real river management challenge: integrating scientists, stakeholders and service agencies. River Research and Applications 22:269–280. doi: 10.1002/rra.910

Röhrs M, Dix A (2010) Rekonstruktion historischer Ereignisse. In: Bell R, Mayer J, Pohl J, et al. (eds) Integrative Frühwarnsysteme für gravitative Massenbewegungen (ILEWS). Monitoring, Modellierung, Implementierung. Klartextverlag, Essen, pp 46–61 & 261–264

Rossi M, Guzzetti F, Reichenbach P, et al. (2010a) Optimal landslide susceptibility zonation based on multiple forecasts. Geomorphology 114:129–142.

Rossi M, Witt A, Guzzetti F, et al. (2010b) Analysis of historical landslide time series in the Emilia-Romagna region, northern Italy. Earth Surf Process Landforms 35:1123–1137.

Rott H, Nagler T (2006) The contribution of radar interferometry to the assessment of landslide hazards. Advances in Space Research 37:710–719. doi: 10.1016/j.asr.2005.06.059

Rougier JC (2013) Quantifying hazard losses. In: Rougier JC, Sparks RSJ, Hill LJ (eds) Risk and uncertainty assessment for natural hazards. Cambridge University Press, Cambridge, pp 19–39

Rougier JC, Beven KJ (2013) Model and data limitations: the sources and implications of epistemic uncertainty. In: Rougier JC, Sparks RSJ, Hill LJ (eds) Risk and uncertainty assessment for natural hazards. Cambridge University Press, Cambridge, pp 19–39

Roy CJ, Oberkampf WL (2011) A comprehensive framework for verification, validation, and uncertainty quantification in scientific computing. Computer Methods in Applied Mechanics and Engineering 200:2131–2144. doi: 10.1016/j.cma.2011.03.016

Ruch C (2014) Ingenieurgeologische Gefahrenhinweiskarte von Baden-Württemberg. In: Landesamt für Geologie, Rohstoffe und Bergbau (LGRB). http://lgrb-bw.de/informationssysteme/geoanwendungen/geogefahren. Accessed 6 May 2014

Rudolf-Miklau F (2007) Austrian Service for Torrent and Avalanche Control. 13.

Von Ruette J, Papritz A, Lehmann P, et al. (2011) Spatial statistical modeling of shallow landslides—Validating predictions for different landslide inventories and rainfall events. Geomorphology 133:11–22. doi: 10.1016/j.geomorph.2011.06.010

Santacana N, Baeza B, Corominas J, et al. (2003) A GIS-based multivariate statistical analysis for shallow landslide susceptibility mapping in La Pobla de Lillet area (Eastern Pyrenees, Spain). Natural Hazards 30:281–295.

Santangelo M, Cardinali M, Rossi M, et al. (2010) Remote landslide mapping using a laser rangefinder binocular and GPS. Natural Hazards and Earth System Science 10:2539–2546. doi: 10.5194/nhess-10-2539-2010

Sapountzaki K, Wanczura S, Casertano G, et al. (2011) Disconnected policies and actors and the missing role of spatial planning throughout the risk management cycle. Natural Hazards 59:1445–1474. doi: 10.1007/s11069-011-9843-3

Sarewitz D, Pielke Jr R (1999) Prediction in science and policy. Technology in Society 21:121–133.

Scheidegger AE (1992) Limitations of the system approach in geomorphology. Geomorphology 5:213–217. doi: 10.1016/0169-555X(92)90004-8

Schicker R, Moon V (2012) Comparison of bivariate and multivariate statistical approaches in landslide susceptibility mapping at a regional scale. Geomorphology 161–162:40–57. doi: 10.1016/j.geomorph.2012.03.036

Schnabel W (2002) Geologische Karte von Niederösterreich 1:200,000.

Schnabel W (1985) Die geologischen Ursachen der Schäden an der II.Wiener Hochquellenleitung bei Scheibbs. Festschrift der MA 31: 75 Jahre II. Wiener Hochquellenleitung

Schrott L (2002) Sediment storage in a mountain catchment. Zeitschrift für Geomorpholgie 175–196.

Schulz WH (2004) Landslides mapped using LIDAR imagery, Seattle, Washington. US Geological Survey Open-File Report 1396:

Schumm SA (1979) Geomorphic thresholds: the concept and its applications. Transactions of the Institute of British Geographers 4:485–515.

Schumm SA (1991) To interpret the Earth. Ten ways to be wrong. Cambridge University Press, Cambridge

Schumm SA, Lichty RW (1965) Time, space, and causality in geomorphology. American Journal of Science 110–119.

Schwab JC, Gori PL, Jeer S (2005) Landslide Hazards and Planning. American Planning Association, Chicago

Schwarz L, Tilch N (2008) Möglichkeiten und Limitierungen der Regionalisierung mittels Neuronaler Netze am Beispiel einer Rutschungsanfälligkeitskarte für die Region Gasen-Haslau. Angewandte Geoinformatik 643–648.

Schweigl J, Hervás J (2009) Landslide Mapping in Austria. 65.

Schweizerische Eidgenossenschaft (2014) Karten der Schweiz - Schweizerische Eidgenossenschaft - map.geo.admin.ch. http://map.bafu.admin.ch/?topic=bafu&lang=de&X=190000.00&Y=660000.00&zoom=1&bgLayer=ch.swisstopo.pixelkarte-grau&catalogNodes=825,826,832,843,849,851,833,838&layers_opacity=0.75&layers=ch.bafu.silvaprotect-hangmuren. Accessed 5 May 2014

Schwenk H (1992) Massenbewegungen in Niederösterreich 1953 - 1990. Jahrbuch der Geologischen Bundesanstalt. Geologische Bundesanstalt, Wien, pp 597–660

Seibert J, Stendahl J, Sørensen R (2007) Topographical influences on soil properties in boreal forests. Geoderma 141:139–148. doi: 10.1016/j.geoderma.2007.05.013

Selby MJ (1993) Hillslope materials and processes, 2nd ed. Oxford University Press, New York

Simoni S, Zanotti F, Bertoldi G, Rigon R (2008) Modelling the probability of occurrence of shallow landslides and channelized debris flows using GEOtop-FS. Hydrological Processes 22:532–545. doi: 10.1002/hyp.6886

Singleton A, Li Z, Hoey T, Muller J-P (2014) Evaluating sub-pixel offset techniques as an alternative to D-InSAR for monitoring episodic landslide movements in vegetated terrain. Remote Sensing of Environment 147:133–144. doi: 10.1016/j.rse.2014.03.003

Skempton AW (1979) Landmarks in early soil mechanics. Proceedings, European Conference on Soil Mechanics. British Geotechnical Society, London, pp 1–26

Slaymaker O (1991) Mountain Geomorphology: A theoretical framework for measurement programmes. Catena 18:427–437.

Soeters R, Van Westen CJ (1996) Slope instability recognition, analysis and zonation. In: Turner AK, Schuster RL (eds) Landslides, Investigation and Mitigation. National Academy Press, Washington, USA, p 129*177

Spencer T, Slaymaker O, Embleton-Hamann C (2009) Landscape, landscape-scale processes and global environmental change: synthesis and new agendas for the twenty-first century. In: Slaymaker O, Spencer T, Embleton-Hamann C (eds) Geomorphology and global environmental change. Cambridge University Press, Cambridge, pp 403–423

Spiegelhalter DJ, Riesch H (2011) Don't know, can't know: embracing deeper uncertainties when analysing risks. Philosophical Transactions of the Royal Society A: Mathematical, Physical and Engineering Sciences 369:4730–4750. doi: 10.1098/rsta.2011.0163

Statistik Austria (2014) STATISTIK AUSTRIA - Bundesländer. http://www.statistik.gv.at/web_de/klassifikationen/regionale_gliederungen/bundeslaender/index.html. Accessed 9 May 2014

Steininger F (1999) Erdgeschichte des Waldviertels, 2nd ed. Waldviertler Heimatbund, Horn

Sterlacchini S, Ballabio C, Blahut J, et al. (2011) Spatial agreement of predicted patterns in landslide susceptibility maps. Geomorphology 125:51–61.

Sterman JD, Rykiel Jr. EJ, Oreskes N, et al. (1994) The meaning of models. Science 264:329–331.

Stockwell DR, Peterson AT (2002) Effects of sample size on accuracy of species distribution models. Ecological modelling 148:1–13.

Stoffel M, Tiranti D, Huggel C (2014) Climate change impacts on mass movements—case studies from the European Alps. Science of The Total Environment in press.

Strahler AN (1952) Dynamic basis of geomorphology. Bulletin of the Geological Society of America 63:923–938.

Strahler AN (1950) Equilibrium theory of erosional slopes approached by frequency distribution analysis. American Journal of Science 248:673–96.

Strahler AN (1980) Systems theory in physical geography. Physical Geography 1:1–27.

Suzen ML, Doyuran V (2004) Data driven bivariate landslide susceptibility assessment using geographical information systems: a method and application to Asarsuyu catchment, Turkey. Engineering Geology 71:303–321.

Tappenden KM (2014) The district of North Vancouver's landslide management strategy: role of public involvement for determining tolerable risk and increasing community resilience. Natural Hazards 72:481–501. doi: 10.1007/s11069-013-1016-0

Tarolli P (2014) High-resolution topography for understanding Earth surface processes: Opportunities and challenges. Geomorphology 295–312. doi: 10.1016/j.geomorph.2014.03.008

Tarolli P, Sofia G, Dalla Fontana G (2010) Geomorphic features extraction from high-resolution topography: landslide crowns and bank erosion. Natural Hazards 1–19.

Taylor DK, Hawley JG, Riddolls BW (1977) Slope Stability in Urban Development. New Zealand Geomechanics Society and New Zealand Department of Scientific and Industrial Research, Wellington, New Zealand

Terzaghi K (1925) Principles of soil mechanics. Reprinted in 1926 as Principles of Soil Mechanics: A Summary of Experimental Studies in Clay and Sand. Engineering News Record 95:742–1068.

Terzaghi K, Peck RB (1967) Soil Mechanics in Engineering Practice. John Wiley & Sons, New York

Thiebes B, Bell R, Glade T, et al. (2013) A WebGIS decision-support system for slope stability based on limit-equilibrium modelling. Engineering Geology 158:109–118. doi: 10.1016/j.enggeo.2013.03.004

Thompson DW (1942) On Growth and Form, 2nd ed. Cambridge University Press, Cambridge, England and Macmillan, New York, N.Y.

Thompson SK (2012) Sampling, 3rd Edition. John Wiley & Sons Inc., Hoboken, New Jersey

Tien Bui D, Pradhan B, Lofman O, et al. (2012) Landslide susceptibility mapping at Hoa Binh province (Vietnam) using an adaptive neuro-fuzzy inference system and GIS. Computers & Geosciences 199–211. doi: 10.1016/j.cageo.2011.10.031

Tilch N, Schwarz L, Hagen K, et al. (2011) Modelling of landslide susceptibility and affected areas - process-specific validation of databases, methods and results for the communities of Gasen and Haslau (AdaptSlide). 305.

Townsend Peterson A, Papeş M, Eaton M (2007) Transferability and model evaluation in ecological niche modeling: a comparison of GARP and Maxent. Ecography 30:550–560. doi: 10.1111/j.2007.0906-7590.05102.x

Trigila A, Iadanza C (2008) Landslides in Italy - Special Report 2008. 40.

Untersweg T, Lipiarski P, Heinrich M (2008) Die digitale Karte quartärer Sedimentgesteine in Österreich: ein "Spin-off" rohstoffgeologischer Bearbeitung. Abhandlungen der geologischen Bundesanstalt 62:117–122.

Varnes DJ (1984) Landslilde hazard zonation: a review of principles and practice. United Nations Educational, Scientificc and Cultural Organization, Paris, France

Varnes DJ (1978) Slope movement types and processes. In: Schuster RL, Krizek RJ (eds) Landslides: Analysis and Control. Transportation and Road Research Board, National Academy of Science, Washington D.C., pp 11–33

Ventura G, Vilardo G, Terranova C, Sessa EB (2011) Tracking and evolution of complex active landslides by multi-temporal airborne LiDAR data: The Montaguto landslide (Southern Italy). Remote Sensing of Environment 115:3237–3248. doi: 10.1016/j.rse.2011.07.007

Vogl F (2008) Statistisches Handbuch des Landes Niederösterreich. 353.

Vorpahl P, Elsenbeer H, Märker M, Schröder B (2012) How can statistical models help to determine driving factors of landslides? Ecological Modelling 239:27–39. doi: 10.1016/j.ecolmodel.2011.12.007

Wasowski J, Bovenga F (2014) Investigating landslides and unstable slopes with satellite Multi Temporal Interferometry: Current issues and future perspectives. Engineering Geology 174:103–138. doi: 10.1016/j.enggeo.2014.03.003

Wenzel WW, Hösl R, Strauss, P. (2013) Erläuterungen zur Niederösterreichischen Bodenkarte 1:900,000. 9.

Wessely G (2006) Geologie der österreichischen Bundesländer - Niederösterreich. Geologische Bundesanstalt, Wien

Van Westen CJ, Asch TWJ, Soeters R (2005) Landslide hazard and risk zonation—why is it still so difficult? Bulletin of Engineering Geology and the Environment 65:167–184. doi: 10.1007/s10064-005-0023-0

Van Westen CJ, Asch TWJ, Soeters R (2006) Landslide hazard and risk zonation—why is it still so difficult? Bulletin of Engineering Geology and the Environment 65:167–184. doi: 10.1007/s10064-005-0023-0

Van Westen CJ, Castellanos E, Kuriakose SL (2008) Spatial data for landslide susceptibility, hazard, and vulnerability assessment: An overview. Engineering Geology 102:112–131. doi: doi: DOI: 10.1016/j.enggeo.2008.03.010

Van Westen CJ, Lulie Getahun F (2003) Analyzing the evolution of the Tessina landslide using aerial photographs and digital elevation models. Geomorphology 54:77–89.

Van Westen CJ, Rengers N, Terlien MTJ, Soeters R (1997) Prediction of the occurrence of slope instability phenomena through GIS-based hazard zonation. Geologische Rundschau 86:404–414.

Van Westen CJ, Seijmonsbergen AC, Mantovani F (1999) Comparing Landslide Hazard Maps. Natural Hazards 20:137–158.

Whitworth MCZ, Giles DP, Murphy W (2005) Airborne remote sensing for landslide hazard assessment: a case study on the Jurassic escarpment slopes of Worcestershire, UK. Quarterly Journal of Engineering Geology and Hydrogeology 38:285–300.

Wieczorek G (1984) Preparing a detailed landslide-inventory map for hazard evaluation and reduction. G Bull Assoc Engng Geol 21:337–342. doi: doi: DOI: 10.1016/0148-9062(85)93910-5

Wiesbauer H, Mazzucco K (1995) Hohlwege in Niederösterreich. 38.

Wills CJ, Perez FG, Gutierrez CI (2011) Susceptibility to Deep-Seated Landslides in California.

Yalcin A, Reis S, Aydinoglu AC, Yomralioglu T (2011) A GIS-based comparative study of frequency ratio, analytical hierarchy process, bivariate statistics and logistics regression methods for landslide susceptibility mapping in Trabzon, NE Turkey. CATENA 85:274–287. doi: 10.1016/j.catena.2011.01.014

Yee TW, Mitchell ND (1991) Generalized additive models in plant ecology. Journal of Vegetation Science 2:587–602. doi: 10.2307/3236170

Yesilnacar E, Topal T (2005) Landslide susceptibility mapping: A comparison of logistic regression and neural networks methods in a medium scale study, Hendek region (Turkey). Engineering Geology 79:251–266.

Yilmaz I (2009) Landslide susceptibility mapping using frequency ratio, logistic regression, artificial neural networks and their comparison: A case study from Kat landslides (Tokat—Turkey). Computers & Geosciences 35:1125–1138. doi: 10.1016/j.cageo.2008.08.007

Zanutta A, Baldi P, Bitelli G, et al. (2006) Qualitative and quantitative photogrammetric techniques for multi-temporal landslide analysis. Annals of geophysics 49:1067–1080.

Zentralanstalt für Meteorologie und Geodynamik (ZAMG) (2014) Klimadaten von Österreich 1971 - 2000. In: Klimadaten von Österreich. http://www.zamg.ac.at/fix/klima/oe71-00/klima2000/klimadaten_oesterreich_1971_frame1.htm. Accessed 12 May 2014

Zezere JL (2002) Landslide susceptibility assessment considering landslide typology. A case study in the area north of Lisbon (Portugal). Natural Hazards and Earth System Sciences 2:73–82.

Zezere JL, de Brum Ferreira A, Rodrigues ML (1999) The role of conditioning and triggering factors in the occurrence of landslides: a case study in the area north of Lisbon (Portugal). Geomorphology 133–146.

Zêzere JL, Reis E, Garcia R, et al. (2004) Integration of spatial and temporal data for the definition of different landslide hazard scenarios in the area north of Lisbon (Portugal). Natural Hazards and Earth System Science 4:133–146.

Zhao W, Tian Y, Wu L, Liu Y (2010) Human impact index in landslide susceptibility mapping. pp 1–6

Zimmermann M, Mani P, Gamma P (1997) Murganggefahr und Klimaänderung - ein GIS-basierter Ansatz. vdf Hochschulverlag AG, ETH Zürich, Zürich

Annex

Contents of the Annex

Contents of the Annex **A-1**

A. Synopsis of the Publications / Manuscripts **A-3**

A.1. Landslide inventories for regional early warning systems.....A-7

A.2. Assessment of landslide age, landslide persistence and human impact using airborne laser scanning DTMs A-15

A.3. Landslide susceptibility modeling with generalized additive models – facing the heterogeneity of large regions A-39

A.4. Landslide inventories for reliable susceptibility maps A-47

A.5. Landslide susceptibility maps for spatial planning in Lower Austria A-55

A.6. Assessing the quality of landslide susceptibility maps – case study Lower Austria A-63

A.7. Landslide inventory mapping for large regions – effectiveness of visually analyzing LiDAR DTM derivatives (subm.).....A-89

A.8. Relative age estimation at landslide mapping on LiDAR derivatives – revealing the applicability of land cover data in statistical susceptibility modeling.....A-123

B. Tables **A-131**

C. Maps..... **A-135**

D. German and English Summary **A-143**

D.1. Zusammenfassung A-143

D.2. Summary.....A-145

E. Eidesstattliche Erklärung..... **A-147**

F. Curriculum Vitae **A-149**

A. Synopsis of the Publications / Manuscripts

In the following the publications and the manuscript subject of this thesis are briefly introduced giving their title, their full citation and status of publication/submission. Furthermore, the contribution of each author, especially the author of this thesis is outlined in a short paragraph. After this section of introducing all publications, copies of the full publications are provided.

A.1. Landslide inventories for regional early warning systems

Petschko, H., *Glade, T., Bell,R., Schweigl, J. & G., Pomaroli (2010), Landslide inventories for regional early warning systems, in: Malet, J.P., Glade, T. & Casagli, N. (Eds.), Proceedings of the International Conference 'Mountain Risks: Bringing Science to Society', Strasbourg, CERG Editions, 277-282.*

Status: Released publication

While the publication was initiated by Thomas Glade, substantial parts of the manuscript preparation and the entire mapping and analysis of the landslides was done by Helene Petschko. Furthermore, the results were obtained by Helene Petschko. Rainer Bell was advising the mapping process and contributed to the publication with constructive feedback. Joachim Schweigl and Gilbert Pomaroli contributed to this publication with their critical revision of the manuscript.

A.2. Assessment of landslide age, landslide persistence and human impact using airborne laser scanning DTMs

Bell, R., ***Petschko, H.,*** *Röhrs, M. & A., Dix (2012), Assessment of landslide age, landslide persistence and human impact using airborne laser scanning digital terrain models, Geografiska Annaler: Series A, Physical Geography, 94(1), 135–156.*

Status: Released publication

The mapping and analysis done at the different sites within Lower Austria was carried out and provided for this publication by Helene Petschko. As the first author of the publication Rainer Bell initiated the writing and provided the concept, the manuscript outline and all manuscript parts dealing with the Swabian Alb. Helene Petschko contributed to the writing process by providing all sections on Lower Austria (study area, method, results and discussion). Furthermore, she contributed with discussions on the methodology and provided feedback on the entire manuscript. The co-authors Matthias Röhrs and Andreas Dix provided their historical expertise on the Swabian Alb and feedback to improve the manuscript.

A.3. Landslide susceptibility modelling with generalized additive models – facing the heterogeneity of large regions

Petschko, H., *Bell, R., Brenning, A. & T., Glade (2012), Landslide susceptibility modelling with generalized additive models - facing the heterogeneity of large regions, in: Eberhardt E., Froese C., Turner A.K., & S. Leroueil (Eds.), Landslides and Engineered Slopes, Protecting Society through Improved Understanding, Taylor & Francis, Banff, Alberta, Canada, 769–777.*

Status: Released publication

The publication was initiated by Helene Petschko sharing a concept and outline with the co-authors. Furthermore, she analyzed the landslide susceptibility and wrote the manuscript. Rainer Bell and Thomas Glade provided their expertise in spatial landslide susceptibility modelling in discussions on the model design and gave feedback on the manuscript. The statistical analysis with generalized additive models was advised by Alexander Brenning. Furthermore, he contributed with discussions on the model design and feedback on the manuscript.

A.4. Landslide inventories for reliable susceptibility maps

Petschko, H., *Bell, R., Leopold, P., Heiss, G. & T., Glade (2013), Landslide inventories for reliable susceptibility maps, in: Margottini, C., Canuti, P. & K. Sassa (Eds.), Landslide Science and Practice, Vol. 1: Landslide Inventory and Susceptibility and Hazard Zoning, Springer, 281-286.*

Status: Released publication

The publication was initiated, designed and written by Helene Petschko. She carried out the statistical analysis as well as the comparison with the Building Ground Register. Rainer Bell gave feedback on the modelling design. Philip Leopold, Gerhard Heiss and Thomas Glade contributed with conceptual discussions and feedback on the manuscript.

A.5. Landslide susceptibility maps for spatial planning in Lower Austria

*Bell, R., Glade, T., Granica, K., Heiss, G., Leopold, P., **Petschko, H.,** Pomaroli, G., Proske, H. & J., Schweigl (2013), Landslide susceptibility maps for spatial planning in Lower Austria, in: Margottini, C., Canuti, P. & K. Sassa (Eds.), Landslide Science and Practice, vol. 1: Landslide Inventory and Susceptibility and Hazard Zoning, Springer, 467-473.*

Status: Released publication

This publication arose from a close collaboration and discussion process of researchers and government authorities. While Rainer Bell wrote the main parts of this manuscript, Helene Petschko supported the writing and provided Figures, Tables, discussion material and broad feedback on the manuscript. Furthermore, the discussion on the choice of the colors was initiated by her. Thomas Glade, Klaus Granica, Gerhard Heiss, Philip Leopold and Herwig Proske contributed with scientific input during the discussion and with feedback on the manuscript. Gilbert Pomaroli and Joachim Schweigl accompanied this discussion process and provided their practical view from outside research institutions and feedback for the manuscript preparation.

A.6. Assessing the quality of landslide susceptibility maps – case study Lower Austria

***Petschko, H.,** Brenning, A., Bell, R., Goetz, J. & T., Glade (2014), Assessing the quality of landslide susceptibility maps – case study Lower Austria, Nat. Hazards Earth Syst. Sci., 14, 95-118, doi:10.5194/nhess-14-95-2014.*

Status: Released publication

The publication was initiated, designed and prepared by Helene Petschko. The review, the statistical modelling and quality analysis was performed by her. Alexander Brenning advised the statistical modelling and the entire analysis. Furthermore, he provided support on writing the methodology sections and extensive feedback on the manuscript. Jason Goetz attended the modelling and supported the manuscript writing with critical feedback. Rainer Bell and Thomas Glade contributed with scientific exchange and critical feedback on the manuscript.

A.7. Landslide inventory mapping for large regions – effectiveness of visually analyzing LiDAR DTM derivatives (subm.)

Petschko, H., *Bell, R. & T., Glade (2014), Landslide inventory mapping for large regions – effectiveness of visually analyzing LiDAR DTM derivatives, Landslides, Springer.*

Status: Submitted manuscript
Date of submission: 02.04.2014, refer to email of Acknowledgement of receipt of the manuscript at "Landslides" Journal, Springer after the references of the manuscript (p. A-120).

The conceptual approach, the effectiveness estimate and the methodology of deriving the main scarp were developed by Helene Petschko. Furthermore, she mapped the landslides and prepared the manuscript. Rainer Bell and Thomas Glade supported the manuscript writing with discussions and extensive feedback on the draft.

A.8. Relative age estimation at landslide mapping on LiDAR derivatives – revealing the applicability of land cover data in statistical susceptibility modelling

Petschko, H., *Bell, R. & T., Glade (2014) Relative Age Estimation at Landslide Mapping on LiDAR Derivatives: Revealing the Applicability of Land Cover Data in Statistical Susceptibility Modelling. In: Sassa, K., Canuti, P., & Y., Yin (Eds.) Landslide Science for a Safer Geoenvironment. Springer International Publishing, 337–343.*

Status: Released publication

The landslide mapping, relative age estimation and writing of the manuscript was initiated and performed by Helene Petschko. Rainer Bell and Thomas Glade provided extensive discussions and critical feedback on the manuscript.

A.1. Landslide inventories for regional early warning systems

Petschko, H., Glade, T., Bell,R., Schweigl, J. & G., Pomaroli (2010), Landslide inventories for regional early warning systems, in: Malet, J.P., Glade, T. & Casagli, N. (Eds.), Proceedings of the International Conference 'Mountain Risks: Bringing Science to Society', Strasbourg, CERG Editions, 277-282.

Landslide inventories for regional landslide early warning systems

H. Petschko, T. Glade & R. Bell
Geomorphic Systems and Risk Research, University of Vienna, Vienna, Austria

J. Schweigl
Geological Survey, Federal State Government of Lower Austria

G. Pomaroli
Department of Spatial Planning and Regional Policy, Federal State Government of Lower Austria

ABSTRACT: Landslide early warning systems are developed and implemented either at specific landslides or for regional assessments. In all cases, the quality of the early warning is heavily dependent on information of previous landslide failures and current grade of activity. Therefore, detailed landslide inventories are one prerequisite for a successful landslide early warning system. In this study, results are presented on using high resolution Lidar imagery and field surveys to establish sound and reliable landslide inventories optimized for statistical landslide susceptibility modeling. The analysis is performed in the study area Waidhofen/Ybbs, one of the most landslide prone regions in Lower Austria. The results show, that the resulting landslide inventories are a major advance. Various previously unknown landslides have been detected, the landslide extent was delineated in more detail and also some indication of activity can be determined. But in particular, the existing landslide inventories could have been improved. This high accurate spatial information is now available for further susceptibility and hazard analysis and has the potential to be in added in future landslide early warning systems. This analysis is part of the research project MoNOE (Methods for landslide susceptibility modelling in Lower Austria) which is funded by the Federal State Government of Lower Austria.

1 GENERAL BACKGROUND

Various definitions of "early warning systems" exist (e.g. Zschau & Küppers 2002). In most recent years, the global UN-ISDR initiative has suggested a common terminology (UNISDR 2009), which is adopted in this contribution.

Early warning schemes for landslides can be classified in the two groups of local and regional systems. While local systems are usually based on monitored data, operated either automatically or manually, the regional systems include preventive long-term warnings based on susceptibility, hazard or risk maps or on previous and recent information on landslide-triggers. Such triggers are commonly rainfall (e.g. Wieczorek & Glade 2005) or earthquakes (e.g. Keefer 2002), or a combination of both. Indeed, both triggers can also function as preparatory factors, e.g. earthquakes can weaken the ground but not initiate the actual movement. Similarly, rainfall can moisture the regolith and increase thus consequent pore water pressures, but not trigger the failure. Examples are described for local systems by e.g. Corsini et al. (2005), while regional assessments of triggers are characterized for rainfall by Guzzetti et al. (2004) and for earthquake by Hancox et al. (2004), to name in all cases one exemplary reference only.

It has been pointed out by various authors, that an early warning system should not focus on the technical approach only (e.g. UN 2006). This is also of major relevance for landslide early warning systems (Glade et al. 2007). Instead, a comprehensive - and finally successful operating – landslide early warning system should include the whole chain of warning starting from monitoring in the field to issuing the warning and finally to suggesting the required actions (Bell et al. 2010). Thus within the technological part a landslide warning system has to include the monitoring, data transmission and storage, analysis, and submission of results (Bell et al. 2008). Within the societal part major topics such as the communication, definition of stakeholders and respective responsibilities, the acceptable and tolerable warning levels as well as the final chain of actions have to be addressed (UNISDR 2009). In most recent years, the accessibility and visualisation of the landslide early warnings get increasingly important (e.g. Breunig et al. 2009, Fan-Chieh et al. 2007).

In all cases, the quality of the landslide early warning is heavily dependent on information of previous failures, recent landslide prone regions and

current grade of activity. Therefore, detailed landslide inventories are one prerequisite for a successful and reliable landslide early warning system on a regional scale.

In this current study, presented results are based on using high resolution Lidar imagery and field surveys to establish sound and reliable landslide inventories for the study area Waidhofen/Ybbs. The study is part of the project MoNOE (Methods for landslide susceptibility modelling in Lower Austria) with the main objective of calculating landslide susceptibility maps for main parts of Lower Austria (10,300 km²).

2 METHODOLOGY

Landslide inventories are commonly compiled from a variety of sources including historical and sedimentary archives, detailed field work, and analysis of remote sensing data. Herein, the spatial determination of landslides has been significantly improved by remote sensing techniques.

Various authors have identified the visual interpretation of airborne laserscanning (ALS) images as particular promising for the assessment of new and optimization of already existing inventories (Haugerund et al. 2003, Schulz 2004, Glenn 2006, Ardizzone et al. 2007, Bell 2007, Proske et al. 2008). In particular the high resolution images with 1m x 1m resolution can be ideally used to delineate single landslides according to morphological forms and structures, including also forested regions (van den Eeckhaut et al. 2007).

Recently acquired ALS datasets with a spatial resolution of 1m x 1m were made available for the MoNOE project by the Department for Hydrology and Geoinformation of the Federal State Government of Lower Austria. The different ALS frames have been merged and complemented in ArcInfo 9.3 in order to get a comprehensive ALS coverage for the whole region. The resulting DTM was used to derive hillshade maps with different azimuth angles and to create contour lines. These datasets form the basis for the landslide mapping. The landslide mapping is mainly carried out by visual interpretation, detection and analysis of different distinctive morphological features such as landslide scarps, fissures, and lobes in order to delineate landslide polygons. Besides the visual interpretation of the DTM derivates, checks with orthophotos and field checks were performed to enhance the quality of the mapping. In order to identify hot spots of the landslide mapping different spatial landslide data were assembled from national and federal institutes such as the Geological Survey of Lower Austria, the Geological Survey of Austria (GBA) and the Austrian Service for Torrent and Avalanche control (WLV).

Due to the large spatial extend and the numerous landslides in various regions, a strategy has been developed to map the landslides comprehensively with the required accuracy and in a reasonable time frame in this project. The strategy is based on the following criteria:

- The landslide mapping is performed in all lithological units of the investigated region. Due to time limitation not all landslides can be mapped. Therefore, a characteristic set of landslides incl. the different landslide types, sizes, and relative ages are mapped within each unit;
- The minimum mapped landslide surface is 100m² including the zones of depletion, transport and accumulation;
- The existing inventories of the National Geological Survey - GBA (GEORIOS, Kociu et al. (2007)), the Geological Survey of the Regional Council in Lower Austria (Building Ground Registry, Schwenk (1992) and the regional recommendation for urban development of the Austrian Service for Torrent and Avalanche Control - WLV in Lower Austria are the basis for the mapping;
- The mapped polygons are classified according to a specific landslide type (flow, slide, complex – but no falls) or to a landslide area (the "landslide area" is here defined as multiple directly adjacent landslides, which cannot be clearly differentiated and thus have not been mapped as separate masses).

3 STUDY REGION

Landslides occur continuously throughout whole Austria (Kociu et al. 1996). The affected sites spread from high alpine regions (e.g. Tyrol) to rolling hill countries (e.g. parts in Lower Austria or Carinthia). Most recent examples of widespread landsliding include the events in Gasen-Haslau (district Weiz, Eastern Styria) 2005, in the Flysch zone in Lower Austria 2009 and in Feldbach (Eastern Styria) 2010.

In Lower Austria, landslides are widespread (Schwenk et al. 1992) and the district Waidhofen/Ybbs shows one of the highest landslide activities in the region. This study area is located in the West of Lower Austria in the south of the Danube and has an area of about 131 km². The area is characterized by four lithological units: Flysch, Klippenzone, Limestone and Dolomite. Many valleys and some foreland basins are covered by Quaternary deposits. Numerous landslides of various types (translational and rotational slides, earth flows, and complex landslides) occurred in the past in all units with different landslide density. Landslide related damage to houses and infrastructure is reported for all units. In the year 2009 the

combination of dense snow cover and snow melting rates in spring with an exceptional wet summer caused hundreds of landslides and extensive economic loss in Lower Austria. The landslides caused damage at farmland, private houses, and some infrastructure lines. The event trigger is somehow typical for this region, because nearly all previously recorded landslide events have been initiated by rainfall. It is expected, that with increasing rainfall intensities and/or amounts due to climate change, landslide susceptibility, hazard and risk will increase significantly. Therefore, local and regional landslide early warning systems might be an important management option for the future in this region.

4 PRELIMINARY RESULTS

All different landslide inventories are displayed for a typical area in Figure 1 in order to display the similarities and differences. The legend refers to the following definitions: "Reported landslides" of the Building Ground Register indicate point information of documents filed in the Geological Survey of Lower Austria; the "Hazard Zone Plans" differentiate into "slides" defined as any downslope movement of earth, debris and rocks and "falls" refers to any type of rock fall; the "Map of Sedimentary Deposits" is a compilation of geological maps and field mapping of loose sediments as visible on the surface; therefore it contains polygons that are assigned as landslides; the "GEORIOS database" refers to "slides" as clearly defined areas of moving material and "area with slides" as displaced areas, which have not been clearly delineated in terms moved and stable areas; and finally the "Inventory – ALS Mapping" refers to mapped landslides according to the Cruden & Varnes 1996 definition that were detected in this survey from ALS imagery. It is evident, that the inventories differ significantly. Some inventories include point information. Unfortunately, it is not reproducible, where the points have been positioned within the landslides. Some of them are on the landslide in various locations ranging from scar, run-out to depositional zone; others are located even outside the landslide body. To complicate the issue even more, some of the locations are not related to any visible landslide location at all, as indicated on the ALS data. Reasons might be a wrong coordinate assigned by the expert, a typing error in the entry, or that the landslide has been removed or the surface has been modified and is thus not visible anymore on the ALS imagery. In contrast, the GEORIOS data generalize the landslides in large areas. Indeed this has to be attributed to the large scale of the respective investigation. The third inventory gives the perimeters of the mapped landslides and shows a very accurate delineation of the landslide. The visual comparison of the inventories shows that the different inventories vary significantly in the regional positioning and in the resolution. This is clearly related to the different aims and purposes of the respective studies and inventories. Therefore, any consequent recommendation for spatial susceptibility, hazard and potential early warning differs greatly in detail as well as in accuracy. It has to be explicitly stressed that the different resolution and accuracy is solely and purely related to the purposes and requirements of each different inventory. While the GBA inventory was established to provide a very broad overview on landslide occurrence on a scale of max. 1:50.000, other inventories do not intend to display the landslide perimeter accurately. Instead they link the reported information to a point only. Other inventories intend to position the landslide precisely for local hazard zone plans. For their purpose the accurate delineation of landslide areas is mapped only at areas close to settlements that are important for sustainable settlement development. Consequently, one has to be very careful in comparing different inventories and judging the quality of each inventory. Nevertheless, if stakeholders are interested on early warning systems, related decisions have to consider all relevant information – also in terms of available inventories. It is of course absolutely important to review all available information, but at the same time, one has to draw the conclusions with great care when comparing the different inventories. For the district Waidhofen/Ybbs, a total of 151 landslides are reported in the building ground registry of the Geological Survey of Lower Austria. Using the DTM created from the ALS data, all landslides have been mapped following the previously described criteria. Hereby, the purpose was to determine the landslide locations for the different types only. Additional information such as detailed volume, grade of activity or even date of occurrence is indeed important but is beyond the purpose of this project. In the resulting inventory (Fig. 2) a total of 691 landslides have been mapped, of which 522 polygons are classified as "slide", 141 polygons as "area with landslides", 25 polygons as "flow", and 3 polygons as "complex". The spatial distribution shows a clear pattern following the lithology. The highest landslide density occurs in the Flysch and Klippenzone that is located in the North of the study area. In the South, in the zone of marly Limestones, comparable few, but very large landslides have been mapped. The zone with mainly Dolomites is located in the center of the study area and there nearly no landslides have been identified. According to the landslide types there is no remarkable difference within the whole district.

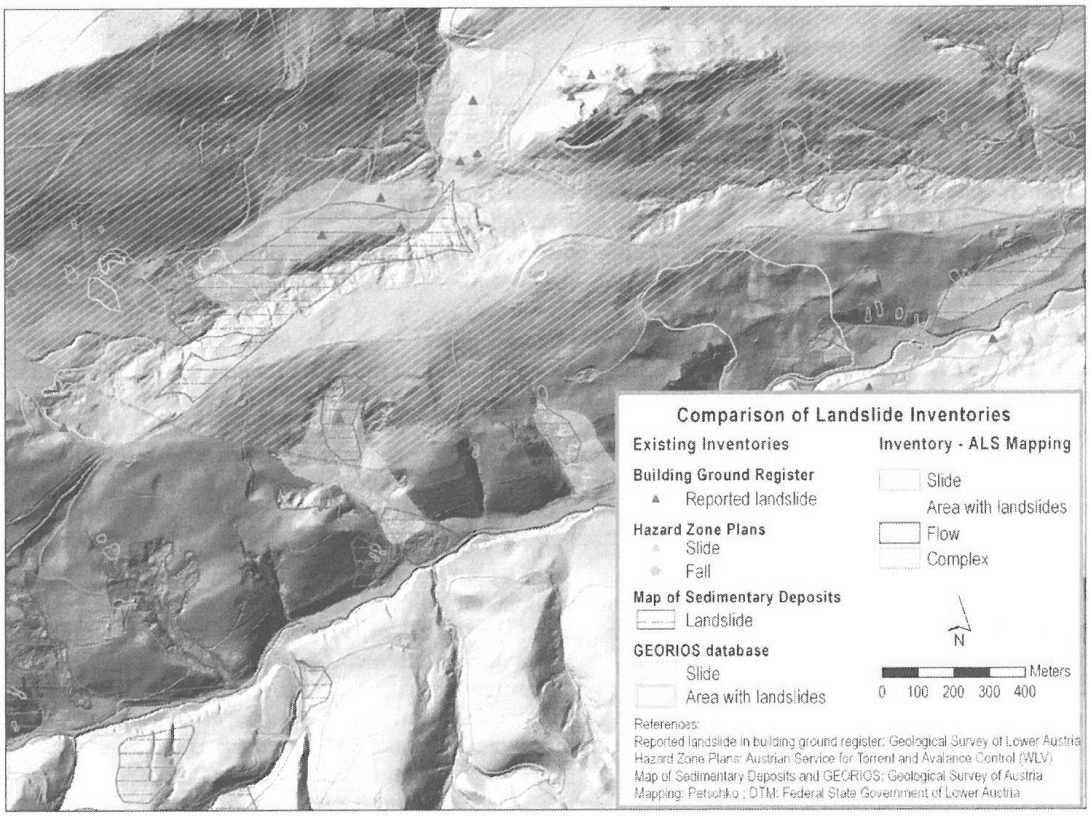

Figure 1. Comparison of existing and newly mapped landslide inventories.

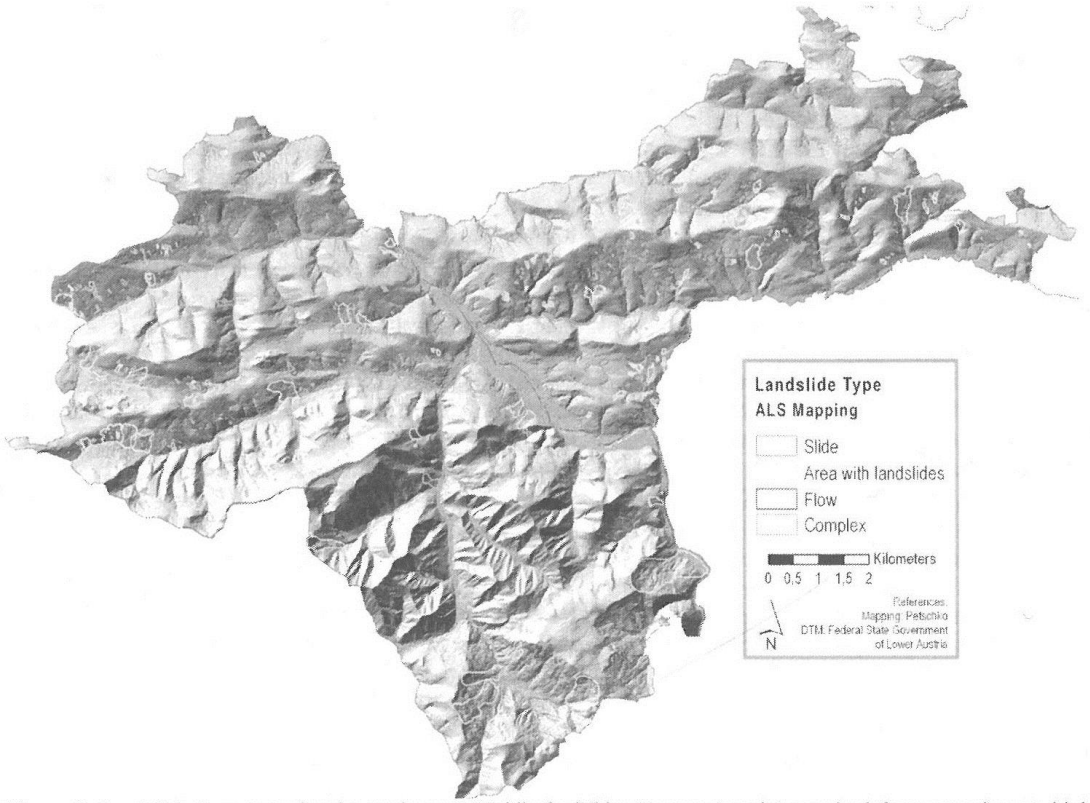

Figure 2. Landslide Inventory for the study area Waidhofen/Ybbs (Lower Austria) acquired from mapping on high resolution DTM's from airborne Laserscanning.

5 CONCLUSIONS AND PERSPECTIVES

The comparison of the existing inventories with the mapping based on high resolution ALS data shows that the accuracy of the location of the landslides and also the number of landslides increased even though not all landslides can be mapped due to time limitation. Consequently, the database for decisions on regional early warning systems and in particular for statistical modeling has been improved remarkably.

The current study is only a small part of the overall project. However, it indicates the importance of compiling different landslide inventories in order to get the best possible landslide information on our environment. This is in particular true for the preparatory work pervious the discussion on the installation of any landslide early warning system.

The landslide early warning system can contain a regional assessment to determine susceptible landslide areas potentially unstable in the future. It can also be established for single landslides, which pose a considerable threat to society. Such systems contain mostly monitoring equipment with consequent analysis concepts and dissemination strategies.

In all cases, spatial landslide inventories are a prerequisite for landslide early warning systems in order to provide reliable and most accurate information on current landslides. These allow the determination of the regions that are most endangered in the future.

ACKNOWLEDGEMENTS

The authors thank the team of the National Geological Survey and the colleagues from the Austrian Service for Torrent and Avalanche Control in Lower Austria for their support. This study was supported by numerous individuals from different agencies within the Federal State Government of Lower Austria, namely the Geological Survey, the Department of Spatial Planning and Regional Policy and the Department for Hydrology and Geoinformation. The authors wish also to thank the project partners from AIT (Austrian Institute of Technology) and Joanneum Research for their valuable input and continuous support. Finally, the authors are grateful for the financial support by the Federal State Government of Lower Austria.

REFERENCES

Ardizzone, F., Cardinali, M., Galli, M., Guzzetti, F., Reichenbach, P. 2007: Identification and mapping of recent rainfall-induced landslides using elevation data collected by airborne Lidar. In *Natural Hazards and Earth System Sciences* 7: 637-650.

Bell, R. 2007. *Lokale und regionale Gefahren- und Risikoanalyse gravitativer Massenbewegungen an der Schwäbischen Alb*. Dissertation. Math.-Natural Science Faculty, University Bonn, Germany.

Bell, R., Mayer, J., Greiving, S., Pohl, J. & Glade, T. (eds.) 2010. *Integrative Frühwarnsysteme für gravitative Massenbewegungen (ILEWS) - Monitoring, Modellierung, Implementierung*. Klartext Verlag, Essen, 270pp.

Bell, R., Petschko, H., Glade, T., Leopold, P., Heiss, G., Proske, H., Granica, K., Schweigl, J. & Pomaroli, G. 2010. Methods for landslide susceptibility modeling in Lower Austria. In *Geophysical Research Abstracts* 12, EGU2010-9869.

Bell, R., Thiebes, B., Glade, T., Becker, R., Kuhlmann, H., Schauerte, W., Burghaus, S., Krummel, H., Janik, M. & Paulsen, H. 2008. The technical concept within the Integrative Landslide Early Warning System (ILEWS). In: Z.-Y. Chen, J.-M. Zhang, K. Ho, F.-Q. Wu & Z.-K. Li (eds.). Proceedings of the 10th International Symposium on Landslides and Engineered Slopes: From the Past to the Future. Xi'an, China, Taylor & Francis Ltd, 293-298.

Breunig, M., Schilberg, B., Kuper, P. V., Jahn, M., Reinhardt, W., Nuhn, E., Mäs, S., Boley, C., Trauner, F.-X., Wiesel, J., Richter, D., Abecker, A., Gallus, D., Kazakos, W. & Bartels, A. 2009. EGIFF – Developing Advanced GI Methods for Early Warning in Mass Movement Scenarios. In Stroink, L. (ed.): GEOTECHNOLOGIEN - Science Report 13. Early Warning Systems in Earth Management. 49–72.

Corsini, A., Pasuto, A., Soldati, M. & Zannoni, A. 2005. Field monitoring of the Corvara landslide (Dolomites, Italy) and its relevance for hazard assessment. In *Geomorphology* 66(1-4): 149-165.

Cruden, D. & Varnes, D.J. 1996. Landslide types and processes. In: Turner, A.K., und Schuster, R.L., Hrsg., 1996: *Landslides: investigation and mitigation*. Washington, D.C., S. 36-75.

Guzzetti, F., Cardinali, M., Reichenbach, P., Cipolla, F., Sebastiani, C., Galli, M. & Salvati, P. 2004. Landslides triggered by the 23 November 2000 rainfall event in the Imperia Province, Western Liguria, Italy. In *Engineering Geology* 73(3-4): 229-245.

Keefer, D.K. 2002. Investigating landslides caused by earthquakes - a historical review. In *Surveys in Geophysics* 23: 473-510.

Petschko, H., Bell, R., Glade, T., Leopold, P. & Schweigl, J. 2010. Compiling a landslide inventory for state wide susceptibility modeling in Lower Austria. In *Geophysical Research Abstracts* 12, EGU2010-8770.

Fan-Chieh, Y., Chien-Yuan, C., Sheng-Chi, L., Yu-Ching, L., Shang-Yu, W. & Kei-Wai, C. 2007. A web-based decision support system for slopeland hazard warning. In *Environmental Monitoring and Assessment* 127(1): 419-428.

Glade, T., Becker, R., Bell, R., Burghaus, S., Danscheid, M., Dix, A., Greiving, S., Greve, K., Jäger, S., Kuhlmann, H., Krummel, H., Paulsen, H., Pohl, J., Röhrs, M. & Thiebes, B. 2007. Integrative Landslides Early Warning Systems. In: L. Stroink (Ed). Early Warning Systems in Earth Management - Geotechnologien Science Report I. Technische Universität Karlsruhe, Germany, 10, 89-100.

Glenn, N.F., Streutker, D.R., Chadwick, D.J., Thackray, G.D. & Dorsch, S.J. 2006. Analysis of LiDAR-derived topographic information for characterizing and differentiating landslide morphology and activity. In *Geomorphology* 73: 131-148 caused by the ML 5.4 Lake Rotoehu earthquake and swarm of July 2004. Report 2004/24, Institute of Geological & Nuclear Sciences Limited, Lower Hutt, New Zealand.

Hancox, G.T., Dellow, G., Mc Saveney, M.J., Scott, B. & Villamor, P. 2004. Reconnaissance studies of landslides.
Haugerund, R.A., Harding, D.J., Johnson, S.Y., Harless, J.L. & Weaver C.S. 2003. High-Resolution Lidar Topography of the Puget Lowland, Washington – A Bonanza for Earth Science. In *GSA Today* 13: 4-10.
Kociu, A., Kautz, H., Tilch, N., Grösel, K., Heger, H. & Reischer, J. 2007. Massenbewegungen in Österreich.- In *Jahrbuch der Geologischen Bundesanstalt* 147(1+2), 215-220.
Proske, H., Granica, K., Hirschmugl, M. & Wurm, M. 2008. Landslide Detection and Susceptibility Mapping using innovative Remote Sensing Data Sources.- In *Proc. Interpraevent* 2, Dornbirn: 219-229.
Schulz, W.H. 2007. Landslide susceptibility revealed by LIDAR imagery and historical records, Seattle, Washington. In *Engineering Geology* 89, 67-87.
Schwenk, H., Spendlingwimmer, R. & Salzer, F. 1992. Massenbewegungen in Niederösterreich, 1953 – 1990.- *Jahrbuch der Geologischen Bundesanstalt* 135(2): 597-660.
UN 2006. *Global Survey of Early Warning Systems*. Geneva.
UNISDR 2009. *Terminology on Disaster Risk Reduction*. Geneva.
Van Den Eeckhaut, M., Poesen, J., Verstraeten, G., Van Acker, V., Nyssen, J., Moeyersons, J., Van Beek, L.P.H. & Vandekerckhove, L. 2007. The use of LIDAR-derived images for mapping old landslides under forest.- In *Earth Surface Processes and Landforms* 32: 754-769.
Wieczorek, G. & Glade, T. 2005. Climatic factors influencing triggering of debris flows. In: Jakob, M. & O. Hungr (Eds): *Debris flow hazards and related phenomena*.- Springer, Heidelberg 325-362.
Zschau, J. & Küppers, A.N. (eds) 2002. *Early warning systems for natural disaster reduction*. Springer, Heidelberg, 834 pp.

A.2. Assessment of landslide age, landslide persistence and human impact using airborne laser scanning DTMs

Bell, R., **Petschko, H.,** Röhrs, M. & A., Dix (2012), Assessment of landslide age, landslide persistence and human impact using airborne laser scanning digital terrain models, Geografiska Annaler: Series A, Physical Geography, 94(1), 135–156.

ASSESSMENT OF LANDSLIDE AGE, LANDSLIDE PERSISTENCE AND HUMAN IMPACT USING AIRBORNE LASER SCANNING DIGITAL TERRAIN MODELS

RAINER BELL[1], HELENE PETSCHKO[1], MATTHIAS RÖHRS[2] and ANDREAS DIX[3]

[1]Department of Geography and Regional Research, University of Vienna, Vienna, Austria
[2]Institute for Applied Remote Sensing, EURAC Research, Bolzano, Italy
[3]Department of Geography, University of Bamberg, Bamberg, Germany

Bell, R., Petschko, H., Röhrs, M. and Dix, A. Assessment of landslide age, landslide persistence and human impact using airborne laser scanning digital terrain models. *Geografiska Annaler: Series A, Physical Geography*, 94, 135–156. DOI:10.1111/j.1468-0459.2012.00454.x

ABSTRACT. Landslides occur worldwide and contribute significantly to sediment budgets as well as to landform evolution. Furthermore, they pose hazards and risks to people and their goods. To assess the role of landslides, information on their age or persistence (i.e. the length of time the morphological characteristics of a landslide remain recognizable in the terrain) is essential. In this study, the potential of airborne laser scanning digital terrain models (ALS DTMs) is analysed for estimating landslide age, landslide persistence and human impact. Therefore, landslides in two study areas, Swabian Alb in Germany and Lower Austria in Austria, are mapped from hillshades of ALS DTMs and combined with historical information on landslide occurrence. It is tested whether the modification of the geomorphological features of landslides can be used to assess landslide age. In the Swabian Alb older landslides might show fresher features than younger ones because of different degrees of human impact, natural erosion and different histories of landslide reactivation. Estimated persistence times range between 27 and 320 years but are minimum values only. In Lower Austria four landslides show estimated minimum persistence times between 4 and 28 years. In Lower Austria 27 landslides disappeared in less than 7 years after occurrence mainly because of planation by farmers. The results show no clear trend in landslide persistence, neither regarding landslide magnitude, nor regarding land use. However, it is evident that human impact plays a major role in landslide persistence.

Key words: airborne LiDAR, human activity, landslide persistence, Lower Austria, orthophoto, Swabian Alb

Introduction

Landslides occur frequently in hilly and mountainous areas. They contribute significantly to landform evolution (e.g. Korup 2009; Crozier 2010; Korup *et al*. 2010) and to sediment budgets (e.g. Jordan and Slaymaker 1991; Johnson *et al*. 2008; Chen 2009). Moreover, they pose a threat to human populations and continue to cause enormous economic damage and fatalities throughout the world (e.g. Schuster 1996; Crozier and Glade 2005). It is important to understand the landslide activity in a given study area to assess the impacts of landslides to sediment budgets and landform evolution. In addition, a detailed landslide inventory is required to adequately assess landslide susceptibility and subsequently landslide hazard and risk.

Since landslide hazard is the probability of a potentially damaging event of a given magnitude in a given area (Varnes 1984; Guzzetti *et al*. 1999), information on frequency and magnitude of landslides in the study area must be known. Thus, information must be gathered on past landslide activities (e.g. Holocene, historic and recent). It is also important to determine the age and/or recurrence intervals of landslides for a wide range of magnitudes because landslides can occur at large spatial-temporal scales (Glade and Crozier 2005). Generally, this information is difficult to obtain and quite often missing. There are various methods available to date single landslides, such as radiocarbon dating, lichenometry, dendrochronology, and optically-stimulated-luminescence (e.g. Lang *et al*. 1999). Regional approaches rely more on interpretation of multi-temporal aerial photographs (e.g. Guzzetti 2005; Guzzetti *et al*. 2006) or analysis of historical archives (e.g. Glade 2001; Guzzetti and Tonelli 2004). However, setting up a landslide inventory with occurrence dates remains a very challenging task, usually due to limited financial resources. Also, identifying landslides by interpretation of multi-temporal aerial photography is

© The authors 2012
Geografiska Annaler: Series A, Physical Geography © 2012 Swedish Society for Anthropology and Geography
DOI:10.1111/j.1468-0459.2012.00454.x

rather time consuming, imagery is usually only available for the last several decades and does not always provide the exact date of the landslide occurrence. Exploitation of historical archives might give information on landslide activity over several centuries, but is very time consuming and often incomplete. Thus, additional methods are necessary to enable the preparation of accurate landslide inventories that include an assessment for the approximate age of landslides.

For more than a decade *Airborne Laser Scanning* (*ALS*), also known as airborne *LiDAR* (*Light Detection And Ranging*), has been used to provide high-resolution *Digital Terrain Models* (*DTMs*), which enable many new investigations in geomorphology. The most important advantage of laser scanning, compared to all other methods for deriving DTMs, is that it can scan through vegetation. These types of DTMs are possible because the laser pulse can have multiple return signals; thus, the laser pulse is able to measure a first return, which in a forest is typically backscatter from tree canopies, and a second return that represents the reflection of the signal from an earth surface. As a result, the first and last return can be differentiated giving first the height of vegetation and second that of the terrain elevation. Modern full-waveform laser scanners are able to record the complete waveform of all echoes backscattered from a single pulse emission (Mallet and Bretar 2009). This new technique not only enables the mapping of vegetation in 3D (Wagner *et al*. 2008), but also improves the accuracy of the DTMs. Currently, vertical accuracy of ALS DTMs is <0.1 m (Mallet and Bretar 2009) in non-vegetated areas and planimetric accuracy is <0.5 m (Höfle *et al*. 2009).

The number of studies using ALS DTMs has significantly increased in recent years. In landslides studies ALS data is used to map landslides (e.g. Ardizzone *et al*. 2007; Bell 2007; Van Den Eeckhaut *et al*. 2007; Schulz 2007; Booth *et al*. 2009; Corsini *et al*. 2009; Haneberg *et al*. 2009; Kellerer-Pirklbauer *et al*. 2012; Petschko *et al*. 2010), to model landslides and their runout (e.g. Stolz and Huggel 2008; Gillon *et al*. 2009; Haneberg *et al*. 2009; Jaboyedoff and Labiouse 2011; Scheidl and Rickenmann 2010; Thiebes *et al*. 2010; Pomaroli *et al*. 2011; Kappes *et al*. 2011) as well as to asses landslide susceptibility (e.g. Bell 2007; Schulz 2007; Jaboyedoff *et al*. 2008; Pomaroli *et al*. 2011), and hazards (e.g. Baum *et al*. 2005; Bell 2007; Haneberg *et al*. 2009; Conway *et al*. 2010) and risk (e.g. Bell 2007).

However, the potential of ALS data is still not completely explored. Within this study, the focus lies on the investigation of the potential of ALS data in combination with information on the dates of landslide initiation to assess landslide age, landslide persistence and human impact for two study areas, the Swabian Alb in Germany and the Federal Province of Lower Austria in Austria and to evaluate the potential for preparing accurate landslide inventories.

Theoretical background

Within this study, landslide definitions refer to the widely used classifications of Cruden and Varnes (1996) and Dikau *et al*. (1996). If landslides occur, they first show a distinct morphology (e.g. sharp scarps and lateral flanks, hummocky topography) but these features can be modified over time either by natural erosion processes or by human impact until they become unidentifiable. The onset of geomorphological landforms and their disappearance over time were defined by Brunsden (1993) as persistence of landforms. He restricted it not only to landslide processes, but also to all geomorphological processes acting on the earth surface. Crozier (2010) defines landslide persistence as "the length of time the morphological characteristics of a landslide remain recognizable in the terrain" (p. 12). McCalpin (1984) was the first who tried to find criteria to assess the preliminary age of landslides based on geomorphological features, which was modified by Keaton and DeGraff (1996), including the renaming of the four activity state classes (see Table 1 and Fig. 1). McCalpin (1984) focused on landslides in a part of the Rocky Mountains, in which human impact could be more or less neglected. Furthermore, McCalpin (1984) and Keaton and DeGraff (1996) did not differentiate between various orders of landslide magnitudes. The description of the different classes seems to be appropriate for a huge range of different study areas. However, the estimated age intervals are only valid for study areas with similar environmental conditions and cannot be transferred to other study areas without modification. Surprisingly, only a few research studies continued the work of McCalpin (1984) and Keaton and DeGraff (1996) to try to estimate geomorphic changes of landslides and respective time intervals needed for these changes. Landslide persistence was investigated by Guthrie and Evans (2007). They found significant differences of the persistence between various

© The authors 2012
Geografiska Annaler: Series A, Physical Geography © 2012 Swedish Society for Anthropology and Geography

Table 1. Criteria for preliminary age classification of landslides for inventory mapping in the Rocky Mountains (based on Keaton and DeGraff 1996 and McCalpin 1984).

Activity state	Main scarp	Lateral flanks	Internal morphology	Vegetation	Toe relationships	Estimated age (years)
Active, reactivated, or suspended; dormant-historic (A)	Sharp; unvegetated	Sharp; unvegetated; streams at edge	Undrained depressions; hummocky topography; angular blocks separated by scarps	Absent or sparse on lateral and internal scarps; trees tilted and/or bent	Main valley stream pushed by landslide; floodplain covered by debris; lake may be present	<100 (historic)
Dormant-young (B)	Sharp, partly vegetated	Sharp, partly vegetated; small tributaries to lateral flanks	Undrained and drained depressions; hummocky topography; internal cracks	Younger or different type or density than adjacent terrain; older tree trunks may be bent	Same as for active class but toe may be modified by modern stream	100 to 5000 (Late Holocene)
Dormant-mature (C)	Smooth, vegetated	Smooth, vegetated; tributaries extend onto body of slide	Smooth, rolling topography; disturbed internal drainage network	Different type or density than adjacent terrain but same age	Terraces covered by slide debris; modern stream not constricted but wider upstream floodplain	5000 to 10 000 (Early Holocene)
Dormant-old or relict (D)	Dissected; vegetated	Vague lateral margins; no lateral drainage	Smooth, undulating topography; normal stream pattern	Same age, type and density as adjacent terrain	Terraces cut into slide debris; uniform modern floodplain	>10 000 (Late Pleistocene)

Note: Activity states dormant-stabilized and dormant-abandoned may have features of any age classification; the stabilized and abandoned states must be interpreted from other conditions.

landslide types and landslide magnitudes, ranging between *c*. 10 and 200 years for debris slides and debris flows and between *c*. 500 and more than 10 million years for rock slides and rock avalanches. However, they did not analyse the influence of human impact. Numerous studies on landslide mapping using ALS data are available as mentioned before. Many recognized the difficulties in mapping old landslides due to the altered features, but only few correlated landslide age with the modification of the geomorphological features using ALS data (e.g. Glenn *et al*. 2006).

Methods and data

To assess landslide age, landslide persistence and human impact different methods were applied. The most important prerequisite for all of these methods is a landslide inventory containing information on the date of occurrence and the location and spatial extent of the events. Therefore landslide inventory mapping and an analysis of different archive data were performed. Landslide mapping was carried out by interpretation of multiple hillshades of the available ALS DTMs. For the Swabian Alb the ALS DTM was produced with a spatial resolution of 1 m × 1 m from flights that were carried out between 2002 and 2004 (Landesamt für Geoinformation und Landentwicklung Baden-Württemberg, http://www.lgl-bw.de, 30-July-11). The ALS DTM of Lower Austria with a spatial resolution of 1 m × 1 m was compiled from flights in 2008 and 2009 (Federal Province of Lower Austria, http://www.intermap1.noel.gv.at, 30-July-11). From these multiple hillshades were computed using eight different light source azimuths (N, NE, E, SE, S, SW, W, NW) to prevent important parts of the landslides being not visible because of shadow effects. The landslide mapping focused on drawing major and minor scarps, cracks, landslide blocks and deposition areas. Furthermore, the boundaries of landslides were mapped to allow calculation of landslide area.

© The authors 2012
Geografiska Annaler: Series A, Physical Geography © 2012 Swedish Society for Anthropology and Geography

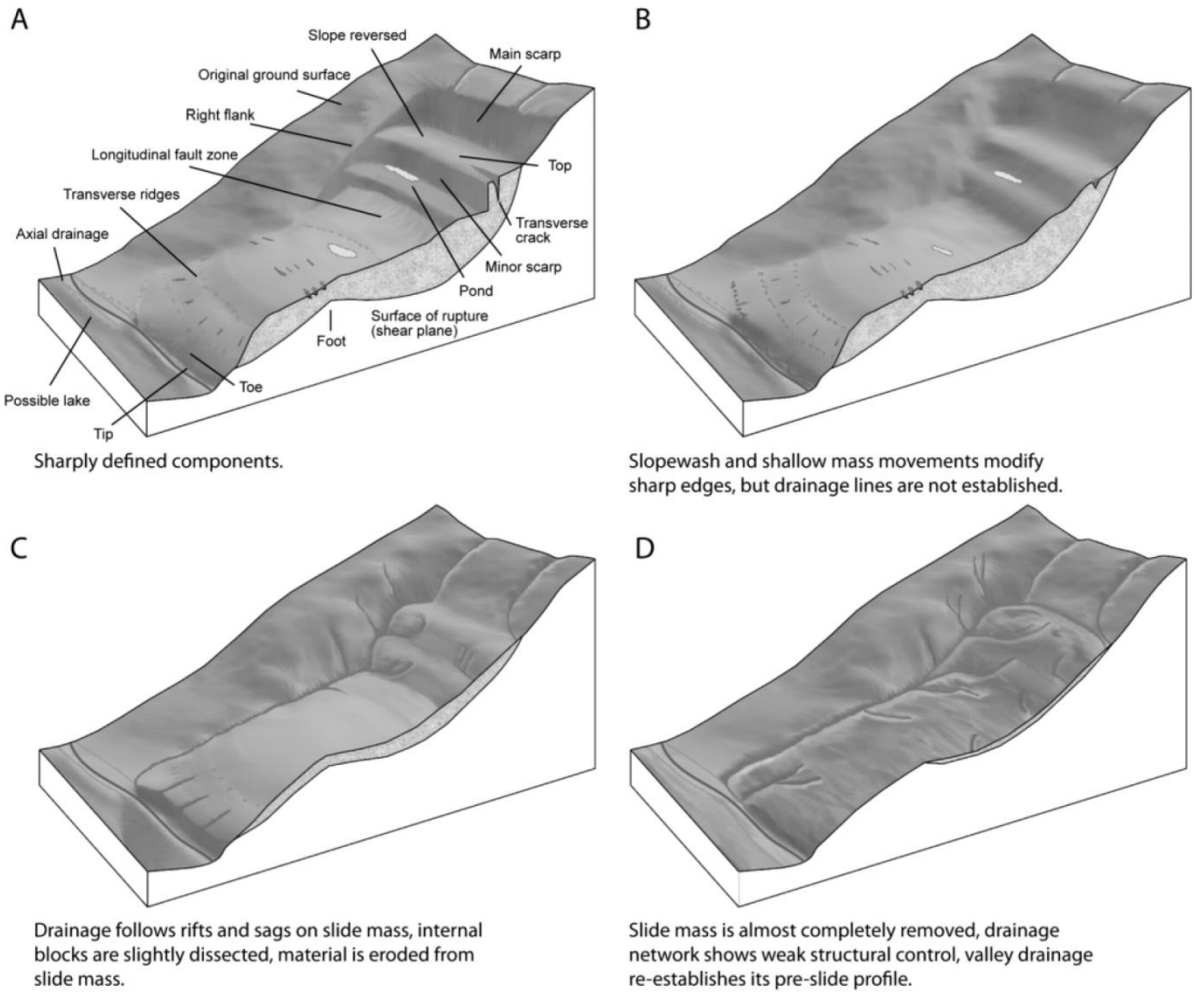

Fig. 1. Sketches of the geomorphological changes over time of an idealized landslide (based on McCalpin (1984) and Keaton and DeGraff (1996). A = active, reactivated, suspended or dormant-historic; B = dormant-young; C = dormant-mature; D = dormant-old (see also Table 2)).

To analyse the effects of the modification of geomorphological features of landslides over time and to determine the persistence of the landslides, the freshness of landslides was assessed using the approach developed by McCalpin (1984) and Keaton and DeGraff (1996). Criteria used are given in Table 1 and assessed by visual interpretation of DTM hillshades. Landslide mapping based on the ALS DTM were proofed by field investigations on all sites in the Swabian Alb and for selected sites in Lower Austria. In addition, it was necessary to gather additional information on the age of the investigated landslides. Due to different data available in the study areas in Lower Austria and in the Swabian Alb different methods were applied, respectively. An overview on the studies carried out and methods applied in the study areas is presented in Table 2.

For Lower Austria (Waidhofen/Ybbs) landslide age was determined by analysing information available from the Building Ground Register (BGR) of the Geological Survey of Lower Austria in comparison to a landslide inventory containing 691 landslides that was mapped by Petschko *et al.* (2010) using ALS data and by mapping landslides from digital orthophotos from 2002/2004 or 2007 with a pixel resolution of 25 cm and 12.5 cm, respectively. The BGR is a database that consists of about 2000 entries on landslides, which occurred and were reported since 1953 in Lower Austria. Their location is stored in a point shapefile. Furthermore, for each landslide reports on damage to houses, streets or agricultural land are available. The analysis of the BGR was mainly based on the comparison of the location of the landslide points of the BGR (151 points) to the landslide polygons

© The authors 2012
Geografiska Annaler: Series A, Physical Geography © 2012 Swedish Society for Anthropology and Geography

Table 2. Overview on studies carried out in different study areas.

	Swabian Alb	Lower Austria
Landslide mapping	Based on ALS DTM and field investigations	Based on ALS DTM, digital orthophotos and field investigations
Landslide age	Based on historical archives	Based on digital orthophotos and Building Ground Register (BGR)
Land use	No information on land use for the whole time of large landslides persisting on earth surface were available	Based on land cover data set derived from satellite imagery
Human impact on landslide	Based on historical archives and field investigations	Based on ALS DTM, digital orthophotos and field investigations
Landslide persistence	Derivation of minimum landslide persistence, since investigated landslides are still recognizable in the field / ALS DTM	Derivation of maximum landslide persistence for 27 landslides which were visible in orthophotos of 2002/2004 and/or 2007 and vanished in the ALS DTM of 2008/2009 Derivation of minimum landslide persistence for 4 landslides which are still recognizable in the field / ALS DTM

which had been mapped by Petschko *et al*. (2010). To get more detailed information on the location of the landslide points old maps, which were attached to the reports of each landslide in the BGR, were also analysed. If these landslides could be accurately located and were still visible in the DTM a minimum landslide persistence was calculated. With this analysis only two landslides from the existing inventory have been identified that were reported in the BGR and are still visible on the ALS. These two landslides were analysed in more detail in the current study. The mapping on the orthophotos was focused on fresh landslides, which were characterized by a missing vegetation cover, either on the entire landslide body or on the main scarp of the landslide only. Because of the missing vegetation cover it can be assumed that these landslides occurred in the year of which the orthophoto was taken or at maximum one year earlier. Applying these criteria 29 landslides were mapped on the digital orthophotos from the years 2002/2004 or 2007. For these landslides it was checked whether these are still visible on the digital orthophotos of 2007 and/or on the ALS DTM derivatives of 2008/2009 and their persistence was obtained. A maximum landslide persistence was calculated when the landslide was already obliterated in the digital orthophotos of 2007 or the ALS DTM. Maximum landslide persistence means that e.g. if the fresh landslide is visible in the images of 2002 but not in the images of 2007 the maximum landslide persistence is determined with 6 years, as no detailed information on the exact time of disappearance is available. The actual persistence time might be shorter because the landslide might have disappeared already 1 to 5 years earlier. If the landslide is still visible in the ALS DTM then a minimum landslide persistence was calculated starting from the year of occurrence until the year of the ALS DTM origin.

For the Swabian Alb historical analysis was carried out by analysing various archives storing information on landslides in the Swabian Alb (Hauptstaatsarchiv Stuttgart, Staatsarchive Ludwigsburg und Sigmaringen, Stadtarchiv Mössingen und Gemeindearchiv Bad Überkingen). The focus was on the investigation of hand written sources and historical maps. First findings aids (Findbücher) were analysed, promising documents ordered and read. If landslide records were found, copies of the documents were ordered. Subsequently, handwritten sources were transcribed and most important information extracted. More detailed information can be found in Röhrs and Dix (2010). The important information collected comprises of the date of landslide occurrence, the size of the event and its location. Reliability of historical records is evaluated in each case. This encompasses e.g. the evaluation of the source and the author, the closeness of timing and location of the historical document in relation to the landslide event, the context in which the landslide was reported and the critical comparison with other historical documents from the same period or reporting the same landslide event. In addition to ALS and historical data, orthophotos from 2003 with a resolution of 25 cm were used to evaluate the visibility of the landslides and therefore the

© The authors 2012
Geografiska Annaler: Series A, Physical Geography © 2012 Swedish Society for Anthropology and Geography

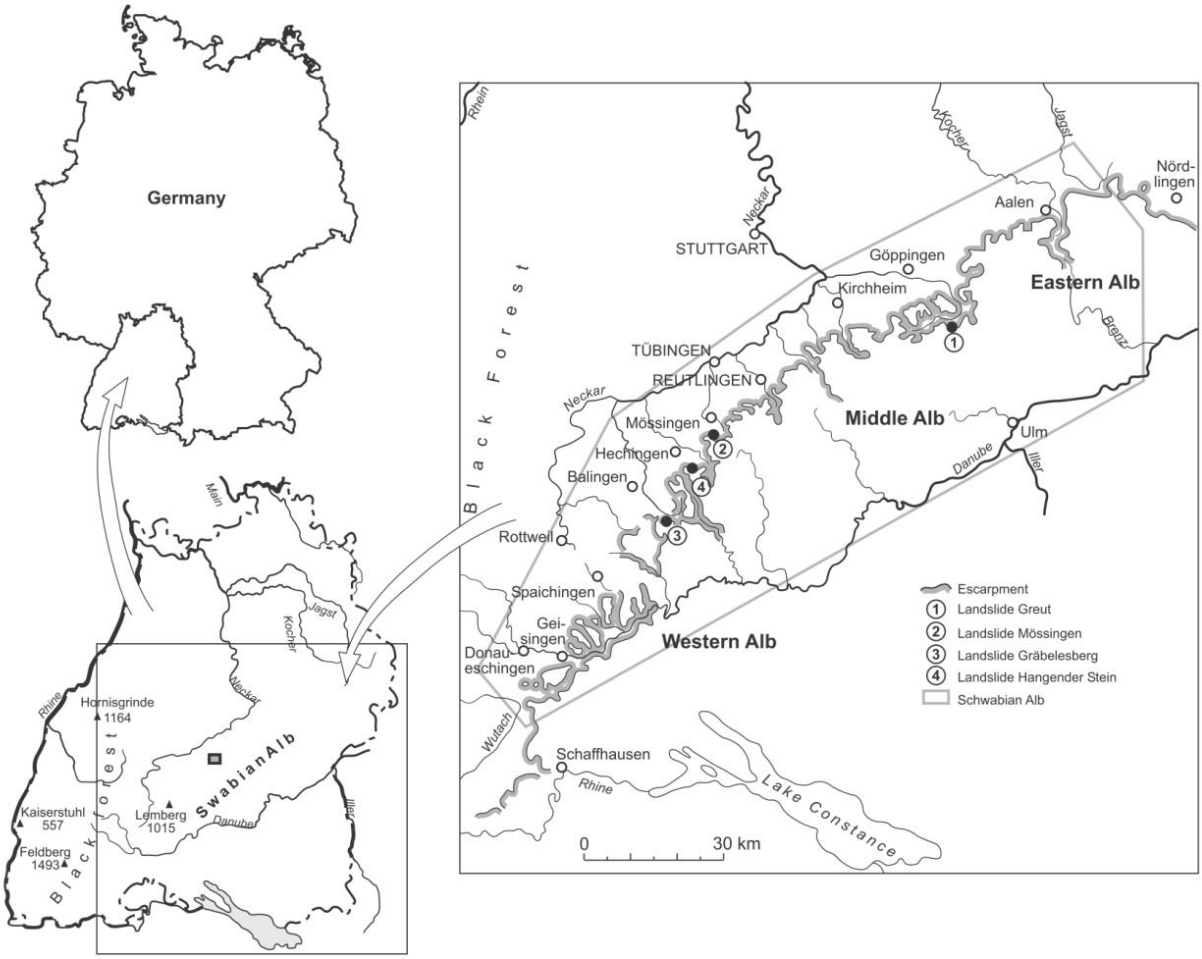

Fig. 2. Study area Swabian Alb in southwestern Germany.

landslide persistence. For the Swabian Alb only minimum landslide persistences were calculated ranging from the date of landslide occurrence to the year of the ALS DTM origin.

The influence of landslide size and land use and therefore the effect of human impact on the preservation of the geomorphological features of the landslides was also studied. Landslide size was derived within the *Geographical Information System* (*GIS*) based on the polygon boundaries of the mapped landslides and compared to the information of historical sources if available. The influence of land use was only investigated in the study area of Lower Austria, since comparable information for the older landslides in the Swabian Alb was not available. The information on land use/land cover for the entire Province of Lower Austria was given by a satellite imagery-derived land cover dataset that was obtained using a supervised classification on a composite of various satellite images of the years 2007 and 2008 (Aster, Landsat TM5, Landsat TM7 and ALOS/AVNIR). For the district Waidhofen/Ybbs Aster images cover the whole area, so that for the detailed investigation land cover information with a resolution of 15 m × 15 m could be used (H. Proske, pers. comm. 2011). Furthermore, the influence of humans on triggering landslides was estimated by the analysis of the watershed of a landslide. Therefore the watershed of a hillslope was analysed what was performed by mapping the natural and the artificially increased watershed in a GIS according to the local topography, morphology and road network.

Study areas

Swabian Alb

The locations of the Swabian Alb, as well as of the landslides investigated, are shown in Fig. 2. The

© The authors 2012
Geografiska Annaler: Series A, Physical Geography © 2012 Swedish Society for Anthropology and Geography

Swabian Alb is part of the South-German Cuesta landscape and covers about 10 000 km^2. It is a lower mountain range, which rises up to 800 m in the East and up to about 1000 m in the West. The height difference between escarpment and valley bottom is *c.* 200–300 m. Lithology is rather homogeneous and consists of Jurassic sedimentary rocks with limestone overlaying marls and clay (see Geyer and Gwinner 1997; Wagenplast 2005; Bell 2007 for details). Slopes in clay are rather gentle (<15°), steeper in the marls (15–30°) and the limestones built up the escarpment. Average yearly rainfall varies between 800 mm and 1300 mm and gradually rises from the drier south-western parts due to lee effects of the Black Forest to the wetter north-eastern parts (Bell 2007). Due to these environmental conditions the region is prone to landslides that are mainly triggered by rainfall events but also snow melting (Bell 2007). Since the Swabian Alb is one of the seismically most active regions in Germany (strongest events in the twentieth century occurred in 1911, 1943 and 1978 (Rothe 2005); in general earthquake magnitudes range up to around ML = 6 (Meyenfeld 2008)), landslides might also be triggered by seismic events but so far only two landslides are known to be seismically induced (Bell 2007). In the Upper Fils-Valley, in which the landslide Greut (investigated in this study) is located, Brennecke (2006) mapped 525 landslides in an area of approx. 80 km^2 based on ALS data and multi-temporal aerial photo interpretation, demonstrating the landslide susceptibility in that area (results are also published in Bell 2007). Assuming the representativeness of this inventory for the whole Swabian Alb, probably more than 20 000 landslides could be mapped in the Swabian Alb.

In the Swabian Alb four study sites were chosen for which essential information on landslide age and ALS data were available: landslide Gräbelesberg (48° 12′ 27.61″ N, 8° 55′ 15.93″ E) in the eastern part of the Western Alb, landslide Hangender Stein (48° 18′ 9.34″ N, 9° 0′ 13.70″ E) and landslide Mössingen (48° 22′ 35.14 ″ N, 9° 3′ 53.01″ E) in the western part of the Middle Alb and landslide Greut (48° 35′ 55.88″ N, 9° 44′ 57.08″ E) in the eastern part of the Middle Alb (Fig. 2).

Lower Austria

The Federal Province of Lower Austria is located in the north-east of Austria mostly at the Alpine foreland (Fig. 3). The study area has a size of 10 200 km^2 and is very heterogeneous regarding its morphology and land cover. This heterogeneity results from the geological setting with five major geological units that leave a characteristic imprint on the morphology. These units are the Bohemian Massif, the Molasse Zone and related basin sediments, the Flysch- and Klippen Zone, the Northern Calcareous Alps and different types of the eastalpine crystalline (Wessely *et al.* 2006). These units show very contrasting properties concerning their slope stability and occurring landslide types. Schwenk (1992) showed that the Bohemian Massif and large parts of the Northern Calcareous Alps are mainly affected by rock falls, whereas most of the shallow and rotational slides reported in Lower Austria occurred in the Molasse Zone, the eastalpine crystalline and particularly in the Flysch- and Klippen Zone.

The main triggers of slides in Lower Austria are extreme rainfall and/or high snow melt rates in spring (Schwenk 1992; Schweigl and Hervás 2009). The spatial distribution of rainfall in Lower Austria shows a distinctive gradient with high precipitation rates of up to 1700 mm per year in the South-West to the lowest annual precipitation rates in the North-East with about 500 mm (Hydrographic Service of Lower Austria, http://www.noel.gv.at/Externeseiten/wasserstand/htm/wndcms.htm, 02-Mar-11).

In this study three sites in Lower Austria for the analysis were chosen as indicated in Fig. 3. The first site is the Achleiten locality (48° 9′ 28.63″ N, 14° 40′ 26.33″ E), situated in the Molasse Zone along the Danube River. This site is mainly characterized by the occurrence of the Schlier Formation that is dominated by fine grained sediments and is often affected by slides (Schweigl and Hervás 2009). The second study site is the Waidhofen/Ybbs district (47° 57′ 36.83″ N, 14° 46′ 22.19″ E), characterized by the Flysch- and Klippen Zone and the Northern Calcareous Alps, in which the Stritzlödt study site is also located (47° 59′ 5.85″ N, 14° 49′ 14.48″ E). The Flysch- and Klippen Zone contains sandstone with high amounts of clays and marls. Therefore, this formation shows a very smooth morphology with open slopes and moderate slope angles and is highly susceptible to shallow and deep seated slides. In contrast, the Northern Calcareous Alps are dominated by limestone and dolomites with only small amounts of marls. The morphology of this geological unit is characterized by steep slopes and deeply incised streams. The third study site is located in

© The authors 2012
Geografiska Annaler: Series A, Physical Geography © 2012 Swedish Society for Anthropology and Geography

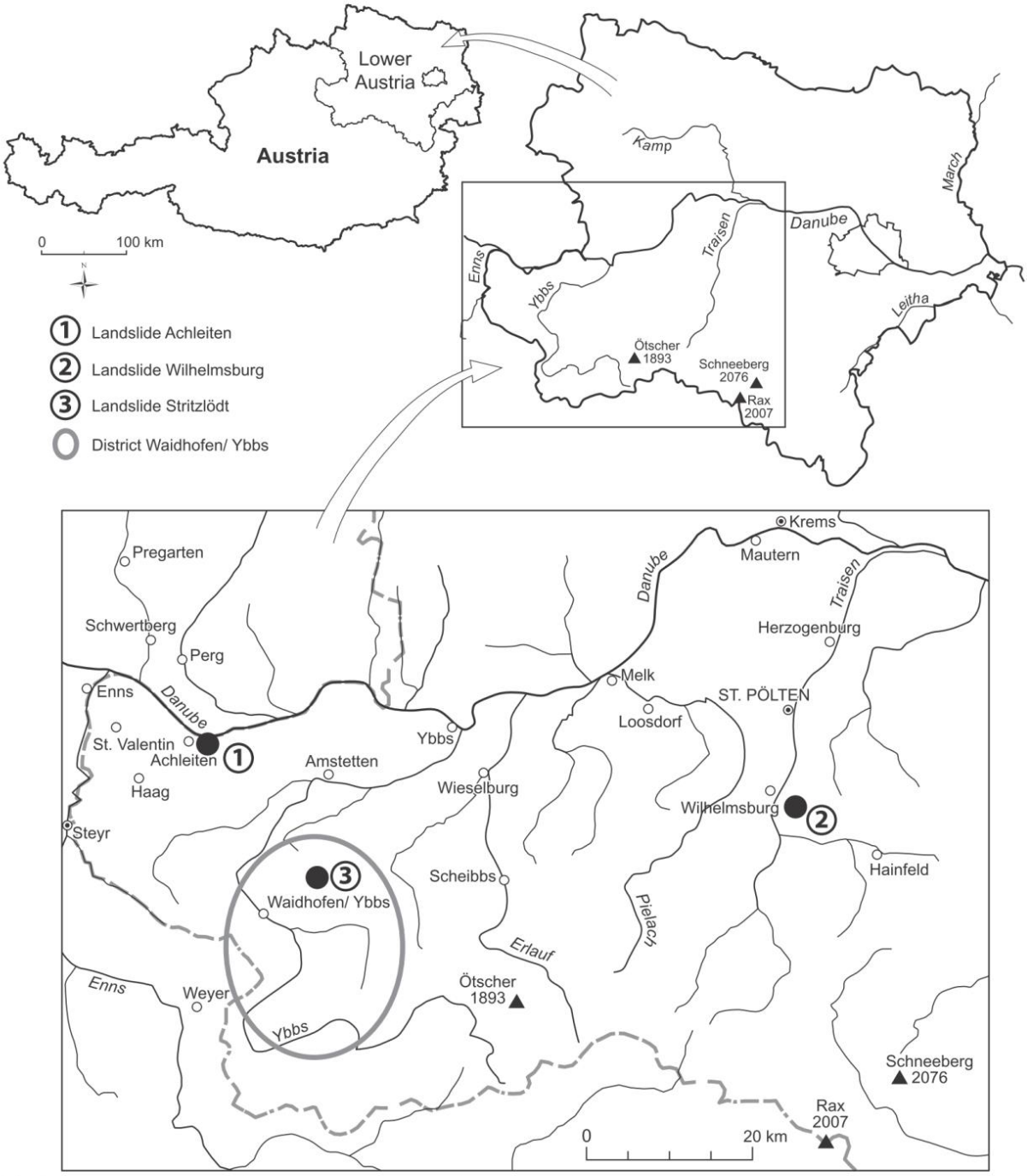

Fig. 3. Study area Lower Austria, a provincial state in northeastern Austria.

the Flysch Zone near the town of Wilhelmsburg at a slope orographically right to the Kreisbach river (48° 5′ 19.91″ N, 15° 37′ 41.41″ E). This site was chosen because of a recently active slide that was first reported in 1996 in the BGR and was still active in 2009. Unfortunately, information on the current activity state is missing.

Results

Within this section first the results of relative age determination are shown based on examples from the Swabian Alb, followed by the influence of human impact on landslides, mainly demonstrated using examples from Lower Austria. Finally,

© The authors 2012
Geografiska Annaler: Series A, Physical Geography © 2012 Swedish Society for Anthropology and Geography

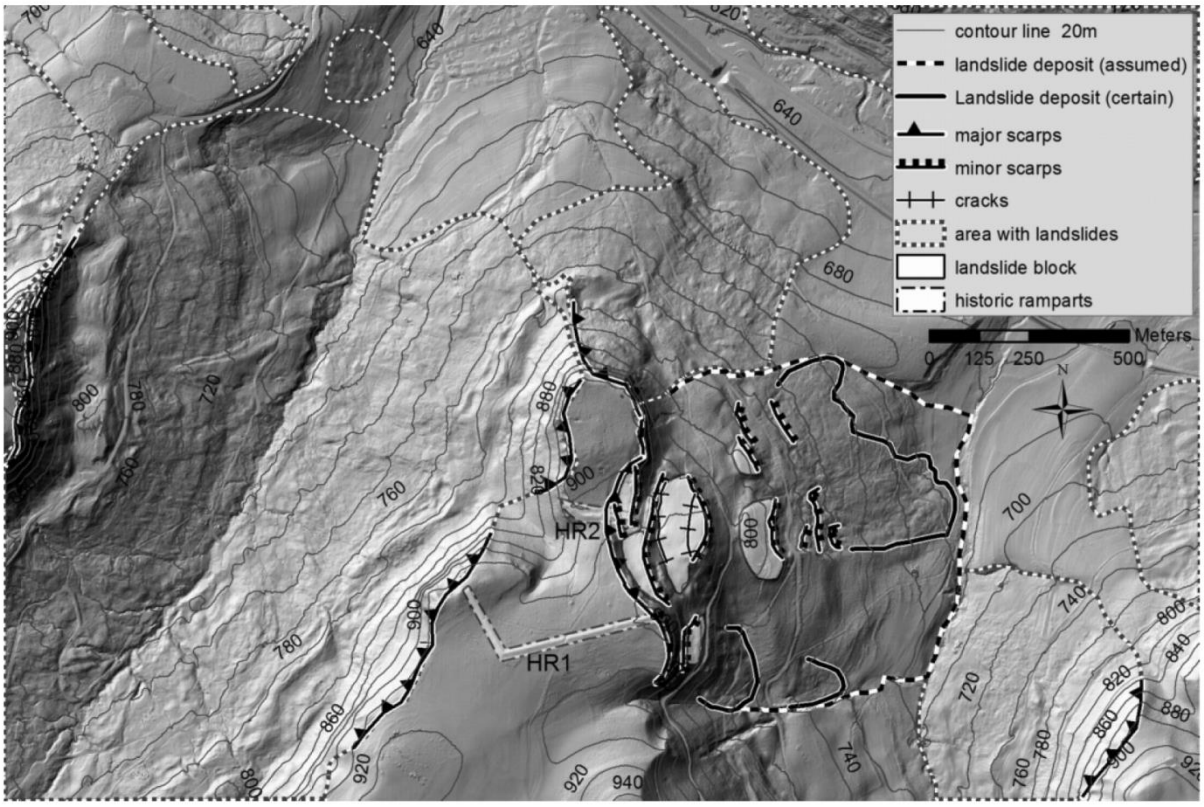

Fig. 4. Morphological features of the landslides at the Gräbelesberg mapped on ALS hillshade. Historical ramparts were displaced by the landslide.

results on landslide persistence in the Swabian Alb and in Lower Austria are presented.

Relative age of landslides

To assess the relative age of landslides based on the modification of geomorphological features over time, landslides of known age are analysed in four study sites in the Swabian Alb.

Landslide Gräbelesberg At the Gräbelesberg numerous landslide phenomena can be found as well as historical ramparts (HR1 and HR2 in Fig. 4). The latter show that the spur of the Gräbelesberg was settled in historic times. The landslide block in Fig. 4 is assumed to be of Pleistocene age (Geological Map 1 : 25 000, 7719 Balingen). This assumption is in line with several other authors who suppose that most of such big landslides occurred in the Pleistocene (e.g. Bleich 1960; Terhorst 1997, 2001), although none of these big landslides have, as yet, been accurately dated.

The detailed analysis of the ALS hillshade shows that the historical rampart HR2 was displaced by the landslide event. Field investigations proved this observation. Until now two different dates of origin for the ramparts are available. On the one hand proofs of the Hallstatt culture were found (i.e. younger than 800 BC) and on the other hand finds (a strap end) could be dated to the sixth century AD (Schmitt 2005). Since the landslide modified rampart HR2, it seems to be younger than 800 BC and therefore much younger than expected before. It might also be that a larger reactivation displaced this historical rampart, which must still be proven by further investigations.

Nowadays, orthophotos show that the whole area is covered in forest, except some small patches of grassland close to the valley bottom. The geomorphological features of the old landslide were significantly altered over time. Furthermore, recent landslide activities are mapped in Fig. 4. The largest landslide block in the upper central part shows some cracks, which seem to be still active. Even though this must be proven by further and more detailed field investigations, potential reactivations of this landslide block might have prevented this feature from further alteration or vanishing.

© The authors 2012
Geografiska Annaler: Series A, Physical Geography © 2012 Swedish Society for Anthropology and Geography

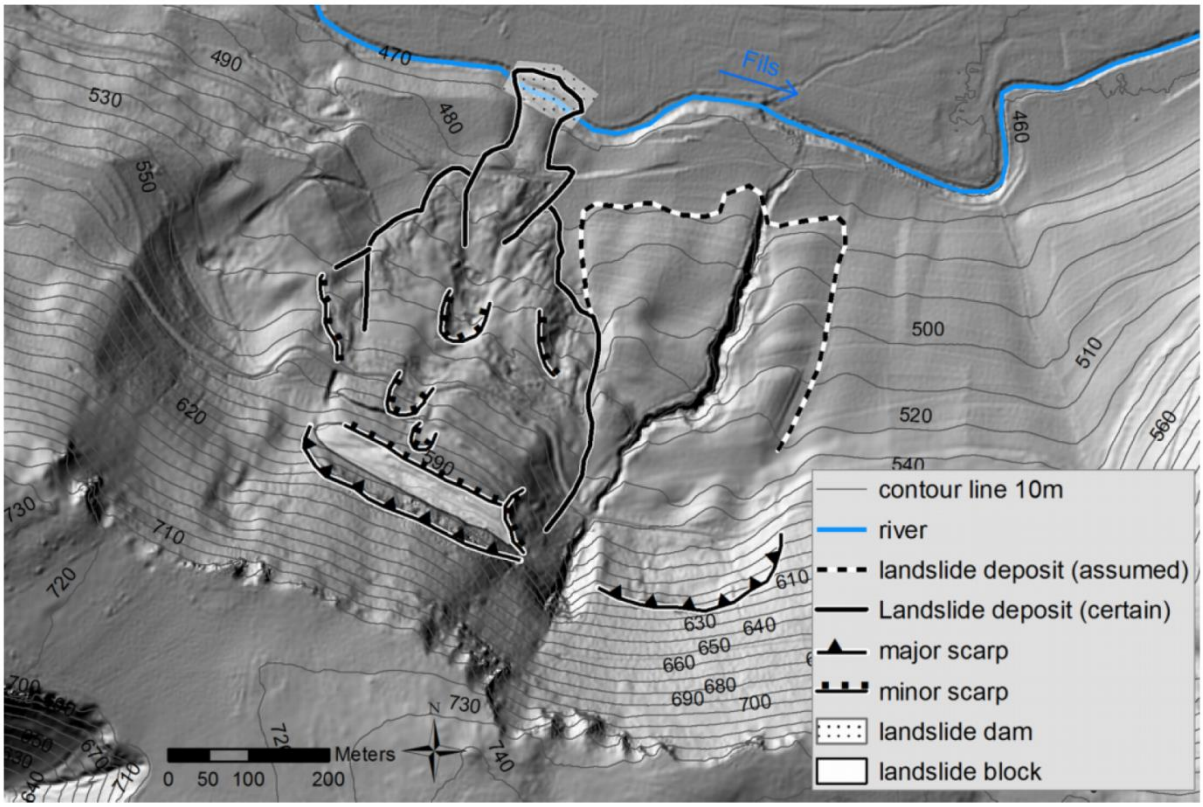

Fig. 5. Morphological features of the landslide Greut 1805 which dammed the river Fils and another landslide (mapped on ALS hillshade).

Landslide Greut 1805 For this landslide detailed historical information is available from official administrative letters and protocols from 1805 only dealing with this landslide event and its management. Thus, these documents are evaluated to be highly accurate regarding timing and location of the landslide. Unfortunately, a sketch of the landslide referred to in the protocols got lost. The landslide Greut occurred on 27–28 February 1805 and involved an area of 40 Jauchert (1 Jauchert = 3.309 m^2) forest, $9^1/_4$ Jauchert agricultural land and $4^1/_4$ Tagwerk ("a full day's work", 1 Tagwerk = 3.408 m^2) grassland which altogether is approx. 177 000 m^2. The landslide is clearly visible in the ALS hillshade (Fig. 5) with geomorphological features of the landslide like main and minor scarps as well as the different parts of the landslide toe. Within the middle part of the landslide material moved all the way down to the river Fils and dammed it. Even though it looks like the middle part could also be a reactivation of the initial movement, historical records reveal that this already happened in 1805. This is also proven by comparison of the landslide size mentioned in the historical documents to the GIS based analysis of the mapped landslide in Fig. 5, which is, with 160 000 m^2, in the same order of magnitude.

The dam was dug up manually by about 100 men to prevent a catastrophic flood following a dam-break. Considering the age of about 200 years, the geomorphological features are still very well preserved, meaning that the landslide shows a distinct morphology although no reports on major reactivations are known. It is assumed that this is mainly, because the whole area of the landslide was likely covered under forest for the whole time, except the first years after failure, when the forest cover was at least partly destroyed by the landslide itself.

East of the 1805 landslide another landslide was mapped. Its main scarp is still clearly visible but more material was removed in the upper parts. Landslide features in the lower parts are much softer and rounded. Also the channel was able to incise up to 6 m in the meantime. Unfortunately, no age of this older landslide is available. The local field name "Greut" means "clearing of forest". This can mean a man-made clearing of the forest

© The authors 2012
Geografiska Annaler: Series A, Physical Geography © 2012 Swedish Society for Anthropology and Geography

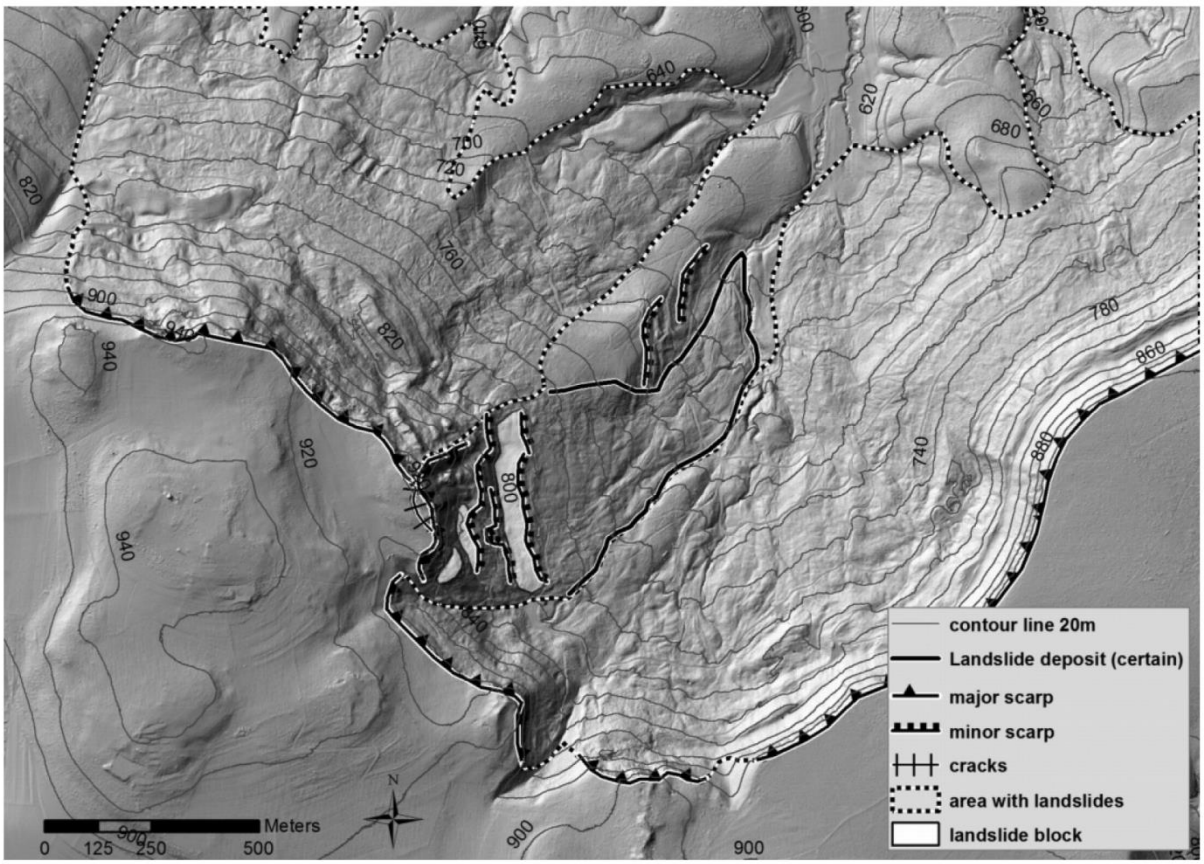

Fig. 6. Morphological features of the landslide Hangender Stein 1879 and surrounding landslide areas (mapped on ALS hillshade).

but also a natural clearing of the forest by landslides, forest fires or wind throw. The field name existed before 1805. Since historical information shows that the area was for centuries under forest owned by the community and considering the steep slope of that area it is more likely that the clearing was caused by natural processes than by human activity. This is also supported when comparing this situation with other communities, for which information on man-made clearing is available. Since more landslide than forest fires and wind throws are reported from that area and its surroundings and taking the morphology into account it seems to be more likely that the local field name "Greut" refers to pre-1805 landslide activity.

Landslide Hangender Stein 1879 The name Hangender Stein ("hanging rock") refers to the deep cracks at the escarpment, which also clearly appear in the ALS hillshade above the main scarp (Fig. 6). The historical analysis revealed that a landslide occurred in 1879 at this location, covering an area of about 315 000 m^2. Based on this information a landslide was mapped using the ALS hillshades. Digitizing the boundaries started at the main scarp and followed the main geomorphological features visible in the hillshade (Fig. 6). After mapping, the planimetric and real area of the landslide was calculated in GIS and resulted in 283 000 m^2 and 309 000 m^2, respectively. Both values are rather close to the landslide area mentioned in the historical report, meaning that at least the order of magnitude is the same. Within the landslide, main and minor scarps as well as different landslide blocks are visible. However, the geomorphological features are not as clear as at the landslide Greut, although the latter is some decades older. Especially, the boundaries are not always clear, which is related to the high landslide activity in the entire area. Thus, there is some uncertainty in the exact location of the landslide boundaries. Studying the vicinity of the mapped landslide, many other landslides can be seen, indicating that almost all slopes are affected by landsliding. Therefore, in many places the exact boundaries are very difficult or impossible to map. Unfortunately,

© The authors 2012
Geografiska Annaler: Series A, Physical Geography © 2012 Swedish Society for Anthropology and Geography

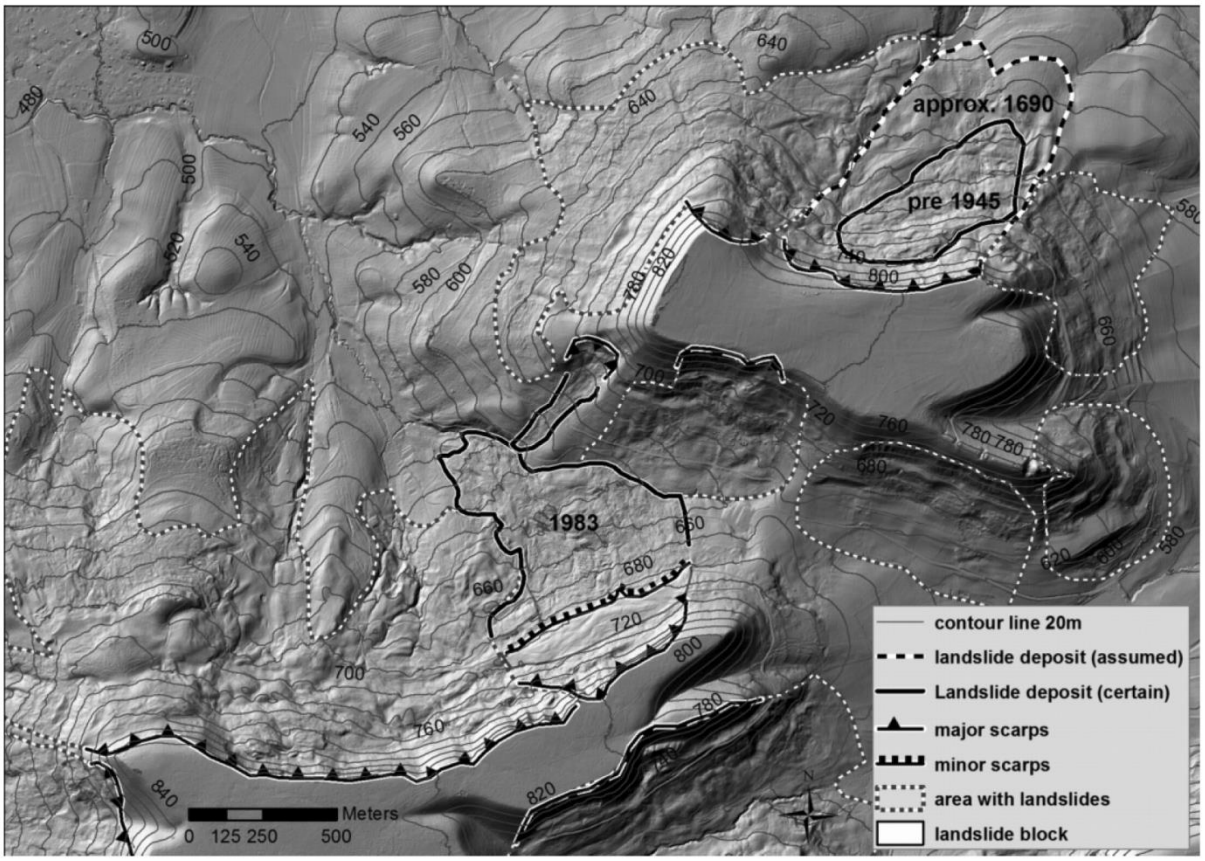

Fig. 7. Morphological features of the landslide Mössingen 1983 and landslides at Farrenberg (mapped on ALS hillshade).

no more dated landslide events are known in the area shown in Fig. 6. The entire area is forested so that landslide morphologies are rather well preserved.

Landslide Mössingen 1983 The Mössingen landslide occurred on 12 April 1983. It involved an estimated volume of 6 million m^3 and covers an area of about 500 000 m^2 (Fundinger 1985; Bibus 1986; Schädel and Stober 1988). The landslide itself was a reactivation of a pre-existing landslide. The landslide block located just below the main scarp rotated slightly (indicated by tilted trees) and moved a few metres further down, with all the trees remaining almost intact on top of the landslide block. However, the rest of the forest was destroyed. Studying the morphology of the landslide area of 1983, it is surprisingly hard to draw the boundaries by using the ALS hillshades only, even though it is the youngest analysed event with a substantial landslide area and volume. Finally, the boundaries were defined by the help of a landslide map of the event which was prepared by interpreting post-event aerial photographs and field mapping (Fundinger 1985, see Fig. 7).

In the same area two more landslides were mapped (Fig. 7). The larger one occurred around 1690 AD, but the exact date is not reported in historical documents. It is reported that the landslide was visible from the Black Forest like the Mössingen landslide is today. Thus, it was assumed that the landslide must have had a similar size. To be visible the landslide must have occurred at the northern slope of the Farrenberg. The geomorphological features of this landslide were heavily modified over time, so that the exact boundaries were more difficult to draw (Fig. 7). Within this landslide, a reactivation occurred which could be dated to pre 1945 resulting from a multi-temporal aerial photo interpretation (M. Galli, pers.com. 2007). This reactivated landslide shows much fresher geomorphological features than the initial movement of 1690 AD.

Similar to the Hangender Stein area, the entire area shows a high level of recent landslide activity (confirmed by field investigations and multi-

© The authors 2012
Geografiska Annaler: Series A, Physical Geography © 2012 Swedish Society for Anthropology and Geography

temporal aerial photo interpretation), which is preserved well because of the widespread forest cover. However, the high landslide activity in some places hampers the mapping of single landslides in the ALS hillshade, since large parts of the whole area seems to slide from time to time creating a palimpsest of landslides of different sizes and ages, so that distinct morphologies of single landslides cannot be easily seen.

Human impact on landslides

Human impact on the landslides in the Swabian Alb shown in the previous section is less intensive. However, at the landslide Gräbelesberg human activity was beneficial to improve the estimation of landslide age. And at the landslide Greut humans took some influence in removing the landslide dam. In the following examples of Lower Austria it is shown that human impact (on preparatory factors and on the morphology) can be quite significant.

Landslide area Achleiten In the Achleiten area almost all slopes facing towards the north and therefore towards the Danube river are showing widespread landslide activity (Fig. 8). To some extent the geomorphological features visible in the ALS hillshade are comparable to the locations Hangender Stein (Fig. 6) and Mössingen (Fig. 7). Also in the Achleiten area it is difficult to map single landslides.

Comparisons of the digital orthophoto (Fig. 8a) and the ALS hillshade (Fig. 8b) indicate clearly the extreme extent of modification of earth surface and geomorphological features by humans. In the central part of the images rather old landslide features were heavily altered and smoothed by farming activities. In the eastern part the building of farmhouses and converting forest into grassland modified another huge landslide area. Unfortunately, so far no information on timing and extent of human activities is available, which leads to some uncertainties and prevent the quantification of the modifications caused by humans. Nevertheless, this example impressively shows what extent human impact can have. In this case only a part of the landslide was altered, but it can be assumed that similar effort was taken on smaller landslides as well so that their morphological footprint completely disappeared on the ALS DTM, as shown in the following example of the landslide Stritzlödt.

Landslide Stritzlödt 2007 In Stritzlödt a fresh landslide is visible in the digital orthophoto of the year 2007 (Fig. 9a). This landslide covers an area of about 2800 m^2. Comparisons with the ALS hillshade, which originates from the year 2008, show that no fresh geomorphological indications of landslide activity are visible anymore (Fig. 9b). Thus, the landslide vanished during this period because of planation by the farmer. Natural erosion as explanation can be excluded since the erosional pattern would be different and so far experience in that area shows that natural erosion does not remove landslides of that size that fast.

Landslide Wilhelmsburg According to the records of the Building Ground Register of the Geological Survey of Lower Austria the first landslide movement at Wilhelmsburg dates back to the 1996. Reactivations were reported in 2006 as well as in 2009. These landslides were triggered either by rainfall or snow melting. The boundaries of the landslide areas are shown in Fig. 10. During fieldwork it became obvious that anthropogenic channels and an anthropogenic sunken road (Hohlweg) play a major role in current landslide activities and probably also in historical landslide activities due to substantial influence on the surface water drainage. Therefore, the channels as well as the natural and artificially enlarged watersheds were mapped based on the ALS hillshade. Calculating the respective areas in GIS demonstrates that the natural watershed of 0.1 km^2 was enlarged by the anthropogenic channels and the sunken road by its half (i.e. 0.05 km^2). This leads to a significant water surplus, which could be observed during field work and was confirmed by local people. This additional water seems to be responsible for the ongoing and/or increased landslide activity.

Landslide persistence

In this study landslide persistence is either given as minimum persistence, when the landslides are still visible in the ALS hillshades or as maximum persistence when the landslide already disappeared but no absolute time period could be determined. Within this section, nine landslides of the Swabian Alb and 31 landslides of Lower Austria that have available age information are analysed.

In Fig. 11 landslide persistence of the larger landslides in the Swabian Alb and smaller landslides in Lower Austria is shown. It is clearly demonstrated that larger landslides persist much longer in the landscape. The three landslides of the Swabian Alb which show a lower persistence are

© The authors 2012
Geografiska Annaler: Series A, Physical Geography © 2012 Swedish Society for Anthropology and Geography

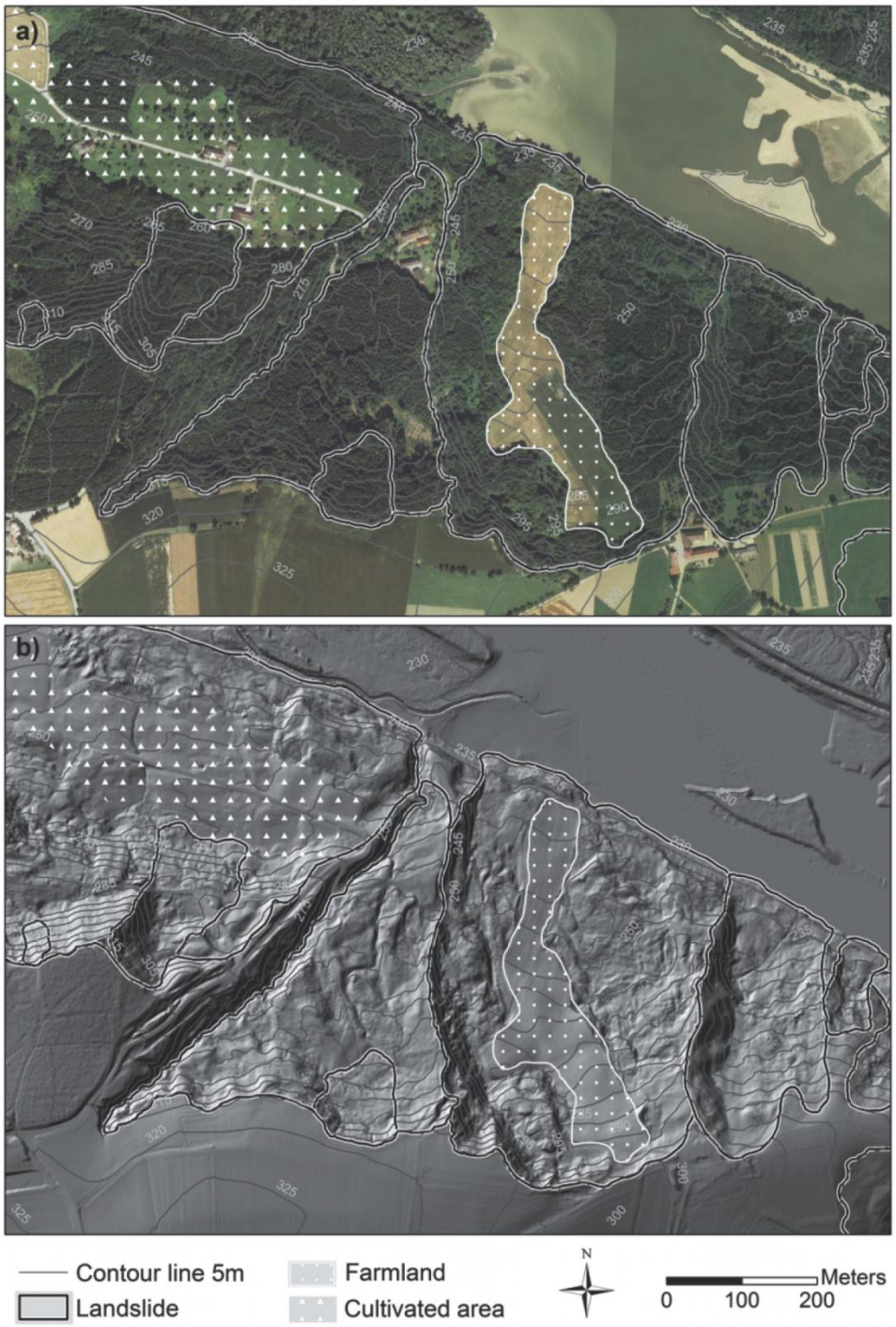

Fig. 8. Digital orthophoto (a) and ALS hillshade (b) of the Achleiten area showing a landslide morphology altered by human activity.

the youngest large landslides. They probably will be identifiable in the landscape for decades, centuries or even much longer. A clear difference is that landslide persistence for all landslides of the Swabian Alb are minimum values whereas in Lower Austria 27 of 31 landslides show maximum persistence values.

In Lower Austria the longest persistence of the investigated landslides is less than 30 years. This is due to the generally much lower magnitude of landslides with known age; in both study areas there is no clearly identifiable trend, except that there is a general tendency that persistence increases with landslide size. However, this

© The authors 2012
Geografiska Annaler: Series A, Physical Geography © 2012 Swedish Society for Anthropology and Geography

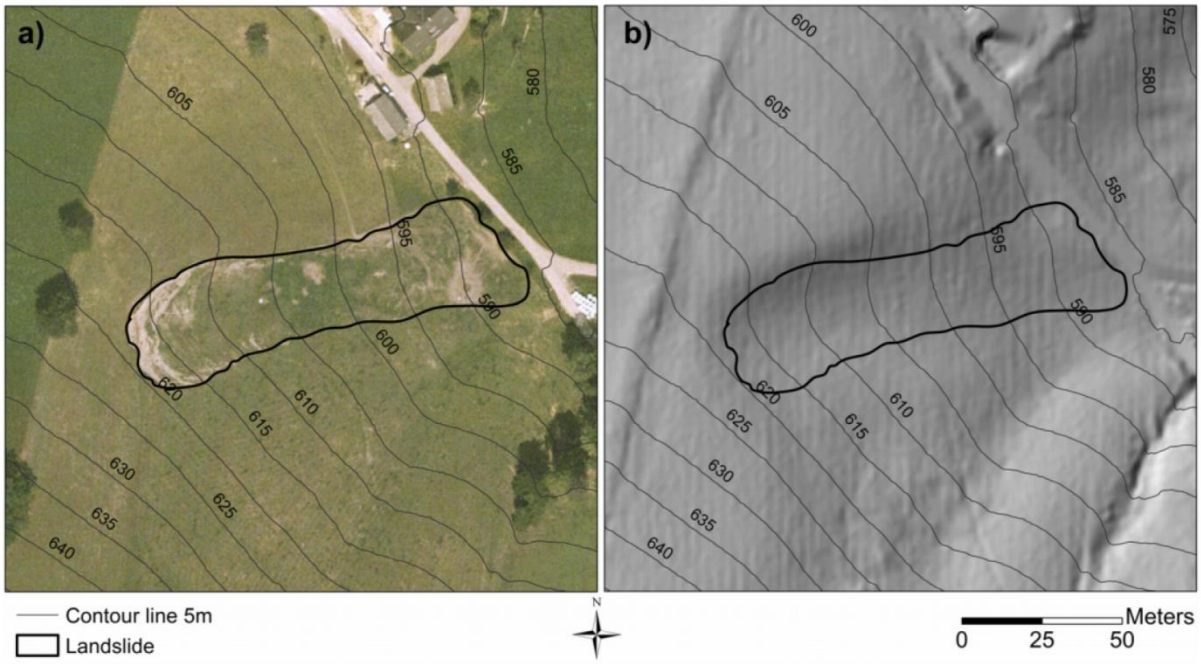

Fig. 9. Digital orthophoto from 2007 (a) and ALS hillshade from 2008 (b) of the Stritzlödt landslide, which disappeared by planation.

assumption is only valid when landslides from the Swabian Alb are compared to the ones of Lower Austria. Within the subsets of each region no clear trend can be seen so that also large landslides can have a short persistence. Nevertheless, it must be stated that in Lower Austria larger landslides can be found with assumed higher persistence, but these landslides lack information on age.

Beside the magnitude of landslides the landslide persistence is dependent on land use. This could only be analysed using the data from Lower Austria, particularly inventory data from Waidhofen/Ybbs. Table 3 shows the land use summarized for all 691 landslides mapped (by Petschko*et al.* 2010) in comparison to the land use of the 31 landslides for which landslide age information is available. Twenty-seven of these 31 landslides have already disappeared from the earth surface and are not visible in the ALS hillshades. Whereas 38% of all mapped landslides are located in currently forested areas, only 16% of the disappeared landslides occurred in forested areas, 23% of the disappeared landslides happened on agricultural land, and the majority of 48% on grasslands. Most of these landslides disappeared due to human activities, mainly planation. Nine landslides vanished within one year, e.g. the landslide Stritzlödt, which covered an area of about 2800 m^2 (Fig. 9). The largest disappeared landslide was approx. 20 000 m^2 in area. In contrast, the two landslides with the longest persistence of 28 and 23 years in the data set are only 1000 m^2 (rough pasture) and 2000 m^2 (mixed forest) in area, respectively and these are only minimum values. Details are given in Fig. 12, in which only the 31 landslides are displayed for which landslide age information is available. For all other landslides information on the age is missing. The results show no clear trend in landslide persistence, neither regarding landslide magnitude, nor regarding land use. However, it is evident that human impact plays a major role in landslide persistence and that human impact depends on land use type. This is supported by the observation that e.g. no landslide in mixed forests disappeared within one year.

Discussion

Within this study, we analysed the potential of high-resolution ALS data in combination with orthophotos and historical information for the estimation of landslide age, for assessing human impact on landslides and to get information on landslide persistence.

It is shown that distinct geomorphological features are visible in the ALS hillshades and can be used for detailed analyses of landslides. The examples from the Swabian Alb demonstrate that

© The authors 2012
Geografiska Annaler: Series A, Physical Geography © 2012 Swedish Society for Anthropology and Geography

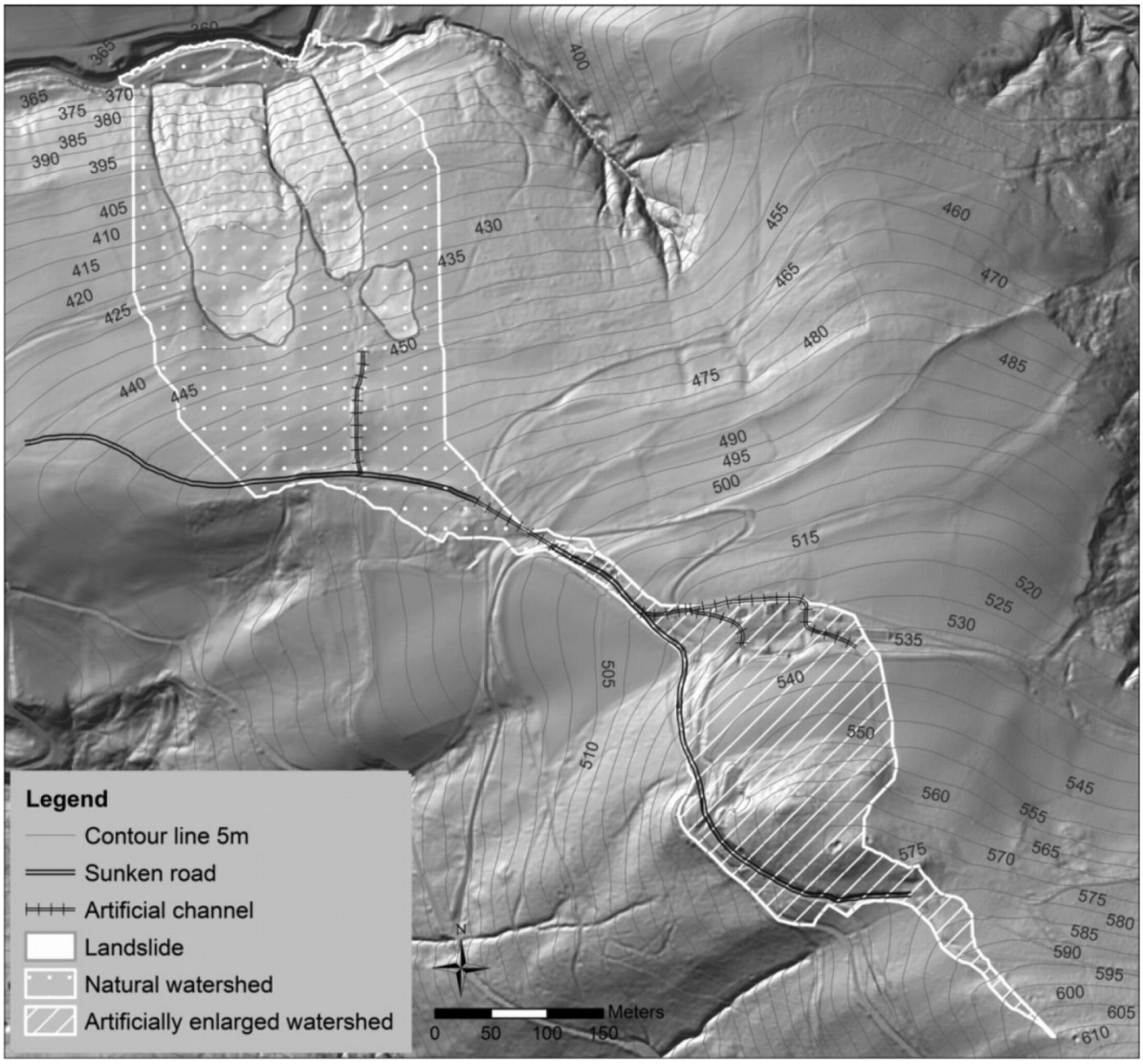

Fig. 10. Landslide Wilhelmsburg with mapped natural and artificially enlarged watersheds (mapped on ALS hillshade).

these geomorphological features are modified over time, but that there is no easy and direct correlation with time. It turned out that older landslides might look younger than younger ones and might thus be much easier to map. The reason for this might be that the whole area shows too high landslide activity so that even the boundaries of young and large landslides like the 1983 event from Mössingen cannot be simply recognized within the ALS hillshade. Other reasons might be different degrees of human impact and/or natural erosion. A major challenge is to quantify the effect of episodic or more or less continuous reactivations, which will leave their footprint in the landscape and, of course, in the ALS hillshade. Unfortunately, such information on reactivations is often not available, as it was not for this study. Multi-temporal landslide inventories, derived from multiple remote sensing imagery (i.e. aerial photographs, ALS DTM), regular field mapping over a long time period or more information from archives could be a way to counter this challenge. Considering these challenges and limitations of the mapping, no landslide age classification system could yet be set up.

The example of the Gräbelesberg shows that human impact can be helpful to date landslides to some extent when these are younger than human structures that are modified by the respective landslide. In this case, ALS hillshade analysis was essential in understanding that the large landslide

© The authors 2012
Geografiska Annaler: Series A, Physical Geography © 2012 Swedish Society for Anthropology and Geography

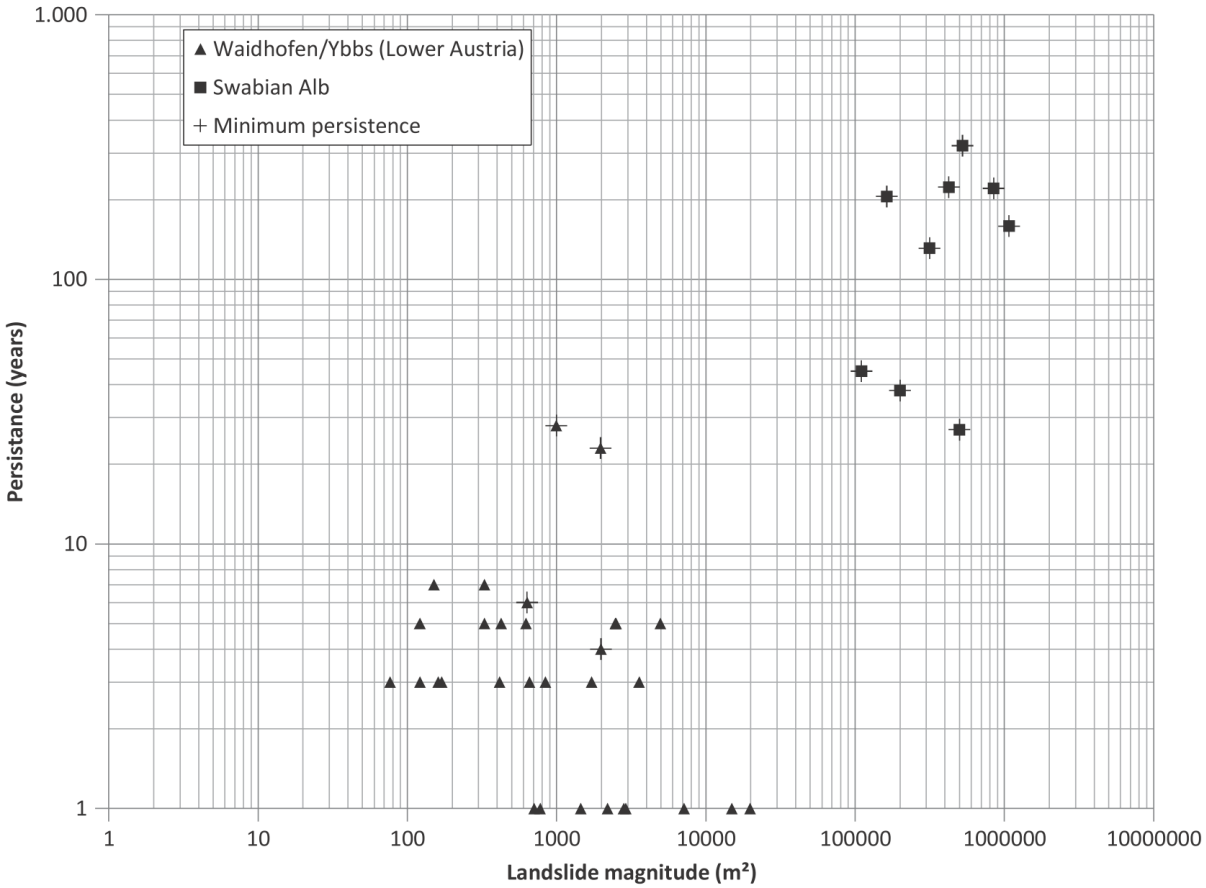

Fig. 11. Persistence of landslides of various magnitudes in the Swabian Alb and Lower Austria. (Marked landslides show a minimum persistence, all others a maximum persistence.)

Table 3. Land use of mapped and disappeared landslides in Lower Austria.

Landslide data	Coniferous forest (Count/%)	Mixed forest (Count/%)	Deciduous forest (Count/%)	Arable land (Count/%)	Grassland, pasture (Count/%)	Rough pasture (Count/%)	Sum (Count/%)
All mapped landslides (N = 691)	57/8	155/23	48/7	157/23	148/21	126/18	691/100
Disappeared landslides (N = 31)	0/0	5/16	0/0	7/23	15/48	4/13	31/100

movement affected human structures. Due to forest cover it is hard to see this feature in the field if one does not know that special attention should be put on this during field work. This shows the high potential of using ALS DTM data for landslide mapping.

It could also be shown, that ALS data can support the evaluation of decisions made in historic times as the following example illustrates. At least three cases at the end of the eighteenth and beginning of nineteenth century are known in the Swabian Alb where landslides dammed the river and were dug up manually by humans to prevent a catastrophic dam-break flood. This was illustrated by the example of the landslide Greut. However, in that case it is hard to understand why they tried to dig through the moving landslide mass instead of shifting the river course so that the river would have done the work by removing the landslide toe. Furthermore the advantage of having historical

© The authors 2012
Geografiska Annaler: Series A, Physical Geography © 2012 Swedish Society for Anthropology and Geography

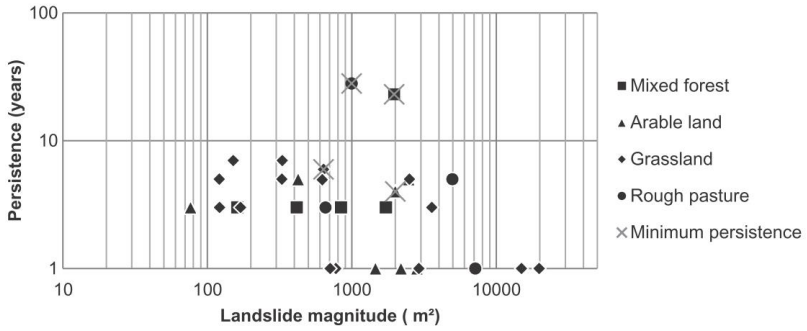

Fig. 12. Persistence of disappeared landslides depending on landslide magnitude and land-use in Lower Austria. (Marked landslides show a minimum persistence, all others a maximum persistence.)

information on landslides could be shown. Only by additional historical analysis it was possible to determine that the middle part of the Greut slide moved within the initial movement and thus was no reactivation. This is an exclusive insight we have on an event which is important when evaluating the relative landslide age.

The examples from Lower Austria clearly demonstrate the enormous consequences human impact can have on the lifetime of landslides and on the modification of geomorphological features of landslides. It shows that landslide mapping and the estimation of landslide age might be heavily hampered by farming and other human activities. Although not shown in this study, other cases in which human impact on altering the morphology of a landslide is of importance include the presence of roads and other linear infrastructure. If landslides occur on transportation lines, then landslide masses are immediately removed to ensure the usage of the infrastructure. Depending on respective location and size of landslides, in many cases, the landslide scarps should still be visible in ALS hillshades.

Regarding landslide persistence, focusing only on the alteration of geomorphological features ignoring landslide magnitude like McCalpin (1984) and Keaton and DeGraff (1996) did can be misleading. The work carried out by Guthrie and Evans (2007) was a step forward, since they integrated landslide magnitude and also investigated different landslide processes; the latter was not a focus of this study because all landslides analysed are of the process type slide. The comparison of the BGR data and the previously mapped landslides in Waidhofen/Ybbs showed that two events out of 151 are still visible in the ALS hillshade maps. This visibility may be highly influenced by the quality of the spatial accuracy of the BGR point data and by the human impact. In the past the BGR points were digitized on a map with a scale of 1 : 50 000. Only recently more effort was spent on a high accuracy of the location of the points. Furthermore, it is highly probable that intensive remediation works (i.e. planation) were taken following the landslide events reported in the BGR, so that many of these landslides disappeared. The two landslides from Lower Austria, which show the longest persistence (28 and 23 years for the landslide magnitudes 1000 m^2 and 2000 m^2, respectively, Figs 11 and 12), fit quite well with the persistence of debris slides of similar magnitudes (approx. 10 to 30 years) calculated by Guthrie and Evans (2007). Of course, in comparing these results all potential differences in environmental and geological conditions are ignored. Therefore, it is surprising that these results are in such good agreement. However, taking land use/human impact into account, the persistence of landslides of such magnitudes might be lowered to one year or even less as the results of this study show. Taking the largest landslide (20 000 m^2 in area) from Lower Austria, which disappeared within one year, the differences increase to 63 years, since the persistence calculated by Guthrie and Evans (2007) would be in the order of 64 years. Thus, landslide persistence depends not only on landslide magnitude but also heavily on land use or human impact.

Substantial differences in landslide persistence exist between the results of this study and the estimations given by Crozier (2010) for different landslide geomorphology systems in New Zealand. Landslide persistence there ranges between 50 and 100 years (destabilized regolith hill country) and >365 000 years (alpine). These rather high persistence values result from the approach that focuses on the oldest dated landslides in the particular system. In contrast, in this study analysed land-

© The authors 2012
Geografiska Annaler: Series A, Physical Geography © 2012 Swedish Society for Anthropology and Geography

slides with available age information are much younger and, therefore, give much shorter landslide persistence times. Especially the results from the Swabian Alb give only minimum persistence times. Applying the same approach like Crozier (2010) in the Swabian Alb, much higher persistence values for landslides might be found there as well. The persistence values of the landslides in Lower Austria are really low and mostly maximum values. The differences compared to Crozier (2010) are mainly a result of the enormous extent of human impact on the landslides. But as stated earlier, larger landslides with much longer estimated persistence times can also be found in Lower Austria.

Conclusion and outlook

It seems that estimating landslide age based solely on geomorphic criteria is not as simple as McCalpin (1984) and Keaton and DeGraff (1996) suggested for the Rocky Mountain type climate/environment. There are huge differences from geomorphic system to geomorphic system and from landslide to landslide. Very important seems to be the rate of reactivations or continuously slow movements, which might force the landslide to look much younger than the initial movement, even though slow movements might be only in the range of mm per year and only shallow. Furthermore, it turned out in this study that landslide magnitude and human impact are important parameters regarding the estimation of landslide age as well as of landslide persistence. Especially on agricultural land landslide features might be removed within a year, months or even weeks, loosing information on landslide activity in the respective study area. Whereas at the local scale it is self-evident that people who suffered damage from a landslide tend to recover from the event as soon as possible, such information is of vital importance when accurate landslide inventories are to be prepared at regional scale.

This study demonstrated that ALS data has a huge potential in setting up concepts, which finally might be used to estimate landslide age and persistence and to derive classification systems for landslide alteration. However, much more work has to be carried out and many more landslides must be analysed to set up preliminary age classifications for landslides depending on landslide magnitude, human impact and different landslide processes. High-resolution ALS data seem also to allow for quantification of the relationship between landslide age and landslide morphology, for example by analysing terrain roughness or similar indices. However, such studies demand for a larger and multi-temporal landslide database with more dated landslide events. Setting up such large and accurate landslide databases is the most critical and time consuming step to enable more detailed analysis on the quantification of landslide age. Whereas for the last decades interpretation of aerial photographs and digital orthophotos might provide an important data source, this study has proven the high value of detailed historical analysis to get age information on much older landslides. In addition, much effort should be spent in deciphering the history of landslide reactivations and potential landslide palimpsests, since these might hamper or even prevent the setup of a correlation of landslide morphology and landslide age. However, it seems to be worthwhile to explore further the potential of ALS data in assessing landslide age and persistence also in a quantitative manner.

As stated in the introduction, no detailed analysis of landslide activity could be conducted. However, in future studies this should also be analysed. In particular, it should be investigated whether differences exist between dormant and relict landslides. To enable such studies, detailed information on landslide activity based on field mapping and measurements are needed. If subsequently these activity states could be differentiated based on ALS analyses this would be very beneficial for a large range of research questions.

Assessing the landslide age, persistence and setting up accurate landslide inventories at regional scale is of crucial importance not only for sediment budget approaches, but also for landform evolution. Especially in landform evolution studies landslides are often ignored; although landslides control the evolution of landforms in many parts of the world (e.g. Crozier 2010). Furthermore, information on landslide age and persistence is essential in assessing landslide hazards and risks.

Acknowledgements

Research was carried out within the following three projects: InterRISK (Interdisciplinary risk analysis and evaluation of recent landslides in the Swabian Alb), ILEWS (Integrative landslide early-warning systems) and MoNOE (Method development for landslide susceptibility modelling in Lower Austria). We highly appreciate the finan-

© The authors 2012
Geografiska Annaler: Series A, Physical Geography © 2012 Swedish Society for Anthropology and Geography

cial support of the German Research Foundation (DFG) for the project InterRISK (GL 347/3), of the German Ministry for Education and Research (BMBF) for the project ILEWS and of the Provincial Government of Lower Austria for the project MoNOE. Special thanks are given to the State Institute for Environment, Measurements and Nature Conservation Baden-Württemberg (LUBW) and the Provincial Government of Lower Austria for providing data. We thank H. Proske and K. Granica (Joanneum Research, Graz) for providing land cover raster layers for Lower Austria. Finally, we are very grateful to Thiery Oppikofer, an anonymous reviewer and the associate editor A. Kellerer-Pirklbauer for their constructive comments on an earlier version which helped to significantly improve the manuscript.

Rainer Bell, Department of Geography and Regional Research, University of Vienna, Universitätsstr. 7, A-1010 Vienna, Austria.
Email: rainer.bell@univie.ac.at

Helene Petschko, Department of Geography and Regional Research, University of Vienna, Universitätsstr. 7, A-1010 Vienna, Austria.
Email: helene.petschko@univie.ac.at

Matthias Röhrs, Institute for Applied Remote Sensing, EURAC research, Via Esperanto 3, I-39100 Bolzano, Italy.
Email: matthias.roehrs@eurac.edu

Andreas Dix, Department of Geography, University of Bamberg, Am Kranen 12, Hochzeitshaus (216), D-96045 Bamberg, Germany.
Email: andreas.dix@uni-bamberg.de

References

Ardizzone, F., Cardinali, M., Galli, M., Guzzetti, F. and Reichenbach, P., 2007. Identification and mapping of recent rainfall-induced landslides using elevation data collected by airborne Lidar. *Natural Hazards and Earth System Science*, 7, 637–650.

Baum, R.L., Coe, J.A., Godt, J.W., Harp, E.L., Reid, M.E., Savage, W.Z., Schulz, W.H., Brien, D.L., Chleborad, A.F., Mckenna, J.P. and Michael, J.A., 2005. Regional landslide-hazard assessment for Seattle, Washington, USA. *Landslides*, 2, 266–279.

Bell, R., 2007. *Lokale und regionale Gefahren- und Risikoanalyse gravitativer Massenbewegungen an der Schwäbischen Alb*. PhD diss, Mathematisch-Naturwissenschaftlichen Fakultät. Rheinische Friedrich-Wilhelms-Universität, Bonn, Germany. http://hss.ulb.uni-bonn.de/2007/1107/1107.htm, 17-Feb-12.

Bibus, E., 1986. Die Rutschung am Hirschkopf bei Mössingen (Schwäbische Alb). Geowissenschaftliche Rahmenbedingungen -Geoökologische Folgen. *Geoökodynamik*, 7, 333–360.

Bleich, E., 1960. Das Alter des Albtraufs. *Jahreshefte des Vereins für Vaterländische Naturkunde in Württemberg*, 115, 39–92.

Booth, A.M., Roering, J.J. and Perron, J.T., 2009. Automated landslide mapping using spectral analysis and high-resolution topographic data: Puget Sound lowlands, Washington, and Portland Hills, Oregon. *Geomorphology*, 109, 132–147.

Brennecke, M., 2006. *Erstellung einer Inventarkarte gravitativer Massenbewegungen an der Schwäbischen Alb. Kartierungaus aus Luftbildern und einem digitalen Höhenmodell*. Diploma thesis (unpublished), Department of Geography, University of Bonn, Germany.

Brunsden, D., 1993. The persistence of landforms. *Zeitschrift für Geomorphologie*, Suppl. 93, 13–28.

Chen, C.Y., 2009. Sedimentary impacts from landslides in the Tachia River Basin, Taiwan. *Geomorphology*, 105, 355–365.

Conway, S.J., Decaulne, A., Balme, M.R., Murray, J.B. and Towner, M.C., 2010. A new approach to estimating hazard posed by debris flows in the Westfjords of Iceland. *Geomorphology*, 114, 556–572.

Corsini, A., Borgatti, L., Cervi, F., Dahne, A., Ronchetti, F. and Sterzai, P., 2009. Estimating mass-wasting processes in active earth slides – Earth flows with time-series of high-resolution DEMs from photogrammetry and airborne LiDAR. *Natural Hazards and Earth System Science*, 9, 433–439.

Crozier, M.J., 2010. Landslide geomorphology: An argument for recognition, with examples from New Zealand. *Geomorphology*, 120, 3–15.

Crozier, M.J. and Glade, T., 2005. Landslide hazard and risk: issues, concepts, and approach. In: Glade, T., Anderson, M.G. and Crozier, M.J. (eds), *Landslide Hazard and Risk*. Wiley, Chichester. 1–38.

Cruden, D.M. and Varnes, D.J., 1996. Landslide types and processes. In: Turner, A.K. and Schuster, R.L. (eds), *Landslides: Investigation and Mitigation*. National Academey Press, Washington, DC. 36–75.

Dikau, R., Brunsden, D., Schrott, L. and Ibsen, M. (eds), 1996. *Landslide Recognition. Identification, Movement and Causes*, John Wiley and Sons Ltd, Chichester.

Fundinger, A., 1985. *Ingenieurgeologische Untersuchung und geologische Kartierung (Dogger/Malm) der näheren Umgebung der Rutschungen am Hirschkopf bei Mössingen und am Irrenberg bei Thanheim (Baden-Württemberg).* Diploma thesis (unpublished), Geowissenschaftliche Fakultät Eberhard-Karls-Universität Tübingen, Germany.

Geyer, O.F. and Gwinner, M.P., 1997. *Die Schwäbische Alb und ihr Vorland. – Sammlung geologischer Führer*, Gebrüder Bornträger, Berlin, Stuttgart.

Gillon, K.A., Wooten, R.M., Latham, R.L., Witt, A.W., Douglas, T.J., Bauer, J.B. and Fuemmeler, S.J., 2009. Integrating GIS-based geologic mapping, LiDAR-based lineament analysis and site specific rock slope data to delineate a zone of existing and potential rock slope instability located along the grandfather mountain window-Linville Falls shear zone contact, Southern Appalachian Mountains, Watauga County, North Carolina. *43rd U.S. Rock Mechanics Symposium and 4th U.S.-Canada Rock Mechanics Symposium*.

© The authors 2012
Geografiska Annaler: Series A, Physical Geography © 2012 Swedish Society for Anthropology and Geography

Glade, T., 2001. Landslide hazard assessment and historical landslide data – an inseparable couple? In: Glade, T., Frances, F. and Albini, P. (eds), *The Use of Historical Data in Natural Hazard Assessments*. Kluwer Academic Publishers, Dordrecht. 153–168.

Glade, T. and Crozier, M.J., 2005. A review of scale dependency in landslide hazard and risk analysis. In: Glade, T., Anderson, M.G. and Crozier, M.J. (eds), *Landslide Hazard and Risk*. Wiley, Chichester. 75–138.

Glenn, N.F., Streutker, D.R., Chadwick, D.J., Thackray, G.D. and Dorsch, S.J., 2006. Analysis of LiDAR-derived topographic information for characterizing and differentiating landslide morphology and activity. *Geomorphology*, 73, 131–148.

Guthrie, R.H. and Evans, S.G., 2007. Work, persistence, and formative events: the geomorphic impact of landslides. *Geomorphology*, 88, 266–275.

Guzzetti, F., 2005. *Landslide hazard and risk assessment*. PhD Diss. Mathematisch-Naturwissenschaftlichen Fakultät., Rheinische Friedrich-Wilhelms-Universität Bonn, Germany. http://hss.ulb.uni-bonn.de/2006/0817/0817.htm, 17-Feb-12.

Guzzetti, F. and Tonelli, G., 2004. Information system on hydrological and geomorphological catastrophes in Italy (SICI): a tool for managing landslide and flood hazards. *Natural Hazards and Earth System Sciences*, 4, 213–232.

Guzzetti, F., Carrara, A., Cardinali, M. and Reichenbach, P., 1999. Landslide hazard evaluation: a review of current techniques and their application in a multi-scale study, Central Italy. *Geomorphology*, 31, 181–216.

Guzzetti, F., Galli, M., Reichenbach, P., Ardizzone, F. and Cardinali, M., 2006. Landslide hazard assessment in the Collazzone area, Umbria, Central Italy. *Natural Hazard and Earth System Science*, 6, 115–131.

Haneberg, W.C., Cole, W.F. and Kasali, G., 2009. High-resolution lidar-based landslide hazard mapping and modeling, UCSF Parnassus Campus, San Francisco, USA. *Bulletin of Engineering Geology and the Environment*, 68, 263–276.

Höfle, B., Mandlburger, G., Pfeifer, N., Rutzinger, M. and Bell, R., 2009. Potential of airborne LiDAR in geomorphology – a technological perspective. *Geophysical Research Abstracts*, 11, EGU2009-4630.

Jaboyedoff, M. and Labiouse, V., 2011. Technical Note: Preliminary estimation of rockfall runout zones. *Natural Hazards and Earth System Science*, 11, 819–828.

Jaboyedoff, M., Pedrazzini, A., Horton, P., Loye, A. and Surace, I., 2008. Preliminary slope mass movements susceptibility mapping using LIDAR DEM. In: *Proceedings of 61st Canadian Geotechnical Conference*. 419–426.

Johnson, R.M., Warburton, J. and Mills, A.J., 2008. Hillslope-channel sediment transfer in a slope failure event: Wet Swine Gill, Lake District, northern England. *Earth Surface Processes and Landforms*, 33, 394–413.

Jordan, P. and Slaymaker, O., 1991. Holocene sediment production in Lillooet River Basin, British Columbia: a sediment budget approach. *Geographie Physique et Quaternaire*, 45, 45–57.

Kappes, M., Malet, J.-P., Remaître, A., Horton, P., Jaboyedoff, M. and Bell, R., 2011. Assessment of debris-flow susceptibility at medium-scale in the Barcelonette Basin, France. *Natural Hazards and Earth System Science*, 11, 627–641.

Keaton, J.R. and DeGraff, J.V., 1996. Surface observations and geologic mapping. In: Turner, A.K. and Schuster, R.L. (eds), *Landslides – Investigation and Mitigation*. National Research Council, Washington, DC. 178–230.

Kellerer-Pirklbauer, A., Lieb, G.K., Avian, M. and Carrivick, J., 2012. Climate change and rock fall events in high mountain areas: numerous and extensive rock falls in 2007 at Mittlerer Burgstall, Central Austria. *Geografiska Annaler: Series A, Physical Geography*, 94, 59–78. doi:10.1111/j.1468-0459.2011.00449.x

Korup, O., 2009. Linking landslides, hillslope erosion, and landscape evolution. *Earth Surface Processes and Landforms*, 34, 1315–1317.

Korup, O., Densmore, A.L. and Schlunegger, F., 2010. The role of landslides in mountain range evolution. *Geomorphology*, 120, 77–90.

Lang, A., Moya, J., Corominas, J., Schrott, L. and Dikau, R. 1999. Classic and new dating methods for assessing the temporal occurrence of mass movements. *Geomorphology*, 30, 33–52.

Mallet, C. and Bretar, F., 2009. Full-waveform topographic lidar: state-of-the-art. *ISPRS Journal of Photogrammetry and Remote Sensing*, 64, 1–16.

McCalpin, J., 1984. Preliminary age classification of landslides for inventory mapping. In: *Proceedings of the 21st Engineering Geology and Soils Engineering Symposium, University of Idaho, Moscow*. 99–120.

Meyenfeld, H., 2008. *Modellierungen seismisch ausgelöster gravitativer Massenbewegungen für die Schwäbische Alb und den Raum Bonn und Erstellen von Gefahrenhinweiskarten*. Ph.D. diss. Mathematisch-Naturwissenschaftlichen Fakultät, Rheinische Friedrich-Wilhelms-Universität Bonn, Germany. http://hss.ulb.uni-bonn.de/2009/1692/1692.htm, 17-Feb-12.

Petschko, H., Glade, T., Bell, R., Schweigl, J. and Pomaroli, G., 2010. Landslide inventories for regional early warning systems. In: Malet, J.-P., Glade, T. and Casagli, N. (eds), *Proceedings of the International Conference 'Mountain Risks: Bringing Science to Society', Firenze, 24–26 November 2010*. 277–282.

Pomaroli, G., Bell, R., Glade, T., Heiss, G., Leopold, P., Petschko, H., Proske, H. and Schweigl, J., 2011. Darstellung der Gefährdung durch gravitative Massenbewegungen im Bundesland Niederösterreich als Grundlage der Raumplanung. *Wildbach und Lawinenverbau*, 166, 198–212.

Röhrs, M. and Dix, A., 2010. Rekonstruktion historischer Ereignisse. In: Bell, R., Mayer, J., Pohl, J., Greiving, S. and Glade, T. (eds), *Integrative Frühwarnsysteme für gravitative Massenbewegungen (ILEWS). Monitoring, Modellierung, Implementierung*. Klartext Verlag, Essen. 46–61, 261–264.

Rothe, P., 2005. *Die Geologie Deutschlands. 48 Landschaften im Portrait*. Wissenschaftliche Buchgesellschaft, Darmstadt.

Schädel, K. and Stober, I., 1988. Rezente Großrutschungen an der Schwäbischen Alb. *Jahreshefte des Geologischen Landesamtes Baden-Württemberg*, 30, 431–439.

Scheidl, C. and Rickenmann, D., 2010. Empirical prediction of debris-flow mobility and deposition on fans. *Earth Surface Processes and Landforms*, 35, 157–173.

© The authors 2012
Geografiska Annaler: Series A, Physical Geography © 2012 Swedish Society for Anthropology and Geography

Schmitt, G., 2005. *Die Alemannen im Zollernalbkreis*. PhD diss. Fachbereich 07, Geschichts- und Kulturwissenschaften, Universität Mainz, Germany.

Schulz, W.H., 2007. Landslide susceptibility revealed by LIDAR imagery and historical records, Seattle, Washington. *Engineering Geology*, 89, 67–87.

Schuster, R.L. 1996. Socioeconomic significance of landslides. In: Turner, A.K. and Schuster, R.L. (eds), *Landslides – Investigation and Mitigation*. National Research Council, Washington, DC. 12–35.

Schweigl, J. and Hervás, J., 2009. *Landslide Mapping in Austria*, JRC Scientific and Technical Report EUR 23785 EN, Office for Official Publications of the European Communities, Luxembourg. http://eusoils.jrc.ec.europa.eu/ESDB_Archive/eusoils_docs/other/EUR23785EN.pdf, 01-Mar-11.

Schwenk, H., 1992. Massenbewegungen in Niederösterreich 1953–1990. *Jahrbuch der Geologischen Bundesanstalt.* Geologische Bundesanstalt, Vienna. 597–660.

Stolz, A. and Huggel, C., 2008. Debris flows in the Swiss National Park: the influence of different flow models and varying DEM grid size on modeling results. *Landslides*, 5, 311–319.

Terhorst, B., 1997. *Formenschatz, Alter und Ursachenkomplexe von Massenverlagerungen an der schwäbischen Juraschichtstufe unter besonderer Berücksichtigung von Boden- und Deckschichtenentwicklung*, Tübinger Geowissenschaftliche Arbeiten, Reihe D, 2, Tübingen.

Terhorst, B., 2001. Mass movements of various ages on the Swabian Jurassic escarpment: geomorphologic processes and their causes. *Zeitschrift für Geomorphologie, Supplement Volume*, 125, 105–127.

Thiebes, B., Bell, R. and Glade, T. 2010. Physikalisch basiertes Frühwarnmodell. In: Bell, R., Mayer, J., Pohl, J., Greiving, S. and Glade, T. (eds), *Integrative Frühwarnsysteme für gravitative Massenbewegungen (ILEWS). Monitoring, Modellierung, Implementierung*. Klartext Verlag, Essen. 130–140, 265–266.

Van Den Eeckhaut, M., Poesen, J., Verstraeten, G., Vanacker, V., Nyssen, J., Moeyersons, J., Van Beek, L.P.H. and Vandekerckhove, L., 2007. Use of LIDAR-derived images for mapping old landslides under forest. *Earth Surface Processes and Landforms*, 32, 754–769.

Varnes, D.J., 1984. *Landslides Hazard Zonation: A Review of Principles and Practice*. UNESCO, Paris.

Wagenplast, P., 2005. *Ingenieur geologische Gefahren in Baden-Württemberg*, Landesamt für Geologie, Rohstoffe und Bergbau Baden-Württemberg, Freiburg i. Br.

Wagner, W., Hollaus, M., Briese, C. and Ducic, V., 2008. 3D vegetation mapping using small-footprint full-waveform airborne laser scanners. *International Journal of Remote Sensing*, 29, 1433–1452.

Wessely, G., Draxler, I., Gangl, G., Gottschling, P., Heinrich, M., Hofmann, T., Lenhardt, W., Matura, A., Pavuza, R., Peresson, H. and Sauer, R., 2006. *Geologie der österreichischen Bundesländer, Niederösterreich*. Geologische Bundesanstalt, Vienna.

Manuscript received 19 Mar., 2011, revised and accepted 9 Dec., 2011

© The authors 2012
Geografiska Annaler: Series A, Physical Geography © 2012 Swedish Society for Anthropology and Geography

A.3. Landslide susceptibility modeling with generalized additive models – facing the heterogeneity of large regions

Petschko, H., Bell, R., Brenning, A. & T., Glade (2012), Landslide susceptibility modelling with generalized additive models - facing the heterogeneity of large regions, in: Eberhardt E., Froese C., Turner A.K., & S. Leroueil (Eds.), Landslides and Engineered Slopes, Protecting Society through Improved Understanding, Taylor & Francis, Banff, Alberta, Canada, 769–777.

Landslides and Engineered Slopes: Protecting Society through Improved Understanding – Eberhardt et al. (eds)
© 2012 Taylor & Francis Group, London, ISBN 978-0-415-62123-6

Landslide susceptibility modeling with generalized additive models—facing the heterogeneity of large regions

H. Petschko, R. Bell & T. Glade
Department of Geography and Regional Research, University of Vienna, Austria

A. Brenning
Department of Geography and Environmental Management, University of Waterloo, Ontario, Canada

ABSTRACT: Landslide susceptibility maps are prepared worldwide on local, regional or national scale to identify regions or hillslopes that might be prone to landslides in future. Furthermore, with increasing frequency provincial governments and other stakeholders demand for susceptibility maps on the scale of a province or a state aiming at hazard mitigation. Especially on regional to national scale special adjustments have to be applied to statistical modeling methods to achieve a good characterization of the study area and to derive reliable susceptibility maps. In the analysis of large study areas new challenges arise regarding data availability and the proper consideration of its lithologic and/or morphologic heterogeneity. The main objective of this study is to model landslide susceptibility for shallow landslides for the province Lower Austria (15,850 km²). In our study design we propose to fit and validate a Generalized Additive Model (GAM) for regions that have unique morphological characteristics, which facilitates the identification of respective predisposing factors for landslides that might vary among the morphological units.

1 INTRODUCTION

Landslides cause enormous economic losses as well as fatalities worldwide. To prevent from future damage landslide susceptibility maps have been identified as a powerful tool. These maps can be implemented in spatial planning strategies, which is an important step to avoid future economic losses and fatalities. Numerous publications show that landslide susceptibility maps have been derived on different scales ranging from local site scale to continental scale (Günther et al., 2011, Dikau & Glade 2003, Bobrowsky & Domínguez-Cuesta 2011, Malet et al., 2011, Ferentinou et al., 2011, Trigila et al., 2011).

The main objective of our ongoing project is to derive consistent landslide susceptibility maps for shallow landslides in the province of Lower Austria. These maps should be ready to use by municipal authorities on a scale of 1:25,000. However, in this study we focus on one aspect of the project, which addresses the high heterogeneity of Lower Austria regarding the morphology and the challenges that arise with that.

Our hypothesis is that this heterogeneity is mainly associated with changes in lithology that brings along spatially variable characteristics of slope stability and predisposing factors of landslides. To meet these challenges a study design has to be set up to facilitate the best characterization of the study area. The analysis of this hypothesis and the study design are presented in detail in this contribution.

We use the statistical method of generalized additive models (GAM) for modeling. The application of GAMs for landslide susceptibility modeling is relatively new (Brenning 2008, Jia et al., 2008, Park & Chi 2008, Goetz et al., 2011) whereas generalized linear models (linear or logistic regression) have widely been facilitated to landslide susceptibility modeling (e.g., in Atkinson & Massari 1998, 2011, Bell 2007, Brenning 2005, Van Den Eeckhaut et al., 2006). The main difference between these approaches is the possibility to model nonlinear relationships between dependent (location of landslide points) and explanatory variables (i.e., slope angle, profile and planar curvature) with a GAM (Hastie & Tibshirani 1990, Brenning 2008).

2 DATA

The data available comprehensively for the entire study area contain information on the location of landslides and on the topography, land cover and lithology. The landslide inventory mapping performed to identify the location of former landslides is described in section 4.1. The most important data set for derivation of topographic parameters is a DTM with a resolution of 1 m × 1 m that was

accomplished by airborne laserscanning (ALS) data. Additionally, an orthophoto from the year 2007 was available. Both, the DTM and the orthophoto are by courtesy of the Provincial Government of Lower Austria. Furthermore, land cover data derived from satellite imagery by our project partners from "Joanneum Research" (Graz) with a resolution of 10 m × 10 m and a lithological map with a scale of 1:200,000 (Source: Geological Survey of Austria, enhanced by Austrian Institute of Technology-AIT) are available. More details on the data preparation and usage in the analysis are given in Section 4.1.

3 STUDY AREA

Lower Austria is the North-Eastern province of Austria (Fig. 1a). The entire province has a size of about 19,000 km². Landslide susceptibility maps have to be modeled in particular for a region mainly south of the Danube with an area of about 15,850 km².

However, to develop the study design three districts of Lower Austria, namely Amstetten, Baden and Waidhofen/Ybbs, were chosen as test study area in this study. These represent the main geological units of Lower Austria but cover a smaller area of 2072 km² which is of advantage regarding shorter data preparation and computation times. Furthermore these districts show differences in the landslide density in the inventory data, which was of importance to test the performance of the model.

The main geological units in Lower Austria are the Bohemian Masif with granites and gneiss, the Molasse Zone with clastic sediments, the Flysch Zone with sandstone and marls, the Klippen Zone with clays and marls, the Northern Calcareous Alps (N.Calc. Alps) with dolomites and limestone (with marls) and in the south the Eastalpine Zone of Paragneiss, Schists and Phyllites.

Figure 1 shows the lithological units and respective bedrock materials in the test study area. In Table 1 their relative area, landslide density and mean arithmetic slope angle is presented. According

Figure 1. a) Location of Lower Austria and the capitals of the districts Amstetten, Baden and Waidhofen/Ybbs. The grey colour shows a hillshade map of the study area. b) Lithological map of the test districts. N. Calc. Alps = Northern Calcareous Alps. Data source: Geological Survey of Austria and AIT.

Table 1. Comparison of the lithological units in the test districts: (a) Proportion of sampled points in the unit to sampled points in the test study area (2% of all grid cells), (b) Landslide density compared to the entire study area, (c) Arithmetic mean of the general slope angle and (d) Landslide rate (Ratio of slide sample points to non-slide sample points).

Lithological unit	a) Sampled points (%)	b) Landslide density (%)	c) Mean slope angle (°)	d) Landslide rate (%)
Alluvial deposits	11.3	0.5	3	0.04
Debris	1.6	2.1	17	1.25
Loess, Loam	4.3	4.1	5	0.93
Landslide deposits	0.5	2.3	17	4.25
Quaternary fluvial terrace	13.4	3.7	4	0.26
"Wr. Becken" (Sand, gravel)	12.4	0.4	3	0.03
Molasse Zone (Clastic Sediments)	7.4	3.4	7	0.45
"Schlier" (Clay, Silt)	2.0	10.2	7	5.15
Flysch Zone (Sandstone, Marl)	18.3	61.8	14	3.34
Klippen Zone (Clay, Marl)	0.9	6.4	16	7.69
N. Calc. Alps (Dolomite)	17.9	2.9	25	0.15
N. Calc. Alps (Limestone with marls)	7.2	1.8	20	0.71
Bohemian Masif (Granite)	2.7	0.5	14	0.19

to the bedrock material the lithological units show very different geotechnical characteristics which have an influence on the general slope stability. The Flysch Zone, for example, contains sandstones and marls which are known for being more prone to landslides in Lower Austria compared to lithological units containing dolomites, limestones or granites.

4 METHODS

4.1 *Data preparation*

The data on DTM, land cover and lithology, which comprises the data basis for the sampling of the explanatory variables, was set to the same spatial extent and resampled to a raster with 10 m × 10 m resolution. The land cover grid was reclassified from ten classes (coniferours forest, mixed forest, deciduous forest, arable land, pasture, rough pasture, snow & ice, debris, fallow land and settlement) to five classes: "Forest", "Arable & Fallow Land", "Pasture", "Settlement" and "Snow, ice, debris".

The landslide data, which gives the dependent variable for the modeling, is comprised of point data that was mapped on derivatives of the ALS DTM (Hillshade maps with different azimuth angles (315°, 45°, 135°), contour lines with a spacing of 4 m and slope angle maps) The landslides were detected visually on the hillshade and orthophoto imagery by interpreting and identifying the specific morphology that landslides leave after occurring (i.e., concave main scarp, convex accumulation zone, significant changes in slope angle and visible fissures or cracks). One point was set in the main scarp area at each detected landslide because there the landslide boundaries are easy to detect what results in high relative accuracy in the location of the points (Van Den Eeckhaut et al., 2006). Furthermore tests with different types of inventory data showed that using points in the main scarp still results in satisfactory evaluation values and susceptibility maps (Petschko et al., in press).

The following grids were derived from the DTM and were obtained by the respective SAGA modules: aspect angle, slope angle, topographic wetness index (SAGA wetness index, see Boehner et al., 2002), catchment height, catchment slope angle, catchment area, curvature, horizontal curvature and vertical curvature. Additionally curvature was derived with different window sizes in order to analyze which variables characterize the morphology and the present landslide distribution best. This datasets were computed in GRASS GIS applying the module r.param.scale (Wood 1996) with a rectangle size of nine pixels (profile curvature, planar curvature and maximum curvature, as defined by Wood 1996).

4.2 *Analysis of heterogeneity/homogeneity zones*

The heterogeneity of the study area mainly results from the different morphology that is strongly connected to a change in lithology and geotechnical characteristics. This was analyzed in more detail by four methods to show the differences between the lithological units: (1) a visual interpretation of the hillshade map overlain with the lithological map was performed. (2) This visual interpretation was analyzed in more detail by an exploratory comparison of mean slope angle in each lithological unit. (3) The distribution of landslides according to slope angle was tested with spineograms plotting slope angle with landslide/no landslide points for each lithological unit. (4) Another indication of the heterogeneity of the area might be the selection of different explanatory variables for each lithological unit when fitting a model with stepwise variable selection (see 4.3). This would reflect differences in the predisposing factors to landslides of each lithological unit. Therefore the count of selection of each variable in the models for all 13 lithological units was analyzed.

4.3 *Modeling with generalized additive models*

The analysis of the heterogeneity/homogeneity zones showed that besides the geotechnical characteristics also the mean slope angle changes in most cases with changes in the lithological unit. For the modeling and our study design this has the following implication: to model this relationship between slope angle and lithological unit correctly, the implementation of an interaction term is needed that describes this relationship exactly (Hastie & Tibshirani 1990, p. 264). As the lithological units describe major changes in geotechnical characteristics of the material our proposed study design is to fit a GAM (R package "gam" described by Hastie 2006) for each lithological unit instead of for the entire study area.

The sample points for the modeling were merged out of two datasets: (1) sample points that were selected randomly in the area outside of landslides with a density of 2% of all grid cells of the test study area (408,918 points) and (2) all mapped landslide points (4055). Subsequently the values of all explanatory grids were extracted to this merged "original sample" to derive a data frame with all information on explanatory and dependent variables. To facilitate the modeling in the lithological units this "original sample" was split according to the extent of the lithological units and the "landslide rate" showing the ratio of original sample

points storing information on "slides" to points storing information on "no slides" was obtained. From these new samples respective subsamples were selected according to a relation 1:1 (slides:no slides). With this subsamples a GAM was fitted for each lithological unit. For fitting the models we used a combined backward and forward stepwise variable selection in R based on Akaike's Information Criterion (AIC, Akaike 1974). The AIC can be applied to automatically determine the best fit of variables for a model as it evaluates the significance of the variables and penalizes for model complexity. During the stepwise variable selection the following choices of using the variable in the model are made and tested by the GAM (Hastie 1991): (1) omitting the variable, (2) use the variable linearly and (3) use the variable with a smooth function which is estimated nonparametically. By comparing the resulting AIC for each model fitted with different variable selections, the GAM decides on the model with the best combination of variables. For the curvature all variables derived with window sizes of three and nine pixel were put at choice. Furthermore, slope was made available once as general slope angle and once as catchment slope angle.

4.4 *Validation with AUROC*

In general a statistical validation provides a comparison of the modeled susceptibility with the present location of landslide points. The resulting susceptibility maps of the lithological units were validated by the calculation of the area under the receiver operating curve (AUROC, Hosmer & Lemeshow 2000). The ROC curve plots all combinations of sensitivities (percentage of correctly classified landslide points) against the false-negatives (percentage of wrong classified non-landslide points). Then the area under this curve is calculated which results in values between 0–1. Values form 0–0.5 show that the model could not discriminate between slides and no slide points whereas a value of 1 shows perfect discrimination (Brenning 2005). This calculation is facilitated by creating a test data set additionally to the training data set that was used for fitting the model. More details on this method can be found in Brenning (2005) and Begueria (2006).

5 RESULTS & DISCUSSION

5.1 *Data preparation*

A total of 4055 main scarps of slides were identified for the study area by mapping the landslides on basis of the ALS DTM derivatives. The landslide density and landslide rate of each lithological unit is presented in Table 1 (b and d).

5.2 *Analysis of heterogeneity/homogeneity zones*

The visual interpretation showed that with the change of the lithological units also the morphology changes distinctly. The results of exploratory analysis showed significant differences of the mean slope angle in most lithological units, although few units have similar mean slope angles (Table 1c).

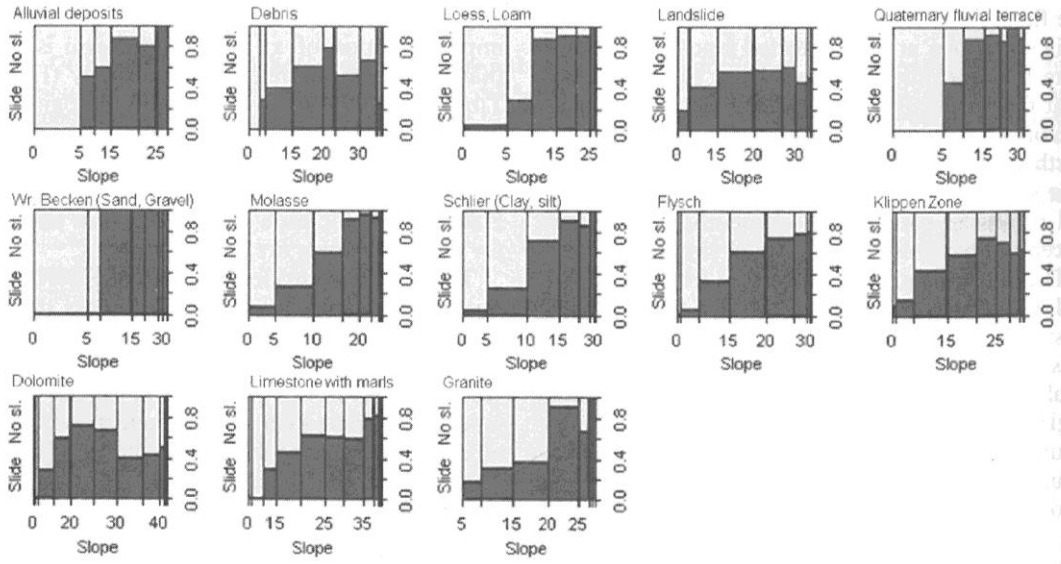

Figure 2. Spineograms for each lithological unit showing the relation of slide / no slide points for the respective slope angle.

The Flysch Zone, for example, has a mean slope angle of 14° which is 11° lower than the mean slope angle of about 25° of the Dolomites of the Northern Calcareous Alps. In the resulting spineograms (Fig. 2) the proportion of landslides to no landslides according to the detected slope angle is plotted taking into account the relative area of the respective slope unit which is shown by the width of the bars. Therefore you can identify at which slope angle most of the landslides occurred and how this proportion evolves with rising slope angles. Comparing for example the Flysch Zone with the Dolomites we see that in both units more landslides (proportion larger than 50%) occurred starting from a slope angle of 15°. While in the Flysch the proportion of slides to no slides rises with increasing slope angles in the Dolomites this proportion drops below 50% at a slope angle of 30°. In general, flat areas with up to 5° show percentage of landslides close to zero. However, the zones of "Loess & Loam", "Molasse" and "Schlier" 5–10% of landslides occurred at these slope angles up to 5°, which has also been recognized during field work. Furthermore in the usually flat lithological units "Alluvial deposits" and the "Wr. Becken (Sand, Clays)" the spineograms show mapped landslides and slope angles of up to 25°. This high slope angles may occur along roads, where the slope was steepened artificially, or at deeply incised streams as we saw in the field at the river Ybbs. Additionally it may be related to some uncertainties in the delineation of the zones in the original geological map.

The results of the fourth method to analyze the heterogeneity are presented in the modeling section.

5.3 *Modeling with generalized additive models*

The original rate of "slide" to "no slide" sample points is presented in Table 1d (Landslide rate) and shows especially in the "Klippen", "Schlier", "Landslide" and "Flysch Zone" a high landslide rate. The other units, particularly the "Alluvial deposits" and the "Wr. Becken (Sand, gravel)" show a comparably low landslide rate. Besides showing the differences in the relative landslide susceptibility of each unit, this emphasizes that there is a different effect of reducing the original sample to a subsample with a ratio of 1:1. This has to be considered at producing the resulting susceptibility maps to ensure the comparability of the lithological units.

Table 2 shows the counts of selection of each variable with a possible maximum count of 13. The total numbers show, that the variable slope angle was used in the model of 11 lithological units. The topographic wetness index was selected in seven of the models mostly in a smoothed form (four out of seven models). Horizontal curvature and catchment aspect have been used in 6 lithological units while profile and planar curvature have never been selected. This table emphasizes that for each lithology different variables have been selected either in their normal linear ("Sum N") or in using a smooth function transforming the variable ("Sum S").

Table 2. Results of stepwise variable selection. The numbers represent the count of usage of each variable in the 13 models for different lithological units. "Sum N" = variable used linearly, "Sum S" = variable is used with a smoothing function, "Total" shows the total count of usage. n.a. = not applicable.

Variable	Sum N	Sum S	Total
Slope angle	11	0	11
Catchment slope angle	1	0	1
Catchment area	1	2	3
Catchment height	2	1	3
Catchment aspect	1	5	6
Curvature	1	3	4
Horizontal curvature	5	1	6
Vertical curvature	4	0	4
Profile curvature (9)	0	0	0
Planar curvature (9)	0	0	0
Maximum curvature (9)	4	0	4
North (Aspect)	1	0	1
East (Aspect)	2	0	2
Arable & Fallow Land	4	n.a.	4
Pasture	4	n.a.	4
Snow, ice, debris	2	n.a.	2
Settlement	2	n.a.	2
Topographic wetness index	3	4	7

5.4 *Validation with AUROC*

The AUROC value was calculated for the susceptibility map of each lithological unit after fitting a model respectively, where the best combination of variables was determined according to the AIC. The resulting AUROC values show the quality of the respective best fit model. The comparison of the AUROC values shows eleven units having AUROC values between 0.66 and 0.95. The highest AUROC value has the unit "Wr. Becken (Sand, Gravel)" with 1 whereas the lowest AUROC value was calculated for the unit "Dolomite" with 0.55. According to these results we state that in each lithological unit the model was able to discriminate between slide and no slide points successfully. However, there are differences in the performance. This is related to the different landslide sample size in each of the units. Especially at very small sample sizes the model tends to overfit (AUROC = 1), which means that the model fits too closely to the

present data and is less capable of capturing minor fluctuations in the data.

6 CONCLUSIONS

Within this study we have shown the details on the differences of the lithological units regarding geotechnical characteristics and also the morphology (which was described by analyzing the mean slope angle). The visual comparison of the hillshade map and the lithological map showed that the lithological map gives an acceptable good delineation of the morphological units. More details on the heterogeneity of the test study area were shown by the results of the exploratory analysis of the slope angle for each lithological unit and interpretation of the spineograms of landslide occurrence and slope angle. According to the findings there we conclude that there are some uncertainties in the delineation of the lithological units but still they give very important information on different geotechnical characteristics.

According to the findings in the analysis of the heterogeneity we propose that in our study design it is necessary to fit a model for these units respectively. In order to avoid the usage of interaction terms to guarantee for an easier interpretation of the model for the stakeholders, and to still be able to give a good characterization of the study area on the aimed output scale, we decided to fit one GAM for each of these lithological units. The results show that with the GAM a model can be fitted for each lithological unit with a resulting AUROC value, which shows a good ability of the model to discriminate between slide and no slide points. However, some units may be affected by low number of landslide samples which has to be analyzed in more detail. Especially when switching to modeling the entire province of Lower Austria this effect may probably change or disappear. The analysis showed that we may consider merging lithological units with similar mean slope angles when the geotechnical characteristics are similar as well. Furthermore it should be considered to integrate the units debris and landslides in their surrounding units. This has to be analyzed in more detail for the application in Lower Austria.

The results of the variable selection for each unit show that different variables were selected for the model of each lithological unit while only the variable slope angle was used in nearly every model. This supports the hypothesis that each lithological unit may be characterized best by different predisposing factors. This in turn emphasizes the necessity to fit a model for each lithological unit in order to give the best characterization regarding landslide susceptibility in the province of Lower Austria.

ACKNOWLEDGEMENTS

The study was carried out in the project MoNOE (Method development for landslide susceptibility modeling in Lower Austria) therefore, the authors are grateful for the funding and data provided by the Provincial government of Lower Austria. Furthermore we want to thank the Geological Survey of Austria for providing data and our project partners and stakeholders for fruitful discussions.

REFERENCES

Akaike, H. 1974. A new look at the statistical model identification. *IEEE Transactions on Automatic Control* 19(6): 716–723.

Aleotti, P. & Chowdhury, R. 1999. Landslide hazard assessment: summary review and new perspectives. *Bulletin of Engineering Geology and the Environment* 58: 21–44.

Atkinson, P. & Massari, R. 2011. Autologistic modelling of susceptibility to landsliding in the central apennines, Italy. *Geomorphology* 130(1–2): 55–64.

Atkinson, P., Jiskoot, H., Massari, R. & Murray, T. 1998. Generalized linear modelling in geomorphology. *Earth Surface Processes and Landforms* 23(13): 1185–1195.

Beguería, S. 2006. Validation and Evaluation of Predictive Models in Hazard Assessment and Risk Management. *Natural Hazards* 37(3): 315–329.

Bell, R. 2007. Lokale und regionale Gefahren- und Risikoanalyse gravitativer Massenbewegungen an der Schwäbischen Alb. *Dissertation thesis*, Rheinische Friedrich-Wilhelms-Universität Bonn, Bonn, Germany.

Bobrowsky, P.T. & Domínguez-Cuesta, M.J. 2011. A proposed landslide susceptibility map of Canada based on GIS. In F. Catani, C. Margottini, A. Trigila & C. Iadanza (eds), *The second World Landslide Forum—Abstract Book*: 280. Italy: ISPRA.

Boehner, J., Koethe, R. Conrad, O., Gross, J., Ringeler, A. & Selige, T. 2002. Soil Regionalisation by Means of Terrain Analysis and Process Parameterisation. In: Micheli, E.,Nachtergaele, F., Montanarella, L. [Ed.]: Soil Classification 2001. European Soil Bureau, Research Report No. 7, EUR 20398 EN, Luxembourg. pp. 213–222.

Brenning, A. 2005. Spatial prediction models for landslide hazards: review, comparison and evaluation. *Natural Hazards and Earth System Sciences* 5: 853–862.

Brenning, A. 2008. Statistical Geocomputing combining R and SAGA: The Example of Landslide susceptibility Analysis with generalized additive Models. SAGA—Seconds Out, *Hamburger Beiträge zur Physischen Geographie und Landschaftsökologie* 19: 23–32. Germany.

Dikau, R. & Glade, T. 2003. Nationale Gefahrenhinweiskarte gravitativer Massenbewegungen.- In: Liedtke H., Mäusbacher R. & Schmidt K.-H. (eds.), *Relief, Boden undss Wasser.—Nationalatlas Bundesrepublik Deutschland*: 98–99. Institut für Länderkunde, Leipzig.

Fell, R., Corominas, J., Bonnard, C., Cascini, L., Leroi, E., Savage, W. Z. & on behalf of the JTC-1 Joint Technical Committee on Landslides and Engineered Slopes, 2008. Guidelines for landslide susceptibility, hazard and risk zoning for land-use planning. *Engineering Geology* 102(3–4): 99–111.

Ferentinou, M. & Chalkias, C. 2011. Mapping Mass Movement Susceptibility across Greece with the use of GIS, Artificial Neural Network and Statistical Methods. In F. Catani, C. Margottini, A. Trigila & C. Iadanza (eds), *The second World Landslide Forum—Abstract Book*: 91. Italy: ISPRA.

Glade, T. & Crozier, M.J. 2005. A review of scale dependency in landslide hazard and risk analysis. In: Glade, T., Anderson, M. & M. Crozier (eds): *Landslide hazard and risk:* 75–138. Chichester.

Goetz, J.N., Guthrie, R.H. & Brenning, A. 2011. Integrating physical and empirical landslide susceptibility models using generalized additive models. *Geomorphology* 129: 376–386.

Günther, A., Reichenbach, P., Malet, J.-P., Hervás, J., Foster, C., Van Den Eeckhaut, M. & Guzzetti, F. 2011. New developements in harmonized landslide susceptibility mapping over Europe in the framework of the European Soil Thematic Strategy. In F. Catani, C. Margottini, A. Trigila & C. Iadanza (eds), *The second World Landslide Forum—Abstract Book*: 100. Italy: ISPRA.

Hastie, T.J. 1992. Generalized additive models. In Chambers, J.M. & Hastie, T.J., *Statistical Models in S.* Wadsworth \& Brooks/Cole.

Hastie, T.J. & Tibshirani, R. 1990. Generalized additive models, Chapman & Hall/CRC, London.

Hervas, J. (ed.) 2007. Guidelines for Mapping Areas at Risk of Landslides in Europe. Proceedings of the Experts Meeting held on 23–24 October 2007. Institute for Environment and Sustainability Joint Research Centre (JRC), Ispra: Italy.

Hosmer, D.W. & Lemeshow, S. 2000. Applied logistic regression, John Wiley & Sons, New York, 2.nd edn., p. 373.

Jia, G., Yuan, T., Liu, Y. & Zhang, Y. 2008. A static and dynamic factors-coupled forecasting model or regional rainfall-induced landslides: a case study of Shenzhen. *Science in China, Series E: Technological Sciences* 51: 164–175.

Park, N.W. & Chi, K.H. 2008. Quantitative assessment of landslide susceptibility using high-resolution remote sensing data and a generalized additive model. *International Journal of Remote Sensing* 29: 247–264.

Petschko, H., Bell, R., Leopold, P., Heiss, G. & Glade, T. (2011). Landslide inventories for reliable susceptibility maps. In F. Catani, C. Margottini, A. Trigila & C. Iadanza (eds), *The second World Landslide Forum—Proceedings*. Italy: ISPRA. In Press.

Soeters, R. & van Westen, C.J. 1996. Slope instability recognition analysis and zonation, In Turner, K.T & R.L. Schuster (eds), *Landslides: Investigation and Mitigation.* Transportation Research Board National Research Council, Special Report 247: 129–177. Washington D.C.

Trigila, A., Casagli, N., Catani, F., Crosta, G., Esposito, C., Frattini, P., Iadanza, C., Scarascia Mugnozza, G., Segoni, S., Spizzichino, D. & Tofani, V. 2011. Landslide susceptibility mapping at national scale: the Italian case study. In F. Catani, C. Margottini, A. Trigila & C. Iadanza (eds)., *The second World Landslide Forum—Abstract Book*: 158. Italy: ISPRA.

Van den Eeckhaut, M., VanWalleghem, T., Poesen, J., Govers, G., Verstraeten, G. & Vandekerckhove, L. 2006. Prediction of landslide susceptibility using rare events logistic regression: A case-study in the Flemish Ardennes (Belgium).—*Geomorphology* 76(3–4): 392–410.

Wood, J. 1996. The Geomorphological characterisation of Digital Elevation Models. Dissertation, Department of Geography, University of Leicester, U.K.

A.4. Landslide inventories for reliable susceptibility maps

Petschko, H., Bell, R., Leopold, P., Heiss, G. & T., Glade (2013), Landslide inventories for reliable susceptibility maps, in: Margottini, C., Canuti, P. & K. Sassa (Eds.), Landslide Science and Practice, Vol. 1: Landslide Inventory and Susceptibility and Hazard Zoning, Springer, 281-286.

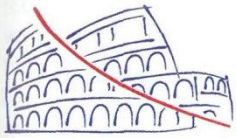

Landslide Inventories for Reliable Susceptibility Maps in Lower Austria

Helene Petschko, Rainer Bell, Philip Leopold, Gerhard Heiss, and Thomas Glade

Abstract

Landslide inventories, their accuracy and the stored information are of major importance for landslide susceptibility modelling. Working on the scale of a province (Lower Austria with about 10,000 km^2) challenges arise due to data availability and its spatial representation. Furthermore, previous studies on existing landslide inventories showed that only few inventories can be used for statistical susceptibility modelling. In this study two landslide inventories and their resulting susceptibility maps are compared: the Building Ground Register (BGR) of the Geological Survey of Lower Austria and an inventory that was mapped on the basis of a high resolution LiDAR DTM. This analysis was performed to estimate minimum requirements on landslide inventories to allow for deriving reliable susceptibility maps while minimizing mapping efforts. Therefore a consistent landslide inventory once from the BGR and once from the mapping was compiled. Furthermore, a logistic regression model was fitted with randomly selected points of each landslide inventory to compare the resulting maps and validation rates. The resulting landslide susceptibility maps show significant differences regarding their visual and statistical quality. We conclude that the application of randomly selected points in the main scarp of the mapped landslides gives satisfactory results.

Keywords

Landslide inventory mapping • Minimum requirements • Archive data • LiDAR DTM • Lower Austria

Introduction

Landslide inventories form the most important data basis for subsequent landslide susceptibility, hazard or risk analysis. Therefore, their quality regarding location and representativeness of the recorded events highly affects the possible quality of its further applications. Working on the scale of a province (in this case Lower Austria), it is of high importance to have data that represents the actual landslide density. Depending on the available archives and their particular purpose the data may show a large range in information quality and quantity. Therefore, a major drawback may be the locally restricted information (Glade 1996). Traditionally landslide inventories consist either of archive data collected in a database from different data sources such as newspapers, archives of churches or national and municipal authorities (Guzzetti et al. 1994; Glade 1996; Glade et al. 2001) or of landslides mapped by the interpretation of topographic maps or aerial photographs (Brardinoni et al. 2003; Duman et al. 2005). New methods for landslide inventory mapping arose with the availability of high resolution

H. Petschko (✉) • R. Bell • T. Glade
Department of Geography and Regional Research, University of Vienna, Universitaetsstrasse 7, 1010 Wien, Vienna, Austria
e-mail: helene.petschko@univie.ac.at

P. Leopold • G. Heiss
Health and Environment Department, Environmental Resources and Technologies, AIT – Austrian Institute of Technology GmbH, Konrad Lorenz Straße 24, 3430 Tulln, Austria

C. Margottini et al. (eds.), *Landslide Science and Practice*, Vol. 1,
DOI 10.1007/978-3-642-31325-7_37, © Springer-Verlag Berlin Heidelberg 2013

remote sensing data, e.g. satellite imagery and LiDAR data, resulting in a "revolution in geomorphology" (Anders and Seijmonsbergen 2008) and in increasing levels of sophistication in terrain mapping (Petley 2010). These new methods contain the identification and mapping of landslides on the hillshade of a LiDAR DTM (Chigira et al. 2004; Schulz 2004; Ardizzone et al. 2007; Bell 2007; Van Den Eeckhaut et al. 2007) and the semi-automated object based mapping of landslides on LiDAR and/or satellite images (van Asselen and Seijmonsbergen 2006; Booth et al. 2009; Martha et al. 2010; Mondini et al. 2011).

As a detailed knowledge on the inventories used for susceptibility modelling is important and as we want to reduce the mapping effort to its possible minimum we set the following three objectives for this study: (1) to analyse the database and documents of the Building Ground Register regarding further information on main triggers and size of events and to identify points that store information on landslide events, (2) to map landslide polygons by interpreting the morphology provided by hillshades of the LiDAR DTM and (3) to compare the resulting inventories and thereby to identify minimum requirements of a landslide inventory for subsequent statistical landslide susceptibility modelling. These minimum requirements may help to define future steps of landslide inventory mapping for the entire province of Lower Austria with respect to the implementation of the resulting susceptibility maps for spatial planning strategies.

This study is part of the project MoNOE (Method development for landslide susceptibility modelling in Lower Austria) that is presented by Bell et al. (this volume).

Study Area

The study area is Lower Austria and focuses particularly on the districts which are identified as prone to landslides according to the prevalent lithology and morphology. In a first project phase, three districts (Amstetten, Waidhofen/Ybbs and Baden) are chosen as test study area to develop a methodology for inventory homogenization and mapping. The three districts have been selected according to their geological setting and landslides based on the number of present entries in the Building Ground Register. All main geological units of Lower Austria are covered and the landslide density differs significantly. In Amstetten and Waidhofen/Ybbs numerous landslide information is available. In contrast, Baden has a similar geological setting but only very few reported landslides. The area of these districts totals 2,072 km^2. For a detailed map on the distribution of the landslide inventories in Lower Austria refer to Bell et al. (this volume).

In Lower Austria, several extensive inventories are available: the "Building Ground Register" (BGR) is a database maintained by the Geological Survey of Lower Austria and consists of reports on landslide events recorded since 1953; the "GEORIOS" database and the "Map of sedimentary deposits" are both provided by the Geological Survey of Austria and contain mainly polygons but also lines and points on mapped landslides. Detailed analysis of these inventories in a previous study showed that these are of varying quality (Petschko et al. 2010) so that the way they are used for landslide susceptibility modelling has to be adopted.

Materials/Data

For a general overview on geodata applied in this study refer to Bell et al. (this volume). In the present study the LiDAR DTM with a resolution of 1 × 1 m and its derivatives (hillshade, slope map, contour lines) were the most important data source. Furthermore orthophotos with a resolution of 25 × 25 cm (taken in the period 1999–2005) and of 12.5 × 12.5 cm (taken in the period 2007–2009) were used during the mapping as a reference on the current land cover.

Landslide Inventory: Building Ground Register

The archive of the Building Ground Register stores reports and studies on e.g. supervision of quarries or underground investigations of parcel land since 1953. Additionally, this archive contains approx. 1,500 studies on reported landslide events (slide, fall) until the year 2009 (Pomaroli et al. 2011). The minimum information provided for each landslide event is a short report that includes the date or the period (month, season and year) of occurrence, the location, the geological setting and a comment on the event trigger (Schwenk 1992). The main information on each event is available in a database which is connected to a point shape-file. Originally the points were mapped at a scale of 1:50,000, but nowadays they are mapped on orthophotos (spatial resolution 25 cm) and on the parcel land map of Lower Austria (1:1,000) with higher accuracy.

Methods

Building Ground Register

The Building Ground Register database is complemented with additional information stored in the event related analogue documents and reports. The entries of the database are analysed with respect to date, main trigger, size and setting (natural or engineered slope) of the event. Especially the latter information is important for the selection of points for

the modelling: only the points indicating landslides on natural slopes are selected as input data to model the susceptibility of natural slopes. The anthropogenic engineered slopes are not considered (Pomaroli et al. 2011).

Inventory Mapping on LiDAR DTM

The method for landslide inventory mapping on the basis of a LiDAR DTM and its derivatives was earlier described in Petschko et al. (2010) and tested for the district Waidhofen/Ybbs. This method is now applied for the districts Amstetten and Baden; therefore we summarize the main details on the mapping method here. The mapping is based on the visual interpretation of the morphology that is visualized by hillshades with different azimuth angles and contour lines, both calculated from the LiDAR DTM (Petschko et al. 2010). With respect to the application of the resulting inventory in statistical modelling we decided to map landslide polygons with a representative density while covering each lithological unit (Petschko et al. 2010). Furthermore, several landslide types are differentiated: slide, flow and complex (following Cruden and Varnes 1996). In case of large areas with several slides of different ages one large polygon was mapped covering the entire area and attributed as "area of slides" (Petschko et al. 2010).

Comparison and Minimum Requirements of Inventories

The resulting inventories are analysed regarding their differences and possible advantages or drawbacks of using the one or the other dataset for modelling landslide susceptibility. Besides the accuracy of the location of the landslides and the density of information also the effort of mapping and the implementation of the resulting maps in spatial planning are important. Therefore, the visual differences of the maps have to be taken into account.

This comparison is facilitated by fitting a number of different models with logistic regression (generalized linear models in R) (e.g. Atkinson et al. 1998; Brenning 2005). For a detailed description of the logistic regression modelling method used here refer to Leopold et al. (this volume). The input datasets for the models are: aspect, flow accumulation, slope angle, slope length, land cover, geology, landform classification and the topographic wetness index as explanatory variables and landsides as dependent variable. Three landslide input parameters are used: (1) randomly selected points form the BGR; (2) points that are randomly sampled in the entire slide polygon and (3) points that are randomly sampled in the main scarp of the slide. For the inventory mapped on the basis of the LiDAR DTM we only use landslides classified as "slide" in the model.

The resulting landslide susceptibility maps are compared both statistically and visually. Therefore the statistical significance of the input datasets and the area-under-ROC (AUROC) values of all maps are compared. The validation of the resulting maps is performed by calculating a ROC plot and the AUROC that allows evaluating the model's performance independently of determined thresholds in the probability values (Beguería 2006). By the usage of training datasets (for each inventory) and the same independent test dataset that is derived of the entire landslide body a "success" and a "prediction" rate was calculated (Chung and Fabbri 2003). Furthermore, the resulting map is also visually evaluated according to geomorphological "quality" (Bell 2007) and to major differences between the susceptibility maps modelled with points from BGR and LiDAR mapping. Therefore, the aimed user-optimized visualisation (Bell et al. this volume) is applied to the resulting maps and the differences between the maps are analysed.

Results

Building Ground Register

The analysis of the completed database of the Building Ground Register shows that 694 events have been reported in the three test districts (BGR green points in Amstetten and Waidhofen/Ybbs are shown in Fig. 1d). It is obvious that these are purely the reported events; the real number of failures can be assumed to be much higher. Landslides that occurred in anthropogenic engineered slopes can successfully be identified by the review of the reports and are excluded from this analysis. The main trigger of the reported events was rainfall (76 %) and snow-melt (12 %). The landslides occurred on pasture (43 %) and affected infrastructure (23 %). The maximum reported landslide size was 75,000 m^2 but the average size is 1,885 m^2 with an average depth of 1.9 m^2 only. During the completion of the BGR database it was noticed that the location of the points (at the main scarp, the parcel land, or at the location of damage) differs and is not exact at each point.

Inventory Mapping on LiDAR DTM

The landslide inventory mapping resulted in a total number of 2,014 polygons. The main mapped landslide type is "slides" (1,518 polygons). 413 polygons are classified as "area with

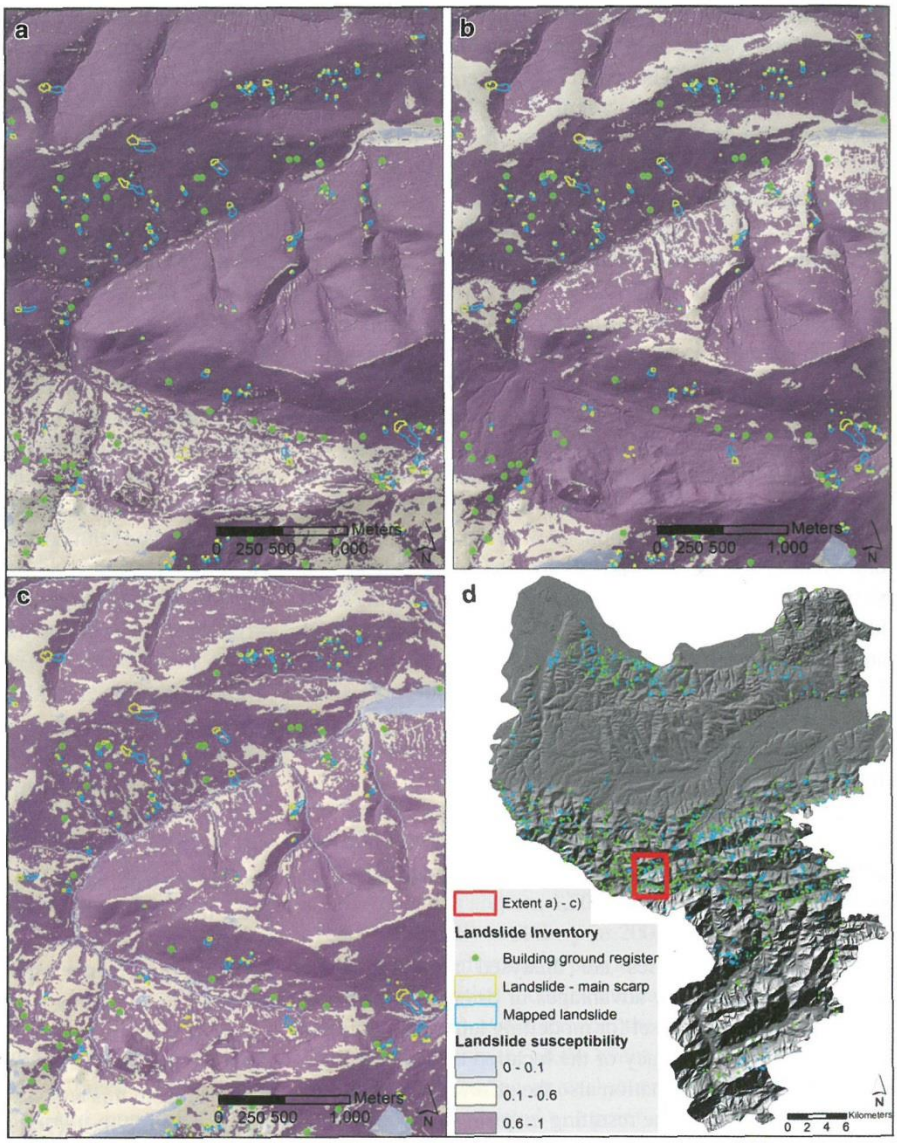

Fig. 1 Comparison of results from logistic regression modelling with (**a**) Points of the Building Ground Register, (**b**) randomly selected points within the mapped landslide polygons and (**c**) randomly selected points within the main scarp of the mapped landslides and the parameters: aspect, slope angle, slope length, lithology, landform classification, land cover, flow accumulation and topographic wetness index. The same classification according to probability values is applied to each susceptibility map. Figure 1. (**d**) shows the landslide inventories (BGR and mapped landslides) in Amstetten and Waidhofen/Ybbs superimposed on the LiDAR hillshade map (Data source: DTM – Provincial Government of LowerAustria)

slides". The resulting inventory on "slides" is presented in Fig. 1d with blue polygons.

During the mapping on the basis of the LiDAR DTM, the respective results have been compared with the points from the BGR. This comparison showed, that only few points can be related to a morphological feature visible on the hillshade. This may be mainly due to the BGR mapping scale (1:50,000) or the size or the age of the event. In some cases agricultural land use is another possible reason for the disappearing of landslides. It was observed that landslides that are mainly located on pastures are very quickly remediated (Bell et al. in prep.).

Comparison and Minimum Requirements of Inventories

In Table 1 a comparison of the analysed Building Ground Register and the mapped landslide inventory regarding number of landslides is presented. In general, more landslides have been mapped than there are stored in the BGR. This is of major advantage in the district Baden where only little information on landslides was available. Furthermore, the representativeness of the BGR could be tested by the comparison of the percentage of landslides mapped (LiDAR) and

Table 1 Comparison of building ground register and mapped landslide inventory for the districts Amstetten, Baden and Waidhofen/Ybbs regarding number of entries/mapped polygons and percentage of these in the three districts. Additionally, the area of the district is stated

District	Number of mapped polygons	Mapped polygons (%)	Number of entries in BGR	BGR entries (%)	District area (km^2)
Amstetten	1,213	60	535	77	1,187
Baden	107	5	7	1	754
Waidhofen/ Ybbs	694	34	151	22	131

Table 2 Comparison of the results of the validation of the modelling results. The "success rate" was calculated with the training dataset on landslides (BGR, scarp or body) and the "prediction rate" was calculated with the test dataset from points from the entire landslide (body). (*not enough observations)

Landslide inventory	"Success rate" AUROC training	"Prediction rate" AUROC test (with landslide bodies)
BGR	–*	0.76
Landslide body	0.87	0.87
Landslide scarp	0.89	0.84

reported in the BGR. This shows that the reported landslide density in Baden is lower than the mapped landslide density.

In Table 2 the comparison of the calculated area-under-ROC values is presented. The "prediction rate" was calculated with a test dataset with points in the landslide body as general reference. The prediction rate is significantly lower in the model with the BGR as input data than at the models of the mapped landslides.

Figure 1 shows the results of the landslide susceptibility modelling with the different landslide inventory point samples. The visual differences of these maps are related to the susceptibility zones. When modelling with the mapped landslides, the susceptibility of the hill slopes is more differentiated between high and medium classes. These differences are particularly occurring at upper and local ridges since the geomorphological quality of the maps (b) and (c) can be stated as higher than the quality of map (a). Comparing the results from modelling with landslide body or main scarp it is shown (Fig. 1b, c) that fewer areas are classified as highly susceptible but the overall impression is similar.

Discussion and Conclusions

The BGR contains very important information at least on the year of occurrence and its major advantage is the long timeline it covers. Some drawbacks are the accuracy of the location of the points that were mapped on a scale of 1:50,000 and the fact that only reported events are stored in this database.

Nevertheless, as the comparison of BGR and mapped inventory particularly for the district Baden shows, the mapping on LiDAR DTM is a valuable additional data source in areas with sparse information on landslides. Furthermore, a higher mapping accuracy can be achieved within short time due to the availability of LiDAR data with a high resolution. Therefore, the landslide mapping can be performed to obtain a representative landslide density and distribution over the entire province with high accuracy regarding the location of the points.

The visual comparison of the landslide susceptibility maps is of course highly dependent on the chosen classification thresholds. As they are once defined (refer to Bell et al. (this volume)) the differences in the possible resulting map can be analysed. This comparison shows that the differences between the usage of BGR or mapped landslides are significant, whereas the maps derived from the usage of points in the entire landslide body or main scarp are quite similar.

Keeping in mind the limited resources and the end-user optimized visualization of the maps we conclude that mapping landslide points in the main scarp area gives satisfying results to derive a representative landslide density in the entire province, which subsequently leads to reliable landslide susceptibility maps. Thus, for the rest of the districts a LiDAR mapping based landslide inventory will be prepared by mapping landslide points in the main scarp area instead of complete landslide polygons. The latter would not be feasible for such a large area, mainly due to limited resources.

Acknowledgments The authors thank several institutions and individuals for their support: the colleagues from the Geological Survey of Austria and from the Austrian Service for Torrent and Avalanche Control for providing inventory data; the Provincial Government of Lower Austria in particular the colleagues from the Geological Survey and the Department of Spatial Planning and Regional Policy for inventory data. Thanks to them also for supporting the MoNOE-project and for numerous fruitful discussions. Thanks also to the Department for Hydrology and Geoinformation for providing LiDAR and orthophoto data.

Finally, the authors are grateful for financial support of the Provincial Government of Lower Austria.

References

Anders NS, Seijmonsbergen H (2008) Laser altimetry and terrain analysis – a revolution in geomorphology. GIM International. November 2008, pp 36–39

Ardizzone F, Cardinali M, Galli M, Guzzetti F, Reichenbach P (2007) Identification and mapping of recent rainfall-induced landslides using elevation data collected by airborne Lidar. Nat Hazards Earth Syst Sci 7(6):637–650

Atkinson P, Jiskoot H, Massari R, Murray T (1998) Generalized linear modelling in geomorphology. Earth Surf Proc Land 23 (13):1185–1195

Beguería S (2006) Validation and evaluation of predictive models in hazard assessment and risk management. Nat Hazards 37(3):315–329

Bell R (2007) Lokale und regionale Gefahren- und Risikoanalyse gravitativer Massenbewegungen an der Schwäbischen Alb. Dissertation thesis, Rheinische Friedrich-Wilhelms-Universität Bonn, Bonn, Germany. http://hss.ulb.uni-bonn.de/2007/1107/1107.pdf

Bell R, Petschko H, Röhrs M Dix A (in prep) Assessment of landslide age, human impact and landslide persistence using airborne laser scanning DTMs. Geografiska Annaler Series A

Bell R, Glade T, Granica K, Heiss G, Leopold P, Petschko H, Pomaroli G, Proske H, Schweigl J (this volume) Landslide susceptibility maps for spatial planning in Lower Austria. In: Proceedings of the 2nd world landslide forum, Rome, 3–7 Oct 2011

Booth AM, Roering JJ, Perron JT (2009) Automated landslide mapping using spectral analysis and high-resolution topographic data: Puget Sound lowlands, Washington, and Portland Hills, Oregon. Geomorphology 109(3–4):132–147

Brardinoni F, Slaymaker O, Hassan MA (2003) Landslide inventory in a rugged forested watershed: a comparison between air-photo and field survey data. Geomorphology 54(3–4):179–196

Brenning A (2005) Spatial prediction models for landslide hazards: review, comparison and evaluation. Nat Hazards Earth Syst Sci 5:853–862

Chigira M, Duan F, Yagi H, Furuya T (2004) Using an airborne laser scanner for the identification of shallow landslides and susceptibility assessment in an area of ignimbrite overlain by permeable pyroclastics. Landslides 1(3):203–209

Chung CJF, Fabbri AG (2003) Validation of spatial prediction models for landslide hazard mapping. Nat Hazards 30(3):451–472

Cruden DM, Varnes DJ (1996) Landslide types and processes. In: Turner AK, Schuster RL (eds) Landslides, investigation and mitigation. National Academy, Washington, D.C., pp 36–75

Duman TY, Çan T, Emre Ö, Keçer M, Dogan A, Ates S, Durmaz S (2005) Landslide inventory of northwestern Anatolia, Turkey. Eng Geol 77(1–2):99–114

Glade T (1996) The temporal and spatial occurrence of landslide-triggering rainstorms in New Zealand. Heidelberger Geographische Arbeiten 104:237–250

Glade T, Frances F, Albini P (eds) (2001) The use of historical data in natural hazard assessments. Kluwer Academic Publishers, The Netherlands

Guzzetti F, Cardinali M, Reichenbach P (1994) The AVI project: a bibliographical and archive inventory of landslides and floods in Italy. Environ Manage 18(4):623–633

Leopold P, Heiss G, Petschko H, Bell R, Glade T (this volume) Susceptibility maps for landslides using different modelling approaches. In: Proceedings of the 2nd world landslide forum. Rome, 3–7 Oct 2011

Martha TR, Kerle N, Jetten V, van Westen CJ, Kumar KV (2010) Characterising spectral, spatial and morphometric properties of landslides for semi-automatic detection using object-oriented methods. Geomorphology 116(1–2):24–36

Mondini AC, Guzzetti F, Reichenbach P, Rossi M, Cardinali M, Ardizzone F (2011) Semi-automatic recognition and mapping of rainfall induced shallow landslides using optical satellite images. Remote Sens Environ 115(7):1743–1757

Petley D (2010) Landslide hazards. In: Alcántara-Ayala I, Goudie AS (eds) Geomorphological hazards and disaster prevention. Cambridge University Press, Cambridge, NY, pp 63–75

Petschko H, Glade T, Bell R, Schweigl J, Pomaroli G (2010) Landslide inventories for regional early warning systems. Malet JP, Glade T, Casagli N (eds) In: Proceedings of the international conference "Mountain risks: bringing science to society". CERG Editions, Strasbourg

Pomaroli G, Bell R, Glade T, Heiss G, Leopold P, Petschko H, Proske H, Schweigl J (2011) Darstellung der Gefährdung durch gravitative Massenbewegungen im Bundesland Niederösterreich als Grundlage der Raumplanung. Skolaut C (ed) Wildbach- und Lawinenverbau - Zeitschrift für Wildbach-, Lawinen-, Erosions- und Steinschlagschutz. Verein der Diplomingenieure der Wildbach und Lawinenverbauung Österreichs, Villach, pp 198–212

Schulz WH (2004) Landslides mapped using LIDAR imagery, Seattle, Washington. US Geological Survey Open-File Report, 1396(11)

Schwenk H (1992) Massenbewegungen in Niederösterreich 1953–1990. Jahrbuch der Geologischen Bundesanstalt. Geologische Bundesanstalt, Wien, pp 597–660

Van Asselen S, Seijmonsbergen AC (2006) Expert-driven semi-automated geomorphological mapping for a mountainous area using a laser DTM. Geomorphology 78(3–4):309–320

Van Den Eeckhaut M, Poesen J, Verstraeten G, Vanacker V, Nyssen J, Moeyersons J, van Beek LPH, Vandekerckhove L (2007) Use of LIDAR-derived images for mapping old landslides under forest. Earth Surf Proc Land 32(5):754–769

A.5. Landslide susceptibility maps for spatial planning in Lower Austria

Bell, R., Glade, T., Granica, K., Heiss, G., Leopold, P., **Petschko, H.,** Pomaroli, G., Proske, H. & J., Schweigl (2013), Landslide susceptibility maps for spatial planning in Lower Austria, in: Margottini, C., Canuti, P. & K. Sassa (Eds.), Landslide Science and Practice, vol. 1: Landslide Inventory and Susceptibility and Hazard Zoning, Springer, 467-473.

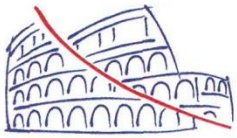

Landslide Susceptibility Maps for Spatial Planning in Lower Austria

Rainer Bell, Thomas Glade, Klaus Granica, Gerhard Heiss, Philip Leopold, Helene Petschko, Gilbert Pomaroli, Herwig Proske, and Joachim Schweigl

Abstract

Landslides threaten most parts of the provincial state of Lower Austria and cause damage to agricultural land, forests, infrastructure, settlements and people. Thus, the project "MoNOE" (Method development for landslide susceptibility modelling in Lower Austria) was initiated by the provincial government to tackle these problems and to reduce further damage by landslides. The main aim is to prepare landslide susceptibility maps for slides and rock falls and to implement these maps into the spatial planning strategies of the provincial state.

Landslide susceptibility maps are either prepared by statistical (for slides) or empirical or process-based (for rock falls) approaches. Final maps are combined to a single landslide susceptibility map and optimised for the end-users (spatial planners and local authorities). It shows that a difference exists between the best scientific maps and the best maps for spatial planning purposes. This involves questions about the best number of susceptibility classes, its thresholds and ideal colours.

Keywords

Landslide inventory • Landslide susceptibility • Spatial planning • LiDAR DTM • Lower Austria

Introduction

Landslides occur frequently in Lower Austria – a federal province of Austria (e.g. Schwenk 1992). Since 1953 more than 1,500 landslides have been studied by the Geological Survey of Lower Austria and stored in the Building Ground Register (BGR). These landslides mainly have caused damage to agricultural land, forests and infrastructure, but also threaten settlements and people. Therefore, the project "MoNOE" (Method development for landslide susceptibility modelling in Lower Austria) is funded by the provincial government. The main objectives of this project are:

1. Design of a method for landslide susceptibility modelling for a large study area (about 10,200 km^2)
2. Production of landslide susceptibility maps (for rock falls and slides)
3. Implementation of the susceptibility maps into the spatial planning strategies of the provincial state of Lower Austria

R. Bell (✉) • T. Glade • H. Petschko
Department of Geography and Regional Research, University of Vienna, Universitätsstrasse 7, 1010 Wien, Vienna, Austria
e-mail: rainer.bell@univie.ac.at

K. Granica • H. Proske
Joanneum Research Forschungsgesellschaft mbH, DIGITAL - Institute for Information and Communication Technologies, Graz, Austria

G. Heiss • P. Leopold
Health and Environment Department, AIT – Austrian Institute of Technology GmbH, Environmental Resources and Technologies, Tulln, Austria

G. Pomaroli
Department of Spatial Planning and Regional Policy, Office of the Lower Austrian Provincial Government, St. Pölten, Austria

J. Schweigl
Office of the Lower Austrian Provincial Government, Geological Survey, St. Pölten, Austria

C. Margottini et al. (eds.), *Landslide Science and Practice*, Vol. 1,
DOI 10.1007/978-3-642-31325-7_60, © Springer-Verlag Berlin Heidelberg 2013

Together with the heterogeneous geology and the aim to implement the landslide susceptibility maps in spatial planning strategies of the state this poses huge challenges towards the development of new and suitable methods for modelling landslide susceptibility. Limitations are given by restricted (digital) data availability for such large areas, e.g. geology is only available at a scale 1:200,000 for the entire study area. Since reliable landslide inventories are an essential prerequisite for high quality susceptibility maps, all available digital landslide information was gathered and evaluated. Furthermore, basic geodata had to be prepared and homogenized.

Subsequently, susceptibility modelling for slides and rock falls was carried out independently. However, since the final landslide susceptibility map shall comprise both processes in one map, approaches for combining single process susceptibility maps have to be developed. Due to the need to optimise final landslide susceptibility maps for spatial planners and local authorities, the maximum number of susceptibility classes and respective thresholds and colours for each class has to be defined. Consequently, the difference between the best scientific landslide susceptibility map and the best map for spatial planning purposes is analysed. Beside all this, human impact on landslides is analysed, mainly at local scale. However, depending on the results it will be tested whether parameters can be derived that can be integrated into regional scale landslide susceptibility modelling.

Study Area

The study area Lower Austria covers an area of approx. 10,200 km^2, which is about 2/3 of the provincial state of Lower Austria. It is located in the northeast of Austria (Fig. 1). Only districts which are prone to landslides and where landslides have been recorded by the Geological Survey of Lower Austria are investigated.

The main geological units of Lower Austria comprise the Northern Calcareous Alps, the Flysch Zone, the Molasse Zone and related units (Vienna basin and Waschbergzone), the Eastalpine Crystalline (Paragneiss and Quarzphyllite), the Bohemian Massif (Granite and Gneiss) and quaternary sediments (fluvial terraces and alluvial deposits) (Fig. 1). Deatails on the geology can be found in Wessely (2006). Based on the BGR inventory most of the registered landslides occurred in the Flysch Zone, followed by the Molasse Zone and the Northern Calcareous Alps (Schwenk 1992, see also Fig 1).

The pattern of total rainfall distribution in the study area follows mainly the topography and shows its maximum in the high mountain area of the Northern Calcerous Alps in the southwest with approx. 1,700 mm and dropping down to the northeast to approx. 500 mm (www.noe.gv.at, 2011).

Detailed information on spatial planning laws in Lower Austria is given in Pomaroli et al. (2011).

Materials/Data

To model landslide susceptibility, essential digital information on landslides and basic geodata must be gathered. Various landslide inventories were available (Table 1). Their spatial representation is shown in Fig. 1. Furthermore, numerous basic geodata was collected, which is listed in Table 2.

Methods

Various methods are applied for the different tasks of the project.

In a first step all available data on landslide inventories were gathered and their potential regarding the applicability for susceptibility modelling was analysed in detail. Furthermore, basic geodata were collected, prepared and homogenised. A new land cover classification was created by deriving it from satellite images.

Whereas slide susceptibility is modelled using statistical approaches (Weights of Evidence and Logistic regression), rock fall susceptibility is modelled based on two steps. First, rock fall release areas are determined by empirical slope thresholds depending on geology (lithology as well as tectonics), followed by modelling the run-out using empirical and process-based run out models. Both susceptibility maps are verified in the field. Furthermore, slide susceptibility maps are validated using common validation criteria like AUROC, success and prediction rate curves.

Final slide and rock fall susceptibility maps are combined and optimised for end-user needs. This is jointly developed with the spatial planners and geologists of the provincial government.

Results

Analysing all available landslide inventories, it turned out that only the landslide inventory based on the Building Ground Register of the Provincial Geological Survey could be used to some extent for slide susceptibility modelling. Furthermore, the need for preparing a new and homogenized landslide inventory based on LiDAR DTM interpretation became evident. Detailed results on the landslide inventories and minimum requirements for susceptibility modelling are presented in Petschko et al. (in this volume).

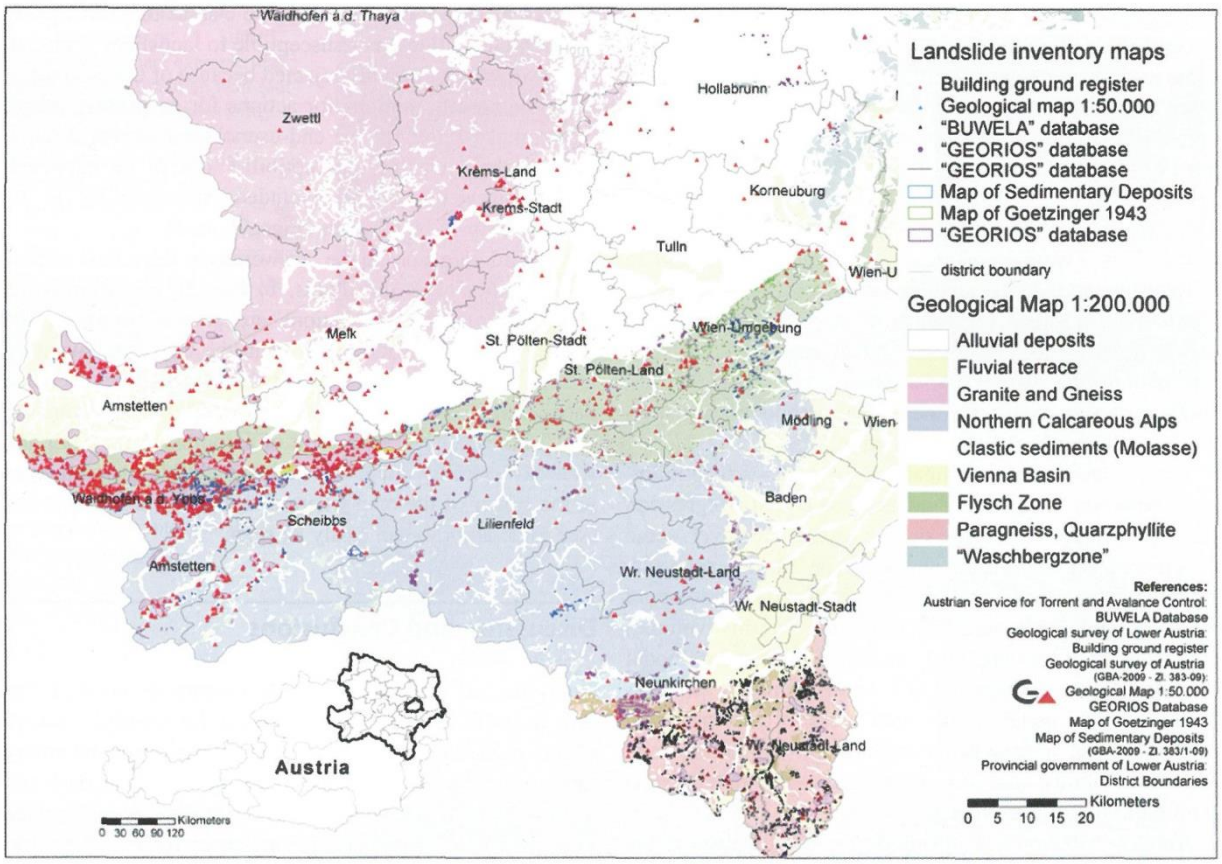

Fig. 1 Location, geology and available landslide inventories of the study area Lower Austria

Table 1 Available landslide inventories in Lower Austria (Note: N.T. = No information on time of mapping/of the events available)

Type	Source	Scale
Building ground register (BGR)	Geological Survey of Lower Austria	1:50,000; Lower Austria; Points; since 1953
Hazard maps and Hazard zoning maps	Austrian Service for Torrent and Avalanche Control – WLV	1:50,000, 1:2,000; Lower Austria – areas surrounding settlements; Polygons (in Tiff); N.T.
Localisation of Slides and Falls	Austrian Service for Torrent and Avalanche Control – WLV	1:50,000; Lower Austria, Points; N.T.
Geomorphological maps (Mapping, archive data)	BUWELA Project WLV, southeast of Lower Austria	ca. 1:50,000, "Bucklige Welt", Points; N.T.
GEORIOS Database	Geological Survey of Austria	1:50,000; Lower Austria, Points, Lines, Polygons; N.T.
Map of unconsolidated rocks	Geological Survey of Austria	1:50,000; Lower Austria, Points, Polygons; N.T.

Table 2 Available basic geodata in Lower Austria (Note: NÖGIS = webgis of the provincial state of Lower Austria, BMLFUW = Federal Ministry for Agriculture, Forestry, Environment and Water Management)

Type	Source	Scale
Geological Map, GK200	Geological Survey of Austria	1:200,000
Geological Map, GK50	Geological Survey of Austria	1:50,000, Parts of Lower Austria
Map of unconsolidated rocks	Geological Survey of Austria	1:50,000
Land cover	Joanneum Research	10 m resolution, derived from satellite data
Various Geodata (Roads, Rivers, Train, Settlements, etc.)	NÖGIS	1:50,000; 1:10.000; 1:1,000
Precipitation and designed rainfall	Hydrology / BMLFUW	Station records, 6 km resolution
Orthophotos	NÖGIS	12.5–25 cm resolution
Digital terrain model	NÖGIS	1 m resolution, Airborne LiDAR

Regarding the preparation of the basic geodata, it turned out that the geological map at a scale of 1:200,000 showed some major errors in representing alluvial areas. These areas reach up to 200 m upslope in many cases. This aspect was corrected within this project. Furthermore, there was the need to simplify the geological map to lithological relevant parameters.

So far, susceptibility modelling was carried out in three test districts (Waidhofen/Ybbs, Amstetten, and Baden) to develop methods to be applied subsequently in the whole study area. Whereas for Waidhofen/Ybbs and Amstetten the BGR landslide inventory shows sufficient landslide information, the district Baden shows only seven entries, but was chosen to test and develope methods in a district with insufficient landslide information.

First results of the comparison of slide susceptibility maps based on Weights of Evidence and Logistic regression show to a great extent quite similar results. However, some differences are significant and must be further analysed. Detailed information on this comparison is given in Leopold et al. (in this volume). Proske et al. (in this volume) concludes that applying first an empirical run-out model for rock fall susceptibility and subsequently a process-based run-out model in hot spot areas of the empirical model provide a reasonable solution for modelling rock fall susceptibility for such large areas. For details it is referred to the respective paper.

This contribution is focussed on the combination of the rock fall and slide susceptibility maps and the end-user optimisation.

Intensive discussions with the representatives of the provincial government resulted first in the decision that the common traffic light colours (green, yellow, red, or dark green, light green, yellow, orange, red) should not be used for the final landslide susceptibility classes ranging from low to high or very low to very high, although these colours are the most intuitive ones, enabling an easy way to read and understand the maps. The reason for this is that the colours yellow and red are used within the hazard zoning maps of the Austrian Service for Torrent and Avalanche Control. Whereas there are strict regulations including e.g. the prohibition of new building activities connected with the different hazard zones, the final landslide susceptibility map will have only a status of indication. To prevent misunderstandings and misinterpretations especially at the local authorities it was decided not to use these colours. Several alternative colour schemes were tested which resulted so far in the usage of the colours beige and purple, in addition to transparent for "susceptibility not to be expected" (Figs. 2b, c, d).

Parallel to the discussion of the colours the final number of different susceptibility classes had to be decided. The scientists preferred four to five classes to more exactly differentiate within areas susceptible to landslides (Fig. 2a). However, this was finally rejected because of the difficulties to define specific options for actions for each class, which would make sense for the end-users. Thus, it was decided to take three classes (susceptibility not to be expected, susceptibility not to be excluded, susceptibility to be expected) for the final maps (Figs. 2b, c, d).

A third question to be answered is the value of the susceptibility class thresholds. In Fig. 2b (conservative),c (progressive) different options are shown based on the percentage of landslide pixels from the landslide inventory used in modelling. The final decision is still being discussed between the scientists and the provincial state government. Fig. 2d presents the first result of a combined rock fall and slide susceptibility map. The high susceptible rock fall areas in the center of the map where slide susceptibility is minor (see Figs. 2b or c) can easily be seen.

Discussion and Conclusions

Analysing all available landslide inventories showed that only the BGR inventory is of some use for landslide susceptibility modelling. It clearly turned out that a new inventory must be prepared. With regard to the available data and especially the large size of the whole study area we decided to prepare such a new landslide inventory based on interpretation of the LiDAR DTM. Historical landslide information (e.g. the BGR) was not directly integrated in the newly mapped inventory since the available information is not comprehensive for the entire study area and has limitations in the accuracy of the location. However, historical landslide information was used as orientation in analysing the LiDAR DTM. Details on the preparation of the LiDAR landslide inventory can be found in Petschko et al. (2010) and in Petschko et al. (in this volume).

First modelling results for rock fall susceptibility as well as slide susceptibility are very promising for the three test districts. However, some more analyses and validations have to be carried out before the developed approaches can be applied to the whole study area.

A major decision regarding the end-user optimisation has already been taken, i.e. the number of susceptibility classes. Final decisions for the ideal colours and the susceptibility class thresholds are shortly before reached.

The project has demonstrated so far that close cooperation between scientists and representatives of the provincial state government is essential to prepare high quality and end-user optimised landslide susceptibility maps. Although the results show that there is a difference between the best

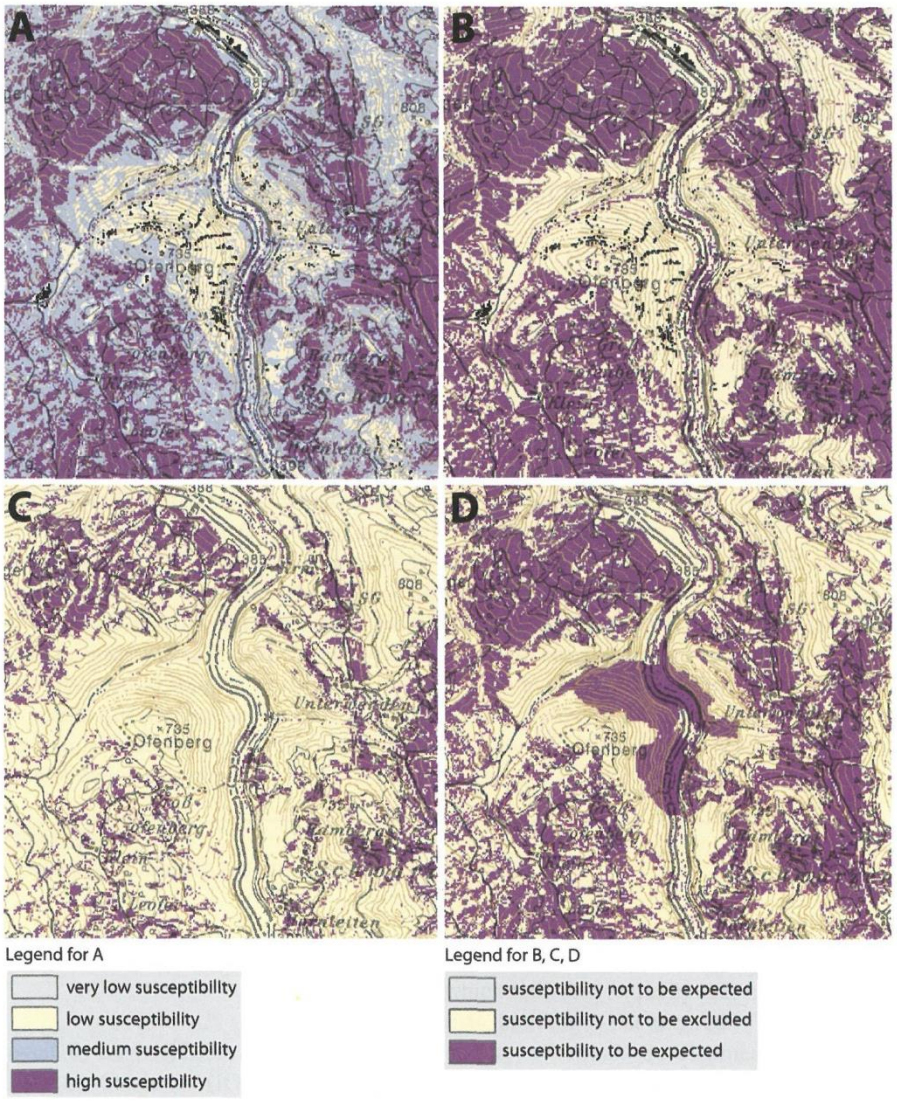

Fig. 2 Different landslide susceptibility maps. (**A**) Slide susceptibility map, example of a preferred scientific map with four classes; (**B**) Slide susceptibility map, example preferred for implementation into spatial planning strategies, class thresholds: lowest class = 1 % of landslide pixels – 40 % of the study area, highest class = 80 % of landslide pixels – 21 % of the study area; (**C**) Slide susceptibility map, like B but class thresholds: lowest class = 0.1 % of landslide pixels – 26 % of the study area, highest class = 50 % of landslide pixels – 8 % of study area; (**D**) Combined slide and rock fall susceptibility map, preferred for implementation into spatial planning strategies

scientific map and the best map for implementation in spatial planning strategies, this way it is ensured that only landslide susceptibility maps are produced which will have clear options for action for each susceptibility class and therefore will be more easily accepted by responsible spatial planners and local authorities.

Acknowledgments The authors thank several institutions and individuals for their support: the colleagues from the Geological Survey of Austria and from the Austrian Service for Torrent and Avalanche Control for providing inventory data; the Provincial Government of Lower Austria in particular the colleagues from the Geological Survey and the Department of Spatial Planning and Regional Policy for inventory data. Thanks to them for supporting the MoNOE-project and for numerous fruitful discussions. Thanks also to the Department for Hydrology and Geoinformation for providing LiDAR and orthophoto data.

Finally, the authors are grateful for financial support of the Provincial Government of Lower Austria.

References

Leopold P, Heiss G, Petschko H, Bell R, Glade T (this volume) Susceptibility maps for landslides using different modelling approaches. In: Proceedings of the 2nd world landslide forum, Rome, 3–7 Oct 2011

Petschko H, Bell R, Leopold P, Heiss G, Glade T (this volume) Landslide inventories for reliable susceptibility maps. In: Proceedings of the 2nd world landslide forum, Rome, 3–7 Oct 2011

Petschko H, Glade T, Bell R, Schweigl J, Pomaroli G (2010) Landslide inventories for regional early warning systems. In: Malet J-P, Glade T, Casagli N (eds) Proceedings of the international conference '*Mountain Risks: Bringing Science to Society*', Firenze, 24–26 November 2010, pp 277–282

Pomaroli G, Bell R, Glade T, Heiss G, Leopold P, Petschko H, Proske H, Schweigl J (2011) Darstellung der Gefährdung durch gravitative Massenbewegungen im Bundesland Niederösterreich als Grundlage der Raumplanung. In: Wildbach und Lawinenverbau. Zeitschrift für Wildbach-, Lawinen-, Erosions- und Steinschlagschutz, Society of

Engineers in the Austrian Torrent and Avalanche Control, Wien, 74, 166, pp 198–212
Proske H, Bauer C, Granica K (this volume) Different approaches of Rockfall Susceptibility Maps in Lower Austria. In: Proceedings of the 2nd world landslide forum, Rome, 3–7 Oct 2011
Schwenk H (1992) Massenbewegungen in niederösterreich 1953–1990. In: Jahrbuch der geologischen bundesanstalt. Geologische Bundesanstalt, Wien, pp 597–660
Wessely G (2006) Geologie der österreichischen Bundesländer. Niederösterreich, Wien
www.noe.gv.at (2011) Rainfall for the period 1971–2000 in Lower Austria, http://www.noe.gv.at/ExterneSeiten/Wasserstand/folder_n_lt/niederschlag/bemessung/n_1971_2000.htm. Accessed 25 June 2011

A.6. Assessing the quality of landslide susceptibility maps – case study Lower Austria

Petschko, H., Brenning, A., Bell, R., Goetz, J. & T., Glade (2014), Assessing the quality of landslide susceptibility maps – case study Lower Austria, Nat. Hazards Earth Syst. Sci., 14, 95-118, doi:10.5194/nhess-14-95-2014.

Nat. Hazards Earth Syst. Sci., 14, 95–118, 2014
www.nat-hazards-earth-syst-sci.net/14/95/2014/
doi:10.5194/nhess-14-95-2014
© Author(s) 2014. CC Attribution 3.0 License.

Natural Hazards and Earth System Sciences
Open Access

Assessing the quality of landslide susceptibility maps – case study Lower Austria

H. Petschko[1], A. Brenning[2], R. Bell[1], J. Goetz[1,2], and T. Glade[1]

[1]Department of Geography and Regional Research, University of Vienna, Austria
[2]Department of Geography and Environmental Management, University of Waterloo, Ontario N2L 3G1, Canada

Correspondence to: H. Petschko (helene.petschko@univie.ac.at)

Received: 27 February 2013 – Published in Nat. Hazards Earth Syst. Sci. Discuss.: 10 April 2013
Revised: 11 October 2013 – Accepted: 27 November 2013 – Published: 16 January 2014

Abstract. Landslide susceptibility maps are helpful tools to identify areas potentially prone to future landslide occurrence. As more and more national and provincial authorities demand for these maps to be computed and implemented in spatial planning strategies, several aspects of the quality of the landslide susceptibility model and the resulting classified map are of high interest. In this study of landslides in Lower Austria, we focus on the model form uncertainty to assess the quality of a flexible statistical modelling technique, the generalized additive model (GAM). The study area (15 850 km^2) is divided into 16 modelling domains based on lithology classes. A model representing the entire study area is constructed by combining these models. The performances of the models are assessed using repeated k-fold cross-validation with spatial and random subsampling. This reflects the variability of performance estimates arising from sampling variation. Measures of spatial transferability and thematic consistency are applied to empirically assess model quality. We also analyse and visualize the implications of spatially varying prediction uncertainties regarding the susceptibility map classes by taking into account the confidence intervals of model predictions. The 95 % confidence limits fall within the same susceptibility class in 85 % of the study area. Overall, this study contributes to advancing open communication and assessment of model quality related to statistical landslide susceptibility models.

1 Introduction

Landslides occur in mountainous as well as in hilly or coastal regions worldwide and have often been an underestimated hazard. In general, people and governing authorities are not sufficiently aware of the potential locations and consequences of landslides (Hervás, 2003). However, in Austria authorities and residents have become more aware of landslide hazards because of recent major landslide events, which affected many residents, caused significant damage to infrastructure and private properties and were reported and discussed on the local media (Damm et al., 2010). These include events in August 2005 in Gasen and Haslau and incidents in 2009 in the district of Feldbach and in the province of Lower Austria, where about 4000 landslides occurred in total (Schwarz and Tilch, 2008; Hornich and Adelwöhrer, 2010; Abteilung Feuerwehr und Zivilschutz, Amt der NÖ Landesregierung, 2010; BMLFUW, 2010). While in the past in Austria practices of post-disaster recovery and reconstruction were applied, recently more and more national and provincial authorities have been demanding pre-disaster mitigation tools, which help to prevent future damage caused by natural hazards such as landslides. Aiming at avoidance of the hazard, zonation plans can be facilitated in prospective land use planning to prevent development in undesirable locations or undesirable types of development (Schwab et al., 2005). In this context landslide susceptibility maps have proven to be a powerful tool, as they give coherent information on the spatial probability on where landslides, or landslide scarps, might occur (Brabb, 1984; Glade et al., 2005; Guzzetti et al., 2000, 2006; Varnes, 1984). The term landslide susceptibility is hereby defined by Brabb (1984) as the likelihood of

Published by Copernicus Publications on behalf of the European Geosciences Union.

a landslide occurring in an area with given local terrain attributes. The frequency or time of occurrence of the future landslides is not assessed within susceptibility zoning (Fell et al., 2008).

This study was embedded in a project preparing landslide susceptibility maps for the province of Lower Austria (15 850 km^2) with an aimed output map scale of 1 : 25 000 (Glade et al., 2012). Generally, landslide hazard zonation for determining slope instability due to landslides is based on simple landslide inventories or heuristic, statistical (including machine learning) or deterministic approaches (Soeters and Van Westen, 1996). Although these approaches are dealing with landslide hazards (spatial and temporal occurrence probability of landslides) the same categorization can be applied for susceptibility maps. Statistical landslide susceptibility models are particularly useful for modelling large areas on a medium scale (1 : 25 000–1 : 500 000) to get an overview of which slopes or slope sections might be prone to landslides in future (Fell et al., 2008). According to the resulting susceptibility maps, hot spots can be identified where more detailed analysis of the slope stability should follow (Van Westen et al., 1997). For this study a statistical approach was regarded as suitable considering the aimed output map scale, the size of the study area, the available data and the limited availability of additional resources for preparing input data (such as a more detailed landslide inventory or soil parameters).

The central assumption of landslide susceptibility modelling is based on James Hutton's (1726–1797) concept of uniformitarianism, "the past and the present are keys to the future" (Orme, 2002). Thus, statistical estimation of the possible future location of landslides is usually based on the conditions (e.g. local terrain attributes) of past landslides (Varnes et al., 1984; Carrara et al., 1993). Presently, several statistical and machine learning techniques are available for application to landslide susceptibility modelling. The most common are logistic regression (e.g. Atkinson et al., 1998; Ayalew and Yamagishi, 2005; Van Den Eeckhaut et al., 2006), bivariate models such as weights of evidence (e.g. Neuhäuser and Terhorst, 2007; Schicker and Moon, 2012) and machine learning techniques such as artificial neural networks (e.g. Nefeslioglu et al., 2008; Pradhan and Lee, 2009) and support vector machines (e.g. Marjanović et al., 2011; Pradhan, 2013). Detailed reviews and comparison of different models can be found, among others, in Guzzetti et al. (1999), Dai et al. (2002), Brenning (2005), Glade and Crozier (2005), Guzzetti (2005), Rossi et al. (2010) and Vorpahl et al. (2012). However, the more flexible machine learning algorithms often tend to overfit (Sect. 5.2), while linear models might not be flexible enough to portray possible nonlinearity in the relationship between landslide occurrence and the explanatory variables (Brenning, 2005; Nefeslioglu et al., 2008; Goetz et al., 2011). In this study the nonlinear generalized additive model (GAM, Hastie and Tibshirani, 1990) was selected for the susceptibility modelling. The GAM is widely used in ecological modelling (Guisan et al., 2002) and has recently been introduced to landslide susceptibility modelling (Brenning, 2008; Jia et al., 2008; Park and Chi, 2008; Goetz et al., 2011; Vorpahl et al., 2012). It is an extension of the generalized linear models (GLMs, such as logistic regression) that can model nonlinear relationships between response and explanatory variables while being less prone to overfitting in geomorphological modelling than the more flexible methods (Hastie and Tibshirani, 1990; Brenning, 2009; Goetz et al., 2011).

Since the application of the landslide susceptibility map resulting from this study is planned for implementation by municipal authorities, our main focus is to identify different aspects of quality (depending on input data, model performance and provided analysis of prediction uncertainties). Accordingly, the purpose of this study is to review the characteristics that describe quality, to analyse the (statistical) model quality and to assess and visualize the uncertainty of the prediction.

Likewise, this paper presents a review on considerations on quality in statistical landslide susceptibility maps (Sect. 2); background information on the study area and the landslides (Sect. 3); a description of the data sources and the input data preparation (Sect. 4); a detailed section on the methods used assessing the model form uncertainty and prediction uncertainty within a topographically heterogeneous study area (Sect. 5) and a thorough presentation of the results (Sect. 6) followed by a critical discussion (Sect. 7). The paper ends with a short conclusion highlighting the main findings of this study (Sect. 8).

2 Considerations on the quality of statistical landslide susceptibility models and resultant maps

As it comes to the application of the landslide susceptibility maps, which is associated with constructing a decisive reality (Egner and Pott, 2010) for the municipality and the land use planners, a detailed and transparent assessment of its quality is necessary. This very broad term of quality can be interpreted in several ways and in several stages of the process of preparing a landslide susceptibility map as described, amongst others, by Carrara (1993), Carrara et al. (1995), Ardizzone et al. (2002), and Guzzetti et al. (2006). In general, good quality refers to input data, a model or result (e.g. susceptibility map) which includes relatively low uncertainties.

Landslide susceptibility modelling is inherently riddled with uncertainties. In engineering and risk assessment a basic distinction between aleatory and epistemic uncertainties is very common (Hoffman and Hammonds, 1994; Oberkampf et al., 2004; Roy and Oberkampf, 2011; Hill et al., 2013). Many processes and conditions leading to landslide occurrence are known and mappable, known but not collectable, or are simply unknown (Carrara et al., 1999). The

imperfect understanding of the complexity of this hazardous phenomenon arising from the missing knowledge (Ardizzone et al., 2002; Kunz et al., 2011) is generally referred to as epistemic uncertainty (Hoffman and Hammonds, 1994; Hora, 1996; Oberkampf et al., 2004). Epistemic uncertainty is often divided into input uncertainty, parametric uncertainty and structural or model form uncertainty (Roy and Oberkampf, 2011; Rougier and Beven, 2013). Naturally, these uncertainties can be reduced by improving knowledge of the subject (Spiegelhalter and Riesch, 2011). Unavoidable uncertainty arising from the natural variability and/or randomness of the natural hazard process can be distinguished as aleatory uncertainty (Rougier and Beven, 2013; Rougier, 2013). Although these distinctions can be applied, the organization of uncertainties is dependent on the study objectives (Hora, 1996; Roy and Oberkampf, 2011).

In the following, we will discuss quality by addressing uncertainty issues associated with statistical modelling regarding input data (parametric uncertainty), model performance (model form uncertainty) and the final susceptibility map. Details on other types of uncertainties which might be more important for other types of susceptibility assessment (e.g. deterministic) or on the propagation of uncertainties can be found e.g. in Hoffman and Hammonds (1994), Draper (1995), Oberkampf et al. (2004), Karam (2005), Helton et al. (2010) and Rougier (2013).

2.1 Quality of input data

Achieving a good quality of the final landslide susceptibility map starts with the quality of the input data set for the modelling. Besides the geomorphological relevance, the spatial resolution and accuracy of the geo-environmental as well as the landslide inventory data is important (van Westen et al., 2008). During the preparation of all input data (done by mapping or measuring) subjectivity, the experience of the mapper, measuring errors or imprecision in computer processes are sources of parametric uncertainty (Mosleh, 1986; Ardizzone et al., 2002; Elith et al., 2002; van Westen et al., 2005, 2008). Furthermore, possible incompleteness, not only in a sense of full spatial coverage but also of general availability of important thematic information on (predisposing or preparatory) factors determining the landslide susceptibility influences the quality and makes the susceptibility assessment more difficult (Carrara et al., 1999; Ardizzone et al., 2002; Van Westen et al., 2005). This source of epistemic uncertainty can rarely be reduced and other assessments of the uncertainty have to be selected. The quantitative assessment of parametric uncertainty and incorporation in subsequent hazard and risk assessment is still a challenge (Ardizzone et al., 2002; Oberkampf et al., 2004; Roy and Oberkampf, 2011). Therefore, estimation on the completeness of the landslide inventory and details on the collecting and mapping method giving information on the accuracy and the location of the landslide point/line/polygon (main scarp or entire landslide body) are very important. This influences the further usage of the input data set and the feasible interpretation of the susceptibility maps substantially.

2.2 Quality of statistical model form

Every model is a simplification of reality. Therefore, while modelling landslide susceptibility, it should be expected that some discrepancies regarding the ability to explain all the processes involved in the phenomenon would naturally occur (Rougier and Beven, 2013). Every modelling result is highly dependent on the input data, the assumptions made to set up the model design and the selection and performance of an appropriate model. These assumptions also define the limitations of the model, its result and the allowed interpretation of it. Quantifying this part of the model form uncertainty is challenging. However, model validation procedures have been developed and are commonly applied to assess the model performance and therefore the model form uncertainty (Roy and Oberkampf, 2011).

The prediction skills (Guzzetti et al., 2006) can be analysed quantitatively with various performance measures and estimation techniques, and qualitatively by considering expert knowledge of a particular study area. Qualitative methods analyse the geomorphic plausibility of the map (Demoulin und Chung, 2007; Bell, 2007). Common quantitative performance measures are success/prediction rate (Chung and Fabbri, 2003, 2008), confusion matrix or error rates (Beguería, 2006a; Brenning, 2005), and cost curves (Frattini et al., 2010). Among the performance estimation techniques and measures, cross-validation using a single hold-out method and the area under receiver operating characteristic curve (AUROC) value based on ROC plots (Beguería, 2006a; Brenning, 2005; Frattini et al., 2010) are usually applied (i.e. Chung and Fabbri, 1999, 2003; Fabbri et al., 2003; Remondo et al., 2003; Brenning, 2005; Beguería, 2006a; Frattini et al., 2010; Rossi et al., 2010).

In single hold-out methods the data set is split in one single training and test sample. The training sample is used to fit the model and the test sample is used to determine the model performance. This results in a single estimate of the performance measure (e.g. one single AUROC value) without providing a measure of precision of the estimator. The estimate depends on the (random) sample used for modelling the susceptibility and testing the model's performance, which may itself have "peculiar" random characteristics that would be different for a different test set. Repeated k-fold cross-validation solves this problem by using, one after another, different subsets or partitions of the data set as test and training sets, thus effectively using the entire data set for performance estimation (Brenning, 2012a, b). In addition, repeating this procedure for different data partitioning reduces sampling variability and allows for the determination of the precision of the performance estimator (see Sect. 5.3 for details).

Depending on the partitioning method (randomly or spatially) to obtain the folds, these statistical estimation methods can further provide a means for assessing the non-spatial transferability of a model onto a different, independent random sample, and the spatial transferability into a spatially separate area. Spatial transferability refers to the capability of the model to generalize empirical relationships learned on a training data set, and to transfer these relationships to (usually adjacent) regions without major loss in predictive performance (Brenning, 2005; Von Ruette et al., 2011). This (non-) spatial transferability describes the model form uncertainty besides other performance measures such as the AUROC value.

In addition, aleatory uncertainties are of importance in the modelling stage, because even if all parameters were known perfectly, some deviance (or discrepancy) of the model results in nature might still occur due to the natural variability of the process (Elith et al., 2002, Rougier and Beven, 2013).

2.3 Quality of final susceptibility map – visualizing prediction uncertainties

One important model uncertainty which can be visualized in a map is the prediction uncertainty arising from using a statistical model. The output of a statistical model for spatial modelling is usually comprised of a single probability value for each unit of the prediction surface (grid cells, slopes or terrain units). These individual probability values represent an estimated conditional mean value of the predicted probability (Hosmer and Lemeshow, 2000). Therefore, there is a prediction uncertainty or possible range, as determined by the standard error of the predicted probabilities, of probability estimates for each unit of the susceptibility map (Guzzetti et al., 2006). The analysis of the standard error of the predicted probabilities and the prediction uncertainty analysis are independent of any class thresholds. Estimating the standard error was analysed and presented in previous research (e.g. Guzzetti et al., 2006; Van den Eeckhaut et al., 2009; Rossi et al., 2010; Sterlacchini et al., 2011). However, the way it affects the appearance of the classified landslide susceptibility map is of interest for planning purposes as considering these prediction uncertainties might result in overlaps of different susceptibility classes. Naturally, the amount of overlapping raster cells and therefore the uncertainty in the final classified map might be dependent on the number of classes and the selected thresholds for the classification.

3 Lower Austria and landslide occurrence

The Austrian province of Lower Austria covers a total area of 19 177 km^2, 15 850 km^2 of which constitute our study area (Fig. 1).

The variation of material and topographic characteristics across Lower Austria can be attributed to the diverse lithology (Petschko et al., 2012). The predominant material types include gravel, sand in the alluvial deposits and fluvial terraces; loess and loam; marl with a high amount of silt in the Molasse Zone and Schlier Zone; sandstone and marlstone of the Rheno-danubian Flysch Zone and Mélange Zone; limestone, dolostone and the igneous rocks of the Austroalpine Unit; and gneisses and granites in the Bohemian Massif (Fig. 1, Table 1).

The median slope angle was used as a simple proxy of the topographic characteristics to highlight the diverse conditions across Lower Austria. The median slope angle ranges from a minimum of $< 1°$ (alluvial deposits) to a maximum of 27° (Austroalpine Unit with dolostone; Table 1).

Land use patterns and variation on precipitation also contribute to the diverse geography of Lower Austria. The land use (40 % agricultural land, 40 % forest, 13 % grassland) is unevenly distributed across the province. Areas south of the Danube and the relatively flat northeast region of the province are predominantly used as agricultural land. The steeper slopes in the south and southwest are mainly forest-covered (coniferous and deciduous forest; Eder et al., 2011). The spatial distribution of the mean annual precipitation rate shows a gradient between the northeast (400–500 mm) and the southwest regions (1600–1700 mm) (Hydrographischer Dienst des Landes Niederösterreich, 2011).

Many different landslide types including rockfalls, earth slides, debris slides and debris flows, can be found in Lower Austria (classified according to Cruden and Varnes, 1996; and Dikau et al., 1996). While rockfall and debris flows typically occur in the southern lithology (Austroalpine Unit), earth- and debris slides occur all over the province with different densities (Table 1), sizes and depths. Only earth- and debris slides which were mapped with one point in the main scarp of each slide were within the scope of this study; recent examples of these landslide types are shown in Fig. 2.

The earth- and debris slides in Lower Austria are mainly triggered by heavy rainfall or rapid snowmelt events (Schwenk, 1992; Schweigl and Hervás, 2009). The Mélange lithology has the maximum landslide density of 5.5 landslides km^{-2}. The Rheno-danubian Flysch Zone and the Zone of Molasse with Schlier also have high landslide densities (> 4 landslides km^{-2}). The lithological properties and topographic characteristics of these units are highly susceptible to earth- and debris slides (Gottschling, 2006; Wessely, 2006). These densities were calculated from the landslide inventory described in Sect. 4.1.

4 Data sources and preparation

The susceptibility modelling in this study was based on an airborne laser scanning digital terrain model (LiDAR-DTM) with a resolution of 1 m × 1 m, acquired between 2006 and

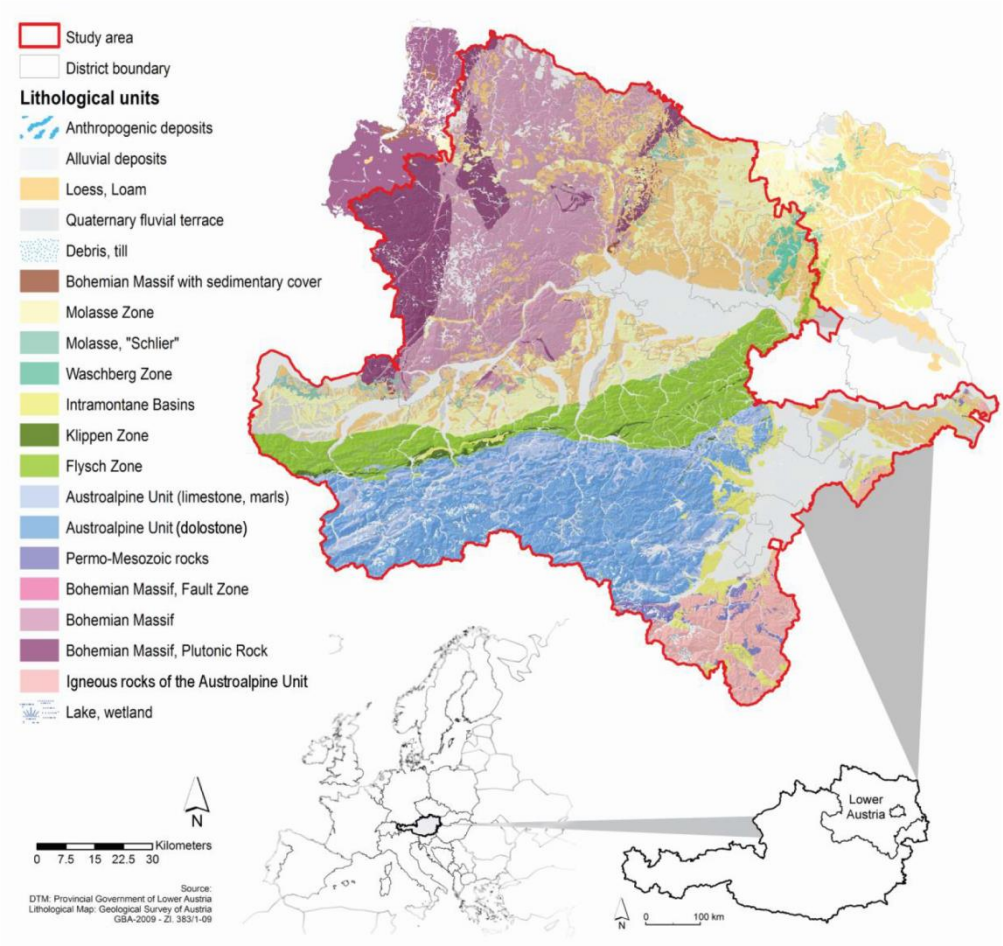

Fig. 1. Location and lithology of Lower Austria.

Table 1. Lithological units of Lower Austria: landslides and topography.

Code	Merged units	Name	Material[+]	Area (km^2)	No. of slides	Landslide density (No. km^2)	Median slope (°)
1	0124	Anthropogenic deposits		2.93	0	0	3.1
2	02297	Alluvial deposits	Gravel, sand,	3739.17	194	0.05	0.9
10	10	Loess, Loam	Sand, loam, loess-loam, drifting sand	2849.22	329	0.12	2.8
24	0124	Quaternary fluvial terrace	Gravel, sand, loess loam,	747.79	222	0.30	2.2
35	35	Debris, till	Debris, till, scree material, rock avalanche material	217.19	177	0.81	16.6
37	3786	Bohemian Massif with sedimentary cover	Sandstone, claystone, conglomerate	30.95	0	0	12.2
39	39	Molasse Zone	Marl, sand, gravel, silt	1462.46	428	0.29	4.7
58	58	Molasse, Schlier	Fine sandy-silty marl in the circum-Alpine Tertiary basins	117.43	501	4.27	4.8
86	3786	Waschberg Zone	Marl, sand, limestone, clay	123.50	52	0.42	5.8
104	104	Intramontane Basins	Sand, gravel, breccia, clay, marl	737.26	291	0.39	5.2
120	120	Mélange Zone, Klippen Zone	Dominantly penninic metasediments and phiolites as well as insignificant Austroalpine elements, Ybbsitzer and Grestener Klippen Zone	73.46	404	5.50	11.9
126	126	Rheno-danubian Flysch Zone	Interbedded sandstone, marlstone to mudstone, marl	1365.96	6281	4.60	12.6
179	179	Austroalpine Unit with limestone, marls and sandstone	Limestone, marl, shale, sandstone, gypsum, conglomerate	785.85	1636	2.08	20.2
191	191	Austroalpine Unit with dolostone	Dolostone, limestone	2148.57	1419	0.66	27.1
230	230	Permo-Mesozoic rocks (overlying the Austroalpine igneous rocks)	Carbonate rocks, siliciclastics, porphyry (mostly metamorphics)	116.43	88	0.76	19.5
239	239	Igneous rocks of the Austroalpine Unit	Orthogneiss, Paragneiss, Mica-schist, Phyllite	614.35	586	0.95	15.1
251	251 259	Bohemian Massif, Fault Zone	Tectonic fault zone	11.81	0	0	7.0
259	251259	Bohemian Massif	Paragneiss, mica-schist, phyllite, orthogneiss, Gföhl Gneiss, Granulite	2398.93	227	0.09	6.1
276	276	Bohemian Massif, plutonic rock	Granite, plutonic rock	1606.85	52	0.03	6.5
297	02297	Lake, wetland	Limnic sediments, wetland	38.77	2	0.05	3.5

[+] sorted according to frequency of occurrence, after geological map

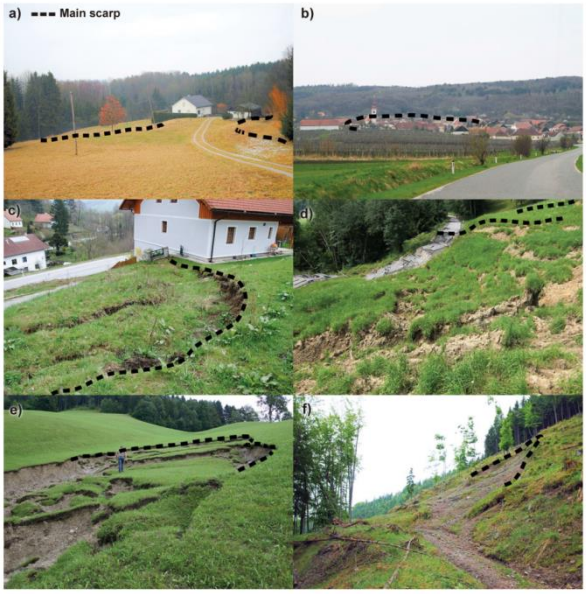

Fig. 2. Examples of landslides (earth- and debris slides) typical of the respective lithological unit **(a)** landslide in Molasse Zone at Strengberg, **(b)** the village "Waitzendorf" located on a landslide in Molasse with Schlier, **(c)** translational landslide in the Rheno-danubian Flysch Zone at Brand, **(d)** rotational landslide/flow in the Rheno-danubian Flysch Zone at Stössing, **(e)** landslide in Austroalpine Unit (Limestone, Marls) at Dippelreith, **(f)** landslide in Austroalpine Unit (with Dolostone) at Kleinzell. Pictures taken by: **(a)**, **(b)**, **(c)**, **(f)** Petschko (2010, 2011, 2012); **(d)** Bertsch (2009); **(e)** BGR (2006).

2009. LiDAR-DTMs are very useful for mapping landslides and representing the morphology of the study area, even in forest areas (Van den Eeckhaut et al., 2007; Razak et al., 2011).

Considering the detailed resolution we have given in the LiDAR-DTM and the rather coarse resolution given in the soil data (50 m × 50 m) we had to find a compromise for the analysis and output of the susceptibility map. We decided an output resolution of the maps of 10 m × 10 m would be suitable to produce 1 : 25 000 scale maps; we are still able to take advantage of the high resolution of the topographic data but also avoid wrong signals in the modelling from very local variations in the derivatives of the high-resolution DTM (Van Westen et al., 2008). The resampling to a 10 m × 10 m resolution was done by bilinear interpolation. Nevertheless, we are aware that this artificial improvement of the soil data resolution does not increase the data accuracy.

4.1 Response variable – landslide inventory

The landslide inventory originates from previous research where earth- and debris slides were mapped from a high-resolution LiDAR-DTM (Petschko et al., 2010; Glade et al., 2012, Petschko et al., 2013a). This inventory consisted of points located in each landslide's main scarp and includes 12 889 earth- and debris slides (Table 1). However, no attributes (landslide type, estimated age, land use, time/date of occurrence etc.) were assigned to each point.

Considering the large study area and the aimed result of a susceptibility map with three classes, a point inventory was preferred over a polygon inventory (Petschko et al., 2013a, c). The decision to map one point per landslide was aimed at increasing mapping effectiveness, avoiding uncertainty related to mapping landslide polygon boundaries, reducing spatial autocorrelation of the case samples (e.g. landslides) and providing equal treatment of small and large landslide samples (Carrara, 1993; Atkinson and Massari, 1998; Van den Eeckhaut et al., 2006; Heckmann et al., 2013; Petschko et al., 2013a). A comparison of modelling landslide susceptibility with sampling either a single point for the main scarp or a random point anywhere in a landslide polygon was conducted by Petschko et al. (2013c). They observed only small differences between the predictive model performances and classified susceptibility maps for the two landslide sampling schemes.

The landslide mapping focussed on distinct and easily detectable morphologies that remain visible after the occurrence of a landslide (McCalpin, 1984). Very old landslides and landslides that were not visible in the available imagery, were not included in the inventory; the full slide with scarp, transportation and accumulation area had to be discernible in the LiDAR-DTM hillshade to be included in the inventory (Petschko et al., 2013a). In areas where human activity on land use was very high, such as agricultural areas, the ability to identify landslides was particularly challenging (Bell et al., 2012). We assume that in agricultural areas fewer landslides were mapped than actually occurred; however, the full extent of the incompleteness of the inventory obtained in the study area remains unknown.

4.2 Explanatory variables

Geomorphically meaningful, explanatory variables available for this study represented terrain conditions, soil properties and potential tectonic activity.

Several terrain attributes were derived from the LiDAR-DTM as proxies for geomorphic and hydrological processes. We used SAGA GIS (Conrad, 2007) to calculate slope angle (°), slope aspect (°, transformed using the sine and cosine representing east versus west and north versus south; Brenning, 2009), overall curvature (all calculated with second-degree polynomial approximation; Zevenbergen and Thornes, 1987), a topographic wetness index (SAGA wetness index; Boehner et al., 2002), catchment height and catchment area calculated with multiple flow direction algorithm (Freeman, 1991; Quinn et al., 1991), as well as convergence indices, calculated with 10 m and 50 m radius, respectively, to represent morphological changes on different

scales. Data preparation was performed within the R package RSAGA (Brenning, 2011).

Van Westen et al. (2008) had discussed the relevance of most of these terrain attributes to landslide susceptibility. The relationship of slope angle with landslide activity is well known from general slope stability literature (e.g. Crozier, 1986). Slope aspect can be used as a proxy for bedding orientation. It may also reflect differences in intensity of solar radiation, which controls the local temperature and evaporation and therefore soil moisture (Van Westen et al., 2008). Curvature represents convex and concave surfaces related to local morphology (3×3 grid cells). The topographic wetness index was used as a proxy for the soil moisture and ground water level (Beven and Kirkby, 1979; Seibert et al., 2007). The position of the landslide on the slope and the distance from the ridge was represented by the variable catchment height. The catchment area was calculated for the subcatchments and gives a local representation of the contributing area. Convergence indices were calculated to represent the slope morphology on two different scales by using two different window sizes for the calculation (10 and 50 m). Positive values indicate ridges while negative values indicate local depressions.

Information on the soil properties is also very important as they have an effect on the infiltration capacity and water storage in the soil, which ultimately influences the disposition to landslides (Crozier, 1986). From the soil data set of Eder et al. (2011) we extracted four gridded variables representing permeability ($mm\,d^{-1}$; average value of the top 20 cm, and minimum value within 100 cm profiles) and void space (%; average value of the top 20 cm, and average of 100 cm profiles), which may be considered as a proxies for the infiltration capacity.

Available tectonic vector data included fault lines and nappe boundaries (Kurz, 2012). The proximity to a fault line might refer to the occurrence of weakened material that has already been strongly tectonically influenced, reworked and mechanically fragmented. This material generally has lower shear strength and may therefore be more prone to landslides (Crozier, 1986). Furthermore, earth- and debris slides might occur with higher density close to nappe boundaries, as these indicate a distinct difference in the material and permeability. For example, many earth- and debris slides have been observed where the nappe boundary of the Austroalpine Unit with limestone overlays the Rheno-danubian Flysch Zone. The higher water permeability of the Austroalpine limestone on top of denser sandstones and marlstones of the Flysch Zone can result in increased soil water availability at the boundary zone and presence of boundary springs (Schnabel, 1985). The fault lines and nappe boundaries were included in the susceptibility analysis by calculating grids representing the Euclidean distance from the respective features.

Land cover data for Lower Austria was also available for this study, but was not included in the analysis. Since the ages of the landslides were not available in the inventory, it would not be accurate to associate the landslide distribution with present land cover conditions (Petschko et al., 2013b). We simply do not know how land cover had historically changed and influenced all of the landslides in this inventory, which is important to understand the changing conditions of slope stability (Glade, 2003; Beguería, 2006b; Van Den Eeckhaut et al., 2009; Bathurst et al., 2010). For example, areas which are forested today might not have been forested for a long time period in the past, e.g. due to influences of mining ore in the study area (Lettner and Wrbka, 2011). Therefore, the landslide susceptibility models were prepared focussing on local terrain conditions (Brabb, 1984), which are relatively static compared to the dynamic nature of land cover (Van Westen et al., 2008).

5 Methods

5.1 Modelling of heterogeneous areas

The heterogeneity of geotechnical and topographical characteristics over a study area should be considered when modelling landslide susceptibility (Lee et al., 2008; Blahůt et al., 2010). Modelling separately in lithology units is one approach to addressing this heterogeneity (Petschko et al., 2012). This approach avoids the use of interaction terms to represent lithology-dependent processes and preparatory factors, and thus facilitates easier interpretation of the models. Fitting the model with individual modelling domains based on the lithology units is expected to improve overall predictive performance by accurately representing the diversity of geotechnical conditions across the study area (Blahůt et al., 2010; Petschko et al., 2012; Trigila et al., 2013).

Accordingly, the study area was divided into 16 modelling domains based on a simplified 1 : 200 000 lithological map (Fig. 1; Schnabel, 2002; Bell et al., 2013). The lithological map gives details on the parent material available for soil formation. This determines the geotechnical characteristics on a scale of 1 : 200 000. Data on the parent material was used as a proxy for these characteristics, as no appropriate geotechnical data covering the entire study area was available. Lithology units with no observed landslides were merged with geotechnically similar units to create homogenous modelling domains (Table 1). The final susceptibility map of the province was obtained by merging the individual susceptibility maps of the 16 domains.

5.2 Generalized additive model

Among the currently available methods for landslide susceptibility modelling a generalized additive model (GAM) is a compromise between the nonlinear predictive flexibility of machine learning algorithms and the smooth, yet linear, predictions of GLMs such as logistic regression. The model fit of the GAM can be easily interpretable, unlike most machine learning algorithms (Brenning, 2008; Goetz et al., 2011). In

addition, the GAM is more suitable for representing the non-linear response of slope stability to changing site conditions than the GLM (Goetz et al., 2011).

The basic design of a GAM is to replace the linear function of each co-variate as used in a GLM with an empirically fitted smooth function to "let the data show the appropriate functional form" (Hastie and Tibshirani, 1990). Thus a GAM allows the combination of linear and nonlinear smoothing functions in an additive manner to describe the relationship between explanatory and response variables. In the case of the logistic additive model for binary (presence/absence) response variables, the response variable is not modelled directly, but using the logit of the occurrence probability $p(\boldsymbol{x})$ conditional on explanatory variables $\mathbf{x} = (x_1, \ldots, x_m)^T$ (Hastie and Tibshirani, 1990):

$$\begin{aligned} &\operatorname{logit}(\boldsymbol{x}) = \log\left(p(\boldsymbol{x}) \big/ (1 - p(\boldsymbol{x}))\right) \\ &= \beta_0 + \beta_1 f_1(x_1) + \ldots + \beta_m f_m(x_m) \end{aligned} \tag{1}$$

where the functions f_i are nonparametric smoothers. The quantity

$$\operatorname{odds}(\boldsymbol{x}) = p(\boldsymbol{x}) \big/ (1 - p(\boldsymbol{x})) \tag{2}$$

is referred to as the odds. Thus, the logistic GAM is additive at the logit level, but increases in f_i have a multiplicative effect on the odds.

We used a combined backward and forward stepwise variable selection based on the Akaike Information Criterion (AIC), which measures the goodness-of-fit while penalizing for model complexity to obtain a parsimonious model (Akaike, 1974). Smaller models help to keep the estimated coefficient standard errors small and prevent the model from overfitting, which occurs when the number of variables in the model is large relative to the number of landslide samples (Hosmer and Lemeshow, 2000). Overfitting refers to an algorithm or model that performs very well on the available training data to which it is fitted, but poorly on future or new test data and therefore produces unreliable predictions (Hand, 1997; Hosmer and Lemeshow, 2000).

Our study design was a case-control study with the mapped landslide samples as cases and randomly selected non-landslide samples as controls. The landslide susceptibility maps were derived for each modelling domain from a model (GAM_1–GAM_{16}) using all landslide samples while the model performance is assessed using cross-validation, i.e. subsamples of landslide cells (Sect. 5.3). The sampling of non-landslide cells for the entire study area was based on a density of 2 % of all grid cells. An equal number of cases and controls (1 : 1) was used for each model fitted; the landslide samples were matched to an equal number of randomly selected non-landslide samples. This gives the sample size in the respective modelling domain.

It was necessary to adjust each model's raw predictions based on the corresponding sampling rate to account for the general relative landslide susceptibility of each modelling domain. We adjusted the prediction by considering the sampling rate (τ_0/τ_1) of each domain, using Eq. (3),

$$\operatorname{odds}^*(\boldsymbol{x}) = \tau_0 \big/ \tau_1 \times \operatorname{odds}(\boldsymbol{x}), \tag{3}$$

where

$$\tau_0 = \text{number of sampled non-landslide cells} \big/ \text{total number of non-landslide cells} \tag{4}$$

and

$$\tau_1 = \text{number of sampled landslide cells} \big/ \text{total number of landslide cells} \tag{5}$$

and odds ($\boldsymbol{x}$) is the unadjusted prediction, in our case, based on training a model with an equal number of landslides to non-landslides (1 : 1) in each domain. The odds*($\boldsymbol{x}$) gives the adjusted odds (Scott and Wild, 1986; Hosmer and Lemeshow, 2000). As all landslides were used in this step, τ_1 =1. The adjusted probability $p^*(\boldsymbol{x})$ was calculated from odds*($\boldsymbol{x}$) which was therefore comparable among different modelling domains. GAM modelling was performed with the gam package within the open-source statistical software R (Hastie, 2011; R Development Core Team, 2011).

The adjusted probabilities of landslide susceptibility of the merged map were further classified into discrete classes of low, medium and high susceptibility based on thresholds related to the percentage of observed landslides falling within each susceptibility class. This was a result of testing different thresholds and checking them in the field according to the best geomorphic and planning plausibility. A threshold for the low susceptibility class was selected so that 5 % of the observed landslides having the lowest predicted probabilities would fall within this class. An additional 25 % of the observed landslides would fall within the medium susceptibility class, while the high susceptibility class contained the 70 % of the landslides with the highest predicted probabilities. The corresponding class thresholds of 0.00209 and 0.0141 were also applied to classify the maps corresponding to the approximate upper and lower confidence limits calculated for each grid cell at the 95 % confidence level (refer to Sect. 5.5).

5.3 Spatial and non-spatial cross-validation

The assembly of the test data for performance assessment can be achieved in three ways: (1) random subsampling, (2) spatial subsampling and (3) temporal partitioning of the landslide data (Chung and Fabbri, 2003). As there was no information on the landslide age or time of occurrence available for temporal partitioning, we focused on testing random and spatial subsampling of cases and controls within each homogeneous modelling domain.

We used non-spatial and spatial k-fold cross-validation to assess each model's predictive performance as a measure of

the model's non-spatial and spatial transferability (Kohavi, 1995; Townsend Peterson et al., 2007). With random subsampling traditional non-spatial cross-validation was performed. Furthermore, spatial cross-validation was applied by spatial subsampling based on k-means clustering classification of point coordinates (Ruß and Brenning, 2010). In k-fold cross-validation, k (here: $k = 5$) randomly or spatially selected disjoint subsamples, or folds, are derived. The model was fitted k times on the combined data of k-1 folds and tested on the data of the remaining fold by applying the fitted model to the test fold and calculating the performance measure (Kohavi, 1995).

In order to obtain results that are independent of a particular partitioning, cross-validation was repeated r times (here: $r = 20$), and the median and interquartile range of the 20 outcomes was calculated. This resulted in 100 different estimates of the performance measures.

We use the AUROC as a performance measure, which was derived by comparing the sensitivity of a model (proportion of true positives) to the specificity (more precisely, 1-specificity, or false positives rate; Hosmer and Lemeshow, 2000). The AUROC takes values between 0 and 1 where a value of 0.5 would be achieved by pure chance agreement between predictions and observations and a value of 1 represent perfect discrimination (Brenning, 2005; Guzzetti et al., 2006); however, this may also indicate overfitting. Thus, the AUROC measures the model's ability to discriminate landslide and non-landslide cells (Hosmer and Lemeshow, 2000).

Spatial and non-spatial cross-validation was also applied to test the effects of reducing the sample size on the interquartile range of the AUROC values and the thematic consistency within one domain. This was performed within the modelling domain Flysch Zone. The cross-validation was applied 9 times (with 5 folds and 20 repetitions each) while the sample size of the training sample (including landslide and non-landslide samples) is reduced from 12 562 to 6400, 3200, 1600, 800, 400, 200, 100 and to 50 samples. The test sample was determined constant with a sum of 2000 landslide and non-landslide sample cells. Spatial and non-spatial cross-validation was performed with the sperrorest package in R (Brenning, 2012b).

5.4 Transferability and thematic consistency indices

The non-spatial and spatial transferability were expressed by the interpretation of the estimated interquartile range (IQR) of the AUROC values resulting from the non-spatial and spatial cross-validation of each modelling domain. The lower the estimated IQR, the better we considered the non-spatial and spatial transferability of the model within the modelling domain. However, sample size differences among modelling domains result in differences in sampling variability of AUROC estimators, which then has an influence on the IQR of AUROC among cross-validation repetitions. In order to account for this contribution to sampling variability and be able to provide a transferability measure that was comparable among modelling domains, the IQR had to be adjusted according to the sample size. We define a transferability index by adjusting the estimated interquartile range (IQR) for the contribution of test-set estimation to sampling variability. For this purpose, we calculated the approximate standard error (SE) of the AUROC (AUC) estimator on a test set of N landslide and N non-landslide samples using the equation presented by Hanley and McNeil (1982):

$$\mathrm{SE} = \Big(\mathrm{AUC} \times (1 - \mathrm{AUC}) + (N-1) \times (Q_1 - \mathrm{AUC}^2) + (N-1) \times (Q_2 - \mathrm{AUC}^2)\Big) \Big/ N^2. \quad (6)$$

The quantities Q_1 and Q_2 were calculated from the AUROC (AUC) value as shown by the following equations:

$$Q_1 = \mathrm{AUC} \big/ (2 - \mathrm{AUC}) \quad (7)$$

$$Q_2 = 2 \times \mathrm{AUC}^2 \big/ (1 + \mathrm{AUC}). \quad (8)$$

Since the IQR is approximately equal to 1.35 times the corresponding standard deviation under normal distribution, we used the following equation to remove the contribution of SE to the IQR of the AUROC, and refer to this quantity as the transferability index T:

$$T = \sqrt{\mathrm{IQR}^2 - (1.35 \times \mathrm{SE})^2}. \quad (9)$$

When slightly negative terms occurred under the square root due to the approximation used, these values were replaced by a value of zero.

A higher value of T indicates a greater variation in predictive performance among models fitted to cross-validation training partitions, which can be interpreted as a poorer transferability. We refer to the transferability calculated by spatial (non-spatial) cross-validation as spatial (non-spatial) transferability T_{sp} (T_{nsp}).

Furthermore, the results of the non-spatial and spatial cross-validation provide an estimate on the variable importance and the thematic consistency in each modelling domain. Based on the 100 models fitted on the different cross-validation training sets within each modelling domain, using stepwise variable selection we assess the importance of each variable in predicting landslide susceptibility using its selection frequency (Goetz et al., 2011). This variable-selection frequency can also be interpreted as a proxy for the thematic consistency of the model (Guzzetti et al., 2006). The thematic consistency is an additional measure to the transferability index showing the model's (and the stepwise variable selection's) sensitivity to sample variation. A high thematic consistency is preferable and describes a good quality of the model (Guzzetti et al., 2006). To formalize this concept, we introduce a thematic consistency index that measures the agreement between variable choices among cross-validation repetitions. In analogy to the Gini impurity index

used in classification (Hand, 1997), we define the consistency index C by

$$C = (p_1(1-p_1) + \ldots + p_m(1-p_m)) \,/\, (0.25 \times m), \quad (10)$$

where p_i is the proportion of models that include the ith predictor variable out of m predictors. The consistency index is calculated for each modelling domain and for spatial (C_{sp}) and non-spatial cross-validation (C_{nsp}). Good thematic consistency is achieved when each variable has a selection frequency either close to 0 % or 100 %, resulting in a p_m(1-p_m) value near 0. Therefore, a low value of C indicates a strong consistency among models. Selection frequencies around 50 % indicate weak thematic consistency and produce p_m(1-p_m) values of up to 0.25 m and a maximum C value of 1.

5.5 Spatially varying prediction uncertainties

The basis for the visualization of the landslide susceptibility map is the predicted probability of the occurrence of landslides of each grid cell, which is computed from the predicted logit. These predictions are subject to uncertainty due to sampling variability and model error, which can be expressed by the standard error of model predictions. This standard error further provides a means to determine approximate upper and lower confidence limits for the predicted logit and ultimately the predicted probability. These limits define an interval within which the true logit or probability of sites with given values of the explanatory variables is located with the chosen confidence of, for example, 95 % (Hosmer and Lemeshow, 2000). In other words, we have strong confidence that the true probability of landslide occurrence at a given type of location is within the confidence interval, but we would hesitate to claim that the true probability falls within any narrower range of values within the confidence interval.

In this study, confidence interval estimates for the predicted logit and probability are of special interest in order to assess the implications of spatially varying uncertainties for the interpretation of the final classified susceptibility map. Since the available GAM implementation (Hastie, 2011) does not provide standard errors or confidence intervals for "new" objects that are not included in the training sample, we proceed as follows to estimate standard errors for each location in the prediction map. We first compute standard errors on the logit and probability levels for all sample cells. A lookup table is then used to transfer these standard errors to all grid cells of the raster based on the similarity of the values of explanatory variables used by the model. Tolerance thresholds were applied to each explanatory variable to identify suitable observations in the training sample that match any given prediction location and therefore have similar standard errors. Several tolerance thresholds were tested for each modelling domain to maximize the R^2 obtained by comparing, on the training sample, standard errors estimated by table lookup to the standard errors calculated by the GAM implementation. This results in a raster data set which gives an estimation of the standard error of the predicted logit for each grid cell.

Based on these approximated standard errors we estimate the approximate upper and lower limit of a 95 % confidence interval of the predicted logit using a normal approximation. These logit-scale confidence intervals are further converted to the probability level and adjusted based on each modelling domain's sampling rate (Sect. 5.2). The approximate upper and lower confidence limits and the predicted probability are used to compare the spatially varying uncertainties in a classified landslide susceptibility map. Therefore, the classified susceptibility map is compared to the classified maps of upper and lower confidence limits to assess potential areas and grid cells in which overlaps of the susceptibility classes (high, medium or low) may occur.

Furthermore, the approximate logit-scale standard errors from each model's predictions are used as relative uncertainty indices of the susceptibility map within each domain. This uncertainty index allows for a more nuanced visualization of prediction uncertainties within each domain, knowing, however, that its interpretation is only applicable within the domain since no adjustment for the domain-specific sampling rate is applied to this index.

To communicate the possible effects of the prediction uncertainty on the classified susceptibility map, a static way of visualization of the results was selected (Elith et al., 2002). Therefore, the classified susceptibility map was presented alongside a map of possible class overlaps considering the upper and lower confidence limits and with a map of the standard errors (unclassified).

A flow chart of the analysis in this study points out the relation of the different aspects of quality raised in Sect. 2 with the presented methods and measures (Fig. 3).

6 Results

6.1 Landslide susceptibility map

The three classes of the final landslide susceptibility map classified according to the proportion of landslides included covered 75 % (low susceptibility), 19 % (medium susceptibility) and 6 % (high susceptibility) of the total study area (Fig. 4).

The variable frequency analysis showed that different subsets of the available 15 explanatory variables were included in the GAMs (GAM_1–GAM_{16}) for the different modelling domains (Table 2). The total number of variables used in the models (GAM_1–GAM_{16}) ranged from four variables in the Bohemian Massif with plutonic rock and Waschberg Zone, including Bohemian Massif with sedimentary cover domains (52 landslides each), to 11 variables used in the model for the Flysch Zone (6281 landslides, Table 3). The number of

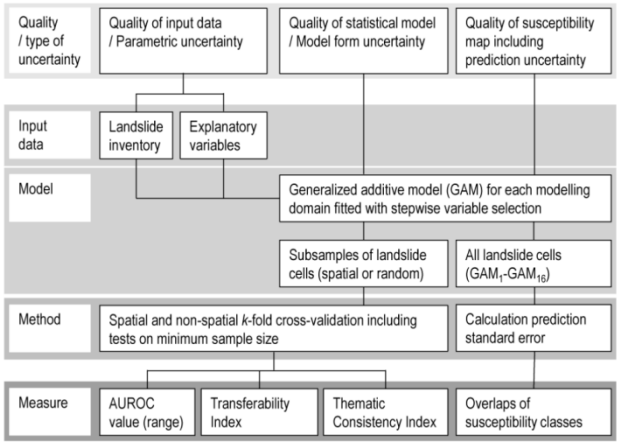

Fig. 3. Flow chart presenting the methods and measures applied within this study assessing the quality of input data, quality of statistical model and quality of final susceptibility map.

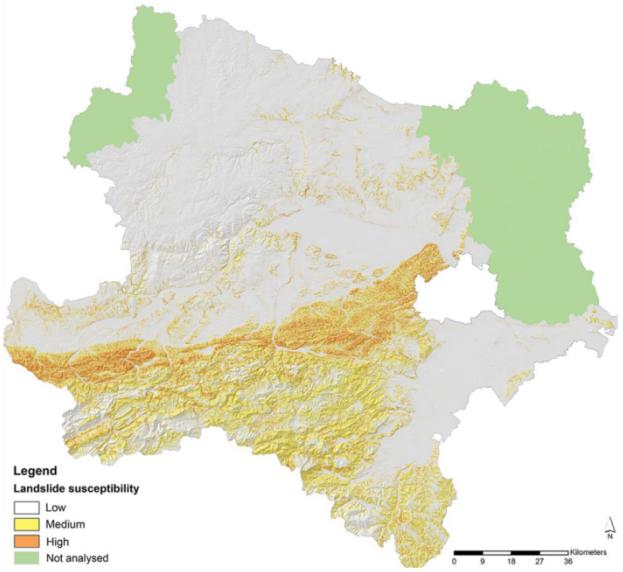

Fig. 4. Resulting classified landslide susceptibility map for Lower Austria. Data source: LiDAR-DTM hillshade – Provincial Government of Lower Austria.

variables included in the models generally increased with the number of observations in the training sample, which was attributed to the AIC's penalization based on model complexity relative to sample size. Furthermore, 65 % of the variables were used in a smoothed form (Table 2). However, mainly linear model terms were selected in four modelling domains. A similar overall frequency of nonlinear model terms was obtained in the models fitted within the cross-validation procedures (71 % nonlinear overall) with very similar results for the spatial and non-spatial techniques (refer to Table 2 for details). Two domains (Loess, Loam and Waschberg Zone and Bohemian Massif with sedimentary cover) primarily used linear model terms in spatial and non-spatial cross-validation. Additionally, in the Bohemian Massif with plutonic rock (only in spatial cross-validation) and in the alluvial deposits including lake and wetland (only in non-spatial cross-validation) high proportions of linear terms were observed.

6.2 Spatial and non-spatial cross-validation

In general, spatial cross-validation had a larger range of AUROC values than non-spatial cross-validation over all cross-validation repetitions (Fig. 5). However, the median AUROC values were very similar; non-spatial cross-validation had only slightly higher median values. The highest median AUROC values of 0.98 (spatial) and 0.99 (non-spatial cross-validation) were found in the alluvial deposits including lakes and wetland domain. With the exception of the Permo-Mesozoic rocks domain, all median AUROC values are higher than 0.74 (Fig. 5). In this domain the largest differences of median AUROC values between spatial (0.53) and non-spatial cross-validation (0.79) were found. Furthermore, the lowest 1st quartile AUROC value, which was higher performing with non-spatial cross-validation (0.73) than spatial cross-validation (0.35), was found for the Permo-Mesozoic rocks domain. Additionally, this domain showed the highest interquartile range of AUROC values (0.42) with spatial cross-validation and the second highest (0.11) with non-spatial cross-validation.

Three domains had very high AUROC values of the 3rd quartile, which ranged from 0.97 to 1 in the spatial and non-spatial cross-validation. These were the loess and loam, the Bohemian Massif with plutonic rock and the alluvial deposits including lakes and wetland domains.

The poorest spatial and non-spatial transferabilities assigned at $T_{sp} > 0.10$ and $T_{nsp} > 0.04$ were obtained in the three modelling domains with the smallest sample sizes (Table 3). Transferability tended to be better in domains with larger sample sizes and/or higher landslide densities, but was unrelated to median AUROC. Among the domains with larger sample sizes, the Austroalpine Unit with dolostone stood out with relatively poor spatial transferability ($T_{sp} = 0.098$) in addition to its relatively low median AUROC of 0.75. Spatial transferabilities were best ($T_{sp} < 0.03$) for igneous rocks of the Austroalpine Unit, the Molasse Zone and the Schlier Zone.

Reducing the sample size from using the total number of landslide and non-landslide samples in the case-control sample (12 562) to 50 samples within a modelling domain (Flysch Zone) still resulted in acceptable median AUROC values (> 0.76) for all sample sizes. However, the median AUROC values decreased from 0.84 to 0.76 in both the spatial and non-spatial cross-validation (Fig. 6) with very little difference between both approaches. While the AUROC values stay relatively constant until a sample size of 3200,

Table 2. Variable frequency for the model using all landslide cells (GAM_1–GAM_{16}) and variable-selection frequency of variables used linearly (*N*) or with a smoothing function (*S*) in spatial (spCV) and non-spatial (nspCV) cross-validation. All values are summarized over all modelling domains.

	Variable frequency (GAM_1–GAM_{16})		Variable frequency total (GAM_1–GAM_{16})	Relative variable-selection frequency from cross-validation					
	N	*S*		All spCV	All nspCV	*N* spCV	*N* nspCV	*S* spCV	*S* nspCV
Slope angle	2	13	15	91.8	95.7	9.1	17.3	82.8	78.4
Curvature	2	10	12	53.8	58.6	7.1	1.5	46.7	57.1
Topographic wetness index	4	7	11	68.3	61.4	15.9	13.5	52.3	47.9
Catchment height	4	6	10	55.6	65.0	26.3	21.1	29.3	43.9
Convergence Index (10)	3	6	9	48.8	44.1	16.5	19.8	32.3	24.4
Euclidian distance to tectonic lines	4	5	9	53.4	53.3	23.6	18.3	29.8	34.9
Euclidian distance to nappe boundaries	4	5	9	74.2	56.1	24.1	11.8	50.1	44.3
Convergence Index (50)	3	5	8	56.1	64.3	21.3	26.3	34.8	38.0
Void space (0–20 cm)	3	4	7	0.3	0.2	0.0	0.1	0.3	0.1
Catchment area (log)	2	4	6	43.4	45.0	4.9	10.2	38.6	34.8
Permeability (0–20 cm)	3	1	4	36.9	23.7	15.3	8.3	21.6	15.4
East aspect	2	1	3	9.4	6.5	5.2	4.8	4.2	1.8
North aspect	2	0	2	11.8	19.5	8.1	17.9	3.7	1.6
Void space (mean 0–100 cm)	0	2	2	0.0	0.0	0.0	0.0	0.0	0.0
Permeability (min)	0	0	0	1.1	4.9	0.5	0.4	0.6	4.5

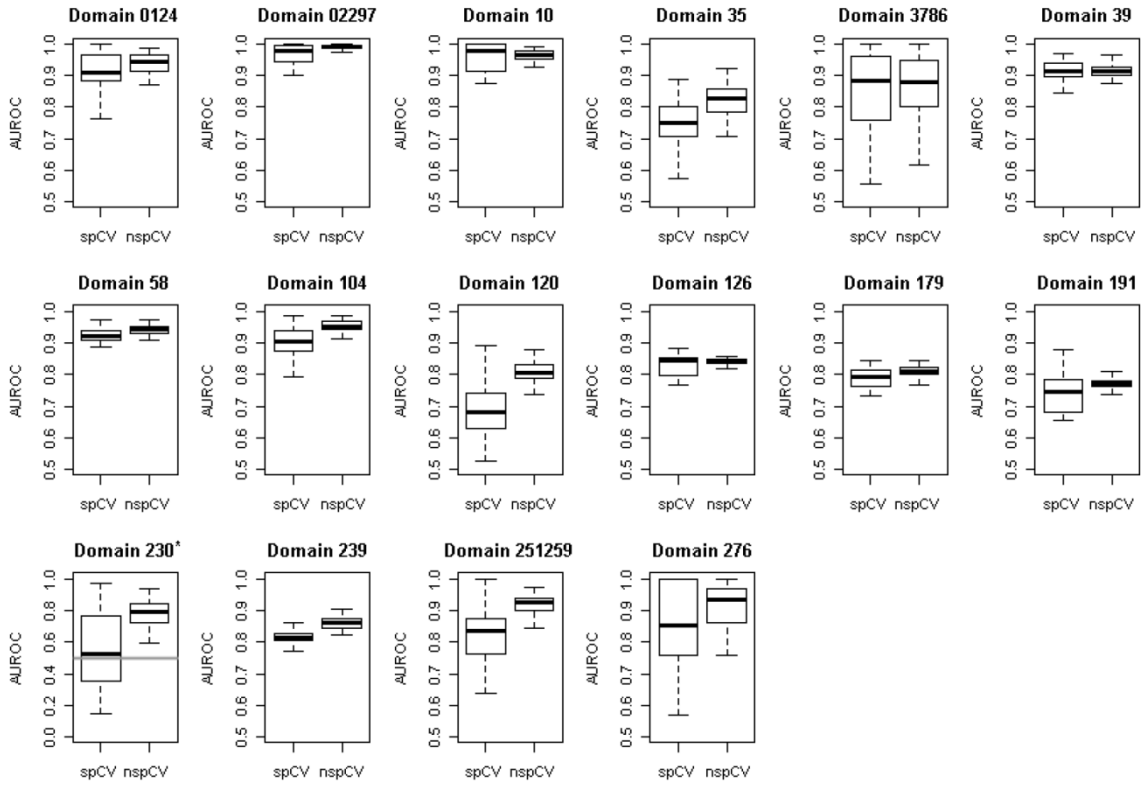

Fig. 5. Box plots showing the range of AUROC values resulting from repeated *k*-fold cross-validation with spatial subsampling (spCV) and non-spatial subsampling (nspCV) for each modelling domain. The *y* axis limits for this domain range from 0 to 1 and a grey line marks the 0.5 value.

they started to decrease more rapidly from there on as the sample size decreases. Despite that, the interquartile ranges were substantially higher with spatial cross-validation, and generally increased with decreasing sample sizes in both spatial (0.052–0.087) and non-spatial (0.011–0.059) cross-validation. Below a sample size of about 400 (spatial cross-

Table 3. Number of selected variables for the models GAM_1–GAM_{16}. Median AUROC values, transferability and thematic consistency of the modelling domains for spatial (spCV) and non-spatial (nspCV) cross-validation. Lower index values T_{sp}, T_{nsp} and C_{sp}, C_{nsp} indicate strong spatial and non-spatial transferability and thematic consistency, respectively. Minimum (Min.), maximum (Max.) and range of standard error (SE) of the prediction on logit level. R^2 obtained by comparing standard errors estimated by the lookup table to the standard errors calculated by the GAM implementation.

Domain	Name	No. of selected variables	Median AUROC spCV	Median AUROC nspCV	Transferability index T_{sp}	Transferability index T_{nsp}	Consistency index $C_{sp}C_{nsp}$	Consistency index	Min. SE (logit)	Max. SE (logit)	SE range (logit)	R^2
239	Igneous rocks of the Austroalpine Unit	7	81.7	86.2	0.000	0.000	0.247	0.151	0.12	1.61	1.49	0.77
58	Molasse, Schlier	6	92.2	94.3	0.015	0.000	0.364	0.191	0.19	2.35	2.16	0.87
39	Molasse Zone	6	91.4	91.4	0.029	0.000	0.418	0.326	0.19	2.63	2.44	0.76
35	Debris, till	7	75	82.7	0.042	0.023	0.352	0.253	0.25	3.61	3.36	0.76
02297	Alluvial deposits including lakes and wetlands	7	97.9	99.3	0.042	0.000	0.339	0.389	0.44	3.12	2.68	0.76
179	Austroalpine Unit with limestone, marls and sandstone	8	79.5	81.2	0.046	0.000	0.176	0.109	0.08	1.63	1.55	0.84
126	Rheno-danubian Flysch Zone	11	84.5	84.1	0.051	0.002	0.099	0.180	0.05	1.62	1.57	0.82
104	Intramontane basins	7	90.8	95.4	0.052	0.000	0.164	0.324	0.25	2.20	1.94	0.79
0124	Quaternary fluvial terrace and anthropogenic deposits	6	90.8	94.3	0.070	0.033	0.363	0.283	0.23	1.69	1.46	0.86
10	Loess, Loam	5	97.8	96.7	0.084	0.010	0.349	0.174	0.27	8.73	8.46	0.90
251259	Bohemian Massif including Fault Zone	6	83.4	92.5	0.091	0.000	0.377	0.251	0.24	1.73	1.49	0.79
120	Mélange Zone, Klippen Zone	8	68.1	80.7	0.098	0.000	0.210	0.081	0.19	1.84	1.65	0.51
191	Austroalpine Unit with dolostone	9	74.7	77	0.098	0.000	0.162	0.068	0.09	1.66	1.57	0.75
3786	Waschberg Zone including Bohemian Massif with sedimentary cover	4	88.4	88	0.170	0.102	0.424	0.235	0.35	4.38	4.03	0.62
276	Bohemian Massif, plutonic rock	4	85.6	93.4	0.208	0.073	0.419	0.323	0.37	16.25	15.88	0.67
230	Permo-Mesozoic rocks (overlying the Austroalpine igneous rocks)	6	52.4	79	0.397	0.045	0.519	0.319	0.27	2.92	2.65	0.57

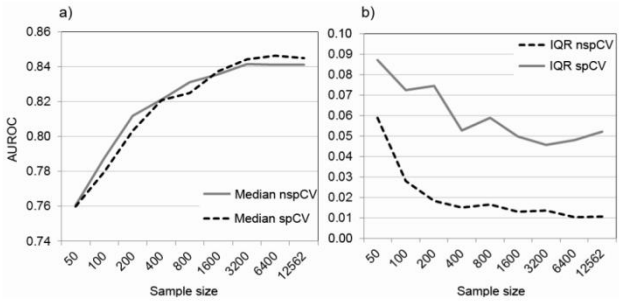

Fig. 6. (a) Median AUROC value and **(b)** interquartile range of AUROC values (IQR) at reduced sample sizes (numbers given refer to the total number of equally distributed landslide and non-landslide points) in the Flysch Zone (Domain 126) resulting from spatial cross-validation (spCV, grey line) and non-spatial cross-validation (nspCV, black dashed line).

validation) and 200 (non-spatial cross-validation) the interquartile range of the AUROC values sharply increased as the sample size decreased; thus the transferability of the model decreased substantially for sample sizes smaller than 400 (spatial cross-validation) and 200 (non-spatial cross-validation). In addition, the smaller sample sizes led to lower thematic consistency of the model.

6.3 Variable importance and thematic consistency

In the comparison of the models fitted within the 16 modelling domains (GAM_1–GAM_{16}), topographic variables were more important than the available variables on soil properties. Out of a maximum of 16 selections, the variable slope angle was selected 15 times within the stepwise variable selection, whereas the minimum permeability value was not selected at all (Table 2). However, this only shows the result of one specific random sample and variable selection. According to the relative variable-selection frequency resulting from the two cross-validation approaches, the variable importance for predicting the landslide susceptibility also changed distinctly between the modelling domains. All modelling domains (except the domain of the Permo-Mesozoic rocks) had slope angle as the most important variable. It was selected on average in 91.8 and 95.7 % of the model repetitions in spatial and non-spatial cross-validation. Another important variable was catchment height, which was selected 55.6 % (spatial) and 65 % (non-spatial) of the repetitions. In the spatial cross-validation the Euclidian distance to nappe boundaries was the second most important variable as it was selected in 74.2 % of the models (non-spatial selection frequency 56.1 %, rank 6). The topographic wetness index (68.3 % / 61.4 %), the convergence index (50 pixel radius; 56.1 % / 64.3 %) and the curvature (53.8 % / 58.6 %) were also among the top ranking variables in both cross-validation approaches. Void space (mean 0–100 cm) was not selected in any of the model runs, while void space (0–20 cm) was selected by less than 1 % of the models and the minimum permeability was included in 1.1 % (spatial cross-validation) to 4.9 % (non-spatial cross-validation) of the models on average over all modelling domains.

Overall the thematic consistency was stronger within the non-spatial cross-validation because training sets are less variable when the data are partitioned randomly as opposed to spatially (Table 3). A strong thematic consistency was assigned for a consistency index of C_{sp}, $C_{nsp} < 0.20$ and was found for seven domains in the non-spatial cross-validation but only for four domains in the spatial cross-validation. The strongest thematic consistency was observed in the Flysch Zone ($C_{sp} = 0.099$) in spatial cross-validation and in

the Austroalpine Unit with dolostone ($C_{nsp} = 0.068$) and the Klippen Zone ($C_{nsp} = 0.081$) in the non-spatial cross-validation. These domains had a very large sample size and landslide density and also a good spatial or non-spatial transferability. While in spatial cross-validation the domains with the smallest sample size and poorest spatial transferability had the weakest thematic consistency, in non-spatial cross-validation the consistency index was unrelated to sample size and transferability. Among these, the Waschberg Zone (including the Bohemian Massif with sedimentary cover domain) gave very contrasting results. It showed a weak thematic consistency in spatial cross-validation but a medium consistency index in non-spatial cross-validation. The weakest thematic consistency was found for the Permo-Mesozoic rocks ($C_{sp} = 0.519$) and the alluvial deposits including lakes and wetlands ($C_{nsp} = 0.389$) domains. In non-spatial cross-validation the thematic consistency was stronger with lower median AUROC values. However, in spatial cross-validation the median AUROC values and the thematic consistency were unrelated.

6.4 Spatially varying prediction uncertainties

The largest range of logit-scale standard errors was obtained for the Bohemian Massif with plutonic rock domain (0.37–16.24; Table 3), whereas the Quaternary fluvial terrace had the minimum range (0.22–1.69). The highest standard error of 16.24 was in the Bohemian Massif with plutonic rock domain, while the median of the highest standard errors over all domains was 2.27. After the transformation from logit-scale to probability scale the typical distribution of the standard error was the following: the range of the standard error of the predicted probability was largest for medium probabilities that were in the medium susceptibility class. The minimum range of the standard errors was typically obtained at the minimum and maximum probability that were contained in the low and high susceptibility class. Nevertheless, the lowest standard errors were computed at the minimum predicted probability.

Within the study area of Lower Austria seven types of susceptibility class uncertainties in the classified landslide susceptibility maps were identified by the analysis of overlaps between the susceptibility classes (Figs. 7 and 8). Most commonly, for about 85 % of the grid cells, there were no overlaps of different susceptibility classes either with the lower or the upper confidence limit meaning that in all maps the susceptibility class was the same. The most common overlaps were found for the low susceptibility class where 6 % of the grid cells were classified with low susceptibility in the predicted probability map but with medium susceptibility in the upper confidence limit map (Fig. 7). Moreover, 2 % of the study area experienced overlaps of the medium class in the predicted probability map to the high susceptibility class in the upper confidence limit map. Even fewer grid cells, 0.03 % had a range from the low class in the predicted probability map to the high class in the upper confidence limit map.

The results of the analysis of spatially varying uncertainties were presented by maps chosen in two exemplary modelling domains with contrasting landslide densities, the Flysch Zone ($4.6\,km^{-2}$) and the Bohemian Massif ($0.09\,km^{-2}$, Fig. 8). The range of the standard errors of the predicted logit of these domains was very similar. While the standard errors range from 0.05 to 1.6 in the Flysch Zone, the Bohemian Massif had a range from 0.24 to 1.73 (Table 3). With this minimum value the Flysch Zone gives the lowest standard error in the study area. The R^2 resulting from using the lookup table to transfer the standard errors to all grid cells range from 0.51 (in the Mélange Zone) to 0.9 (in Loess, Loam; Table 3). In the Flysch Zone the computed R^2 was 0.82 which is only slightly better than in the Bohemian Massif (0.79).

Comparing the classified maps from the Flysch Zone to the Bohemian Massif it can be seen that the grid cells showing an overlap in the Flysch Zone were much more scattered, pixel-wise, and mainly occurred at the boundaries of the susceptibility classes (Fig. 8). In the centre of the high susceptible class no overlaps occurred. However, in the Bohemian Massif the overlaps mainly occurred between the medium and high susceptibility classes and generally covered the entire class or larger areas, instead of single grid cells only. Both maps shared a low frequency of dark blue and dark green grid cells, which showed overlaps from the low class to the high class (either from lower confidence limit to predicted probability or from predicted probability to upper confidence limit). Furthermore, the overlaps of classes were occurring equally in- and outside of permanent settlement areas, which was important when considering the map for future planning purposes (Fig. 8).

7 Discussion

7.1 Quality of input data

Practical challenges in this study arise from the size of the study area and the intended output map scale of 1 : 25 000. The size of the study area brings along some limitations regarding the availability of data sources that offer a full spatial coverage and a reasonable map scale. This introduces a number of parametric uncertainties into the modelling. Generally a complete, unbiased inventory would be desirable, as for example a full inventory that was mapped directly in the aftermath of a landslide event (single landslide or multiple landslides triggered at the same time) in the area of the susceptibility map (Van Westen et al., 2008). This would allow for the inclusion of land cover or precipitation data in the modelling which might be helpful to learn even more about the landslides in the area and to build scenarios on future landslide susceptibility (or hazard/risk; Begueria, 2006b; Tarolli et al., 2011). However, a complete inventory is rarely

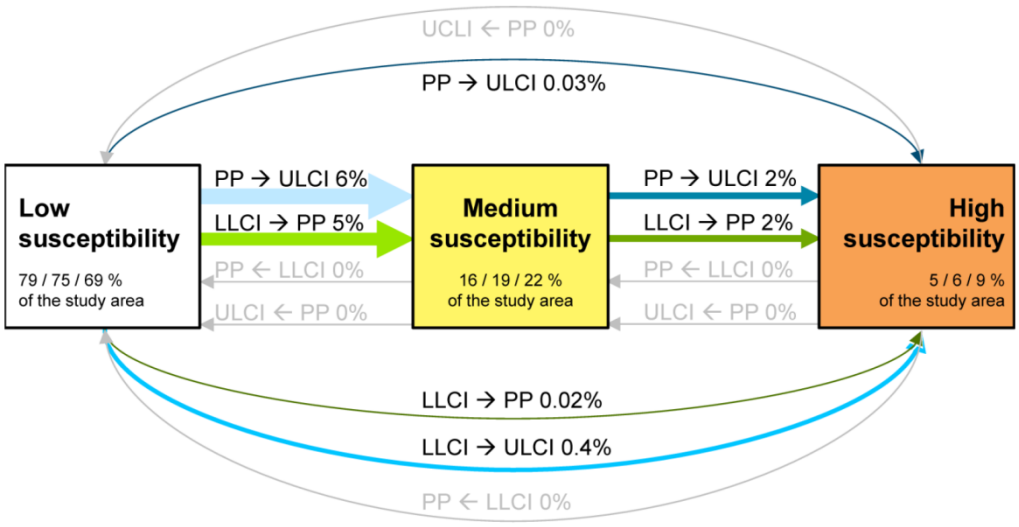

Fig. 7. Susceptibility class uncertainty expressed by types of overlaps between susceptibility maps at the lower confidence limit (LLCI) or the upper confidence limit (ULCI) at the 95 % confidence level relative to the class in the predicted probability map (PP). With the susceptibility class the percentage of area in the maps of LLCI, PP and ULCI is given in the box. The arrow thickness is relative to the percentage of affected area. Possible types of overlaps, which did not occur in the study area, are indicated with grey arrows. Next to the type of overlap the percentage of affected area related to the study area is given. In 85 % of the study area, the 95 % confidence limits fall within the same susceptibility class (not indicated here).

available. Particularly for historical inventories, the level and type of completeness is unknown, while it is known that they are generally incomplete (Malamud et al., 2004). Even a substantially complete inventory, which would be useful in statistical modelling as it includes a substantial fraction (random sample) of all landslides at all scales, land use types, lithological units or slope angles, cannot be reached for historical inventories (Malamud et al., 2004). This originates from the observation that landslides and their visibility on aerial photographs or other base maps (e.g. hillshades derived from airborne laser-scanning DTMs) are highly influenced by new landslides, reactivation, erosion, land use type and anthropogenic activities (Bell et al., 2012; Malamud et al., 2004; McCalpin, 1984, Van Westen et al., 2008). Furthermore the mapping and identification of landslides is highly dependent on the experience and knowledge of the investigator (Van Westen et al., 1999; Harp et al., 2002; Ardizzone et al., 2002). If these influences on the completeness are not random they might introduce a bias in the inventory and furthermore in the sampling which results in a model bias or systematic modelling error.

In our study area it is assumed that the inventory is not complete as it originates from recent data sources (not multitemporal) only and the visibility of landslides in the LiDAR-DTM or orthophoto is influenced by human impact depending on the land use type (Bell et al., 2012). Furthermore, a drawback is that no information on the time of occurrence of the landslide is available. However, the type of incompleteness was not analysed for the entire study area. Therefore, it is not clear if the missing landslides are missing completely at random or are biased toward absence in certain land uses or lithological units. The implications of an incomplete inventory on the model performance (shown by the AUROC value) were estimated by performing the repeated *k*-fold cross-validation using training and test samples. The results show rather high AUROC values for most modelling domains, which indicates that even with an incomplete inventory (training sample) the prediction of landslides of the test sample was successful for most cases. However, sample size is of importance for the model performance. For the discussion of this please see Sect. 7.4.

7.2 Quality of statistical model form

7.2.1 Study design to meet the heterogeneity of the study area

Observed variable-selection frequencies showed that different explanatory variables were relevant in different domains, which provides additional justification to the decision to model susceptibility in each modelling domain separately. Additionally, not only the different choice of the variables is important but also the way the variables are fitted or smoothed according to the sample in the respective domain. Previous studies showed that within each lithological unit landslides occur at different slope angles (Blahůt et al., 2010; Muenchow et al., 2012; Petschko et al., 2012). Similar differences within lithological units or terrain types might be

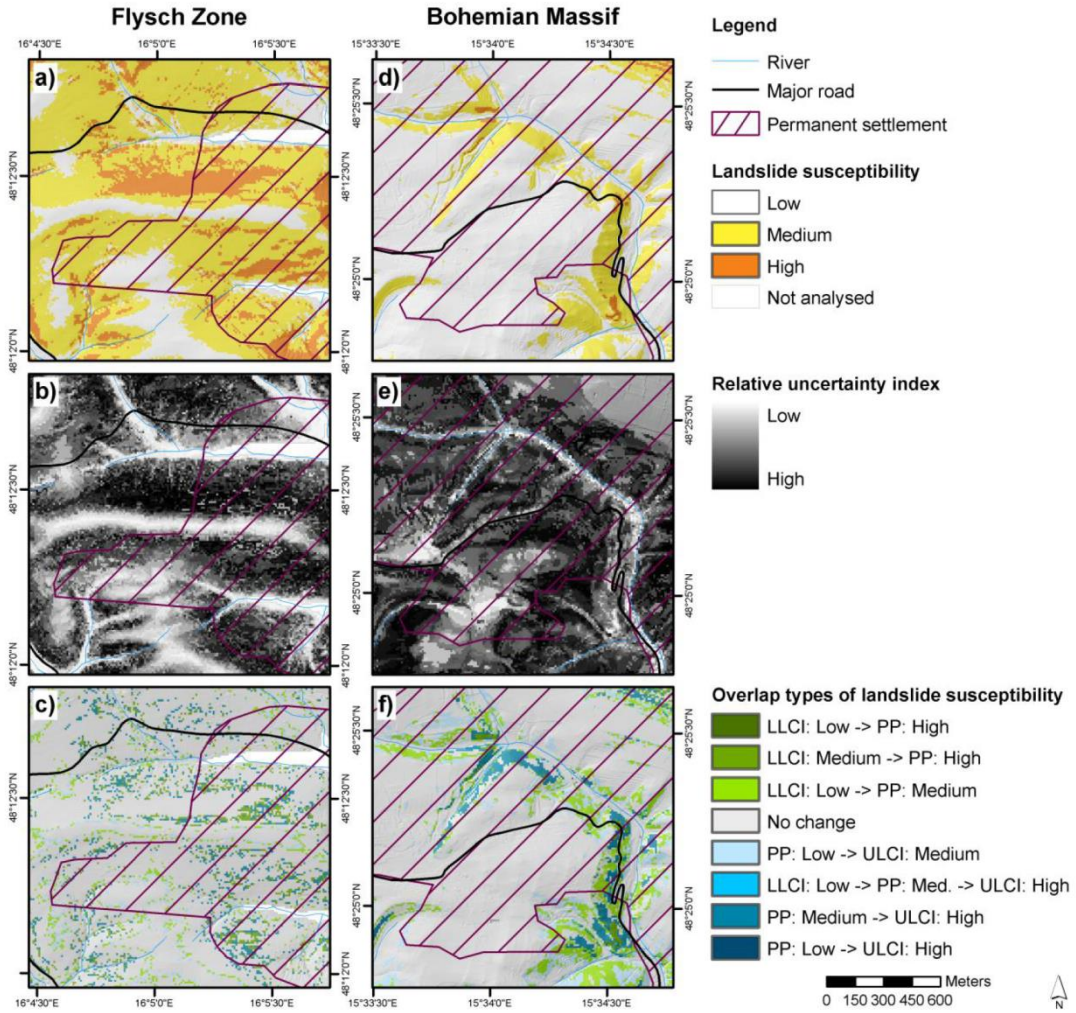

Fig. 8. Landslide susceptibility map (target scale 1 : 25 000) and map uncertainty in an example area. **(a)**, **(d)** Susceptibility map; **(b)**, **(e)** relative uncertainty index; **(c)**, **(f)** susceptibility class uncertainty. Panels **(a–c)** correspond to an area in the Flysch Zone (very high landslide density), **(d–f)** are in the Bohemian Massif (very low landslide density). The susceptibility class uncertainty refers to differences between susceptibility maps at the lower confidence limit (LLCI) or the upper confidence limit (ULCI) at the 95 % confidence level relative to the class in the predicted probability map (PP) in panels **(a)** and **(d)**. Data sources: LiDAR-DTM hillshade, river, major road and settlement – Provincial Government of Lower Austria.

present for other explanatory variables as well, as the geomorphic and geologic characteristics change (Lee et al., 2008). Facing this, our study design gives much more flexibility to represent the characteristics of the study area. Furthermore, it incorporates information on lithology by adjusting the odds of the prediction with the sampling rate of cells in each lithological unit.

However, one may argue that with this approach problems occur at the boundaries of the lithological units. Inaccuracies in the delineation of the lithological map of the area have effects on the model results as the landslides might be assigned incorrect lithological information. This may lead to an underestimation of effect sizes as data from different (true) lithological units would be mixed. Similar mixing effects may occur for quantitative predictor variables as well, for example as a function of positional accuracy for scale and resolution. In regression this effect is known as dilution, which may introduce a bias of estimated regression coefficients toward zero (Frost and Thompson, 2000). As this would also occur using the lithological map as a factor instead of as a mask for partitioning the study area, the boundary inaccuracies are not only a problem in the applied study design.

7.2.2 Spatial and non-spatial cross-validation

We assessed the model form uncertainty by deriving a model performance estimate and thematic consistency by spatial and non-spatial cross-validation. Cross-validation estimation of a model's predictive performance is a crucial step in predictive modelling because estimation on the training set is always too optimistic (Hosmer and Lemeshow, 2000; Brenning, 2005). Cross-validation results in bias-reduced performance estimates as the test partitions used in each repetition do not overlap with the training sample (Brenning, 2005). In particular spatial cross-validation is recommendable for spatial data, which may be subject to spatial autocorrelation (Brenning, 2005, 2012a).

The median AUROC values estimated by spatial and non-spatial cross-validation were generally similarly high in this study. However, the median AUROC values and the transferability index clearly showed that non-spatial cross-validation provided a more optimistic or even overoptimistic assessment of the model performance and transferability in contrast to spatial cross-validation. Therefore, spatial and temporal cross-validation should be preferred for performance estimation (Chung and Fabbri, 2008). While spatial performance and transferability do not necessarily reflect a model's predictive performance in the time domain, they provide a more realistic assessment of its ability to generalize from the available data than non-spatial approaches (Brenning, 2005).

The spatially and non-spatially least transferable models in this study were associated with domains that had the smallest sample sizes. The relationship of sample size on predictive abilities has also been shown in other spatial modelling studies (Stockwell and Peterson, 2002; Hjort and Marmion, 2008). However, we believe that the cases of high variation in AUROC values may be also related to the cross-validation sampling variation as indicated by the difference between T_{sp} and lower T_{nsp}, and possibly the proportion of stable and unstable terrain in a modelling domain.

Heterogeneity of landslide conditions (e.g. related to topography or land use) in the cross-validation samples is more likely to occur if samples are partitioned spatially, such as the case in spatial cross-validation. Here, similar characteristics of the explanatory variables in both training and test sample are assumed and necessary (Guzzetti et al., 2006). If this assumption is not met by the data (e.g. a rock type or land use class is missing in the test sample) the transfer of the fitted model to the test sample and the estimation of the model performance are difficult (or impossible) (Guzzetti et al., 2006). In our study some model domains might have high contrast between stable (e.g. large flat areas) and unstable (e.g. steep areas) terrain which gives potential for greater variation of sampled terrain conditions; it may be possible that in some samples one terrain condition is overrepresented relative to others. The sampling strategy may be improved further by masking low-lying flat areas that are not typically susceptible to landslides (Van den Eeckhaut et al., 2009; Goetz et al., 2011). Consequently, the sample may have more potential to capture the differentiating conditions of stable and unstable terrain in an area that is generally susceptible to landslides (e.g. steep hillslopes). This might lead to a smaller variation in the AUROC values.

The high importance of topographic variables in the susceptibility modelling goes along with findings in other studies (Guzzetti et al., 2006; Begueria, 2006b; Van Westen et al., 2008; Guns and Vanacker, 2012). However, it was rather surprising that the soil data on permeability and void space was not selected more often during the stepwise-variable selection. This might be related to the poor resolution of the soil data (50 m × 50 m) and to the usage of topographic data as a proxy for hydrological and soil characteristics (soil moisture and thickness). A strong correlation between the topographic wetness index and soil characteristics was found amongst others by Seibert et al. (2007). Furthermore, the higher resolution of the topographic variables might be of advantage for better describing the local conditions of landslide susceptibility.

Whereas a very strong thematic consistency was generally found for domains with a large sample size and sampling rate, domains with a small sample size and rate showed a high variability in the variable-selection frequencies which gave a weak thematic consistency. Therefore, the weak thematic consistency might also be associated with a poor spatial and non-spatial transferability, both originating from a small sample size and a small sampling rate. This relation was stronger for the spatial cross-validation, while the thematic consistency from non-spatial cross-validation was unrelated.

Generally, the usage of rather static data in the modelling was a necessity resulting from the available landslide inventory. However, this does not give the possibility to include dynamic data on triggers into the modelling or to design scenarios of future landslide susceptibility considering land cover or precipitation change. A clear source of model form uncertainty is the concept of uniformitarianism in modelling. This implies that the predisposing and triggering factors of landslides do not change in future. However, natural variability of landslide triggering mechanisms and also of the climate system might cause future changes. Currently, the influence of climate change on current or future landslide activity is debated. However, no clear evidence on these possible future changes was found in many regions (e.g. Crozier, 2010; Huggel et al., 2012). Additionally, it might be possible that the most important data set explaining the susceptibility might still be missing. This might happen although expert knowledge on geomorphology was applied in selecting geomorphologically relevant data. Moreover, it has to be stated that this type of susceptibility map was designed for the main scarps of landslides. A classified map might cover the possible runout of landslides but by definition does not show how the initiated landslides might move downslope and endanger further areas (Demoulin and Chung, 2007).

7.3 Quality of final susceptibility map – visualizing prediction uncertainties

This analysis of prediction uncertainty is an improvement of previous landslide susceptibility studies (Guzzetti et al., 2006; Van den Eeckhaut et al., 2009; Rossi et al., 2010, Sterlacchini et al., 2011), as it not only showed an uncertainty index of the predicted probability on a grid cell basis but additionally provided information on where the susceptibility class uncertainties were located. Some model uncertainties within this method arise from using the lookup table for transferring the prediction standard error to all grid cells as shown by the range of resulting R^2. This method might be improved or substituted by a function assigning the standard errors to all grid cells.

It was found that in the classified map the majority of grid cells did not change. However, there are differences between the modelling domains where some domains had larger overlaps of different susceptibility classes than others. Special attention should be given to the low susceptibility class. Here, the highest percentage of overlapping classes and underestimation of the susceptibility were detected.

The visualization of these spatially varying uncertainties is of special interest for future land use and development planning usually performed by non-landslide experts. In the aftermath of this study each landslide susceptibility class will be related to, not legally binding, recommendations for the designation of new building areas. Therefore, a misclassification (e.g. low instead of medium susceptibility) might lead to an interpretation by the municipality or landowner that underestimated landslide susceptibility. Knowledge about the susceptibility class overlaps might outline where more caution and detailed investigations are necessary. Additionally, it also shows where no uncertainties are expected, which might help to avoid costs for slope investigations.

There is a need to communicate the research results and their quality with appropriate explanations for the local officials, environmental managers and the public to raise awareness and knowledge about it, which leads to an easier understanding and incorporation of the results into the decision-making process (Knuepfer and Petersen, 2002; Rogers, 2006; Brierley, 2009; Hill et al., 2013). This analysis might aid good acceptance of the landslide susceptibility maps in the local governments, as instead of a fuzzy statement on involved uncertainties, these are clearly shown in a map on grid cell level (Guzzetti et al., 2006; Luoto et al., 2010). Furthermore, the preparation of the susceptibility maps showing the class overlaps contributes to an easier understanding of the possible effects of the prediction uncertainties.

The question if the policy-makers or stakeholders are really interested in knowing more about the uncertainty is discussed conversely. The study of Brugnach et al. (2006) pointed out that the confidence in modelling results is dependent on the way the uncertainties are addressed. Policy-makers were missing more information on the uncertainty of any model result. Therefore, the modelling results should be presented with a measure of uncertainty or confidence indicator (Brugnach et al., 2006). In habitat suitability modelling the visualization of uncertainty was identified as relevant to inform decision-makers about areas with extreme error, but also about areas which are particularly well modelled (Elith et al., 2002). This openly addresses the uncertainties involved in the maps instead of giving an impression of certainty (Elith et al., 2002). However, interviews of Klimeš and Blahůt (2012) showed that local governments do not want any information on uncertainties.

Nevertheless, the spatially verying prediction uncertainties might have severe consequences on buildings and their inhabitants if an event occurred within the uncertainties of the method used to delineate the hazard zones. The converse discussion shows that more or better communication with the stakeholders or policy-makers (also during the modelling process) is necessary to learn about uncertainties and enlarge confidence into the modelling (Brugnach et al., 2006). However, the way the uncertainties are presented to the stakeholder has to be adapted by the scientist to ensure the success of the communication. The visualization of some aspects of the quality of landslide susceptibility maps, such as the spatially varying prediction uncertainty, can enhance the communication among experts and decision-makers to facilitate informed decisions (Kunz et al., 2011).

Additionally, further aspects of considering and communicating the effects of epistemic uncertainty are still open research fields in susceptibility modelling. A clear assessment of these is necessary to evaluate on their consequences on the susceptibility (or hazard or risk) map.

7.4 Considerations on sample size

Summarizing the previously discussed findings some considerations on a minimum sample size might be possible. While the transferability index is less strongly related to sample size or sampling rate, the thematic consistency index shows a stronger relationship to them. Generally, larger sample sizes and sampling rates result in better thematic consistency and transferability of the model. Furthermore, the minimum standard error of the prediction was lower with larger sample size (Table 3).

The effect of a reduced sample size on the median and interquartile range AUROC values was assessed in the Flysch domain. We found that the median AUROC remained satisfactory high but decreased as sample size decreased, while the interquartile range of the AUROC increased. Even with the smallest sample size the model still achieved a good discrimination between landslide and non-landslide cells according to the median AUROC value. Summarizing the results, a minimum sample size with a sum of around 400 slide and non-slide cells might be recommended for the methods applied in this study. This size leads to an acceptable transferability and thematic consistency of the model in spatial

cross-validation in the analysed modelling domain. However, examples from successfully fitting a susceptibility model with smaller sample sizes (10 landslides with 15 cells each in an area of 177 km^2; Demoulin and Chung, 2007) give a very contrasting result. This shows that for small sample sizes other modelling methods (statistical or heuristic) might be more suitable. However, some difficulties arise in the modelling with small samples, which might create the need for a larger sample or for selecting a different method. The sample needs to be substantially complete to represent all local terrain conditions (Malamud, et al., 2004). However, increasing the sample size can only be done by enlarging the landslide inventory (e.g. by selecting a larger study area, mapping more landslides). This is challenging, as in some regions no additional data on landslides (or resources for mapping more landslides) might be available due to a general low susceptibility of the area or to missing data.

Giving a recommendation on a minimum sample size is challenging, as this study showed that the general trends found for sample size and sampling rate do not apply for all modelling domains. Therefore, we highlight that the resulting quality estimates (transferability index, consistency index and prediction uncertainty) might additionally be dependent on a combination of the domain size and the landslide density (landslides per km^2). Also, dependencies on local terrain conditions and their homogeneity in the modelling domain might exist. In this context the provision of the presented quality estimates is recommended, as these clearly show the quality of the results which might be lower compared to studies with larger sample sizes.

Moreover, the geomorphic plausibility of the susceptibility map has to be analysed. Previous studies found that high performance measures do not always guarantee high geomorphic plausibility of the map (Bell, 2007; Trigila et al., 2013). It might be possible that with a smaller sample size the geomorphic plausibility of the map is lower. However, the influence of a small sample size on the geomorphic plausibility of the susceptibility map is unclear. Nevertheless, analysing this was beyond the scope of this study.

8 Conclusions

The high quality of landslide susceptibility maps is defined by the low aleatory and epistemic uncertainties involved in the susceptibility modelling. This was analysed in terms of landslide susceptibility model performance and spatially varying prediction uncertainties of the final classified susceptibility map. The analysis gives an overview and some estimates on the epistemic and aleatory uncertainties involved in statistical susceptibility modelling. However, the effect of the propagation of all the single uncertainties on the final map and subsequently to hazard and risk maps has to be analysed further. Considering the present results in high model performance, analysis and visualization of prediction uncertainties, the applied model and resulting classified landslide susceptibility map are regarded to be of high quality.

The applied study design with modelling in the different domains provides a high flexibility for representing the characteristics of the heterogeneous study area. Opposed to single hold-out validation the repeated k-fold cross-validation provides a measure on the precision of the estimator and is independent of the one (random) test sample. The spatial cross-validation gave a more realistic assessment of the model performance and spatial transferability from the available data than non-spatial approaches. This aids as an estimate on the model form uncertainty, which is considered to be low.

A recommendation on an appropriate minimum sample size might be given considering the presented analysis in different modelling domains and the tests on reducing the sample size. According to the results, the larger the sample size the better is the transferability and thematic consistency. Therefore, also the quality of the statistical model form increases with sample size. However, not all modelling domains follow this trend. This might be related to a combined influence of the heterogeneity or homogeneity of the local terrain conditions, the size of the domain and its landslide density. A minimum sample size of around 400 slide and non-slide cells (200 each) might be recommended for the methods applied in this study.

Only rather static data on local terrain conditions could reasonably be included in the analysis given the landslide inventory, with no known landslide age. The stepwise variable selection resulted in a satisfactory thematic consistency. Among the geomorphologically relevant variables, topographic variables were selected with a higher frequency than soil variables. This might be related to the spatial resolution of the respective data. However, this result goes along with comparable studies having topographic variables as the most frequently selected variables. The final landslide susceptibility map gives a good representation of the landslide susceptibility based on topography although the map does not include possible landslide triggers.

Regarding the susceptibility class uncertainties we conclude that the majority of the study area is not affected by class uncertainties. Special attention has to be drawn to possible overlaps of the low and medium susceptibility class in the predicted probability map and the map of the upper confidence limit. A misclassification in the low class might result in an underestimation of the susceptibility. This might have adverse effects on the municipality or landowner if the recommendations for the assignment of building areas might not be restrictive enough.

We discussed that there is a need to assess, minimize and communicate uncertainties involved in susceptibility modelling. The analysis results need to be communicated in an understandable manner to the stakeholder to allow for informed decisions instead of giving an impression of certainty. A possible example was shown by the visualization of the

prediction uncertainty and its effects on the classified landslide susceptibility map.

Acknowledgements. This study was conducted within the research project MoNOE – Method development for landslide susceptibility maps for Lower Austria funded by the Provincial Government of Lower Austria. The data on the topography, soil and tectonic lines was provided by courtesy of the Provincial Government of Lower Austria and the geological data by the Geological Survey of Austria (GBA-2009–Zl.383/1-09). The authors are thankful for the support and provision of additional data (landslide archive, simplified geological map and land cover map) of the Geological Survey of Lower Austria and the Department of Spatial Planning and Regional Policy and of the project partners Austrian Institute of Technology and Joanneum Research. We are grateful for the comments of two anonymous referees who helped to substantially improve the quality of this manuscript.

Edited by: P. Reichenbach

References

Abteilung Feuerwehr und Zivilschutz, Amt der NÖ Landesregierung: Zusammenfassung Ereignisse 2009, available at: http://www.noe.gv.at/Land-Zukunft/Katastrophenschutz/Archiv/zusammenfassung_ereignisse_2009.wai.html, (last access: 9 December 2010), 2010 (in German).

Akaike, H.: A new look at the statistical model identification, IEEE T. Automat. Contr., 19, 716–723, 1974.

Ardizzone, F., Cardinali, M., Carrara, A., Guzzetti, F., and Reichenbach, P.: Impact of mapping errors on the reliability of landslide hazard maps, Nat. Hazards Earth Syst. Sci., 2, 3–14, doi:10.5194/nhess-2-3-2002, 2002.

Atkinson, P., Jiskoot, H., Massari, R. and Murray, T.: Generalized linear modelling in geomorphology, Earth Surf. Proc. Land., 23, 1185–1195, 1998.

Bathurst, J. C., Bovolo, C. I., and Cisneros, F.: Modelling the effect of forest cover on shallow landslides at the river basin scale, Ecol. Eng., 36, 317–327, doi:10.1016/j.ecoleng.2009.05.001, 2010.

Beguería, S.: Validation and Evaluation of Predictive Models in Hazard Assessment and Risk Management, Nat. Hazards, 37, 315–329, 2006a.

Beguería, S.: Changes in land cover and shallow landslide activity: A case study in the Spanish Pyrenees, Geomorphology, 74, 196–206, 2006b.

Bell, R.: Lokale und regionale Gefahren- und Risikoanalyse gravitativer Massenbewegungen an der Schwäbischen Alb, Rheinische Friedrich-Wilhelms-Universität Bonn, Bonn. available at: http://hss.ulb.uni-bonn.de/2007/1107/1107.pdf, (last access: 20 March 2012), 2007.

Bell, R., Petschko, H., Röhrs, M., and Dix, A.: Assessment of landslide age, landslide persistence and human impact using airborne laser scanning digital terrain models, Geogr. Ann. A, 94, 135–156, 2012.

Bell, R., Petschko, H., Proske, H., Leopold, P., Heiss, G., Bauer, C., Goetz, J. N., Granica, K., and Glade, T.: Methodenentwicklung zur Gefährdungsmodellierung von Massenbewegungen in Niederösterreich MoNOE – Vorläufiger Endbericht, Projektbericht, Universität Wien, Wien., 2013.

Beven, K. J. and Kirkby, M. J.: A physically based, variable contributing area model of basin hydrology, Hydrolog. Sci. Bullet., 24, 43–69, 1979.

Blahůt, J., van Westen, C. J., and Sterlacchini, S.: Analysis of landslide inventories for accurate prediction of debris-flow source areas, Geomorphology, 119, 36–51, doi:10.1016/j.geomorph.2010.02.017, 2010.

BMLFUW: Nachhaltig geschützt – Naturgefahrenmanagement im Unwetterjahr 2009, Jahresbericht, Bundesministerium für Land- und Forstwirtschaft, Umwelt und Wasserwirtschaft (Lebensministerium), Wien, available at: http://www.forstnet.at/article/articleview/82437/1/4932, (last access: 3 December 2010), 2010.

Boehner, J., Koethe, R., Conrad, O., Gross, J., Ringeler, A., and Selige, T.: Soil Regionalisation by Means of Terrain Analysis and Process Parameterisation, Research Report, European Soil Bureau, Luxembourg, 2002.

Brabb, E. E.: Innovative approaches to landslide hazard mapping, 4th International Symposium on Landslides, 16–21 September, Toronto, Canada, 307–324, 1984.

Brenning, A.: Spatial prediction models for landslide hazards: review, comparison and evaluation, Nat. Hazards Earth Syst. Sci., 5, 853–862, doi:10.5194/nhess-5-853-2005, 2005.

Brenning, A.: Statistical Geocomputing combining R and SAGA: The Example of Landslide susceptibility Analysis with generalized additive Models, SAGA – Seconds Out, 19, 23–32, 2008.

Brenning, A.: Benchmarking classifiers to optimally integrate terrain analysis and multispectral remote sensing in automatic rock glacier detection, Remote Sens. Environ., 113, 239–247, 2009.

Brenning, A.: RSAGA: SAGA Geoprocessing and Terrain Analysis in R, available at: http://CRAN.R-project.org/package$=$RSAGA, (last access: 22 January 2013), 2011.

Brenning, A.: Improved spatial analysis and prediction of landslide susceptibility: Practical recommendations, in Landslides and Engineered Slopes, Protecting Society through Improved Understanding, edited by: Eberhardt, E., Froese, C., Turner, A. K., and Leroueil, S., Taylor & Francis, Banff, Alberta, Canada., 789–795, 2012a.

Brenning, A.: Spatial cross-validation and bootstrap for the assessment of prediction rules in remote sensing: the R package "sperrorest", IEEE Int. Geosci. Remote Se., 23, 5372–5375, 2012b.

Brierley, G.: Communicating Geomorphology, J. of Geography in Higher Educ., 33, 3–17, 2009.

Brugnach, M., Tagg, A., Keil, F., and Lange, W. J.: Uncertainty Matters: Computer Models at the Science-Policy Interface, Water Resources Management, 21, 1075–1090, doi:10.1007/s11269-006-9099-y, 2006.

Carrara, A.: Uncertainty in evaluating landslide hazard and risk, in Prediction and Perception of Natural Hazards, 101–109, Kluwer Academic Publishers, the Netherlands, 1993.

Carrara, A., Cardinali, M., Guzzetti, F., and Reichenbach, P.: GIS technology in mapping landslide hazard, in Geographical Information Systems in Assessing Natural Hazards, edited by: Carrara, A. and Guzzetti, F., Kluwer Academic Publishers, the Netherlands, 135–175, 1995.

Carrara, A., Guzzetti, F., Cardinali, M., and Reichenbach, P.: Use of GIS technology in the prediction and monitoring of landslide hazard, Nat. Hazards, 20, 117–135, 1999.

Chung, C. J. F. and Fabbri, A. G.: Probabilistic prediction models for landslide hazard mapping, Photogramm. Eng. Rem. S., 65, 1389–1399, 1999.

Chung, C. J. F. and Fabbri, A. G.: Validation of spatial prediction models for landslide hazard mapping, Nat. Hazards, 30, 451–472, 2003.

Chung, C. J. and Fabbri, A. G.: Predicting landslides for risk analysis-Spatial models tested by a cross-validation technique, Geomorphology, 94, 438–452, 2008.

Conrad, O.: SAGA – Entwurf, Funktionsumfang und Anwendung eines Systems für Automatisierte Geowissenschaftliche Analysen, PhD thesis, University of Göttingen, Germany, available at: http://hdl.handle.net/11858/00-1735-0000-0006-B26C-6, (last access: 27 February 2013), 2007 (in German).

Crozier, M. J.: Landslides: causes, consequences and environment, Croom Helm, London, Sydney, Dover, New Hampshire, 1986.

Crozier, M. J.: Deciphering the effect of climate change on landslide activity: A review, Geomorphology, 124, 260–267, 2010.

Cruden, D. M. and Varnes, D. J.: Landslide types and processes, Landslides, Investigation and Mitigation, edited by: Turner, A. K. and Schuster, R. L., Transportation Research Board Special Report 247, Washington DC, USA, 36–75, 1996.

Dai, F. C., Lee, C. F., and Ngai, Y. Y.: Landslide risk assessment and management: an overview, Eng. Geol., 64, 65–87, 2002.

Damm, A., Eberhard, K., and Patt, A.: Risikowahrnehmung von Erdrutschen: Ergebnisse einer empirischen Untersuchung in der Südoststeiermark, Wegener Zentrum für Klima und Globalen Wandel, International Institute for Applied Systems Analysis (IIASA), Graz, Wien, 2010.

Demoulin, A. and Chung, C.-J. F.: Mapping landslide susceptibility from small datasets: A case study in the Pays de Herve (E Belgium), Geomorphology, 89, 391–404, 2007.

Dikau, R., Brunsden, D., Schrott, L., and Ibsen, M. L.: Landslide recognition: identification, movement, and causes, Wiley, Chichester, 1996.

Draper, D.: Assessment and Propagation of Model Uncertainty, J. R. Stat. Soc. B, 57, 45–97, 1995.

Eder, A., Sotier, B., Klebiner, K., Sturmlechner, R., Dorner, J., Markat, G., Schmid, G. and Strauss, P.: Hydrologische Bodenkenndaten der Böden Niederösterreichs (HydroBodNÖ) (Data on hydrological soil characteristics of soils in Lower Austria), unpublished final Report, Bundesamt für Wasserwirtschaft, Institut für Kulturtechnik und Bodenwasserhaushalt; Bundesforschungszentrum für Wald, Institut für Naturgefahren, Petzenkirchen, Innsbruck, 2011 (in German).

Egner, H. and Pott, A.: Risiko und Raum: Das Angebot einer Beobachtungstheorie, in Geographische Risikoforschung – Zur Konstruktion verräumlichter Risiken und Sicherheiten, edited by: Egner, H. and Pott, A., Franz Steiner Verlag, Stuttgart, 9–35, 2010 (in German).

Elith, J., Burgman, M. A., and Regan, H. M.: Mapping epistemic uncertainties and vague concepts in predictions of species distribution, Ecol. Model., 157, 313–329, 2002.

Fabbri, A. G., Chung, C. J. F., Cendrero, A., and Remondo, J.: Is prediction of future landslides possible with a GIS?, Nat. Hazards, 30, 487–503, 2003.

Fell, R., Corominas, J., Bonnard, C., Cascini, L., Leroi, E., and Savage, W. Z.: Guidelines for landslide susceptibility, hazard and risk zoning for land use planning, Eng. Geol., 102, 85–98, doi:10.1016/j.enggeo.2008.03.022, 2008.

Frattini, P., Crosta, G., and Carrara, A.: Techniques for evaluating the performance of landslide susceptibility models, Eng. Geol., 111, 62–72, 2010.

Freeman, G. T.: Calculating catchment area with divergent flow based on a regular grid, Comput. Geosci., 17, 413–422, 1991.

Frost, C. and Thompson, S.: Correcting for regression dilution bias: comparison of methods for a single predictor variable, J. R. Stat. Soc. Ser. A, 163, 173–190, 2000.

Glade, T.: Landslide occurrence as a response to land use change: a review of evidence from New Zealand, Catena, 51, 297–314, 2003.

Glade, T. and Crozier, M. J.: A review of Scale Dependency in Landslide Hazard and Risk Analysis, in Landslide Hazard and Risk, edited by: Glade, T., Anderson, M., and Crozier, M. J., John Wiley and Sons, Ltd, Chichester, England, 75–138, 2005.

Glade, T., Anderson, M. G. and Crozier, M. J.: Landslide Hazard and Risk, John Wiley and Sons, Ltd, Chichester, England, 2005.

Glade, T., Petschko, H., Bell, R., Bauer, C., Granica, K., Heiss, G., Leopold, P., Pomaroli, G., Proske, H., and Schweigl, J.: Landslide susceptibility maps for Lower Austria – Methods and Challenges, vol. 1, edited by: Koboltschnig, G., Hübl, J., and Braun, J., International Research Society INTERPRAEVENT, Grenoble, France, 497–508, 2012.

Goetz, J. N., Guthrie, R. H., and Brenning, A.: Integrating physical and empirical landslide susceptibility models using generalized additive models, Geomorphology, 129, 376–386, 2011.

Gottschling, P.: Massenbewegungen, in Geologie der Bundesländer – Niederösterreich, Geologische Bundesanstalt, Wien, 335–340, 2006 (in German).

Guisan, A., Edwards, T. C., and Hastie, T.: Generalized linear and generalized additive models in studies of species distributions: setting the scene, Ecol. Model., 157, 89–100, 2002.

Guns, M. and Vanacker, V.: Logistic regression applied to natural hazards: rare event logistic regression with replications, Nat. Hazards Earth Syst. Sci., 12, 1937–1947, doi:10.5194/nhess-12-1937-2012, 2012.

Guzzetti, F.: Landslide hazard and risk assessment, Dissertation, Rheinischen Friedrich-Wilhelms-Universität Bonn, Bonn, November, 2005.

Guzzetti, F., Carrara, A., Cardinali, M., and Reichenbach, P.: Landslide hazard evaluation: a review of current techniques and their application in a multi-scale study, Central Italy, Geomorphology, 31, 181–216, 1999.

Guzzetti, F., Cardinali, M., Reichenbach, P., and Carrara, A.: Comparing Landslide Maps: A Case Study in the Upper Tiber River Basin, Central Italy, Environ. Manage., 25, 247–263, 2000.

Guzzetti, F., Reichenbach, P., Ardizzone, F., Cardinali, M., and Galli, M.: Estimating the quality of landslide susceptibility models, Geomorphology, 81, 166–184, 2006.

Hand, D.: Construction and Assessment of Classification Rules, Wiley, West Sussex, 1997.

Hanley, J. A. and McNeil, B. J.: The meaning and use of the area under a receiver operating characteristic (ROC) curve, Radiology, 143, 29–36, 1982.

Harp, E. L., Castañeda, M. R., and Held, M. D.: Landslides triggered by Hurricane Mitch in Tegucigalpa, Honduras., US Geological Survey Open-File Report, USGS, 2002.

Hastie, T.: gam: Generalized Additive Models, available at: http://CRAN.R-project.org/package$=$gam, (last access: 27 February 2013), 2011.

Hastie, T. and Tibshirani, R.: Generalized additive models, Chapman and Hall/CRC, London, 1990.

Heckmann, T., Gegg, K., Gegg, A., and Becht, M.: Sample size matters: investigating the effect of sample size on a logistic regression debris flow susceptibility model, Nat. Hazards Earth Syst. Sci. Discuss., 1, 2731–2779, doi:10.5194/nhessd-1-2731-2013, 2013.

Helton, J. C., Johnson, J. D., Oberkampf, W. L., and Sallaberry, C. J.: Representation of analysis results involving aleatory and epistemic uncertainty, Int. J. Gen. Syst., 39, 605–646, 2010.

Hervás, J.: Lessons Learnt from Landslide Disasters in Europe, European Commission Joint Research Centre, Institute for Environment and Sustainability, Ispra (VA), Italy, 2003.

Hill, L. J., Sparks, R. S. J. and Rougier, J. C.: Risk assessment and uncertainty in natural hazards, in Risk and uncertainty assessment for natural hazards, edited by: Rougier, J. C., Sparks, R. S. J., and Hill, L. J., 1–18, Cambridge University Press, Cambridge, 2013.

Hjort, J. and Marmion, M.: Effects of sample size on the accuracy of geomorphological models, Geomorphology, 102, 341–350, 2008.

Hoffman, F. O. and Hammonds, J. S.: Propagation of uncertainty in risk assessments: the need to distinguish between uncertainty due to lack of knowledge and uncertainty due to variability, Risk Analysis, 14, 707–712, 1994.

Hora, S. C.: Aleatory and epistemic uncertainty in probability elicitation with an example from hazardous waste management, Reliability Engineering and System Safety, 54, 217–223, 1996.

Hornich, R. and Adelwöhrer, R.: Landslides in Styria in 2009/Hangrutschungsereignisse 2009 in der Steiermark, Geomechanics and Tunnelling, 3, 455–461, 2010 (in German).

Hosmer, D. W. and Lemeshow, S.: Applied logistic regression, Wiley, New York, NY, 2000.

Huggel, C., Clague, J. J., and Korup, O.: Is climate change responsible for changing landslide activity in high mountains?, Earth Surf. Process. Landforms, 37, 77–91, 2012.

Hydrographischer Dienst des Landes Niederösterreich: Wasserstandsnachrichten und Hochwasserprognosen Niederösterreich, available at: http://www.noel.gv.at/Externeseiten/wasserstand/wiskiwebpublic/maps_N_0.htm?entryparakey$=$N, (last access: 2 March 2011), 2011 (in German).

Jia, G., Tian, Y., Liu, Y., and Zhang, Y.: A static and dynamic factors-coupled forecasting model of regional rainfall-induced landslides: A case study of Shenzhen, Sci. China Ser. E, 51, 164–175, 2008.

Karam, K. S.: Landslide hazards assessment and uncertainties, PhD Thesis, Massachusetts Institute of Technology, 2005.

Klimeš, J. and Blahůt, J.: Landslide risk analysis and its application in regional planning: an example from the highlands of the Outer Western Carpathians, Czech Republic, Nat. Hazards, 64, 1779–1803, 2012.

Knuepfer, P. L. and Petersen, J. F.: Geomorphology in the public eye: policy issues, education, and the public, Geomorphology, 47, 95–105, 2002.

Kohavi, R.: A study of cross-validation and bootstrap for accuracy estimation and model selection, 14, 1137–1145, 1995.

Kunz, M., Grêt-Regamey, A., and Hurni, L.: Visualization of uncertainty in natural hazards assessments using an interactive cartographic information system, Nat. Hazards, 59, 1735–1751, 2011.

Kurz, W.: Erstellung einer digitalen, strukturgeologischen, tektonischen Karte von Niederösterreich (Endbericht), unpublished final report, Karl-Franzens-University Graz, Graz, 2012 (in German).

Lee, C.-T., Huang, C.-C., Lee, J.-F., Pan, K.-L., Lin, M.-L., and Dong, J.-J.: Statistical approach to earthquake-induced landslide susceptibility, Eng. Geol., 100, 43–58, 2008.

Lettner, C. and Wrbka, T.: Historical Development of the Cultural Landscape at the Northern Border of the Eastern Alps: General Trends and Regional Peculiarities, edited by: Balázs, P. and Konkoly-Gyuró, E., 109–121, University of West Hungary Press, Sopron, Hungary, 2011.

Luoto, M., Marmion, M., and Hjort, J.: Assessing spatial uncertainty in predictive geomorphological mapping: A multi-modelling approach, Comput. & Geosci., 36, 355–361, 2010.

Malamud, B. D., Turcotte, D. L., Guzzetti, F., and Reichenbach, P.: Landslide inventories and their statistical properties, Earth Surf. Proc. Land., 29, 687–711, 2004.

Marjanović, M., Kovačević, M., Bajat, B. and Voženílek, V.: Landslide susceptibility assessment using SVM machine learning algorithm, Eng. Geol., 123, 225–234, 2011.

McCalpin, J.: Preliminary age classification of landslides for inventory mapping, In: Proceedings 21st annual Enginnering Geology and Soils Engineering Symposium, 5–6 April, University of Idaho, Moscow, 99–111, 1984.

Mosleh, A.: Hidden sources of uncertainty: judgment in the collection and analysis of data, Nucl. Eng. Des., 93, 187–198, 1986.

Muenchow, J., Brenning, A., and Richter M.: Geomorphic process rates of landslides along a humidity gradient in the tropical Andes, Geomorphology, 139, 271–284, 2012.

Nefeslioglu, H. A., Gokceoglu, C., and Sonmez, H.: An assessment on the use of logistic regression and artificial neural networks with different sampling strategies for the preparation of landslide susceptibility maps, Eng. Geol., 97, 171–191, 2008.

Neuhäuser, B. and Terhorst, B.: Landslide susceptibility assessment using "weights-of-evidence" applied to a study area at the Jurassic escarpment (SW-Germany), Geomorphology, 86, 12–24, 2007.

Oberkampf, W. L., Helton, J. C., Joslyn, C. A., Wojtkiewicz, S. F., and Ferson, S.: Challenge problems: uncertainty in system response given uncertain parameters, Reliability Engineering & System Safety, 85, 11–19, doi:10.1016/j.ress.2004.03.002, 2004.

Orme, A. R.: Shifting paradigms in geomorphology: the fate of research ideas in an educational context, Geomorphology, 47, 325–342, 2002.

Park, N.-W. and Chi, K.-H.: Quantitative assessment of landslide susceptibility using high-resolution remote sensing data and a generalized additive model, Int. J. Remote Sens., 29, 247–264, 2008.

Petschko, H., Glade, T., Bell, R., Schweigl, J. and Pomaroli, G.: Landslide inventories for regional early warning systems, in: Proceedings of the International Conference Mountain Risks: Bringing Science to Society', Firenze, 24–26 November 2010, edited by: Malet, J. P., Glade, T., and Casagli, N., CERG Editions, Strasbourg, 277–282, 2010.

Petschko, H., Bell, R., Brenning, A., and Glade, T.: Landslide susceptibility modeling with generalized additive models – fac-

ing the heterogeneity of large regions, in: Landslides and Engineered Slopes, Protecting Society through Improved Understanding, Vol. 1, edited by: Eberhardt, E., Froese, C., Turner, A. K., and Leroueil, S., Taylor & Francis, Banff, Alberta, Canada, 769–777, 2012.

Petschko, H., Bell, R., Glade, T., Leopold, P., and Heiss, G.: Landslide inventories for large regions – mapping effectiveness of visually analyzing LiDAR derivatives, in prep., 2013a.

Petschko, H., Bell, R., and Glade, T.: Relative age estimation at landslide mapping on LiDAR derivatives – revealing the applicability of land cover data in statistical susceptibility modelling, Proceedings of the World Landslide Forum 3, 2–6 June 2014, Beijing, submitted, 2013b.

Petschko, H., Bell, R., Leopold, P., Heiss, G., and Glade, T.: Landslide inventories for reliable susceptibility maps in Lower Austria, in: Landslide Science and Practice. Volume 1: Landslide Inventory and Susceptibility and Hazard Zoning, edited by: Margottini C, Canuti P, Sassa K, Springer, 281–286, 2013c.

Pradhan, B.: A comparative study on the predictive ability of the decision tree, support vector machine and neuro-fuzzy models in landslide susceptibility mapping using GIS, Computers & Geosciences, 51, 350–365, 2013.

Pradhan, B. and Lee, S.: Landslide risk analysis using artificial neural network model focusing on different training sites, Int. J. Phy. Sci., 4, 1–15, 2009.

Quinn, P. F., Beven, K. J., Chevallier, P., and Planchon, O.: The prediction of hillslope flow paths for distributed hydrological modelling using digital terrain models, Hydrol. Process., 5, 59–79, 1991.

R Development Core Team: R: A Language and Environment for Statistical Computing, R Foundation for Statistical Computing, Vienna, Austria. available at: http://www.R-project.org, (last access: 27 February 2013), 2011.

Razak, K. A., Straatsma, M. W., Van Westen, C. J., Malet, J.-P., and De Jong, S. M.: Airborne laser scanning of forested landslides characterization: Terrain model quality and visualization, Geomorphology, 126, 186–200, 2011.

Remondo, J., González, A., De Terán, J. R. D., Cendrero, A., Fabbri, A., and Chung, C. J. F.: Validation of landslide susceptibility maps; examples and applications from a case study in Northern Spain, Nat. Hazards, 30, 437–449, 2003.

Rogers, K. H.: The real river management challenge: integrating scientists, stakeholders and service agencies, River Res. Appl., 22, 269–280, 2006.

Rossi, M., Guzzetti, F., Reichenbach, P., Mondini, A. C., and Peruccacci, S.: Optimal landslide susceptibility zonation based on multiple forecasts, Geomorphology, 114, 129–142, 2010.

Rougier, J. C.: Quantifying hazard losses, in Risk and uncertainty assessment for natural hazards, edited by: Rougier, J. C.,Sparks, R. S. J. , and Hill, L. J., 19–39, Cambridge University Press, Cambridge., 2013.

Rougier, J. C. and Beven, K. J.: Model and data limitations: the sources and implications of epistemic uncertainty, in Risk and uncertainty assessment for natural hazards, edited by: Rougier, J. C., Sparks, R. S. J., and Hill, L. J., 19–39, Cambridge University Press, Cambridge., 2013.

Roy, C. J. and Oberkampf, W. L.: A comprehensive framework for verification, validation, and uncertainty quantification in scientific computing, Comput. Methods Appl. M., 200, 2131–2144, 2011.

Ruß, G. and Brenning, A.: Data mining in precision agriculture: management of spatial information, Lect. Notes in Comput. Sci., 6178, 350–359, 2010.

Schicker, R. and Moon, V.: Comparison of bivariate and multivariate statistical approaches in landslide susceptibility mapping at a regional scale, Geomorphology, 161–162, 40–57, 2012.

Schnabel, W.: Die geologischen Ursachen der Schäden an der II. Wiener Hochquellenleitung bei Scheibbs, in: Festschrift der MA 31: 75 Jahre II. Wiener Hochquellenleitung, edited by: Magistrat der Stadt Wien, MA 31-Wasserwerke, Wien, 1985 (in German).

Schnabel, W.: Geologische Karte von Niederösterreich 1 : 200 000, Geologische Bundesanstalt, Wien, Austria, 2002 (in German).

Schwab, J. C., Gori, P. L., and Jeer, S.: Landslide Hazards and Planning, Planning Advisory Service Report, American Planning Association, Chicago, 2005.

Schwarz, L. and Tilch, N.: Möglichkeiten und Limitierungen der Regionalisierung mittels Neuronaler Netze am Beispiel einer Rutschungsanfälligkeitskarte für die Region Gasen-Haslau, Beiträge zum 20. AGIT-Symposium, Angewandte Geoinformatik, 2–4 July 2008, Salzburg, Austria, 643–648, 2008 (in German).

Schweigl, J. and Hervás, J.: Landslide Mapping in Austria, JRC Scientific and Technical Reports, European Commission Joint Research Centre, Institute for Environment and Sustainability, Italy, available at: http://eusoils.jrc.ec.europa.eu/ESDB_Archive/eusoils_docs/other/EUR23785EN.pdf, (last access: 1 March 2011), 2009.

Schwenk, H.: Massenbewegungen in Niederösterreich 1953–1990, in: Jahrbuch der Geologischen Bundesanstalt, Geologische Bundesanstalt, Wien, 135, 597–660, 1992 (in German).

Scott, A. J. and Wild, C. J.: Fitting logistic models under case-control or choice based sampling, J. Roy. Stat. Soc. B, 48, 170–182, 1986.

Seibert, J., Stendahl, J., and Sørensen, R.: Topographical influences on soil properties in boreal forests, Geoderma, 141, 139–148, 2007.

Soeters, R. and Van Westen, C. J.: Slope instability recognition, analysis and zonation., in Landslides, Investigation and Mitigation, edited by: Turner, A. K. and Schuster, R. L., 129–177, National Academy Press, Washington, USA, 1996.

Spiegelhalter, D. J. and Riesch, H.: Don't know, can't know: embracing deeper uncertainties when analysing risks, Philosophical Transactions of the Royal Society A: Mathematical, Physical and Engineering Sciences, 369, 4730–4750, 2011.

Sterlacchini, S., Ballabio, C., Blahůt, J., Masetti, M., and Sorichetta, A.: Spatial agreement of predicted patterns in landslide susceptibility maps, Geomorphology, 125, 51–61, 2011.

Stockwell, D. R. and Peterson, A. T.: Effects of sample size on accuracy of species distribution models, Ecol. Model., 148, 1–13, 2002.

Tarolli, P., Borga, M., Chang, K.-T., and Chiang, S.-H.: Modeling shallow landsliding susceptibility by incorporating heavy rainfall statistical properties, Geomorphology, 133, 199–211, 2011.

Townsend Peterson, A., Papeş, M., and Eaton, M.: Transferability and model evaluation in ecological niche modeling: a comparison of GARP and Maxent, Ecography, 30, 550–560, 2007.

Trigila, A., Frattini, P., Casagli, N., Catani, F., Crosta, G., Esposito, C., Iadanza, C., Lagomarsino, D., Mugnozza, G., Segoni, S., Spizzichino, D., Tofani, V., and Lari, S.: Landslide Susceptibility Mapping at National Scale: The Italian Case Study, in Landslide Science and Practice, edited by: Margottini, C., Canuti, P., and Sassa, K., 287–295, Springer Berlin Heidelberg, 2013.

Van den Eeckhaut, M., Vanwalleghem, T., Poesen, J., Govers, G., Verstraeten, G., and Vandekerckhove, L.: Prediction of landslide susceptibility using rare events logistic regression: a case-study in the Flemish Ardennes (Belgium), Geomorphology, 76, 392–410, 2006.

Van den Eeckhaut, M., Poesen, J., Verstraeten, G., Vanacker, V., Nyssen, J., Moeyersons, J., Van Beek, L. P. H., and Vandekerckhove, L.: Use of LIDAR-derived images for mapping old landslides under forest, Earth Surf. Proc. Land., 32, 754–769, 2007.

Van den Eeckhaut, M., Moeyersons, J., Nyssen, J., Abraha, A., Poesen, J., Haile, M., and Deckers, J.: Spatial patterns of old, deep-seated landslides: A case-study in the northern Ethiopian highlands, Geomorphology, 105, 239–252, 2009.

Van Westen, C. J., Rengers, N., Terlien, M. T. J., and Soeters, R.: Prediction of the occurrence of slope instability phenomena through GIS-based hazard zonation, Geologische Rundschau, 86, 404–414, 1997.

Van Westen, C. J., Asch, T. W. J., and Soeters, R.: Landslide hazard and risk zonation—why is it still so difficult?, B. Eng. Geol. Environ., 65, 167–184, 2005.

Van Westen, C. J., Castellanos, E., and Kuriakose, S. L.: Spatial data for landslide susceptibility, hazard, and vulnerability assessment: An overview, Eng. Geol., 102, 112–131, 2008.

Varnes, D. J.: Landslilde hazard zonation: a review of principles and practice, United Nations Educational, Scientific and Cultural Organization, Paris, France, 1984.

Von Ruette, J., Papritz, A., Lehmann, P., Rickli, C., and Or, D.: Spatial statistical modeling of shallow landslides – Validating predictions for different landslide inventories and rainfall events, Geomorphology, 133, 11–22, 2011.

Vorpahl, P., Elsenbeer, H., Märker, M., and Schröder, B.: How can statistical models help to determine driving factors of landslides?, Ecol. Model., 239, 27–39, 2012.

Wessely, G.: Geologie der österreichischen Bundesländer – Niederösterreich, Geologische Bundesanstalt, Wien, 2006 (in German).

Zevenbergen, L. W. and Thornes, J. B.: Quantitative analysis of land surface topography, Earth Surf. Proc. Land., 12, 47–56, 1987.

A.7. Landslide inventory mapping for large regions – effectiveness of visually analyzing LiDAR DTM derivatives (subm.)

Petschko, H., Bell, R. & T., Glade (2014), Landslide inventory mapping for large regions – effectiveness of visually analyzing LiDAR DTM derivatives, Landslides, Springer.

Submitted Manuscript:

Landslide inventory mapping for large regions – effectiveness of visually analyzing LiDAR DTM derivatives

Petschko, H., Bell, R., Glade, T.

University of Vienna, Department of Geography and Regional Research, Universitätsstrasse 7, 1010 Vienna, helene.petschko@univie.ac.at, +431427748628

Abstract (max. 250 words)

Landslide inventories are the most important data source for landslide process, susceptibility, hazard and risk analysis. Not only the modelling or the analysis of the process benefits from a highly accurate, precise and informative inventory, but also the model performance assessment profits from a good quality inventory. The objective of this study was to identify an effective method for mapping a landslide inventory for a large study area (19,186 km²). This inventory should in particular be optimized for statistical susceptibility modelling to derive a classified landslide susceptibility map with a high quality. Therefore, we mapped landslides representatively as polygons but also substantially complete with a point in the main scarp only and developed a method to automatically derive the main scarp form the landslide polygon within GIS. The effectiveness of the mapping methods was estimated semi-quantitatively taking into account the requirements on an inventory given by the analysis type (e.g. statistical susceptibility modelling, hazard or risk analysis).

The resulting landslide inventories outline the heterogeneity of the study area regarding the landslide susceptibility but also the occurring landslide processes. The obtained effectiveness estimate demonstrates that none of our mapped inventories is perfect for the assessed analysis

types. However, opposed to mapping polygons, mapping the points in the main scarp is most effective for statistical susceptibility modelling within large study areas.

The advantages, drawbacks and effectiveness of landslide mapping on the basis of LiDAR DTM derivatives compared to other imagery were discussed. We conclude that mapping landslide points visually interpreting LiDAR DTM derivatives is of high effectiveness considering its application in statistical susceptibility modelling deriving a classified susceptibility map for large regions.

Keywords: visual analysis, landslide inventory, mapping effectiveness, LiDAR digital terrain model, statistical susceptibility modeling

1. Introduction

Landslide inventories are a very important source to better understand landslide processes, their activity, magnitude and frequency, predisposing and preparatory factors, landslide susceptibility, and also contribute to related vulnerability and risk analysis (Soeters and Van Westen 1996; Fell et al. 2008; Ghosh et al. 2012). Furthermore, landslide inventories are required to evaluate the success and predictive power of any modeling approach (heuristic, deterministic or statistic as summarized by Soeters and Van Westen (1996)) used to model landslide susceptibility or hazard (Chung and Fabbri 2003; Beguería 2006).

Therefore, the availability of landslide inventories is of high importance independently from the specific modeling approach used or the size of the study area. Moreover, the quality of the landslide inventory regarding complete or substantially complete spatial and temporal information on landslide occurrence in the past (Malamud et al. 2004), amount of stored information (e.g. date of occurrence, trigger, caused damage), positional accuracy of the mapped landslide and correctness in the assigned landslide type/age/extent is decisive for its usability (Soeters and Van Westen 1996; Ardizzone et al. 2002; Glade et al. 2005; Galli et al. 2008; van Westen et al. 2008; Guzzetti et al. 2012; Petschko et al. 2014b).

Amongst all characteristics of an inventory the positional accuracy of single landslides is probably the most important and also the minimum requirement (Aleotti and Chowdhury 1999; Fell et al. 2008; Malamud et al. 2004). Mistakes in the location of the landslide can lead to wrong results in the susceptibility modeling or at the evaluation of the model performance (Malamud et al. 2004; van Westen et al. 2008). This may have significant consequences, e.g. if these maps are applied within land use development plans or zonings.

However, fulfilling all the quality characteristics of an inventory is a challenging task, given the subjectivity involved in the mapping and the limitations associated with the available data source (e.g. archive, aerial photograph, satellite imagery, LiDAR), the mapping technique (mapping in the field, digitizing analogue or digital data sources, or (semi-) automated mapping) and human activity influencing the visibility of landslides (Cardinali et al. 2000; Ardizzone et al. 2002; van Westen et al. 2008; Fiorucci et al. 2011; Bell et al. 2012). All these challenges increase working on

large study areas, such as Lower Austria (19,186 km²), on a small to medium scale (1:25,000; Fell et al., 2008), as the available resources (time, people, funds) for mapping landslides are usually restricted (Van Westen et al. 1997).

Landslide inventory mapping methods are manifold and refine permanently with new technologies and aperture in combination with a wide availability of geographical information system (GIS) software (Guzzetti et al. 2012). All methods share the need of identifying discernible features remaining after landslide occurrence either visually or by (semi-) automated techniques and are specifically addressed since approximately three decades (e.g. Carrara and Merenda 1976; McCalpin 1984; Wieczorek 1984; Guzzetti 2005).

An overview on traditional but also recent developments and techniques in landslide inventory mapping is given by Van Westen et al. (2008) and Guzzetti et al. (2012). Traditional methods of landslide inventory mapping include geomorphological field mapping (Carrara and Merenda 1976; Brunsden 1985; Brunsden 1993; Zezere et al. 1999; Brardinoni et al. 2003), evaluation of historical archives (Schwenk 1992; Ibsen and Brunsden 1996; CNR-IRPI-Turin 1998; Glade et al. 2001; Rossi et al. 2010; Röhrs and Dix 2010; Pereira et al. 2014) and landslide identification and mapping on the basis of stereoscopic interpretation of aerial photographs (Mantovani et al. 1996; Carrara et al. 2003; Van Westen and Lulie Getahun 2003; Duman et al. 2005; Zanutta et al. 2006).

Recent improvements in aperture and imagery production introduce more effectiveness in reconnaissance as well as desktop mapping of landslides, making it easier to map landslides with higher precision in large areas (van Westen et al. 2008; Guzzetti et al. 2012). These include GPS equipped binoculars (Santangelo et al. 2010) and high resolution remote sensing imagery such as (stereoscopic) optical satellite imagery (e.g. Fiorucci et al. 2011; Ardizzone et al. 2013), imagery derived from airborne or terrestrial SAR (synthetic aperture radar; e.g. Colesanti and Wasowski 2006; Herrera et al. 2010; Cigna et al. 2012) and airborne or terrestrial laser scanning data (e.g. Schulz 2004; Jaboyedoff et al. 2010). Examples for recent developments in landslide mapping and semi-automated detection on the basis of high resolution satellite data were presented amongst others by Whitworth et al. (2005), Barlow et al. (2006), Fiorucci et al. (2011), Harp et al. (2011), Mondini et al. (2011). Object-oriented approaches revealing landslides by the combined analysis of DTM and optical satellite data were amongst others presented by Martha et al. (2010) and Martha et al. (2012).

Mapping on derivatives of airborne laser scanning data allows insights underneath the forest cover (e.g. Chigira et al. 2004; Schulz 2004; Haneberg et al. 2005; Glenn et al. 2006; Bell 2007; Van Den Eeckhaut et al. 2007; Anders and Seijmonsbergen 2008), which is beneficiary mapping a historical landslide inventory storing all (visible) landslides occurred in the past. The inventory reaches a new level of spatial coverage paired with high precision in the positioning accuracy of the landslide feature despite the fact, that the age of occurrence is unknown (Petschko et al. 2010).

More advanced methods based on the usage of derivatives from digital terrain models (DTMs) of airborne laser scanning data (LiDAR data) deal with the semi-automated detection of landslides (e.g. van Asselen and Seijmonsbergen 2006; McKenna et al. 2008; Dalyot et al. 2008; Booth et al. 2009; Tarolli et al. 2010). Furthermore, an object-oriented approach was applied to identify landslides under forest (Van Den Eeckhaut et al. 2012).

Our objective is assessing and comparing the effectiveness of landslide inventory mapping visually analyzing airborne LiDAR DTM derivatives using polygon or point features. We define mapping effectiveness as an estimate comparing the time per person needed for mapping a specific number of landslides (and their attributes) with the highest possible quality in a given area, with the planned usage (analysis type) of the resulting inventory. In other words effectiveness takes into account a cost benefit ratio between having as much information on single landslides as possible and necessary for amongst other analysis types statistical landslide susceptibility modeling with grid cells as terrain unit (e.g. on the location, extent, area, relative age) using as few resources as manageable.

In this study we focused on the requirements on a landslide inventory used in statistical landslide susceptibility modeling creating a landslide susceptibility map with a scale of 1:25,000 with three classes used for land use planning strategies (Petschko et al. 2013; Petschko et al. 2014b). This assessment and comparison aims to identify an effective method for landslide mapping (points or polygons) in the entire province Lower Austria, providing a substantially complete historical inventory. Our study areas in Lower Austria were the districts Amstetten, Baden and Waidhofen/Ybbs. We focused on sliding processes according to Cruden and Varnes (1996), therefore rock fall and debris flow processes were not considered.

2. Materials

The LiDAR DTM was available with a spatial resolution of 1 m x 1 m. Within the test districts it was generated from data of airborne laser scanner flight campaigns between 2006 and 2009 (Amt der NÖ Landesregierung 2013). Four different LiDAR platforms were used, as the flight campaigns were operated by different companies and in different years: Riegl LMS-Q560 (Riegl 2010), ALTM 3100 (Optech 2008a), ALTM Gemini (Optech 2008b) and Leica ALS50 (Leica Geosystems 2003; Amt der NÖ Landesregierung 2013).

The within ArcGIS 9.3 computed derivatives from the LiDAR DTM were hillshade maps calculated with different azimuth angles (315°, 135°, 45°), a slope map displayed in inverted greyscale and contour lines with a spacing of 4 m (Petschko et al. 2013; Figure 1). Furthermore, orthophotos with a spatial resolution of 25 cm and 12.5 cm taken in the periods between 2000-2004 and 2007-2008 respectively were available in the test districts (Amt der NÖ Landesregierung 2013).

The information on lithology was derived from the geological map of Lower Austria at the scale 1:200,000 (Schnabel 2002).

3. Methods

The need for mapping a new landslide inventory for Lower Austria was pointed out in a previous study visually comparing existing landslide inventories with the newly available opportunity to positional accuracy given by the LiDAR data (Petschko et al. 2010). Furthermore, an assembly of all existing inventories showed areas with different landslide density which can be attributed to the reporting activity of municipalities and to the focus of the geologist mapping in the area (Schwenk

1992; Kociu et al. 2007). While traditionally landslides were mapped on topographic maps (1:50,000), a new level of positioning precision of the landslide mapping can be reached with recently available high resolution data (orthophotos, LiDAR DTM; Petschko et al. 2010). This allows the production of a landslide inventory suitable for the aimed output scale of the susceptibility map (1:25,000).

Whereas the following sections describe the methods of mapping polygons and points in more detail, we first present the similarities of the methods. Both methods (mapping polygons or points) were based on the mapping on remote sensing imagery (LiDAR derivatives and orthophotos; Figure 2). The mapping method in both applications was to visually interpret the imagery regarding discernible (morphological) features remaining after landslide occurrence (Carrara and Merenda 1976; McCalpin 1984; Wieczorek 1984; Schulz 2004; Guzzetti 2005). At sliding processes these features include: a steep concave main scarp, possibly also concave minor scarps or cracks, a landslide toe characterized by a steep convex form, irregular hummocky morphology sometimes with ridges across the slide direction and longitudinal cracks in the toe area (Varnes 1984). At minimum a transition from a concave main scarp to a convex toe must be visible to consider the form being a slide (Guzzetti 2005). This might be recognized by a distinct change of the slope angle or of a river course due to landslide deposits (Cardinali et al. 2000).

Additional signs for landslide occurrence are abrupt vegetation changes from dense vegetation cover (forest, brushes or grassland) to no cover (McCalpin 1984). This is best visible for recent landslides on corresponding orthophotos, as on old landslides the vegetation might be regrown. Also, the forests and brushes were filtered and erased in the LiDAR DTM.

The landslide mapping should always be done at a larger scale than the susceptibility or hazard zoning maps to provide a thorough inventory (Cascini 2008). Given the aimed scale of the susceptibility map and the detail of the LiDAR DTM, hillshade maps and orthophotos were screened for landslide morphology on a scale of 1:2,000. However, the mapping (and digitizing) of the landslides was done at any larger scale necessary (1:200 – 1:2,000) to ensure a smooth and correct delineation of the landslide polygons and accurate and precise positioning of the landslide points.

Both methods include the mapping of easy discernible landslides with usually rather fresh looking morphology only. Considering easy detectable landslides only, accelerates the mapping process, as the decision on the delineation or placing a point is done faster. Furthermore, it reduces uncertainties introduced by erroneous delineation of the landslides without clear boundaries (Malamud et al. 2004; Van Den Eeckhaut et al. 2006).

Another mapping criterion was the identification of all parts of the landslide (main scarp and toe) before outlining the polygon or setting the point. This reduces possible errors in the mapping due to misinterpretation of morphological convergent forms of landslide (scarp) features. Morphological convergence describes the presence of similar forms resulting from different natural but also anthropogenic processes (Antonini et al. 2002). Manmade features such as quarries or embankments built at houses or roads can have a similar appearance to sliding processes on the LiDAR DTM derivatives. This misinterpretation was avoided by checking the land cover on the orthophoto. Furthermore detailed field surveys of exemplary, characteristic and representative sites

were performed. This was done to revise the desktop mapping regarding the identification of landslides, the delineation of landslide boundaries and morphological convergence.

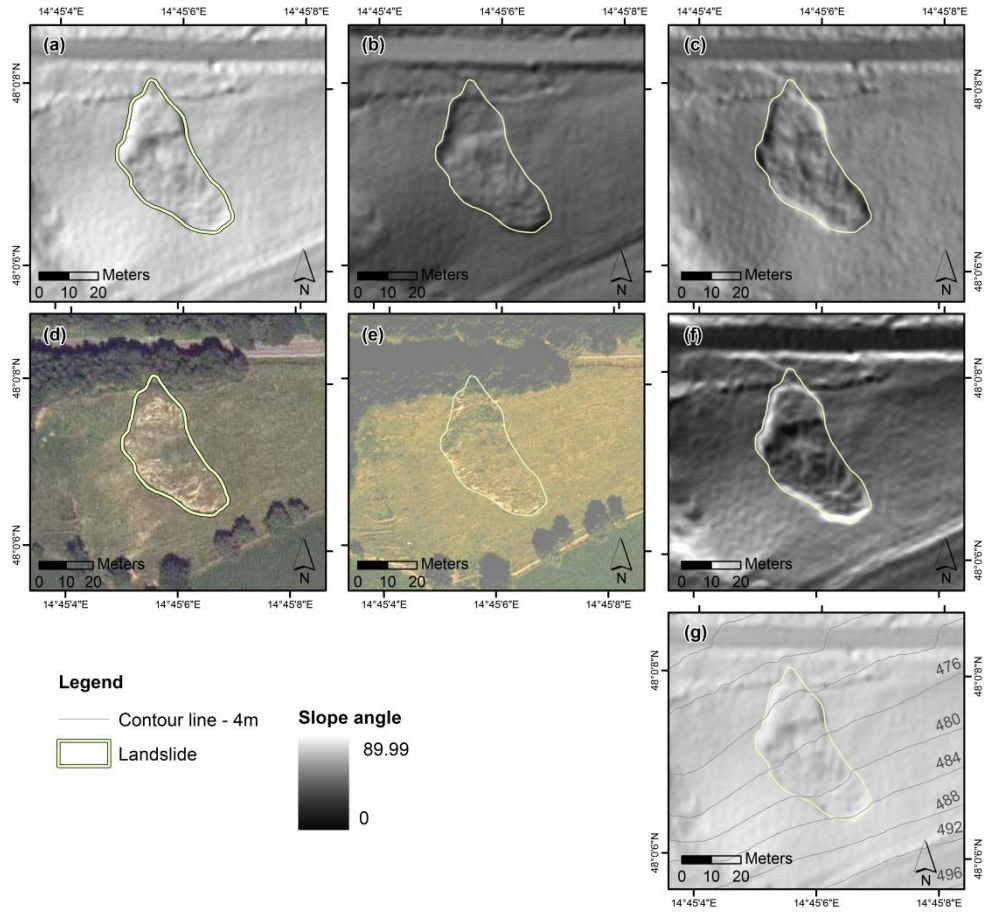

Fig. 1 A comparison of materials used for the landslide mapping: (a) Hillshade map derived from the LiDAR DTM with an azimuth angle of 315°; (b) Hillshade map derived with an azimuth angle of 135°; (c) Hillshade map derived with an azimuth angle of 45°; (d) Orthophoto (25cm x 25cm) acquired between 2000-2004; (e) Orthophoto (12,5cm x 12,5cm) acquired between 2007-2008; (f) Slope map derived from the LiDAR DTM; (g) Contour lines derived from the LiDAR DTM with 4m spacing. Source: DTM and orthophotos: Provincial Government of Lower Austria; Landslide mapping: own survey.

3.1 Landslide polygons – mapping and derivatives

Although the availability of a high resolution LiDAR DTM, an area-wide mapping of all visible landslides with polygons is a challenging task given restricted resources and a very high density of landslides as for example in the Flysch Zone (Petschko et al. 2010). To meet this challenge we further developed and tested a strategy to map a representative subset of landslides as polygons (as previously presented in Petschko et al. 2010 and Petschko et al. 2013) in the three test districts.

Our main principle was to map a characteristic subset of landslide polygons (without distinguishing between main scarp, transport and accumulation zone) in all lithological units, while ascertaining to map a representative number of landslides of all sizes and types in each unit.

This results in a landslide inventory with functional completeness (Malamud et al. 2004) designed for statistical modeling.

Each mapped landslide polygon was assigned with the following attributes: landslide type, relative landslide age, certainty of mapping and certainty of the assigned type. The mapped landslide types grouped according to Cruden and Varnes (1996) were (shallow and rotational) earth and debris slides, earth flows, complex and we introduced an "area with slides" (Petschko et al. 2013). This area includes a slope with several landslides of different relative age, size and maybe also type, which occurred very close or upon each other. As in this area the single landslide boundaries were difficult to distinguish, especially for very old, or strongly overlapping landslides, an "area with slides" was delineated (Petschko et al. 2010). This was done to increase the mapping effectiveness by reducing the mapping time while increasing the mapping accuracy. The relative age was estimated according to the appearance of the slide morphology in the imagery after an approach presented by McCalpin (1984). This approach and its results are presented and discussed in more detail in Petschko et al. (2014a).

The certainty of mapping and the assigned landslide type was expressed as "certain", where the type and landslide boundaries are clear and easy to detect. "Uncertain" was assigned to polygons where the boundaries were transitional and unclear or where the landslide type was ambiguous. Landslides assigned as "uncertain" were not included in the further analysis.

In addition, the mapping strategy includes the mapping of landslides larger than 100m² only, as this represents the area of a grid cell (10m x 10m) planned to be applied in susceptibility modeling (Petschko et al. 2014b). Furthermore, landslides below this size might be difficult to delineate on basis of the LiDAR derivatives.

3.1.1 Automated derivation of main scarps from landslide polygons

Many statistical landslide susceptibility modeling approaches use the information of the landslide main scarp rather than of the entire body. More distinct results of the modeling can be achieved by using points in the main scarp only (Van Den Eeckhaut et al. 2006; Van Den Eeckhaut et al. 2009; SpatialModels Inc. 2006). Furthermore, by subsampling one point for each main scarp spatial autocorrelation of the landslide samples can be avoided (Carrara 1993; Atkinson et al. 1998; Van Den Eeckhaut et al. 2006; Guns and Vanacker 2012). However, the extent of the main scarp is not always available within a landslide inventory and the mapping of the main scarp alongside with the landslide polygon needs additional resources.

Therefore, an automated derivation of main scarps from landslide polygons was tested to show the potential of the mapped features. Successfully implementing this automated approach might accelerate the mapping process, as only one polygon per landslide has to be mapped and therefore it potentially enhances the mapping effectiveness.

We propose a similar method as presented within the Spatial Prediction Modeling System (SPMS, Spatial Models Inc. 2006). Using the elevation data stored in a DTM, the landslide part with the highest elevation is assigned as trigger area or main scarp (SpatialModels Inc. 2006). Furthermore, the percentage of the area to be allocated as main scarp can be selected by the user within SPMS.

Likewise, we developed a raster based approach within ArcGIS 9.3 using the mapped landslide polygons and a DTM.

The LiDAR DTM was resampled to a spatial resolution of 10m x 10m, as this allowed faster computation and is the selected susceptibility modeling resolution (Petschko et al. 2014b). Furthermore, the DTM was masked by the landslide polygons resulting in a raster containing the landslides with elevation information for each grid cell.

Within the proposed approach a group of the highest grid cells per landslide was assigned as main scarp. Therefore, the minimum (Min_{pne}) and maximum (Max_{pne}) elevation (e) and the elevation range ($Max_{pne} - Min_{pne}$) within each landslide polygon (pn) was determined within ArcGIS 9.3. Considering differences in the elevation range between the landslide polygons we calculated a dynamic threshold value (T_{pne}) giving the lowest elevation of the main scarp for each landslide.

$$T_{pne} = Max_{pne} - P \times (Max_{pne} - Min_{pne}) \quad (1)$$

The dynamic nature of the threshold value originates from the percentage value (P) representing the percentages of the elevation range assigned for the main scarp. This gives the opportunity to consider the elevation differences of each landslide polygon in the derivation of the main scarp. In contrast, a static value subtracted from the maximum elevation might not be equally appropriate for very small or very large landslides.

Given this threshold value (T_{pne}) the grid cells of the main scarp were determined using a conditional statement within the raster calculator. Within this statement the cells of the landslides with a value lower than the threshold value were excluded from the landslide.

Moreover, we tested different percentages (P; 30%, 35% and 40%) of the elevation range and visually compared the computed main scarps with rasterized expert mapped main scarps. We visually identified the appropriate percentage value resulting in a good agreement with the expert mapping.

Comparisons of the size of the entire body and the main scarp of the slides were prepared for each lithological unit to characterize the landslides and main scarps.

3.2 Mapping of landslide points in the main scarp

While the polygons are marking the entire landslide body, we used points to map the main scarp only. The landslide main scarp is the most distinct discernible part of a landslide and therefore comparably easy and fast to detect on any imagery. At the main scarp the best accuracy of the mapping can be achieved as the boundary between stable terrain and the failed mass particularly at the lateral boundaries but also the toe of the landslide is often transitional (Malamud et al. 2004; Van Den Eeckhaut et al. 2006). This is not only a matter of the resolution of the imagery but was also recognized during field mapping (refer also to Santangelo et al. (2010) for similar findings).

While the data and imagery used for the mapping was identical in this approach, the main difference between mapping polygons and points in the main scarp was the mapping of all easy discernible landslides instead of a representative sample. Furthermore, no attributes describing the landslide type, relative age or certainty of mapping were assigned to the points. Despite assigning attributes to a single point is simple, this process is very time consuming for the huge sum of

points (Malamud et al. 2004). Additionally, the mapping was focusing on slides only excluding any flow, complex or areas of slides from the inventory. Areas with slides and very old slides were not considered in this mapping, as the decision of placing the point in the main scarp was very difficult and the information of single landslides is of higher importance for the modeling.

The location of the point within the main scarp was selected patterned on a random sample done within GIS in the main scarp as usually applied in susceptibility modeling (e.g. Atkinson et al. 1998). Therefore, the point was manually set fast and at random locations in the main scarp of the identified landslide.

3.3 Comparing landslide polygons and points – effectiveness estimate

As an estimate on the success of the representative mapping of the landslide polygons we calculated and compared the landslide density of each inventory (polygon or point) and the landslide ratio (RR_l) within the lithological units (l). The landslide density (D_l) is calculated dividing the number of landslides mapped in the lithological unit (N_l) by the area of the unit (km²; A_l) ($D_l = N_l/A_l$). The landslide ratio (RR_l) was derived dividing the percentage of earth and debris slides mapped as polygons within the lithological unit by the respective percentage of earth and debris slide points within each lithological unit. The landslide ratio gives an estimate on the success of the representative mapping of landslides as polygons, assuming the landslide point mapping being substantially complete. Values greater than 1 ($RR_l > 1$) indicate an overrepresented mapping of earth and debris slide polygons. Hence, values less than 1 ($RR_l < 1$) signal an underrepresented mapping of earth and debris slide polygons within the respective lithological unit.

Furthermore, the median slope angle of the different inventories was compared for the different lithological units as one proxy for the topographic characteristics. The median and range (minimum to maximum) of the slope angle of the landslide polygons, the extracted main scarps and of the mapped points in the main scarp was derived using the LiDAR DTM slope map. This gives an overview on representativeness and also on the general characteristics of landslides in the study area.

We assembled a record of the needed resources (person months, working 40h/week) for the mapping of both inventories. This allowed estimations on the demand for mapping the entire province, given the landslide mapping rate.

Considering the usage of the obtained inventory within statistical susceptibility modeling the advantages and drawbacks of the applied mapping methods are discussed reflecting on examples from literature and the needs given in Table 1. Therefore, the obtained inventories are compared to inventories mapped by other methods (based on aerial photographs, high resolution satellite images, semi-automated detection) as presented by Guzzetti et al. (2012) and in Table 4.

Assessing the effectiveness of the mapping of a given inventory (*i*) considering the type of analysis (*a*), we defined a semi-quantitative mapping effectiveness estimate (*Ee*).

The proposed effectiveness estimate

$$Ee_{ia} = \frac{N_i / PM_i / A_i}{M} \times w_{ia} \quad (2)$$

takes into account the ratio of the number of landslides mapped (N) in the study area, the used resources given by the person months (PM; working 40h/week) and the study area size (A; km²). This landslide mapping rate was divided by the maximum value (M) of this rate of all compared inventories to obtain a value ranging between zero and one. Furthermore, the importance of the inventory (*i*; mapped polygons or points) for a specific analysis or application (*a*) was considered assigning a weight (w_{ia}).

This weight is obtained by comparing the general requirements of the given type of analysis and the characteristics of the respective earth and debris slide inventory. Therefore, we identified different requirements for four analysis types: (1) characterization of the landslide process, (2) statistical landslide susceptibility modelling (using grid cells), (3) hazard and (4) risk analysis. The requirements we generally identified for all analysis types according to general practice and recommendations in literature, are specifically seen in the context of the analysis of earth and debris slides (Tab. 1): knowing the accurate landslide extent and / or location; knowing the date of occurrence; distinction between landslide zones (scarp, transportation and accumulation zone); information on the landslide runout length and/or angle of reach; landslide type; landslide volume; knowing the location of the main scarp; available multi temporal information on the landslide extent; one feature (polygon/point) representatively; one feature (polygon/point) substantially complete available per landslide and information on the triggering conditions (Van Westen et al. 1997; Guzzetti et al. 2006; Van Westen et al. 2006; Fell et al. 2008; van Westen et al. 2008). As these requirements are not equally important for every analysis type we differentiated between five levels of requirements on the landslide inventory given the analysis type: “absolutely necessary (++)”, “necessary (+)”, “helpful (o)”, “not necessary (-)”, and “adverse (--)”. For example for statistical susceptibility modelling using grid cells as terrain units, the accurate landslide location is “absolutely necessary”, whereas information on the landslide extent was considered as “helpful”. We compared our mapped point and polygon inventory to the previously defined requirements evaluating if the inventory met the requirements and assigned up to three stars (***) according to the level of the essential information (Table 1). For example the “absolutely necessary” accurate location of the landslides requirement was met by both our inventories. Therefore, both inventories score three stars (***). However, if one essential was not met, negative stars were assigned. For example the polygon inventory did not provide the date of occurrence which is a “helpful” characteristic of the inventory for statistical modelling. Therefore, for this inventory and requirement one negative star (-*) was assigned. Where the information could be obtained with some simple further analysis of the inventory (such as the automated derivation of main scarps) only the half amount of stars was given. The requirements indicated for the risk analysis show the expectations on the results of the hazard analysis and data required for evaluating the vulnerability and consequences of the hazard (Fell et al. 2008). As the data requirements for the specific analysis types is also scale dependent the mapping or analysis scale was set to range from medium (1:100,000 – 1:25,000) to detailed scale (> 1:5,000; Fell et al. 2008).

Tab. 1 Weights (w_{ia}) assigned for the importance of the polygon or point earth and debris slide inventory (inv.) mapped in the test study area for the listed analysis type. The requirements on the earth and debris slide inventory are listed and the requirements of the different analysis types are assigned using the following coding: "++" = absolutely necessary; "+" = necessary, "o" = helpful, "-" = not necessary, "--" = adverse (refer to Fell et al., 2008, Van Westen et al., 1997, 2008). We compared the information given by our inventory of points in the main scarp (Point) and our inventory of polygons marking the entire earth and debris slide body (Polygon) to the defined requirements (Requ.). Waves (~) or up to three stars (***) were assigned respectively if the requirements were met by the inventory: absolutely necessary characteristic given → "***"; necessary characteristic given → "**", helpful characteristic given → "*", not necessary characteristic given → "Δ", adverse characteristic given → "-#". If information could be obtained by some further analysis of the inventory only half of the stars were assigned. If information was required but not given by the inventory corresponding negative stars (e.g. "-***") were allocated. A wave is half a star and the sign "Δ" equals zero. The risk analysis does not include the required hazard analysis. The requirements indicated for the risk analysis show the expectations on the results of the hazard analysis and data required for evaluating the vulnerability and consequences of the hazard. The weight (w_{ia}) is the sum of the stars and waves times 100 for each inventory divided by the potential sum of stars of the respective analysis type. The resulting effectiveness estimate (Ee_{ia}; Eq. 2) is given in the last row. The mapping or analysis scale range of the listed analysis types is from medium (1:100,000 – 1:25,000) to detailed scale (> 1:5,000; Fell et al., 2008).

	Analysis Type											
Information required / given from inventory for specific analysis	Landslide process / Evolution analysis - Morphometric analysis			Statistical earth and debris slide susceptibility modeling			Hazard analysis			Risk analysis		
	Requ.	Point inv.	Polygon inv.	Requ.	Point inv.	Polygon inv.	Requ.	Point inv.	Polygon inv.	Requ.	Point inv.	Polygon inv.
Accurate landslide extent	++	-***	***	o	-*	*	++	-***	***	++	-***	***
Accurate landslide location	++	***	***	++	***	***	++	***	***	++	***	***
Date of occurrence	++	-***	-***	o	-*	-*	++	-***	-***	++	-***	-***
Distinction of landslide zones (Depletion, transportation and accumulation zone)	++	-***	-***	o	~	~	+	-**	-**	+	-**	-**
Landslide runout length and/or angle of reach	++	-***	***	o	-*	*	++	-***	*~	++	-***	*~
Landslide type distinguished	++	***	***	++	***	***	++	***	***	++	***	***
Landslide volume	+	-**	*	-	Δ	Δ	+	-**	*	++	-***	*~
Location of main scarp known	+	**	*	++	***	*~	+	**	*	o	*	~

Multi temporal information on the landslide extent	++	-***	-***	-	Δ	Δ	+	-**	-**	o	-*	-*
One feature (point/ polygon) per landslide representative for entire study area	o	*	*	++	***	***	++	***	***	++	***	***
One feature (point/ polygon) per landslide substantially complete in study area	o	*	-*	++	***	-***	++	***	-***	++	***	-***
Trigger or triggering conditions	+	-**	-**	o	-*	-*	++	-***	-***	+	-**	-**
Sum of (potiental) stars and waves	29	-9	3	20	11.5	8	32	-4	2.5	30	-4	4.5
Total weight (w_{ia}) for inventory for given application		-31.0	10.3		57.5	40.0		-12.5	7.8		-13.3	15.0
Value "N/PM/km² / M"[#]		1	0.17		1	0.17		1	0.17		1	0.17
Effectiveness estimate (Ee_{ia}) [#] of inventory for given application		**-31.0**	**1.8**		**57.5**	**6.9**		**-12.5**	**1.3**		**-13.3**	**2.6**

[#] According to equation (2)

As the different analysis types reached a different potential total amount of stars, scored if all requirements would be fulfilled, the sum of all stars (and waves = half a star) obtained by the inventory was divided by the potential amount of stars of the analysis type and multiplied by 100. This resulted in the weight (w_{ia}) for the inventory for a given application ranging from 0-100. Therefore, the larger the resulting value of the effectiveness estimate the higher the effectiveness of the inventory for the given analysis type. An effectiveness estimate below zero corresponds to a very low or no effectiveness of the given inventory for the analysis type.

The inventory mapping method with the highest effectiveness for statistical landslide susceptibility modelling using grid cells as terrain unit was applied for mapping landslides in the entire province Lower Austria.

4. Study area

The three test districts Amstetten, Baden and Waidhofen/Ybbs were selected for assessing the most effective method of inventory mapping applicable for Lower Austria. The districts are considered as representative of the lithology and topography of Lower Austria (Figure 2). Furthermore, they are characterized by a different number of reported landslides (mainly slide processes) in the so called "Building Ground Register", an archive run by the Geological Survey of Lower Austria (Schwenk 1992). This allowed us to test the mapping in areas of different landslide documentation density.

The lithology of the test study area includes clastic sediments of the Molasse Zone, a unit of Loess and Loam, sandstone interbedded with marl in the Flysch Zone, limestone (with marls) and dolostone in the Austroalpine Unit, granite and gneiss in the Bohemian Massif and sand, gravel and clay in the Intramontane Basin (Figure 1; Wessely 2006). These units showed a very distinct general susceptibility to landslides given by the differences in the predominant material (Petschko et al. 2010; Petschko et al. 2014b). Furthermore, the lithological map of the study area contains a unit named "landslide deposits". This unit was assigned for areas where landslides were observed abundantly and no information on the underlying lithology is available (Wessely 2006). However, not all landslides visible in the LiDAR DTM were assigned as "landslide deposits" in the lithological map. Furthermore, drawbacks of the map scale (1:200,000) have to be considered.

The main landslide processes (as defined by Cruden and Varnes (1996)) in Lower Austria are shallow and deep seated earth and debris slides, but also earth and debris flows and rock falls occur. In this study we focus on sliding processes mainly. Most slide processes were reported in the Flysch Zone (Schwenk 1992). Furthermore, many slides are documented in the Klippen Zone, Molasse Zone and the Austroalpine Unit with limestone and marl (Schwenk 1992). During the past 60 years (1953-2011) 535 landslides were reported in the Building Ground Register for the district Amstetten (1187km²), 7 landslides were documented in Baden (754km²) and 151 landslides were filed for Waidhofen/Ybbs (131km²) (Petschko et al. 2013). Associated damage occurred mainly on farmland (43%) as well as on private houses and on infrastructure (23%) (Petschko et al. 2010; Petschko et al. 2012).

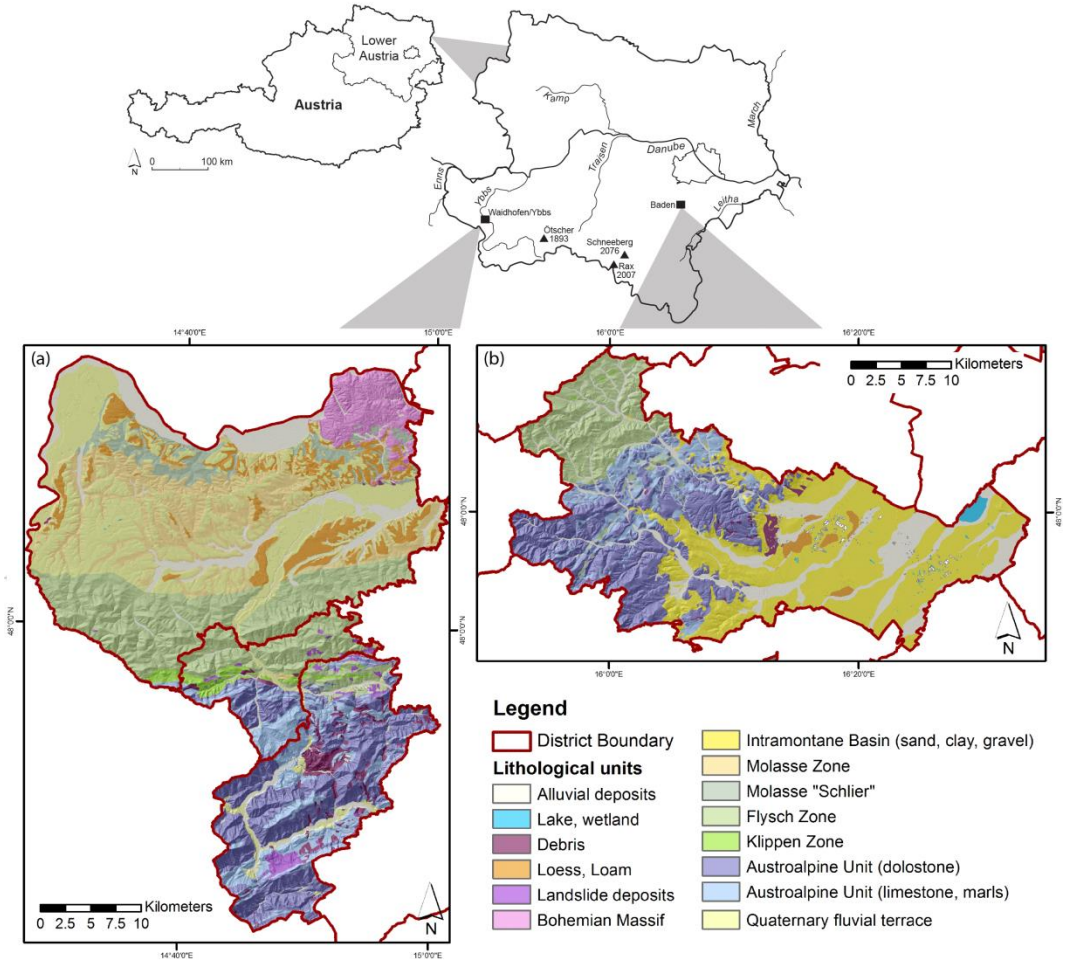

Fig. 2 Location and lithology of the three test districts (a) Amstetten, Waidhofen/Ybbs and (b) Baden. Source: DTM: Provincial Government of Lower Austria; Lithological map: Geological Survey of Austria (GBA-2009-Zl. 383/1-09).

The main triggers of landslides in Lower Austria are exceptional rainfall and/or intensive snow melt events (Schwenk 1992; Schweigl and Hervás 2009). Earthquakes occur rarely (Eisinger et al. 1992) but have not been analyzed as a landslide trigger in Lower Austria so far. The distribution of the mean annual precipitation rates (between 2001 and 2010) throughout Lower Austria shows a gradient from low rates in the northeast (500mm) to high rates in the southwest (1600mm – 1700mm, Hydrographischer Dienst des Landes Niederösterreich 2011). Likewise, the station Hinterlug in the district Waidhofen/Ybbs showed a mean annual precipitation of 1379mm with a daily maximum of 130.5mm measured on the September 6, 2007 (Hydrographischer Dienst des Landes Niederösterreich 2011). At the station Alland in Baden comparably low mean annual precipitation rates of 820mm were recorded whereas the daily maximum in this period is very high (131.4mm, measured on the June 6, 2002; Hydrographischer Dienst des Landes Niederösterreich 2011).

5. Results

5.1 Landslide polygons and points in the main scarp

Compared to existing landslide inventories the mapping of landslides on the LiDAR DTM derivatives revealed a large number of additional, previously unknown landslides in our test districts. 1213 landslide polygons and 2709 landslide points in Amstetten, 107 polygons and 219 points in the main scarp in Baden and 694 landslide polygons and 1061 landslide points were mapped in Waidhofen/Ybbs. This totals to 2014 mapped landslide polygons (including 1834 landslides assigned as certain and thereof 1437 slides) and 3994 points in the main landslide scarp in our test districts. (Tab. 2, Fig. 3). Among these mainly earth and debris slides (75.7%) and "areas with slides" (20.3%), but also landslides classified as earth flows (3.8%) and complex landslides (0.2%) were mapped. Nearly half of the landslides were considered to be of "old" relative age (48%) whereas 34% were assigned as "young", 10% as "very old" and 8% as "very young" (Petschko et al. 2014a).

The lithological unit with the most landslides is the Rheno-danubian Flysch Zone (1021 landslide polygons, 2373 points). However, looking at sliding processes only the highest landslide density (D_l) was found for the Mélange Zone or also called Klippen Zone (5.09 landslide polygons / km²; 13.85 points / km²; Tab. 2). The Rheno-danubian Flysch Zone ranks fourth (2.23 polygons / km²; 6.41 points / km²) following the unit of landslide deposits (4.3 polygons / km²; 7.03 points / km²) and the Molasse, Schlier unit (4.17 polygons / km²; 8.79 points / km²). Only few landslide polygons or points in the main scarp were mapped in the alluvial deposits, Intramontane Basin and Bohemian Massif (Tab. 2). This comparison shows a clear difference in the landslide density of mapped landslide polygons and points and therefore suggests a high heterogeneity in the study area regarding landslide susceptibility.

We analyzed the success of the representative mapping of landslide polygons by comparing the landslide ratio (RR_l) assuming that the points in the main landslide scarp represent a substantially complete sample. Generally the results show both, an underrepresented and overrepresented mapping of earth and debris slide polygons within the lithological units of the test districts (Tab. 2). The landslide ratio values range from zero (in the Bohemian Massif) to a maximum of 1.7 (in the Landslide deposits) times as many polygons as points. Besides, the presented minimum and maximum values showing the highest under- and overrepresentation of polygons, earth and debris slide polygons were comparably high overrepresented in the lithological units of Debris and Intramontane Basin. Apart from the Bohemian Massif, where no landslide polygons were mapped, the Austroalpine Unit with limestone, marl and sandstone shows the highest underrepresentation of polygons (RR_l = 0.7). Unlike, nearly the same percentage of earth and debris slide polygons or points was found for the Rheno-danubian Flysch Zone (RR_l = 0.97) and for the Mélange Zone (RR_l = 1.02).

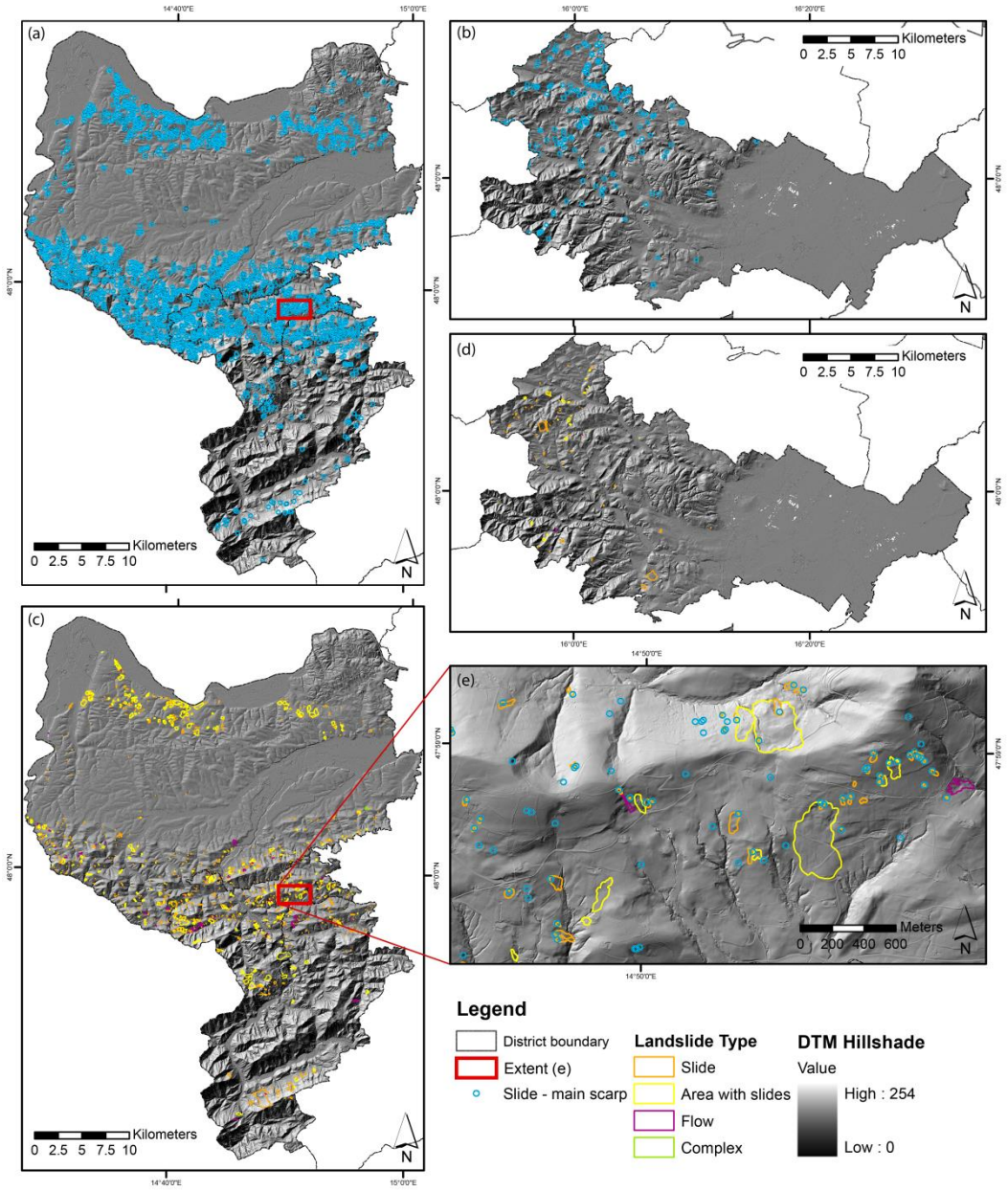

Fig. 3 Comparison of resulting landslide inventories. Landslides mapped with points (a, b) and with polygons (c), (d) presented in a zoomed in example (e). Source: DTM: Provincial Government of Lower Austria; Landslide mapping: own survey.

The mapping of the polygons of all landslide types mapped as "certain" required the setting of 160,316 vertices (points) to delineate the polygons within 4 person months. The polygons of the type earth and debris slide were mapped with 100,256 vertices (points) within 1.5 person months. Compared to the total points set in the main earth and debris slide scarp this results in a ratio 25:1. However, it has to be kept in mind, that the landslide polygons were only mapped representatively (about a third of the landslides mapped with a point). Therefore, to map one earth and debris slide with a polygon around 75 vertices have to be set opposed to one single point set in the main scarp.

Tab. 2 Comparison of the number of mapped polygons (N_{pnl}, N_{psnl}) and points (N_{ptl}), of the landslide density of mapped polygons (D_{pnl}, D_{psnl}) and points (D_{ptl}), of the landslide percentage within each lithological unit (R_{pnl}, R_{psnl}, R_{ptl}) and the landslide ratio (RR_l) in the test study area in the lithological units. Furthermore, the median slope angle within the lithological units is presented.

ID	Lithological unit	Landslide count (N_l)			Area lith. unit (A, km²)	Landslide density ($D_l = N_l/A_l$)			Landslide percentage within lithological unit ($R_l = N_l/\Sigma N_l*100$)			Landslide ratio ($RR_l = R_{psnl}/R_{ptl}$)	Median slope angle (°)		
		Polygons all landslide types (N_{pnl})	Polygons " Slides" (N_{psnl})	Points (N_{ptl})		Polygons (D_{pnl})	Polygons "Slides" (D_{psnl})	Points (D_{ptl})	Polygons ($R_{pnl,}$ %)	Polygons "Slides" ($R_{psnl,}$ %)	Points ($R_{pt,l}$ %)		Slide polygon	Main scarp slide polygon	Main scarp slide point
11	Alluvial deposits	8	6	20	231.5	0.04	0.03	0.09	0.44	0.42	0.50	0.83	19	21	17
13	Debris	55	44	81	33.5	1.64	1.31	2.42	3.00	3.06	2.03	1.51	18	19	20
14	Loess, Loam	70	47	165	88.4	0.79	0.53	1.87	3.81	3.27	4.13	0.79	10	12	14
15	Landslide deposits	66	55	90	12.8	5.16	4.30	7.03	3.60	3.83	2.25	1.70	20	15	18
21	Quaternary fluvial terrace	50	44	145	275.1	0.18	0.16	0.53	2.72	3.06	3.63	0.84	10	14	14
22	Intramontane Basin	6	6	11	274.6	0.02	0.02	0.04	0.33	0.42	0.28	1.52	7	n.a.	12
31	Molasse Zone	45	35	135	150.9	0.30	0.23	0.89	2.45	2.44	3.38	0.72	8	10	15
32	Molasse, Schlier	261	189	398	45.3	5.76	4.17	8.79	14.22	13.15	9.96	1.32	8	10	13
41	Rheno-danubian Flysch Zone	1021	826	2373	370.4	2.76	2.23	6.41	55.64	57.48	59.41	0.97	15	16	19
42	Mélange Zone, Klippen Zone	127	91	248	17.9	7.10	5.09	13.85	6.92	6.33	6.21	1.02	14	18	19
51	Austroalpine Unit with dolostone	54	44	109	367.0	0.15	0.12	0.30	2.94	3.06	2.73	1.12	23	25	25
52	Austroalpine Unit with limestone, marl and sandstone	72	50	198	149.6	0.48	0.33	1.32	3.92	3.48	4.96	0.70	25	25	26
61	Bohemian Massif	0	0	21	55.7	0.00	0.00	0.38	0.00	0.00	0.53	0.00	n.a.	n.a.	20
TOTAL ($\sum N_{psn} / \sum N_{pt}$)		1835	1437	3994	2072.7	0.89	0.69	1.93							

5.2 Automated derivation of main scarps from landslide polygons

The automated derived main landslide scarps, using different percentage values of the elevation range assigned as main scarp, gave rather similar results (Fig. 4). Despite, with the visual comparison of the automated derived and rasterized expert mapped main landslide scarps we identified the derived main scarps with the best agreement with the rasterized expert mapped main scarps. As a result, 35% of the elevation range assigned as the main scarp gave the closest representation of the main scarps.

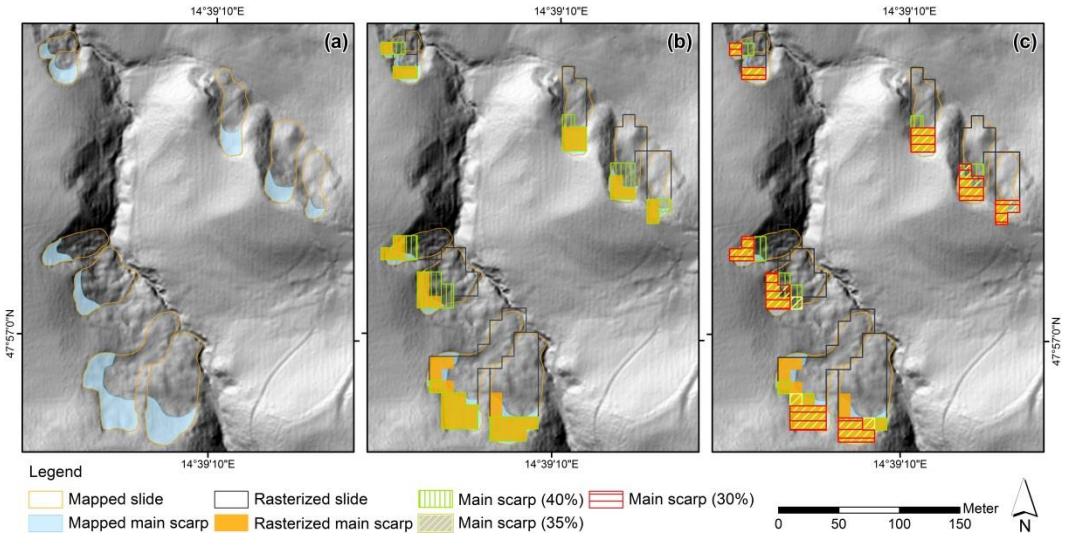

Fig. 4 Derivation of the main scarp within ArcGIS. (a) Mapped landslide including main scarp. Rasterized main scarps and scarps derived with ArcGIS using (b) 40% and (c) 35% and 30% of the elevation range assigned as the main scarp. Source: DTM: Provincial Government of Lower Austria; Landslide mapping: own survey.

Looking at the size (area in m²) of the landslide polygons and the derived main scarps we observed a distinct change between size of the entire polygon and the main scarp. 75% of the earth and debris slide bodies showed a size between 477m² and 2257m², whereas 75% of the main scarps of earth and debris slides ranged between 100m² to 600m² (Tab. 3). Besides, the size of the earth and debris slide polygons and derived main scarps changed with the lithological unit, as shown best by the median of the boxplots (Fig. 5). The largest earth slide was mapped within the landslide deposits (1,844,305m²) but the smallest landslide was found in the debris, till unit (59m²). This shows that despite our expectation, also landslides smaller than 100m² can be mapped on the LiDAR derivatives.

By extension, the median slope angle of the mapped earth and debris slides distinctly changed between the different lithological units (Tab. 2). Comparing the median slope angle of the entire earth and debris slide polygon and the derived main scarp revealed a trend toward a steeper slope angle of the main scarp. This matches the general understanding of the distribution of slope angles in an earth slide area (Varnes 1984). Also the points mapped in the main scarp showed a steeper

slope angle than the polygons. Compared to the automated derived main scarp the median slope angles of the points were different in some lithological units (e.g. the Rheno-danubian Flysch Zone (16°, 19°) or the alluvial deposits (21°, 17°). However, the median slope angles were similar or identical in the Quaternary fluvial terrace (14°, 14°), the Mélange Zone (18°, 19°) and the Austroalpine Unit with dolostone and with limestone, marl and sandstone (25°, 25°; 25°, 26°; refer to Tab. 2). An analysis of the minimum and maximum values of the slope angle within the derived main earth and debris slide scarps and the mapped points (not presented here) showed that the points mainly fit into the range of values given by the main scarps derived from the earth and debris slide polygons. These results show the dependency of the median slope angle of the mapped landslides points on the selected location to map the main scarp. Furthermore, landslides which were mapped as point but not as polygon might have slightly different median slope angles.
Generally, these results emphasize the heterogeneity of the study area also in terms of earth and derbis slide characteristics.

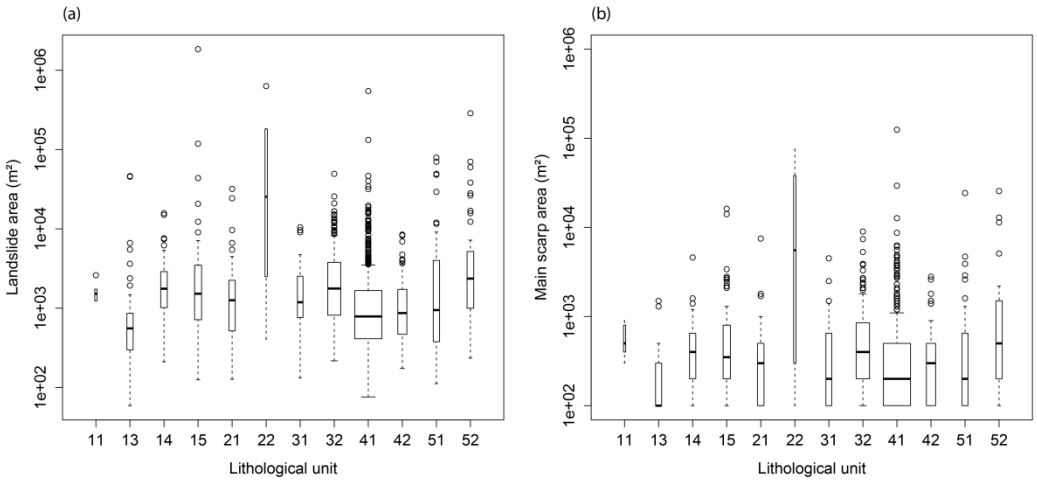

Fig. 5 Comparison of the area of mapped earth and debris slide processes (a) and their derived main scarps (b) presented with boxplots for each lithological unit. The Bohemian Massif is not presented here, as no earth and debris slide polygons were mapped in that lithological unit. The width of the bars is relative to the number of landslides in the respective lithological unit. Numbers of the lithological units refer to the respective numbers given in Table 2.

5.3 Effectiveness estimate

The mapping of 1834 landslide polygons took 2.67 times as many person months (PM, working 40h/week; 4 PM) as mapping 3994 landslide points (1.5 PM; Tab. 4). This results in a landslide mapping rate of 459 and 2663 landslides per person month respectively (Tab. 4). Taking into account the size of the study area we found that 518km² (mapping polygons) and 1382km² (mapping points) were mapped per person month. Compared to studies using different mapping methods (e.g. mapping from aerial photographs or satellite images) presented by Guzzetti et al. (2012) the area mapping (and digitizing) rates were comparable but mainly higher using LiDAR imagery in Lower Austria (Tab. 4). This area mapping rate was mainly dependent on the production scale of the inventory and less on the mapping method (Tab. 4).

Tab. 3 Landslide size in m² for the entire landslide body and the automated derived main scarp. The minimum (Min), maximum (Max) and median of the landslide (main scarp) polygon area are given. While the size of the landslide bodies was derived from the polygons, the area of the main scarps was calculated based on the 10m x 10m grid, thus the minimum area cannot be smaller than 100m². The main scarps of complex features were not analysed (n.a.).

Landslide Type	Landslide size - body (m²)					Landslide size - main scarp (m²)				
	Min	1st Quartile	Median	3rd Quartile	Max	Min	1st Quartile	Median	3rd Quartile	Max
All types	59	595.0	14080.	4203.0	1844305	100	200	400	1300	154800
Slides	59	477.0	971.0	2257.0	1844305	100	100	300	600	124900
Area with slides	356	4624.3	10871.5	36689.0	746785	100	1375	3750	11125	154800
Flow	274	1615.8	3282.5	13400.3	123566	100	500	1100	4400	56100
Complex	1546	3229.0	3740.0	17724.0	51935	n.a.	n.a.	n.a.	n.a.	n.a.

Tab. 4 can be found at the end of this publication due to its page size.

Unlike, the landslide mapping rate seems to be depending on the mapping method (as shown by the imagery type used). Using aerial photographs, a lower landslide mapping rate was achieved than by mapping on satellite or LiDAR imagery (Tab. 4). The largest landslide mapping rate was achieved using satellite imagery for automated detection of landslides (Tab. 4; Mondini et al. 2011).

We assessed the requirements of statistical landslide susceptibility modelling on the landslide inventory and compared these to the information given by each of the mapped inventories. We obtained a weight (w_{ia}) 57.5 for mapping landslides with points and 40 for mapping with polygons (Tab. 1). Accordingly, the resulting effectiveness estimate (Ee_{ia}) was 57.5 (points) and 6.9 (polygons; Tab. 1).

Comparing this to other analysis types as evaluated according to the requirements listed in literature (e.g. Fell et al. 2008; van Westen et al. 2008), the effectiveness estimates were ranging from -31 (using points for the analysis of the landslide process) to +2.6 (using landslide polygons analyzing landslide risk; Tab. 1). Except for the statistical modelling of landslide susceptibility the mapping of landslide points in the main scarp had very low (or no) effectiveness for the other assessed analysis types (Tab. 1). The effectiveness estimate of mapping landslide polygons was highest for risk analysis, considering the identified requirements on the results of the hazard modelling and on the data for assessing the hazard consequences for this analysis from literature (e.g. Fell et al. 2008; van Westen et al. 2008).

According to our objective of statistically modelling landslide susceptibility in a large study area, visualization of the final map in three classes (Petschko et al. 2013) and the respective effectiveness estimate the mapping of points was the preferable and acceptable method for Lower Austria. Consequently, our mapping team for the remaining districts mapped points in the main landslide scarp for the entire province (Fig. 6). Applying the methods to the study area Lower Austria revealed new insight into the presence of landslides in the province as 13,166 landslides were mapped in total (Fig. 6). Compared to previously existing landslide inventories, such as the Building Ground Register of the Geological Survey of Lower Austria, we identified up to 10 times more landslides in some districts.

6. Discussion

We successfully mapped landslides of different types and size in forested but also open land using derivatives from a LiDAR DTM and orthophotos. The result of a historical landslide inventory clearly distinguishing between single landslides (polygons or points) can be used for further analysis such as susceptibility modelling. However, no information is available on the time of occurrence of the landslides and the age can only be estimated relatively (McCalpin 1984).

Analyzing landslide triggering conditions an event inventory is beneficiary as it represents only landslides and related losses occurred and mapped after a trigger event (Van Westen et al. 2006). Compiling these, other landslide mapping methods (e.g. stereoscopic interpretation of multi temporal aerial or satellite images (e.g. Fiorucci et al. 2011; Ardizzone et al. 2013) are preferable

to using LiDAR DTMs due to currently high costs of the data acquisition and low availability of multi temporal and event related data.

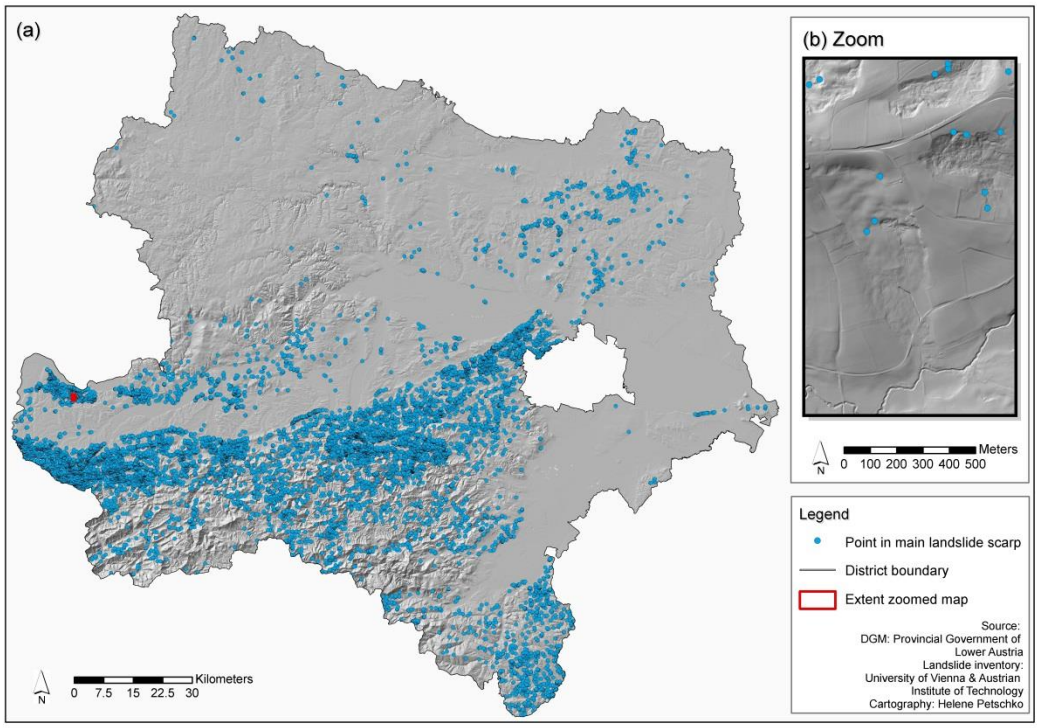

Fig. 6 (a) Resulting landslide inventory mapped using LiDAR DTM derivatives and orthophotos in Lower Austria (number of mapped main earth slide scarps = 13,166). (b) Zoom to the earth and debris slides mapped in the Molasse, Schlier area in Amstetten (refer to location marked in (a) as red dot). Source: DTM: Provincial Government of Lower Austria; Landslide mapping: own survey.

Generally the visual analysis of optical imagery (aerial photographs, satellite images) is well suitable creating an event inventory as "fresh" landslides are characterized by missing vegetation due to the landslide process (McCalpin 1984; Guzzetti et al. 2012). Inventories resulting from these methods can give a detailed insight into the landslide process including the date of occurrence, the related trigger or in the multi temporal context into the evolution of landslides over years. However, some drawbacks of aerial photograph interpretation are the time consuming collection and digitizing process which might create transfer errors, the high costs for aerial photographs and the therefore restricted study area size (Tab. 4; Baeza et al. 2010; Guzzetti et al. 2012). Furthermore, problems of landslide identification in forested areas might occur (Brardinoni et al. 2003; Van Den Eeckhaut et al. 2007).

For mapping landslides in large areas semi-automated methods are very promising, as cloud free satellite data is usually available briefly after an event (e.g. typhoon; Martha et al. 2010; Mondini et al. 2011; Martha et al. 2012). These methods work best for large, deep seated landslides or debris flows, where the morphological and vegetational footprint of the landslide is obvious. Also the comparison of the landslide mapping rate (N/PM) showed, that these methods are very fast in detecting landslides over a large area (Tab. 4; Mondini et al. 2011). However, regarding the mapping or detection of single events most of these advanced methods are currently lacking the

possibility to delineate single landslides but the results are zones containing several landslides. This is of disadvantage especially when the landslide inventory should be used as a basis for susceptibility modeling, where the exact location of each landslide must be known, and also the information on how many landslides are in a certain area is important (Petschko et al. 2014b). Therefore, an (additional) "old-fashioned" visual interpretation to identify the single landslides is still of high importance in landslide inventory mapping. Consequently, the mapping effectiveness is reduced.

The representative mapping of a subset of landslides with a polygon was very successful for the Rheno-danubian Flysch Zone and the Mélange Zone. Within three units out of 13 a rather high overrepresentation of mapped polygons was found (Landslide deposits, Debris and Intramontane Basis). However, the expert based representative mapping of earth and debris slides was surprisingly successful. Nevertheless, the performed expert estimation of the representativeness during the mapping might be considered as not effective and highly subjective. It seems that there is a tendency that subjectivity in mapping landslides is influenced by landslide density. While an overrepresentation of mapped landslide polygons was observed in relatively small lithological units showing a high landslide density, in lithological units with low landslide density the mapped landslide polygons were underrepresented.

However, the idea of mapping a representative sample only in the sense of creating a substantially complete inventory might be attractive for statistical modelling of landslide susceptibility (Calvello et al. 2013). A more sophisticated representative mapping approach inspired by geospatial sampling techniques might be preferable. For example mapping all visible landslides in a limited number of quadrats (of a specific size) randomly located in the study area / lithological unit. This methodology is patterned on the quadrat count method widely used in ecology (Krebs 1999; Christman 2000; Ver Hoef 2002; Thompson 2012). Other approaches working with terrain mapping units of different size related to the analysis scale tested the mapping of landslides over a portion of the area for landslide susceptibility zoning (Calvello et al. 2013). They derived landslide distribution zoning maps for terrain units where no landslide mapping was performed. These are intermediate products between an inventory and a susceptibility map which can be used for landslide susceptibility or hazard zoning (Calvello et al. 2013). In this way full landslide information from a relatively small area can be used to calibrate and validate a model used to transfer the landslide distribution zoning maps (Calvello et al. 2013).

While these spatial sampling methods sound appealing, the heterogeneity of the study area regarding lithology, morphology, landslide size and density, and land cover poses a challenge identifying a satisfactory and still applicable sampling technique (e.g. using randomly located quadrats of a specific size or mapping landslides over a portion of the area only). Fitting a statistical susceptibility model within each lithological unit requires information on the landslide density of each unit (Petschko et al. 2014b). Furthermore, the irregular shape and differing landslide density e.g. from east to west of a lithological unit are challenging (Fig. 1, Fig. 6). In a previous study we assessed the spatial transferability of landslide susceptibility models in lithological units in Lower Austria (Petschko et al. 2014b). The spatial transferability is a comparison of changes in the model performance dividing the sample of landslide and non-

landslide points spatially in training and test samples (Townsend Peterson et al. 2007; Ruß and Brenning 2010). This simulates the modelling of the landslide susceptibility in only one subarea and applying it to the remaining area. Our results showed that the spatial transferability is very different for each lithological unit and rather low in units with small sample sizes (Petschko et al. 2014b). Furthermore, the comparison of the median slope angles of derived main scarps and mapped points showed differences of up to 6°. These examples illustrate the challenges of defining an appropriate geospatial sampling design characterizing heterogeneous study areas. Moreover, in this study the analysis using grid cells as terrain units was part of the objective.

Apart from that, the substantial completeness of the earth and debris slide points inventory might be questioned. In agricultural land the vegetational and morphological footprint of landslides is potentially removed naturally by erosion or anthropogenically rather quickly by farming or remediation activities (Fiorucci et al. 2011; Bell et al. 2012). Therefore, the landslides are not visible on the LiDAR imagery anymore. Accordingly, the point inventory might have a bias of unknown extent towards underrepresenting landslides in agricultural, not forested, land (Bell et al. 2012; Petschko et al. 2014a; Petschko et al. 2014b). This is a further drawback of the limited availability of multi temporal or event related LiDAR data. However, more detailed analysis is necessary to assess the presence or absence of a potential bias in our study area.

The automated derivation of the main landslide scarp was performed using a 10m x 10m grid cell size. Although the results are promising and rather satisfactory, the performance needs to be assessed quantitatively and different grid cell sizes could be tested. Any prediction (or in our case model to derive the main scarp) is of no value if its performance is not assessed (Chung and Fabbri 2003; Chung and Fabbri 2008; Fabbri et al. 2003). The geographical discrepancy of derived and mapped main landslide scarps could be quantified on a raster base or by a method proposed and adopted by Carrara (1993) and Galli et al. (2008). Facilitating this, the error index and the degree of matching of the derived main landslide scarps could be determined quantitatively instead of visually. Furthermore, using the derived scarps in subsequent analysis the possible introduction of a bias into the landslide sample has to be considered, if the mismatch of the mapped and derived main scarp is too big or not random.

The mapping (or usage) of points in the main landslide scarp leads to a limited representation of the landslide process. However, modelling with one point (per landslide or scarp) only is a standard method used in susceptibility modelling (e.g. Atkinson et al. 1998; Beguería 2006; Van Den Eeckhaut et al. 2006; Felicísimo et al. 2012). Furthermore, it is common to use the main scarp area only in the susceptibility analysis (Dai and Lee 2002; Fernández et al. 2003; Remondo et al. 2003; Santacana et al. 2003). This must be considered in the further usage of the inventory e.g. in susceptibility modelling as the result only shows the probability of landslide initiation, not of the run out (Petschko et al. 2014b). Assessing the entire landslide extent (e.g. for hazard or risk analysis) the run out of the individual earth and debris slides has to be estimated. One possible run out modelling solution was proposed by Tobler et al. (2013).

The proposed effectiveness estimate helped to assess the requirements of different analysis types on the inventory in a structured way. Although it might be considered as rather subjective or experimental, the resulting effectiveness estimate gave a good summary of the benefits and

drawbacks of the respective inventory using it for different analysis types. This table on the effectiveness estimate should help to identify priorities in assigning resources for landslide inventory mapping, especially in large heterogeneous study areas.

Neither of the mapped landslide inventories is “perfect” for the listed analysis types as shown by the effectiveness estimate. Analyzing landslide hazard and risk, more attributes to the landslide polygons (e.g. trigger conditions, date of occurrence, consequences including caused damage) as necessary for the analysis are missing (e.g. Fell et al. 2008). Additionally, the results and discussion outlined limitations in the general representativeness of both mapped inventories due to the performed mapping approach.

The effectiveness of the mapping might also be discussed or compared using the landslide mapping rate per square kilometer (N/PM/km²). However, this estimate is not reliable comparing study areas of different size. By extension, the size of areas with flat topography in the different study areas is unknown. This has a huge influence on this rate, as in flat areas no landslides can be mapped and consequently the rate is lowered substantially. Therefore, interpreting the effectiveness measure is only feasible within the same study area. Another possibility would be to consider only areas which can be prone to landslides a priori excluding flat areas from the study area. Therefore, we did not compare the mapping effectiveness for using the one or the other mapping method (e.g. aerial photographs, satellite imagery) as presented in Table 4 to map landslides in large study areas.

What we did not include into the effectiveness measure is the quality of the final susceptibility map (Petschko et al. 2014b). We assessed the change in the model performance and the visualization of a susceptibility map with three classes using randomly sampled points in the entire polygon or the main landslide scarp only in a logistic regression model in a previous study (Petschko et al. 2013). The resulting area under the receiver operating characteristic curve (AUROC) values were only slightly higher using points in the polygon than using points in the main scarp. Additionally, the appearance of the classified landslide susceptibility maps was similar (Petschko et al. 2013). The present study showed that this similarity can not be attributed to a similar size of the rasterized landslide body and main scarp (Fig. 5). From this modelling perspective, not only from the effectiveness estimate, we considered mapping the points in the main scarp only as effective method still resulting in reliable classified susceptibility maps for Lower Austria (Petschko et al. 2013).

7. Conclusions

Generally, in the best case the landslide mapping is performed briefly after a landslide event, delineating landslide polygons and assigning as many attributes as possible. Similarly, the availability of multi temporal data is required to analyze the potential bias of the landslide inventory towards an underrepresentation in agricultural land. However, this is a question of available resources (data, time and trained people), the study area size and the number of landslides occurred in this area. The restricted (multi temporal) availability and high acquisition costs are clear limitations of the LiDAR DTM used in this study. Nevertheless, the LiDAR DTM

has proven to be of advantage for identifying and mapping landslide morphology also in forested areas throughout Lower Austria.

We conclude that mapping points in the main landslide scarp only is the most effective landslide inventory mapping method, in particular considering its usage in statistical landslide susceptibility modelling deriving classified susceptibility maps for large and heterogeneous study areas. However, the effectiveness estimate showed that on the long term perspective the mapping of landslide polygons is beneficiary for upcoming hazard and risk analysis. The representative mapping of landslide polygons within the lithological units was only partly successful. Therefore, the testing of more sophisticated geospatial sampling methods, such as the quadrat method taking into account the heterogeneity of the study area is strongly recommended.

We successfully implemented the automatic derivation of main scarps from polygons which helps minimizing the resources needed for landslide mapping and increasing the mapping effectiveness. However, a quantitative assessment of the mismatch is pending.

The proposed effectiveness estimate might be considered as rather experimental and subjective. Despite this, it aims to help expressing the importance of an inventory for a specific analysis type in a semi-quantitative way. Naturally, this effectiveness estimate can be expanded or adapted for other analysis types as well. Moreover, if resources are limited and the subsequent analysis type is defined, identifying or considering the listed requirements as done in assessing the effectiveness estimate might be helpful to identify the most effective mapping method.

8. Acknowledgements

This study was carried out within the research project “MoNOE – method development for landslide susceptibility modelling in Lower Austria” funded by the Provincial Government of Lower Austria. The authors are thankful for the provision of data by the Geological Survey of Austria and Lower Austria, the Austrian Service for Torrent and Avalance Control and the Provincial Government of Lower Austria. We want to thank the landslide inventory mapping team including Dr. Philip Leopold’s team of the Austrian Institute of Technology and our research assistants Mag. Christine Gassner and Ekrem Canli MSc. for their substantial work mapping landslide points in the province Lower Austria.

9. References

Aleotti P, Chowdhury R (1999) Landslide hazard assessment: summary review and new perspectives. Bull Eng Geol Environ 58:21–44.

Amt der NÖ Landesregierung (2013) Niederösterreich Atlas. In: Niederösterr. Atlas. http://atlas.noe.gv.at. Accessed 28 Oct 2013

Anders NS, Seijmonsbergen H (2008) Laser Altimetry and Terrain Analysis - A revolution in Geomorphology. GIM Int 36–39.

Antonini G, Ardizzone F, Cardinali M, et al. (2002) Surface deposits and landslide inventory map of the area affected by the 1997 Umbria-Marche earthquakes. Boll Soc Geol It Volume speciale n.1:843–853.

Ardizzone F, Cardinali M, Carrara A, et al. (2002) Impact of mapping errors on the reliability of landslide hazard maps. Nat Hazards Earth Syst Sci 2:3–14.

Ardizzone F, Fiorucci F, Santangelo M, et al. (2013) Very-High Resolution Stereoscopic Satellite Images for Landslide Mapping. In: Margottini C, Canuti P, Sassa K (eds) Landslide Sci. Pract. Springer Berlin Heidelberg, pp 95–101

Van Asselen S, Seijmonsbergen AC (2006) Expert-driven semi-automated geomorphological mapping for a mountainous area using a laser DTM. Geomorphology 78:309–320. doi: doi: DOI: 10.1016/j.geomorph.2006.01.037

Atkinson P, Jiskoot H, Massari R, Murray T (1998) Generalized linear modelling in geomorphology. Earth Surf Process Landf 23:1185–1195.

Baeza C, Lantada N, Moya J (2010) Influence of sample and terrain unit on landslide susceptibility assessment at La Pobla de Lillet, Eastern Pyrenees, Spain. Environ Earth Sci 60:155–167. doi: 10.1007/s12665-009-0176-4

Barlow J, Franklin S, Martin Y (2006) High spatial resolution satellite imagery, DEM derivatives, and image segmentation for the detection of mass wasting processes. Photogramm Eng Remote Sens 72:687–692.

Beguería S (2006) Validation and Evaluation of Predictive Models in Hazard Assessment and Risk Management. Nat Hazards 37:315–329. doi: 10.1007/s11069-005-5182-6

Bell R (2007) Lokale und regionale Gefahren- und Risikoanalyse gravitativer Massenbewegungen an der Schwäbischen Alb. Rheinische Friedrich-Wilhelms-Universität Bonn (available at http://hss.ulb.uni-bonn.de/2007/1107/1107.htm, 29 March 2014)

Bell R, Petschko H, Röhrs M, Dix A (2012) Assessment of landslide age, landslide persistence and human impact using airborne laser scanning digital terrain models. Geogr Ann Ser Phys Geogr 94:135–156.

Booth AM, Roering JJ, Perron JT (2009) Automated landslide mapping using spectral analysis and high-resolution topographic data: Puget Sound lowlands, Washington, and Portland Hills, Oregon. Geomorphology 109:132–147.

Brardinoni F, Slaymaker O, Hassan MA (2003) Landslide inventory in a rugged forested watershed: a comparison between air-photo and field survey data. Geomorphology 54:179–196.

Brunsden D (1985) Landslide types, mechanisms, recognition, identification. In: Morgan CS (ed)pp 19–28

Brunsden D (1993) Mass movement; the research frontier and beyond: a geomorphological approach. Geomorphology 7:85–128.

Calvello M, Cascini L, Mastroianni S (2013) Landslide zoning over large areas from a sample inventory by means of scale-dependent terrain units. Geomorphology 33–48.

Cardinali M, Ardizzone F, Galli M, et al. (2000) Landslides triggered by rapid snow melting: the December 1996 – January 1997 event in Central Italy. In: Claps P, Siccardi F (eds) Proc. 1st Plinius Conf. Bios Publisher, Cosenza, Maratea, pp 439–448.

Carrara A (1993) Uncertainty in evaluating landslide hazard and risk. Predict. Percept. Nat. Hazards. Kluwer Academic Publishers, Netherlands, pp 101–109.

Carrara A, Crosta G, Frattini P (2003) Geomorphological and historical data in assessing landslide hazard. Earth Surf Process Landf 28:1125–1142.

Carrara A, Merenda L (1976) Landslide inventory in northern Calabria, southern Italy. Geol Soc Amer Bull 87:1153–1162.

Cascini L (2008) Applicability of landslide susceptibility and hazard zoning at different scales. Eng Geol 102:164–177

Chigira M, Duan F, Yagi H, Furuya T (2004) Using an airborne laser scanner for the identification of shallow landslides and susceptibility assessment in an area of ignimbrite overlain by permeable pyroclastics. Landslides 1:203–209.

Christman MC (2000) A Review of Quadrat-Based Sampling of Rare, Geographically Clustered Populations. J Agric Biol Environ Stat 5:168–201.

Chung CJ, Fabbri AG (2008) Predicting landslides for risk analysis–Spatial models tested by a cross-validation technique. Geomorphology 94:438–452.

Chung CJ., Fabbri AG (2003) Validation of spatial prediction models for landslide hazard mapping. Nat Hazards 30:451–472.

Cigna F, Bianchini S, Casagli N (2012) How to assess landslide activity and intensity with Persistent Scatterer Interferometry (PSI): the PSI-based matrix approach. Landslides 10:267–283.

CNR-IRPI-Turin (1998) Determinazione delle fasce fluviali di alcuni corsi d'acqua lombardi ai fini urbanistici: Torrente Stafora. Final report. CNR-IRPI-Turin, Torino, Italy

Colesanti C, Wasowski J (2006) Investigating landslides with space-borne Synthetic Aperture Radar (SAR) interferometry. Eng Geol 88:173–199.

Cruden DM, Varnes DJ (1996) Landslide types and processes. In: Turner AK, Schuster RL (eds) Landslides Investig. Mitig. Transportation Research Board Special Report 247, Washington D.C, pp 36–75.

Dai FC, Lee CF (2002) Landslide characteristics and slope instability modeling using GIS, Lantau Island, Hong Kong. Geomorphology 42:213–228.

Dalyot S, Keinan E, Doytsher Y (2008) Landslide Morphology Analysis Model Based on LiDAR and Topographic Dataset Comparison. Surv Land Inf Sci 68:155–170.

Van Den Eeckhaut M, Kerle N, Poesen J, Hervás J (2012) Object-oriented identification of forested landslides with derivatives of single pulse LiDAR data. Geomorphology 173-174:30–42.

Van Den Eeckhaut M, Moeyersons J, Nyssen J, et al. (2009) Spatial patterns of old, deep-seated landslides: A case-study in the northern Ethiopian highlands. Geomorphology 105:239–252.

Van Den Eeckhaut M, Poesen J, Verstraeten G, et al. (2007) Use of LIDAR-derived images for mapping old landslides under forest. Earth Surf Process Landf 32:754–769.

Van Den Eeckhaut M, Vanwalleghem T, Poesen J, et al. (2006) Prediction of landslide susceptibility using rare events logistic regression: a case-study in the Flemish Ardennes (Belgium). Geomorphology 76:392–410.

Duman TY, Çan T, Emre \Ö, et al. (2005) Landslide inventory of northwestern Anatolia, Turkey. Eng Geol 77:99–114.

Eisinger U, Gutdeutsch R, Hammerl C (1992) Beiträge zur Erdbebengeschichte von Niederösterreich. Amt der NÖ Landesregierung, Landesamtsdirektion, Wien.

Fabbri AG, Chung CJF, Cendrero A, Remondo J (2003) Is prediction of future landslides possible with a GIS? Nat Hazards 30:487–503.

Felicísimo ÁM, Cuartero A, Remondo J, Quirós E (2012) Mapping landslide susceptibility with logistic regression, multiple adaptive regression splines, classification and regression trees, and maximum entropy methods: a comparative study. Landslides.

Fell R, Corominas J, Bonnard C, et al. (2008) Guidelines for landslide susceptibility, hazard and risk zoning for land use planning. Eng Geol 102:85–98.

Fernández T, Irigaray C, El Hamdouni R, Chacón J (2003) Methodology for landslide susceptibility mapping by means of a GIS. Application to the Contraviesa area (Granada, Spain). Nat Hazards 30:297–308.

Fiorucci F, Cardinali M, Carlà R, et al. (2011) Seasonal landslide mapping and estimation of landslide mobilization rates using aerial and satellite images. Geomorphology 129:59–70.

Galli M, Ardizzone F, Cardinali M, et al. (2008) Comparing landslide inventory maps. Geomorphology 94:268–289.

Ghosh S, van Westen CJ, Carranza EJM, et al. (2012) Generating event-based landslide maps in a data-scarce Himalayan environment for estimating temporal and magnitude probabilities. Eng Geol 128:49–62.

Glade T, Anderson MG, Crozier, M.J. (2005) Landslide Hazard and Risk. John Wiley & Sons, Ltd, Chichester, England.

Glade T, Frances F, Albini P (2001) The use of historical data in natural hazard assessments. Kluwer Academic Publishers.

Glenn NF, Streutker DR, Chadwick DJ, et al. (2006) Analysis of LiDAR-derived topographic information for characterizing and differentiating landslide morphology and activity. Geomorphology 73:131–148.

Guns M, Vanacker V (2012) Logistic regression applied to natural hazards: rare event logistic regression with replications. Nat Hazards Earth Syst Sci 12:1937–1947.

Guzzetti F (2005) Landslide hazard and risk assessment. Dissertation, Rheinischen Friedrich-Wilhelms-Universität Bonn. (available at http://hss.ulb.uni-bonn.de/2006/0817/0817.htm, 29 March 2014)

Guzzetti F, Mondini A, Cardinali M, et al. (2012) Landslide inventory maps: New tools for an old problem. Earth-Sci Rev 112:42–66.

Guzzetti F, Reichenbach P, Ardizzone F, et al. (2006) Estimating the quality of landslide susceptibility models. Geomorphology 81:166–184.

Haneberg WC, Creighton AL, Medley EW, Jonas DA (2005) Use of LiDAR to assess slope hazards at the Lihir gold mine, Papua New Guinea.

Harp EL, Keefer DK, Sato HP, Yagi H (2011) Landslide inventories: The essential part of seismic landslide hazard analyses. Eng. Geol.

Herrera G, Notti D, García-Davalillo JC, et al. (2010) Analysis with C- and X-band satellite SAR data of the Portalet landslide area. Landslides 8:195–206.

Ver Hoef J (2002) Sampling and geostatistics for spatial data. Ecoscience 9:152–161.

Hydrographischer Dienst des Landes Niederösterreich (Hydrographic Service of Lower Austria) (2011) Wasserstandsnachrichten und Hochwasserprognosen Niederösterreich. http://www.noel.gv.at/Externeseiten/wasserstand/wiskiwebpublic/maps_N_0.htm?entryparakey=N. Accessed 2 Mar 2011

Ibsen ML, Brunsden D (1996) The nature, use and problems of historical archives for the temporal occurrence of landslides, with specific reference to the south coast of Britain, Ventnor, Isle of Wight. Geomorphology 15:241–258.

Jaboyedoff M, Oppikofer T, Abellán A, et al. (2010) Use of LIDAR in landslide investigations: a review. Nat Hazards 61:5–28.

Kociu A, Kautz H, Tilch N, et al. (2007) Massenbewegungen in Österreich. Jahrb. Geol. Bundesanst. Geologische Bundesanstalt, Wien, pp 215–220

Krebs CJ (1999) Ecological Methodology, 2nd edition. Addison-Wesley Educational Publishers Inc., Benjamin Cummings, Menlo Park, CA.

Leica Geosystems (2003) ALS50 Airborne Laser Scanner, product description. 10.

Malamud BD, Turcotte DL, Guzzetti F, Reichenbach P (2004) Landslide inventories and their statistical properties. Earth Surf Process Landf 29:687–711.

Mantovani F, Soeters R, Van Westen CJ (1996) Remote sensing techniques for landslide studies and hazard zonation in Europe. Geomorphology 15:213–225.

Martha TR, Kerle N, Jetten V, et al. (2010) Characterising spectral, spatial and morphometric properties of landslides for semi-automatic detection using object-oriented methods. Geomorphology 116:24–36.

Martha TR, Kerle N, van Westen CJ, et al. (2012) Object-oriented analysis of multi-temporal panchromatic images for creation of historical landslide inventories. ISPRS J Photogramm Remote Sens 67:105–119.

McCalpin J (1984) Preliminary age classification of landslides for inventory mapping. Moscow, Idaho, pp 99–111.

McKenna JP, Lidke DJ, Coe JA (2008) Landslides Mapped from LIDAR Imagery, Kitsap County, Washington. US Geol Surv Open-File Rep 1292:81.

Mondini AC, Guzzetti F, Reichenbach P, et al. (2011) Semi-automatic recognition and mapping of rainfall induced shallow landslides using optical satellite images. Remote Sens Environ 115:1743–1757.

Optech (2008a) ALTM 3100. 2.

Optech (2008b) ALTM Gemini. 2.

Pereira S, Zêzere JL, Quaresma ID, Bateira C (2014) Landslide incidence in the North of Portugal: Analysis of a historical landslide database based on press releases and technical reports. Geomorphology In Press.

Petschko H, Bell R, Glade T (2014a) Relative age estimation at landslide mapping on LiDAR derivatives – revealing the applicability of land cover data in statistical susceptibility modelling. Landslide Risk Mitig. Safer Geoenvironment. Springer, p In Press.

Petschko H, Bell R, Leopold P, et al. (2013) Landslide inventories for reliable susceptibility maps in Lower Austria. In: Margottini C, Canuti P, Sassa K (eds) Landslide Sci. Pract. Springer, pp 281–286

Petschko H, Bell, R., Brenning A, Glade T (2012) Landslide susceptibility modeling with generalized additive models - facing the heterogeneity of large regions. In: Eberhardt E, Froese C, Turner AK, Leroueil S (eds)Taylor & Francis, Banff, Alberta, Canada, pp 769–777

Petschko H, Brenning A, Bell R, et al. (2014b) Assessing the quality of landslide susceptibility maps – case study Lower Austria. Nat Hazards Earth Syst Sci 14:95–118.

Petschko H, Glade T, Bell R, et al. (2010) Landslide inventories for regional early warning systems.

Remondo J, González A, De Terán JRD, et al. (2003) Validation of landslide susceptibility maps; examples and applications from a case study in Northern Spain. Nat Hazards 30:437–449.

Riegl (2010) LMS-Q560 Airborne Laser Scanner for Full Waveform Analysis. Austria, Japan, USA.

Röhrs M, Dix A (2010) Rekonstruktion historischer Ereignisse. In: Bell R, Mayer J, Pohl J, et al. (eds) Integr. Frühwarnsysteme Für Gravitative Massenbewegungen ILEWS Monit. Modellier. Implementierung. Klartextverlag, Essen, pp 46–61 & 261–264.

Rossi M, Witt A, Guzzetti F, et al. (2010) Analysis of historical landslide time series in the Emilia-Romagna region, northern Italy. Earth Surf Process Landf 35:1123–1137.

Ruß G, Brenning A (2010) Data mining in precision agriculture: management of spatial information. Lect Notes Comput Sci 350–359.

Santacana N, Baeza B, Corominas J, et al. (2003) A GIS-based multivariate statistical analysis for shallow landslide susceptibility mapping in La Pobla de Lillet area (Eastern Pyrenees, Spain). Nat Hazards 30:281–295.

Santangelo M, Cardinali M, Rossi M, et al. (2010) Remote landslide mapping using a laser rangefinder binocular and GPS. Nat Hazards Earth Syst Sci 10:2539–2546.

Schnabel W (2002) Geologische Karte von Niederösterreich 1:200,000.

Schulz WH (2004) Landslides mapped using LIDAR imagery, Seattle, Washington. US Geol. Surv. Open-File Rep. 1396:

Schweigl J, Hervás J (2009) Landslide Mapping in Austria. 65.

Schwenk H (1992) Massenbewegungen in Niederösterreich 1953 - 1990. Jahrb. Geol. Bundesanst. Geologische Bundesanstalt, Wien, pp 597–660

Soeters R, Van Westen CJ (1996) Slope instability recognition, analysis and zonation. In: Turner AK, Schuster RL (eds) Landslides Investig. Mitig. National Academy Press, Washington, USA, p 129*177

SpatialModels Inc. (2006) Spatial Prediction Modeling System User's Guide. 132.

Tarolli P, Sofia G, Dalla Fontana G (2010) Geomorphic features extraction from high-resolution topography: landslide crowns and bank erosion. Nat Hazards 1–19.

Thompson SK (2012) Sampling, 3rd Edition. John Wiley & Sons Inc., Hoboken, New Jersey

Tobler D, Riner R, Pfeifer R (2013) Runout Modelling of Shallow Landslides Over Large Areas with SliDepot. In: Margottini C, Canuti P, Sassa K (eds) Landslide Sci. Pract. Springer, Heidelberg, pp 239–245

Townsend Peterson A, Papeş M, Eaton M (2007) Transferability and model evaluation in ecological niche modeling: a comparison of GARP and Maxent. Ecography 30:550–560.

Varnes DJ (1984) Landslilde hazard zonation: a review of principles and practice. United Nations Educational, Scientificc and Cultural Organization, Paris, France

Wessely G (2006) Geologie der österreichischen Bundesländer - Niederösterreich. Geologische Bundesanstalt, Wien

Van Westen CJ, Asch TWJ, Soeters R (2006) Landslide hazard and risk zonation—why is it still so difficult? Bull Eng Geol Environ 65:167–184.

Van Westen CJ, Castellanos E, Kuriakose SL (2008) Spatial data for landslide susceptibility, hazard, and vulnerability assessment: An overview. Eng Geol 102:112–131.

Van Westen CJ, Lulie Getahun F (2003) Analyzing the evolution of the Tessina landslide using aerial photographs and digital elevation models. Geomorphology 54:77–89.

Van Westen CJ, Rengers N, Terlien MTJ, Soeters R (1997) Prediction of the occurrence of slope instability phenomena through GIS-based hazard zonation. Geol Rundsch 86:404–414.

Whitworth MCZ, Giles DP, Murphy W (2005) Airborne remote sensing for landslide hazard assessment: a case study on the Jurassic escarpment slopes of Worcestershire, UK. Q J Eng Geol Hydrogeol 38:285–300.

Wieczorek G (1984) Preparing a detailed landslide-inventory map for hazard evaluation and reduction. G Bull Assoc Engng Geol 21:337–342.

Zanutta A, Baldi P, Bitelli G, et al. (2006) Qualitative and quantitative photogrammetric techniques for multi-temporal landslide analysis. Ann Geophys 49:1067–1080.

Zezere JL, de Brum Ferreira A, Rodrigues ML (1999) The role of conditioning and triggering factors in the occurrence of landslides: a case study in the area north of Lisbon (Portugal). Geomorphology 133–146.

Acknowledgement of receipt of the manuscript at “Landslides” Journal, Springer

Betreff: Acknowledgement of Receipt
Von: "Editorial Office" <marieveth.chua@springer.com>
Datum: 02/04/2014 12:04 AM
An: "Helene Petschko" <helene.petschko@univie.ac.at>

Dear Helene Petschko:

Thank you for submitting your manuscript, "Landslide inventory mapping for large regions - effectiveness of visually analyzing LiDAR DTM derivatives", to Landslides.

During the review process, you can keep track of the status of your manuscript by accessing the following web site:

http://lasl.edmgr.com/

Your username is: HPetschko-967
Your password is: petschko48465

If you have any questions, please contact us.

With kind regards,

The Editorial Office
Landslides

(02.04.2014)

Tab. 4 Details on the mapping area, scale, data source, number of investigators (P), time, person months (PM), number of landslides mapped (N), area mapping rate, area mapping and digitizing rate and landslide mapping rate of the inventories compared for the inventories of this study with international examples published by Guzzetti et al. (2012). The original table of Guzzetti et al. (2012) was updated (marked with *), partly simplified to include sliding processes mainly (where replicable from the publications) and additional information on the number of mapped landslides was added. It is distinguished between different types of inventory: G=geomorphological / historical inventory; E= event inventory; M= multi temporal inventory. Furthermore the type of imagery is stated: AP = Aerial photograph; SI = Satellite images; LI = (airborne) LiDAR derivatives (Guzzetti et al., 2012). The time for digitizing an inventory mapped analogue on aerial photographs was only considered where the information was available in the publications. Sources: (1) Cardinali et al. 1990, (2) Guzzetti and Cardinali 1989, (3) Antonini et al. 2002a, (4) Galli et al. 2008, (5) Cardinali et al. 2000, (6) Guzzetti et al. 2004, (7) Mondini et al., 2011, (8) Ardizzone et al. 2007, (9) Fiorucci et al. 2011, (10) Petschko et al. 2013 and this contribution, (11) this contribution, (12) Glade et al. 2012 and this contribution. [+] No information on single landslide polygons is available, only on areas affected by landslides.

ID	Study area	Size	Type	Scale		Imagery			Investigators (P)		Time [Months]		Person months (PM)	Number of landslides (N)	Area mapping rate	Area mapping and digitizing rate	Landslide mapping rate	
		[km²]		Production	Publication	Type	Sets	Scale/resolution	Mapping	Digitizing	Mapping	Digitizing	Mapping + digitizing		[km²/P/month]	[km²/P/month]	[N/PM]	[N/PM/km²]
1	New Mexico, USA	315,194	G	1:100,000	1:500,000	AP	1(2)	1:31,500; 1:12,000; 1:58,000	2	n.i.	18	n.i.	36	9000	8755	n.i.	250	0.0008
2	Umbria, Italy	8456	G	1:25,000	1:100,000	AP	1	1:33,000	2	1	9	2	20	5270	470	423	264	0.0312
3	Umbria, Italy	8456	G	1:10,000	1:25,000	AP	2(1)	1:33,000; 1:13,000;1:73,000	4	4	28	20	192	47414	100	44	247	0.0292
4	Collazzone, Italy	79	M	1:10,000	1:10,000	AP	5	1:13,000; 1:33,000	2	1	5	1	11	2564	8	7	233	2.9505
5	Umbria, Italy	1500	E	1:10,000	1:10,000	AP	1	1:20,000	2	n.i.	6	n.i.	12	4000	125	n.i.	333	0.2222
6	Imperia, Italy	500	E	1:10,000	1:10,000	AP	2(1)	1:13,000, 1:5000; 1:55,000	2	n.i.	2	n.i.	4	1204	125	n.i.	301	0.6020
7	Messina, Italy *	9.4	E	1:10,000	1:10,000	AP	2	1:3500, 1:4500	2.5	2	0.58	0.16	1.8	821	6	5	463	49.2282
		9.4	E	1:10,000	1:10,000	SI	2	0.6 m x 0.6 m	2		0.16		0.3	821	29		2545	270.755[+]
8	Collazzone, Italy	10	E	1:10,000	1:10,000	LI	1	2 m x 2 m	1		2		2	47	5		24	2.3500
9	Collazzone, Italy	79	S	1:10,000	1:10,000	SI	2	1 m x 1 m, 0.5 m x 0.5 m	1		3		3	542	26		288	0.6793
10	Test districts - polygons, Austria	2073	G	1:2,000	1:10,000	LI	1	1 m x 1 m	1		4		4	1834	518		459	0.2212
11	Test districts - points, Austria	2073	G	1:2,000	1:10,000	LI	1	1 m x 1 m	1		1.5		1.5	3994	1382		2663	1.2846
12	Lower Austria	19,186	G	1:2,000	1:25,000	LI	1	1 m x 1 m	5		3.2		16	13166	1199		823	0.0429

A.8. Relative age estimation at landslide mapping on LiDAR derivatives – revealing the applicability of land cover data in statistical susceptibility modeling

Petschko, H., Bell, R. & T., Glade (2014) Relative Age Estimation at Landslide Mapping on LiDAR Derivatives: Revealing the Applicability of Land Cover Data in Statistical Susceptibility Modelling. In: Sassa, K., Canuti, P., & Y., Yin (Eds.) Landslide Science for a Safer Geoenvironment. Springer International Publishing, 337–343.

Relative Age Estimation at Landslide Mapping on LiDAR Derivatives: Revealing the Applicability of Land Cover Data in Statistical Susceptibility Modelling

Helene Petschko, Rainer Bell, and Thomas Glade

Abstract

In statistical landslide susceptibility modelling the identification of appropriate explanatory variables describing the predisposing and preparatory factors for the landslides of a given inventory is important. In this context information on the age and the respective land cover at the time of occurrence is beneficiary. The potential of mapping very old (or prehistoric) landslides using LiDAR derivatives has not been analysed yet. Additionally, performing a visual interpretation of derivatives of a single LiDAR DTM it is not possible to assign the accurate age or date of the occurrence of the event to each mapped landslide. Therefore, commonly no information on the land cover at the time of landslide occurrence for these very old landslides (but also for younger ones) is available. The objective of this study is, to estimate the relative age of landslides during the mapping and to explore differences of the recent land cover distribution in the relative ages of the landslides. This is performed to evaluate the sustainability of including recent land cover data into susceptibility modelling. The relative age of the landslides is estimated for each landslide according to its morphological footprint on the LiDAR DTM derivatives and to its appearance on the orthophoto. The different relative ages assigned are "very old", "old", "young" and "very young". The study area is located in three districts of Lower Austria, namely Amstetten, Baden and Waidhofen/Ybbs. The resulting inventory includes 1834 landslides and shows that the "very old" and "old" landslides (60 % of all mapped landslides) are mainly covered by forest (~60 % of all land cover types). We conclude that using this inventory including recent land cover data in the susceptibility model is not appropriate for Lower Austria. There is a potential of mapping "old" or "very old" landslides on the LiDAR derivatives. The absolute age remains unknown.

Keywords

Landslide inventory mapping • LiDAR derivatives • Relative landslide age • Recent land cover map

Introduction

As no detailed information on the date of occurrence of the landslides can be determined from the LiDAR derivatives (or other remote sensing techniques, Van Westen et al. 2005) the age of the landslides can only be estimated relatively in the study area. Whereas the determination of relative landslide age is very common in studies mapping landslides on aerial photographs or orthophotos (e.g. Ardizzone et al. 2002;

H. Petschko (✉) • R. Bell • T. Glade
Department of Geography and Regional Research, University of Vienna, Universitaetsstrasse 7 1010, Vienna, Austria
e-mail: helene.petschko@univie.ac.at; rainer.bell@univie.ac.at; thomas.glade@univie.ac.at

K. Sassa et al. (eds.), *Landslide Science for a Safer Geoenvironment*, Vol. 2,
DOI 10.1007/978-3-319-05050-8_53, © Springer International Publishing Switzerland 2014

Table 1 Land cover evaluated for landslide polygons according their landslide type and relative landslide age

Land cover unit	Study area (%)	All landslides (%)	Slide (%)	Area with slides (%)	Flow (%)	Complex (%)	Young (%)	Very young (%)	Old (%)	Very old (%)
Coniferous forest	12.77	19.97	25.72	16.60	11.80	16.60	5.80	0.92	16.89	23.65
Mixed forest	13.89	20.04	20.05	19.52	24.96	10.14	13.27	7.18	26.04	17.65
Deciduous forest	13.65	20.19	18.08	21.86	21.74	24.46	11.91	5.19	17.90	22.91
Arable land	17.70	15.93	10.66	19.08	19.89	19.01	29.81	20.89	18.01	13.14
Grassland, pasture	10.14	11.25	10.21	11.85	12.10	20.66	22.03	38.08	10.05	10.10
Rough pasture	10.48	8.21	9.96	7.09	8.85	8.37	13.58	23.45	8.47	7.16
Snow, Ice	0.02	0.00	0.00	0.01	0.00	0.00	0.00	0.00	0.00	0.01
Debris	9.38	1.54	3.73	0.15	0.01	0.00	0.09	3.63	0.08	2.39
Fallow land	9.76	2.49	1.41	3.36	0.54	0.63	3.35	0.53	2.25	2.58
Housing settlement	1.66	0.31	0.20	0.39	0.10	0.13	0.15	0.11	0.32	0.32
Water	0.41	0.01	0.00	0.01	0.00	0.00	0.00	0.00	0.00	0.01
NA	0.14	0.06	0.00	0.09	0.00	0.00	0.01	0.00	0.00	0.09

Cardinali et al. 2002; Guzzetti et al. 2003; Guzzetti 2005; Zanutta et al. 2006), in studies using LiDAR derivatives as mapping basis only few attention is dedicated to this topic so far (e.g. Bell et al. 2012). Therein the potential mapping of "very old" (prehistoric (Schulz 2004)) landslides and its effects on the subsequent application of the inventory are not considered or analysed yet. The quality of the inventory and the information on the landslides stored in it are of importance for any application of the inventory (Ardizzone et al. 2002; Guzzetti et al. 2012; Petschko et al. 2014; Van Westen et al. 2005). Precisely in the context of this study the inventory is a basis for statistical susceptibility modelling in Lower Austria (Petschko et al. 2014) where the resulting susceptibility map is dependent on the model input data and their geomorphological relevance. In this context the landslide age or event date is of importance, as trigger factors or also the land cover is considered as an explanatory variable for landslide susceptibility modelling. However, if the inventory contains "very old" (or prehistoric) landslides, they cannot be related to a trigger event (Van Westen et al. 2005) and the recent land cover information might not match the land cover at the time of the occurrence of the mapped landslides.

This study is aimed to analyse the potential of LiDAR derivatives to map landslides of different age and to assess the landslide age in a relative manner within the study area. Furthermore, the objective is to compare the relative landslide age with the recent land cover map. This is done to evaluate the sustainability of including recent land cover data into susceptibility modelling using a landslide inventory originating from visual analysis of LiDAR derivatives.

Study Area

The study area is located in the three districts Amstetten (1,187 km^2), Baden (754 km^2) and Waidhofen/Ybbs (131 km^2) in the province of Lower Austria. These districts show a high heterogeneity regarding their land cover, topography and susceptibility to landslides (Petschko et al. 2012). Whereas 40 % of the study area is covered by forest (coniferous, mixed and deciduous forest) 48 % of the area is covered by farmland (arable land, (rough) pasture and fallow land, Table 1). However, the predominant land cover type changes distinctly, as for example in the districts Amstetten and Waidhofen/Ybbs the North is mainly covered by farmland but the South is dominated by forest (Fig. 1).

The main lithological units in the study area are (from North to south) the Bohemian Massif, the Molasse Zone (including the "Schlier"), the Loess and Loam, the Flysch and Klippen Zone and the Austroalpine Unit with dolostone or with limestone and marls.

Landslides are abundant especially in the Flysch and Klippen Zone, as an existing landslide inventory resulting

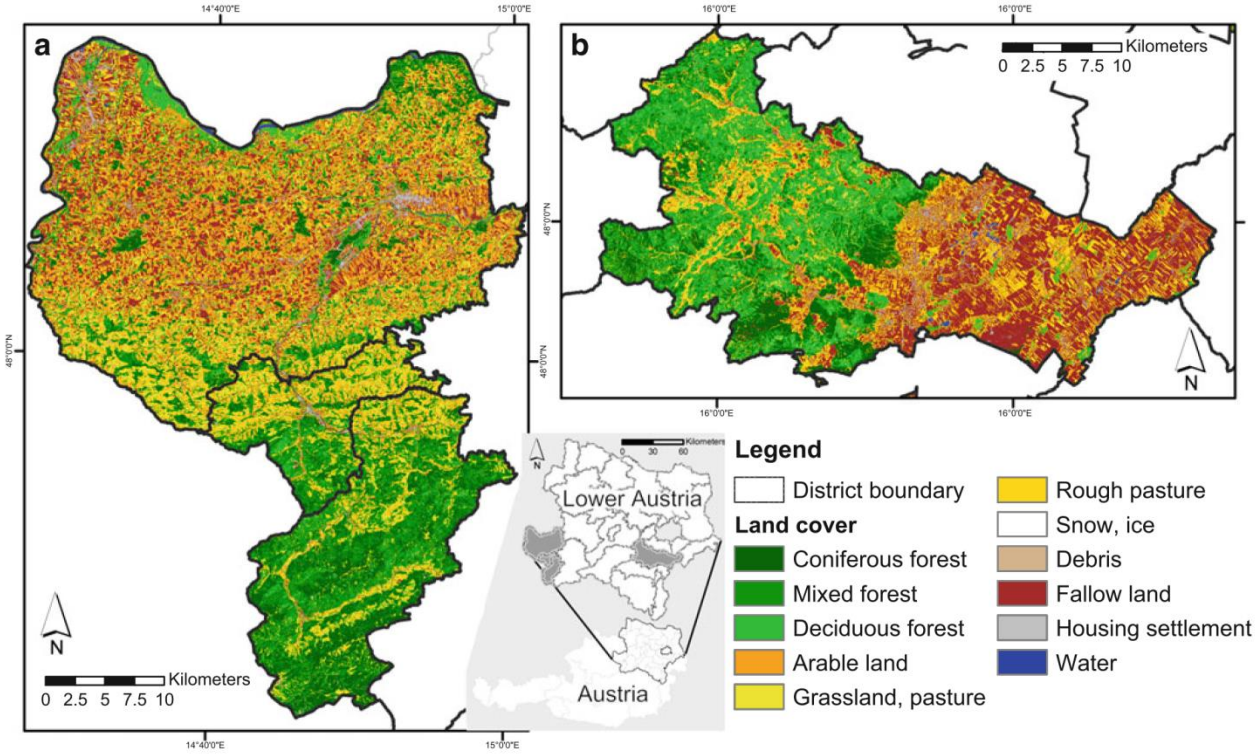

Fig. 1 Land cover in the study area in Lower Austria ((**a**) Amstetten, Waidhofen/Ybbs, (**b**) Baden)

from an archive of the Geological Survey of Austria (building ground register (BGR)) shows (Petschko et al. 2013; Schwenk 1992). The landslides mainly occurred under very wet conditions either due to heavy rainfall, rapid snow melt events or a combination of both (Schweigl and Hervás 2009).

Data

Data available in this study include a high resolution LiDAR DTM (1 × 1 m, acquired in 2006–2009, multiple acquisition years were necessary to cover the entire area), an orthophoto from 2002 (25 × 25 cm) and a land cover map derived from ASTER data (resampled to 10 × 10 m; 2007).

Methods

Landslide Inventory Mapping

During the landslide mapping the specific morphological features, which are left after a landslide event occurred, are visually analysed and used to identify landslides, also in forested areas. The landslide inventory mapping was performed in a previous study (Petschko et al. 2013) by visually interpreting hillshade maps of different azimuth angle (315°, 135°, 45°, (as used by Schulz 2004)), a slope map, contour lines with 4 m elevation difference and an orthophoto to delineate landslide polygons (Petschko et al. 2013). The mapping scale for identifying landslides was 1:2,000, however the polygons have been digitized at a scale of 1:200–1:1,000. During the mapping of the landslides different types were distinguished: "slide" (earth and debris slide), "flow" and "complex" following Cruden and Varnes (1996) (Petschko et al. 2013; Petschko et al. 2010). Areas with many landslides of different generations and where the delineation of single landslides was hardly possible were mapped as an "area of slides" (Petschko et al. 2010). Furthermore, the certainty of the delineation of the polygon was assigned as certain or uncertain for each polygon.

Relative Age Estimation

The relative age estimation is based on an approach proposed by McCalpin (1984) interpreting the morphology and the "freshness" of the morphological features that remain visible after the occurrence of a landslide on LiDAR DTM derivatives and orthophotos.

According to this concept the landslide morphology experiences a transformation starting from a feature showing every landslide detail (e.g. main and minor scarps, landslide

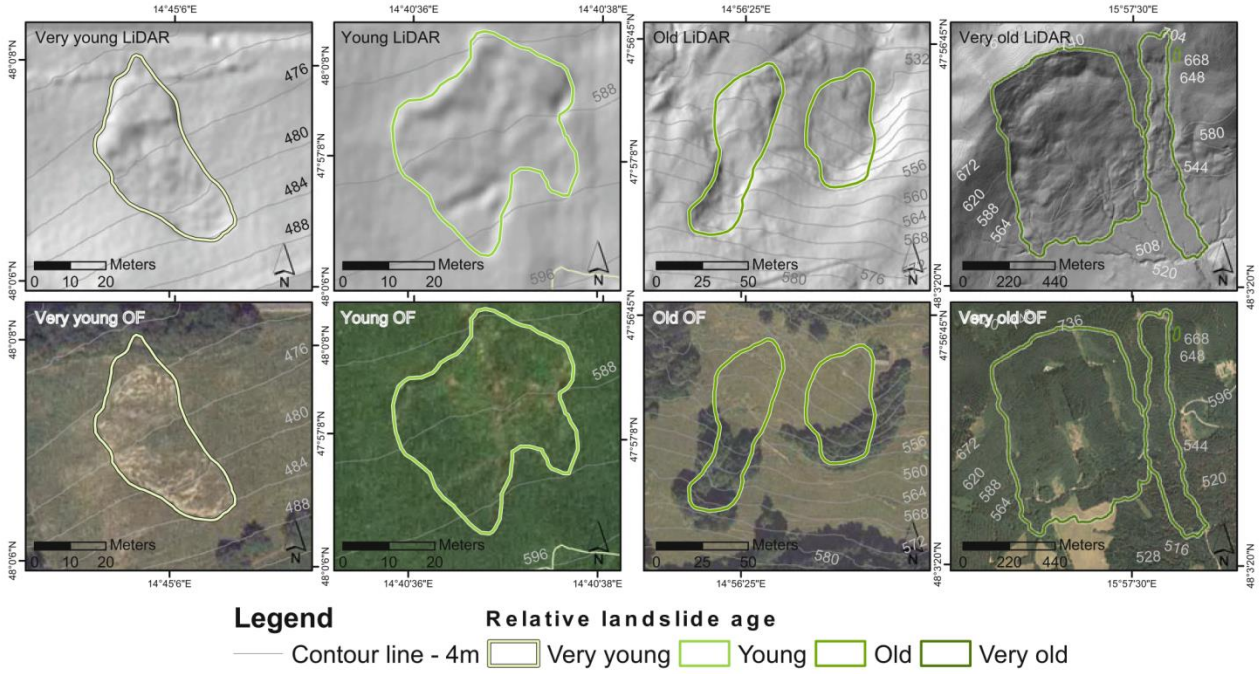

Fig. 2 Relative landslide age as estimated by the morphology visible on the LiDAR derivatives and by the vegetation cover visible on the orthophoto (OF). The relative age classes were defined "very young", "young", "old" and "very old". Note the different size of the four presented landslides as indicated by the scale bar

toe and fissures) very clear. The older the landslide gets and the longer it is exposed to erosion the more features of erosion will be visible. First the landslide forms will get smoother, later erosion and incision of streams will occur and reshape the morphology (Bell et al. 2012; McCalpin 1984). Furthermore, the vegetation cover is of importance to assess the relative age of the landslides (McCalpin 1984). We assume that in our study area the first occurrence of landslides is mainly on open land (not forested land). In literature this assumption is often related to the reinforcing effect of tree roots on the slope stability (Rickli and Graf 2009). In the field we learned that often after the landslide occurred farming of the land became more difficult and it was abandoned to forest growth.

Adapted after McCalpin (1984) we assign (1) "very young" to landslides which are not vegetated at least at the main scarp and which show a very fresh, rugged morphology (Fig. 2); (2) "young" to landslides which are fully vegetated (grass) and have a smoother morphology, which shows first modifications of the original topography due to erosion and deposition; (3) "old" to landslides which still show a distinct main scarp but a smooth morphology with dense vegetation cover (partly brushes or forest); (4) "very old" to landslides which are characterized by a very smooth morphology, by the re-establishing of the valley drainage pre-slide profile and by a dense vegetation cover. This vegetation cover is of the same age or density as the surrounding vegetation. This relative age estimation was performed for each landslide and landslide type during the mapping process.

Comparison of Land Cover and Relative Landslide Age

The land cover of the mapped landslides was derived from the available land cover map on a grid cell base. Therefore, only the landslides classified as certain in their delineation and type were analysed further. This landslide inventory was split according to the assigned landslide age in four data sets. Each of this data set was used to mask the land cover map in ArcGIS (Version 9.3). Therewith the amount of pixel in each land cover class per landslide age was determined.

Results and Discussion

Landslide Inventory Mapping

The resulting landslide inventory contains 2,014 landslides of which 1,834 are considered to be of high certainty regarding the delineation and type of process (Petschko et al. 2013). The main mapped landslide type was "slide"

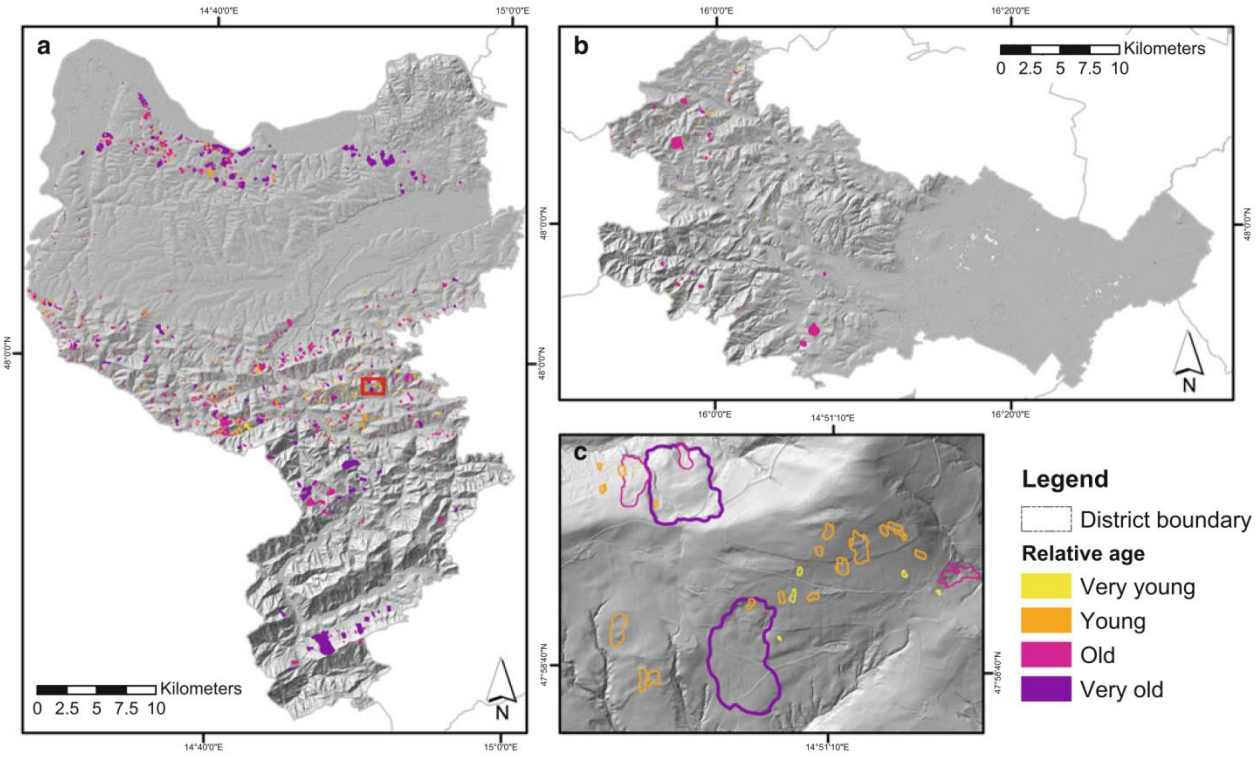

Fig. 3 Results of the relative landslide age estimation for (**a**) Amstetten and Waidhofen/Ybbs, (**b**) Baden. (**c**) Zoom to an example area. The relative age classes were defined "very young", "young", "old" and "very old"

(75 %). 20.5 % of the polygons of the landslide inventory were classified as "area with slides".

Analysing all landslide types we found that these landslides are mainly located in forested areas (20.2 % in deciduous forest, 20 % in mixed forest and 19.9 % in coniferous forest, Table 1). Around 16 % of all landslides are located in arable land and 11 % are covered by grassland or pasture. Within the different landslide types the variation of land cover (forest (coniferous, mixed and deciduous)/no forest (arable land, grassland, pasture, fallow land and rough pasture)) is minor (Table 1). "Slides" (earth and debris slides) show the largest proportion of forested cells (64 %) whereas "complex landslides" only show a forest cover for 51 % of the cells. However, these results show, that more than half of the landslide cells are covered by forest.

Relative Age Estimation

With the relative age estimation we found that 8 % of the landslides were classified as "very young", 10 % as "very old", 34 % as "young" and nearly half of the landslides (48 %) were assigned as "old" (Fig. 3). During the mapping of "young" or "very young" landslides the combined interpretation of orthophoto and LiDAR derivatives was found to be effective. In this way, also landslides with a very short travel distance and a clear but small main scarp could be easily identified. However, for "old" and "very old" landslides the availability of LiDAR derivatives is important. On orthophotos (or aerial photographs) the vegetation cover (mainly forest) does not allow the interpretation of the morphology and therefore the identification of a landslide, as shown in Fig. 2 with the "very old" landslide, is not possible (Brardinoni et al. 2003). Nevertheless, the interpretation of the LiDAR derivatives only might be misleading due to effects of morphological convergence (Antonini et al. 2002) or the conservation effect of forest cover on the landslide morphology. Examples for morphological convergence found in the study area are quarries or artefacts in the DTM due to the removal of single trees, houses and infrastructure. The conservation effect describes morphology that appeared to be fresh and "young" but the type of vegetation (forest), field checks and the starting re-establishing of the valley drainage in the lower part of the landslide revealed the landslide to be "very old" (Fig. 2). Therefore, the comparison with the vegetation cover (grass or forest) during the mapping is of high importance.

Furthermore, regarding the completeness of the inventory it has to be taken into account, that in agriculturally used areas the persistence of the landslide morphology is restricted.

Among the landslides with low persistence mainly "young" or "very young" landslides are not visible on the orthophoto or the LiDAR derivatives anymore (Bell et al. 2012). In these areas, the visibility of landslides is influenced by the activity of local farmers. Immediately after a landslide event smaller landslides are levelled to ensure the harvest or the usability of the area as pasture (Bell et al. 2012; Fiorucci et al. 2011). However, the number of landslides with low persistence and therefore landslides that are potentially missing from the inventory is unknown (Petschko et al. 2014).

In general it has to be pointed out that the relative landslide age estimated in this study is only applicable to the study area and its specific setting (e.g. topography, geology, vegetation, climate (Antonini et al. 2002)). Therefore, comparisons to the relative age of other areas are not possible.

Comparison of Land Cover and Relative Landslide Age

In contrast to the results of the land cover of all mapped landslides the splitting of the data into the different classes of relative age reveals large differences between the classes "very young" to "very old". In more detail we found that the percentage of the grid cells covered with forest (coniferous, deciduous or mixed) increases the older the landslides were estimated. An exception to this general trend is the mixed forest. Here the "old" landslides show the highest proportion of forested grid cells (26 %, Table 1). All forest types summed up, 13 % of the "very young" landslides, 31 % of the "young" landslides, 61 % of the "old" and 64 % of the "very old" landslides are covered by forest.

With 38 % the land cover class grassland and pasture covers a large area of the "very young" landslides. This land cover class was found for only 10 % of the "very old" landslides. Combining all not forested land cover classes (open land) we found that these cover 83 % of the "very young", 69 % of the "young", 39 % of the "old" and 33 % of the "very old" landslides.

These findings match the assumption that landslides mainly occur on open land and the forest grows after abandonment of the land. However, a Swiss study on six event landslide inventories in a lithological similar region showed, that directly after a rainstorm event nearly 50 % of the landslides occurred in forested terrain (Rickli and Graf 2009). Furthermore, a dendrogeomorphology study showed that landslides can reactivate under forest (Van Den Eeckhaut et al. 2009).

Besides, this results show, that also "very young" and "young" landslides are covered by forest (according to the ASTER land cover map). This is clearly contradictory to the age estimation criteria. However, the possible reasons for this misclassified grid cells can be (1) the difference in the resolution of the land cover data and the mapping scale of the landslides, (2) the algorithm used in the masking of the land cover by the landslides or (3) general problems in the supervised classification of the ASTER data.

Conclusions

The results of this study show that landslides of different relative age can be and are mapped when mapping landslides on the basis of LiDAR derivatives of one acquisition time only. Furthermore it was shown, that the interpretation of the morphology only can be misleading. Therefore, the combined usage of LiDAR and orthophotos is necessary. This potential mapping of very old landslides has to be considered before starting the mapping and might be overcome by restricting the mapping criteria on mapping young landslides only. However, the limited persistence of the landslide morphology of "young" and "very young" landslides in agricultural areas has additional influence on the completeness of the inventory.

At modelling with data on recent land cover the relative landslide age has to be accounted for, as no information on past land cover (at the time of the landslide occurrence) is available. Otherwise, there is a chance of introducing an unwanted bias into the susceptibility modelling. One solution can be the exclusion of "old" and "very old" landslides from the modelling sample. The alternative we propose is to use all landslides but to leave the land cover data out of the modelling. This might be considered, as the range of information on the topographical conditions (which are available in a much better spatial resolution as the land cover data) of the landslides might be better represented including the "old" and "very old" landslides in the analysis as well. Furthermore, leaving out the land cover but having better information on the topography can be of interest in case the land cover changes fast, e.g. by logging, and therefore the susceptibility map is soon not up-to-date anymore.

The absolute age of the landslides remains unknown. With the availability of multi-temporal LiDAR imagery the information on landslide age can be improved. However, this was not analysed in this study.

Acknowledgments The authors are thankful for the fruitful collaboration with the project clients and partners of the project "MoNOE—Method development for landslide susceptibility modelling in Lower Austria". We are grateful for the funding and provision of data by the Provincial Government of Lower Austria.

References

Antonini G, Ardizzone F, Cardinali M, Galli M, Guzzetti F, Reichenbach P (2002) Surface deposits and landslide inventory

map of the area affected by the 1997 Umbria-Marche earthquakes. Boll Soc Geol It Volume speciale n.1:843–853

Ardizzone F, Cardinali M, Carrara A, Guzzetti F, Reichenbach P (2002) Impact of mapping errors on the reliability of landslide hazard maps. Nat Hazards Earth Syst Sci 2:3–14

Bell R, Petschko H, Röhrs M, Dix A (2012) Assessment of landslide age, landslide persistence and human impact using airborne laser scanning digital terrain models. Geografiska Annaler: Series A, Physical Geography 94:135–156

Brardinoni F, Slaymaker O, Hassan MA (2003) Landslide inventory in a rugged forested watershed: a comparison between air-photo and field survey data. Geomorphology 54:179–196

Cardinali M, Reichenbach P, Guzzetti F, Ardizzone F, Antonini G, Galli M, Cacciano M, Castellani M, Salvati P (2002) A geomorphological approach to the estimation of landslide hazards and risks in Umbria, Central Italy. Nat Hazards Earth Syst Sci 2:57–72

Cruden DM, Varnes DJ (1996) Landslide types and processes. In: Turner AK, Schuster RL (eds) Landslides, investigation and mitigation. Transportation Research Board Special Report 247, Washington DC, pp 36–75

Fiorucci F, Cardinali M, Carlà R, Rossi M, Mondini AC, Santurri L, Ardizzone F, Guzzetti F (2011) Seasonal landslide mapping and estimation of landslide mobilization rates using aerial and satellite images. Geomorphology 129:59–70

Guzzetti F (2005) Landslide hazard and risk assessment. Dissertation, Rheinischen Friedrich-Wilhelms-Universität Bonn

Guzzetti F, Mondini A, Cardinali M, Fiorucci F, Santangelo M, Chang K-T (2012) Landslide inventory maps: New tools for an old problem. Earth-Sci Rev 112:42–66

Guzzetti F, Reichenbach P, Cardinali M, Ardizzone F, Galli M (2003) The impact of landslides in the Umbria region, central Italy. Nat Hazards Earth Syst Sci 3:469–486

McCalpin J (1984) Preliminary age classification of landslides for inventory mapping. University of Idaho, Moscow, pp 99–120

Petschko H, Bell R, Leopold P, Heiss G, Glade T (2013) Landslide inventories for reliable susceptibility maps in Lower Austria. In: Margottini C, Canuti P, Sassa K (eds) Landslide science and practice. Volume 1: Landslide inventory and susceptibility and hazard zoning. Springer, pp 281–286

Petschko H, Bell R, Brenning A, Glade T (2012) Landslide susceptibility modeling with generalized additive models - facing the heterogeneity of large regions. In: Eberhardt E, Froese C, Turner AK, Leroueil S (eds) Landslides and engineered slopes, protecting society through improved understanding. Taylor & Francis, Banff, Alberta, Canada, pp 769–777

Petschko H, Brenning A, Bell R, Goetz J, Glade T (2014) Assessing the quality of landslide susceptibility maps – case study Lower Austria. Nat Hazards Earth Syst Sci 14:95–118

Petschko H, Glade T, Bell R, Schweigl J, Pomaroli G (2010) Landslide inventories for regional early warning systems. In: Malet JP, Glade T, Casagli N (eds) Mountain risks: bringing science to society. CERG Editions, Strasbourg

Rickli C, Graf F (2009) Effects of forests on shallow landslides–case studies in Switzerland. For Snow Landscape Res 82:33–44

Schulz WH (2004) Landslides mapped using LIDAR imagery, Seattle, Washington. US Geological Survey Open-File Report 1396 (11)

Schweigl J, Hervás J (2009) Landslide Mapping in Austria. JRC Scientific and Technical Reports. European Commission Joint Research Centre, Institute for Environment and Sustainability, Italy. 65p

Schwenk H (1992) Massenbewegungen in Niederösterreich 1953–1990. Jahrbuch der Geologischen Bundesanstalt. Geologische Bundesanstalt, Wien, pp 597–660

Van Den Eeckhaut M, Muys B, Van Loy K, Poesen J, Beeckmann H (2009) Evidence for repeated re-activation of old landslides under forest. Earth Surf Process Landforms 34:352–365

Van Westen CJ, Asch TWJ, Soeters R (2005) Landslide hazard and risk zonation—why is it still so difficult? Bull Eng Geol Environ 65: 167–184

Zanutta A, Baldi P, Bitelli G, Cardinali M, Carrara A (2006) Qualitative and quantitative photogrammetric techniques for multi-temporal landslide analysis. Ann Geophys 49:1067–1080

B. Tables

Table B.1 Variable frequency of variables used linearly (N) or with a smoothing function (S) applying spatial k-fold cross validation (spCV) and k-fold cross validation with random subsampling (CV). The grey shaded cells mark the variable usage in the global model used to compute the susceptibility map.

Homogeneous modelling domain	0124				02297				10				35				3786				39			
spCV / CV	spCV		CV		spCV		CV		spCV		CV		spCV		CV		spCV		CV		spCV		CV	
Count of variables used N or S	N	S	N	S	N	S	N	S	N	S	N	S	N	S	N	S	N	S	N	S	N	S	N	S
Slope angle	0	100	0	100	1	99	92	8	30	70	2	98	51	14	19	75	8	79	49	51	0	100	0	100
North versus South aspect	1	0	78	0	0	0	3	0	35	1	28	8	0	0	47	2	47	2	0	0	7	2	17	2
East versus West aspect	1	0	2	0	6	0	10	4	3	0	0	3	3	2	3	1	2	0	1	0	1	2	2	0
Catchment height	41	59	22	75	3	0	99	0	24	1	5	0	0	76	10	86	49	0	27	68	30	5	33	11
Curvature	21	0	1	2	21	2	5	0	1	1	1	8	0	39	1	81	7	14	2	1	0	7	1	23
Topographic wetness index	1	52	1	23	5	13	1	12	94	3	73	26	24	76	2	92	11	10	6	1	55	2	1	1
Catchment area (log)	2	4	16	0	5	3	57	13	3	7	0	1	31	42	48	38	17	7	15	6	4	27	8	54
Convergence Index (10)	6	0	12	3	29	47	35	1	88	3	94	5	1	1	18	3	12	2	2	0	23	10	40	31
Convergence Index (50)	15	22	7	19	4	0	37	0	5	3	0	16	20	3	1	1	0	8	56	1	8	77	92	3
Permeability (0-20cm)	20	3	0	0	8	45	9	14	20	24	5	6	6	11	1	0	1	0	56	4	49	3	2	0
Permeability (min)	0	0	0	0	3	0	4	9	0	1	0	0	0	0	0	0	0	0	2	0	0	0	0	1
Void space (0-20cm)	0	0	0	0	0	0	0	0	0	0	0	0	0	0	0	0	0	0	0	0	0	0	0	0
Void space (mean 0-100cm)	0	0	0	0	0	0	0	0	0	0	0	0	0	0	0	0	0	0	0	0	0	0	0	0
Euclidian distance to tectonic lines	20	0	9	6	0	87	0	5	29	4	0	0	10	0	2	3	7	3	0	2	52	48	62	38
Euclidian distance to nappe boundaries	6	53	5	90	0	77	11	4	6	84	0	0	94	6	100	0	69	13	2	0	0	88	0	91
Mean variable count	4.28		4.71		4.61		4.33		5.4		3.79		5.07		6.34		3.68		3.56		6		6.16	
Variable count "global" model	6				7				5				7				4				6			
Percentage of total count of variables	31	69	32	68	19	81	84	16	63	37	55	45	47	53	40	60	63	38	62	38	38	62	42	58
Sum of count of variables (N+S)	427		471		458		433		540		379		510		634		368		352		600		613	
Number of earth slides	222				196				329				177				52				428			
Landslide density	0.3				0.05				0.12				0.81				0.42				0.29			

Homogeneous modelling domain	58~				104				120				126				179				191*			
spCV / CV	spCV		CV		spCV		CV		spCV		CV		spCV		CV		spCV		CV		spCV		CV	
Count of variables used N or S	N	S	N	S	N	S	N	S	N	S	N	S	N	S	N	S	N	S	N	S	N	S	N	S
Slope angle	0	100	0	100	0	100	51	0	0	100	0	100	0	100	0	100	0	100	0	100	0	100	0	100
North versus South aspect	7	5	1	0	0	0	11	0	3	2	0	0	0	0	30	0	0	0	0	0	3	46	0	0
East versus West aspect	21	15	1	0	0	1	0	0	2	0	4	0	0	0	0	0	0	0	0	0	20	2	2	9
Catchment height	10	50	0	7	1	1	2	0	0	2	1	3	43	57	0	100	91	9	91	9	0	100	0	100
Curvature	37	63	1	82	0	100	0	100	0	69	0	98	0	100	0	100	0	100	0	100	0	100	0	100
Topographic wetness index	26	64	66	34	1	90	7	69	1	92	0	100	0	100	0	100	0	63	0	99	0	100	0	100
Catchment area (log)	5	0	11	6	4	4	0	19	0	30	2	3	0	100	0	100	0	100	0	100	0	100	0	100
Convergence Index (10)	1	79	69	24	87	5	39	61	2	98	0	100	0	38	0	21	0	99	0	11	0	98	0	83
Convergence Index (50)	28	70	40	60	22	0	55	9	11	88	21	74	0	100	0	100	25	75	1	99	0	100	0	100
Permeability (0-20cm)	0	59	8	72	90	8	24	34	1	4	4	0	0	12	0	7	0	22	0	6	0	85	0	100
Permeability (min)	0	0	0	0	0	0	0	0	5	5	0	0	0	3	0	62	0	0	0	0	0	0	0	0
Void space (0-20cm)	0	5	2	1	0	0	0	0	0	0	0	0	0	0	0	0	0	0	0	0	0	0	0	0
Void space (mean 0-100cm)	0	0	0	0	0	0	0	0	0	0	0	0	0	0	0	0	0	0	0	0	0	0	0	0
Euclidian distance to tectonic lines	n.a.	n.a.	n.a.	n.a.	4	6	0	96	3	97	3	96	42	58	0	100	20	22	37	6	n.a.	n.a.	n.a.	n.a.
Euclidian distance to nappe boundaries	n.a.	n.a.	n.a.	n.a.	20	72	1	99	13	80	0	93	0	100	0	100	82	18	56	44	0	100	0	100
Mean variable count	6.55		5.85		6.16		7.26		7.08		7.02		8.53		9.2		8.26		7.59		9.54		8.94	
Variable count "global" model	6				7				8				11				8				9			
Percentage of total count of variables	21	79	34	66	37	63	28	72	5.8	94	5	95	10	90	3.3	97	26	74	24	76	2.4	98	0.2	100
Sum of count of variables (N+S)	645		585		616		677		708		702		853		920		826		759		954		894	
Number of earth slides	501				291				404				6281				1636				1419			
Landslide density	4.27				0.39				5.5				4.6				2.08				0.66			

Homogeneous modelling domain	230				239				251259				276			
spCV / CV	spCV		CV		spCV		CV		spCV		CV		spCV		CV	
Count of variables used N or S	N	S	N	S	N	S	N	S	N	S	N	S	N	S	N	S
Slope angle	10	11	36	51	10	90	17	83	0	100	0	100	35	61	11	88
North versus South aspect	25	0	36	5	0	0	3	0	0	1	2	0	1	0	31	8
East versus West aspect	1	0	11	9	2	23	32	0	4	1	1	0	17	21	7	2
Catchment height	57	25	2	85	50	46	17	83	0	33	21	74	22	4	8	1
Curvature	26	36	0	78	0	100	0	100	0	6	0	14	0	10	12	27
Topographic wetness index	10	66	12	1	0	100	0	90	10	5	31	8	17	1	16	10
Catchment area (log)	0	67	3	0	0	95	0	100	0	27	0	16	7	4	3	1
Convergence Index (10)	3	0	0	0	0	11	0	36	0	5	6	3	12	20	1	8
Convergence Index (50)	35	6	5	88	98	2	77	23	40	3	15	14	30	0	14	1
Permeability (0-20cm)	16	7	5	1	0	60	0	0	21	1	7	1	13	2	12	1
Permeability (min)	0	0	0	0	0	0	0	0	0	0	1	0	0	0	0	0
Void space (0-20cm)	0	0	0	0	0	0	0	0	0	0	0	0	0	0	0	0
Void space (mean 0-100cm)	0	0	0	0	0	0	0	0	0	0	0	0	0	0	0	0
Euclidian distance to tectonic lines	2	86	3	84	68	12	5	95	73	23	84	16	48	31	88	12
Euclidian distance to nappe boundaries	3	38	0	2	0	19	0	0	14	36	0	0	79	17	14	85
Mean variable count	5.04		5.21		7.86		7.61		4.08		4.14		4.52		4.62	
Variable count "global" model	6				7				6				4			
Percentage of total count of variables	35	65	22	78	29	71	20	80	40	60	41	59	62	38	47	53
Sum of count of variables (N+S)	530		517		786		761		403		414		452		461	
Number of earth slides	88				586				227				52			
Landslide density	0.76				0.95				0.09				0.03			

C. Maps

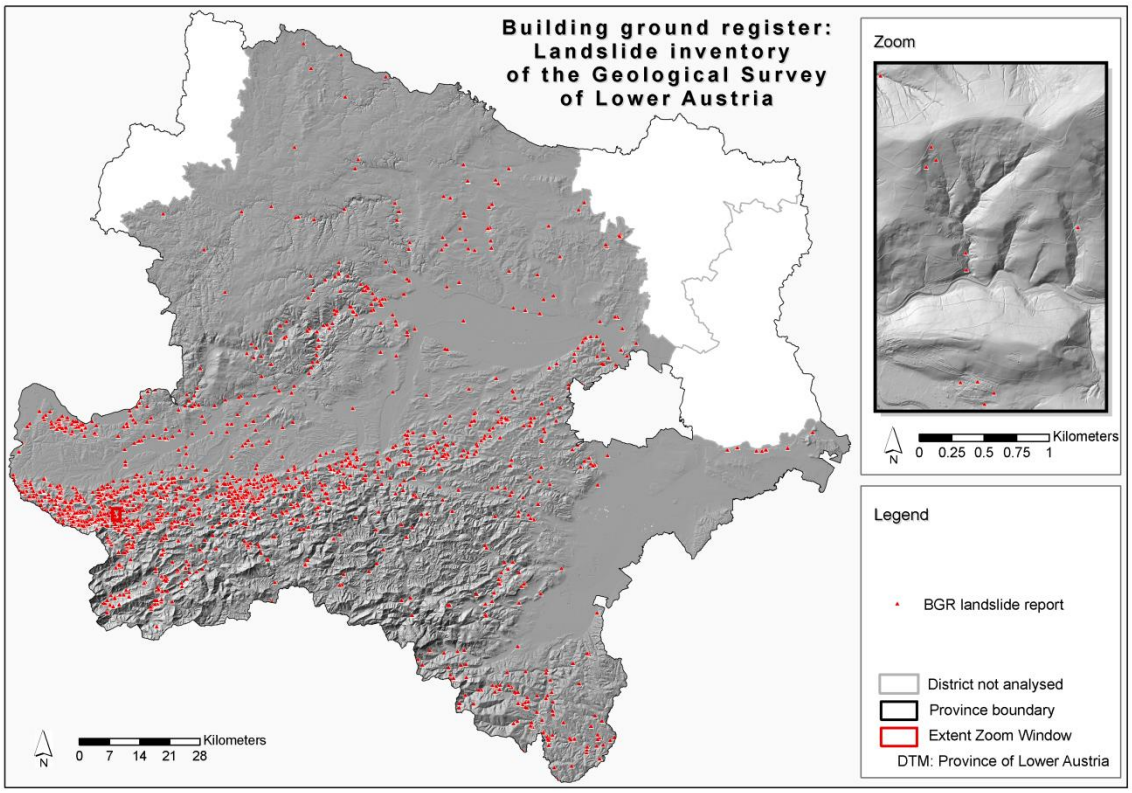

Figure C.1 Map of the Building Ground Register of the Geological Survey of Lower Austria. Source: Geological Survey of Lower Austria

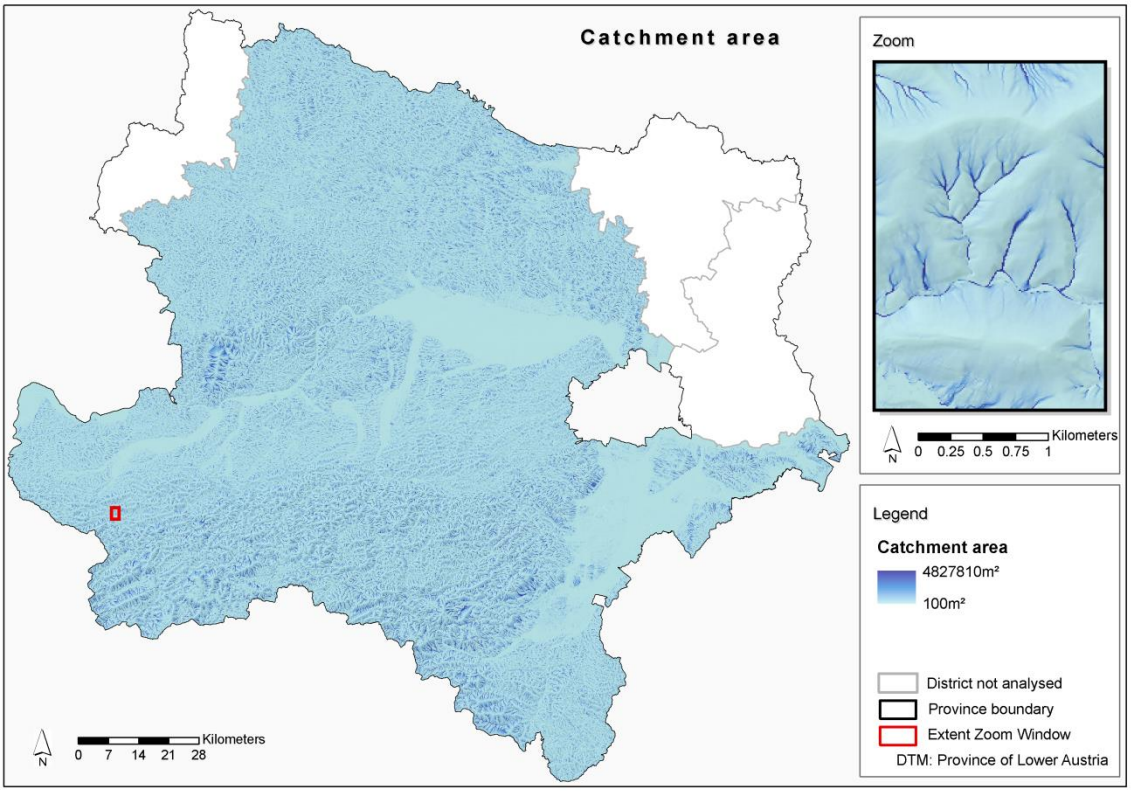

Figure C.2 Explanatory variable: catchment area

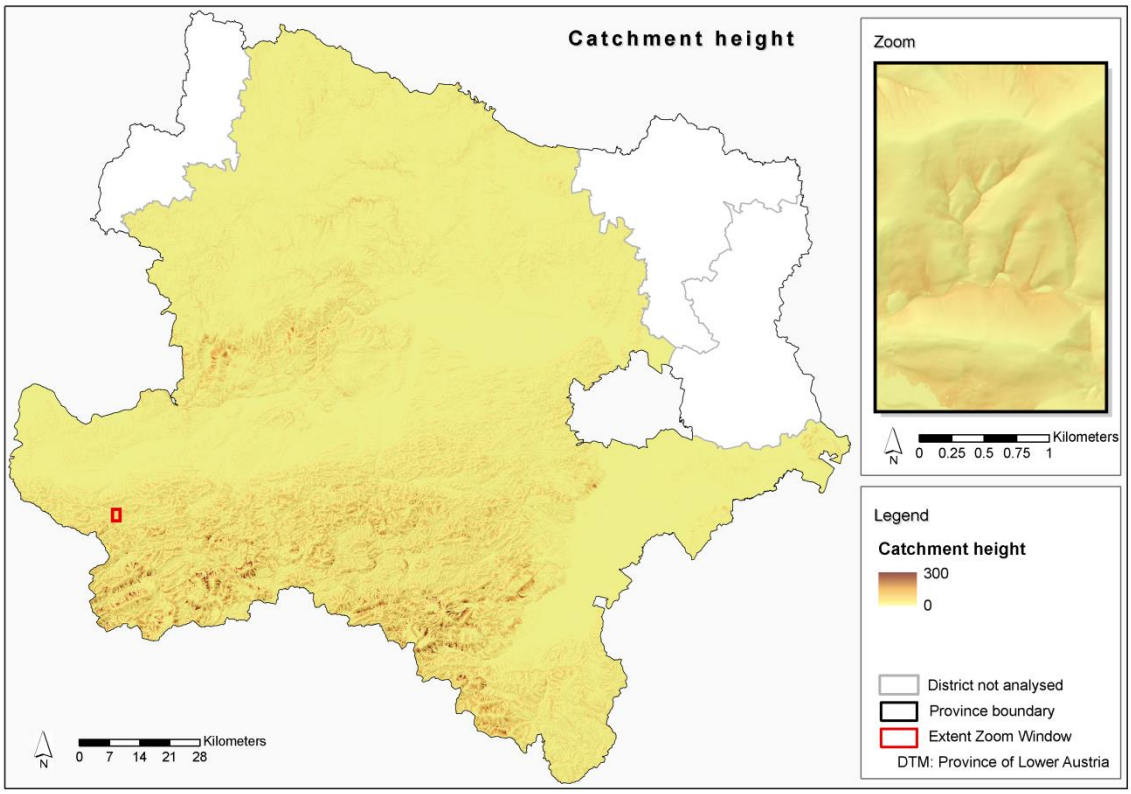

Figure C.3 Explanatory variable: catchment height

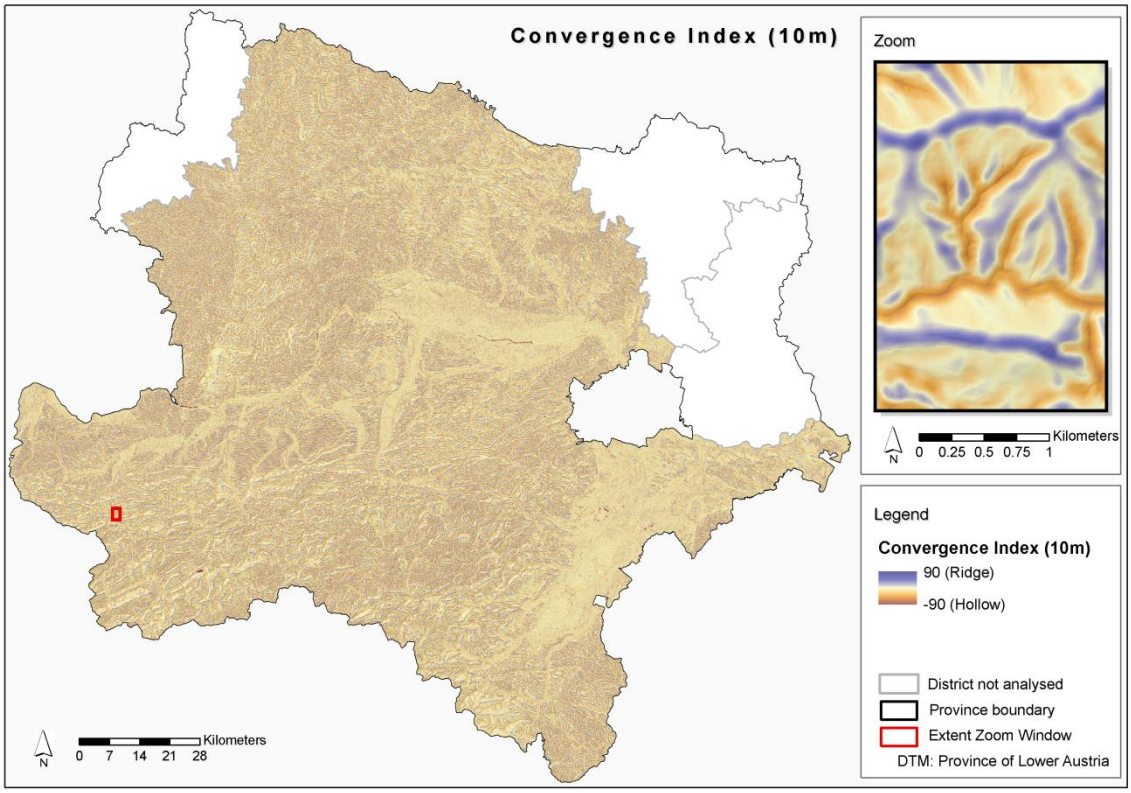

Figure C.4 Explanatory variable: convergence index (10m radius)

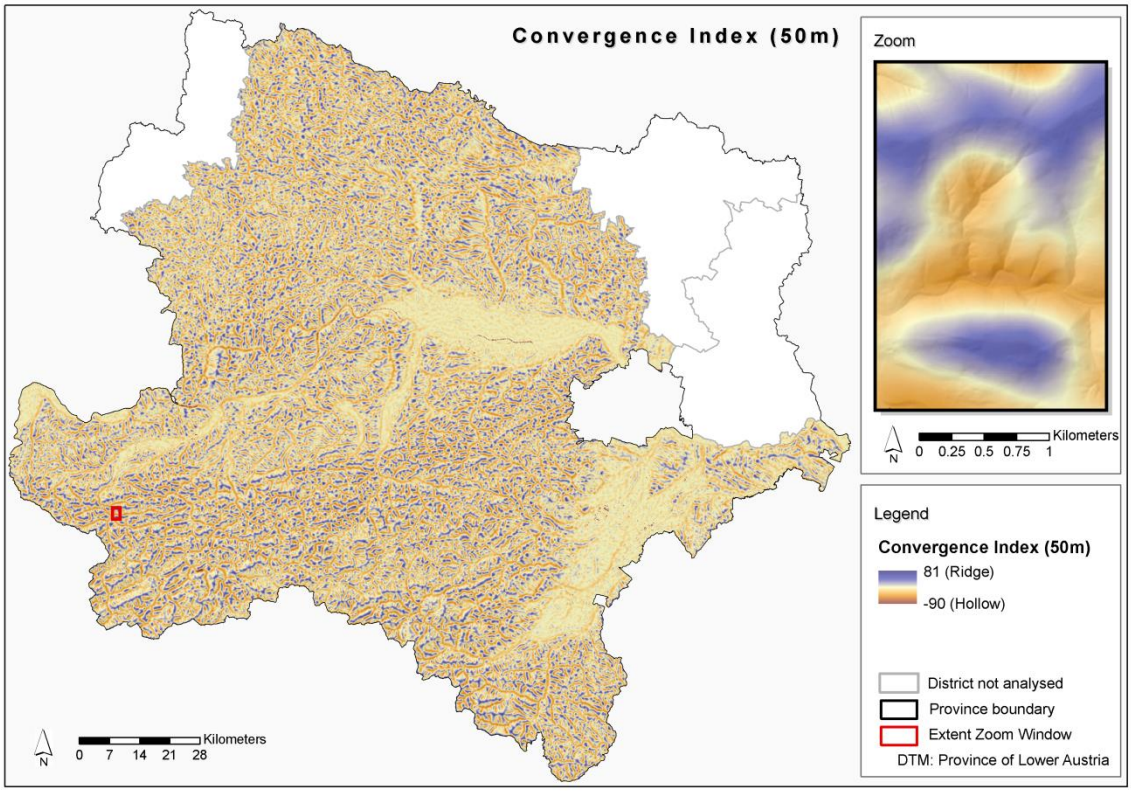

Figure C.5 Explanatory variable: convergence index (50m radius)

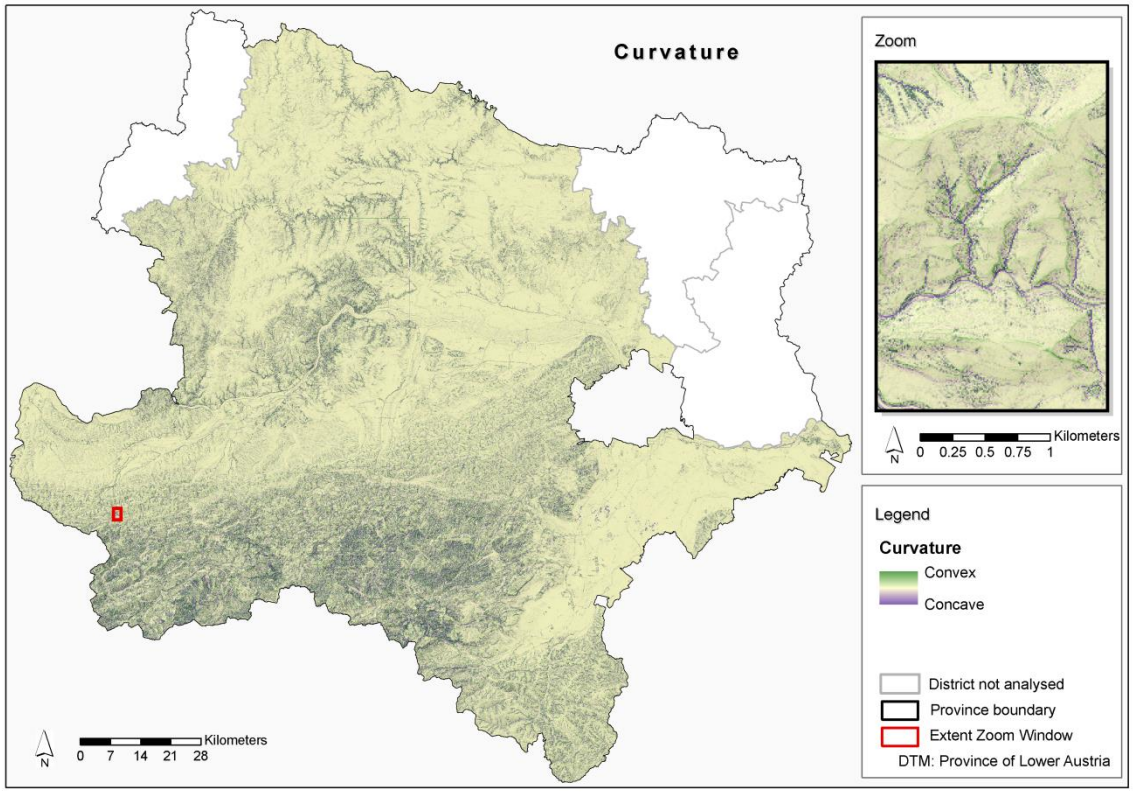

Figure C.6 Explanatory variable: Curvature

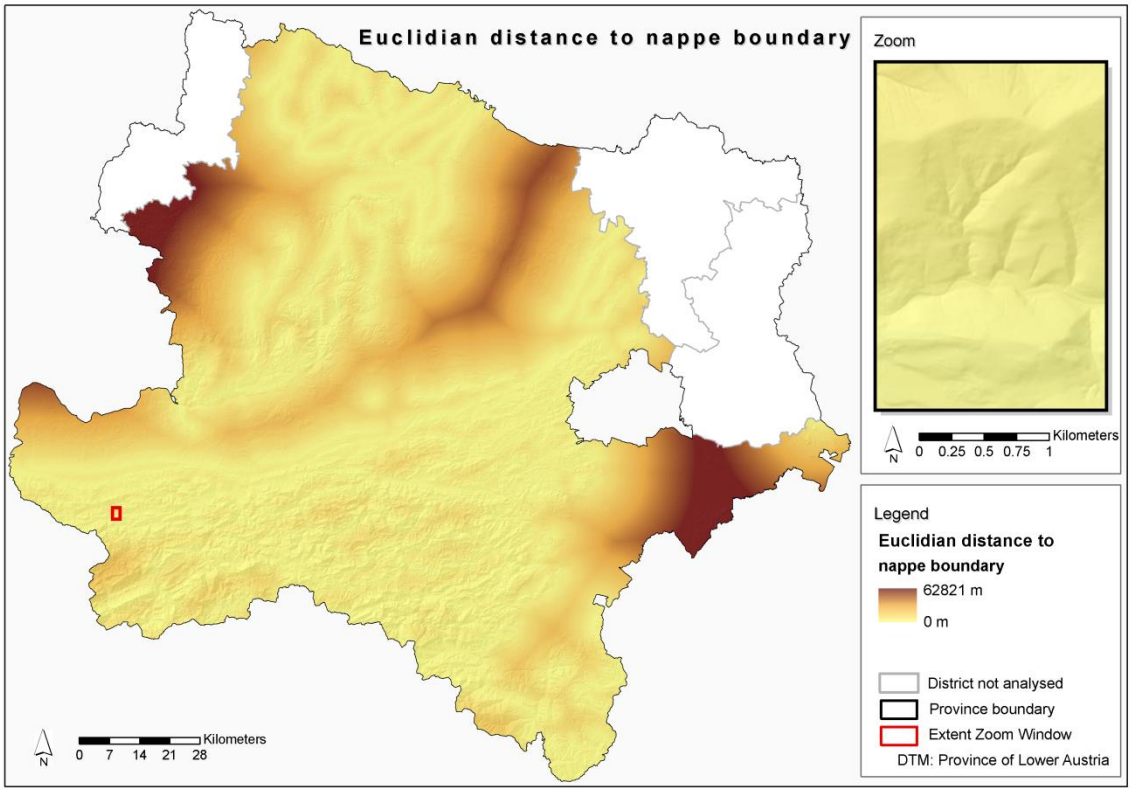

Figure C.7 Explanatory variable: Euclidian distance to nappe boundary

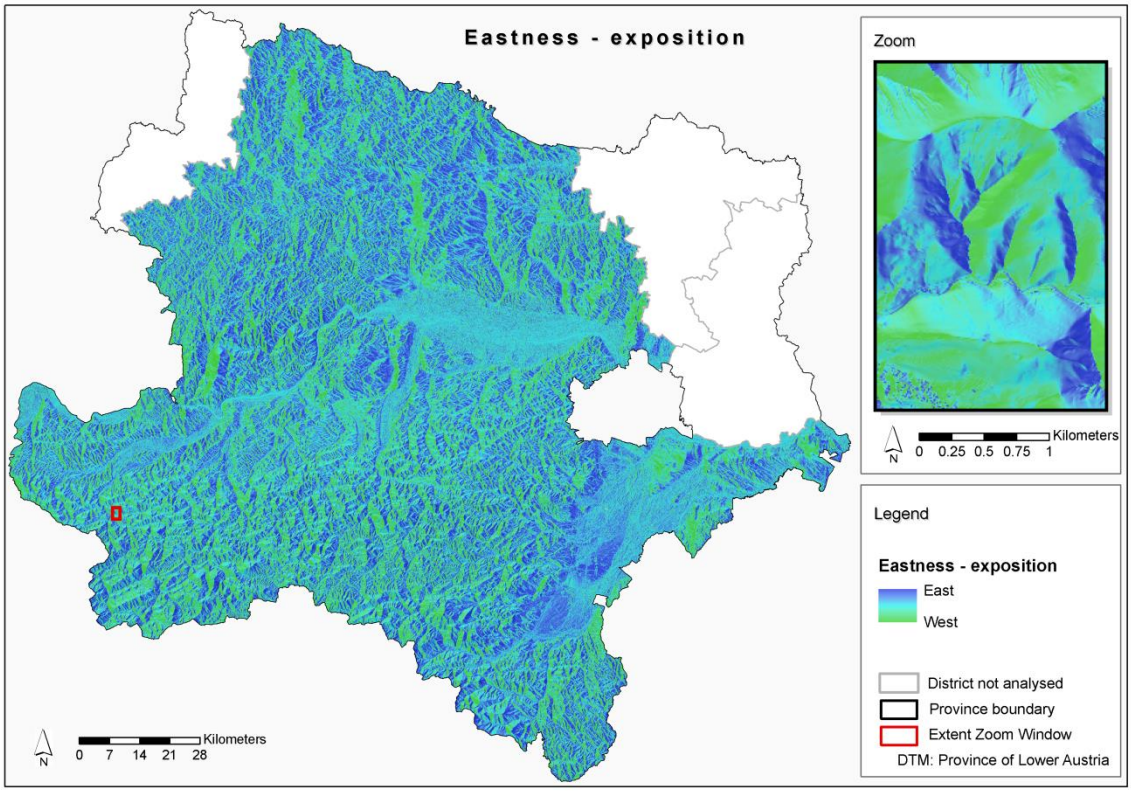

Figure C.8 Explanatory variable: East versus West exposition (Eastness)

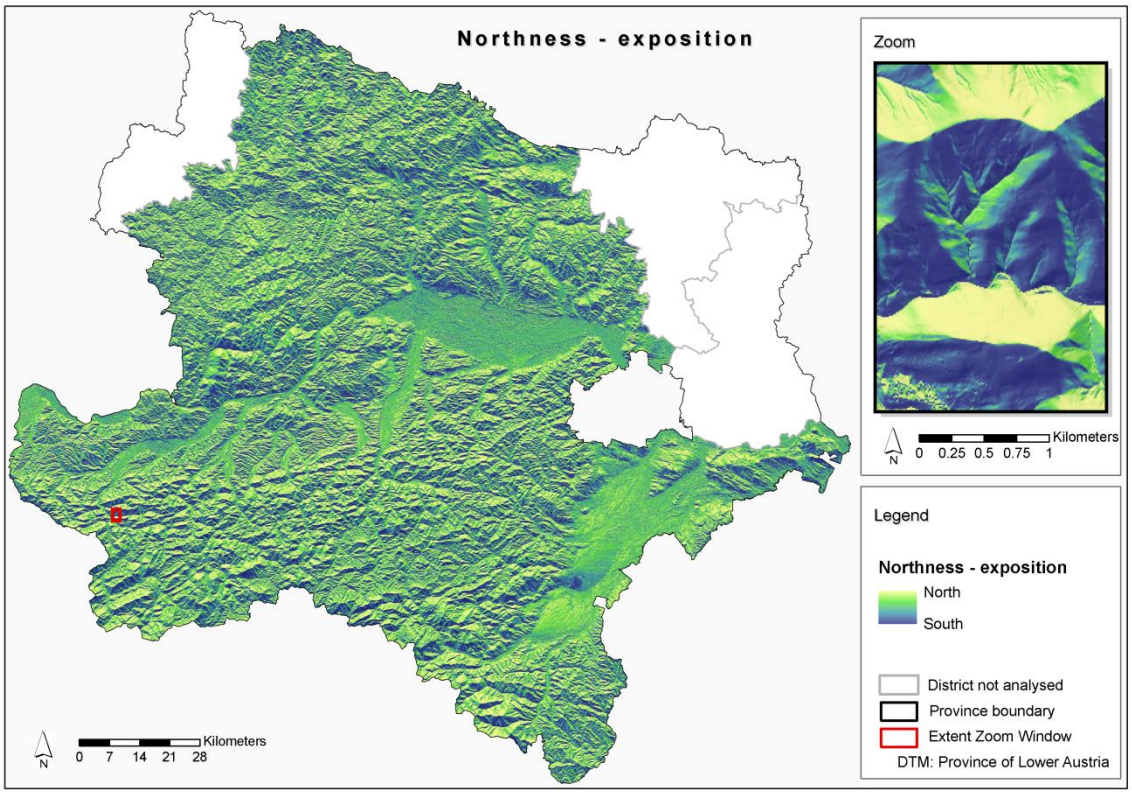

Figure C.9 Explanatory variable: North versus South exposition (Northness)

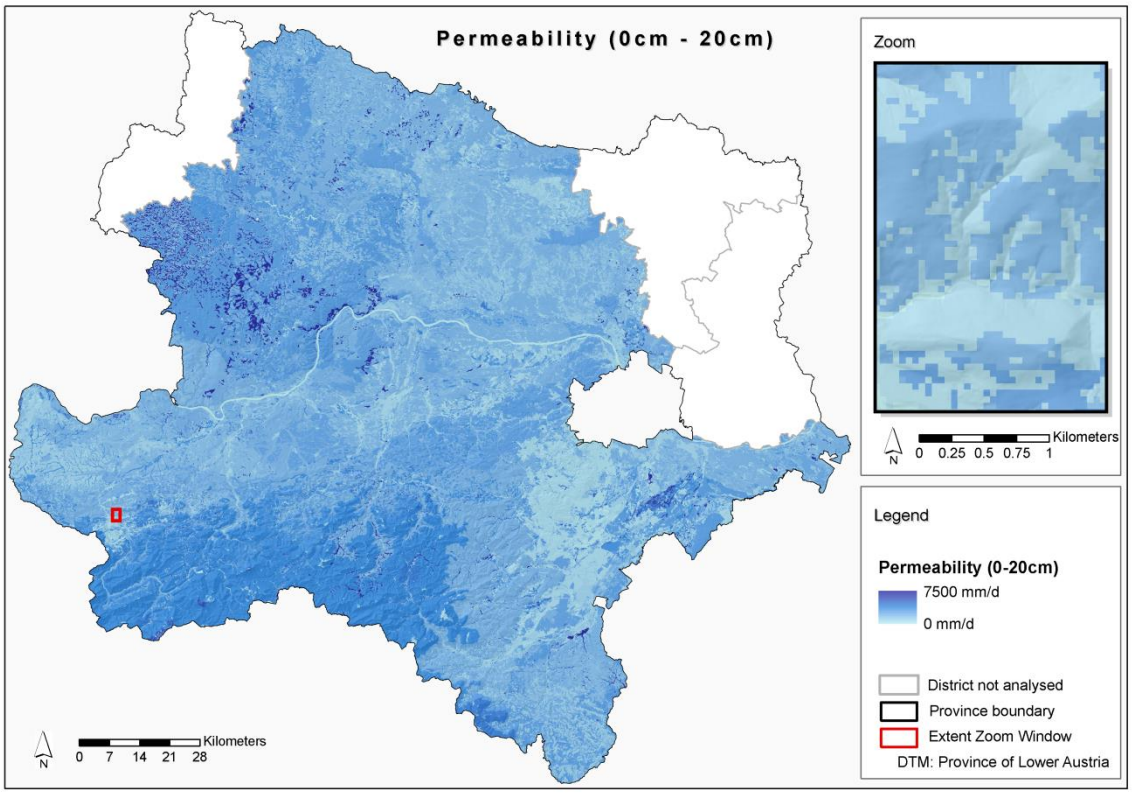

Figure C.10 Explanatory variable: Permeability (0cm - 20cm)

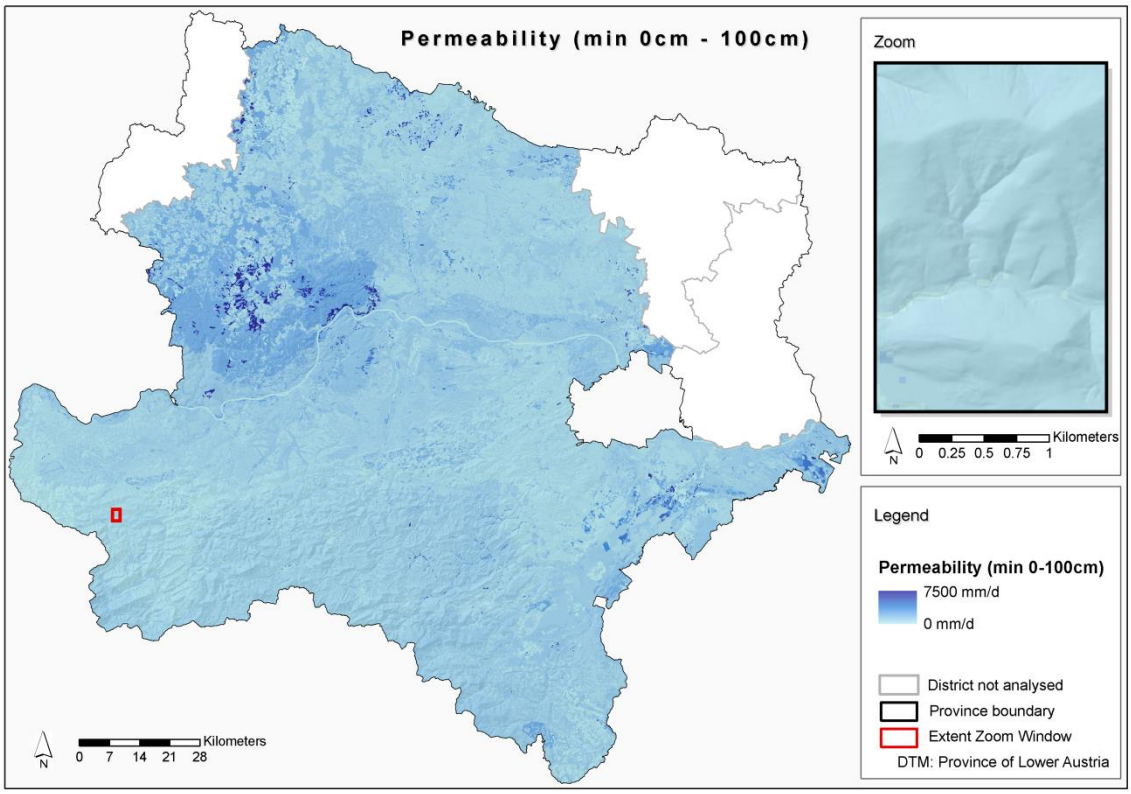

Figure C.11 Explanatory variable: Minimum permeability (0cm - 100cm)

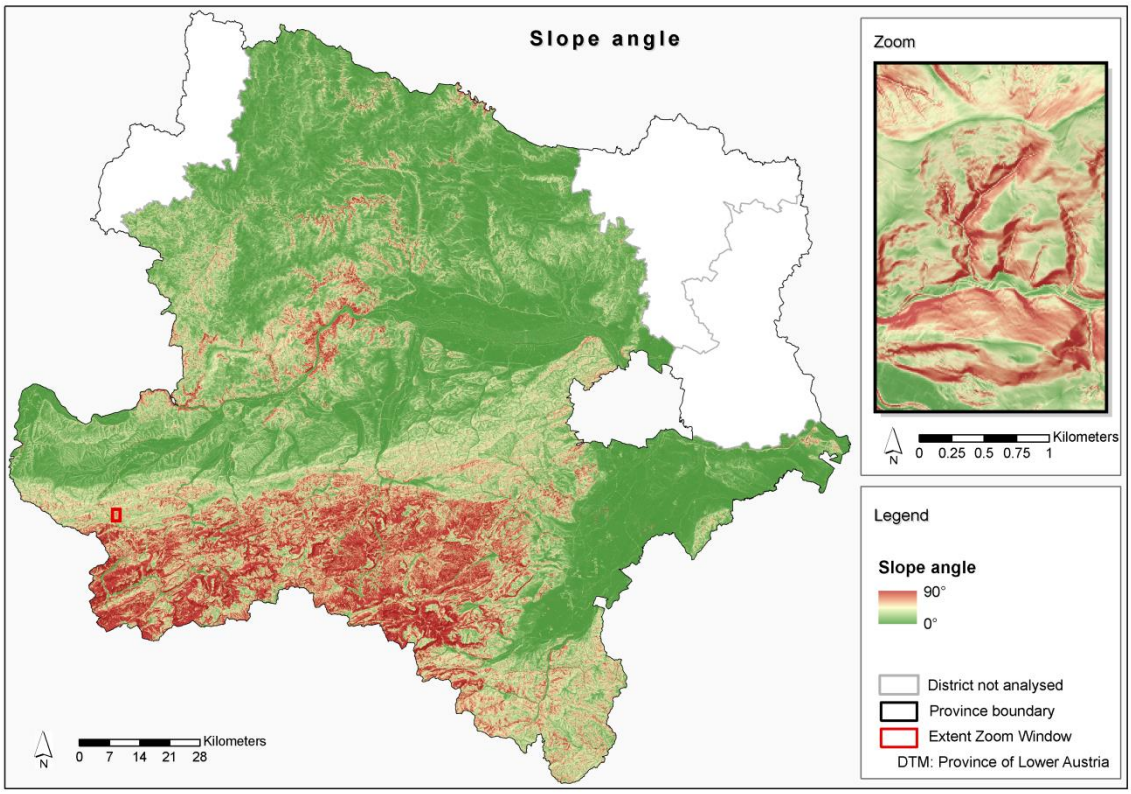

Figure C.12 Explanatory variable: Slope angle

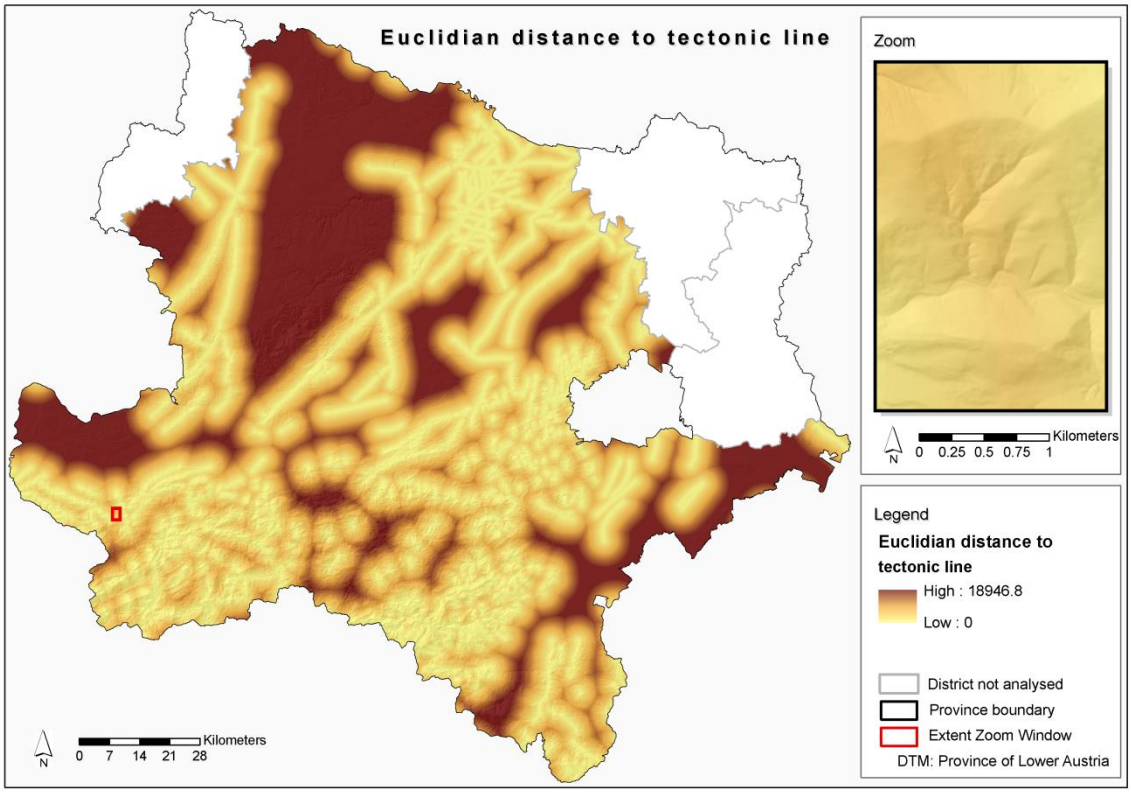

Figure C.13 Explanatory variable: Euclidian distance to tectonic line

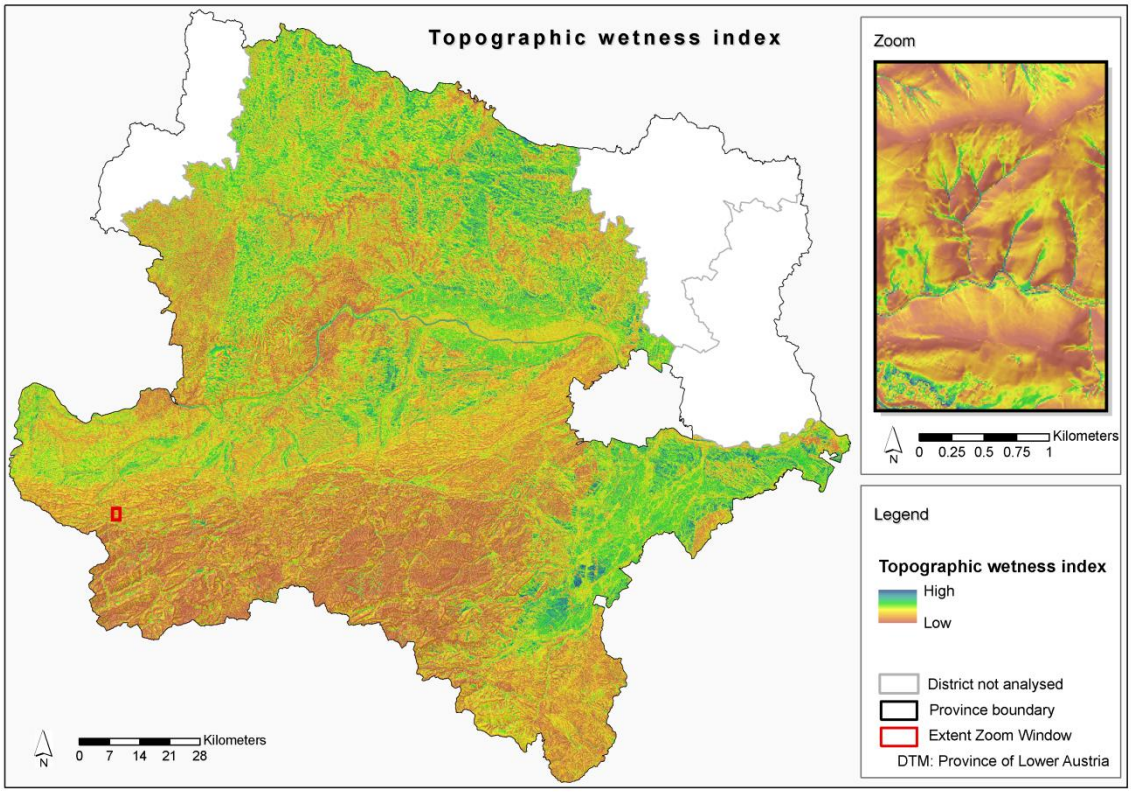

Figure C.14 Explanatory variable: Topographic wetness index

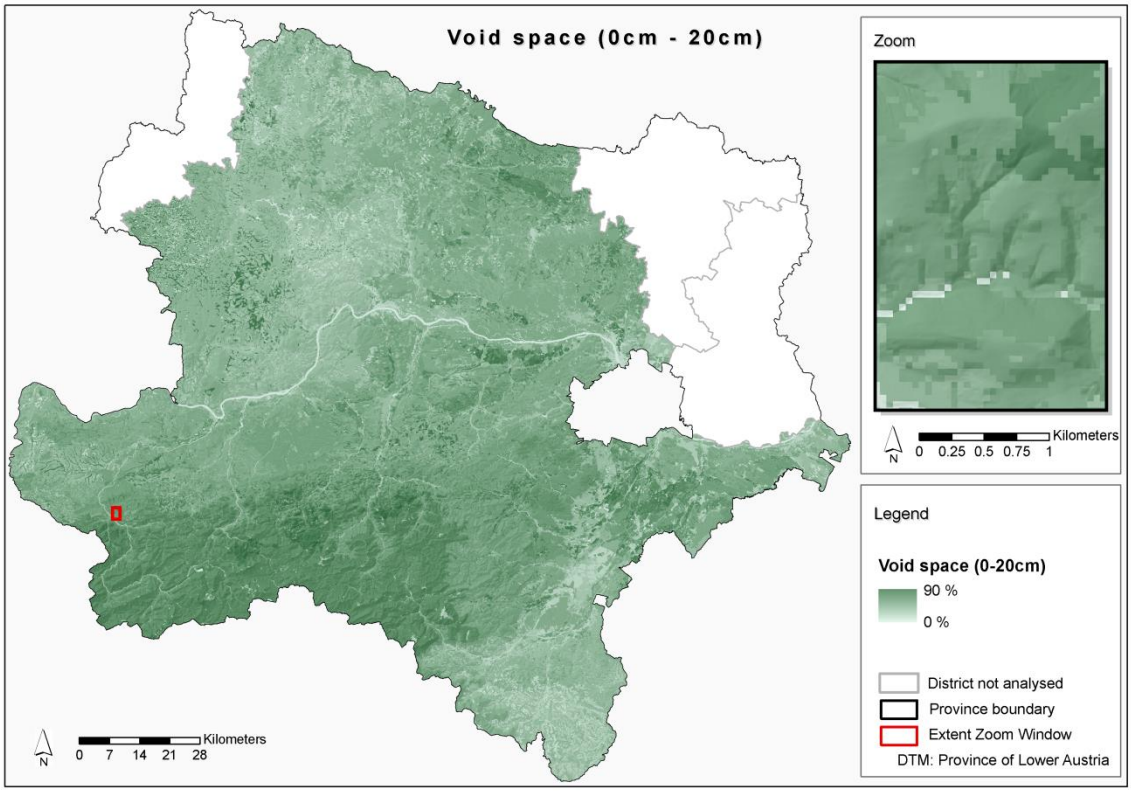

Figure C.15 Explanatory variable: Void space (0cm – 20cm)

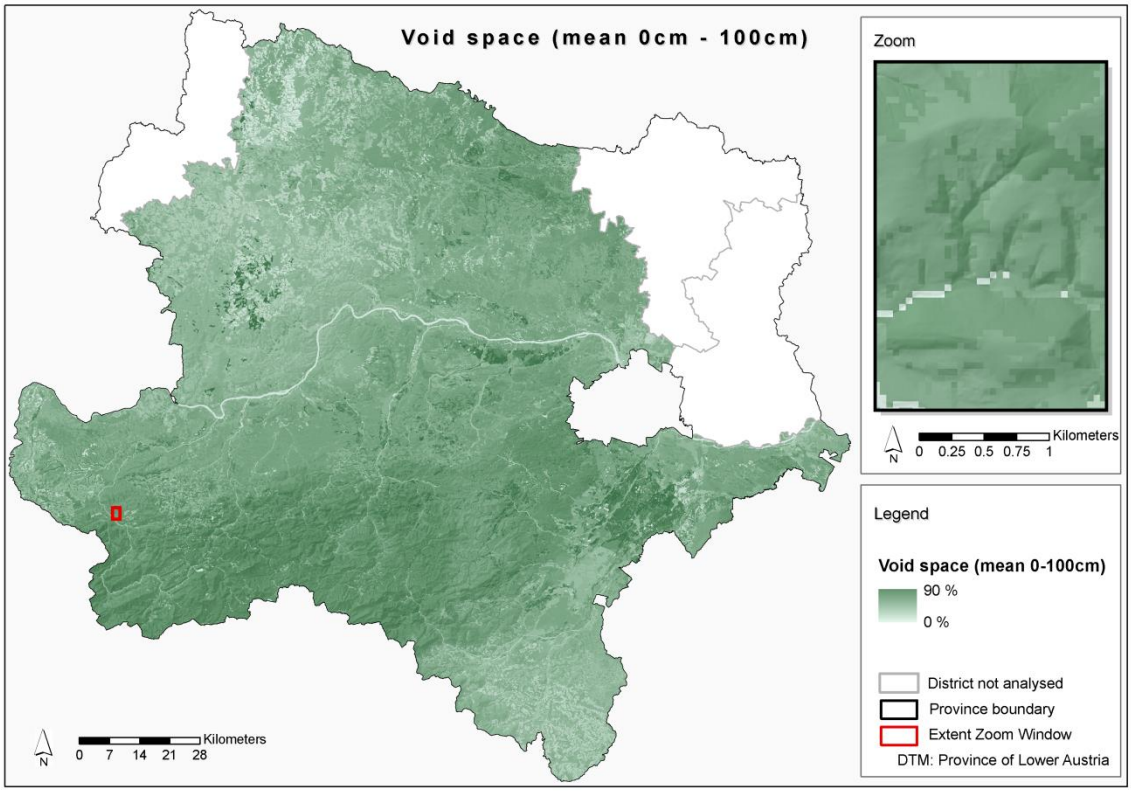

Figure C.16 Explanatory variable: Void space (mean 0cm – 100cm)

D. German and English Summary

D.1. Zusammenfassung

Die Berücksichtigung gravitativer Massenbewegungen, insbesondere Rutschungen, stellt eine besondere Herausforderung in der Raumordnung dar. In diesem Kontext wurden Gefahrenhinweiskarten für gravitative Massenbewegungen als hilfreiche Grundlage identifiziert, welche den Planungsprozess in der örtlichen Raumplanung unterstützen kann. Diese Gefahrenhinweiskarten weisen flächendeckend drei unterschiedliche Klassen aus. Jede Klasse entspricht einer Empfehlung zu Maßnahmen, welche im Fall einer Widmung, bzw. vor einem Bauvorhaben seitens der Gemeinde getätigt werden können. Diese Maßnahmen sollen dazu beitragen unerwünschte Entwicklungsarten (Widmungsarten) zu vermeiden, bzw. möglichen Schäden durch gravitative Massenbewegungen vorzubeugen.

Vor allem in Fällen wo Gefahrenhinweiskarten in der örtlichen Raumplanung zur Anwendung kommen, ist eine Aussage über ihre Qualität und deren zulässigen Interpretation unabkömmlich. Die Qualität einer Gefahrenhinweiskarte wird maßgeblich durch die Eingangsdaten, allen voran dem Inventar zu gravitativen Massenbewegungen, beeinflusst.

In der vorliegenden Dissertation wurden verschiedene Aspekte der Qualität (Modellgüte, thematische Übereinstimmung verschiedener Modellläufe, Übertragbarkeit des Modells auf andere Gebiete) einer Gefahrenhinweiskarte vor allem mit quantitativen Methoden, wie der wiederholten mehrfachen Kreuzvalidierung, untersucht. Speziell bei der Bearbeitung von sehr großen und heterogenen Gebieten entstehen Herausforderungen bezüglich Datenverfügbarkeit, beschränkter Ressourcen zur Kartierung und der Vergleichbarkeit der Gefährdung in allen Bereichen des Untersuchungsgebietes. Diesen Herausforderungen wurde mit Überlegungen zur größtmöglichen Effektivität bei der Kartierung von Rutschungen und einem neuen Forschungsdesign zur statistischen Modellierung der Rutschungsanfälligkeit eines Gebietes begegnet. Die Kartierung erfolgte auf Basis von Schummerungen eines hochauflösenden digitalen Geländemodells. Die Modellierung der Gefährdung wurde innerhalb geotechnisch und topographisch homogener Teilgebiete durchgeführt. Die Vollständigkeit des Inventars und der menschliche Einfluss auf die Auslösung von Rutschungen wurden mittels einer Persistenzanalyse der Morphologie der Rutschung und der Abschätzung des Einflusses von alten Weganalagen auf das Einzugsgebiet einer Rutschung beurteilt.

Zusätzlich wurden Unsicherheiten in der „Vorhersage“ der Rutschungsgefährdung durch die Analyse ihrer Konfidenzintervalle bestimmt. Die Überlappung von Gefährdungsklassen der Gefahrenhinweiskarten der vorhergesagten Auftretens-Wahrscheinlichkeit von Rutschungen und der Konfidenzintervalle der Vorhersage wurde ermittelt. Diese Überlappungen entsprechen den räumlichen Unsicherheiten,

welche auf einer Karte visualisiert wurden. Diese Visualisierung soll die Kommunikation über Unsicherheiten in der Gefährdungsmodellierung mit den Anwendern der Gefahrenhinweiskarte erleichtern bzw. eine Diskussion zum zulässigen Ausmaß von Unsicherheiten ankurbeln.

Im Rahmen dieser Forschungsarbeit konnte eine effektive Methode zur Kartierung von Rutschungen auf Basis des hochaufgelösten digitalen Geländemodells erarbeitet werden. Das resultierende Inventar ist besonders auf die Anforderungen der statistischen Gefährdungsmodellierung von heterogenen Gebieten abgestimmt. Die Ergebnisse bestätigen die Entscheidung für das neue Forschungsdesign, da in jedem homogenen Teilgebiet eine unterschiedliche Variablenauswahl zur besten Charakterisierung der Rutschungsanfälligkeit geführt hat. Des Weiteren konnten Unterschiede bezüglich der Modellgüte, je nach Größe der verwendeten Stichprobe zum Modellieren festgestellt werden. Teilgebiete mit sehr großen Stichproben zeigten eine geringere Spannweite der Validierungsmaße auf als Teilgebiete mit kleinen Stichprobengrößen.

Die Darstellung der Überlappung von verschiedenen Gefährdungsklassen, welche durch Berechnung der Konfidenzintervalle der Vorhersage ermittelt wurden, mit der ursprünglichen Gefahrenhinweiskarte zeigen deutlich Bereiche mit sehr großen Unsicherheiten aber auch mit sehr kleinen Unsicherheiten auf. Die Bearbeitung der Fortpflanzung von Unsicherheiten der Eingangsdaten zu Unsicherheiten der Modellierung ist eine der Perspektiven dieser Forschungsarbeit.

D.2. Summary

Landslide susceptibility maps have been identified as powerful tool for the identification of areas susceptible to landslides. As they provide spatial information on the level of susceptibility these maps are very valuable for spatial planning strategies.

The scope of this thesis was the statistical modelling of landslide susceptibility of a large and heterogeneous area, including the preparation of an inventory with high positional accuracy and the evaluation of different aspects of quality of the landslide susceptibility map. Landslides of the type earth and debris slides were visually mapped on the basis of high resolution LiDAR DTM derivatives. Assessing the effectiveness of mapping landslides for statistical susceptibility modelling the mapping of polygons and points was compared according to resources needed for the mapping and the potential output. Furthermore, the persistence and relative age of the landslide forms was assessed to estimate the incompleteness of the inventory mapped solely using LiDAR DTM derivatives and the sustainability of using land cover as explanatory variables.

The landslide susceptibility modelling was performed using generalized additive models. Information on their quality is of high importance, as the final landslide susceptibility maps may be implemented in spatial planning practices. The model performance was assessed applying a repeated *k*-fold cross-validation, once with random subsampling and once with spatial subsampling. This was done to estimate the range of performance measures using different samples for the modelling and to assess the transferability of the model. Furthermore, a good susceptibility model can be described by a high thematic consistency, which selects similar sets of input variables within each model run. As the study area was very large and heterogeneous, as defined by a large range of lithological units and geotechnical characteristics present in the area, a new study design had to be developed. This was done to characterize the landslide susceptibility of the study area in its best possible way and to allow for the comparison of the susceptibility throughout the study area. The new study design included modelling within homogeneous modelling domains. The uncertainty of the modelling result was visualized using the 95% confidence intervals of the predicted probability of landslide susceptibility. These maps were compared with the map of the predicted probability and overlaps of different susceptibility classes were derived. The visualization of these class overlaps might aid stakeholders in the interpretation of the uncertainties of a modelling result and start the discussion about acceptable uncertainty levels.

With the applied methods it was possible to identify an effective landslide inventory mapping method optimized for statistical landslide susceptibility modelling mapping points in the main scarp. Furthermore, the quality of the landslide susceptibility map was assessed quantitatively showing a different transferability and thematic consistency depending on the modelling domain size and the sample size used within the analysis. The visualization of the spatially varying prediction uncertainties was

successful showing areas of high uncertainty and of low uncertainty. This allows the identification of hot spots for future slope stability analysis with more detailed, maybe physically based models.

E. Eidesstattliche Erklärung

Hiermit erkläre ich, Helene Theresia Petschko, geboren am 16.04.1984 in St.Pölten die vorliegende Dissertation selbstständig angefertigt zu haben. Aus fremden Quellen direkt oder indirekt übernommene Informationen und Gedanken sind als solche kenntlich gemacht.

Die Arbeit wurde bisher weder in gleicher noch in ähnlicher Form einer anderen Prüfungsbehörde vorgelegt oder veröffentlicht.

Wien, Juni 2014 .....

F. Curriculum Vitae

Mag. Helene Petschko

Personal information

Adress:	Malfattigasse 19/10 1120 Wien
Mobile	+4369912256131
E-Mail	helene.petschko@univie.ac.at
Web	http://goo.gl/8SN5Y8
Nationality	Austrian

Education Qualifications

PhD candidate for Study of Natural Sciences, Geography

June 2009 - present (expected July 2014), University of Vienna, Department of Geography and Regional Research, Geomorphological Systems and Risk Research Group

Thesis title: Challenges and solutions of mapping and modeling landslide susceptibility for heterogeneous regions – providing maps for spatial planning in Lower Austria

Advisor: Univ.-Prof. Dr. Thomas Glade

Qualification: Dr.rer.nat. (expected July 2014)

Graduate Study of Theoretical and Applied Geography

October 2002 - November 2008, University of Vienna, Department of Geography and Regional Research, Geomorphological Systems and Risk Research Group

Specialization: Applied Geomorphology, Geographical Information and Visualization, and Global Environmental Change

Thesis title: Spatial prediction of landslide susceptibility - a case study in the region Gasen/Haslau in Eastern Styria, Austria (in German)

Advisor: Univ.-Prof. Dr. Thomas Glade

Qualification: Mag.rer.nat. (equivalent with MSc.); Degree with honors

Visiting Scholar at University of Waterloo, Ontario

June 20 - July 27, 2012 & July 05 - July 16, 2011

Faculty of Environment, Geography and Environment, Geomatics working group

Research: Analyzing uncertainties of landslide susceptibility models and resulting maps with the statistical methods in R and SAGA GIS
Modeling of landslide susceptibility maps with the statistical method of generalized additive model

Advisor: Dr. Alexander Brenning

Visiting PhD Student at the Geomorphology Research Group of the National Research Council of Italy (IRPI)

June 05 - 30, 2010, Perugia, Italy

Research: Landslide inventory mapping by stereoscopic interpretation of aerial photographs; Computation of slope units with GRASS GIS (r.watershed)

Advisors: Paola Reichenbach & Mauro Cardinali (Senior research scientists)

Work experience

Research associate

June 2009 - present, University of Vienna

Project title: Methods for landslide susceptibility modelling in Lower Austria

Responsibility:
- Collaborated with government and private research institutions to conduct a large-scale, applied research project
- Coordinated responsibilities of tasks to fulfil upcoming milestones
- Published and presented research results at national and international journals and conferences
- Mapped landslides using LiDAR derivatives and orthophotos and validated with field work
- Supervised graduate assistants that contributed to landslide mapping
- Communicated effectively with national authorities to acquire relevant data
- Analyzed spatial distribution of landslide susceptibility with statistical models
- Designed an easily interpretable map usable by government authorities
- Coordinated and contributed to midterm and final report writing

Funding: Provincial Government of Lower Austria

Project coordinator

June 2009 - November 2011, University of Vienna

Project title: Digitizing and data backup of the "Landslide Event and Damage Archive" of the Geological Survey of Lower Austria

Responsibility:
- Advertised open positions, seeking and interviewing job applicants
- Prepared midterm and final reports
- Supervised graduate project assistants
- Coordinated upcoming tasks with the provincial government of Lower Austria

Funding: Geological Survey of the Provincial Government of Lower Austria

Project assistant

January 2009 - May 2009, University of Vienna, Provincial Government of Lower Austria

Project title: Digitizing and data backup of the "Landslide Event and Damage Archive" of the Geological Survey of Lower Austria

Responsibility:
- Designed a systematic filing and abbreviation system for newly scanned documents on damage and landslide event reports
- Presented, discussed and reported my design and work status with the geologists and secretary of the Geological Survey

Funding: Geological Survey of the Provincial Government of Lower Austria

Teaching experience

- Field class in Physical Geography (undergraduate): July 2010, July 2011, August 2012, August 2013; 1 week each, University of Vienna; Obergurgl, Tyrol, Austria
- Field trip on landslides in Lower Austria (undergraduate and graduate) May 2011, May 2012, May 2013; 1 day, University of Vienna; Amstetten and Waidhofen/Ybbs, Lower Austria
- Lecture with lab on modelling in Physical Geography - Geomorphological Analysis with GIS (graduate): Winter term 2010, University of Vienna
- Field methods in physical geography - landslide surface and subsurface investigation (undergraduate and graduate): June 2009; 1 week, University of Vienna, Wilhelmsburg, Lower Austria

Further activities in science conveyance

- **Children's university workshop**
  July 2011, 2012, 2013; 1 day, University of Vienna, Children's university
  Topics: Workshop for kids of the age from 7-10 on "Global Warming and Glaciers" entitled "From Ice Age to a Meltdown. What is Global warming?"
- **UniClub Vienna "Winter Science Camp"**
  February 2013; 1 day, University of Vienna
  Topic: "Changes of Land Use and Flood Risk? How Geographers analyze the situation in Hinterbrühl", Workshop for Teenagers older than 13
- **Center for teaching methodology - Teaching methodology night**
  November 26, 2010 & November 14, 2012; University of Vienna
  Oral presentations on "Natural hazards and risks - Causes and consequences" and "Climate change and glaciers - Sharing know-how with 7-10 year olds in a playful environment"
- **Community youth progam "Jungschar" - Guide and Manager**
  1999 - 2010; Community of Neidling, Lower Austria
  - From the age of 15 to 26 I was volunteering as a youth guide.
  - From 2005 - 2010 I volunteered as manager and coordinator of this program, a group of 12-15 youth guides and 40 kids (from 9-15 years old).
  - I organized fund raising events, summer camps and events for the community.
  - I shared my geography interests and knowledge with the kids and teenagers in workshops on the local geology or exploring local natural hazard potiental.

Computer skills and Languages

Computer skills:
- GIS Software: ESRI ArcInfo (ArcGIS), ArcView (3.x), GRASS GIS, SAGA GIS, ILWIS
- Statistics: R, SPSS
- Microsoft office: Word, Excel, Power Point
- Adobe: Photoshop, InDesign, Illustrator, Dreamweaver
- Visualization and Layout: I designed a clean layouts of maps, presentations, reports and announcements of events for work related tasks. I also enjoy exploring design elements in my hobbies (painting and photography).

Languages:
- German (first language)
- English (fluent in talking and writing)

Academic/Professional Society Membership and Offices

- Chair, Austrian research group for geomorphology and global environmental change (geomorph.at; elected September 2012, in office since January 2013)
- National delegate to the International Association of Geomorphologists (IAG; 2013 - present)
- Executive board member of the Austrian Association of Geographers (ÖGG; 2013 - present)
- European Geosciences Union (EGU; 2010 - present)

Service to the discipline

- Refereeing activities for the journals Natural Hazards and Earth System Sciences (NHESS), Natural Hazards (NHAZ) and Mountain Research and Development.
- Organization of a poster session for young geomorphologists at the Swiss-Austrian Mountain Days

Awarded Grants

- "Research developement program" grant for international communication awarded from the Austrian Research Association in May 2014 (700€)
- Grant for "scientific research and specialist courses (outgoing)" awarded from the University of Vienna in the summer term 2010 (650 €)
- Grant for the costs of the Mountain Risks Intensive Course on Multi-technique landslide investigation for hazard assessment in 2009 in Switzerland awarded from the Marie Curie Actions Mountain Risks Project (300 €)

List of Publications

Journal publications (peer-reviewed)

Petschko, H., Brenning, A., Bell, R., Goetz, J., & T. Glade (2014), Assessing the quality of landslide susceptibility maps – case study Lower Austria, Nat. Hazards Earth Syst. Sci., 14, 95-118, doi:10.5194/nhess-14-95-2014. Revised and Published Paper.

Petschko, H., Brenning, A., Bell, R., Goetz, J. & T. Glade (2013): Assessing the quality of landslide susceptibility maps – case study Lower Austria, Nat. Hazards Earth Syst. Sci. Discuss., 1, 1001-1050, doi:10.5194/nhessd-1-1001-2013. Discussion Paper.

Bell, R., Petschko, H., Röhrs, M. & A. Dix (2012), Assessment of landslide age, landslide persistence and human impact using airborne laser scanning digital terrain models, Geografiska Annaler: Series A, Physical Geography, 94(1), pp.135–156.

Conference Proceedings (peer-reviewed)

Petschko, H., Bell, R., Brenning, A. & T. Glade (2012), Landslide susceptibility modeling with generalized additive models - facing the heterogeneity of large regions, in: Eberhardt E., Froese C., Turner A.K., & S. Leroueil (Eds.), Landslides and Engineered Slopes, Protecting Society through Improved Understanding, Taylor & Francis, Banff, Alberta, Canada, pp. 769–777.

Glade, T., Petschko, H., Bell, R., Bauer, C., Granica, K., Heiss, G., Leopold, P., Pomaroli, G., Proske, H. & J. Schweigl (2012), Landslide susceptibility maps for Lower Austria - Methods and Challenges, in: Koboltschnig G., Hübl J., & Braun J. (Eds.), Interpraevent Conference Proceedings, International Research Society INTERPRAEVENT, Grenoble, France, pp. 497–508.

Petschko, H., Glade, T., Bell,R., Schweigl, J. & G. Pomaroli (2010), Landslide inventories for regional early warning systems, in: Malet, J.P., Glade, T. & Casagli, N. (Eds.), Proceedings of the International Conference 'Mountain Risks: Bringing Science to Society', Strasbourg, CERG Editions, pp. 277-282.

Conference proceedings

Petschko, H., Bell, R., Glade, T., Goetz, J., Heiss, G. &P. Leopold (2013), MoNOE – Modellierung der Rutschprozesse (in German, Project MoNOE - Modelling of slide processes), NÖ Geotage "Geogene Gefahren und Raumordnung", 19. - 20. September 2013, Rabenstein an der Pielach, Niederösterreich. pp. 77-87.

Bell, R., Petschko, H. & T. Glade (2013), Gefährdungsmodellierung bei gravitativen Massenbewegungen (in German, Landslide susceptibilty modelling methods), NÖ Geotage "Geogene Gefahren und Raumordnung", 19. - 20. September 2013, Rabenstein an der Pielach, Niederösterreich. pp. 54-61.

Book chapter (peer-reviewed)

Petschko H, Bell R, Glade T (2014) Relative Age Estimation at Landslide Mapping on LiDAR Derivatives: Revealing the Applicability of Land Cover Data in Statistical Susceptibility Modelling. In: Sassa K, Canuti P, Yin Y (Eds.) Landslide Science for a Safer Geoenvironment. Springer International Publishing, pp 337–343.

Petschko, H., Bell, R., Leopold, P., Heiss, G. & T., Glade (2013), Landslide inventories for reliable susceptibility maps, in: Margottini, C., Canuti, P. & K. Sassa (Eds.), Landslide Science and Practice, vol. 1: Landslide Inventory and Susceptibility and Hazard Zoning, Springer, pp. 281-286.

Bell, R., Glade, T., Granica, K., Heiss, G., Leopold, P., Petschko, H., Pomaroli, G., Proske, H., & J. Schweigl (2013), Landslide susceptibility maps for spatial planning in Lower Austria, in: Margottini, C., Canuti, P. & K. Sassa (Eds.), Landslide Science and Practice, vol. 1: Landslide Inventory and Susceptibility and Hazard Zoning, Springer, pp. 467-473.

Leopold, P., Heiss, G., Petschko, H., Bell, R. & T. Glade (2013), Susceptibility maps for landslides using different modelling approaches, in: Margottini, C., Canuti, P. & K. Sassa (Eds.), Landslide Science and Practice, vol. 1: Landslide Inventory and Susceptibility and Hazard Zoning, Springer, pp. 353-357.

Popular Science publications

Glade, T., Petschko, H., Bell, R., Leopold, P. & H. Proske (2013), Karten zu gravitativen Massenbewegungen. Möglichkeiten und Grenzen ihrer Aussagekraft. Raumdialog - Magazin für Raumplanung und Regionalentwicklung in Niederösterreich 2, pp. 10–13.

Glade, T., Petschko, H., Bell, R., Leopold, P. & H. Proske (2013), "MoNOE" - Das Projekt: Gefahrenhinweiskarten für gravitative Massenbewegungen in NÖ. Raumdialog - Magazin für Raumplanung und Regionalentwicklung in Niederösterreich 2, pp. 14–17.

Pomaroli, G., R. Bell, T. Glade, G. Heiss, P. Leopold, H. Petschko, H. Proske & J. Schweigl (2011), Darstellung der Gefährdung durch gravitative Massenbewegungen im Bundesland Niederösterreich als Grundlage der Raumplanung (in German: Landslide susceptibility maps for Lower Austria for spatial planning), in: Skolaut C. (Ed.), Wildbach- und Lawinenverbau, Zeitschrift für Wildbach-, Lawinen-, Erosions- und Steinschlagschutz, Verein der Diplomingenieure der Wildbach und Lawinenverbauung Österreichs, Villach, pp. 198-212.

Petschko, H. (2009), Flüsse und Bäche aus dem Wienerwald – Klein aber oho. (in German: Rivers and trenches of the Vienna Forest – small but powerful). in: Embleton-Hamann, C., Keiler, M. & I. Teufl (Eds.): Wien - Umweltstadtführer. Einblicke in die Natur einer Großstadt. Böhlau, Wien, pp. 51-61.

Petschko, H. (2009), Böden und Landwirtschaft in Wien – der Bauer und das liebe Vieh in der Großstadt. (in German: Soils and Agriculture in Vienna), in: Embleton-Hamann, C., Keiler, M. & I. Teufl (Eds.): Wien - Umweltstadtführer. Einblicke in die Natur einer Großstadt. Böhlau, Wien, pp. 101-109.

Petschko, H. und K., Sattler (2009), Rodaun – die zwei Gesichter des Wienerwaldes. (in German: Rodaun – the two faces of the Vienna Forest, a field trip), in: Embleton-Hamann, C., Keiler, M. & I. Teufl (2009): Wien - Umweltstadtführer. Einblicke in die Natur einer Großstadt. Böhlau, Wien, pp. 187-201.

Petschko, H. (2009), Dem Wienfluss entgegen. (in German: Towards the Vienna River, a field trip) In: Embleton-Hamann, C., Keiler, M. & I. Teufl (2009): Wien - Umweltstadtführer. Einblicke in die Natur einer Großstadt. Böhlau, Wien, pp.201-217.

Conference oral presentations

Petschko H, Bell R, Glade T (2014) Relative Age Estimation at Landslide Mapping on LiDAR Derivatives: Revealing the Applicability of Land Cover Data in Statistical Susceptibility Modelling. In: Sassa K, Canuti P, Yin Y (Eds.) Landslide Science for a Safer Geoenvironment. Springer International Publishing, pp 337–343.

Petschko, H., Brenning, A., Goetz, J., Bell, R., & T. Glade (2014), Spatially varying prediction uncertainties and their implications on landslide susceptibility maps. Geophysical Research Abstracts Vol. 16, EGU2014-7041.

Petschko, H., Bell, R., Glade, T., Goetz, J., Heiss, G. &P. Leopold (2013), MoNOE – Modellierung der Rutschprozesse (in German, Project MoNOE - Modelling of slide processes), NÖ Geotage "Geogene Gefahren und Raumordnung", Rabenstein an der Pielach, Niederösterreich, 19. - 20. September 2013.

Bell, R., Petschko, H. & T. Glade (2013), Gefährdungsmodellierung bei gravitativen Massenbewegungen (in German, Landslide susceptibilty modelling methods), NÖ Geotage "Geogene Gefahren und Raumordnung", Rabenstein an der Pielach, Niederösterreich, 19. - 20. September 2013.

Bell, R., Petschko, H. & A. Brenning (2013), Age-dependent footprint of landslides in airborne laser scanning digital terrain models, 8th IAG International Conference on Geomorphology, August 27 - 31, 2013.

Bell, R., Petschko, H., Bauer, C., Glade, T., Granica, K., Heiss, G., Leopold, P., Pomaroli, G., Proske, H. & J. Schweigl, J. (2013), Implementation of landslide susceptibility maps in Lower Austria as part of risk governance. Geophysical Research Abstracts Vol. 15, EGU2013-10204.

Petschko, H., Goetz, J., Brenning, A., Bell, R., & T. Glade (2012), Spatial transferability of landslide susceptibility models for the province Lower Austria. 32nd International Geographical Congress, Cologne, 26.-30. August 2012.

Petschko, H., Bell, R., A. Brenning, and T. Glade (2012), Landslide susceptibility modeling with generalized additive models - facing the heterogeneity of large regions, International Symposium on Landslides and North American Symposium on Landslides "Landslides and Engineered Slopes, Protecting Society through Improved Understanding", Banff, Alberta, Canada, June 3-8 2012.

Petschko, H., Brenning, A., Goetz, J., Bell, R., Glade, T. (2012), Assessing the quality of landslide susceptibility maps for Lower Austria. Geophysical Research Abstracts Vol. 14, EGU2012-7437.

Bell, R. & H. Petschko (2012), Landslide persistence and human impact in Lower Austria assessed by lidar data and aerial photography. Geophysical Research Abstracts Vol. 14, EGU2012-9898.

Petschko, H., Bell, R., Glade, T., Granica, K., Heiss, G., Leopold, P. & H. Proske (2011), Methodenentwicklung zur Gefährdungsmodellierung von gravitativen Massenbewegungen in Niederösterreich – MoNOE. Vortrag bei den NÖ-Geotagen „Gefahr – Wasser – Versorgung", 29.-30. September 2011, Schloss Haindorf bei Langenlois.

Petschko, H., Bell, R., Glade, T., Tilch, N., Schwarz, L. & A. Kociu (2009), Gravitative Massenbewegungen und der Mensch – Spuren des Anthropogenen Einflusses am Beispiel der Region Gasen/Haslau (Oststeiermark). (Landslides and human beings – traces of the human impact on landslide triggering at the case study at Gasen/Haslau (Eastern Styria - Austria)) Presentation in German at meeting of the working group "Natural Hazard and Natural Risk" at the „Deutscher Geographentag" - conference in Vienna, 19.9.2009.

Conference poster presentations

Petschko, H., Bell, R., Glade, T., Goetz, J., Granica, K., Heiss, G., Leopold, P., Pomaroli, G., Bauer, G., Proske, H. & J. Schweigl (2013), Methods for landslide susceptibility assessment - concepts and applications for spatial planning in Lower Austria, 8th IAG International Conference on Geomorphology, August 27 - 31, 2013.

Gassner, C., Promper, C., Petschko, H. & T. Glade (2013), Scenarios of future landslide susceptibility – incorporating changes in land cover and climate. Geophysical Research Abstracts Vol. 15, EGU2013-6786.

Steger, S., Bell, R., Petschko, H. & T. Glade (2013), Exploratory data analysis as an alternative to automated variable selection in statistical susceptibility modeling. A case study for the Flysch Zone (Lower Austria). Geophysical Research Abstracts Vol. 15, EGU2013-10276.

Gassner, C., Petschko, H., Bell, R. & T. Glade (2012), Effect of lithological data of different scales on modelling landslide susceptibility maps. Geophysical Research Abstracts Vol. 14, EGU2012-11262.

Petschko, H., Bell, R., Glade, T., Granica, K., Heiss, G., Leopold, P. & H. Proske (2011), Methodenentwicklung zur Gefährdungsmodellierung von gravitativen Massenbewegungen in Niederösterreich – MoNOE. NÖ-Geotage „Gefahr – Wasser – Versorgung", 29.-30. September 2011, Schloss Haindorf bei Langenlois.

Petschko, H., Bell, R., Brenning, A. & T. Glade (2011), Modelling landslide susceptibility in large and heterogeneous regions with generalised additive models: case study Lower Austria. Geophysical Research Abstracts Vol. 13, EGU2011-6155.

Petschko, H., Bell, R., Glade, T., Leopold, P. & J. Schweigl (2010), Compiling a landslide inventory for state wide susceptibility modelling in Lower Austria. Geophysical Research Abstracts Vol. 12, EGU2010-8770.

Bell, R., Petschko, H., Glade, T., Leopold, P., Heiss, G., Proske, H., Granica, K., Schweigl, J. & G. Pomaroli (2010), Methods for landslide susceptibility modelling in Lower Austria. Geophysical Research Abstracts, Vol. 12, EGU2010-9869.

Bell, R. & H. Petschko (2010), New potentials of laser scanning in landslide hazard assessments. Geophysical Research Abstracts Vol. 12, EGU2010-13645.

Petschko, H., Bell, R., Glade, T., Tilch, N. & A. Kociu (2008), Spatial prediction of landslide hazards – A case study in Gasen/Haslau (Eastern Styria, Austria). Geophysical Research Abstracts, Vol. 10, EGU2008-A-09948.

Oral presentations

Pöppl. R., Petschko, H., Promper, C. & R. Bell (2012), "Climate change and glaciers - Sharing know-how with 7-10 year olds in a playful environment", Teaching methodology night, November 14, 2012, University of Vienna. (in German)

Bell, R. and H. Petschko (2010), Natural hazards and risks - Causes and consequences, Teaching methodology night, November 26, 2010, University of Vienna. (in German)